

Some pages of this thesis may have been removed for copyright restrictions.

If you have discovered material in Aston Research Explorer which is unlawful e.g. breaches copyright, (either yours or that of a third party) or any other law, including but not limited to those relating to patent, trademark, confidentiality, data protection, obscenity, defamation, libel, then please read our [Takedown policy](#) and contact the service immediately (openaccess@aston.ac.uk)

**REACTIVE PROCESSING OF POLYOLEFINS
USING ANTIOXIDANT SYSTEMS**

NENG SRI SUHARTY
Doctor of Philosophy

THE UNIVERSITY OF ASTON IN BIRMINGHAM

March 1993

This copy of the thesis has been supplied on condition that anyone who consults it is understood to recognise that its copyright rest with its author and that no quotation from the thesis and no information derived from it may be published without proper acknowledgement.

ASTON UNIVERSITY

REACTIVE PROCESSING OF POLYOLEFINS USING ANTIOXIDANT SYSTEMS

NENG SRI SUHARTY

Doctor of Philosophy

March 1993

SUMMARY

Various monoacrylic compounds containing a hindered phenol function (e.g. 3,5-di-tert.-butyl-4-hydroxy benzyl alcohol, DBBA and vinyl-3-[3',5'-di-tert.-butyl-4-hydroxy phenyl] propionate, VDBP), and a benzophenone function (2-hydroxy-4-[beta hydroxy ethoxy] benzophenone, HAEB) were synthesised and used as reactive antioxidants (AO's) for Polypropylene (PP). These compounds were reacted with PP melt in the presence of low concentration of a free radical generator such as peroxide (reactive processing) to produce bound-antioxidant concentrates. The binding reaction of these AO's onto PP was found to be low and this was shown to be mainly due to competing reactions such as homopolymerisation of the antioxidant. At high concentrations of peroxide, higher binding efficiency resulted, but, this was accompanied by melt degradation of the polymer. In a special reactive processing procedure, a di- or a trifunctional reactant (referred to as coagent), e.g. tri-methylol propane tri-acrylate, Tris, and Divinyl benzene, DVB, were used with the antioxidant and this has led to an enhanced efficiency of the grafting reaction of antioxidants on the polymer in the melt. The evidence suggests that this is due to copolymerisation of the antioxidants with the coagent as well as grafting of the copolymers onto the polymer backbone.

Although the 'bound' AO's containing a UV stabilising function showed lower overall stabilisation effect than the unbound analogues before extraction, they were still much more effective when subjected to exhaustive solvent extraction. Furthermore, a very effective synergistic stabilising activity was achieved when two reactive AO's containing thermal and UV stabilising functions e.g. DBBA and HAEB, were reactively processed with PP in the presence of a coagent. The stabilising effectiveness of such a synergist was much higher than that of the unbound analogues both before and after extraction.

Analysis using the GPC technique of concentrates containing bound-DBBA processed in the presence of Tris coagent showed higher molecular weight (Mn), compared to that of a polymer processed without the coagent, but was still lower than that of the control processed PP with no additives. This indicates that Tris coagent may inhibit further melt degradation of the polymer. Model reactions of DBBA in liquid hydrocarbon (decalin) and analysis of the products using FTIR and NMR spectroscopy showed the formation of grafted DBBA onto decalin molecules as well as homopolymerisation of the AO. In the presence of Tris coagent, copolymerisation of DBBA with the Tris inevitably occurred, which was followed by grafting of the copolymer onto the decalin. FTIR and NMR results of the polymer concentrates containing bound-DBBA processed with and without Tris, showed similar behaviour as the above model reactions. This evidence supports the effect of Tris in enhancing the efficiency of the reaction of DBBA in the polymer melt. Reactive processing of HAEB in polymer melts exhibited crosslinking formation in the early stages of the reaction, however, in the final stage, the crosslinked structure was 'broken down' or rearranged to give an almost gel free polymer with high antioxidant binding efficiency.

Keywords,

reactive antioxidants, reactive processing, bound antioxidants, antioxidant concentrates

ACKNOWLEDGEMENTS

I wish to acknowledge with gratitude the guidance, advice and encouragement given by my supervisor, Dr. Sahar Al-Malaika. I am thankful to Prof. Gerald Scott for the many valuable discussions.

My thanks are also to Dr.H.H.Sheena for his advice and discussion and to the other research fellows of the Polymer Processing and Performance Research Group, Drs. B.Wirjosentono, T.Koenig and K.B.Chakraborty as well as all research students of the group for their numerous discussions and comradeship during this research work. I am grateful to Dr.M.C.Perry for his discussion and NMR analysis, and to Mr.S.Ludlow and Mrs.L.Store for their technical assistance.

I am indebted to RAPRA Technology Ltd. for providing the molecular weight results described in this thesis.

Thanks are extended to the Ministry of Education and Culture of The Republic of Indonesia for the scholarship and to the University of Sebelas Maret for granting study leave.

Last but not least, I gratefully acknowledge my mother and all my family for their love, immense patience and moral support in all these years.

LIST OF CONTENT

	<u>Page</u>
THESIS TITLE	1
SUMMARY	2
ACKNOWLEDGEMENTS	3
LIST OF CONTENT	4
LIST OF SCHEMES	10
LIST OF TABLES	13
LIST OF FIGURES	19
ABBREVIATIONS AND SYMBOLS	29
<u>CHAPTER ONE</u>	
INTRODUCTION	31
1.1 GENERAL INTRODUCTION	31
1.2 DEGRADATION OF POLYOLEFINS	31
1.2.1 Thermal Oxidative Degradation	32
1.2.2 Photo Oxidative Degradation	33
1.3 STABILISATION OF POLYOLEFINS	36
1.3.1 Synergistic and Antagonistic Effects	40
1.4 CHEMICAL AND PHYSICAL LOSSES OF ANTIOXIDANTS FROM POLYMERS	42
1.5 IMPROVING SUBSTANTIVITY OF ANTIOXIDANTS IN POLYOLEFINS	44
1.5.1 General Approaches	44
1.5.2 Experience at Aston on Bound Antioxidant Using Reactive Processing Procedure	45
1.6 HINDERED PHENOL AS ANTIOXIDANT	48

1.6.2	Chemical Transformation of Hindered Phenols and Their Activity as Thermal Stabilisers for Polyolefins	52
1.7	BENZOPHENONE AS UV ABSORBER OF POLYOLEFINS	57
1.8	OBJECTIVE AND SCOPE OF THE PRESENT WORK	61

CHAPTER TWO

	GENERAL EXPERIMENTAL TECHNIQUES	62
2.1	MATERIALS	62
2.2	SYNTHESIS AND CHARACTERISATION OF ANTIOXIDANTS	64
2.2.1	Preparation of 3,5-di-tert.-butyl-4-hydroxy benzyl alcohol (DBHBA)	65
2.2.2	Preparation of 3,5-di-tert.-butyl-4-hydroxy benzyl acrylate (DBBA)	68
2.2.3	Preparation of 3-(3',5'-di-tert.-butyl-4-hydroxy phenyl) propionic acid (Irganox acid)	72
2.2.4	Preparation of vinyl-3-(3',5'-di-tert.-butyl-4-hydroxy phenyl) propionate (VDBP)	76
2.2.5	Preparation of 2-hydroxy-4-(beta hydroxy ethoxy) benzophenone (HHBP)	80
2.2.6	Preparation of 2-hydroxy-4-(beta acrylate ethoxy) benzophenone (HAEB)	84
2.3	COMPOUNDING	88
2.3.1	Reactive Processing of Polymer Samples	88
2.3.2	Film Preparation	89
2.4	EVALUATION OF BINDING	90
2.4.1	Soxhlet Extraction	90
2.4.2	Assesment of Binding Efficiency of Antioxidants	90
2.5	MEASUREMENT OF MELT FLOW INDEX (MFI)	92
2.6	MEASUREMENT OF INSOLUBLE GEL (GEL CONTENT)	92
2.7	STABILISING ACTIVITY TEST	93
2.7.1	Ultra Violet Irradiation of Polymer Films	93
2.7.2	Thermal Ageing of Polymer Films	94

2.8	MEASUREMENT OF BRITTLE FRACTURE TIME OF POLYMER SAMPLES	95
2.9	FOURIER TRANSFORM INFRARED (FT-IR) SPECTROSCOPY	95
2.10	ULTRA VIOLET SPECTROSCOPY	97
2.11	PROTON AND CARBON-13 NUCLEAR MAGNETIC RESONANCE (NMR) SPECTROSCOPY	98
2.12	GEL PERMEATION CHROMATOGRAPHY	101

CHAPTER THREE

	OPTIMISATION OF GRAFTING EFFICIENCY OF ANTIOXIDANTS CONTAINING HINDERED PHENOL AND BENZOPHENONE FUNCTIONS IN POLYPROPYLENE USING REACTIVE PROCESSING PROCEDURE	133
3.1	OBJECT AND METHODOLOGY	133
3.1.1	Evaluation of Binding Efficiency of Antioxidants in Masterbatch Films	134
3.2	RESULTS	138
3.2.1	Optimisation of Condition to Achieved High Level of Binding of 3,5-di-tert.-butyl-4-hydroxy benzyl acrylate (DBBA) in Polypropylene	138
3.2.2	Effect of Processing Conditions on Efficiency of Binding of DBBA on Polypropylene During Melt Processing	138
3.2.2.1	Effect of processing temperature on the binding efficiency of DBBA in polypropylene	138
3.2.2.2	Effect of processing time on the binding efficiency of DBBA in polypropylene	139
3.2.3	Effect of Chemical Composition on Binding of DBBA on Polypropylene During Melt Processing	140
3.2.3.1	Effect of initiator (Trigonox 101) on the binding efficiency of DBBA in polypropylene	140
3.2.3.2	Effect of DBBA concentration on the binding efficiency	141

3.2.4	Effect of Coagent on Binding Efficiency of DBBA in Polypropylene	143
3.2.4.1	Optimisation of binding efficiency of DBBA in polypropylene using DVB as a coagent	144
3.2.4.2	Optimisation of binding efficiency of DBBA in polypropylene using TMPTA (Tris) as a coagent	146
3.2.4.3	Effect of FRI (Trigonox 101) on the MFI of various polypropylene film controls (unprocessed and processed) and containing 4% Tris or 4% DVB	149
3.2.5	Optimisation of Condition to Achieved High Level Binding Efficiency of 2-hydroxy-4-(beta acrylate ethoxy) benzophenone (HAEB) in Polypropylene	150
3.2.5.1	Effect of processing time on the binding efficiency of HAEB in polypropylene	150
3.2.5.2	Effect of processing temperature on the binding efficiency of HAEB in polypropylene	151
3.2.5.3	Effect of antioxidant's concentration on the binding efficiency of HAEB in polypropylene	152
3.2.5.4	Effect of initiator on the binding efficiency of HAEB in polypropylene	152
3.2.6	Effect of a Coagent, TMPTA (Tris) on the Binding Efficiency of HAEB in Polypropylene	153
3.3	DISCUSSION	156
3.3.1	Reactive Processing Containing DBBA System	156
3.3.2	Reactive Processing Containing HAEB System	160

CHAPTER FOUR

	STABILISING ACTIVITY OF HINDERED PHENOL AND BENZOPHENONE CONTAINING ACRYLIC GROUP IN POLYPROPYLENE EITHER AS A SINGLE OR AS A MIXTURE OF ANTIOXIDANTS	181
4.1	OBJECT AND METHODOLOGY	181

4.2	RESULTS	189
4.2.1	Effect of Reactive Processing on the Photo Stabilising Activity of Derivatives of Hindered Phenol and Benzophenone AO's Containing Acrylic Group	189
4.2.2	Effect of Reactive Processing on the Thermal Stabilising Activity of Derivatives of Hindered Phenol and Benzophenone AO's Containing Acrylic Group	191
4.2.3	Effect of Mixture Antioxidant Activity of Hindered Phenol and Benzophenone Containing Acrylic Group as Mixture AO's on Thermal Stabilising Activity of Polypropylene	193
4.2.4	Effect of Mixture Antioxidant Activity of Hindered Phenol and Benzophenone Containing Acrylic Group as Mixture AO's on UV-Stabilising Activity of Polypropylene.	194
4.3	DISCUSSION	200
4.3.1	Effect of Reactive Processing on Stabilising Activity of Hindered Phenol and Benzophenone in Polypropylene Containing Acrylic Group	200
4.3.2	Synergistic of Hindered Phenol and Benzophenone in polypropylene Containing Acrylic Group	201

CHAPTER FIVE

	ANALYSIS OF MASTERBATCHES CONTAINING DBBA AND HAEB IN POLYPROPYLENE AND MODEL REACTION OF DBBA IN SOLUTION	208
5.1	OBJECT AND METHODOLOGY	208
5.2	RESULTS	213
5.2.1	Analysis of Masterbatches Containing DBBA and HAEB	213
5.2.1.1	Spectroscopically investigations using infra red	213
5.2.1.2	Analysis of antioxidant concentration in masterbatches and the gel content	216

5.2.1.3	Molecular weight distribution (MWD) data of masterbatches containing DBBA or HAEB	229
5.2.2	Polymerisation of DBBA Using Benzene as a Substrate	231
5.2.3	Polymerisation of DBBA-Decalin	234
5.2.4	"Insitu" Polymerisation of DBBA in NMR Sample Tube	237
5.2.5	Homopolymerisation of Tris Coagent in Benzene Substrate	240
5.2.6	Polymerisation of DBBA with Tris in Benzene Substrate	243
5.2.7	Polymerisation of DBBA+Tris with Decalin	245
5.3	DISCUSSION	254
5.3.1	Reactive Processing Mechanism of HAEB and DBBA in Polymer Melts	254

CHAPTER SIX

	CONCLUSIONS AND RECOMMENDATIONS FOR FURTHER WORK	338
6.1	CONCLUSIONS	338
6.2	RECOMMENDATIONS FOR FURTHER WORK	344
	REFERENCES	346

LIST OF SCHEMES

Scheme	Page
1.1 General mechanism of hydrocarbon oxidation	33
1.2 Stabilisation mechanisms of polyolefins	37
1.3 Cyclical regeneration of galvinoxyl (G.) during the melt stabilisation of polypropylene	39
1.4 The first step involved in the stabilising activity of hindered phenols	49
1.5 Transition state in the oxidation of phenolic antioxidant	50
1.6 Chemical transformation of hindered phenol antioxidant	53
1.7 Bifunctional stabilising mechanism of Sumilizer GM	56
1.8 The reaction of Deuterated SGM with AZBN	57
1.9 Tautomerisation of benzophenone	58
2.1 Flowchart for preparation of 3,5-di-tert.-butyl-4-hydroxy benzyl alcohol, DBHBA.	67
2.2 Flowchart for preparation of 3,5-di-tert.-butyl-4-hydroxy benzyl acrylate, DBBA.	71
2.3 Flowchart preparation of 3-(3',5'-di-tert.-butyl-4-hydroxy phenyl) propionic acid, Irganox acid.	75
2.4 Flowchart for preparation of Vinyl-3- (3',5'-di-tert.-butyl-4-hydroxy phenyl) propionate, VDBP.	79
2.5 Flowchart for preparation of 2-hydroxy-4-(beta hydroxy ethoxy) benzophenone, HHBP.	83
2.6 Flowchart for preparation of 2-hydroxy-4-(beta acrylate- ethoxy) benzophenone, HAEB.	87
3.1 Flow chart for a typical reactive processing procedure and polymer test and characterisation	137
3.2 The possibility reaction of DBBA+Tris in polypropylene using reactive processing procedure in the presence of 0.02 m.r Trigonox 101 under standard condition.	158
4.1 Flow diagram for preparation of MB film containing single antioxidant for stabilising activity test.	185
4.2 Flow diagram for preparation MB film containing mixture antioxidants (one stage synergistic system) for stabilising activity test.	186

Scheme	Page
4.3 Flow diagram for preparation MB film containing mixture antioxidants from different MB's, processing separately (two stage synergistic system) for stabilising activity test.	187
4.4 Flow diagram for preparation MB film containing mixture antioxidants from MB and fresh AO, processing separately (two stage synergistic system) for stabilising activity test.	188
5.1 Schematic presentation of procedure used for analysis of MB's containing 6-10% of DBBA or HAEB processed in the presence of various concentration of Trigonox 101 (molar ratio=0-0.02) at 180°C for 10 minutes in a closed mixer torque rheometer.	210
5.2 Schematic procedure of polymerisation DBBA-Decalin in the presence of 0.02 molar ratio (I/DBBA) Trigonox 101 at 180°C for 5 hours.	211
5.3 Schematic procedure of DBBA polymerisation in benzene in the presence of 0.3 molar ratio (I/DBBA) AZBN at 70°C for 25 hours under Argon atmosphere.	212
5.4 Diagram analysis of 5 gram masterbatch containing 10% DBBA in the presence of 0.02 molar ratio of Trigonox 101.	223
5.5 Diagram analysis of 5 gram masterbatch containing 6% DBBA and 4% Tris, processed in the presence of 0.02 molar ratio Trigonox 101.	224
5.6 Diagram analysis of 5 gram masterbatch containing 6% DBBA and 4% DVB processed in the presence of 0.02 molar ratio of Trigonox 101.	225
5.7 Diagram analysis of 5 gram masterbatch containing 10% HAEB processed for 2.5 minutes, in the presence of 0.005 molar ratio Trigonox 101.	226
5.8 Diagram analysis of 5 gram masterbatch containing 10% HAEB processed for 5 minutes, in the presence of 0.005 molar ratio Trigonox 101.	227
5.9 Diagram analysis of 5 gram masterbatch containing 10% HAEB processed for 10 minutes, in the presence of 0.005 molar ratio Trigonox 101.	228
5.10 Schematic procedure of polymerisation Tris in benzene in the presence of 0.03 m.r. (I/Tris), AZBN at 70°C for 5 hours.	251
5.11 Schematic procedure of polymerisation DBBA+Tris (ratio 6/4) in benzene in the presence of 0.02 m.r. (I/DBBA+Tris) AZBN at 70°C for 5 hours.	252
5.12 Schematic procedure of polymerisation DBBA+Tris (ratio 6/4) with decalin in the presence of 0.02 molar ratio (I/DBBA+Tris) Trigonox 101 at 180°C for 5 hours.	253
5.13 Structure of HAEB in polymer (10%) MB's processed with PP in the presence of 0.02 m.r. Trig.101, for 2.5 and 10 minutes under standard condition.	256
5.14 Suggested mechanism of reactive processing of HAEB in PP in the presence of 0.005 m.r. Trig.101, processed at 180°C for 10 minutes in closed mixing condition.	257

Scheme	Page
5.15 Structure of grafted DBBA in polymer (10% MB, processed with polypropylene in presence of 0.02 m.r Trig.101, under standard condition.	262
5.16 Structure of grafted DBBA with Tris coagent in polymer (10% MB, processed with polypropylene in the presence of 0.02 m.r. Trig.101, under standard condition.	263
5.17 Structure of grafted DBBA with DVB coagent in polymer (10% MB, processed with polypropylene in the presence of 0.02 m.r. Trig.101, under standard condition.	266
5.18 Suggested mechanism of reactive processing of grafted DBBA in PP in the presence of 0.02 m.r. of Trig.101, processed at 180°C for 10 minutes in closed mixing condition.	267
5.19 Suggested mechanism of polymerised DBBA with Decalin in the presence of 0.02 m.r.Trig.101 as initiator at 180°C for 5 hours under Argon atmosphere.	268
5.20 Suggested mechanism of reactive processing of grafted DBBA+Tris in PP, in the presence of 0.02 m.r.Trig.101, processed at 180°C for 10 minutes in closed mixing condition.	269
5.21 Suggested mechanism of polymerised DBBA+Tris with Decalin in the presence of 0.02 m.r.Trig.101 as initiator at 180°C for 5 hours under Argon atmosphere.	270

LIST OF TABLES

Table	Page
1.1 Effect of substituents variations in 2,4, and 6 positions on the antioxidant activity of phenols compared to that of unsubstituted phenol.	51
1.2 Typical hindered phenol antioxidants.	51
2.1 Chemical structure of commercial antioxidants are used.	63
2.2 Elemental analysis and major absorption peak in FTIR of DBHBA.	65
2.3 Proton NMR spectrum of 3,5-di-tert.-butyl-4-hydroxy benzyl alcohol, DBHBA in deuterated chloroform.	66
2.4 ¹³ C NMR spectrum of 3,5-di-tert.-butyl-4-hydroxy benzyl alcohol, DBHBA in deuterated chloroform.	66
2.5 Elemental analysis and major absorption peak in FTIR of DBBA.	69
2.6 Proton NMR spectrum of 3,5-di-tert.-butyl-4-hydroxy benzyl acrylate, DBBA in CDCl ₃ .	69
2.7 ¹³ C NMR spectrum of 3,5-di-tert.-butyl-4-hydroxy benzyl acrylate, DBBA in CDCl ₃ .	70
2.8 Elemental analysis and major absorption peak in FTIR of Irganox acid.	73
2.9 Proton NMR spectra of 3-(3',5'-di-tert.-butyl-4-hydroxy phenyl) propionic acid (Irganox acid) in CDCl ₃ .	73
2.10 ¹³ C NMR spectrum of 3-(3',5'-di-tert.-butyl-4-hydroxy phenyl) propionic acid (Irganox acid) in CDCl ₃ .	74
2.11 Elemental analysis and major absorption peak in FTIR of VDBP.	77
2.12 Proton NMR of Vinyl-3- (3',5'-di-tert.-butyl-4-hydroxy phenyl) propionate, VDBP in CDCl ₃ .	77
2.13 ¹³ C NMR of Vinyl-3- (3',5'-di-tert.-butyl-4-hydroxyphenyl) propionate, VDBP in CDCl ₃ .	78
2.14 Elemental analysis and major absorption peak in FTIR of HHBP.	81
2.15 Proton NMR of 2-hydroxy-4-(beta hydroxy ethoxy) benzophenone, HHBP in deuterated chloroform.	81
2.16 ¹³ C NMR of 2-hydroxy-4-(beta hydroxy ethoxy) benzophenone, HHBP in deuterated chloroform.	82
2.17 Elemental analysis and major absorption peak in FTIR of HAEB.	85

Table	Page
2.18 Proton NMR of 2-hydroxy-4-(beta acrylate ethoxy) benzophenone, HAEB in deuterated chloroform.	85
2.19 ¹³ C NMR of 2-hydroxy-4-(beta acrylate ethoxy) benzophenone, HAEB in deuterated chloroform.	86
3.1 Acrylic ester derivatives of hindered phenol and benzophenone antioxidants used.	135
3.1a Various coagent used to extend the binding efficiency of antioxidants.	136
3.1b Binding efficiency and Melt flow index (MFI) of masterbatches (MB's) containing 10% DBBA in polypropylene in the presence of 0.02 m.r. (I/DBBA) Trigonox 101, processed at different temperatures for 10 minutes under closed mixer condition.	139
3.2 Binding efficiency and Melt flow index (MFI) of masterbatches (MB's) containing 10% DBBA in polypropylene in the presence of 0.02 molar ratio, m.r.(I/DBBA) Trigonox 101, processed at various processing time at 180°C under closed mixer condition.	140
3.3 Binding efficiency and Melt flow index (MFI) of masterbatches (MB's) containing 6% & 10% DBBA in polypropylene in the presence of (0-0.03 m.r.) Trigonox 101, processed in standard condition.	141
3.4 Molecular weight distribution data of polymer samples (masterbatches).	142
3.5 Effect of DBBA concentration on the binding efficiency and Melt flow index (MFI) in polypropylene in the presence of 0.02 m.r. Trig. 101, processed in closed mixing condition at 180°C for 10 minutes.	142
3.6 Binding efficiency of DBBA in polypropylene (3%) processed with various co-agents (2%), in the presence of Trigonox 101 (0.002m.r.), in closed mixing condition at 180°C for 10 minutes.	143
3.7 Binding efficiency of DBBA in Polypropylene film processed with various ratio of DVB coagent (total concentration of DBBA+DVB=10%) in the presence of FRI Trigonox 101 (0.002 or 0.02 m.r.), under standard condition.	144
3.8 Effect of FRI concentration on the binding efficiency and MFI of 10% masterbatches (MB's) PP containing DBBA-DVB ratio 6/4, processed in closed mixing condition at 180°C for 10 minutes.	145
3.9 Molecular weight distribution data of polymer samples of 10% MB's PP containing DBBA-DVB ratio 6/4, processed in closed mixing condition at 180°C for 10 minutes.	146
3.10 Binding efficiency of DBBA in PP film processed with various ratio of Tris coagent (total concentration of DBBA+Tris = 10%) in the presence of FRI Trig. 101 0.02 m.r. [I]/[DBBA+Tris], under standard condition.	147
3.11 Effect of FRI concentration on the binding efficiency and MFI of 6% or 10% MB's PP containing DBBA-Tris ratio 6/4, processed in closed mixing condition at 180°C for 10 minutes.	148

Table	Page
3.12 Molecular weight distribution data of polymer samples 10% masterbatches (MB's) PP containing DBBA-Tris ratio 6/4, processed in closed mixing condition at 180°C for 10 minutes.	148
3.13 Effect of FRI on the MFI of various polypropylene film controls (unprocessed and processed) and containing 4% Tris or 4% DVB in various concentration of Trig. 101, processed under standard condition.	149
3.14 Effect of various processing time on binding efficiency of 10% HAEB in PP, in the presence of Trig. 101 (0.005 m.r., I/HAEB), processed in closed mixing condition at 180°C.	151
3.15 Effect of processing temperature on the binding efficiency of HAEB (10% MB) in propylene, in the presence of DCP (0.005 m.r., I/HAEB), processed in closed mixer condition for 10 mins.	151
3.16 Effect of HAEB concentration on binding efficiency in PP, in the presence of DCP (0.005 m.r., I/HAEB), processed in closed mixing condition at 180°C for 10 minutes.	152
3.17 Binding efficiency and MFI of MB's containing 10% HAEB in PP in the presence of various concentrations of FRI dicumyl peroxide or Trig. 101, processed under standard condition.	153
3.18 Binding of HAEB in Polypropylene with Tris co-agent at various ratios HAEB/Tris in masterbatches containing 10% of mixture in the presence 0.005 m.r. of FRI Trig.101, processed in closed mixing condition at 180°C for 10 minutes.	154
3.19 Effect of FRI Trigonox 101 concentration in binding efficiency and MFI of PP MB's containing 10 % mixture of HAEB/Tris ratio 9/1 processed in closed mixing condition at 180°C for 10 minutes.	155
3.20 Effect processing time on binding efficiency and gel content of PP film containing (9% HAEB+1% Tris) in presence 0.005 m.r. of Trig. 101, processed in closed mixing condition at 180°C.	155
4.1 Various antioxidants used in reactive processing	183
4.2 Various commercial antioxidants used in reactive processing.	184
4.3 Binding and uv-stability of bound AO's in PP-films containing 0.4% of AO's (before and after extraction), diluted from 10% MB's processed in the presence of 0.02 m.r. [I]/[AO] Trig. 101.	189
4.4 UV-stability of PP-films containing 0.4% of unbound AO's (before and after extraction) processed without peroxide as conventional additive.	190
4.5 Binding and UV stability of PP-film containing 0.4% of AO in the presence of coagent (before and after extraction), diluted in fresh PP from 10% MB's processed in the presence of 0.02 m.r.[I]/[AO+Coagent) under standard condition.	191

Table	Page
4.6 Thermal stability of PP-films containing 0.4% of bound and unbound AO's (before and after extraction) diluted from 10% MB's processed without and with 0.02 m.r. [I]/[AO+Coagent] Trig. 101 under standard condition.	192
4.7 Thermal stability (at 140°C) of PP-films containing 0.4% of unbound commercial AO (before and after extraction) and PP processed as control.	193
4.8 Thermal stability of PP-films containing 0.4 % of bound mixture of AO's (before and after extraction) diluted from 10% masterbatches processed in the presence of 0.02 molar ratio [I]/[AO ₁ +AO ₂ +Coagent] Trig. 101 under standard condition.	194
4.8a The combination of antioxidant mixtures and coagent in 10% masterbatches.	195
4.9 UV Stability of PP-films containing 0.4% of mixture AO's in varied composition (before and after extraction), diluted in PP from 10% MB's processed in the presence of 0.02 molar ratio [I]/[AO ₁ +AO ₂ +AO ₃ +Tris] Trig. 101, under standard condition.	196
4.10 UV Stability of PP-films containing 0.4% AO's of mixture masterbatches in varied composition (before and after extraction), diluted from 10% MB's processed in the presence of 0.02 molar ratio Trig. 101, under standard condition.	198
4.11 UV Stability of PP-films containing different single AO using various ratio Tris coagent in varied concentration (before and after extraction), diluted from 10% masterbatches processed in the presence optimum Trig.101, under standard condition.	199
4.12 Effect of UV-stabiliser (HOBP) on the uv-irradiated of PP films containing bound DBBA with coagent at 0.4% total AO's mixture MB's (before and after extraction), diluted from 10% masterbatches processed in standard condition.	199
5.1 Binding efficiency, MFI and gel content of 10% masterbatches containing DBBA in polypropylene without and with coagents, in the presence of 0.02 m.r. [I]/([DBBA]+[Coagent]) Trig.101 (processed at 180°C for 10 minutes under closed mixer).	217
5.2 Effect of procesing time on binding efficiency, MFI and gel content of 10% HAEB in polypropylene, in the presence of 0.005 molar ratio [I]/[AO] Trig.101 processed at 180°C under closed mixer condition at different processing time.	218
5.3 Percentage weight of soluble and insoluble fractions (after continuous extraction in different solvents) of masterbatches containing 10% AO's processed in the presence of optimum concentration of Trig.101, at 180°C in closed mixing at different processing times.	220
5.4 Percentage of DBBA in different fractions (after continous separation in different solvents) of 10% total (DBBA with or without coagent) MB's processed with 0.02 m.r. (I/DBBA+Coagent) Trig. 101, at 180°C, for 10 minutes under closed mixer condition.	221

Table	Page
5.5 Percentage weight of soluble and insoluble fractions (after continuous extraction in different solvents) of masterbatches containing 10% HAEB processed in the presence of 0.005 m.r. (I/AO) Trig.101, at 180°C under closed mixer condition at different processing times.	221
5.6 Percentage of HAEB in different fractions (after continuous separation in different solvents) of 10% HAEB masterbatches processed with 0.005 m.r. (I/AO) Trig.101, at 180°C, under closed mixer condition, for various processing time (2.5, 5 and 10 minutes).	222
5.7 The MFI of original MB's, soluble and insoluble fractions (after continuous extraction in different solvents) of MB's containing 10% AO's processed in the presence of optimum concentration of Trig.101, at 180°C in closed mixer condition at different processing times.	222
5.8 Molecular weight distribution (MWD) data of masterbatches containing 10% (DBBA without or with coagent), processed in the presence of 0.02 m.r. (I/DBBA+coagent) Trigonox 101 at 180°C for 10 minutes under closed mixer condition.	230
5.9 Molecular weight distribution (MWD) data of masterbatch's fractions after Soxhlet separation of DBBA MB's containing 10% total (DBBA with or without coagent) processed in the presence of 0.02 m.r. Trig. 101, at 180°C for 10 minutes, in closed mixer condition.	230
5.10 Molecular weight distribution (MWD) data of MB's containing 10% HAEB, processed in the presence of 0.005 m.r.(I/HAEB) Trig.101 at 180°C in closed mixing condition at various processing time.	231
5.11 Proton NMR spectra of polymerised DBBA without decalin in CDCl ₃ (using AZBN in benzene).	233
5.12 ¹³ C NMR spectra of polymerised DBBA without decalin in CDCl ₃ (using AZBN in benzene).	234
5.13 ¹³ C NMR spectrum of polymerised DBBA-decalin in CDCl ₃ .	236
5.14 ¹³ C NMR spectra of DBBA with decalin in NMR sample tube before reaction at 296°K, using Trigonox 101 as initiator.	238
5.15 ¹³ C NMR spectra of DBBA with decalin in NMR sample tube at 373°K, using Trigonox 101 as initiator after 1 hour reaction.	239
5.16 ¹³ C NMR spectra of DBBA with decalin in NMR sample tube at 373°K, using Trig.101 as initiator after 25 hours reaction.	240
5.17 ¹³ C NMR of fresh Tris in CDCl ₃ .	242
5.18 Solid state ¹³ C NMR of polymerised Tris in benzene substrate using AZBN as initiator.	242
5.19 Solid state ¹³ C NMR of polymerised DBBA+Tris in benzene substrate using AZBN as initiator.	245

Table		Page
5.20	Solid state ^{13}C NMR of polymerised DBBA-Tris-Decalin using Trig.101 as initiator.	247
5.21	Solid state ^{13}C NMR of polymerised DBBA with Decalin using AZBN as initiator.	248
5.22	Solid state ^{13}C NMR of xylene soluble MB containing 10% DBBA.	249
5.23	Solid state ^{13}C NMR of xylene soluble MB containing 10% (DBBA+Tris).	250

LIST OF FIGURES

Figure	Page
2.1 Comparison between FTIR spectra of 3,5-di-tert.-butyl-4-hydroxy benzyl alcohol, DBHBA and DTBP, using KBr disc.	103
2.2 FTIR spectrum of 3,5-di-tert.-butyl-4-hydroxybenzyl alcohol, DBHBA in KBr disc.	104
2.2a UV spectrum of 3,5-di-tert.-butyl-4-hydroxybenzyl alcohol, DBHBA in DCM solution.	105
2.3 Proton NMR spectrum of 3,5-di-tert.-butyl-4-hydroxy benzyl alcohol, DBHBA in deuterated chloroform.	106
2.4 Carbon-13 NMR spectrum of 3,5-di-tert.-butyl-4-hydroxy benzyl alcohol, DBHBA in deuterated chloroform.	107
2.5 Comparison between FTIR spectra of 3,5-di-tert.-butyl-4-hydroxy benzyl acrylate, DBBA and DBHBA using KBr disc.	108
2.6 FTIR spectrum of 3,5-di-tert.-butyl-4-hydroxybenzyl acrylate, DBBA in KBr disc.	109
2.6a UV spectrum of 3,5-di-tert.-butyl-4-hydroxybenzyl acrylate, DBBA in DCM solution.	110
2.7 Proton NMR spectrum of 3,5-di-tert.-butyl-4-hydroxy benzyl acrylate, DBBA in CDCl ₃ .	111
2.8 C-13 NMR spectrum of 3,5-di-tert.-butyl-4-hydroxy benzyl acrylate, DBBA in CDCl ₃ .	112
2.9 Comparison between FTIR spectra of 3-(3',5'-di-tert.-butyl-4-hydroxy phenyl) propionic acid, Irganox acid and Irganox 1076 in KBr disc.	113
2.10 FTIR spectrum of 3-(3',5'-di-tert.-butyl-4-hydroxy phenyl) propionic acid, Irganox acid in KBr disc.	114
2.10a UV spectrum of 3-(3',5'-di-tert.-butyl-4-hydroxy phenyl) propionic acid, Irganox acid in DCM solution.	115
2.11 Proton NMR spectrum of 3-(3',5'-di-tert.-butyl-4-hydroxy phenyl) propionic acid, Irganox acid in CDCl ₃ .	116
2.12 C-13 NMR spectrum of 3-(3',5'-di-tert.-butyl-4-hydroxy phenyl) propionic acid, Irganox acid in CDCl ₃ .	117
2.13 Comparison between FTIR spectra of vinyl-3-(3',5'-di-tert.-butyl-4-hydroxy phenyl) propionate, VDBP and Irg. Acid in KBr disc.	118
2.14 FTIR spectrum of Vinyl-3-(3',5'-di-tert.-butyl-4-hydroxy phenyl) propionate, VDBP in KBr disc.	119
2.14a UV spectrum of Vinyl-3-(3',5'-di-tert.-butyl-4-hydroxy phenyl) propionate, VDBP in DCM solution.	120

Figure	Page
2.15 Proton NMR spectrum of Vinyl-3- (3',5'-di-tert.-butyl-4-hydroxy phenyl) propionate, VDBP in CDCl ₃ .	121
2.16 Carbon-13 NMR spectrum of Vinyl-3- (3',5'-di-tert.-butyl-4-hydroxy phenyl) propionate, VDBP in CDCl ₃ .	122
2.17 Comparison between FTIR spectra of 2-hydroxy-4-(beta hydroxy ethoxy) benzophenone, HHBP and DHBP in KBr disc.	123
2.18 FTIR spectrum of 2-hydroxy-4-(beta hydroxy ethoxy) benzophenone, HHBP in KBr disc.	124
2.18a UV spectrum of 2-hydroxy-4-(beta hydroxy ethoxy) benzophenone, HHBP in DCM solution.	125
2.19 Proton NMR spectrum of 2-hydroxy-4-(beta hydroxy ethoxy) benzophenone, HHBP in deuterated chloroform.	126
2.20 Carbon-13 NMR spectrum of 2-hydroxy-4-(beta hydroxy ethoxy) benzophenone, HHBP in deuterated chloroform.	127
2.21 Comparison between FTIR spectra of 2-hydroxy-4-(beta acrylate ethoxy) benzophenone, HAEB and in KBr disc.	128
2.22 FTIR spectrum of 2-hydroxy-4-(beta acrylate ethoxy) benzophenone, HAEB in KBr disc.	129
2.22a UV spectrum of 2-hydroxy-4-(beta acrylate ethoxy) benzophenone, HAEB in DCM solution.	130
2.23 Proton NMR spectrum of 2-hydroxy-4-(beta acrylate ethoxy) benzophenone, HAEB in deuterated chloroform.	131
2.24 Carbon-13 NMR spectrum of 2-hydroxy-4-(beta acrylate ethoxy) benzophenone, HAEB in deuterated chloroform.	132
2.25 Processing chamber of a Brabender torque rheometer (internal-mixer).	89
2.26 Measurement peak area in FT-IR spectroscopy.	96
2.27 Measurement of absorption in UV spectrophotometer.	97
3.1 Infra red spectra of PP film processed in the presence of 6% DBBA and 0.02 m.r. of Trig.101, before and after Soxhlet extraction.	161
3.1a Infra red spectra of PP film processed in the presence of 6% DBBA+ 4% Tris and 0.02 m.r. of Trig.101, before and after Soxhlet extraction.	162
3.1b Infra red spectra of PP film processed in the presence of 6% DBBA+ 4% DVB and 0.02 m.r. of Trig.101, before and after Soxhlet extraction.	163
3.2a Infra red spectra of PP film processed in the presence of 10% HAEB and 0.005 m.r. of Trig.101, before and after Soxhlet extraction.	164

Figure	Page
3.2b UV spectra of PP film processed in the presence of 9% HAEB+1% Tris and 0.005 m.r. of Trig.101, before and after Soxhlet extraction.	165
3.3 Binding efficiency and MFI of MB's containing 10% DBBA in PP in the presence of 0.02 m.r. Trig.101, processed at various processing temperature for 10 minutes under closed mixer condition.	166
3.3a Binding efficiency and MFI of MB's containing 10% DBBA in PP in the presence of 0.02 m.r. Trig.101, processed at various processing time at 180°C under closed mixer condition.	166
3.4 The effect of various Trig. 101 concentration on binding level of 6% DBBA MB's with PP, procesed under standard condition.	167
3.4a The effect of various Trig. 101 concentration on MFI of 6 % DBBA MB's with PP, procesed under standard condition.	167
3.5 Molecular weight distribution curves for, PP processed with: 0.02 m.r. Trig.101, 10% DBBA, 10% DBBA + 0.02 m.r. Trig.101, and 10% DBBA + 0.03 m.r. Trig.101	168
3.6 Effect of DBBA concentration on binding efficiency in PP processed in the presence of 0.02 and 0.03 m.r. Trig.101, under standarad condition.	169
3.7 The effect of DBBA concentration on MFI in PP processed in the presence 0.02 and 0.03 m.r. Trig. 101, under standard condition.	169
3.8 The effect of DVB as a coagent on binding level of antioxidant in PP, in the presence of 0.002 and 0.02 m.r. Trig.101, processed under standard condition.	170
3.9 The effect of Trig.101 concentration on the binding efficiency and MFI of 10% MB's containing DBBA+DVB ratio 6 to 4, processed under standard condition.	170
3.9a Molecular weight distribution curves for, PP processed with: 0.02 m.r. Trig.101, 6% DBBA+4% DVB, 6% DBBA+4% DVB+FRI 0.005m.r., 6% DBBA+4%DVB+FRI 0.02 m.r. and 6% DBBA+4%DVB+FRI 0.03 m.r.	171
3.10 The effect of Tris concentration on the binding efficiency and MFI of 10% MB's containing at various ratio (DBBA+DVB), processed under standard condition.	172
3.11 The effect of Trig.101 concentration on binding efficiency and MFI of 10% MB's containing DBBA+Tris ratio 6/4, processed under standard condition.	172
3.12 Effect of various concentration of Trig.101 on the MFI of PP film containing 4% Tris or 4% DVB processed in closed mixing condition at 180°C for 10 minutes.	173
3.13 Molecular weight distribution curves for, PP processed with: 0.02 m.r. Trig.101, 6% DBBA+4% Tris, 6% DBBA+4% Tris+FRI 0.005m.r., 6% DBBA+4%Tris+FRI 0.02 m.r. and 6% DBBA+4%Tris+FRI 0.03 m.r.	174
3.14 MFI values of 10% (DBBA+Tris) and 4% Tris MB's processed in the presence of different amounts of Trig.101, under standard condition.	173

Figure	Page
3.15 MFI values of 10% (DBBA+DVB) and 4% Tris masterbatches processed in the presence of different amounts of Trig.101, under standard condition.	175
3.16 Effect of various processing time on MFI of 10% HAEB MB's, processed in the presence of Trigonox (0.005 m.r., I/HAEB), at 180°C under closed mixing condition.	175
3.17 Effect of various processing time on the Torque changes of 10% MB's of HAEB in Polypropylene in the presence of 0.005 m.r. (I/HAEB) Trig. 101, processed at 180°C under closed mixing condition.	176
3.18 Effect of processing temperature on the binding efficiency of HAEB (10% MB) in polypropylene, in the presence of DCP (0.005 m.r., I/HAEB), processed in closed mixing condition for 10 minutes.	176
3.19 Effect of HAEB concentration on MFI MB's, processed in the presence of DCP (0.005 m.r, I/HAEB), under closed mixing condition at 180°C for 10 minutes.	177
3.20 Changes in torque during processing of HAEB (10%) in PP in the presence of various concentrations of DCP, processed under standard condition.	177
3.21 Binding efficiency of masterbatches containing 10% HAEB in polypropylene in the presence of various concentrations of FRI dicumyl peroxide or Trigonox 101, processed under standard condition.	178
3.22 Changes in Torque during processing of 10% (HAEB/Tris) at various ratios with PP in the presence of 0.005 m.r., (I)/(HAEB+Tris) Trig.101 processed under standard condition.	178
3.23 Torque recording of various concentration of FRI Trig. 101 in binding efficiency and MFI of PP MB's containing 10 % mixture of HAEB/Tris ratio 9/1 processed in closed mixing condition at 180°C for 10 minutes.	179
3.24 Effect of Trigonox 101 concentration on binding efficiency and MFI of MB's containing HAEB/Tris ratio 9/1, processed under standard condition.	179
3.25 Effect of processing time on binding efficiency and gel content of MB's containing 10% (HAEB+Tris) at ratio 9/1 processed in the presence of 0.005 m.r. Trigonox 101, under standard condition.	180
4.1 Embrittlement time of uv-irradiated diluted-films containing 0.4% of various bound (B) antioxidants and commercial AO's before (Unextracted) and after extraction (Extracted).	203
4.2 Retention activity of uv-irradiated diluted-films containing 0.4% of bound (B) antioxidants and commercial AO's.	203
4.3 Carbonyl index increase during uv-irradiation of diluted masterbatch film containing 0.4% of bound and unbound VDBP, DBBA, and HAEB before extraction.	204

Figure	Page
4.4	Embrittlement time of uv-irradiated diluted masterbatch films containing 0.4% of various bound (B) antioxidants in the presence of coagent and commercial antioxidants, before and after extraction. 204
4.5	ET of thermally aged diluted MB films containing 0.4% of various bound (B) antioxidants with or without coagent, before and after extraction. 205
4.6	Retention Activity of thermal ageing diluted masterbatch films containing 0.4% of various bound (B) antioxidants compared with commercial AO's. 205
4.7	Embrittlement time of UV-irradiated films of (DBBA/HAEB/Tris) MB's having the same concentration of Tris (2%), but at various ratios of DBBA/HAEB (1/1, 1/2, 1/3) processed in the presence of 0.02 m.r. Trig.101, diluted to 0.4% of total AO's content. 206
4.8	Retention Activity of UV-irradiated films of (DBBA/HAEB/Tris) MB's having the same concentration of Tris (2%), but at various ratios of DBBA/HAEB (1/1, 1/2, 1/3) processed in the presence of 0.02 m.r. Trig.101, diluted to 0.4% of total AO's content. 206
4.9	The Embrittlement Time of UV-irradiated films of (DBBA/HAEB/Tris) MB's have the same ratio (1/3) of DBBA/HAEB in the presence of different concentration of Tris coagent content, diluted to 0.4% of total AO's content. 207
4.10	Carbonyl index increase during uv-irradiation of diluted MB films containing 0.4% of bound-DBBA, bound-HAEB and mixtures DBBA/HAEB/Tris weight ratio: 4/4/2, 2.7/5.3/2, and 2/6/2 before extraction. 207
5.1	Comparison of FTIR spectra of PP film containing 10% DBBA processed without peroxide, with that of fresh DBBA in KBr disc, and PP processed without peroxide under standard condition. 271
5.2	Comparison of FTIR spectra of PP film containing 10% DBBA processed without peroxide before and after DCM extraction, and PP processed without peroxide under standard condition. 272
5.3	Comparison of FTIR spectra of PP film containing 10% DBBA+ 0.02 m.r. Trig.101 with that of fresh DBBA using KBr disc, and PP processed without peroxide under standard condition. 273
5.4	Comparison of FTIR spectra of PP film containing 10% DBBA+ 0.02 m.r. Trig.101 before and after DCM extraction, and PP processed without peroxide under standard condition. 274
5.5	Comparison of FTIR spectra of PP film containing 10% DBBA processed with 0.02 m.r. and without peroxide before and after DCM extraction processed under standard condition. 275
5.6	Comparison of FTIR spectra of cold DCM-extract of 10% DBBA MB processed with 0.02 m.r. Trig.101 and with that of fresh DBBA both using KBr disc. 276
5.7	Comparison of FTIR spectra of cold DCM-extract in KBr disc of 10% DBBA MB processed with 0.02 m.r. Trig.101 and with the same MB film but before extraction. 277

Figure	Page
5.8 Comparison of FTIR spectra of cold DCM-extract in KBr disc of 10% DBBA MB processed with 0.02 m.r. Trig.101 and with the same MB film but after extraction.	278
5.8a Comparison of FTIR spectra of 10% MB film containing (DBBA+DVB) processed with 0.02 m.r. Trig.101 before extraction and with that of fresh DBBA in KBr disc.	279
5.8b Comparison of FTIR spectra of 10% MB film containing (DBBA+DVB) processed with 0.02 m.r. Trig.101 before and after extraction and DCM extract from the same MB in KBr disc.	280
5.8c Comparison of FTIR spectra of 10% MB film containing (DBBA+Tris) processed with 0.02 m.r. Trig.101 before extraction and with that of fresh DBBA in KBr disc.	281
5.8d Comparison of FTIR spectra of 10% MB film containing (DBBA+Tris) processed with 0.02 m.r. Trig.101 before and after extraction and DCM extract from the same MB in KBr disc.	282
5.9 Comparison of FTIR spectra of 10% MB film containing HAEB processed without peroxide with that of fresh HAEB in KBr disc and PP processed without peroxide under standard condition.	283
5.10 Comparison of FTIR spectra of 10% MB film containing HAEB processed without peroxide before and after extraction and PP processed without peroxide under standard condition.	284
5.11 Comparison of FTIR spectra of 10% MB film containing HAEB processed with 0.005 m.r. Trig.101 with that of fresh HAEB in KBr disc and PP processed without peroxide under standard condition.	285
5.12 Comparison of FTIR spectra of 10% MB film containing HAEB processed with 0.005 m.r. Trig.101 before and after extraction and PP processed without peroxide under standard condition.	286
5.13 Comparison of FTIR spectra of 10% MB film containing HAEB processed with 0.05 m.r. Trig.101 and without peroxide and PP processed without peroxide under standard condition.	287
5.14 Comparison of FTIR spectra of cold DCM-extract in KBr of 10% HAEB MB processed with 0.005 m.r. Trig.101 and with that of fresh HAEB both using KBr disc.	288
5.15 Comparison of FTIR spectra of cold DCM-extract in KBr of 10% HAEB MB processed with 0.005 m.r. Trig.101 and with the same MB's film but before DCM extraction.	289
5.16 Comparison of FTIR spectra of cold DCM-extract in KBr of 10% HAEB MB processed with 0.005 m.r. Trig.101 and with the same MB's film but after DCM extraction.	290
5.17 Torque recording of various masterbatches: PP processed alone, PP+10%DBBA+0.02m.r.Trig.101, PP+ 6% DBBA+ 4%Tris+ 0.02m.r. Trig.101, and PP+ 6% DBBA+ 4%DVB+ 0.02 m.r. Trig.101.	291

Figure	Page
5.18 Binding Efficiency of various masterbatches: PP+ 0.02 m.r Trig.101, PP+10%DBBA+0.02 m.r. Trig.101, PP+ 6% DBBA+ 4%Tris+ 0.02m.r. Trig.101, and PP + 6% DBBA + 4%DVB + 0.02 m.r.Trig.101.	291
5.19 MFI of various masterbatches: PP+0.02 m.r Trig.101, PP+10% DBBA+ 0.02m.r.Trig.101, PP+6% DBBA+4%Tris+0.02m.r.Trig.101, and PP + 6% DBBA + 4%DVB+0.02 m.r. Trig.101.	292
5.20 Changes in torque during processing of masterbatches containing 10%HAEB + 0.005 m.r. [I]/[AO] Trigonox 101, PP processed without AO in absence and presence 0.005 m.r. of Trigonox 101 is also shown for comparison processing condition, under closed mixer, 10 minutes at 180°C.	292
5.21 Changes in torque during processing and gel content of MB's containing 10% HAEB in the presence of 0.005 m.r.Trig.101, processed at various time (2.5, 5 and 10 minutes) under closed mixer condition at 180°C.	293
5.22 MFI and Gel content of 10% HAEB masterbatches processed in the presence of 0.005m.r. [I]/[AO]) Trigonox 101, at various time processing (2.5, 5 and 10 minutes) under closed mixer condition at 180°C.	293
5.23 Calibration curve of DBBA masterbatches in various concentration.	294
5.24 Calibration curve of DBBA masterbatches in various concentration.	294
5.25 Calibration curve of HAEB masterbatches in various concentration.	295
5.26 The MFI of original MB's, containing 10% HAEB processed in the presence of optimum concentration of Trigonox 101, at 180°C in closed mixer condition at different processing times.	295
5.27 Molecular weight distribution curves of MB's containing 10% of DBBA processed in the presence of 0.02 m.r. Trig.101, compared to that of PP processed with 0.02 m.r. peroxide and unprocessed PP film.	296
5.28 Molecular weight distribution curves of MB's containing: 10% DBBA, 10% (DBBA+DVB) all were processed with 0.02 m.r. Trig.101, and PP processed with 0.02 m.r. Trig.101.	297
5.29 Molecular weight distribution (Mn) data of MB's fractions (after Soxhlet separation) of DBBA MB's containing 10% total (DBBA without or with coagent ratio 6/4) processed in the presence of 0.02 m.r.Trig.101, at 180°C for 10 minutes, in closed mixing condition.	298
5.30 Molecular weight distribution curves of MB's containing 10% DBBA before extraction, toluene extract fraction, xylene extract fraction, compared to that of PP processed with 0.02 m.r. Trig.101.	298
5.31 Molecular weight distribution curves of MB's containing 10% (DBBA+Tris)before extraction, toluene extract fraction, xylene extract fraction, compared to that of PP processed with 0.02 m.r. Trig.101.	299
5.32 Molecular weight distribution curves of MB's containing 10% (DBBA+DVB) before extraction, toluene extract fraction, xylene extract fraction, compared to that of PP processed with peroxide.	299

Figure	Page
5.33 Molecular weight distribution, $[M_n \times 10^{-4}]$ data of MB's containing 10% HAEB, processed in the presence of 0.005 m.r. (I/HAEB) Trig.101 at 180°C in closed mixing condition at various processing time.	301
5.33a Molecular weight distribution curves of MB's containing 10% HAEB processed with 0.005 m.r. Trig.101 for 2.5, 5 and 10 minutes.	302
5.34 Comparison of FTIR spectra of polymerised DBBA without decalin, refluxed at 70°C for 25 hours in the presence of initiator AZBN, with that of fresh DBBA, both in KBr.	303
5.35 Comparison of FTIR spectra of polymerised DBBA without decalin, refluxed at 70°C for 25 hours in the presence of initiator AZBN, with that of DCM-extract of 10% DBBA MB, both in KBr.	304
5.36 Proton NMR spectrum of polymerised DBBA without decalin, refluxed at 70°C for 25 hours in the presence of initiator AZBN in $CDCl_3$.	305
5.37 Carbon-13 NMR spectrum of polymerised DBBA without decalin, refluxed at 70°C for 25 hours in the presence of initiator AZBN in $CDCl_3$.	306
5.38 Comparison of FTIR spectra of polymerised DBBA - Decalin, with that of fresh DBBA, both in KBr.	307
5.39 Comparison of FTIR spectra of polymerised DBBA-Decalin with that of polymerised DBBA without decalin, both in KBr.	308
5.40 Comparison of FTIR spectra of polymerised DBBA-Decalin in KBr disc with that of neat liquid decalin.	309
5.41 Comparison of FTIR spectra of polymerised DBBA-Decalin in KBr disc, with that of PP MB film containing 10% DBBA after DCM extraction.	310
5.42 Comparison of FTIR spectra of polymerised DBBA-Decalin in KBr disc, with that of xylene soluble of MB film containing 10% DBBA.	311
5.43 Carbon-13 NMR spectrum of polymerised DBBA-Decalin run in $CDCl_3$.	312
5.44 Carbon-13 NMR spectrum of fresh Decalin, run in $CDCl_3$.	313
5.45 Carbon-13 NMR spectrum of 10% DBBA solution in decalin at 296°K in the presence of 0.02 m.r. Trig.101 and small amount of deuterated decalin before reaction.	314
5.46 Carbon-13 NMR spectrum of 10% DBBA solution in decalin at 373°K after 1 hour reaction in the presence of 0.02 m.r. Trig.101 and small amount of deuterated decalin before reaction.	315
5.47 Carbon-13 NMR spectrum of fresh decalin at 373°K heated in NMR cavity for 1 hour in the presence of small amount of deuterated decalin.	316
5.48 Carbon-13 NMR spectrum of 10% DBBA solution in decalin at 373°K after 25 hours reaction in the presence of 0.02 m.r. Trig.101 and small amount of deuterated decalin.	317

Figure	Page
5.49 FTIR of fresh Tris as neat liquid.	318
5.49a Comparison of FTIR spectra of polymerised Tris in KBr disc with that of fresh Tris as neat liquid.	319
5.50 Carbon-13 NMR spectrum of fresh Tris in CDCl ₃ .	320
5.51 Carbon-13 NMR spectrum of polymerised Tris, run by solid state NMR.	321
5.52 Comparison of FTIR spectra of polymerised DBBA-Tris with that of fresh DBBA, both in KBr disc.	322
5.53 Comparison of FTIR spectra of polymerised DBBA-Tris with that of polymerised DBBA without decalin, both in KBr disc.	323
5.53a Comparison of FTIR spectra of polymerised DBBA-Tris in KBr disc with that of fresh Tris as neat liquid.	324
5.54 Comparison of FTIR spectra of polymerised DBBA-Tris with that of polymerised Tris, both in KBr disc.	325
5.55 Carbon-13 NMR solid state spectrum of polymerised DBBA-Tris.	326
5.55a Comparison of FTIR spectra of polymerised DBBA-Tris-Decalin with that of fresh DBBA, both in KBr disc.	327
5.56 Comparison of FTIR spectra of polymerised DBBA-Tris-Decalin with that of polymerised DBBA-Tris without decalin, both in KBr disc.	328
5.57 Comparison of FTIR spectra of polymerised DBBA-Tris-Decalin with that of polymerised Tris, both in KBr disc.	329
5.58 Comparison of FTIR spectra of polymerised DBBA-Tris-Decalin in KBr disc with that of polymerised DBBA-Decalin, both in KBr disc.	330
5.59 Comparison of FTIR spectra of polymerised DBBA-Tris-Decalin in KBr disc with that of 10% MB's film containing (DBBA+Tris) after DCM extraction.	331
5.60 Comparison of FTIR spectra of polymerised DBBA-Tris-Decalin in KBr disc with that of xylene soluble of 10% MB's film containing (DBBA+Tris).	332
5.61 Comparison of FTIR spectra of polymerised DBBA-Tris-Decalin with that of polymerised DBBA without decalin, both in KBr disc.	333
5.62 Solid state Carbon-13 NMR spectrum of polymerised DBBA-Tris with Decalin .	334
5.63 Solid state Carbon-13 NMR spectrum of polymerised DBBA with Decalin .	335
5.64 Solid state Carbon-13 NMR spectrum of xylene soluble of 10% MB containing DBBA processed in the presence 0.02 m.r. Trig. 101.	336

Figure		Page
5.64a	Grafted DBBA content of toluene soluble and xylene soluble of 10% MB containing DBBA without and with Tris coagent processed in the presence of 0.02 m.r. Trig.101, under standard condition.	264
5.64b	Molecular weight (e.g. $M_n \times 10^{-4}$) and MFI of 10% MB's containing DBBA without and with coagents (Tris or DVB) processed in the presence of 0.02 m.r. TrigonoX 101, under standard condition.	265
5.65	Solid state Carbon-13 NMR spectrum of xylene soluble of 10% MB containing DBBA-Tris processed in the presence 0.02 m.r. Trig.101.	337

ABBREVIATIONS AND SYMBOLS

A	: absorbance
AATP	: 1-acryloyl 4-acryloxy 2,2,6,6-tetramethyl piperidine
ABS	: acrylonitrile butadiene styrene
ArO-CHD	: aryloxy cyclohexadienones
AOTP	: 4-acryloyloxy 2,2,6,6-tetramethyl piperidine
AO	: antioxidant
AZBN	: azobisisobutyronitrile
BHBM	: 2,6-di-tert.-butyl-4-hydroxy benzyl mercaptan
BHT	: 3,5-di-tert.-butyl-4-hydroxy toluene
CB	: chain breaking
CB-A	: chain breaking acceptor
CB-D	: chain breaking donor
CHD	: cyclohexadienone
CP	: cross polarisation
DBBA	: 3,5, di-tert.-butyl -4-hydroxy benzyl acrylate
DBHBA	: 3,5-di-tert.-butyl-4-hydroxy benzyl alcohol
DCP	: dicumyl peroxide
DCM	: dichloromethane
DHBP	: 2,4-di-hydroxy benzophenone
DTBP	: 2,6-ditert.-butyl phenol
DR-R	: dissociation energy
DVB	: divinyl benzene
ET	: embrittlement time
EBHPT	: 4-ethoxymercaptoacetate-2-hydroxy benzophenone
FTIR	: furier transform infrared
FRI	: free radical initiator
GH	: hydrogalvinoxyl
HALS	: hindered amine light stabiliser
HAEB	: 2-hydroxy-4-(beta acrylate ethoxy) benzophenone
HDPE	: high density polyethylene
HHBP	: 2-hydroxy-4-(beta hydroxy ethoxy) benzophenone
HMBP	: 2-(2-hydroxy-5-vinylphenyl)-2H-benzotriazole
HOBP	: 2-hydroxy-4-octyloxy-benzophenone
Irg. 1076	: n-octadecyl-3-(3',5'-ditert.-butyl-4-hydroxy-hexyl)propionate
Irg. 1010	: pentaerythrityl tetrakis-(3,5-di-tert.-butyl-4-hydroxy phenyl) propionate
Irganox acid	: 3-(3',5'-di-tert.-butyl-4-hydroxy phenyl)
PhO.	: phenoxy radical
JMOD	: J-modulate spin echo
LDPE	: low density polyethylene
MADA	: 4-mercapto acetamido diphenylamine
MFI	: melt flow index
MPDA	: 4-mercapto propionamido diphenylamine
d-MB	: diluted masterbatch
MW	: molecular weight
MWD	: molecular weight distribution
Mn	: number average molecular weight
Mw	: weight average molecular weight
m.r.	: molar ratio, [FRI]/[AO with or without coagent]
NBR	: nitrile butadiene rubber
NMR	: nuclear magnetic resonance
NR	: natural rubber
PD	: peroxide decomposer
PD-C	: catalytic peroxide decomposer
PD-S	: stoichiometric peroxide decomposer
PhOH	: hindered phenol

PP : polypropylene
QM : quinone methide
Sumilizer GM : 2-tert.-butyl-6-(3-tert.-butyl-2-hydroxy-5-methyl benzyl)-4-
methylphenyl acrylate
Tac. : 2,4,6-triallyloxy 1,3,5-triazine
Trig.101 : 2,5-dimethyl 2,5- di-tert. butyl peroxy hexane
Tris/TMPA : trimethylol propane triacrylates
UV : ultra violet
VDBP : vinyl-3-(3',5'-di-tert.-butyl-4-hydroxy phenyl propionate
Tin.770 : bis-(2,2,6,6-tetra methyl piperidine) sebacate

CHAPTER ONE

INTRODUCTION

1.1 GENERAL INTRODUCTION

Polyolefins as a commodity plastic dominate significantly both in household and industrial applications, due to their low price, versatility, ease of processing, in addition to their low weight to volume ratio⁽¹⁾. A major drawback, however, is their susceptibility to oxidative degradation⁽²⁾. A range of antioxidants have, therefore, been used to protect these polymers against oxidation during processing and fabrication and subsequently when subjected to hostile environments during in-service performance^(3,4). This has led to a dramatic increase in their annual production⁽¹⁾. Polyolefins dominate the world thermoplastic market for both antioxidant and light stabiliser usage. The polyolefin industry consumes approximately half the antioxidants and three-quarters of the light-stabilisers produced for thermoplastic polymers^(5,6,7). A major problem associated with the use of antioxidants in polymers is their physical loss especially when subjected to aggressive environments, e.g. oils, solvents and foodstuffs. The loss of antioxidants does not only lead to loss of their intended function (stabilising activity), but also to contamination of the surrounding environment, with adverse consequences such as in the case of food packaging and medicinal applications^(8,9).

1.2 DEGRADATION OF POLYOLEFINS

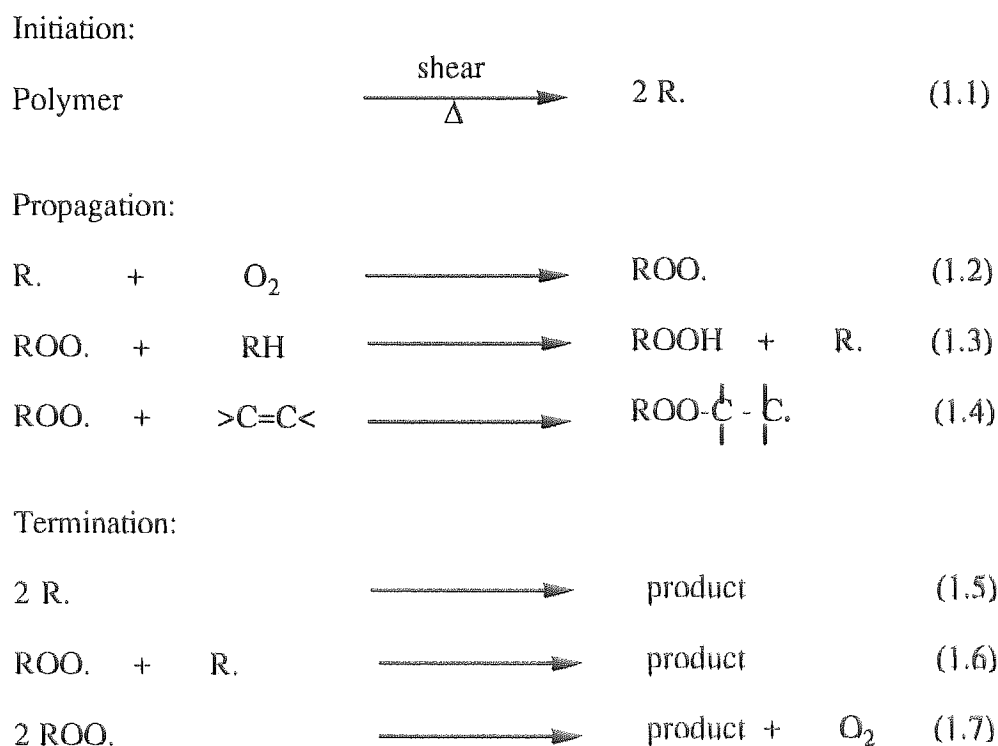
Polymers deteriorate as a result of conditions encountered during two main stages, processing and subsequently in service. In the former, the polymer is subjected to high temperatures and shearing forces in the presence of very small concentration of oxygen for relatively short periods of time such as the case with extrusion and moulding operations. While the long term ageing under the effect of light, heat and mechanical stress, is a more

gradual process. The change in composition and structure of the polymers eventually lead to the deterioration of the useful properties and ultimately to failure of the polymer articles.

1.2.1 Thermal Oxidative Degradation

During melt processing operation the shearing forces applied on the polymer melt cause some of the polymer chains to undergo homolytic scission leading to the formation of macroalkyl radicals, see reaction 1.1 in Scheme 1.1. The rate of this chain scission depends on the dissociation energy (D_{C-C}) of the bonds⁽¹⁰⁾. Ultimately, melt degradation leads to changes in the polymer molecular weight, which is technically very important since the final properties of the polymers depend to a large extent on their molecular weight⁽¹¹⁻¹³⁾. Depending on the structure of the polymer, different reactions may take place during melt processing⁽¹⁴⁻²⁰⁾. In the case of polypropylene for example, the polymer mainly undergoes chain scission leading to a decrease in molecular weight (reflected in an increase of melt flow index, MFI) ^(14,21,22), while in polyethylene, crosslinking reactions dominate leading to a decrease in MFI value^(14,21,24).

In general the mechanism of oxidative degradation of polyolefins has been shown to be very similar to that of low molecular weight hydrocarbons, which was initially proposed by Bolland, Gee and co-workers⁽²⁴⁻²⁷⁾, see Scheme 1.1. It is generally accepted that both thermal and photo degradation is generated by initial formation of macro-alkyl radicals (R.), see reaction 1.1. The macro-alkyl radicals formed then react rapidly with oxygen to give an alkyl-peroxyl radical (ROO.), see reaction 1.2, which abstracts a hydrogen to give hydroperoxides (ROOH), see reaction 1.3. The rate constant of hydrogen abstraction by radical primarily depends on the activation energy. These peroxyl radicals are sensitive to steric and polar effects of the attacking radical and dependent on the reaction temperature.



Scheme 1.1 General mechanism of hydrocarbon oxidation

Peroxy radicals are relatively selective electrophilic species, which abstract tertiary bonded hydrogens in preference to secondary or primary hydrogens⁽²⁸⁻³⁰⁾. In the presence of a double bond, peroxy radicals easily attack the double bond to form saturated new macroperoxy radicals, see reaction 1.4. The termination of the radical chain is due to reactions of free radicals with each other by combination, in which inactive products are formed (see reaction 1.5-1.7). When the oxygen pressure is high, the termination reaction almost exclusively follows reaction 1.7. At low oxygen pressures other termination reactions take place to some extent.

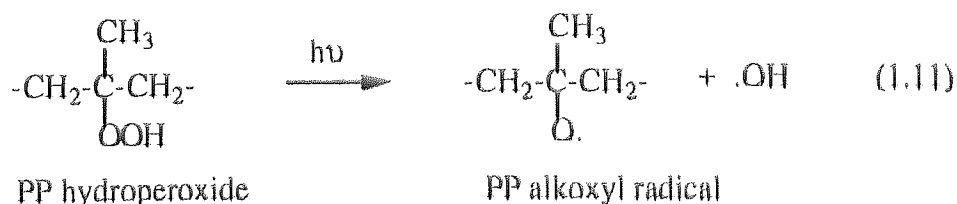
1.2.2 Photo-oxidative Degradation

The main difference between thermal-oxidative and photo-oxidative degradation lies in the nature and rate of the initiating step, i.e. the formation of the first radicals^(31,32). Pure polyolefins, should be stable to ultra violet (UV) light, since these polymers do not absorb

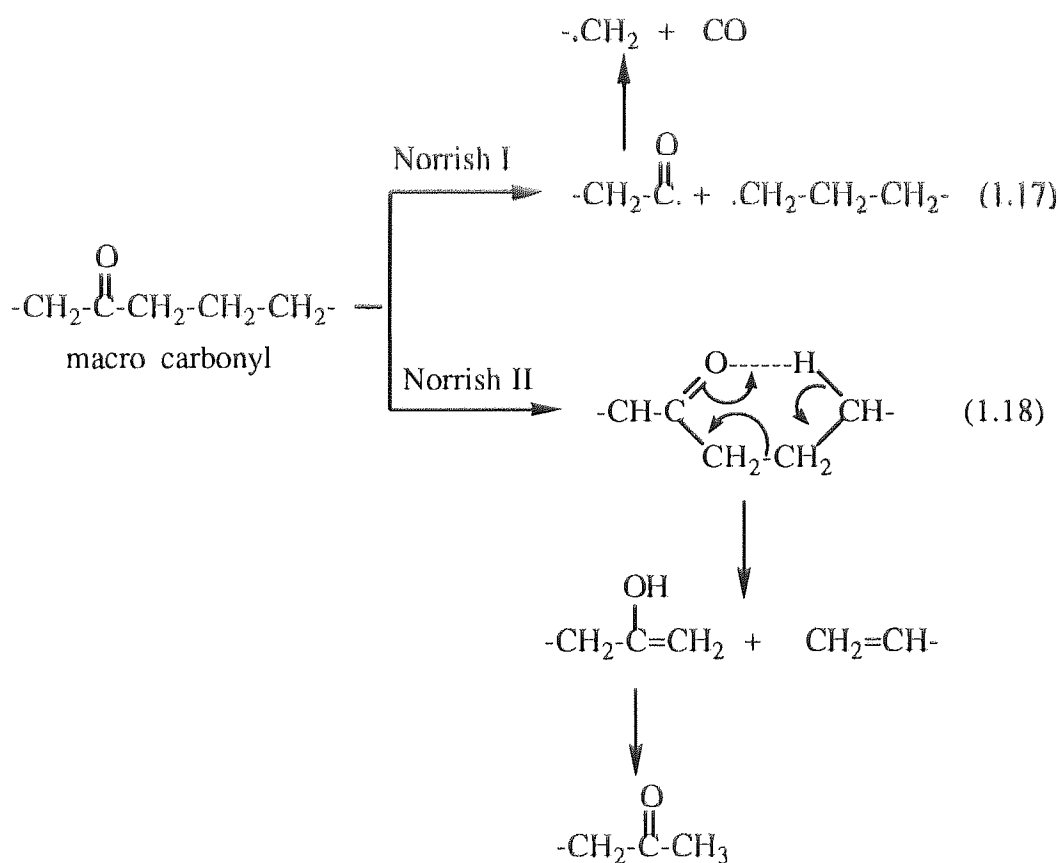
electro-magnetic radiation energy in the wave-length region above 200 nm. However, commercially produced polyolefins normally contain impurities that can absorb at the longer wave-lengths of the sun's spectrum (>285 nm)^(31,32). Photo-oxidative degradation of polyolefins can be initiated by the presence of impurities in the polymers, such as charge transfer complexes, catalyst residues, and various oxidation products formed during manufacture, e.g. hydroperoxides, peroxides and carbonyls compound (33-37). It was shown (22,31,38-41) that hydroperoxides formed during polymer processing play a major role in the initiation of photooxidation while the contribution of carbonyl containing compounds during the early stages of photo-oxidation is negligible. Hydroperoxides are exceptionally photolabile (43-45), leading to alkoxy (RO \cdot) and hydroxyl (\cdot OH) radical formation which can abstract a hydrogen atom from the polymer, which leads to chain scission during the early stages of photo-oxidation (see reaction 1.8, 1.9 and 1.10).



In polypropylene, hydroperoxides undergo photo cleavage by a process which generates reactive macroalkoxy radical (see reaction 1.11), which undergoes β -scission with C-C cleavage (see reaction 1.12 and 1.13) to form backbone ketone (A) and terminal ketones (B), (31,32).



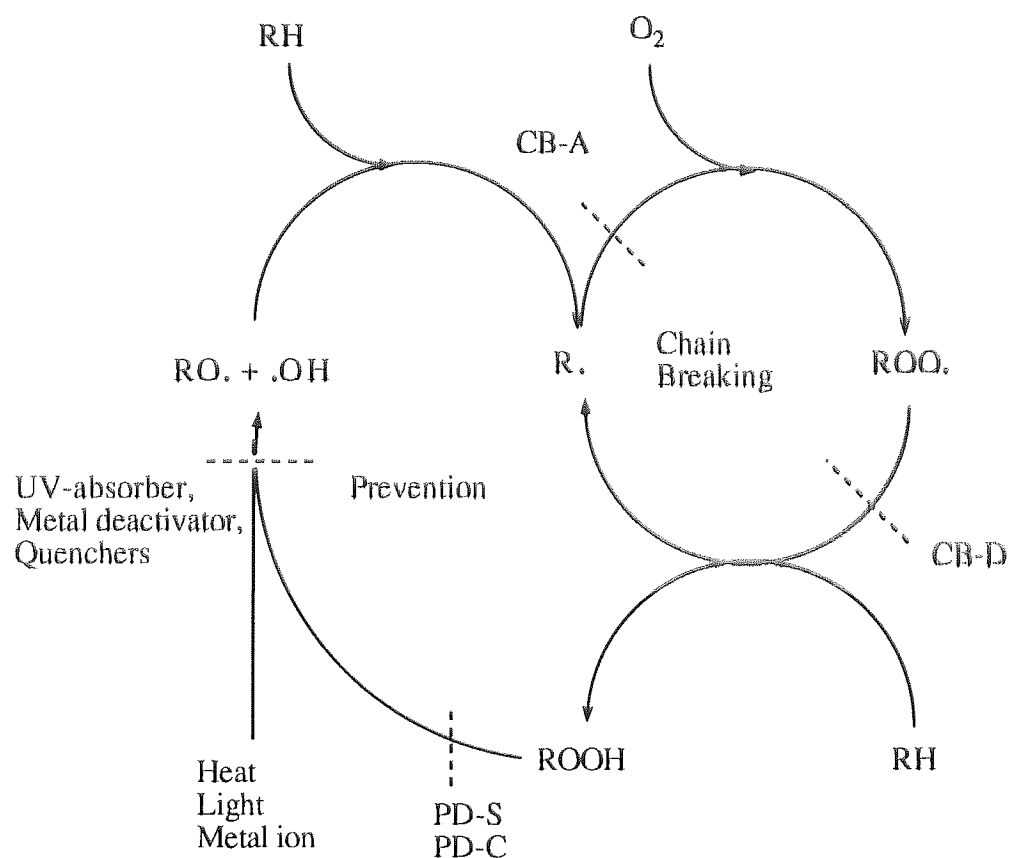
They play a major role during the later stages of oxidation. Ketones undergo two dominant photo cleavages, following Norrish type I and Norrish type II reactions. In the Norrish type I reaction, the bond between the carbonyl group and the adjacent α -carbon is homolytically cleaved producing two radicals, (see reaction 1.17), while the Norrish type II reaction proceed via a non-radical process. This is an intermolecular process that occurs with the formation of a six member cyclic intermediate. Subsequent abstraction of a hydrogen atom from the end carbon results in decomposition into olefins and ketones (31), see reaction 1.18.



1.3. STABILISATION OF POLYOLEFINS

The problems of polymer oxidation can be minimised by using antioxidants that can interfere with the process of oxidation. Therefore, the inhibition of polymer oxidation can be achieved in two ways, firstly, by breaking the primary chain oxidative process using chain-breaking (CB) antioxidants and secondly, by preventing or retarding the

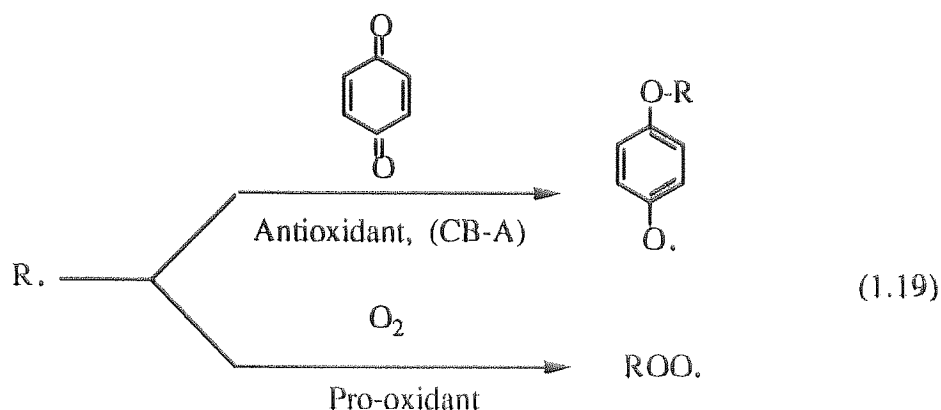
formation of free radical initiator and hydroxides, the most important class here are peroxide decomposer (PD)(46). Scheme 1.2 represents polymer oxidation by two interlinked cycles and shows the points at which the 2 major classes of antioxidants interfere with these cycles (47).



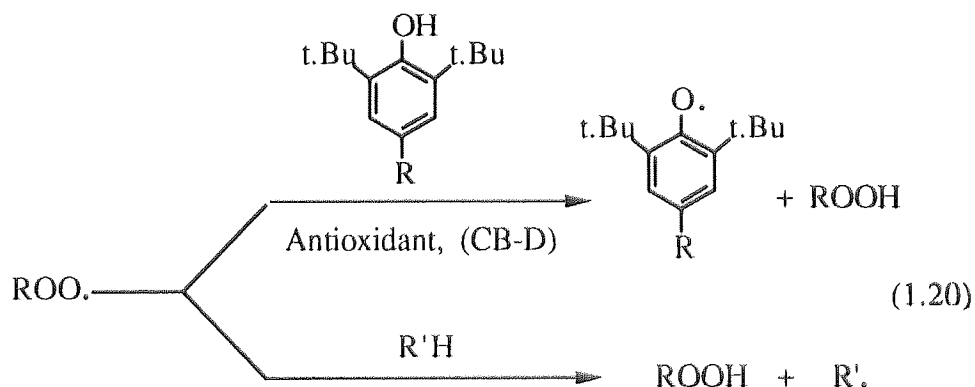
Scheme 1.2 Stabilisation mechanisms of polyolefins

The chain breaking mechanism operates by interrupting the chain oxidative cycle (see Scheme-1.2), by removing the main propagating reactive alkyl ($R\cdot$) and alkyl-peroxy ($ROO\cdot$) radicals. The chain breaking antioxidants act either by accepting an electron or $H\cdot$ (i.e. oxidising the alkyl radical, $R\cdot$) in the absence of oxygen (chain breaking acceptor, CB-A), or by donating an electron or $H\cdot$ to $ROO\cdot$ (i.e. reducing the $ROO\cdot$), these are known as chain breaking donors (CB-D)(47,48). Example of CB-A antioxidants include quinones, stable radicals such as nitroxyls. These have to compete with oxygen for the macroalkyl radicals ($R\cdot$) to show effective antioxidant activity (47-49), (see reaction

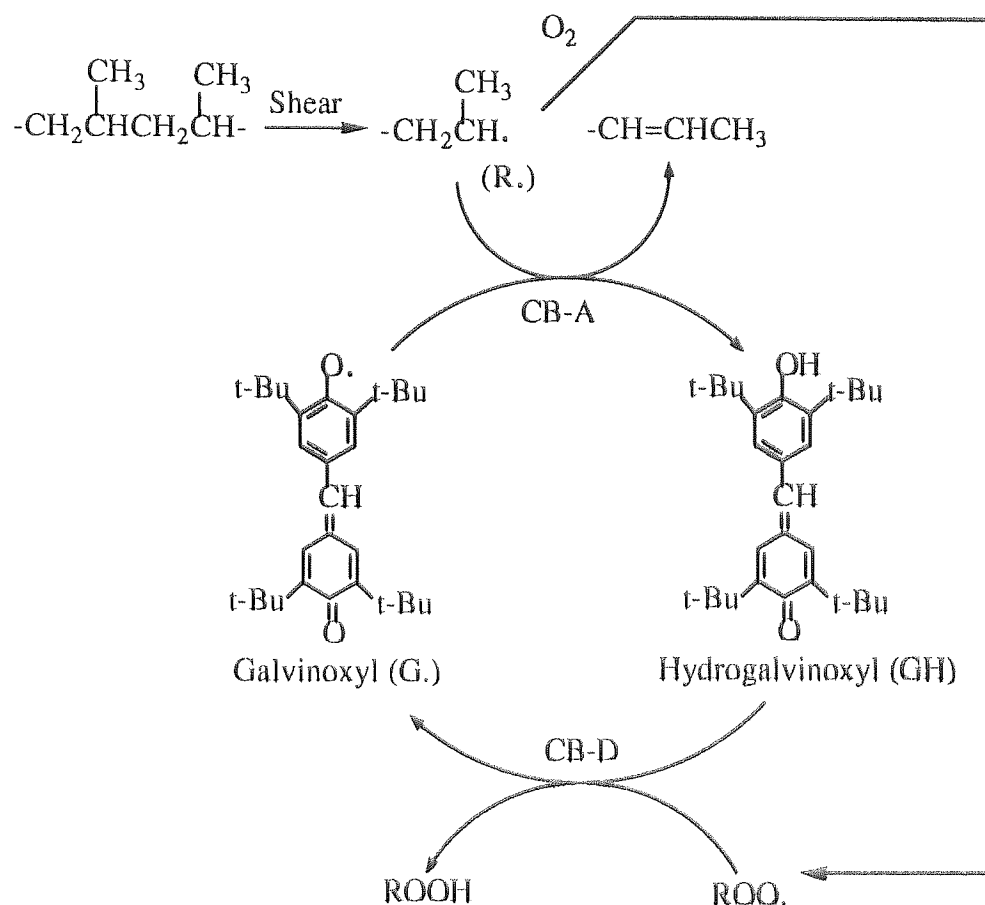
1.19). In general, therefore, molecular requirement for a CB-A antioxidant is similar to that for a polymerisation inhibitor .



Antioxidants that reduce alkyl-peroxy radicals ($\text{ROO}\cdot$) by donating an electron (or $\text{H}\cdot$) are referred to as CB-D. These have to compete with the substrate for the alkyl-peroxy radicals ($\text{ROO}\cdot$), see reaction 1.20 (47-49). Major examples are based on hindered phenols and aromatic amines.



Some antioxidants can act by both CB-A and CB-D mechanisms, (see Scheme 1.3) and are referred to as regenerative antioxidants (47,50-52). For example Galvinoxyl (G.) is particularly effective in polypropylene and in the first minute of mixing in a closed internal mixer at 200°C is converted to the hydrogalvinoxyl (GH)(51,52). The hydrogalvinoxyl (GH) functions as a CB-D antioxidant to donate electron ($\text{H}\cdot$) to alkyl-peroxy radical ($\text{ROO}\cdot$), see Scheme 1.3.

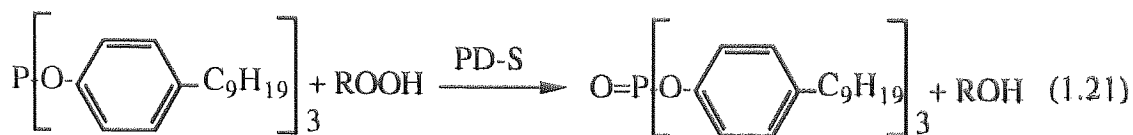


Scheme 1.3 Cyclical regeneration of galvinoxyl (G.) during the melt stabilisation of polypropylene

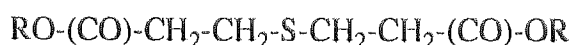
However, as the shear in the mixer decreases due to reduction in polymer melt viscosity, GH is partially re-oxidised to galvinoxyl, G· (CB-D mechanism) by alkyl-peroxy radicals, which then accumulate in the system. Furthermore, the galvinoxyl radical forming from the above reaction may react with alkyl-radicals ($\text{-CH}_2\text{-(CH}_3\text{)C·-H}$, R·) by CB-A mechanism to produce a non radical product (-CH=CH-CH_3) (47,50-52).

The PD mechanism involves decomposition of hydroperoxides in a process that does not lead to the formation of free radicals. Two classes of antioxidants show PD activity, the first are based on phosphates which decompose peroxide stoichiometrically (reduces peroxides to alcohols), see reaction 1.21 (53-58). The second include variety of sulphur compounds such as, thiodipropionate esters (I), dithiocarbamates (II), dithiophosphates

(III), all of which act by catalytically decomposing hydroperoxides (PD-C mechanism) (56,59,60).



Tris-nonyl phenyl phosphite



I

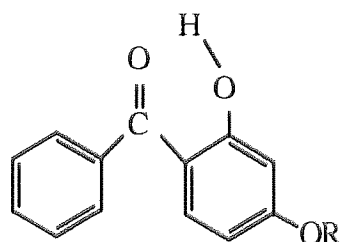


II

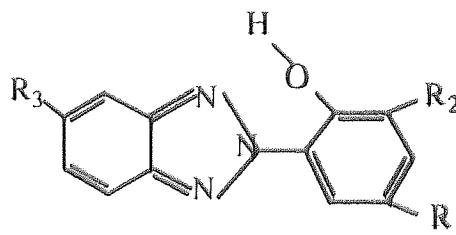


III

UV absorbers are a class of stabilisers that have intense absorption in the region of 290 to 370 nm, but are transparent in the visible region. The best examples of this category are the 2-hydroxybenzophenones (IV) and the benzotriazoles (IVa)⁽³¹⁾. UV absorbers can absorb the harmful radiation (UV energy) that causes photooxidation and convert it to a harmless radiation (61,62), for more detail this will be discussed in Section 1.7.



IV



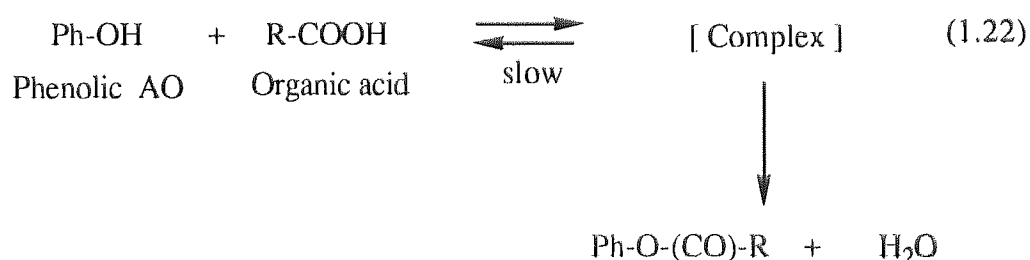
IVa

1.3.1 Synergistic and Antagonistic Effects

In practice, to enhance the activity of a stabilisation system, more than one type of antioxidant which can act by different mechanisms can be employed in order to reinforce

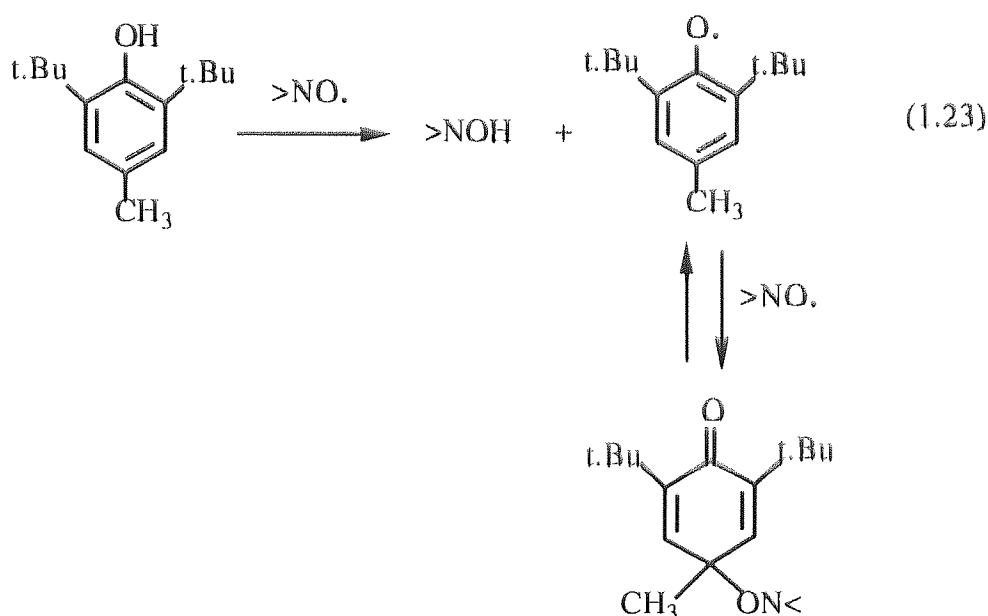
their action. If the overall effect adds to more than the sum of the effect of the individual antioxidants, then this is referred to as 'synergism'^(49,63-65). The mechanism by which the synergistic mixture function, depends on the original mechanism of action of each of the antioxidants in the mixture. Classical examples of synergistic antioxidant systems include combination of hindered phenols and phosphite antioxidants, hindered phenols and substituted thiopropionates, hindered phenols with UV absorbers or sulphur compounds containing UV absorbers (66-68).

Unlike synergism, antagonism reduces the overall effectiveness of combinations of antioxidants. Mar'in and Shlyapnikov⁽⁶⁹⁾ had studied the influence of a higher carboxylic acid (which may be present in oxidised polymer) in phenolic antioxidant systems, which can reduce the effectiveness of antioxidants compared to that of the active individual compounds. This antagonism between phenolic antioxidant and organic acids was found to be caused by formation of an acid-phenol complex and the contribution of phenol esterification reaction becomes considerable only at latter stages of the process, because of its low rate, see reaction 1.22⁽⁶⁹⁾.



Allen and co-workers^(70,71) also reported that under photooxidation conditions hindered amine light stabilisers (HALS)/hindered phenol systems in polyolefins showed antagonistic effects. One reason for this antagonistic effect was suggested to be due to deactivation of the hindered phenolic moiety when used in combination with HALS due to its oxidation by the $>\text{NO}\cdot$ radical⁽⁷²⁻⁷⁴⁾. The hindered phenol oxidises easily by nitroxyl radicals to form phenoxy radical and this is followed by the formation of a benzoquinone, see reaction 1.23.

Sulfur containing antioxidants (as hydroperoxide decomposers) were shown to antagonize the photo-stabilising action of HALS in polyolefins. The antagonistic effect is explained by a mechanism in which sulfur-containing compounds may decompose hydroperoxides in the polymer matrix, resulting in retardation or prevention of the formation of nitroxyl-derived from HALS, since the nitroxyl is considered to be essential for photo-stabilisation (75-79).

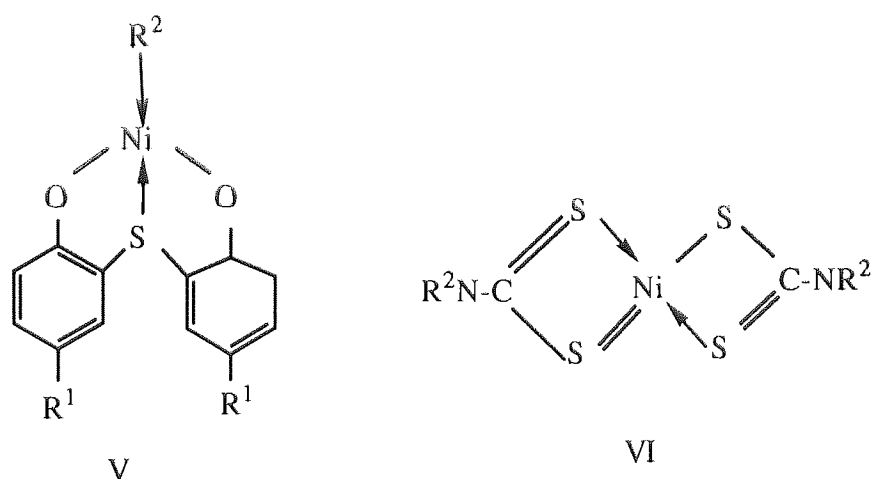


1.4 CHEMICAL AND PHYSICAL LOSSES OF ANTIOXIDANTS FROM POLYMERS.

There are two factors that are responsible for the effectiveness of antioxidants, i.e. the antioxidant's intrinsic behaviour and their retention in the polymer during their useful lifetime. The intrinsic behaviour of antioxidants and the nature of transformation products formed during processing and subsequently under environmental condition depend primarily on the initial chemical structure of the antioxidants. By appropriate modification of the active structural features, the antioxidants may be tailored to improve their effectiveness. However, effectiveness of intrinsically active antioxidants can be useful only if they can be maintained in the polymer during processing and in service^(8,62). Antioxidants can be lost from the polymer by chemical or physical means. The nature of

chemical losses varies from one class of antioxidant to another. The chemical losses in polymers could be undesirable or desirable. Many reviews (31,62,81-84) appeared recently describing the chemical losses of antioxidants from polymers during processing and under effect of UV light and heat. It was reported (81) that 2-hydroxybenzophenone (IV) can be destroyed by hydroperoxides, peroxides and that their losses during photooxidation is largely due to their activity as free radical scavengers.

The Ni complexes, V and VI were shown to be chemically lost during photo oxidation of polyolefins(85-92). Nickel complexes of dithioamides were shown to act as stabilisers by decomposing hydroperoxides and also by scavenging free radicals.



Physical losses of antioxidants are affected not only by the nature of the antioxidants but also the properties of the polymer and its morphology which in turn affect the compatibility and extractability of the antioxidants in the polymer. In addition, processing conditions and the nature of the contact media also contribute to the physical losses (8,93-97). The compatibility and solubility of antioxidants with polymers are associated with the interaction between polymer and antioxidant through their cohesive forces that affect the homogeneity of the antioxidant in the polymer. The degree of compatibility can be improved by incorporating polar groups into the antioxidant molecules(93,97) in the case of polar polymer, or non-polar groups for non-polar polymers. Solubility of antioxidants

depends greatly on temperature, antioxidants may be soluble at the high processing temperatures but may come out of solution when polymers are cooled down to room temperature⁽⁹⁴⁾. Volatility is another major cause of physical loss of antioxidants at elevated temperatures. As the concentration of antioxidant on the surface decreases, the antioxidant in the bulk starts to diffuse to the surface layer leading to more volatilisation (94,96). The extractability or leachability of antioxidants can also affect their performance when polymers are in contact with a dissolving media (e.g. oil, acid, water, detergent solution, food stuffs). Besides the solubility of antioxidants in the media, the diffusion of antioxidants from polymer to the contact media materials also affects the rate of evaporation or leaching of antioxidants. Antioxidants with high diffusion coefficients migrate easily to the polymer surface and this lead ultimately to their loss (8,93,94).

1.5 IMPROVING SUBSTANTIVITY OF ANTIOXIDANTS IN POLYOLEFINS

1.5.1 General Approaches

Improving substantivity of antioxidants in polymers continues to be an area of interest both in industrial and academical institutions. Several approaches to this problem have been described in the literature⁽⁹⁸⁻¹⁰²⁾. The first simple solution is based on increasing the molecular weight of the antioxidants. Some antioxidants, however, still can be lost when subjected to aggressive environments and the bulky structure of the antioxidant can also reduce their compatibility in the polymer (103-107). The second approach is through copolymerisation of the antioxidants during synthesis of the polymer (108,109). Although this approach is technically effective, high cost is involved in producing new speciality polymers for each end use^(98,110-112). The more attractive alternative approach involves modification of the polymer with reactive antioxidants during the processing operation, this approach is referred to here as reactive processing. In a special reactive processing procedure^(98,110-112), antioxidant concentrates (masterbatches) of different polymers were prepared in which the reactive antioxidant becomes highly attached to the polymer

backbone. These antioxidant concentrates can be used as conventional antioxidants by dilution in the same or different thermoplastic polymers. One general problem associated with reactive processing, however, is that several side reactions, such as homopolymerisation of the additive and crosslinking of the polymer, compete with the main grafting reaction. The extent and contribution of the desirable (grafting) and undesirable (side reactions) is greatly dependent on the processing conditions, e.g. time, temperature, molar ratio of initiator to additive and the presence or absence of any co-reactive agent (98,110,113).

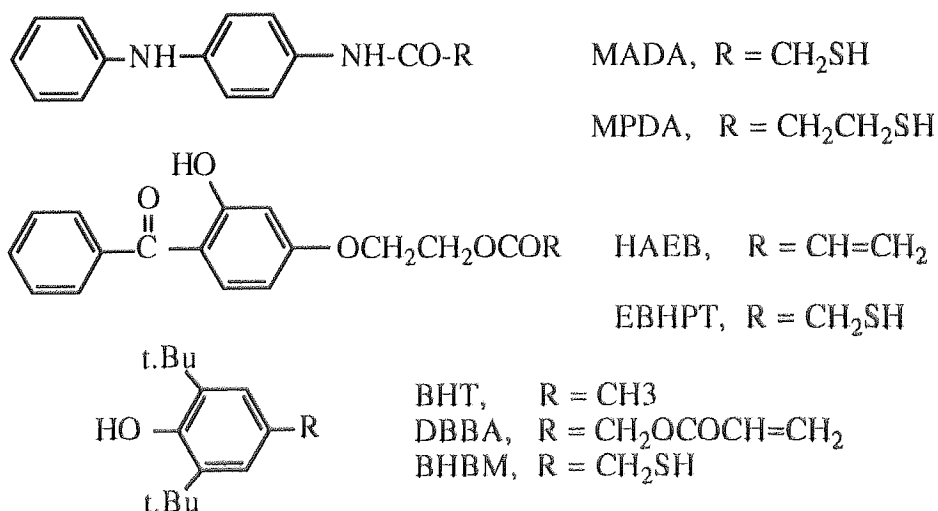
Various workers have shown that under certain aggressive environments the synthetic polymer having chemically bound antioxidants are superior to polymers containing a dispersed antioxidant(113-117). The general methods of increasing the antioxidant substantivity such as copolymerisation and grafting of monomeric antioxidants, and binding of non-polymerisable antioxidants onto polymers have been reviewed (98,100,118).

1.5.2 Experience at Aston on Bound Antioxidants Using a Reactive Processing Procedure

Carrying out chemical reactions of antioxidants in a polymer melt is referred to as reactive processing. Much effort has been devoted at Aston over the last 15 years to chemically attaching antioxidants and other additives to a wide range of polymers during melt processing(98,99,107,110-112,119-131). In most of the work, concentrates of polymer bound-antioxidant (with concentration up to 20%) were prepared and subsequently diluted down in fresh polymer to the normal low antioxidant concentration(107,111,112,119-124,127-131). Reactive processing is normally carried out under oxygen depleted conditions and usually takes place through radical-initiated chemical reactions in which the functionalised antioxidant, becomes attached to the polymer backbone. Careful design of

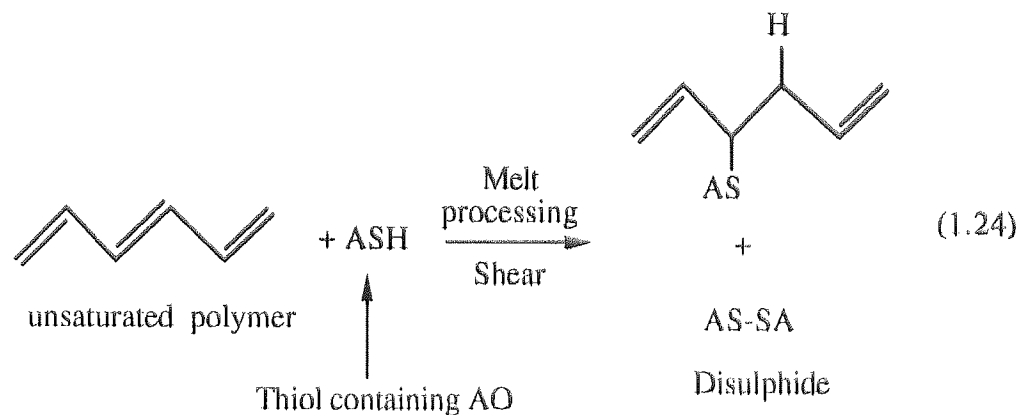
the functionalised antioxidants and control of processing parameters is very important to avoid the large number of undesirable side reactions that compete with the grafting reaction of antioxidants.

Reaction of thiol containing antioxidants in the polymer melt can be initiated mechanochemically by the influence of shear instead of using free radical initiators (98,99,107). It had been reported (119) that thiol containing antioxidants (e.g. 2,6-di-tert.-butyl-4-hydroxy benzyl mercaptan, BHBM) and stabilisers (e.g. 4-ethoxymercaptoacetate-2-hydroxy benzophenone, EBHPT) can be chemically reacted with rubbers and rubber modified plastics (e.g. acrylonitrile butadiene styrene, ABS) in high yields and under conditions of high temperature and high shear during processing. A phenolic thiol antioxidant (BHBM) and two thiol amide (4-mercapto acetamido diphenylamine, MADA and 4-mercapto propionamido diphenylamine, MPDA) have been reacted with nitrile butadiene rubber (NBR) in latex under condition closed and opened internal mixer condition, at 55°C, and high shear during processing (120) to high levels.

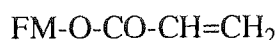


Furthermore, other antioxidants containing thiols group were mechanochemically reacted with both natural rubber (NR)(123) and styrene-butadiene-rubber (SBR)(121) under processing conditions (closed internal mixer at 70°C). This method is particularly suitable for unsaturated polymer such as natural rubber (NR), nitrile butadiene rubber (NBR) and thermoplastic elastomers (e.g. ABS, SBR) but not for saturated hydrocarbon polymers

e.g. polyolefins. Another problem of this approach is that it is difficult to achieve very high levels of binding due to the formation of disulphide (from the thiol antioxidant) which is a major by-product and this can easily be lost from the polymer under aggressive environments (8,107) see reaction 1.24.



More recent efforts at Aston (107,111,112,125,128-130) have concentrated on developing methods for grafting of functional antioxidants on polyolefins. Acrylate monomers, VII (e.g. AATP, AOTP, DBBA, HAEB) and maleate esters, VIII [e.g. Bis (2,2,6,6-tetra methyl piperidiny) maleate, BPM], containing antioxidant functions were reacted with polyolefins in the melt in the presence of a free radical initiator (during processing).

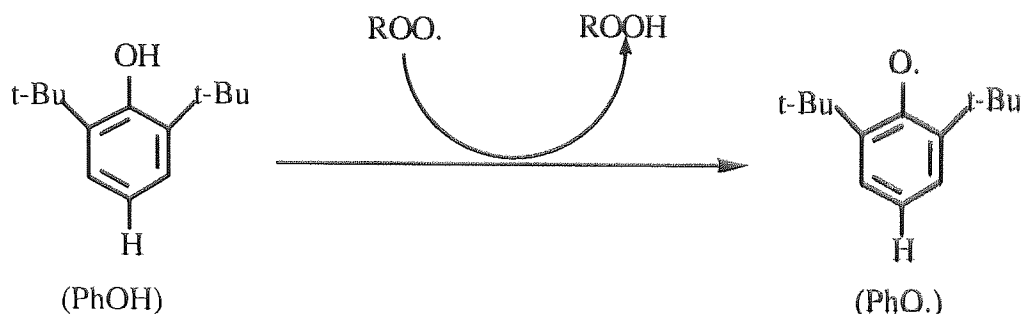


VII

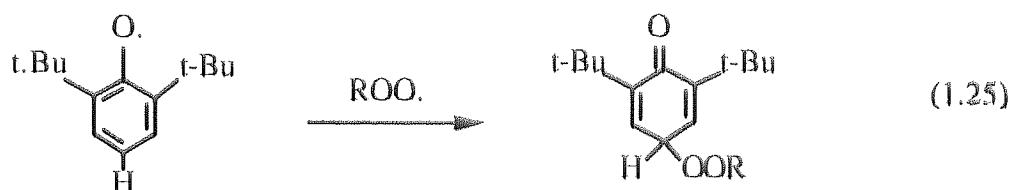


VIII

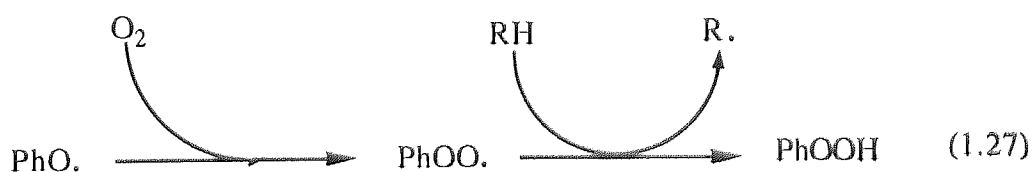
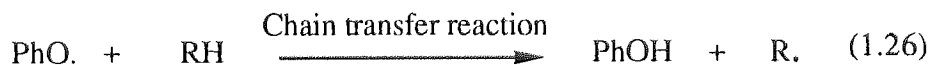
In general, it was shown (99,111,112) that acrylates and methacrylates containing antioxidants (VII) lead to low levels of adduct formation due to effective competition from homo-polymerisation. These antioxidant homopolymers are less effective than the grafted antioxidants since they can leach out under extraction conditions in addition to the fact that they may form phase separation (98,111,113). It was shown that monofunctional antioxidants (e.g. vinyl containing HALS, AOTP) lead to low grafting efficiency due mainly to homopolymerisation of the antioxidant. However, using a multifunctional coagent (e.g. trimethylol propane triacrylate, Tris) was found to enhance the grafting efficiency of the monofunctional antioxidant profoundly (126). Maleate derivatives (e.g. BPM) were shown to give higher binding efficiency than vinyl containing antioxidants



Scheme 1.4 The first step involved in the stabilising activity of hindered phenols

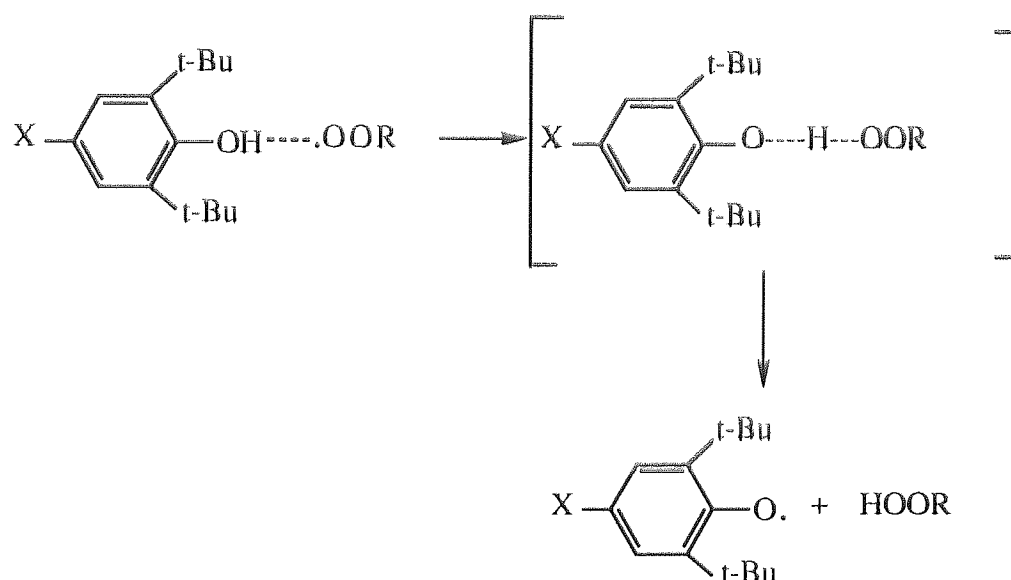


The phenoxy radical formed can also undergoes chain transfer reaction (see reaction 1.26) as well as competing reaction of oxygen with phenoxy radical (PhO·), see reaction 1.27. This reaction become more favourable with less sterically hindered phenols.



The stabilising activity of phenolic antioxidants (PhOH) are strongly dependent on their structure. In general the transition state involves both electron delocalisation and charge separation within the benzene ring of the phenolic antioxidant (see Scheme 6). Consequently, groups in the 2, 4 and 6 positions which extend the delocalisation of the unpaired electron (e.g. phenyl or methyl), increase the activity. Electron-releasing groups (e.g. R₂N, RNH, RO, R) on the para position, on the other hand, decrease the energy of the transition state and consequently increase antioxidant activity, whereas electron-

attracting groups (e.g. Cl, CN, COOH, NO₂) decrease the activity (132,133). The presence of at least one tertiary alkyl group in the ortho position is necessary for the high antioxidant activity. Many of the most effective antioxidants in polyolefins are substituted in both ortho positions by tertiary alkyl groups. This steric enhancement of antioxidant activity is due to the increased stability of the derived phenoxyl radical which reduces the rate of the chain transfer reaction.



Scheme 1.5 Transition State in the oxidation of Phenolic Antioxidant

The relationship between the antioxidant activity of phenols and their structure has been thoroughly studied in petrol (96). A few examples are represented in the Table 1.1 below to show the effect of 2,4, and 6 tri-substituted phenols in petrol.

One of the most widely used and studied hindered phenols is BHT (XII), this is a very volatile antioxidants and therefore is very susceptible to physical loss (2,134). To overcome this problem, a variety of higher molecular weight hindered phenols have been developed commercially such as Irganox 1076, XIII; Irganox 1010, XIV; Antioxidant 2246, XV), see Table 1.2.

Table 1.1 Effect of substituents variations in 2,4, and 6 positions on the antioxidant activity of phenols compared to that of unsubstituted phenol* (96).

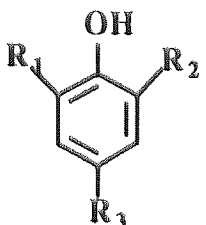
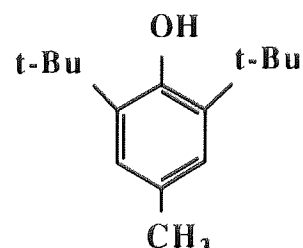
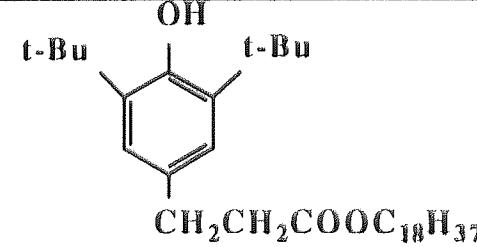
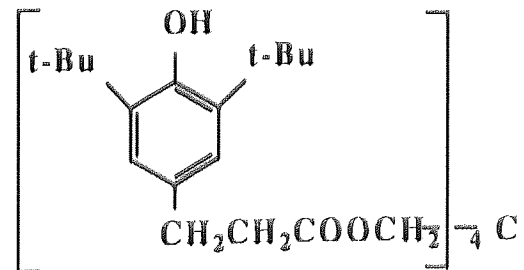
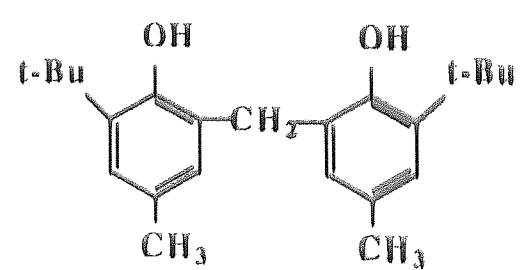
				
No	R ₁	R ₂	R ₃	Antioxidant activity in petrol
1	H	H	H	1*
2	Me	H	H	14
3	H	H	Me	10
4	Me	Me	H	32
5	Me	H	Me	47
6	Me	Me	Me	120
7	Me	Me	t-Bu	20
8	t-Bu	Me	Me	170
9	t-Bu	Me	t-Bu	48
10	t-Bu	t-Bu	Me	100
11	t-Bu	t-Bu	t-Bu	46
12	t-Bu	t-Bu	OMe	200

Table 1.2 Typical Hindered Phenol Antioxidants.

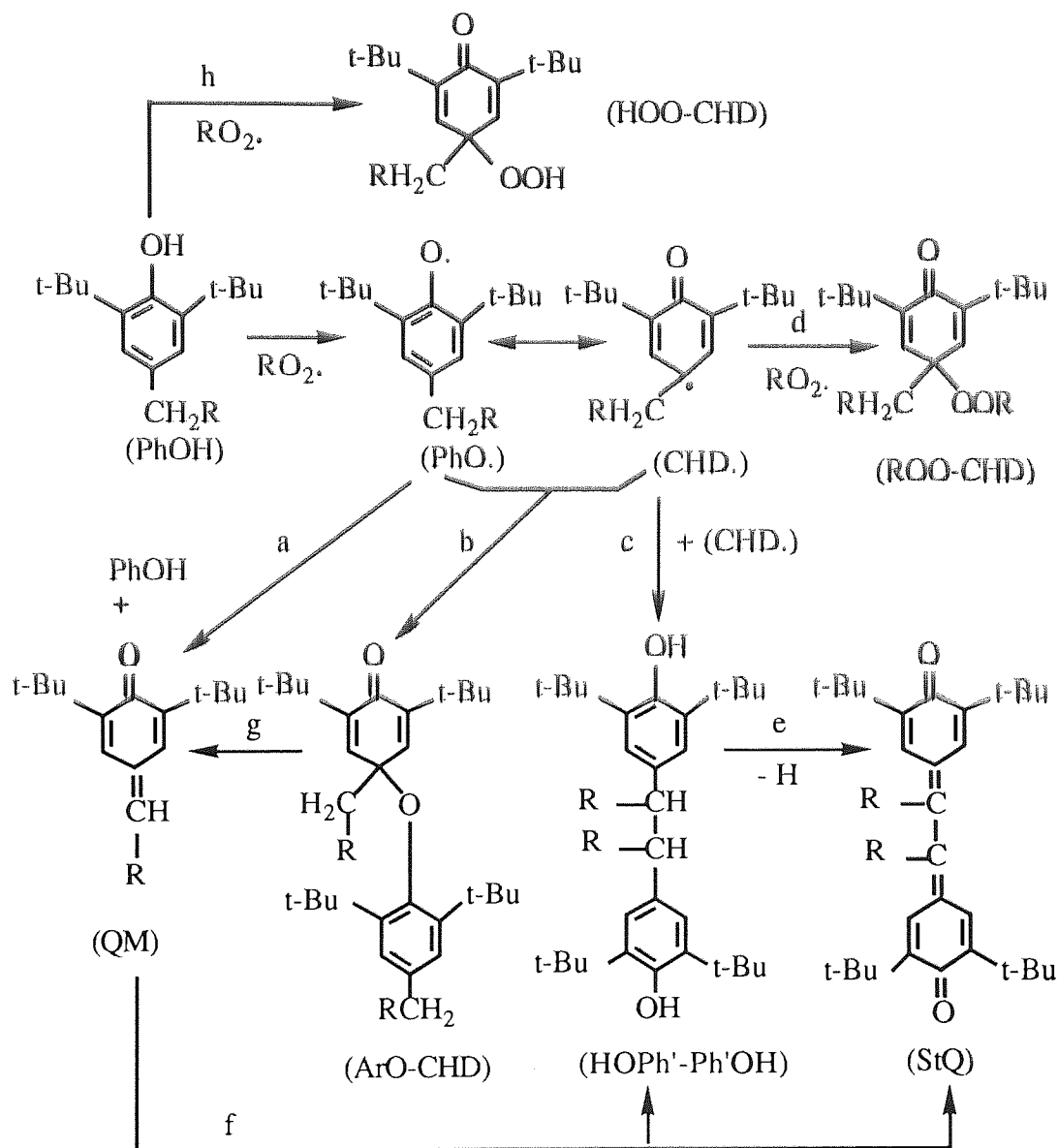
 <p>BHT, IX</p>	 <p>Irganox 1076, X</p>
 <p>Irganox 101, XI</p>	 <p>Antioxidant 2246, XII</p>

1.6.2 Chemical Transformation of Hindered Phenols and their Activity as Thermal Stabilisers for Polyolefins.

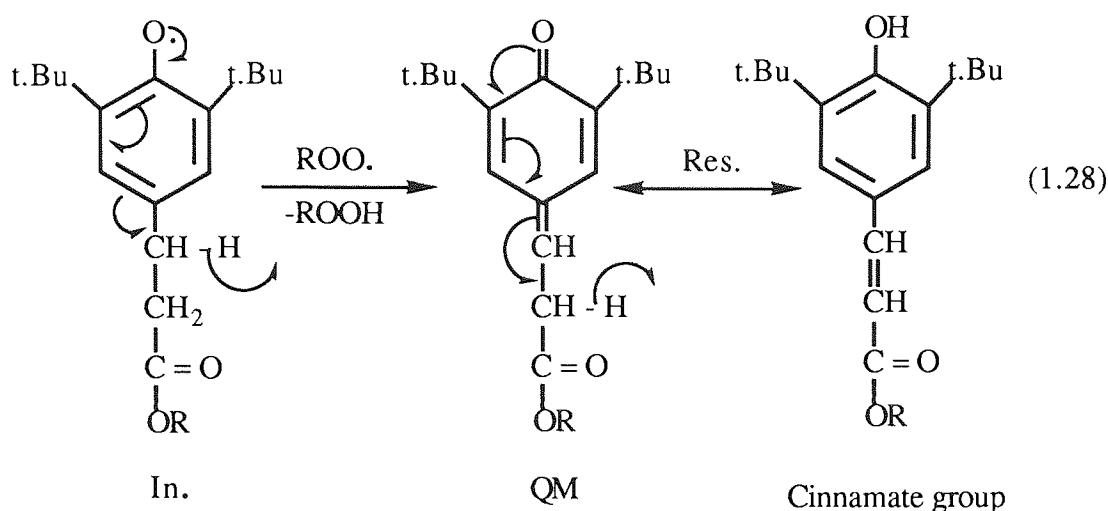
Phenoxy radicals are the first detectable radical species formed during the antioxidant action of hindered phenol, see reaction a Scheme 1.6^(135,136). They are also formed, to some extent, by oxidation with molecular oxygen (O_2 or O_3) at temperature above $150^\circ C$, during sensitised photo-oxidation⁽¹³⁷⁾ and during radiolysis of phenols⁽¹³⁸⁾. The chemistry of phenoxy radicals is decisive for the consecutive transformations of phenols observed in oxidised polymers. The nature of chemical transformations which was examined mainly in model systems has been reviewed extensively^(71,132,135-138) the salient features are summarised in Scheme 1.6.

The main chemistry of the transformation of phenolic antioxidants (PhOH) therefore start with stable phenoxy radicals ($PhO\cdot$) which followed by its further transformations through bimolecular disproportionation lead to a quinone methide, QM (reaction a Scheme 1.6). C-O coupling of $PhO\cdot$ with mesomeric cyclohexadienonyl radical ($CHD\cdot$) leading to aryloxy cyclohexadienones (ArO-CHD), see reaction b Scheme 1.6. C-C coupling of benzyl radicals formed through formal rearrangement of $CHD\cdot$, resulting in phenolic dimers (HOPh-Ph'OH), see reaction c Scheme 1.6. This is followed by combination of $CHD\cdot$ with a second $ROO\cdot$ to form alkylperoxy cyclohexadienone (ROO-CHD), see reaction d Scheme 1.6^(139,140).

It was reported by Gugumus⁽¹⁴¹⁾ that reaction 1.28 is an important mechanistic feature contributing to the efficiency of hindered phenols substituted with a propionate group. After reaction of hindered phenol with alkylperoxy radical to form phenoxy radical ($PhO\cdot$), a second alkylperoxy radical, $ROO\cdot$ (see reaction 1.30) is scavenged by $PhO\cdot$ to give quinone methide (QM) without the formation of ROO-CHD that is an initiator. The process has a CB-regenerative character due to the intramolecular rearrangement of the QM formed which is substituted with a cinnamate group⁽¹⁴¹⁾.

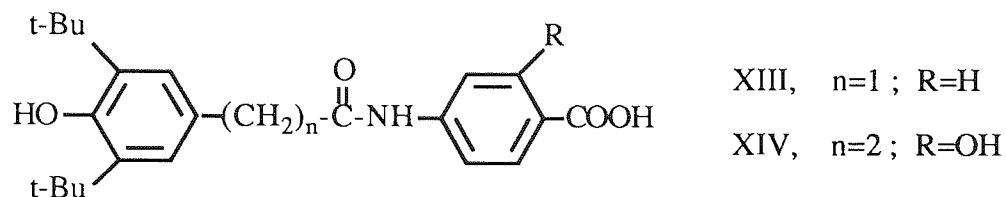


Scheme 1.6 Chemical Transformation of Hindered Phenol Antioxidant
 Where,
 $\text{R} = \text{H}$, BHT ; $\text{R} = \text{CH}_2\text{-(CO)-O-C}_{18}\text{H}_{37}$, Irganox 1076

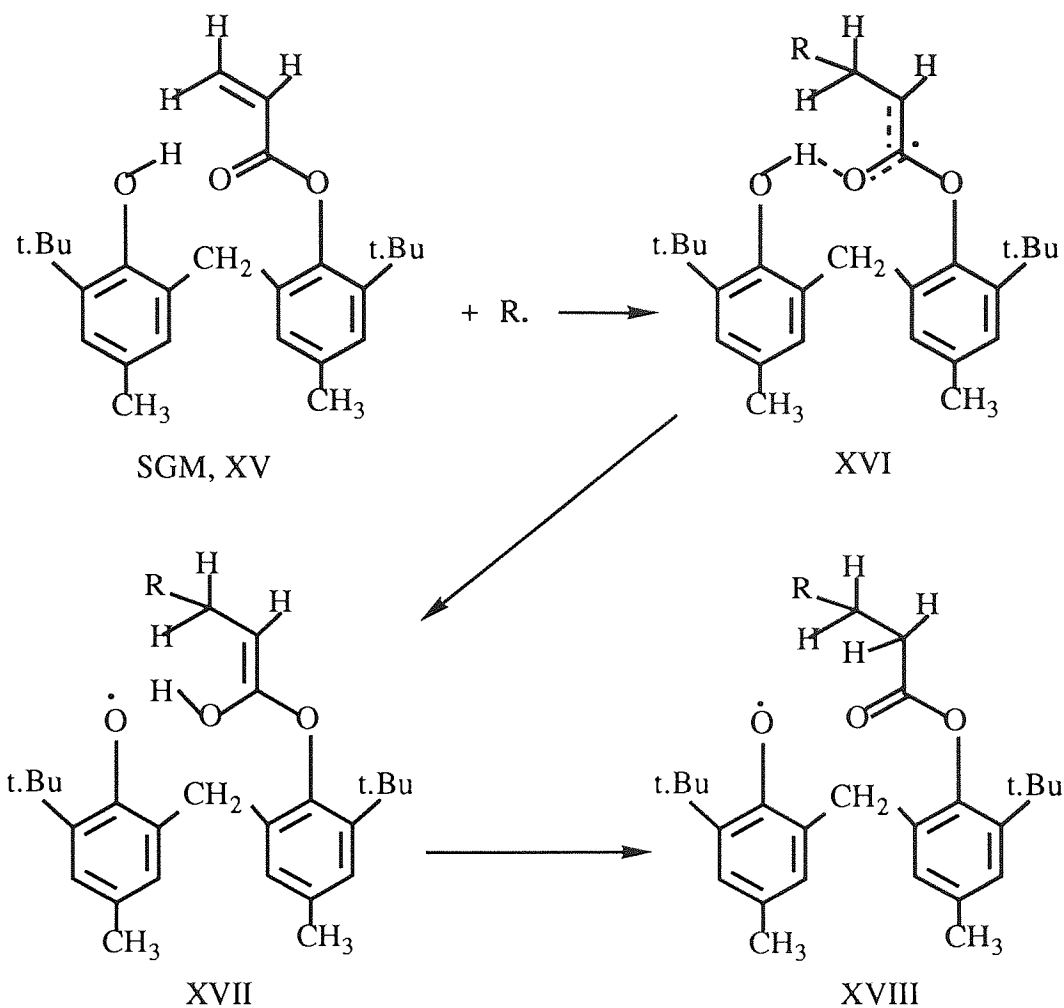


Hindered phenols can be employed as melt stabiliser, due to their ability to trap ROO· radicals and the ability of some of the transformation products, e.g. quinonoid structures, to trap R· (135). The stabilising activity of bound hindered phenols in polymers have been shown to be higher than that of unbound analogues^(98,142,143). Hindered phenols give photosensitive products, hence, are not used alone in photo stabilising polymers, but when used in combinations with UV absorbers synergism in photo stabilisation has been observed^(107,111,112,119-125,131,144). Work at Aston⁽¹⁰⁷⁾ has shown that hindered phenols become effective polypropylene photo stabilisers when grafted to the polymer through their acrylic groups and in combination with small amount of UV stabiliser 2-hydroxy-4-(beta acrylate ethoxy) benzophenone (HAEB). The hindered phenol acts as a radical scavenger, hence it retards the oxidation of the UV stabiliser, HAEB during processing⁽¹⁴⁵⁾. The stabilising activity of combination of bound AATP and a commercial hindered phenol thermal stabiliser, Irganox 1076, has also been examined⁽¹¹¹⁾ in polypropylene and the results showed a very high synergistic effect.

Other functional hindered phenols were chemically bound to polypropylene during processing, e.g. using 3% glycidyl methacrylate, such as, 4-[3',5'-di-tert.-butyl-hydroxyphenylacetamido] benzoic acid (XIII) and 4-[3',5'-di-tert.-butyl-4'-hydroxyphenyl-β-propionamido] salicylic acid (XIV), to give improved thermoxidative stability and better resistance to dry cleaning solvents^(98,142,143).

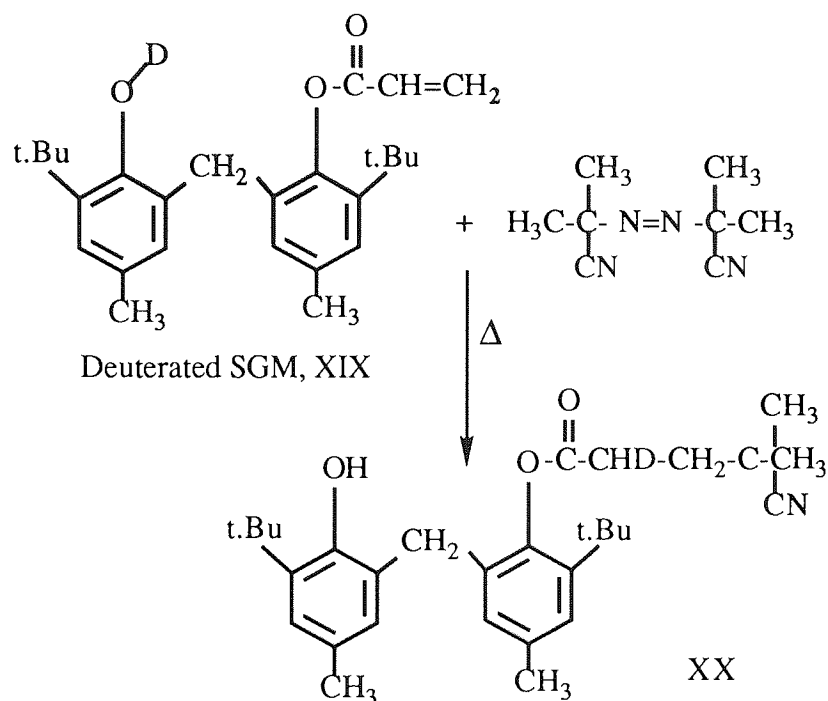
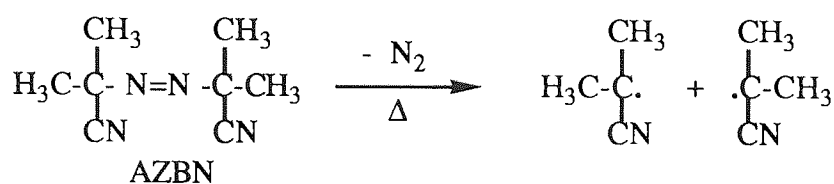


It was also reported ⁽¹⁴⁶⁾ that an acrylate containing hindered phenol, antioxidant [i.e. 2-tert.-butyl-6-(3-tert.-butyl-2-hydroxy-5-methyl benzyl)-4-methylphenyl acrylate, Sumilizer GM, XV] was shown to be an effective thermal stabiliser for butadiene polymers. The stabilising mechanism of the phenolic antioxidant under an oxygen free atmosphere was suggested ⁽¹⁴⁶⁾ to be via a unique bifunctional mechanism, which consists of polymer radical trapping by the acrylate group to give enolate radicals (XVI in Scheme 1.7). This reaction was followed by fast hydrogen atom transfer from intramolecular hydrogen-bonded phenolic hydroxyl group to form stable phenoxyl radicals (XVIII) see reaction Scheme 1.7.



Scheme 1.7 Bifunctional stabilising mechanism of Sumilizer GM

In order to clarify that the hydrogen transfer occurred from intramolecular hydrogen-bonded phenolic hydroxyl groups, these workers⁽¹⁴⁶⁾ have prepared deuterated SGM (see structure, XIX), and examined its action in a model experiment using toluene and AZBN as an initiator at 110°C. It was confirmed by NMR spectra that the transfer from phenolic hydroxyl groups follows route XVI to XVII in Scheme 1.7 and 1.8.

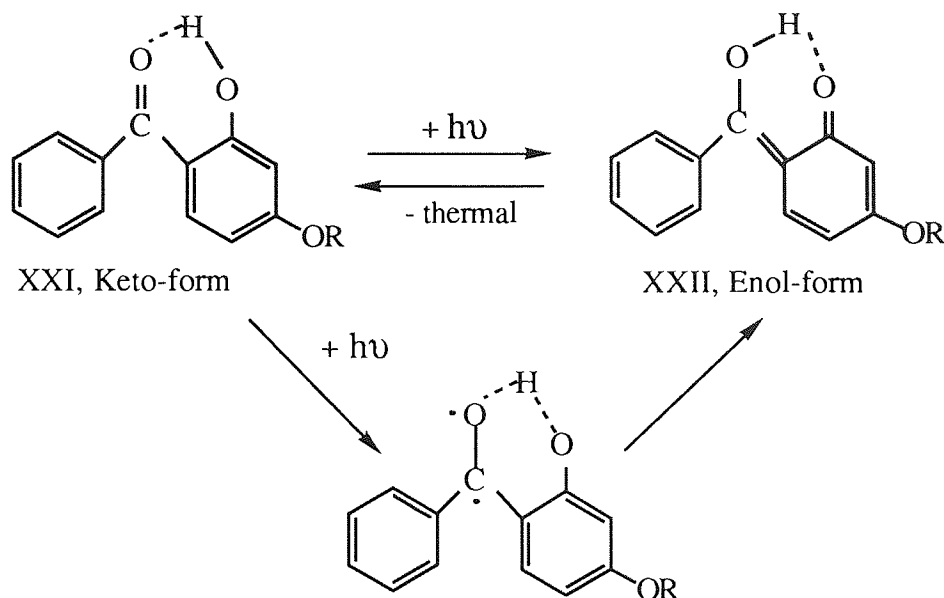


Scheme 1.8 The reaction of Deuterated SGM with AZBN

1.7 BENZOPHENONE AS UV ABSORBER OF POLYOLEFINS

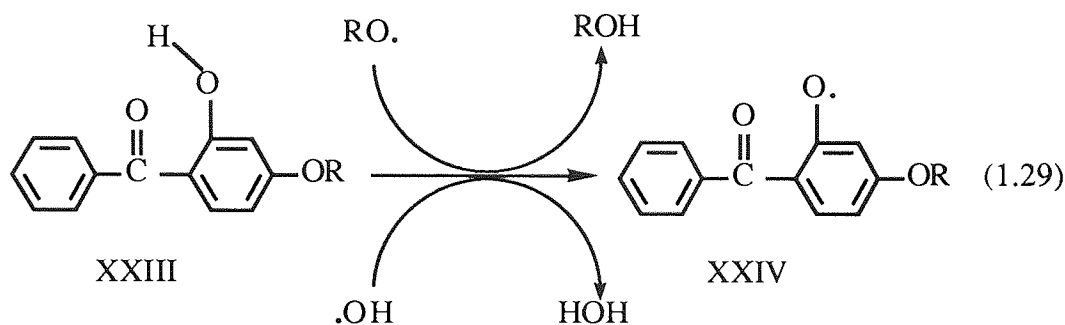
2-hydroxybenzophenones comprise one of the best known UV absorbers, which give effective UV stabilising activity (31,32,61,62,98,147). Early theories on the mode of operation of these stabilisers showed that they absorb the incident harmful sunlight, thereby preventing it from being absorbed by the photoactive impurities or structural units in the polymer^(61,62). Photostability is intimately connected with an energy dissipation mechanism, e.g. 2-hydroxybenzophenones, dissipate their absorbed energy by a mechanism that involves a reversible formation of six-member hydrogen bonded ring (61,62). The rapid keto-enol tautomerisation is involved in deactivation of the excited

state induce by the absorption of light, see Scheme 1.9. The enol form (XXII) of the carbonyl group is assumed to be more stable in the excited state, whereas the ground state is in the keto form (XXI). Alternatively, H \cdot transfer to the carbonyl group may also occur (61,62).

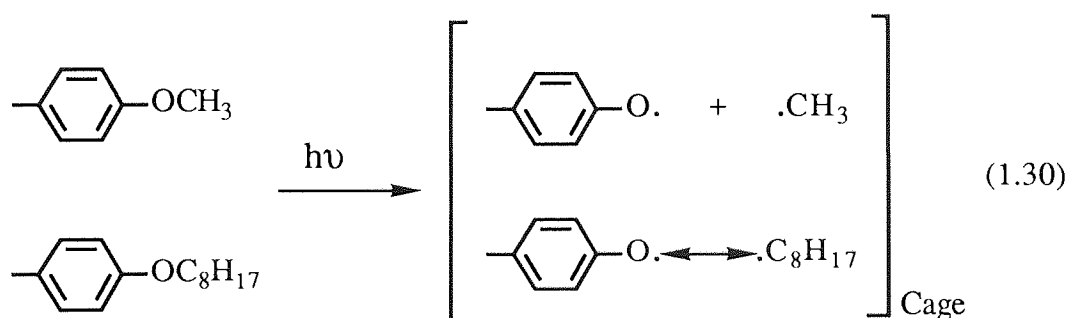


Scheme 1.9 Tautomerisation of benzophenone

It is well known that the photostabilising action of light stabilisers depends very much on prior processing history (31,32). Allen and co-workers⁽¹⁴⁸⁾ have studied this effect for a number of ortho-hydroxybenzophenones. It was shown that the stabilisers photodecompose more rapidly in processed polypropylene compared with unprocessed polymer. It is also noted that the rates of photodecomposition correlate exactly with initial hydroperoxide concentration in the polymer. These results are associated with the following reaction whereby alkoxy (RO \cdot) and hydroxyl (\cdot OH) radicals produced in the photolysis of hydroperoxides abstract the ortho-hydrogen atom on the hydroxyl group from 2-ortho-hydroxybenzophenone (XXIII), see reaction 1.29. The radical product (XXIV) is then no longer capable to undergo tautomeric equilibrium as shown in Scheme 1.8(67,149).



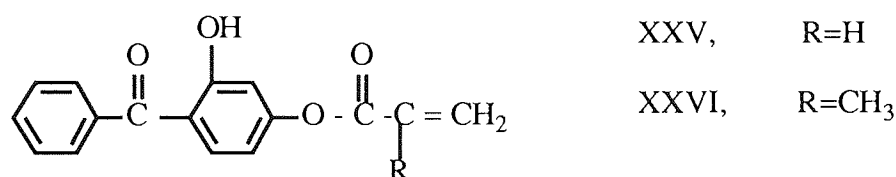
Longer n-alkoxy groups in the 4-position of the benzene ring in hydroxybenzophenone lead to more effective photostabilisation than shorter groups. This could be on two accounts: first longer alkyl groups lead to increase solubility in the polymer⁽⁸⁾, but also, it was suggested that during irradiation these groups may photolyse to give their corresponding alkyl radicals, see reaction 1.30⁽⁶¹⁾.



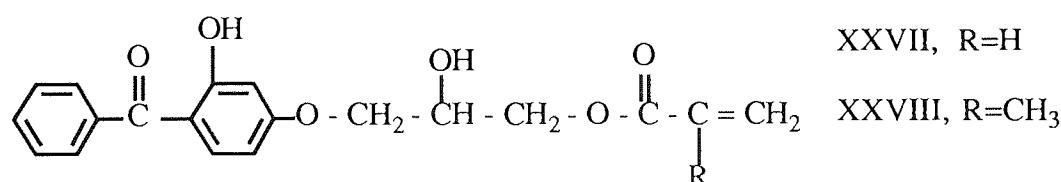
The smaller methyl radicals may escape more easily out of the polymer cage than the larger alkyl (e.g. octyl) radical. In the later case, radical recombination could increase the light stabilising effectiveness of the larger alkyl group substitution of 2-hydroxybenzophenone in solution (150,151,152).

Grafting of functional UV absorber onto polymer backbone has been explored⁽¹⁰²⁾. Although, there are five main classes of UV absorbers: salicylate ester, 2-hydroxybenzophenones, 2-hydroxyphenylbenzotriazoles, α -cyano- β -phenylcinnamate esters, and 4-aminobenzoate esters, only a few monomeric UV stabilisers have been employed in the stabilisation of polyolefins by grafting, primarily the 4-hydroxy-substituted derivatives of 2,4-dihydroxybenzophenone with the methacryloyloxy group as a polymerisable group,

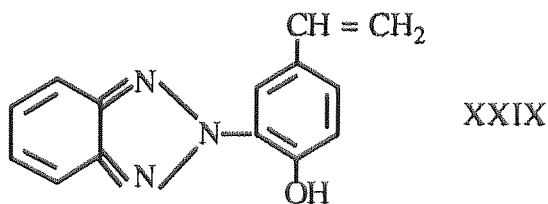
see compound XXV to XXVIII. Both bulk and surface grafting of these monomers have been used for photostabilisation of polyolefins⁽⁹⁸⁾. Munteanu et. al. ⁽⁹⁸⁾ claimed the bulk stabilisation of polyolefins by melt grafting of UV absorbers: 2-hydroxy-4-(meth) acryloyloxy benzophenone (XXV and XXVI) and 2-hydroxy-4-[3'-(meth) acryloyloxy-2'-hydroxypropoxy] benzophenone (XXVII and XXVIII). The polymer, monomeric stabiliser and peroxide were mixed and processed in an extruder or in an internal mixer at 130-200°C, using dilauroyl peroxide for low-temperature and dicumyl peroxide for grafting at high temperatures⁽⁹⁸⁾.



Sharma et. al. ^(153,154) have used a similar approach to graft the UV absorbing monomers XXV and XXVI onto LDPE and PP. In the absence of a free radical initiator, it was found that 17% of the monomer was grafted, but the rest was unreacted and homopolymerised. The chemically grafted UV absorber showed higher UV stabilising effectiveness compared to that of a UV absorber used as an additives (non grafting) ⁽¹⁵⁴⁾.



Burchill and Pinkerton ⁽¹⁵⁵⁻¹⁵⁷⁾ and Ranogajek et al. ⁽¹⁵⁷⁻¹⁵⁹⁾ have reported that gamma-radiation induced surface grafting of 2-hydroxy-4-[3'-(meth)-acryloyloxy-2'-hydroxypropoxy] benzophenone (HMPB, XXVIII) onto LDPE, HDPE and PP film. Vogl et. al. ⁽¹⁶⁰⁾ reported that 2-(2-hydroxy-5-vinylphenyl)-2H-benzotriazole (XXIX) can graft onto polymer molecules.



1.8 OBJECT AND SCOPE OF THE PRESENT WORK

The main objects of the present work are:

1. To synthesis polymer-reactive antioxidants based on hindered phenols, and hydroxybenzophenone structures.
2. To improve the efficiency of binding reactions of these reactive antioxidants into the polypropylene using reactive processing procedures.
3. To investigate the role and mechanism of a number of co-reactive agents on the binding reaction.
4. To study the mechanism of the grafting reaction of DBBA (as a concentrate, MB) in polypropylene melt during processing in the absence and presence of co-agent and the nature of the transformation products. This will be investigated both in polymer and in liquid hydrocarbon model compounds.
5. To investigate the co-operative effects of reactively grafted UV stabiliser (based on benzophenone) and thermal antioxidant (based on hindered phenol) in stabilising polypropylene against UV light and heat.
6. To compare the stabilising effectiveness of the reactively grafted UV stabiliser of that antioxidants with that of commercial antioxidants containing the same antioxidant functional but are used as additives (not grafting)

CHAPTER TWO

GENERAL EXPERIMENTAL TECHNIQUES

2.1 MATERIALS

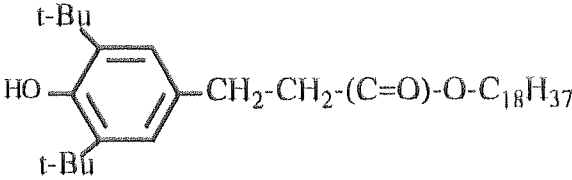
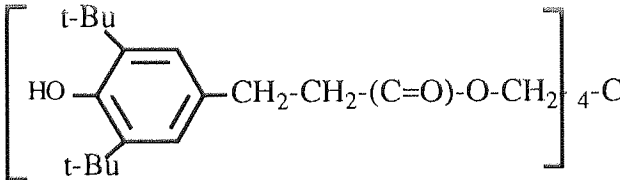
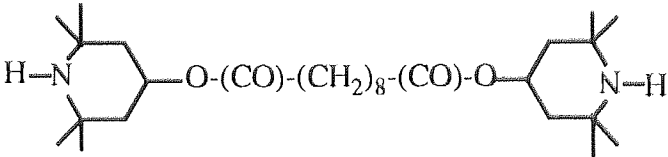
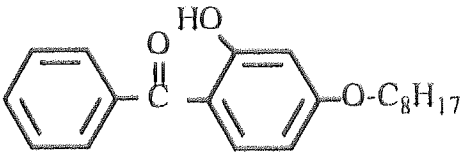
Unstabilised polypropylene (Propathene HF-26) and stabilised commercial polypropylene (HMW 25) were supplied by I.C.I. (Plastic Division) Ltd. Free radical initiators, liquid 2,5-dimethyl 2,5-di-tertiarybutylperoxy hexane (Trigonox 101), dicumylperoxide (DCP, recrystallised from methanol) and azobisiso-butyronitrile (AZBN, recrystallised from diethylether) were supplied by Azko Chemicals Ltd.


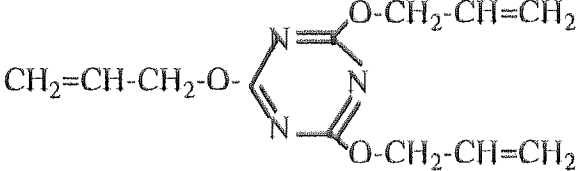
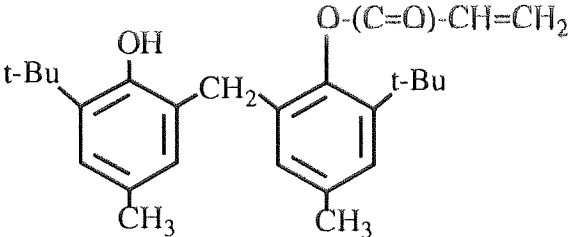
Commercial antioxidants, n-octadecyl-3-(3',5'-di-tert.-butyl-4-hydroxy-hexyl) propionate under the trade name Irganox 1076, pentaerythrityl tetrakis-(3,5-di-tert.-butyl-4-hydroxy phenyl) propionate (Irganox 1010), and bis-(2,2,6,6-tetra-methyl-piperidinyl) sebacate (Tinuvin 770), were kindly donated by Ciba Geigy. 2-hydroxy-4-octyloxy-benzophenone (HOBP) was supplied by American Cyanamid. Trimethylol propane triacrylates (TMPTA=Tris), divinyl benzene (DVB), 2,4,6-triallyloxy 1,3,5-triazine (Tac) were supplied by Ancomer Ltd. The commercial thermal stabiliser 2,2'-methylene-bis-(4-methyl-6-tert.-butyl phenol) mono acrylate (Sumilizer GM) was kindly donated by Sumitomo Chemical Company. Table 2.1 shows chemical structure of the above compounds.

Paraformaldehyde, 2,6-ditert.-butyl phenol, potassium tert.butoxide, anhydrous tert.-butyl alcohol, acrylic acid, 2,4-dihydroxy benzophenone, sodium hydroxide, sulfuric acid, sodium bicarbonate, ethylene chlorohydrine, potassium hydroxide, hydrochloride, absolute ethanol, mercuric acetate, vinyl acetate, sodium acetate, anhydrous magnesium sulfate, ortho-di-chlorobenzene, decahydronaphtaline (decaline), benzene, methylcyclohexane, n-hexane, quinone, dichloromethane (spectroscopic grade) and isooctane were all ex-Aldrich Chemical and were used directly without further purification.

All other solvents were standard laboratory reagents. These include acetone, hexane, dichloromethane (DCM), toluene, xylene, diethyl ether, petroleum ether, methanol, dry toluene, benzene, dichlorobenzene, pentane and chloroform.

Table 2.1 Chemical structure of commercial antioxidants are used

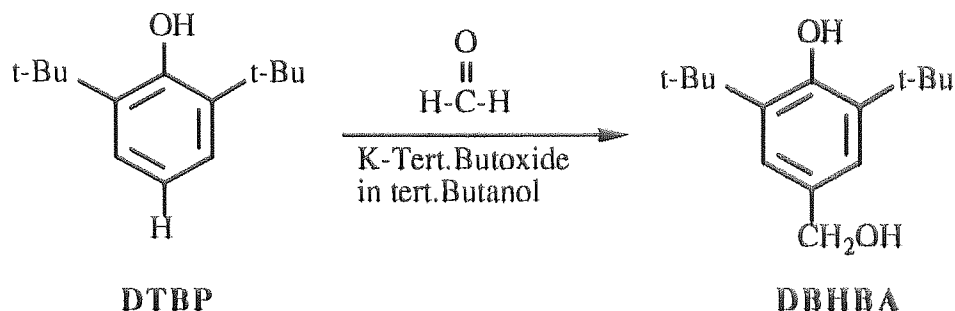
Chemical structure and name	Abreviation
 <p>n-octadecyl-3-(3',5'-di-tert.-butyl-4-hydroxyphenyl propionate</p>	Irganox 1076
 <p>Pentaerythrityl tetrakis-(3,5,-di-tert.-butyl-4-hydroxy phenylpropionate</p>	Irganox 1010
 <p>Bis-(2,2,6,6-tetra methyl piperidine) sebacate</p>	Tinuvin 770
 <p>2-hydroxy-4-octyloxy-benzophenone</p>	Cyasorb UV-351 (HOBP)
Continued.....	

Continued...	
Chemical structure and name	Abreviation
$\left[\text{CH}_2=\text{CH}-(\text{C}=\text{O})-\text{O}-\text{CH}_2 \right]_3-\text{C}-\text{CH}_2-\text{CH}_3$ <p>Trimethylol propane triacrylates</p>	TMPTA (Tris)
 <p>Divinyl benzene</p>	DVB
 <p>2,4,6-triallyloxy 1,3,5-triazine</p>	Tac
 <p>2,2'-methylene-bis-(4-methyl-6-tert.-butyl phenol) mono acrylate</p>	Sumilizer GM

2.2 SYNTHESIS AND CHARACTERISATION OF ANTIOXIDANTS

Various antioxidants based on hindered phenol and benzophenone structures were synthesised according to literatures(96,107,129,161-166). In general, almost all the synthesis produced high yield, the highest yield was obtained by esterification of benzophenone, but lower yield was resulted from esterification of 3-(3',5'-di-tert.-butyl- 4-hydroxy phenyl) propionic acid (Irganox acid). Detailed synthetic procedures and flowcharts of the preparation are shown below.

2.2.1 Preparation of 3,5-di-tert.-butyl-4-hydroxy benzyl alcohol (DBHBA)(161)



61.8 g (0.3 mol) of 2,6-di-tert.-butyl phenol (DTBP), 15 g (0.5 mol) of paraformaldehyde and 3 g (0.03 mol) of potassium tert. butoxide were dissolved in 500 ml of anhydrous tert.-butyl alcohol. The solution was cooled down to 5°C, in ice bath, and continuously stirred using a mechanical stirrer, under nitrogen atmosphere for 2 hours. The reaction mixture was then poured into an ice water and left at room temperature for 24 hours. Two layers were formed, the upper (organic layer) was separated as a reddish solid. The solid product was filtered off and the filtrate was further purified by recrystallisation from n-hexane. White crystals were formed (melting point 136° - 137° C) and after drying under vacuum at room temperature, the yield was 50 %, see Scheme 2.1 (161). Table 2.2 shows the elemental analysis and a major absorption peaks in infrared spectroscopy of the product (see also Figures 2.1 and 2.2 for IR spectra). Figure 2.2a shows the UV spectrum of DBHBA in DCM solution. Tables 2.3 & 2.4 and Figures 2.3 & 2.4 show the proton and ¹³C NMR spectra of DBHBA.

Table 2.2 Elemental analysis and major absorption peak in FTIR of DBHBA

C and H analysis			IR analysis	
Element	% found	% theoretical	cm ⁻¹	Absorption peak
C	75.42	75.00	3567	free OH hydrogen bonded -OH aromatic double bond
H	10.64	10.71	3518	
			1619-1585	

Table 2.3 Proton NMR spectrum of 3,5-di-tert.-butyl-4-hydroxy benzyl alcohol, DBHBA in deuterated chloroform.

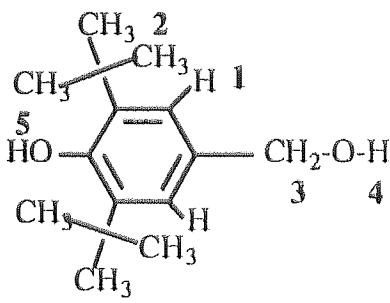
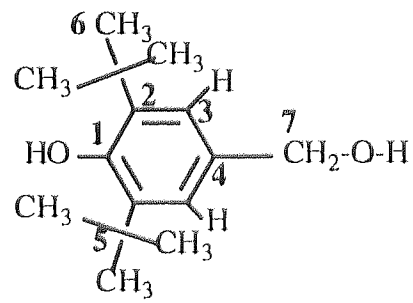
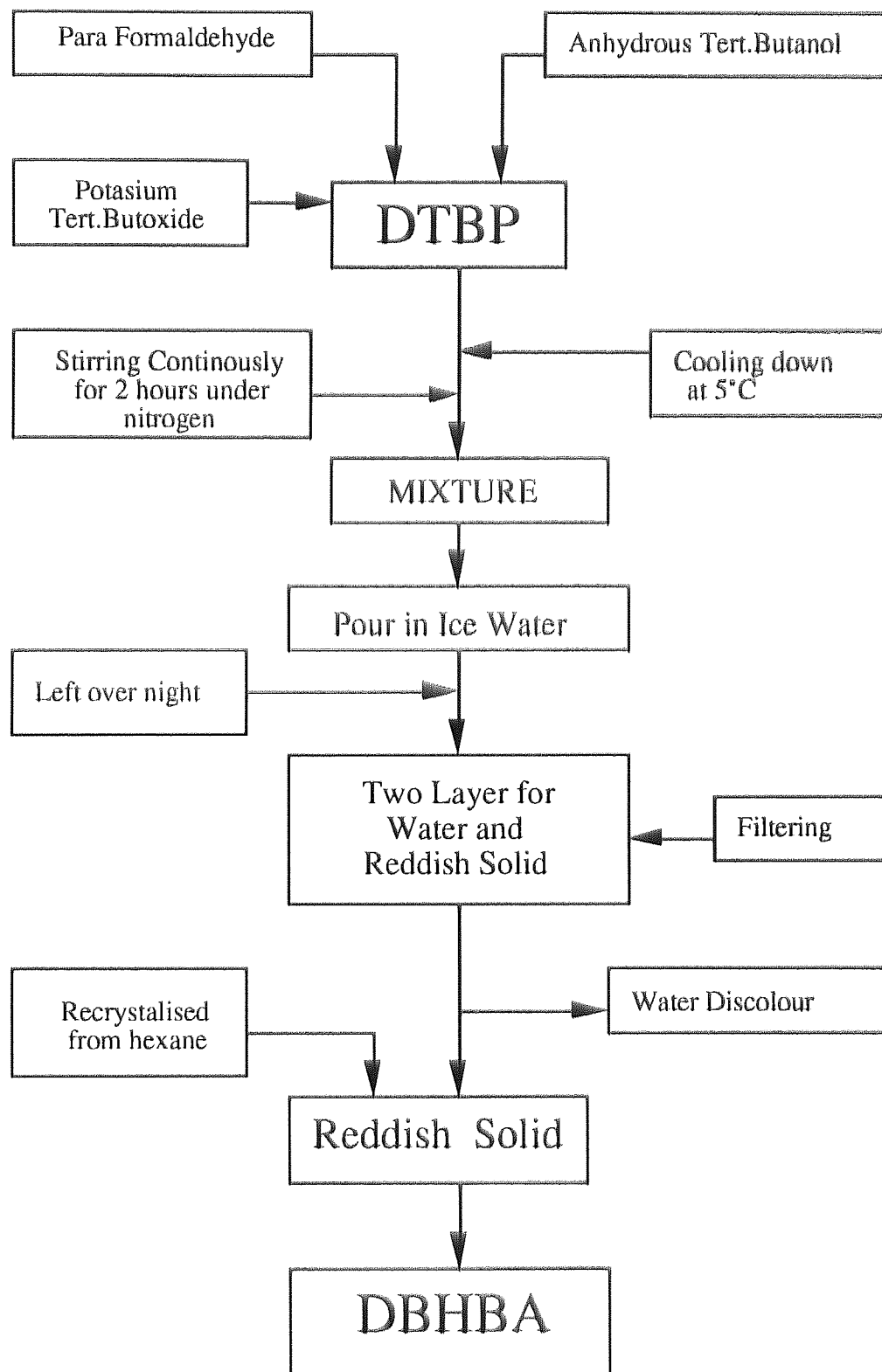
				
H No	δ (ppm)	m'plicity	I (%)	Total H
1	7.19	1	6.8	2
2	1.40	1	60.5	18
3	4.58	1	7.6	2
4	1.89	1	3.6	1
5	5.25	1	3.7	1

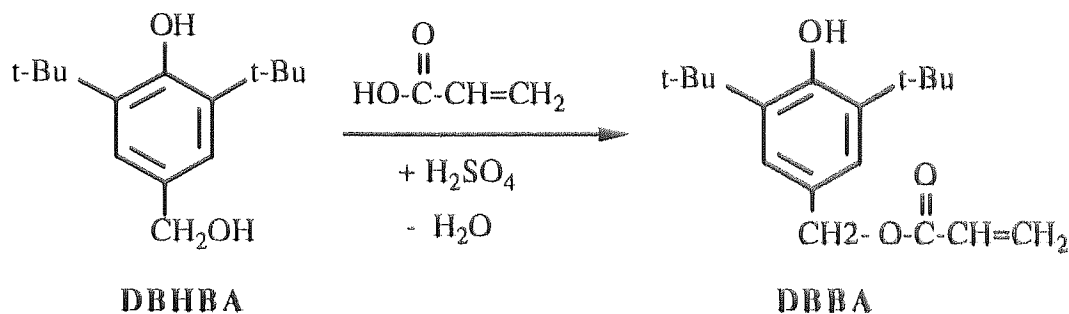
Table 2.4 ^{13}C NMR spectrum of 3,5-di-tert.-butyl-4-hydroxy benzyl alcohol, DBHBA in deuterated chloroform.

				
C No	δ (ppm)	(+)/(-)	I (%)	Total C
1	153.4	(-)	0.3	1
2	136.1	(-)	0.6	2
3	124.4	(+)	3.7	2
4	131.6	(-)	0.5	1
5	34.3	(-)	1.1	2
6	30.2	(+)	12.1	6
7	65.9	(-)	1.6	1



Scheme 2.1 Flowchart for preparation of 3,5-di-tert.-butyl-4-hydroxy benzyl alcohol, DBHBA.

2.2.2 Preparation of 3,5-di-tert.-butyl-4-hydroxy benzyl acrylate (DBBA)(162)



A mixture of 47.2 g (0.2 mol) freshly prepared 3,5-di-tert.-butyl-4-hydroxy benzyl alcohol (DBHBA) and 144 ml (2 mol) of acrylic acid was warmed gently (70°C) under nitrogen gas atmosphere, until a clear solution was obtained. To this solution was added one drop of concentrated sulfuric acid, refluxed for 8 hours and was allowed to remain at room temperature overnight. The reaction mixture was poured into cold water and the organic layer was extracted in diethylether, washed with water, neutralised with aqueous sodium bicarbonate, dried over anhydrous magnesium sulphate and finally the diethylether was evaporated in rotary evaporator. The residue was recrystallised from petroleum ether to give yellowish crystals (melting point, 67 - 68°C), the yields was 60 %, see Scheme 2.2 (162).

Table 2.5 shows the elemental analysis and a major absorption peaks in infrared spectroscopy of the product (see also Figures 2.5 & 2.6 for IR spectra). Figure 2.6a shows UV spectrum of DBBA in DCM solution. Tables 2.6 & 2.7 and Figures 2.7 & 2.8 show the proton and ¹³C NMR spectra of DBBA.

Table 2.5 Elemental analysis and major absorption peak in FTIR of DBBA

C and H analysis			IR analysis	
Element	% found	% theoretical	cm ⁻¹	Absorption peaks
C	75.09	75.50	3588	free OH carbonyl unsaturated aromatic double bond vinyl of acrylic
H	9.19	8.60	1714 1619-1588 1636 & 1408	

Table 2.6 Proton NMR spectrum of 3,5-di-tert-butyl-4-hydroxy benzyl acrylate, DBBA in CDCl₃

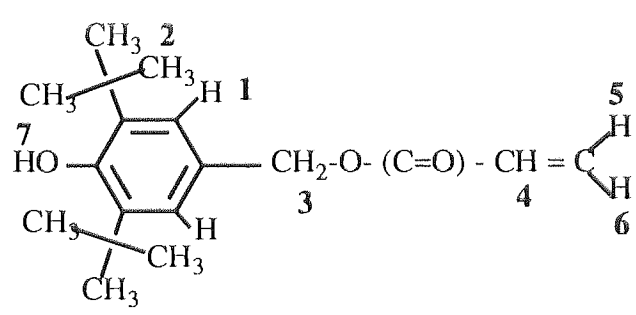
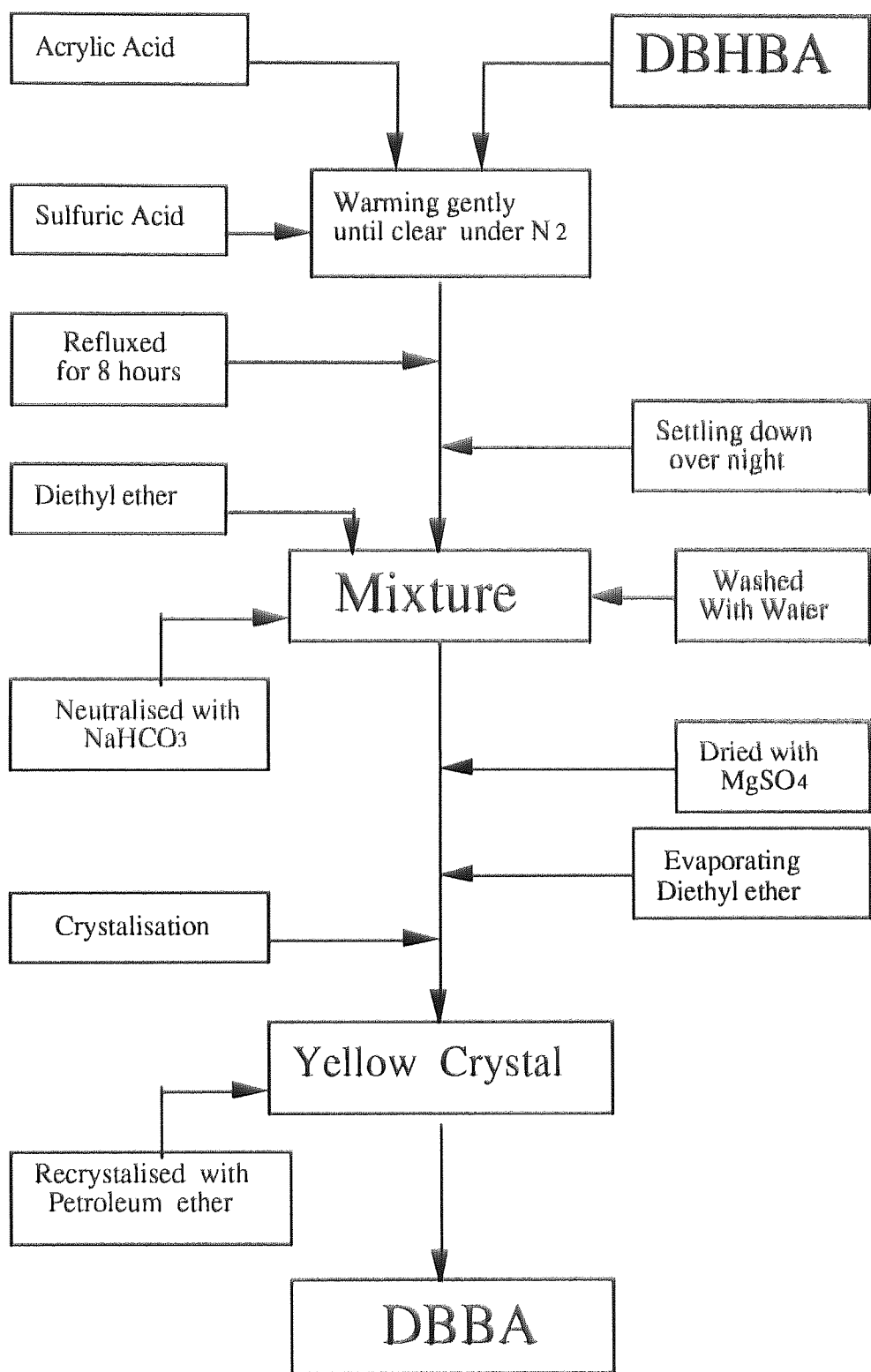
				
H No	δ (ppm)	m'plicity	I (%)	Total H
1	7.23	1	3.6	2
2	1.50	1	31.6	18
3	5.16	1	3.5	2
4	6.15 - 6.23	4	1.7	1
5	6.44 - 6.50	2	1.7	1
6	5.82 - 5.86	2	1.8	1
7	5.35	1	1.8	1

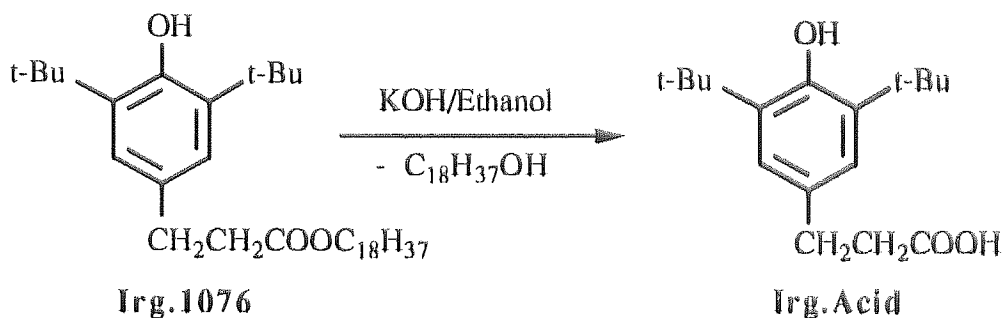
Table 2.7: ^{13}C NMR spectrum of 3,5-di-tert.-butyl-4-hydroxy benzyl acrylate, DBBA in CDCl_3

C No	δ (ppm)	(+)/(-)	I (%)	Total C
1	154.0	(-)	0.4	1
2	136.1	(-)	0.9	2
3	125.8	(+)	4.0	2
4	128.4	(-)	0.6	1
5	34.3	(-)	1.3	2
6	30.2	(+)	12.1	6
7	67.2	(-)	1.8	1
8	166.1	(-)	0.2	1
9	128.6	(+)	1.3	1
10	130.1	(-)	1.4	1



Scheme 2.2 Flowchart for preparation of 3,5-di-tert.-butyl-4-hydroxy benzyl acrylate, DBBA.

2.2.3 Preparation of 3-(3',5'-di-tert.-butyl-4-hydroxy phenyl) propionic acid (Irganox acid)^(96,166)



A mixture of 32.4 gram (0.1 mol) Irganox 1076, 400 ml of freshly prepared 10% aqueous solution of potassium hydroxide and 400 ml of absolute ethanol were placed in three neck round bottom flask. After assembling with a thermometer, condenser, and purged with nitrogen gas the mixture was then refluxed for 6 hours and was cooled down to room temperature. 500 ml of dilute hydrochloride solution was added until smoky white precipitate appeared and was allowed to stand over night. The smoky white precipitate was filtered off and washed with warm water. A white solid was found, which then was recrystallised over methanol to give colourless needle crystal (melting point 171° - 172° C), the yields was 30%, see Scheme 2.3^(96,166).

Table 2.8 shows the elemental analysis and a major absorption peaks in infrared spectroscopy of the product (see also Figure 2.9 and 2.10 for IR spectra), Figure 2.10a shows UV spectrum of the product, Tables 2.9 & 2.10 and Figures 2.11 & 2.12 show the proton and ^{13}C NMR spectra of Irganox acid.

Table 2.8 Elemental analysis and major absorption peak in FTIR of Irganox acid

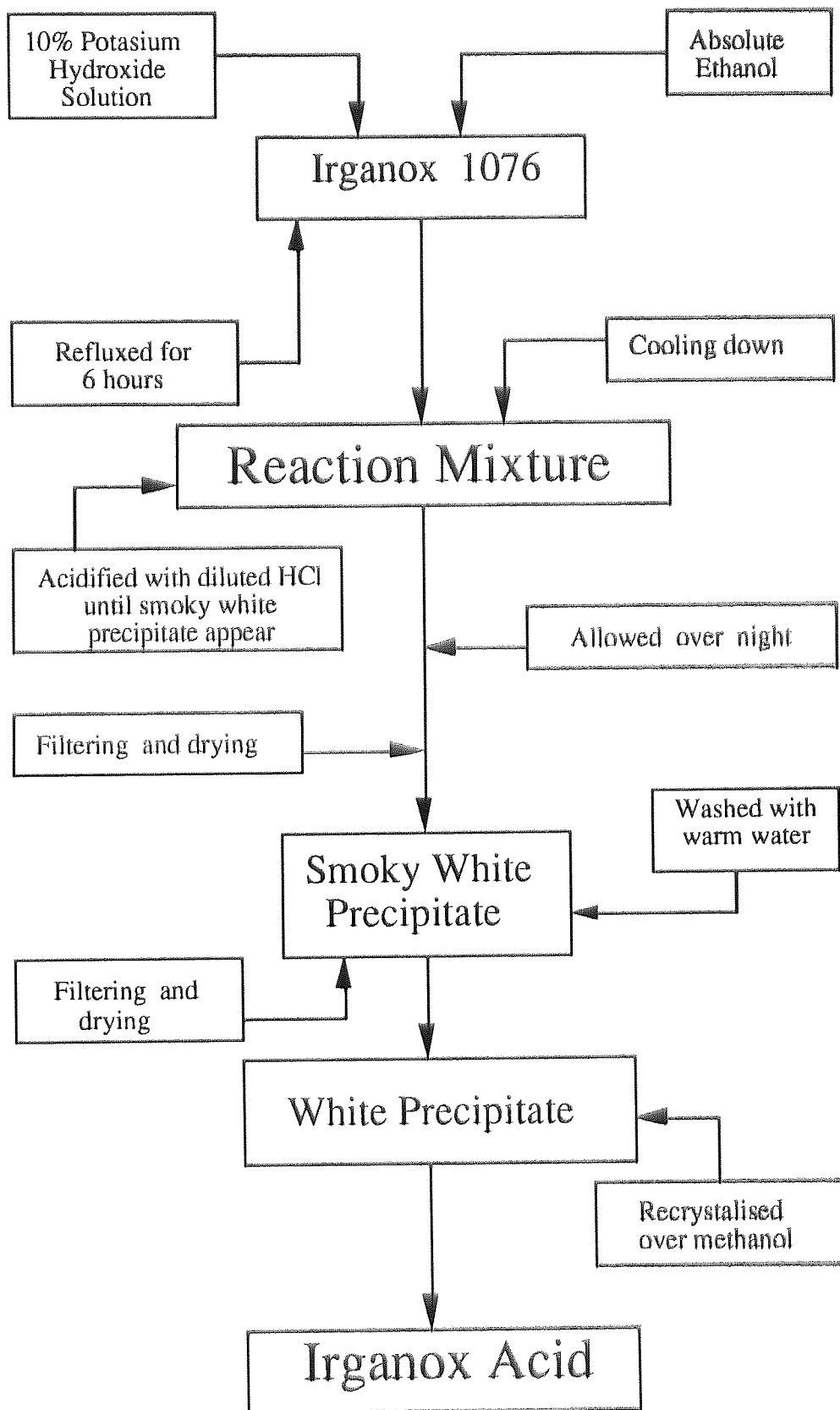
C and H analysis			IR analysis	
Element	% found	% theoretical	cm ⁻¹	Absorption peak
C	73.18	73.35	3587	free OH
H	9.46	9.41	1639-1619	aromatic double bond
			1707	carbonyl of acid, >C=O

Table 2.9 Proton NMR spectra of 3-(3',5'-di-tert.-butyl-4-hydroxy phenyl) propionic acid (Irganox acid) in CDCl₃.

H No	δ (ppm)	m'plicity	I (%)	Total H
1	7.03	1	5.2	2
2	1.44	1	43.5	2
3	2.85 - 2.90	3	4.5	2
4	2.83 - 2.89	3	4.3	1
5	5.12	1	2.2	18

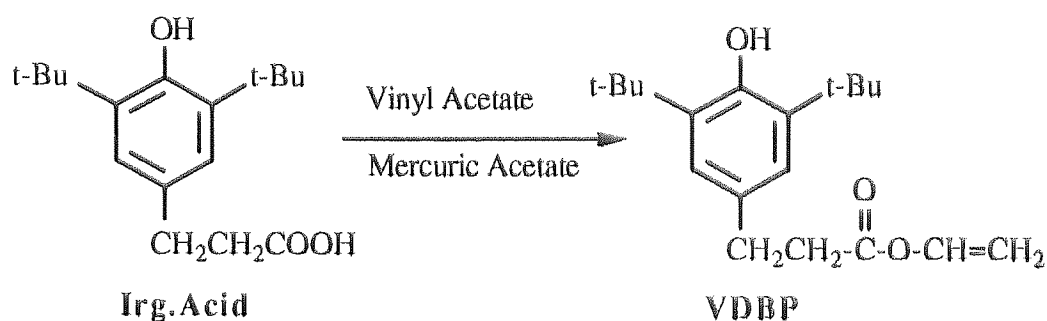
Table 2.10 ^{13}C NMR spectrum of 3-(3',5'-di-tert.-butyl-4-hydroxy phenyl) propionic acid (Irganox acid) in CDCl_3

C No	δ (ppm)	(+)/(-)	I (%)	Total C
1	152.2	(-)	0.5	1
2	136.6	(-)	1.1	2
3	125.1	(+)	4.0	2
4	131.4	(-)	0.8	1
5	31.0	(-)	2.5	2
6	30.5	(+)	12.1	6
7	36.6	(-)	1.9	1
8	34.6	(-)	1.5	1
9	179.7	(-)	0.8	1



Scheme 2.3 Flowchart preparation of 3-(3',5'-di-tert.-butyl-4-hydroxy phenyl) propionic acid, Irganox acid.

2.2.4 Preparation of Vinyl-3-(3',5'-di-tert.-butyl-4-hydroxy phenyl) propionate (VDBP)(96,164,165,166)



27.8 gram (0.1 mol) of freshly prepared Irganox acid, 103.2 gram (1.2 mol) of vinyl acetate, and 0.406 gram (0.0012 mol) of mercuric acetate were placed in a 500 ml three neck round bottom flask which was assembled with thermometer, condenser and purged with nitrogen gas. After adding 4 drops of concentrated sulfuric acid, the mixture was then refluxed for 6 hours at 70° C and cooled down to room temperature. After neutralisation with anhydrous sodium acetate the mixture was then distilled at 70°-80° C to remove unreacted vinyl acetate. This was then continuously distilled in vacuum condition at 10 mmHg and 125° C. The distillate was collected which became yellowish solid on cooling (melting point 60°- 61° C) the yield was 8 %, see Scheme 2.4 (96,164,165,166).

Table 2.11 shows the elemental analysis and a major absorption peaks in infrared spectroscopy of the product (see also Figures 2.13 & 2.14). Figure 2.14a shows UV spectrum of the product. Tables 2.12 & 2.13, and Figures 2.15 & 2.16 show the proton and ¹³C NMR spectra of VDBP.

Table 2.11 Elemental analysis and major absorption peak in FTIR of VDBP

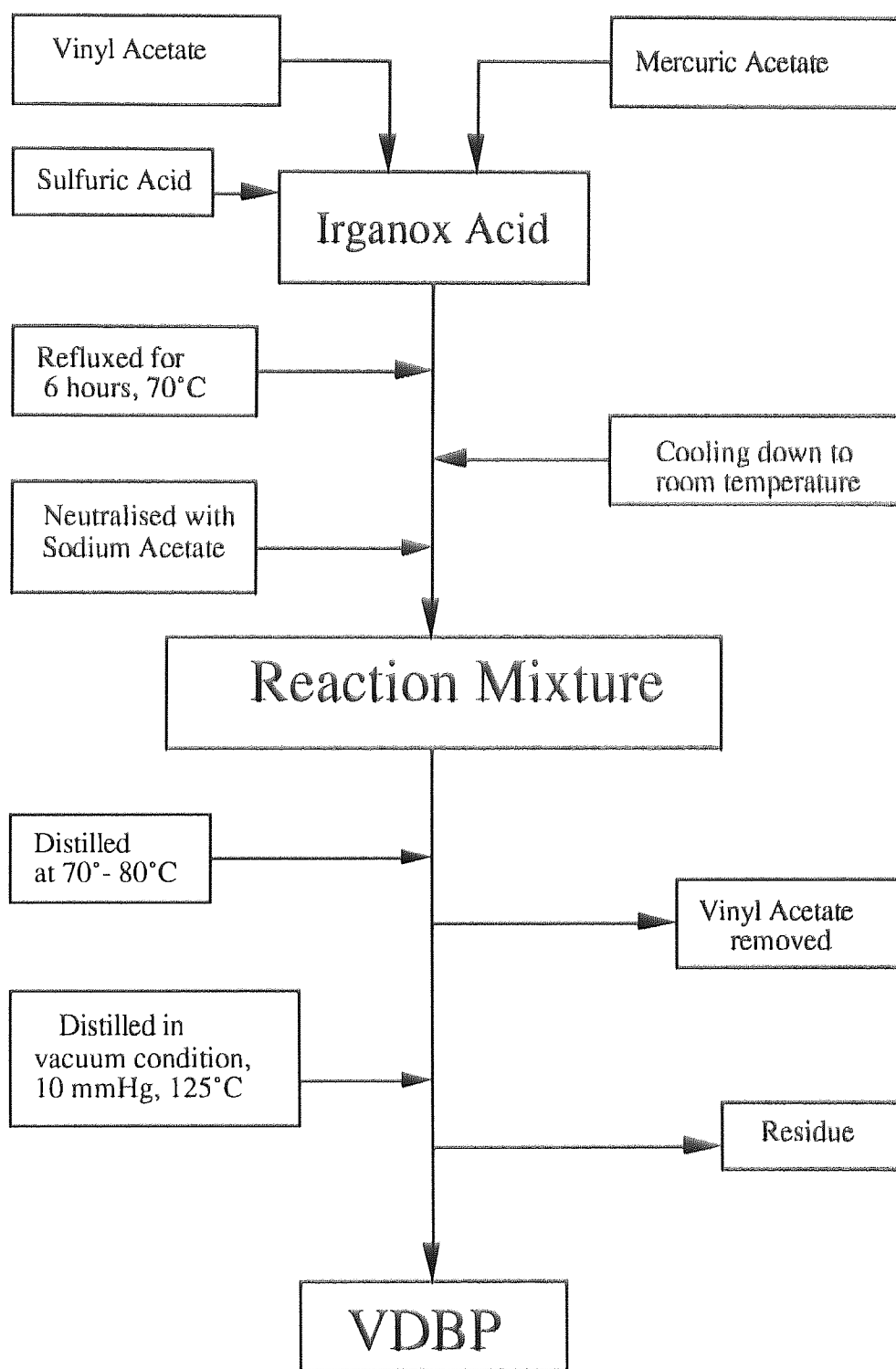
C and H analysis			IR analysis	
Element	% found	% theoretical	cm ⁻¹	Absorption peak
C	75.19	74.96	3628	free OH aromatic C=C unsaturated carbonyl, [-(C=O)-O-] vinyl acrylic
H	9.46	9.27	1617-1588	
			1755 1646 & 1414	

Table 2.12 Proton NMR of Vinyl-3- (3',5'-di-tert.-butyl-4-hydroxy phenyl) propionate, VDBP in CDCl₃.

H No	δ (ppm)	m'plicity	I (%)	Total H
1	7.08	1	6.8	2
2	1.44	1	62.4	18
3	2.66 - 2.70	3	5.1	2
4	2.88 - 2.93	3	4.9	2
5	7.23 - 7.34	4	3.1	1
6	4.87 - 4.91	2	2.6	1
7	4.56 - 4.58	2	2.4	1
8	5.09	1	3.1	1

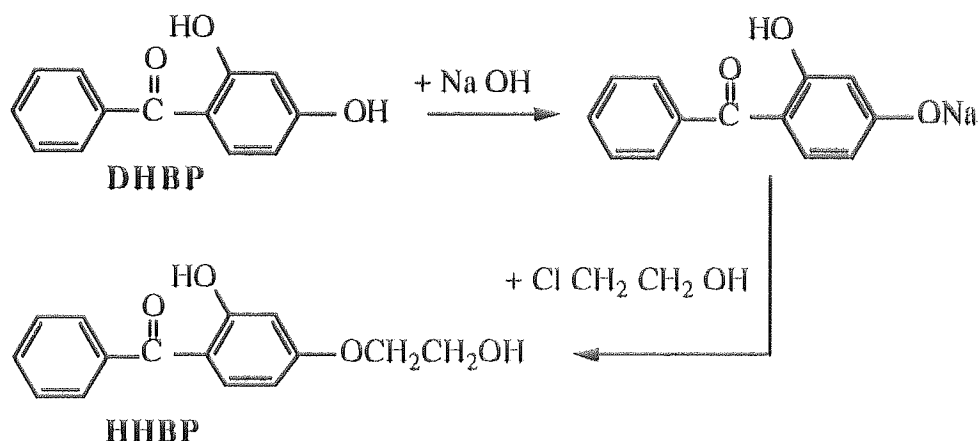
Table 2.13 ^{13}C NMR of Vinyl-3-(3',5'-di-tert.-butyl-4-hydroxyphenyl) propionate, VDBP in CDCl_3 .

C No	δ (ppm)	(+)/(-)	I (%)	Total C
1	152.2	(-)	0.3	1
2	124.7	(+)	0.1	2
3	124.7	(+)	0.1	2
4	130.7	(-)	0.5	1
5	30.8	(-)	1.8	5
6	30.3	(+)	12.0	6
7	36.1	(-)	1.8	1
8	34.2	(-)	1.1	1
9	170.2	(-)	0.3	1
10	141.1	(+)	0.6	1
11	97.6	(-)	1.5	1



Scheme 2.4 Flowchart for preparation of Vinyl-3- (3',5'-di-tert.-butyl-4-hydroxy phenyl) propionate, VDBP.

2.2.5 Preparation of 2-hydroxy-4-(beta hydroxy ethoxy) benzophenone, HHBP(163)



21.4 g (0.1 mol) of 2,4-di-hydroxy benzophenone and 4 g of sodium hydroxyde in 40 ml aqueous were stirred for 1 hour in a 500 ml three neck round bottom flask which was assambled with a thermometer, a condensor, and purged with nitrogen gas. After adding of 10 ml (1.5 mol) of ethylene chlorohydrine, the solution was then refluxed continuously for 5 hours. Water was subsequently added to the refluxed solution and was allowed to stand overnight. After washing with water the solution was stirred with mechanical stirrer until the white solid appeared. The white solid was filtered, dried and recrystalised from methanol-petroleum ether (1:10) to give yellowish needle crystal (melting point 90-91°C), the yields was 70 %, see Scheme 2.5(163).

Table 2.14 shows the elemental analysis and major absorption peaks in infrared spectroscopy of the product (see also Figures 2.17 and 2.18). Figure 2.18a shows UV spectrum of the product. Tables 2.15 & 2.16 and Figures 2.19 & 2.20 show the proton and ¹³C NMR spectra of HHBP.

Table 2.14 Elemental analysis and major absorption peak in FTIR of HHBP

C and H analysis			IR analysis	
Element	% found	% theoretical	cm ⁻¹	Absorption peak
C	69.29	69.77	3463	free OH
H	5.17	5.43	1631-1596	aromatic double bond

Table 2.15 Proton NMR of 2-hydroxy-4-(beta hydroxy ethoxy) benzophenone, HHBP in deuterated chloroform.

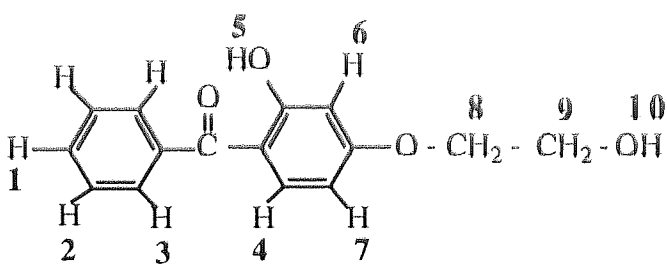
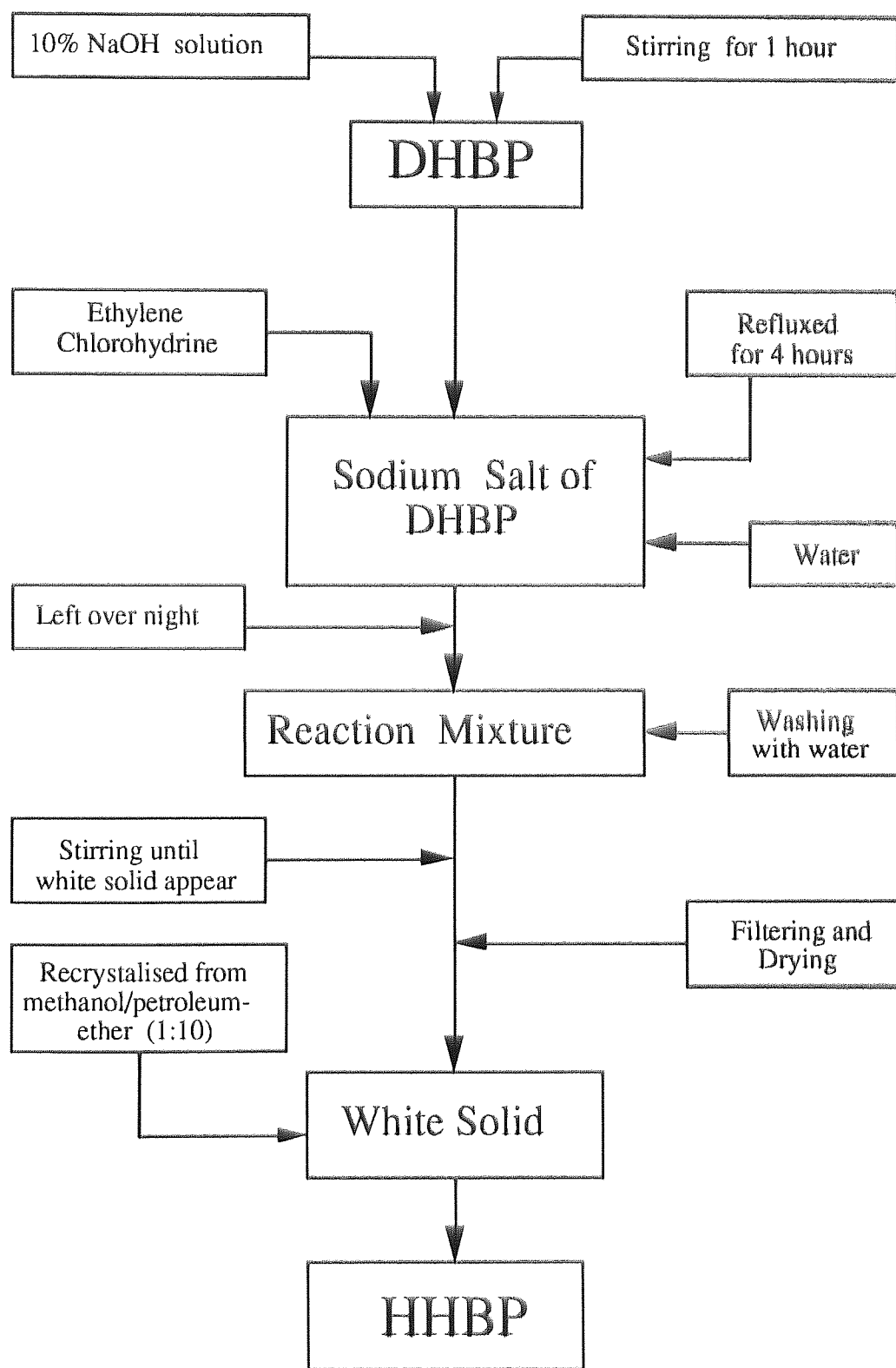
				
H No	δ (ppm)	m'plicity	I (%)	Total H
1)	7.41 - 7.60	m'plet	193.3	1
2)				2
3)				2
6)				1
4	6.46 - 6.47	2	30.1	1
5	12.84	1	32.5	1
7	6.37 - 6.40	2	35.5	1
8	4.00 - 4.09	3	62.7	2
9	3.92 - 3.95	3	64.0	2
10	2.72	1	40.0	1

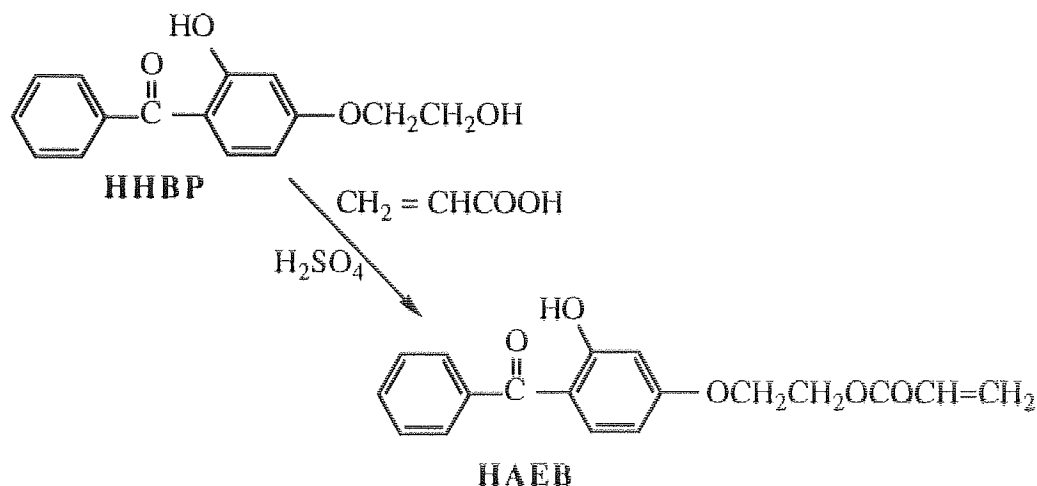
Table 2.16 ^{13}C NMR of 2-hydroxy-4-(beta hydroxy ethoxy) benzophenone, HHBP in deuterated chloroform.

C No	δ (ppm)	(+)/(-)	I (%)	Total C
1	101.76	(+)	4.8	1
2	128.77	(+)	12.1	2
3	128.23	(+)	11.6	2
4	113.29	(-)	1.4	1
5	166.07	(-)	2.4	1
6	138.06	(-)	1.3	1
7	200.00	(-)	1.2	1
8	107.46	(+)	5.3	1
9	135.29	(+)	6.5	1
10	131.47	(+)	6.1	1
11	165.20	(-)	1.8	1
12	69.57	(-)	6.3	1
13	60.89	(-)	6.6	1



Scheme 2.5 Flowchart for preparation of 2-hydroxy-4-(beta hydroxy ethoxy) benzophenone, HHBP.

2.2.6 Preparation of 2-hydroxy-4-(beta acrylate ethoxy) benzophenone, HAEB(163)



24.2 g (0.1 mol) of HHBP, 100 ml of dry toluene, 11.1 ml (0.15 mol) of acrylic acid and 6 drops of concentrated sulfuric acid were mixed in a 500 ml three round bottom flask. The flask was then assembled with a thermometer, a condenser, and purged with nitrogen. The mixture was refluxed for 10 hours and allowed to stand overnight. The light yellow liquid product was washed with excess water and was neutralised with sodium hydrocarbonate solution and then dried with magnesium sulfate anhydrous. After filtering the toluene was evaporated in rotary evaporator, then dried under vacuum at room temperature. The solid was then recrystallised with chloroform to give a white crystals (melting point 67°C), the yield was 90 %, see Scheme 2.5(163).

Table 2.17 shows the elemental analysis and major absorption peaks in infrared spectroscopy of the product (see also Figures 2.21 and 2.22). Figure 2.22a shows UV spectrum of the product. Tables 2.18 & 2.19 and Figures 2.23 & 2.24 show the proton and ^{13}C NMR spectra of HAEB.

Table 2.17 Elemental analysis and major absorption peak in FTIR of HAEB

C and H analysis			IR analysis	
Element	% found	% theoretical	cm ⁻¹	Absorption peak
C	68.81	69.23	3414 (broad)	hydrogenbonded -OH aromatic C=C unsaturated carbonyl, [-(C=O)-O-] vinyl acrylic
H	5.08	5.15	1631-1596	
			1725	
			1636 & 1414	

Table 2.18: Proton NMR of 2-hydroxy-4-(beta acrylate ethoxy) benzophenone, HAEB in deuterated chloroform.

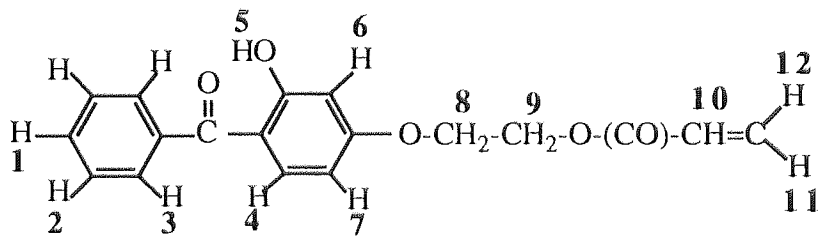
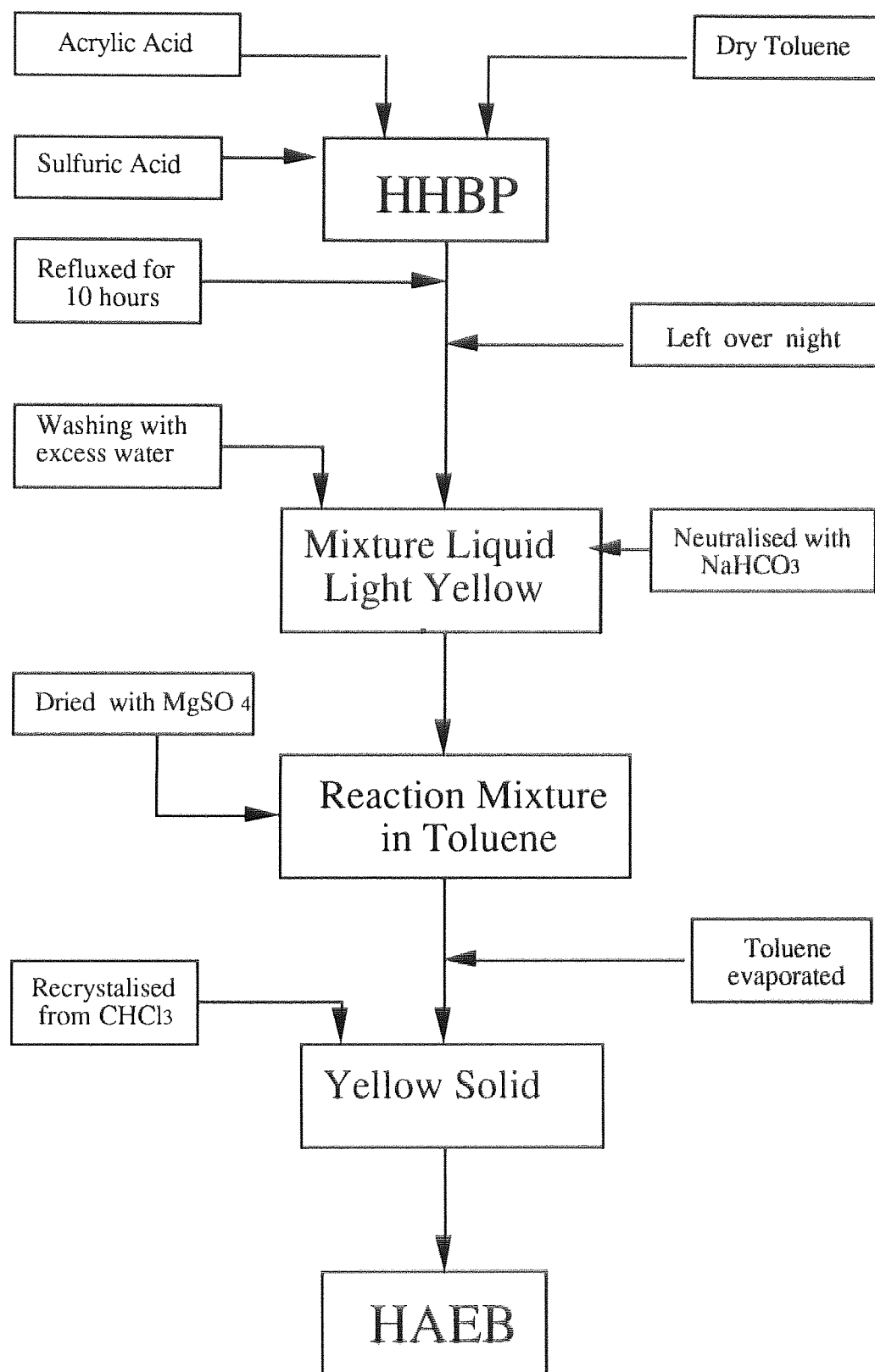
				
H No	δ (ppm)	m'plicity	I (%)	Total H
1)	7.43 - 7.61	m'plet	178.8	1
2)				2
3)				2
6)				1
4)	6.40 - 6.50	m'plet	83.9	1
7)				1
11)				1
5	12.62	1	29.9	1
8	4.40 - 4.52	3	66.1	2
9	4.20 - 4.28	3	54.9	2
10	6.12 - 6.18	4	29.0	1
12	5.82 - 6.09	2	31.5	1

Table 2.19: ^{13}C NMR of 2-hydroxy-4-(beta acrylate ethoxy) benzophenone, HAEB in deuterated chloroform.

C No	δ (ppm)	(+)/(-)	I (%)	Total C
1	101.7	(+)	5.3	1
2	128.8	(+)	12.2	2
3	128.2	(+)	11.7	3
4	113.4	(-)	1.0	1
5	166.1	(-)	2.2	1
6	138.1	(-)	0.8	1
7	200.0	(-)	0.9	1
8	107.4	(+)	0.9	1
9	135.3	(+)	0.7	1
10	131.5	(+)	3.5	1
11	164.9	(-)	1.3	1
12	66.1	(-)	5.9	1
13	62.3	(-)	5.7	1
14	165.8	(-)	0.6	1
15	127.9	(+)	3.4	1
16	131.4	(-)	1.5	1



Scheme 2.6 Flowchart for preparation of 2-hydroxy-4-(beta acrylate-ethoxy) benzophenone, HAEB.

2.3 COMPOUNDING

Polypropylene samples containing 3 - 20% of various antioxidants (agents) were processed in a Hampden Rapra torquerheometer internal mixer with a free radical initiator (FRI) in the presence or absence of another functional compound referred to as a coagent to form concentrates (masterbatches) of the bound-antioxidants. The advantages of using antioxidant masterbatches are that they are easy to supply and can be diluted down to normal antioxidant concentration level (0.1 - 0.2 % antioxidants) in any thermoplastic polymers.

2.3.1. Reactive Processing of Polymer Samples

The antioxidant (agent), coagent (multi functional compound which can enhance the binding level of agent) and free radical initiator concentrations were varied, keeping the total weight of the polymer sample constant (35 gram) to charge the full capacity of the processing chamber. Freshly prepared antioxidant, coagent, free radical initiator (FRI) after dissolving in 10 ml of DCM and unstabilised polypropylene (Propathene ICI, HF-26) were tumble mixed together at room temperature. After exhaustive vacuum evaporation at room temperature, the polymer sample was then processed in a HAMPDEN-RAPRA torquerheometer head fixed on a BRABENDER motor, with a digital torque recording motor. This is essentially an internal mixing chamber containing mixing screws contra rotating at various speeds. The processing may be conducted in the presence of excess oxygen (open to the atmosphere) or under restricted oxygen access sealing the chamber via a pneumatic ram (closed mixing). The processing carried out in this work was done under closed mixing conditions (CM, i.e. restricted oxygen access) only for 10 minutes at 180°C and rotor speed of 60 rotation per minute (RPM). The torque reading was recorded every 15 seconds during the processing operation. Finally, the processed polymer sample (masterbatch) was removed from the processing chamber and chilled in cold water to

prevent further thermal oxidation. The polymer samples were then stored in a cold and dark place.

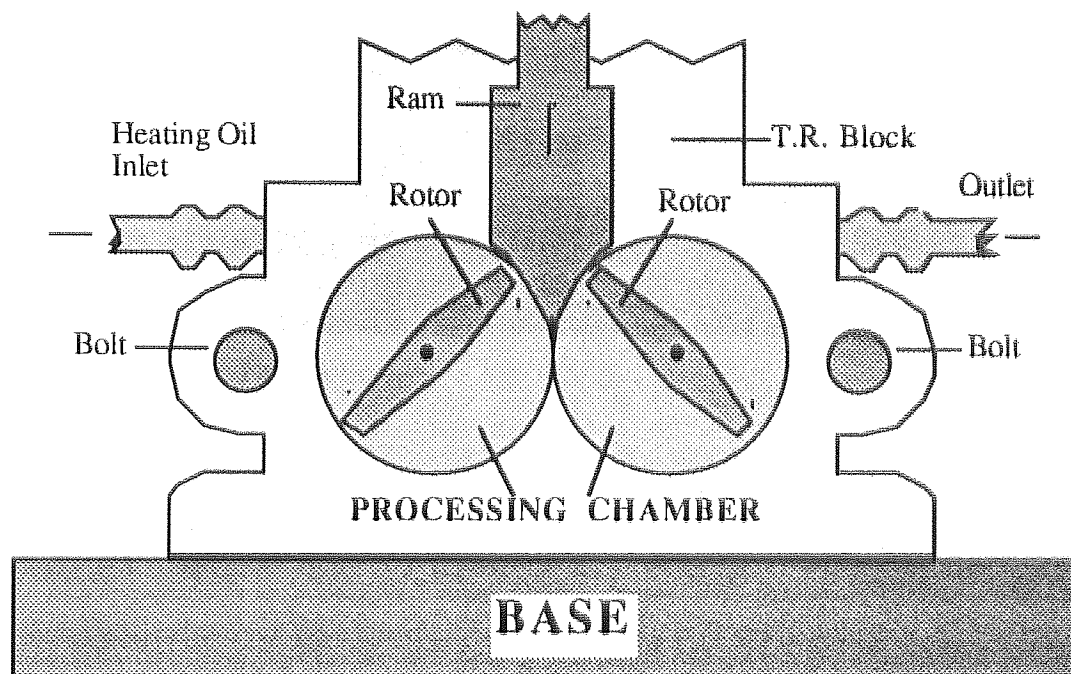


Figure 2.25 Processing chamber of a Brabender torque rheometer (internal - mixer)

Masterbatches of 3%, 6%, 10% and 20% were prepared using the polymer and various molar ratios of radical generator and various percentage of coagent. The dilution of the concentrates prepared in the torquerheometer with fresh unstabilised polymer was carried out using the same equipment.

2.3.2. Film Preparation

Polymer films for uv stability test, thermal ageing and spectroscopic studies were prepared from the processed samples by compression moulding using an electric DANIELS press machine. The polymer concentrate (masterbatch) was placed between two polished stainless steel plates, which were thoroughly cleaned before use to ensure smooth surface and laminated with special grade heat resistance cellophane film to prevent the film sticking to the plates. Control of film thickness (0.1-0.2 mm) was

achieved by using a standard quantity of polymer sample (7 gram), which was preheated for 2 minutes without pressure at 180°C. Pressure of 85kg/cm² was then applied for 1.5 minutes before cooling down to below 100°C by using cold running water. Polymer sample films were selected from section of uniform thickness for further test and investigation.

2.4. EVALUATION OF BINDING

2.4.1 Soxhlet Extraction

Film samples (2 x 3 cm² in size) were exhaustively Soxhlet extracted to remove any unbound antioxidant and other low molecular mass materials, by using a suitable solvent e.g. methanol, acetone or dichloromethane (depending on the solubility of the antioxidant) under nitrogen atmosphere until no antioxidant can be extracted. It was found that 48 hours extraction was sufficient to remove all unbound antioxidant. The extracted films were dried under vacuum at room temperature for 24 hours. Three films were extracted for every sample to establish the experimental error.

2.4.2. Assessment of Binding Efficiency of Antioxidants

Either carbonyl (1730 cm⁻¹) or hydroxyl (3639 cm⁻¹) indices, with peak reference to polypropylene absorption (at 2722 cm⁻¹, of >CH₂) were used to measure the amount of the antioxidants in the polymer sample, since the CH₂ absorption of polypropylene does not change in various heat or UV irradiation environments. The absorption area of carbonyl ester group (>C=O), hydroxyl of (free -OH), and methylene of (>CH₂) group of polypropylene were measured by using a Perkin Elmer FTIR Spectrophotometer model 1700 (see Figure 2.26). The amount of the bound antioxidant was calculated either by comparing either the carbonyl or hydroxyl indices before and after extraction, for three film samples of each antioxidant and the average was taken. The carbonyl index is defined as

ratio of carbonyl absorption area (at 1808 - 1672 cm^{-1}) over that of ($>\text{CH}_2$) group of polypropylene (at 2752 - 2692 cm^{-1}) and similarly the hydroxyl index represents the ratio of hydroxyl absorption area (at 3673 - 3553 cm^{-1}) over that of ($>\text{CH}_2$) group of polypropylene. Binding of the antioxidant (%) is defined as:

$$\% \text{ of Binding} = \frac{\text{Carbonyl or hydroxyl index after extraction}}{\text{Carbonyl or hydroxyl index before extraction}} \times 100 \%$$

e.g. in DBBA carbonyl area index is defined as: $\frac{(\text{area of } 1808 - 1672 \text{ cm}^{-1})}{(\text{area of } 2752 - 2692 \text{ cm}^{-1})}$

e.g. in DBBA hydroxyl area index is defined as: $\frac{(\text{area of } 3673 - 3553 \text{ cm}^{-1})}{(\text{area of } 2752 - 2692 \text{ cm}^{-1})}$

Binding efficiency of antioxidant in masterbatch sample film were carried out in triplicates to establish the experimental error. For example, (B=binding efficiency), $B_1 = 41$, $B_2=42$ and $B_3=37$, hence, the average binding efficiency was taken as 40%. The % error of these binding efficiency calculation was found to be between 3 - 8%.

To improve the binding efficiency of antioxidant an interlinking agent that has more than one functional group was used, referred to as a coagent. In the case of benzophenone masterbatch containing coagent, both carbonyl absorption of benzophenone and that of coagent in the FTIR spectra overlapped in the same area. The amount of benzophenone antioxidant with or without coagent in the masterbatch, therefore, were measured by using UV Spectroscopy by comparing the characteristic absorption intensity at $\lambda = 288 \text{ nm}$ before and after extraction (see Figure 2.27). The binding efficiency (%) of benzophenone was calculated by comparing absorbance of HAEB at $\lambda=288 \text{ nm}$ area before and after extraction.

$$\% \text{ Binding} = \frac{\text{Absorbance area of HAEB at } \lambda=288 \text{ nm, after extraction}}{\text{Absorbance area of HAEB at } \lambda=288 \text{ nm, before extraction}} \times 100 \%$$

2.5 MEASUREMENT OF MELT FLOW INDEX (MFI)

The melt flow index (MFI) is defined as the mass (gram) of the molten polymer extruded through a standard die in a given time (normally 10 minutes). The measurement of the melt viscosity of the polymer is related to the molecular weight. 5 g of finely cut masterbatch samples were used for melt viscosity measurements using Melt Flow Indexer (Davenport) at constant extrusion temperature of $230 \pm 5^{\circ}\text{C}$ for polypropylene. The barrel was then charged with the polymer masterbatch using a charging tool in such a way to exclude air and the charging-time should not exceed one minute. The masterbatch sample was preheated for 4 minutes before putting a load of 2.16 kg to drive the molten masterbatch through a die (diameter $\varnothing = 0.1181 \text{ cm}$). The time interval for the first extrudate or cut-off was 60 seconds and discarded, then 5 successive cut-off's were taken, each at the end of 30 seconds. Any cut off that contained air bubbles was rejected, the average of 5 cut-offs was taken. The MFI was calculated from the amount of polymer melt (in gram) which passed through the die within 10 minutes⁽¹⁶⁹⁾. Every sample was carried out in triplicate to establish the experimental error. For example, $\text{MFI}_1 = 1.65$, $\text{MFI}_2 = 1.72$ and $\text{MFI}_3 = 1.62$, hence, the average MFI was taken as 1.65 g/10 minutes. The % error of these MFI calculation was found between 2 - 4 %.

2.6 MEASUREMENT OF INSOLUBLE GEL (GEL CONTENT)

Polypropylene (PP) is known to be completely soluble in boiling xylene (b.p 135°C). To examine the crosslinking content (which is identified as insoluble gel in xylene extraction), after exhaustive Soxhlet extraction in DCM, to separate the unbound antioxidant, all the masterbatches (containing antioxidant in the presence of free radical

initiator, Trigonox 101, with or without coagent) were further exhaustively Soxhlet extracted in xylene for 48 hours under nitrogen atmosphere. In cases where the gel content was very low, indicating very little crosslinking, the extraction was carried out in toluene (b.p. 110°C) under N₂ in order to separate the high and low molecular weight fraction. The toluene extract was then further extracted in xylene. Concentration of the antioxidant in each fraction were calculated by measuring either hydroxyl or carbonyl indices using FTIR Spectroscopy.

2.7 STABILISING ACTIVITY TEST

2.7.1 Ultraviolet Irradiation of Polymer Films

The masterbatches were diluted down in fresh polypropylene to the normal antioxidant concentration level of 0.2 % and 0.4 % for the purpose of photo stabilising and thermal ageing tests of the stabilised films (thickness of 0.10-0.20 mm). All film samples were irradiated in an ultra-violet light ageing cabinet containing 28 fluorescent-sun lamps and black lamps. The photo stability of the samples films were followed by measuring the embrittlement time (see subsection 2.8) and the increase of carbonyl index along with the control sample of processed polypropylene films.

The ultra-violet cabinet comprised a metal cylinder about 110 cm outer diameter and having a concentric circular rotating sample drum whose circumference was 15 cm from the periphery of the metal cylinder. Twenty eight fluorescent tube lamps were composed of 1 to 3 combination of fluorescent-sun lamps and black lamps, each of 20 watts power and mounted alternately around the periphery of the metallic cylindrical board⁽¹⁶⁸⁾. The rotating arrangement of the sample allows an identical amount of total radiation to fall on each sample. The cylindrical cabinet was opened to the atmosphere on both the lower and upper sides and the circulation of air in the cabinet was ensured by driven ventilation situated under the rotating frame. The film were mounted vertically on the circumference of

a rotating drum fixed inside the cabinet. In this manner, the light beam fell perpendiculary on the surface of the films. the distance of the sample films from the light source was 10 cm and the temperature inside the cabinet with the lights on was around 30° C. In order to maintain long term uniform spectral distribution inside the cabinet, the lamps were replaced sequentially every 300 hours of operation in addition to periodical radiation output measurements.

The radiation output in the UV exposure cabinet was monitored sequentially every six months in order to maintain long term uniform spectral distribution inside the cabinet and also to detect positional variation in output. The measurement is based on the use of polysulphone films as a dosimeter⁽¹⁶⁹⁾. The intensity of uv-irradiation falling on the surface of the films was calculated to be 5.5 W.m⁻². The principle of this method relates to the degree of deterioration of the film, usually in terms of changes in their spectroscopic properties, to the incident radiation dose.

2.7.2 Thermal Ageing of Polymer Films

The accelerated thermal ageing test of processed polymer films were carried out in a Single Cell Wallace oven at 140°C under air atmosphere. Each sample was contained and suspended in a separate cell to prevent cross contamination of the additives by volatilisation and was subjected to an air flow of 3.0 cubic feet/hour (85 liters/hour). The thermal stability of the sample films were followed by measuring the embrittlement time (ET) and the increase of carbonyl index along with the control sample of processed polypropylene films. All tests were carried out triplicate to establish the experimental error. For example, ET₁=266 hours, ET₂=278 hours and ET₃=257 hours, hence, the average embrittlement time was taken 267 hours. The % error of the embrittlement time was between 3 - 4%.

2.8 MEASUREMENT OF BRITTLE FRACTURE TIME OF POLYMER SAMPLES

Film polymer samples of identical size and uniform thickness containing additives along with a control were irradiated or heated and were periodically checked and their times to embrittlement were determined by bending the film back on itself 180° manually. Each polymer samples test was carried out in triplicate.

2.9 FOURIER TRANSFORM INFRARED (FT-IR) SPECTROSCOPY

Fourier Transform Infrared Spectroscopy provides a high resolution and more sensitive mathematical technique compared to that of ordinary Infrared Spectroscopy⁽¹⁷⁰⁾. In addition, the mathematical calculation can be more accurately carried out by using a computer. Like the ordinary infrared spectroscopy, the calculation of absorbance (A) and concentration (C) also follows the Beer-Lambert law.

$$A = \log (I_0/I) = \epsilon c l$$

Where,

A = Absorbance

I_0 = Intensity of radiation effectively entering the sample

I = Intensity of radiation emerging from the sample

ϵ = Extinction coefficient expressed in litres mole⁻¹ cm⁻¹

c = Concentration of absorbing group present in the sample mole/litre

l = Path length of radiation within the sample in cm

In quantitative measurement of infrared spectra of polymer films, one can eliminate experimental error due to thickness variation of the films, using a known reference peak of the polymer, for instance in the case of polypropylene the reference peak is the absorption peak of (>CH₂) group at 2752 - 2692 cm⁻¹. This allows the measurement of an absorption

index of the sample (A_S/A_R), i.e. ratio of absorbance of the sample peak with the absorbance of the reference peak, which is thickness independent. The Beer-Lambert law then can be written in the form,

$$(A_S/A_R) = B c_s$$

where, subscript *s* refers to the sample, *r* represents the reference and **B** is a new constant equal to $\epsilon_s / (\epsilon_r c_r)$. Using the above equation, Zakrzewski and Henniker (171) have found a good straight line when the absorbance ratio of $>C=O$ to $>CH_2$ peaks was plotted against PVA concentration, for the determination of PVA (poly vinyl alcohol) concentration in the copolymer of PVC-PVA (polyvinylchloride-polyvinylalcohol). Problem concerning with the accuracy of measurement of the absorption peak may be overcome by measuring the peak area, instead of peak absorbance, as shown in Figure 2.26. Using an application software (M1700) in the Data Station of the Perkin-Elmer FT-IR machine model 1700, either the area under the curve with the base line of the peak (area of ABC) or the area between the curve with the zero absorbance line (area of EABCD) may be calculated. In this work the total absorption area is taken as the area of ABC.

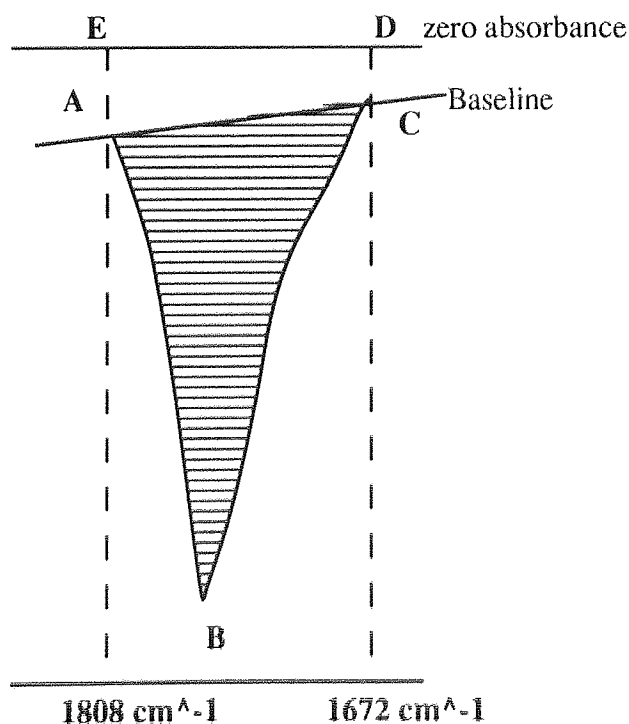


Figure 2.26 Measurement peak area in FT-IR spectroscopy

2.10 ULTRA VIOLET SPECTROSCOPY

Ultra-violet spectra of polymer films with additives and solution spectra were recorded using the Beckman DU-7 ultra violet visible computing spectrophotometer. The instrument was used to assess the binding efficiency of antioxidant by observing the characteristic UV absorption band of additives. An additive free polymer film of identical thickness was used as reference to compensate for the polymer. This was done (as shown in Figure 2.27) by drawing a straight line (base line) tangential to an adjacent absorption maxima or shoulder, then erecting a perpendicular through the analytical wave length until it intersects the base line. At "G" the concentration of chromophore group to be determined is zero and at "F" there appears an absorption peak whose height (BF) serves to calculate the concentration.

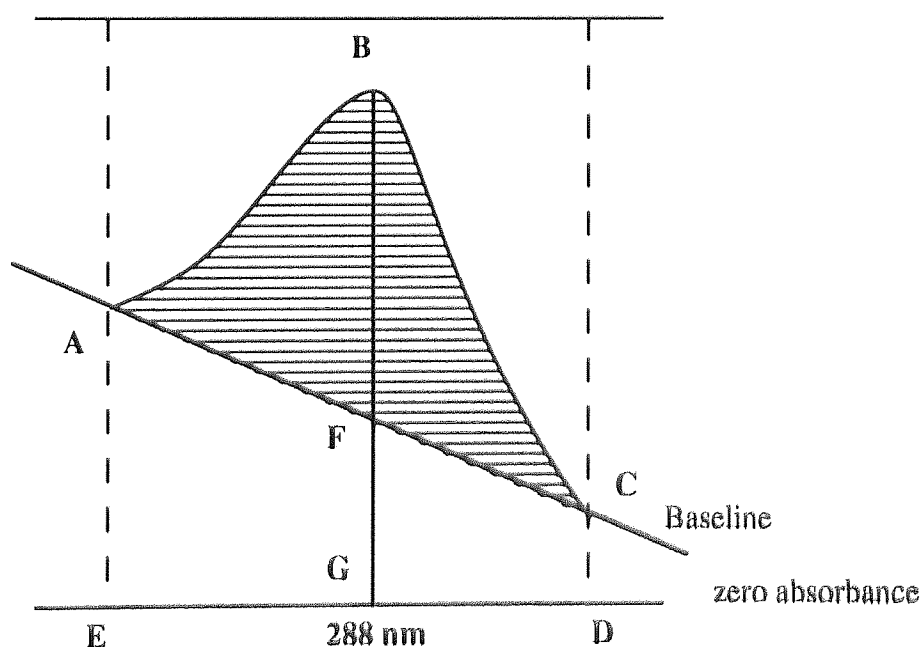


Figure 2.27 : Measurement of absorption in UV spectrophotometer

As it is known that polypropylene alone gives no absorption in that wave length area, the absorbance values were calculated using the combined form of the Beer - Lambert law:

$$A = \log (I_0/I) = \epsilon c l$$

In the case of solution studies, spectra were recorded using quartz cells of 1 cm path length with the spectroscopic solvent serving as external reference(170,171).

2. 11 PROTON AND CARBON-13 NUCLEAR MAGNETIC RESONANCE (NMR) SPECTROSCOPY

Essentially, the atomic nuclei of many elements have a magnetic moment because they are charged and behave as if they were spinning. This magnetic property can be investigated by studying the way in which the nuclei interact with an externally applied magnetic field (B_0). In essence, the field brings about two energy configurations within which the nuclear spins are aligned with or opposed to the field (low and high energy states respectively). The application of radio frequency energy causes some of the spins in the low energy state to go to the higher energy state, bringing about nuclear magnetic resonance (NMR).

Typical types of magnetic nuclei studied are proton ^1H and carbon ^{13}C . Fortunately for the purposes of structural investigation magnetic nuclei come into resonance at slightly different field strengths due to the neighbouring electronic environment of other atoms. As an example, the higher the electron density around the proton, the higher the external magnetic field has to be to promote it to its excited state (high level energy); this nuclei is referred to as 'shielded'. Thus, different shielding of the nuclei causes a spread of NMR signals, or chemical shifts. For instance, protons of tetramethyl silane (TMS) which are surrounded by high electron density due to positive inductive effect (+I) from the silicon atom, appear on the NMR spectrum at a 'chemical shift' on the high magnetic field area (right hand side of the spectrum). On the other hand, the chemical shift of a proton adjacent to a quaternary ammonium ion (R_4N^+) sees low electron density and is deshielded and appears at low field.

In practice, the chemical shifts are expressed in δ -units which for a proton is defined as the difference of the applied magnetic field (in ppm) from TMS (δ of TMS = 0). Another factor affecting the shift of proton NMR signals is due to interaction with their neighbouring proton(s), spin-spin coupling, which in the simple case splits the NMR proton signal into (n+1) signals with intensity ratio which follows the Pascal's triangle formula (n=number of neighbouring protons)(172,173).

The NMR signal of a ^{13}C nucleus is weaker than that of ^1H due to the lower natural abundance of ^{13}C in every carbon atom (only 1.1%), and its lower magnetic moment. Presentation of ^{13}C NMR spectra also uses TMS as standard ($\delta = 0$ ppm), whereas the position of a particular carbon signal is affected by electronic charge, in which the hybridisation state of the carbon atom determine their signal positions, i.e. sp^2 carbon appear on the lowest field ($\delta = 100 - 200$ ppm), followed by sp carbon ($\delta = 70 - 40$ ppm) and sp^3 carbon at highest field (0 - 30 ppm)(174).

The measurements made in the solid state gave much broader resonances compared to those in the solution state. When observing NMR of solids, two distinct situations that depend upon the concentration of magnetic nuclei must be considered. These are the "abundance" and "dilute" spin cases, the meaning of which will soon become self evident. For protons in a typical organic solid, with a high concentration of hydrogen in the sample and 100% natural abundance, homonuclear dipole-dipole interaction are important. In such solids, protons are the abundant spins. The situation for ^{13}C is different. The ^{13}C nuclei are diluted by ^{12}C so even if there is a high concentration of carbon, homonuclear dipole-dipole interactions will occur only at long distances and be very weak. At natural abundance, ^{13}C is a dilute spin. In organic solids, heteronuclear (^1H - ^{13}C) dipole-dipole interaction dominate the ^{13}C broadening (^{13}C - ^{13}C interactions are relatively unimportant because the natural abundance of this isotope is only 1.1%).

The ^1H - ^{13}C dipolar coupling can be removed by high power decoupling. This leaves the carbon chemical shift anisotropy as the dominant broadening mechanism. In order to explain chemical shift anisotropy, it needs to be visualised that in the NMR experiment the local magnetic field at a given carbon is a function of the relative molecular orientation with respect to the external magnetic field. Thus, the observed spectrum for a typical solid would represent a superposition of all possible molecular orientations (anisotropy), as opposed to spectra obtained in liquids, where rapid tumbling of the molecules leads to observation of an average (isotropic) chemical shift (exhibits sharp lines at the chemical shift). However, this broadening can be removed by spinning the solid sample at a rapid rate compared to the resonance bandwidth of a static sample and inclining it at an angle of 54.7° (the "magic angle") with respect to the external field. This process leads to an averaging of the anisotropy and results in a single narrowed absorption at a position characteristic of the isotropic chemical shift.

The sensitivity of ^{13}C NMR spectroscopy is normally limited by the low natural abundance of the magnetic isotope, its small magnetic moment, and long relaxation time. The situation can be improved, however, by the use of cross polarisation (CP). Using an appropriate spectrometer sequence, magnetisation (polarisation) can be transferred from the protons to the carbons, resulting in a significant enhancement in carbon magnetization over the normal value. Moreover, CP allows for in more rapid acquisition of the carbon spectrum. Together, cross polarisation, high power decoupling, and the magic angle spinning procedure allow one to obtain high resolution spectra of solids. Measurements made in solid give ^{13}C spectra with resonances all in (+) values(175).

Measurements of ^{13}C NMR spectra in this work were run in two different ways: solution and solid states. All spectra were recorded on a BRUKER AC 300 High Resolution NMR Spectrometer.

For solution state NMR the sample was dissolved in CDCl_3 and ^{13}C NMR spectra were run at room temperature using the J-modulated spin echo (JMOD) method except where indicated. The JMOD method gives ^{13}C NMR spectra with resonances displayed in a positive (+) and negative (-) manner. For example, methyl ($-\text{CH}_3$) and tertiary ($>\text{CH}-$) carbon peaks appear as positive (+) values, whereas methylene ($-\text{CH}_2-$) and quaternary ($>\text{C}<$) carbon nuclei exhibit (-) values. In the case where polymerisation was carried out "insitu" a routine method was used. The NMR probe temperature was kept at 373°K . The latter method gives ^{13}C NMR spectra with all resonances being (+) values.

2.12 GEL PERMEATION CHROMATOGRAPHY

Gel Permeation Chromatography is one of most important techniques for determination of molecular weight and molecular weight distribution of polymer samples. Molecular weight changes during thermal degradation of low density polyethylene have usually been explained by chain scission or crosslinking⁽¹⁷⁶⁾. A chain scission process shifts the molecular weight distribution (MWD) to lower molecular weight. A molecular enlargement will be observed as an increase of the high molecular weight tail.

The measurement of molecular weight distribution of the masterbatches were carried out at RAPRA polymer characterisation centre using Gel Permeation Chromatography (GPC). The condition of the measurement were as follows:

columns : P.L gel 2x mixed gel, 20 micron packing, 30 cm columns
solvent : 1,2 - dichlorobenzene, stabilised with 2,6 - ditert. butyl - p-cresol
flow rate : 1.0 ml/minute
temperature : 140°C and
calibration : third order polynomial using polystyrene standard

Molecular weight of a polymeric material is determined from the averages of the range of its molecular weights, since polymer materials are polydisperse compounds which contain molecules of different sizes and molecular weights. By definition, there are several methods of calculating average molecular weight of polymer (176).

- Number average molecular weight (M_n), is calculated from the total weight of polymer ($\sum N_i M_i$) divided by its total molecules ($\sum N_i$).

$$M_n = \frac{\sum N_i M_i}{\sum N_i}$$

- Weight average molecular weight (M_w) is based on the average of total weight of the polymer ($\sum N_i M_i$).

$$M_w = \frac{\sum N_i M_i^2}{\sum N_i M_i}$$

- Z-property average molecular weight (M_z). This is theoretical average molecular weight, which is defined as:

$$M_z = \frac{\sum N_i M_i^3}{\sum N_i M_i^2}$$

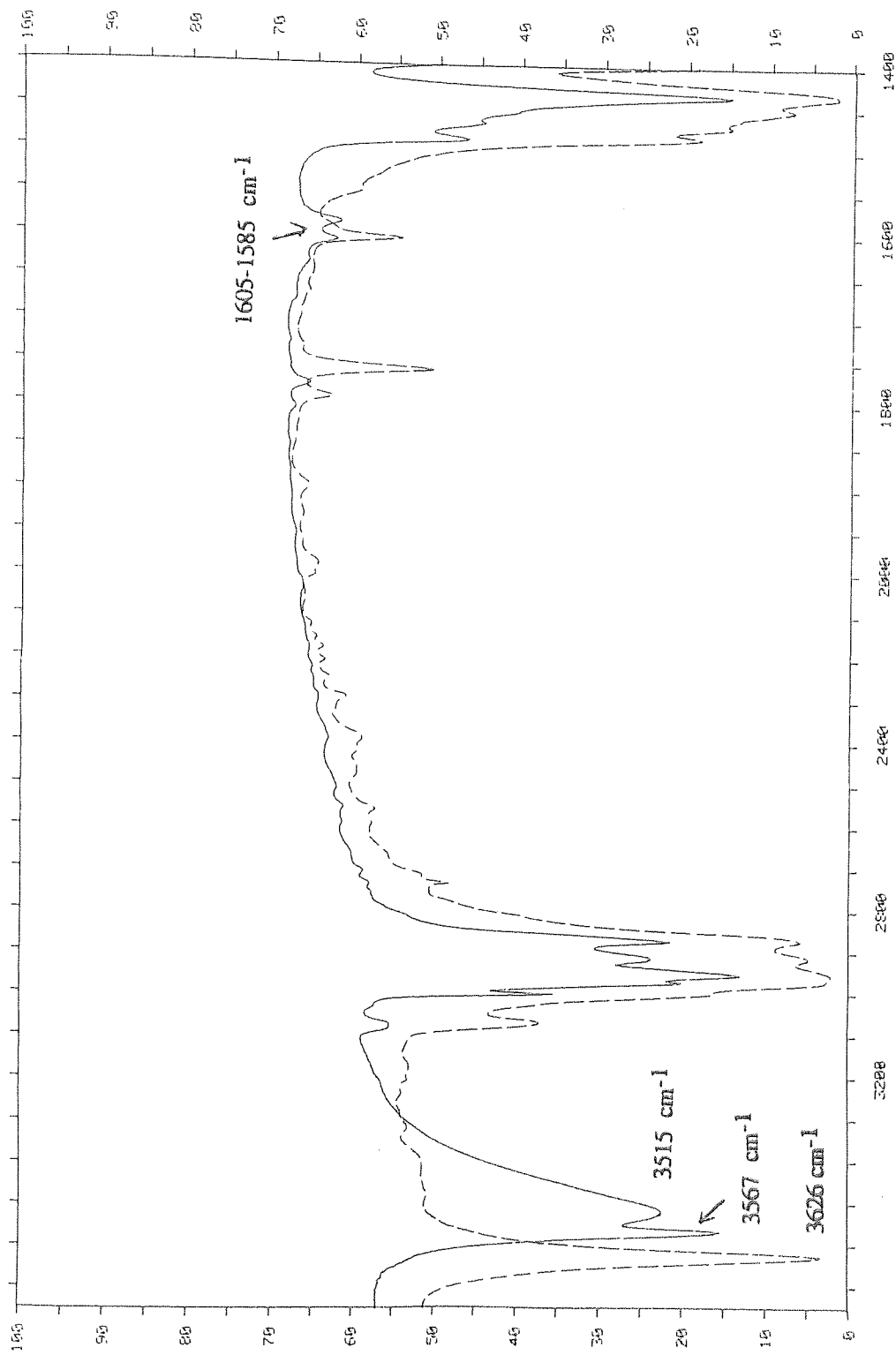


Figure 2.1 Comparison FTIR spectra in region 4000-1400 cm^{-1} of 3,5-di-tert-butyl-4-hydroxy benzyl alcohol, DBHBA (—), with that of DTBP (-----) using KBr disc.

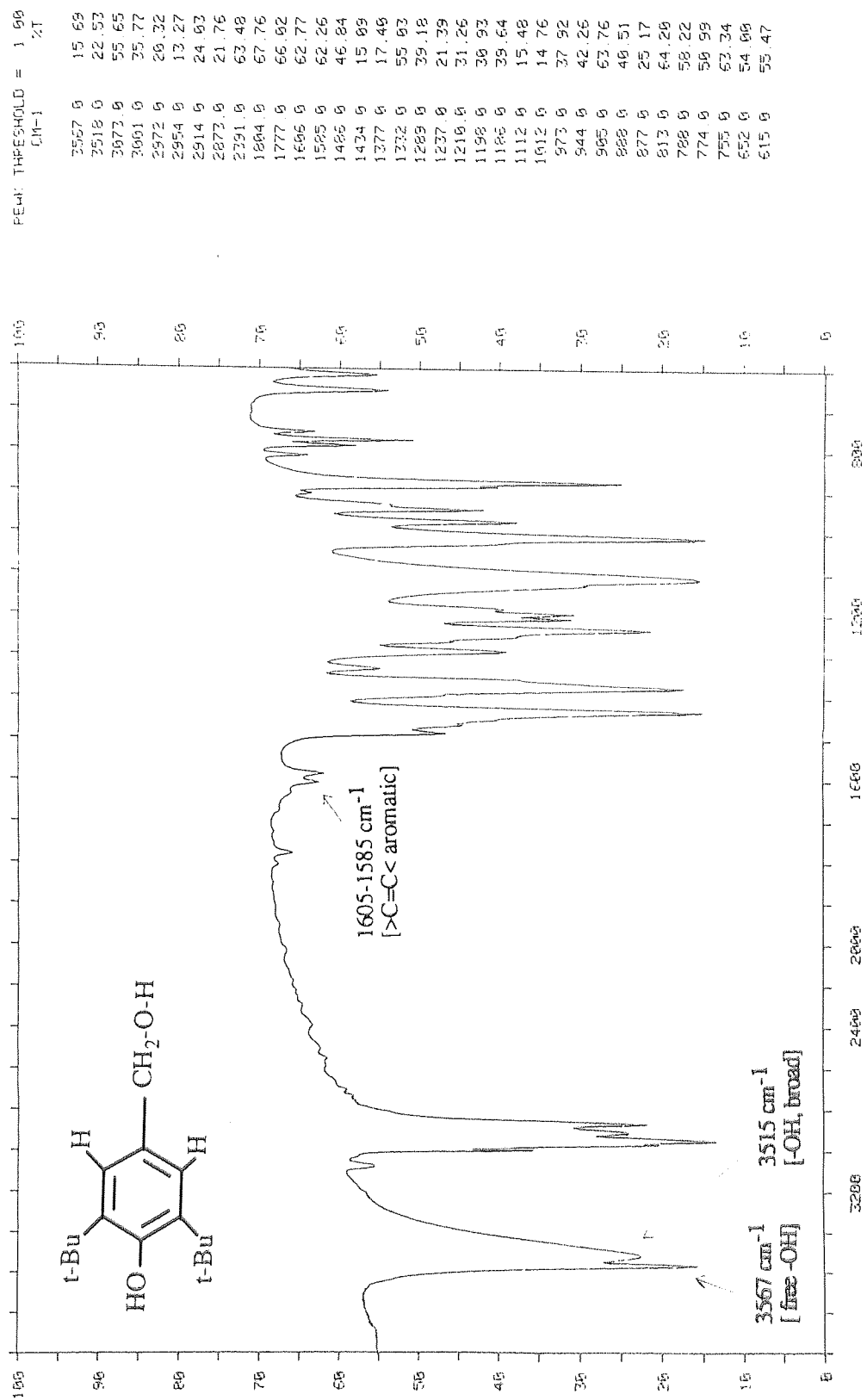
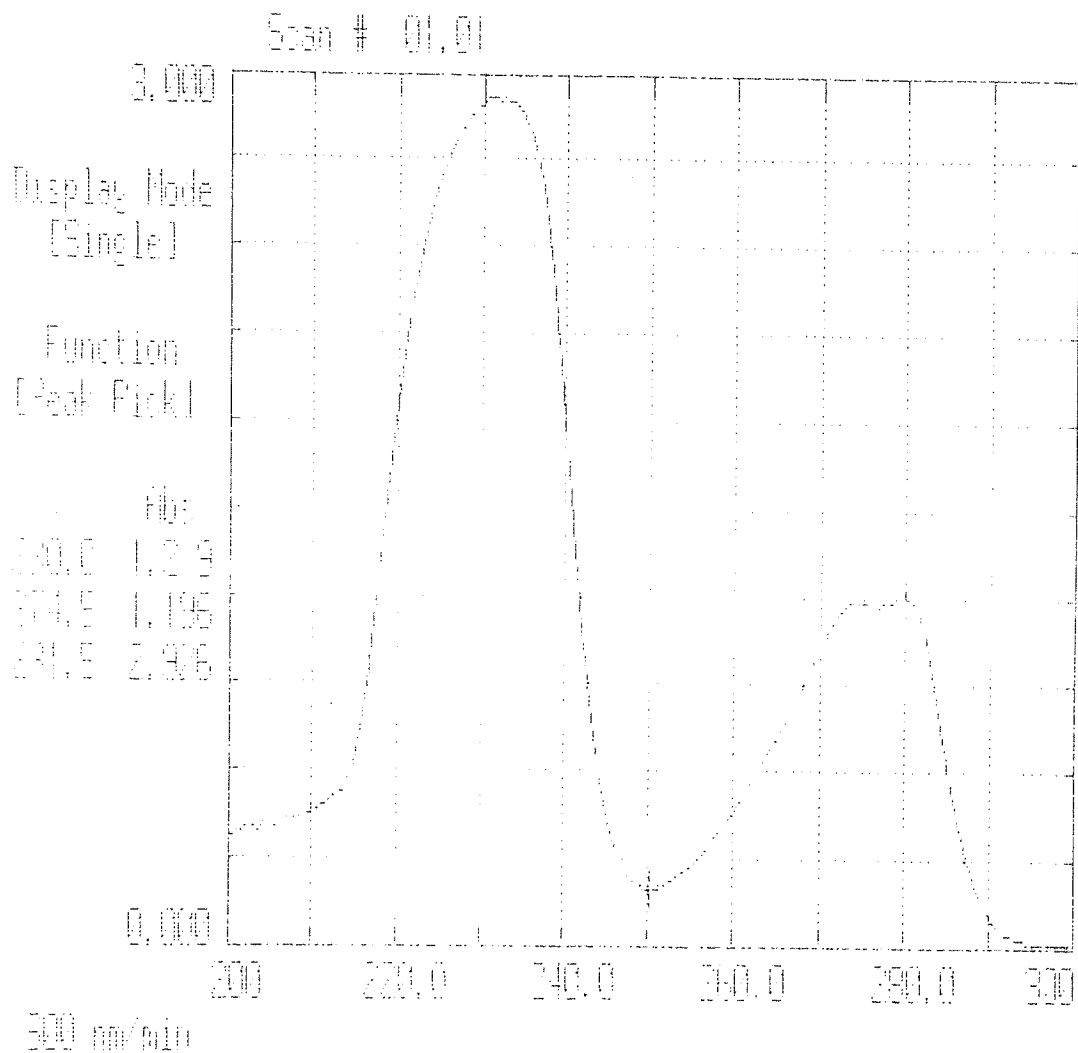
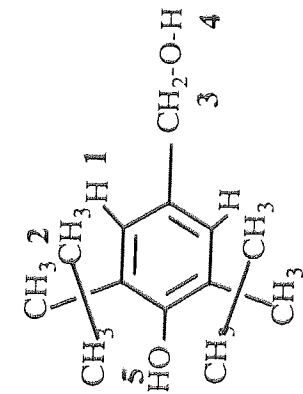


Figure 2.2 FTIR spectrum of 3,5-di-tert-butyl-4-hydroxybenzyl alcohol, DBHBA in KBr disc.



Wavelength (nm)	Abs	Source	Mode	Trace	Wavelength (nm)	Abs
200.0	-0.0304	115-UV	Scan	OFF	250.0	0.1991

Figure 2.2a UV spectrum of 3,5-di-tert.-butyl-4-hydroxybenzyl alcohol, DBHBA in DCM solution.



H No	δ (ppm)	m'plicity	I (%)
1	7.19		6.8
2	1.40	1	60.5
3	4.58	1	7.6
4	1.89	1	3.6
5	5.25	1	3.7

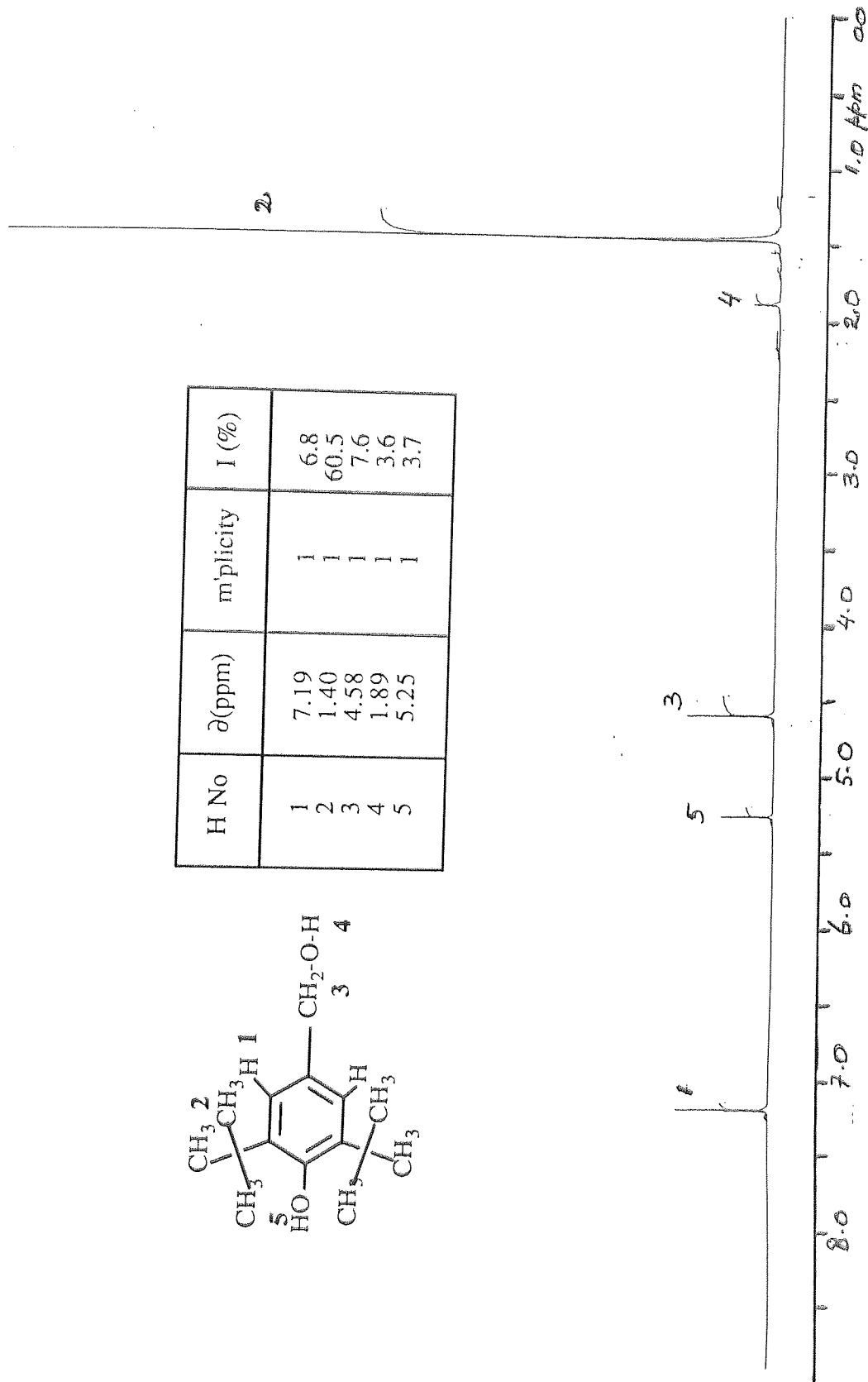


Figure 2.3 Proton NMR spectrum of 3,5-di-tert-butyl-4-hydroxy benzyl alcohol, DBHBA in deuterated chloroform.

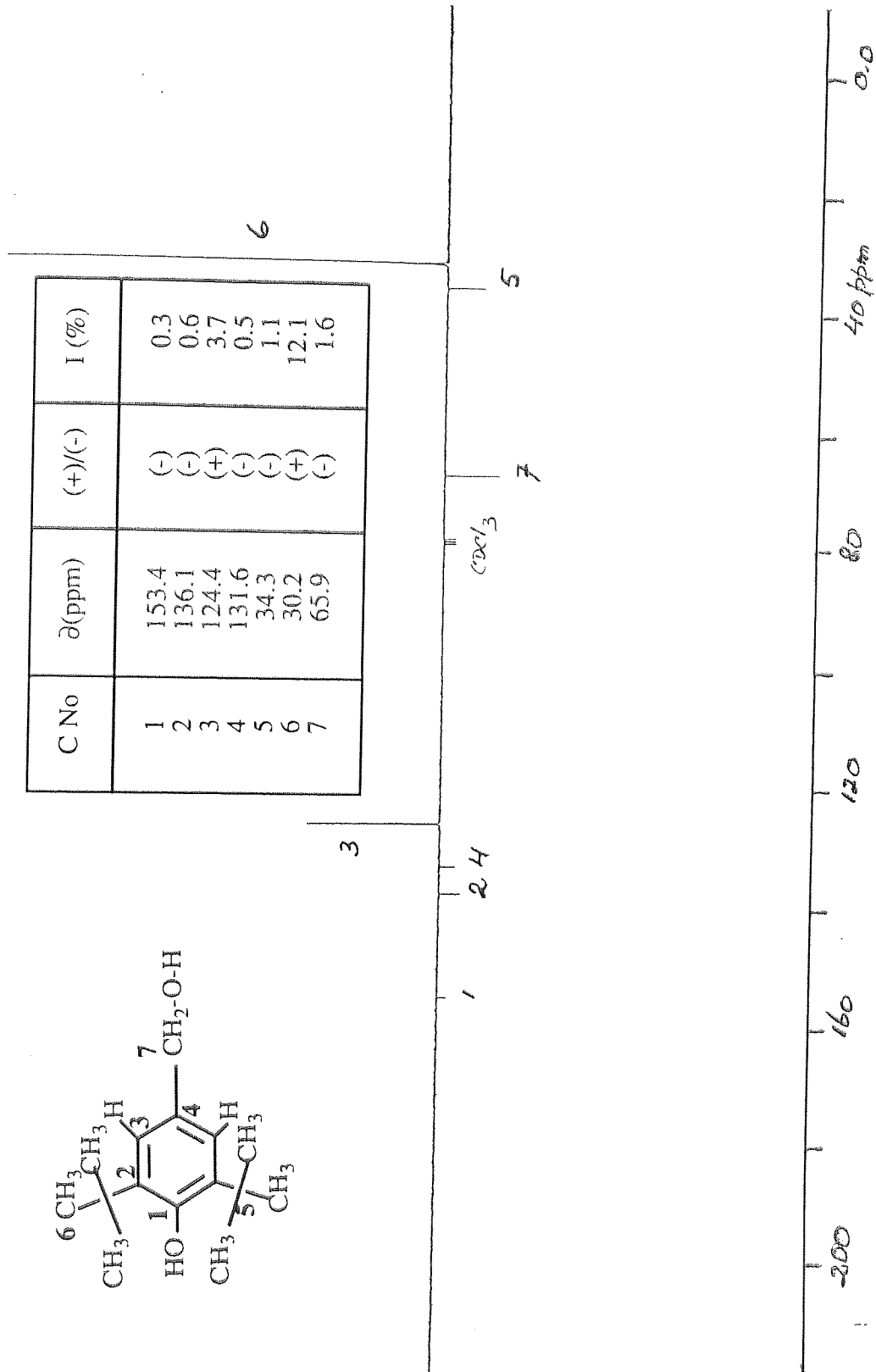


Figure 2.4 Carbon-13 NMR spectrum of 3,5-di-tert-butyl-4-hydroxybenzyl alcohol, DBHBA in deuterated chloroform.

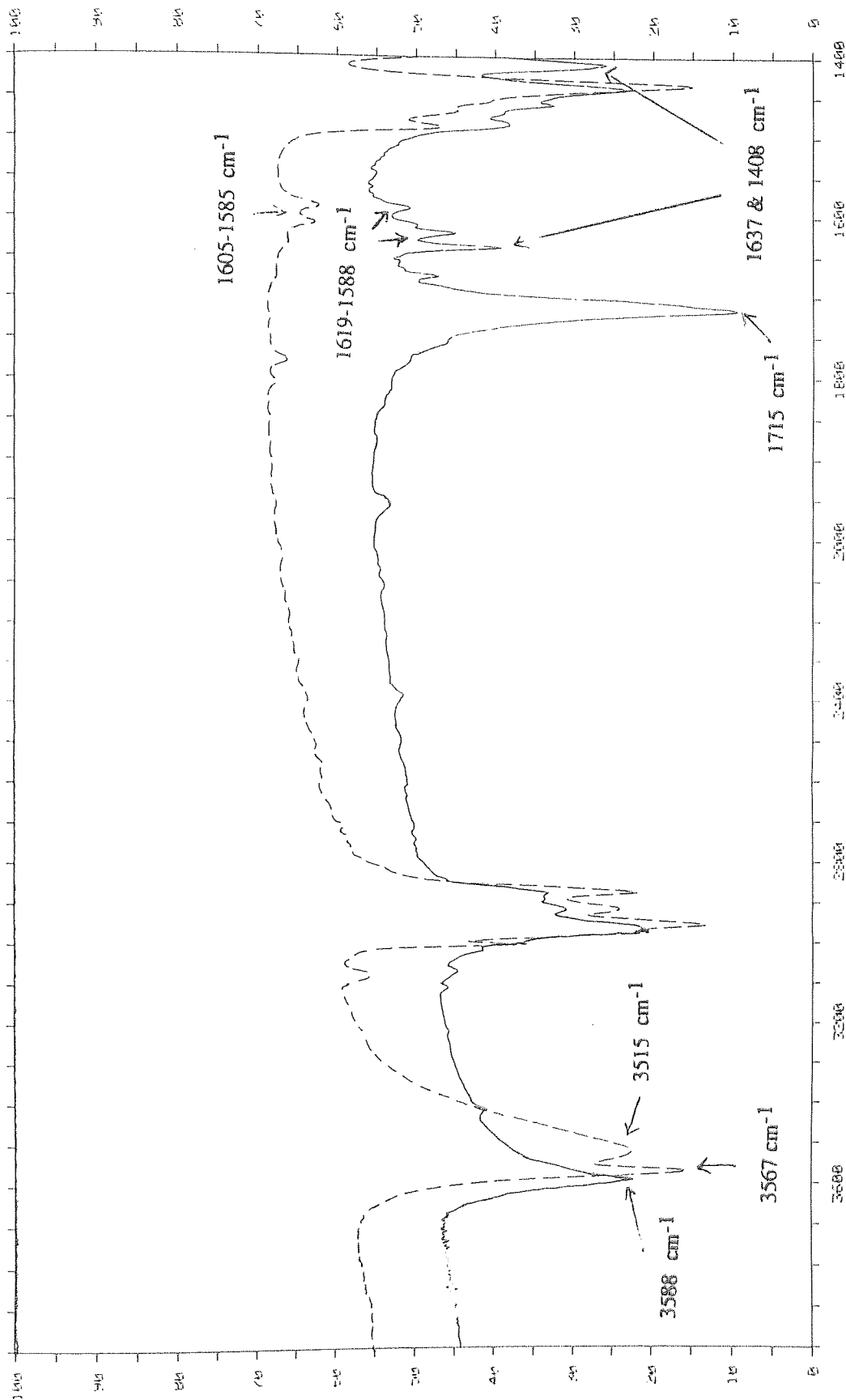


Figure 2.5 Comparison FTIR spectra in region 4000-1400 cm^{-1} of 3,5-di-tert-butyl-4-hydroxy benzyl acrylate, DBBA (—) compared to that of DBHA (-----) using KBr disc.

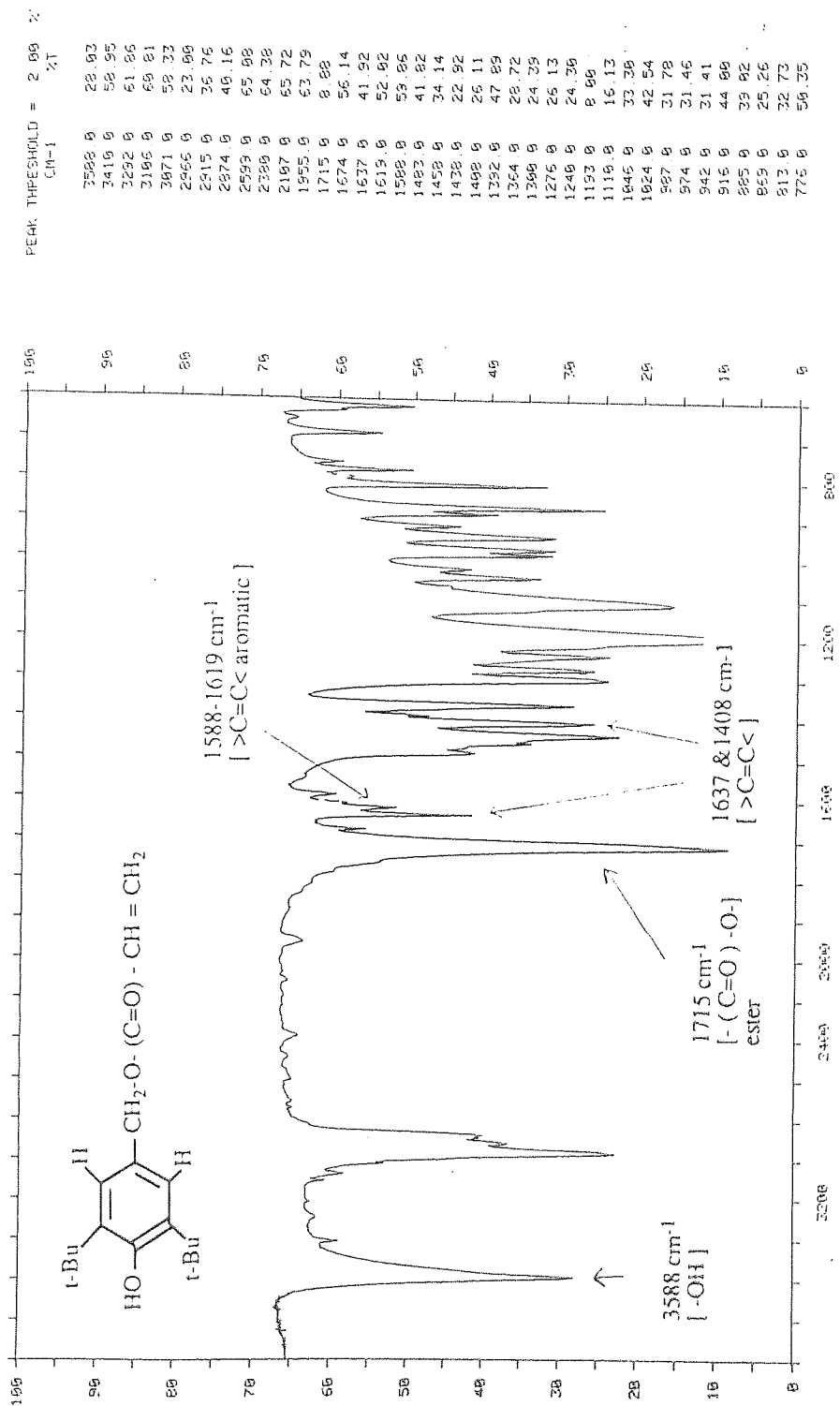


Figure 2.6 FTIR spectrum of 3,5-di-tert-butyl-4-hydroxybenzyl acrylate, DBBA in KBr disc.

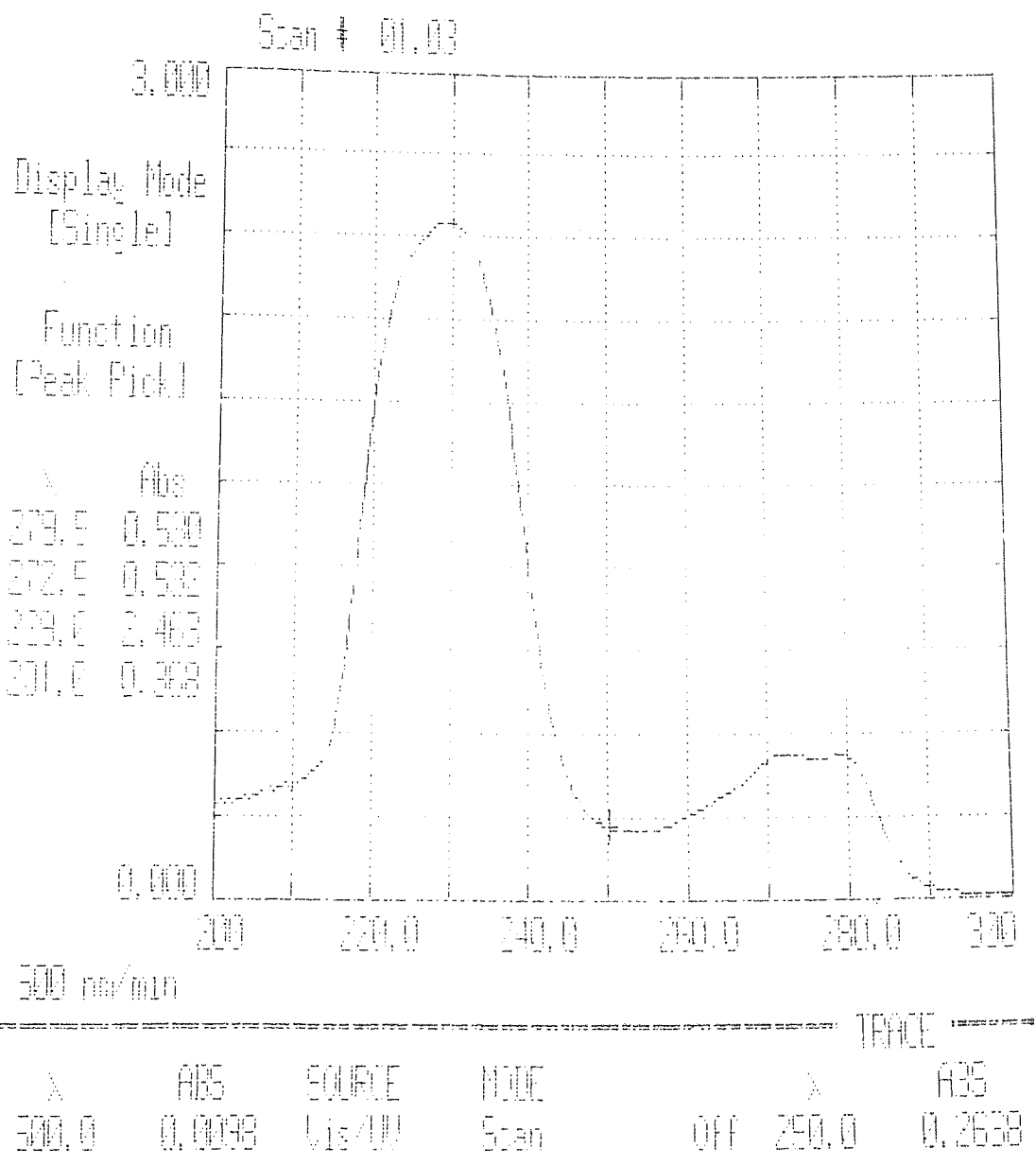


Figure 2.6a UV spectrum of 3,5-di-tert.-butyl-4-hydroxybenzyl acrylate, DBBA in DCM solution

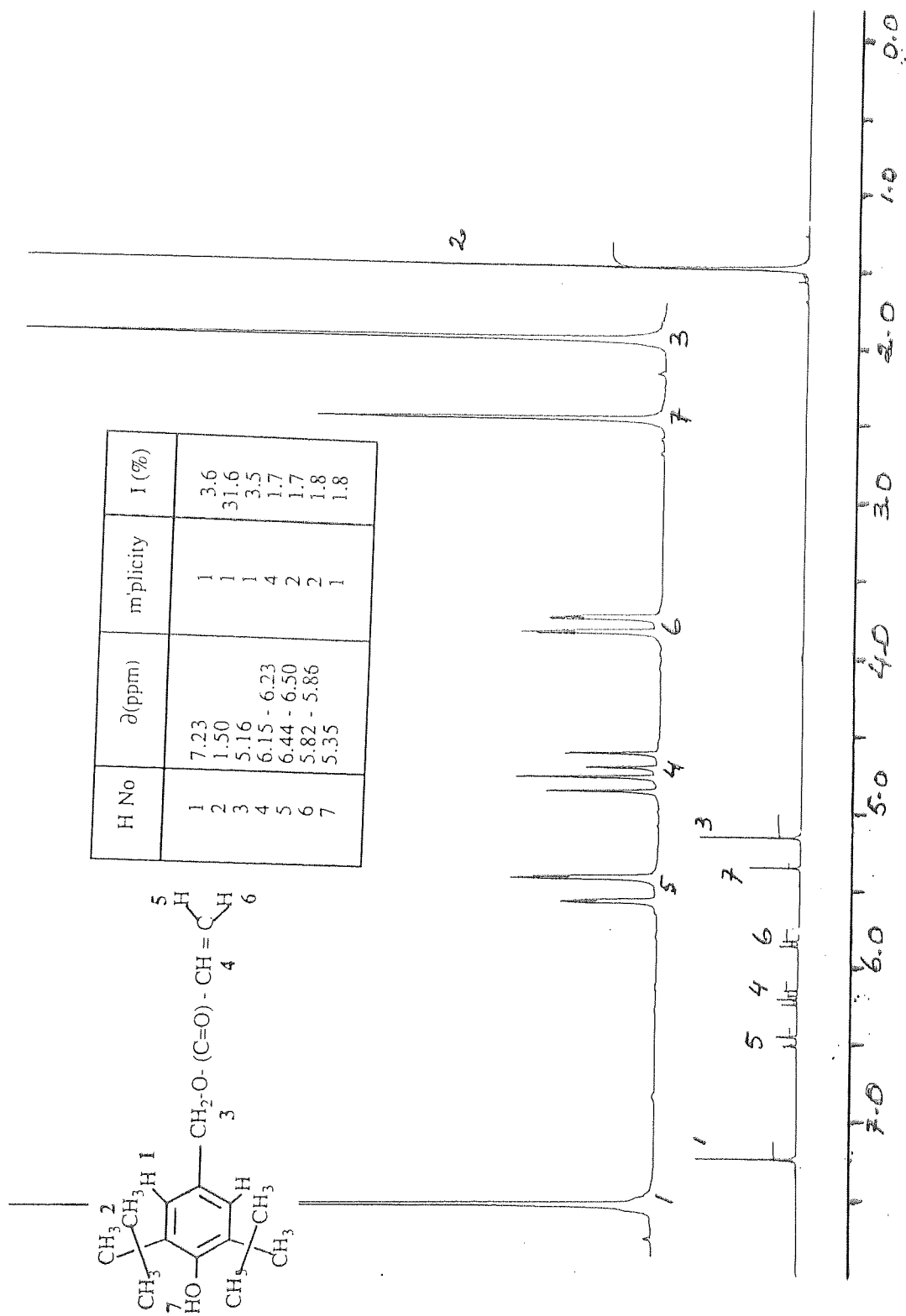


Figure 2.7 Proton NMR spectrum of 3,5-di-tert-butyl-4-hydroxy benzyl acrylate, DBBA in CDCl₃

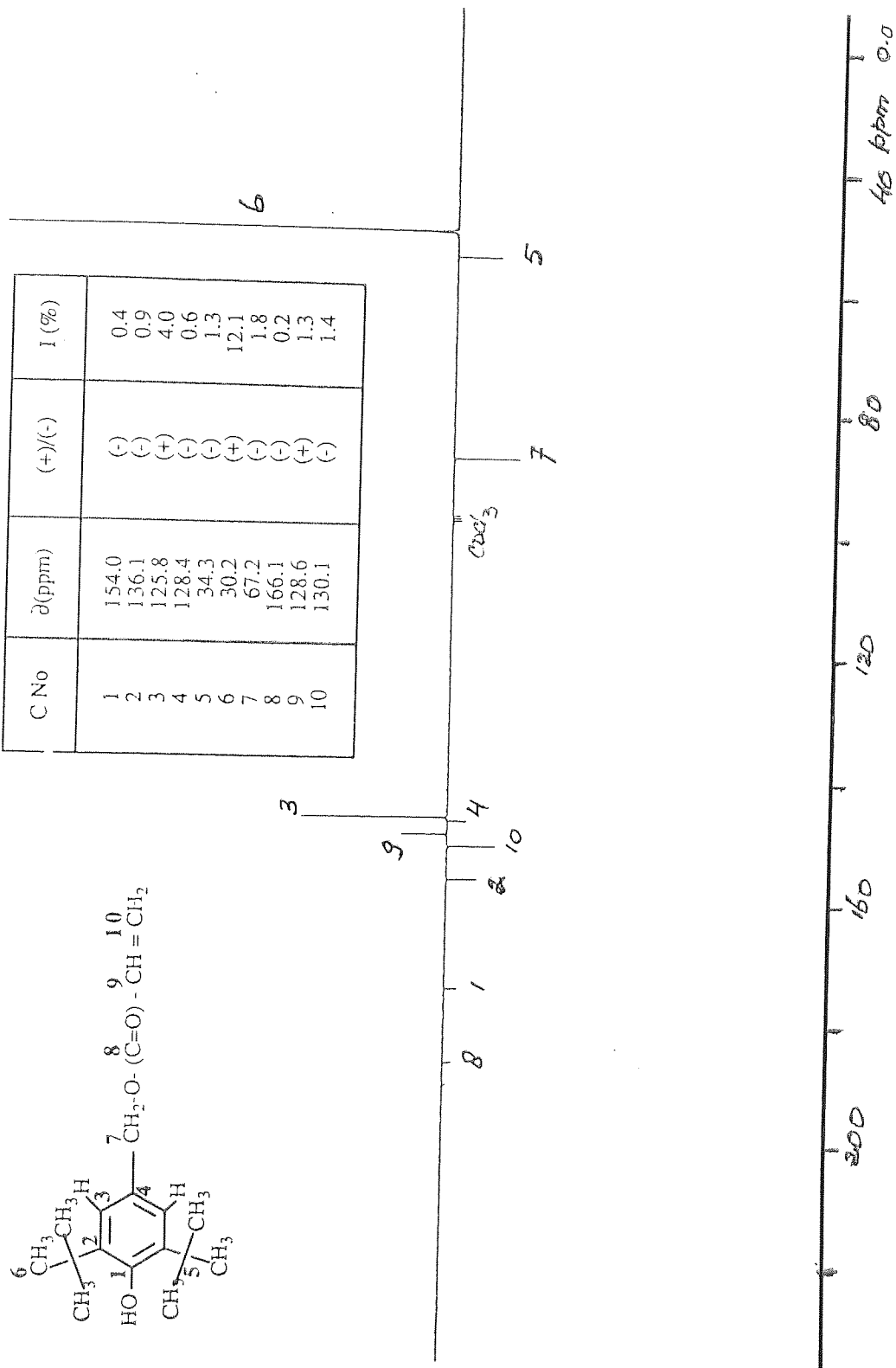


Figure 2.8 C-13 NMR spectrum of 3,5-di-tert-butyl-4-hydroxy benzyl acrylate, DBBA in $CDCl_3$

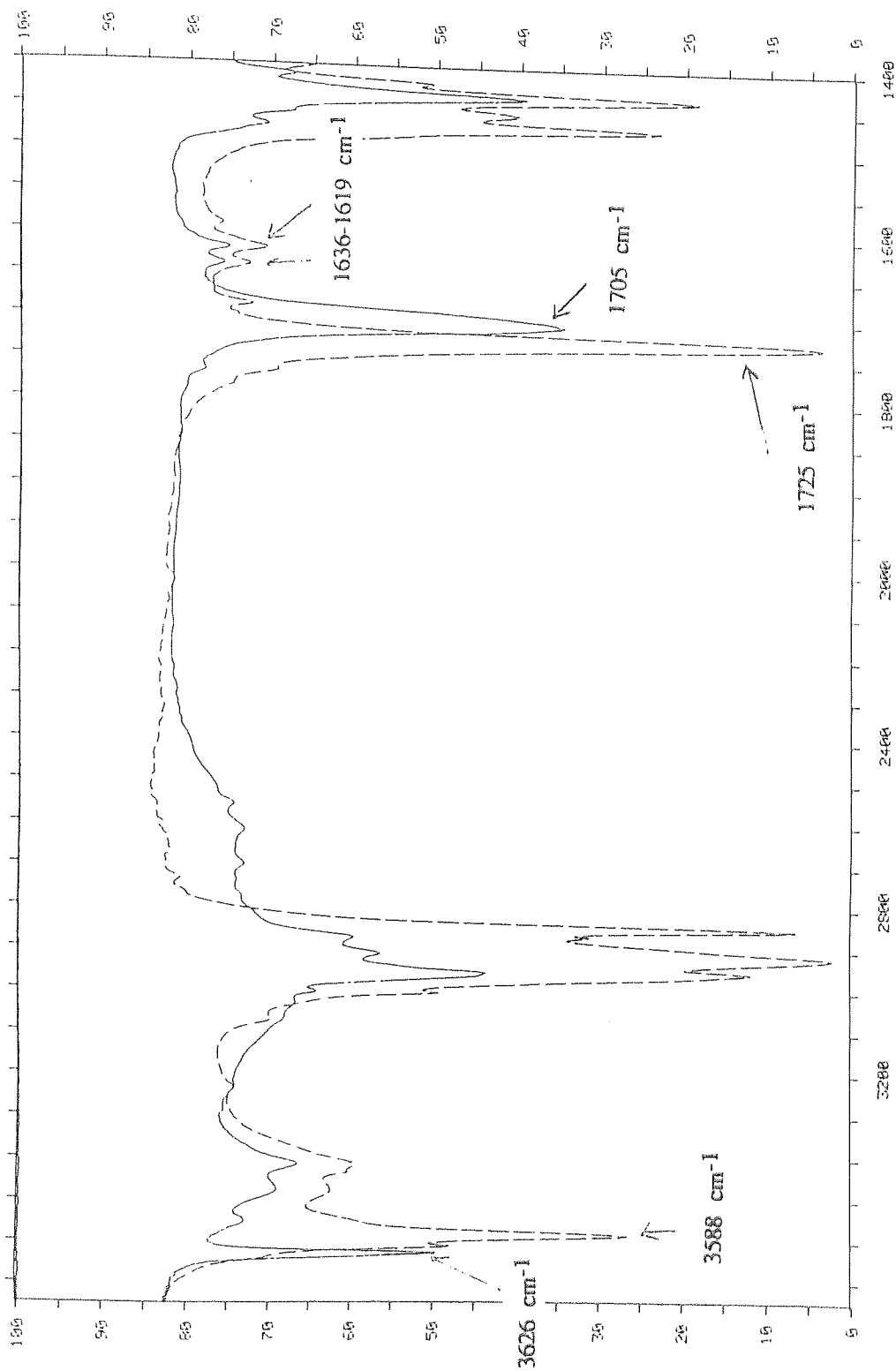


Figure 2.9 Comparison FTIR spectra in region 4000-1400 cm^{-1} of 3-(3',5'-di-tert-butyl-4-hydroxy phenyl) propionic acid, Irganox acid (—) compared to that of Irganox 1076 (----) in KBr disc.

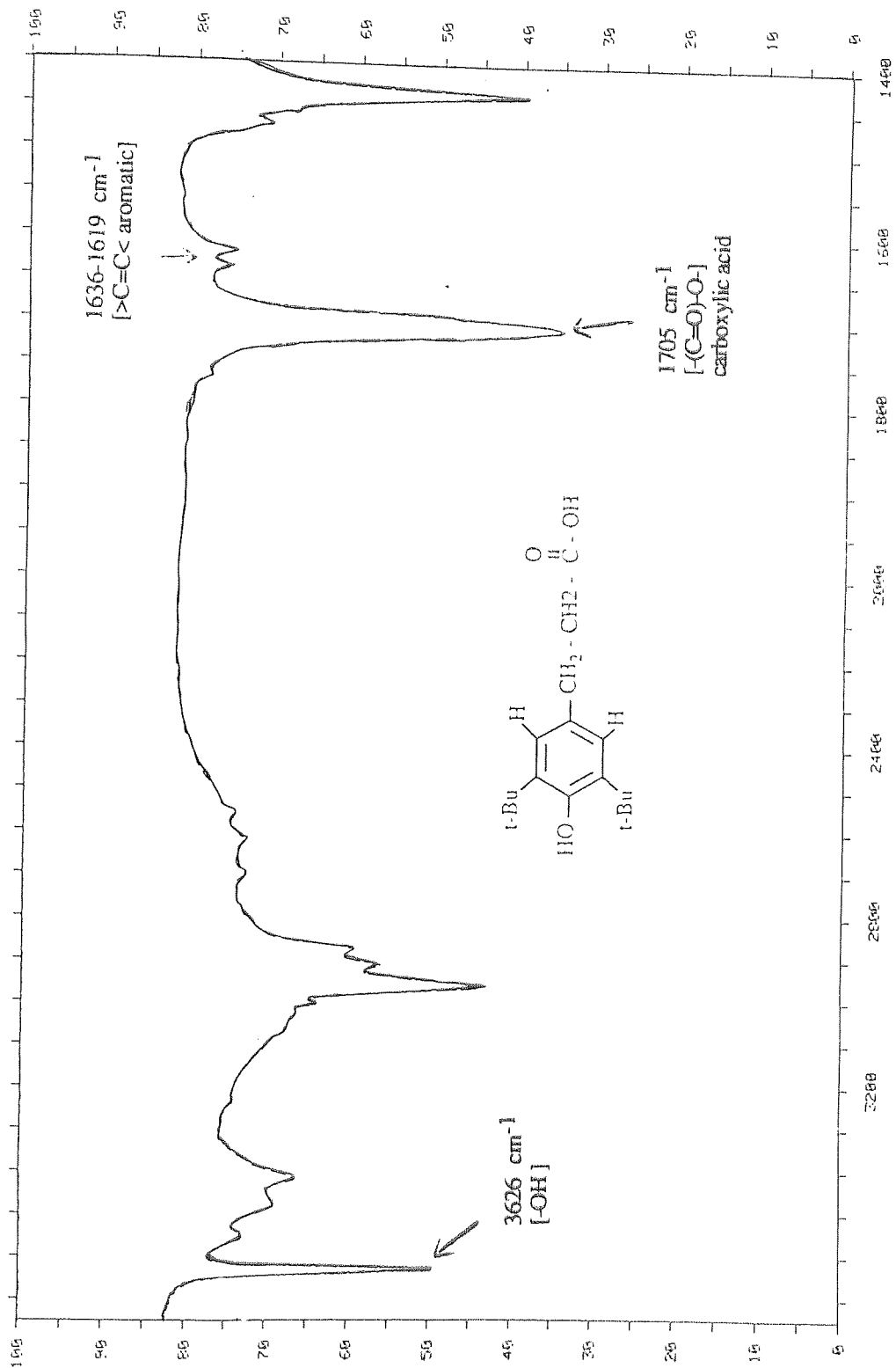


Figure 2.10 FTIR spectrum of 3-(3',5'-di-tert-butyl-4-hydroxy phenyl) propionic acid, Irganox acid in KBr disc.

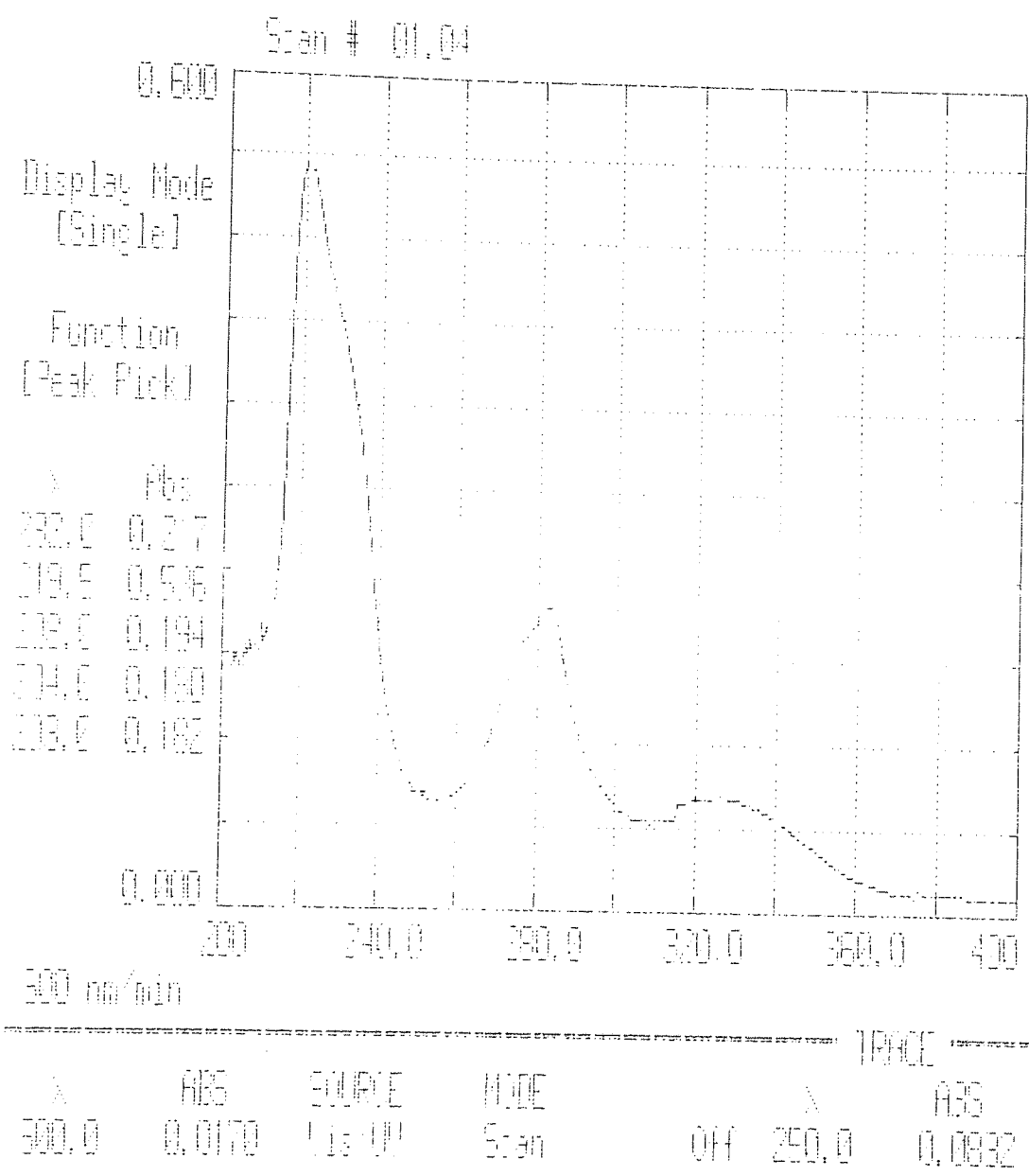


Figure 2.10a UV spectrum of 3-(3',5'-di-tert-butyl-4-hydroxy phenyl) propionic acid, Irganox acid in DCM solution.

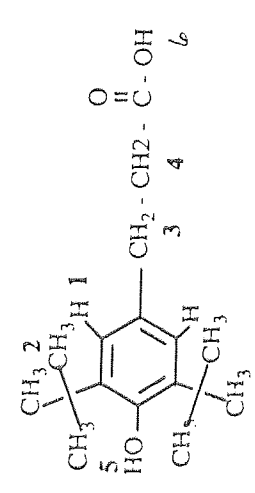
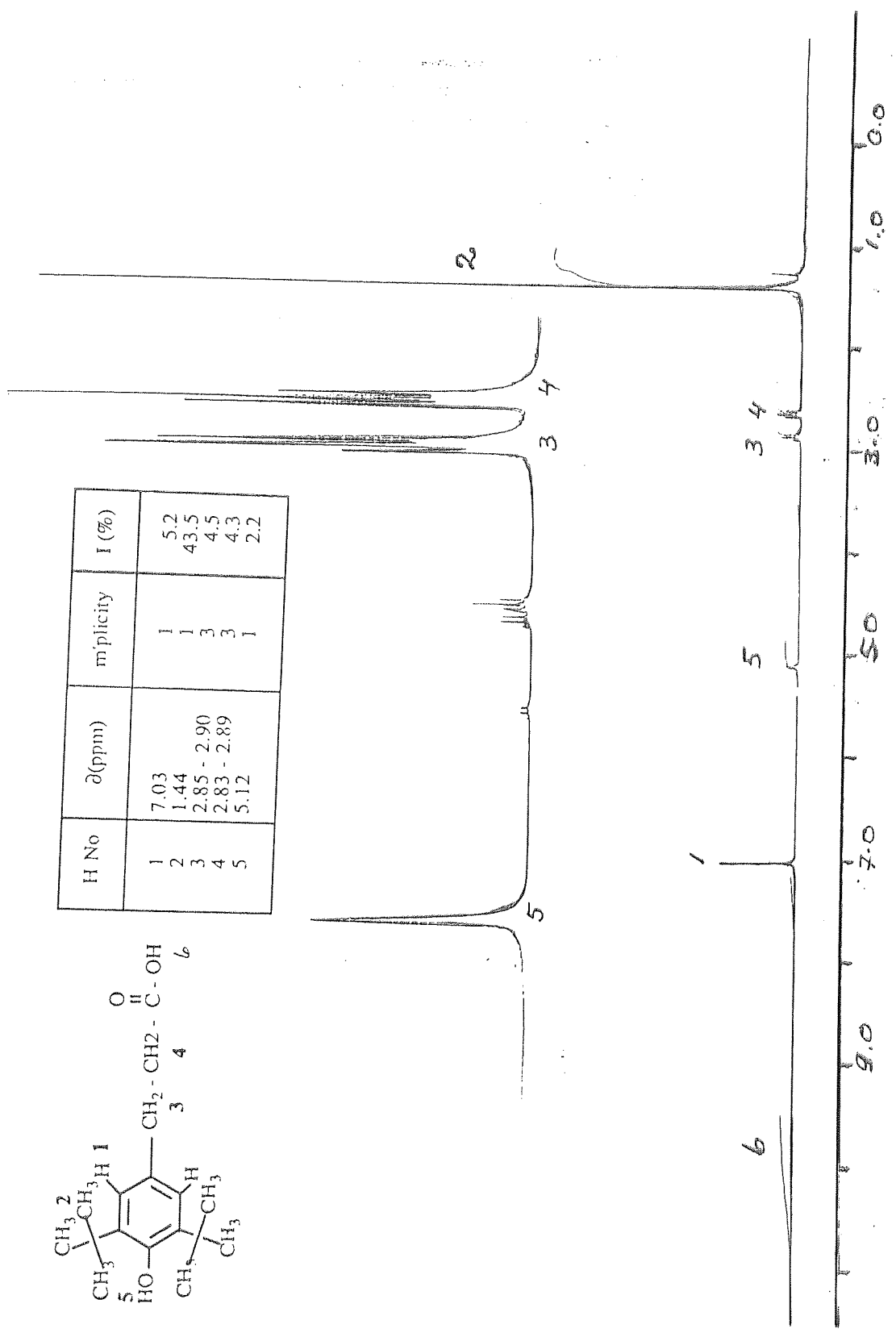


Figure 2.11 Proton NMR spectrum of 3-(3',5'-di-tert-butyl-4-hydroxyphenyl) propionic acid, H_2O acid in CDCl_3 .

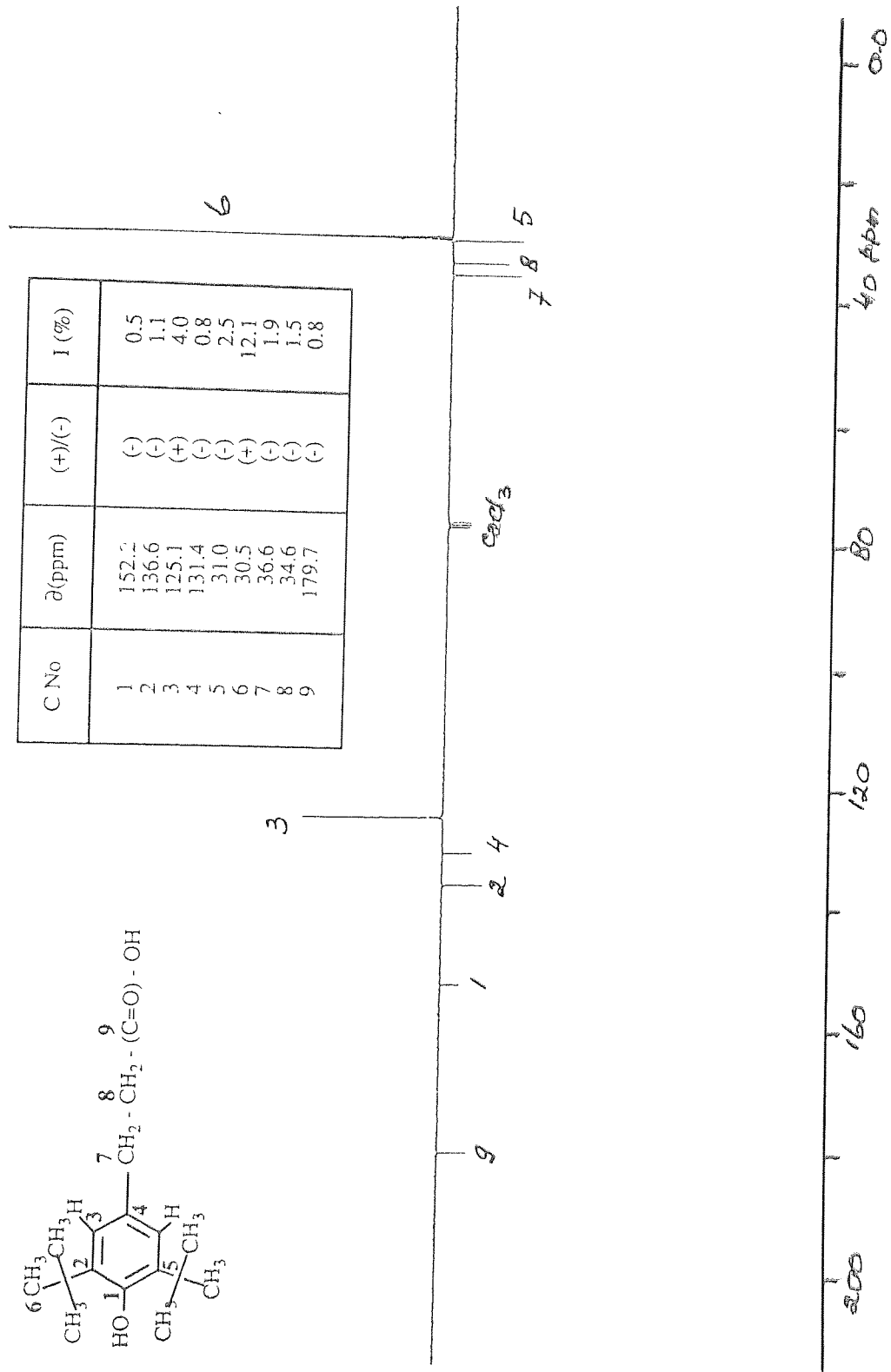


Figure 2.12 C-13 NMR spectrum of 3-(3',5'-di-tert-butyl-4-hydroxyphenyl) propionic acid, Irznox acid in CDCl₃

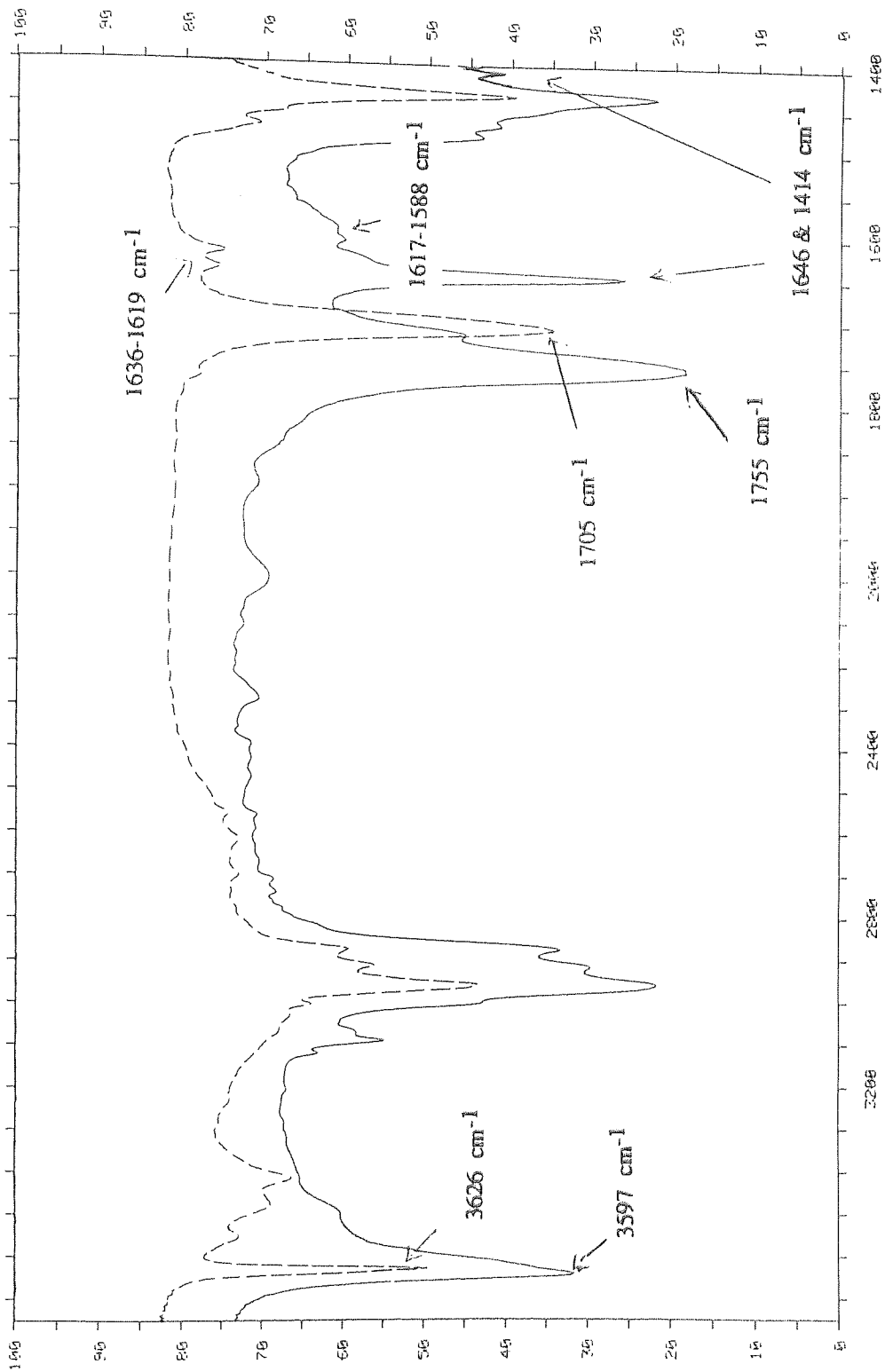


Figure 2.13 Comparison FTIR spectra in region 4000-1400 cm^{-1} of Vinyl-3-(3',5'-di-tert.butyl-4-hydroxy phenyl) propionate, VDBP (—) with that of Irg-Acid (---) in KBr disc.

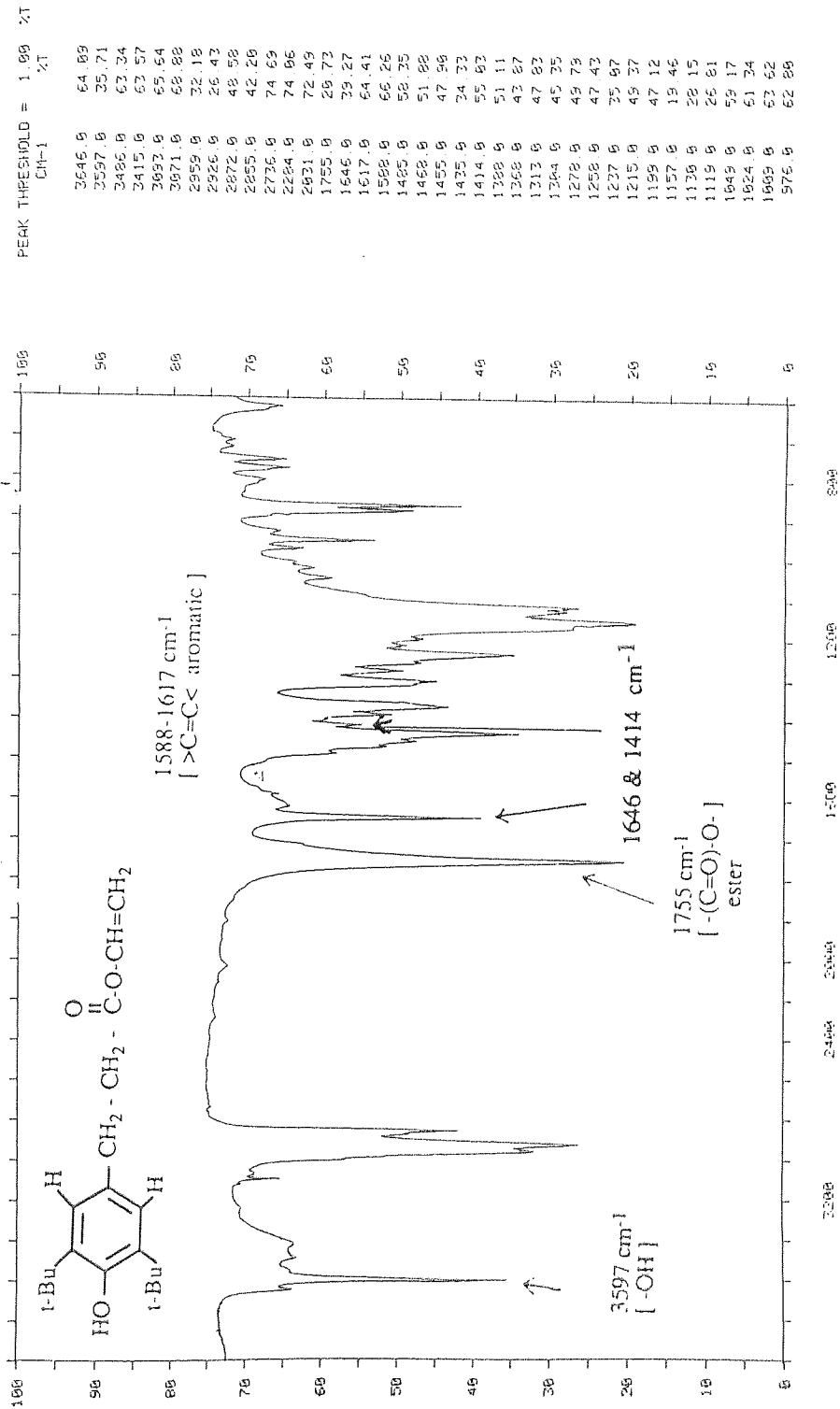


Figure 2.14 FTIR spectrum of Vinyl-3-(3',5'-di-tert-butyl-4-hydroxyphenyl) propionate, VDBP in KBr disc.

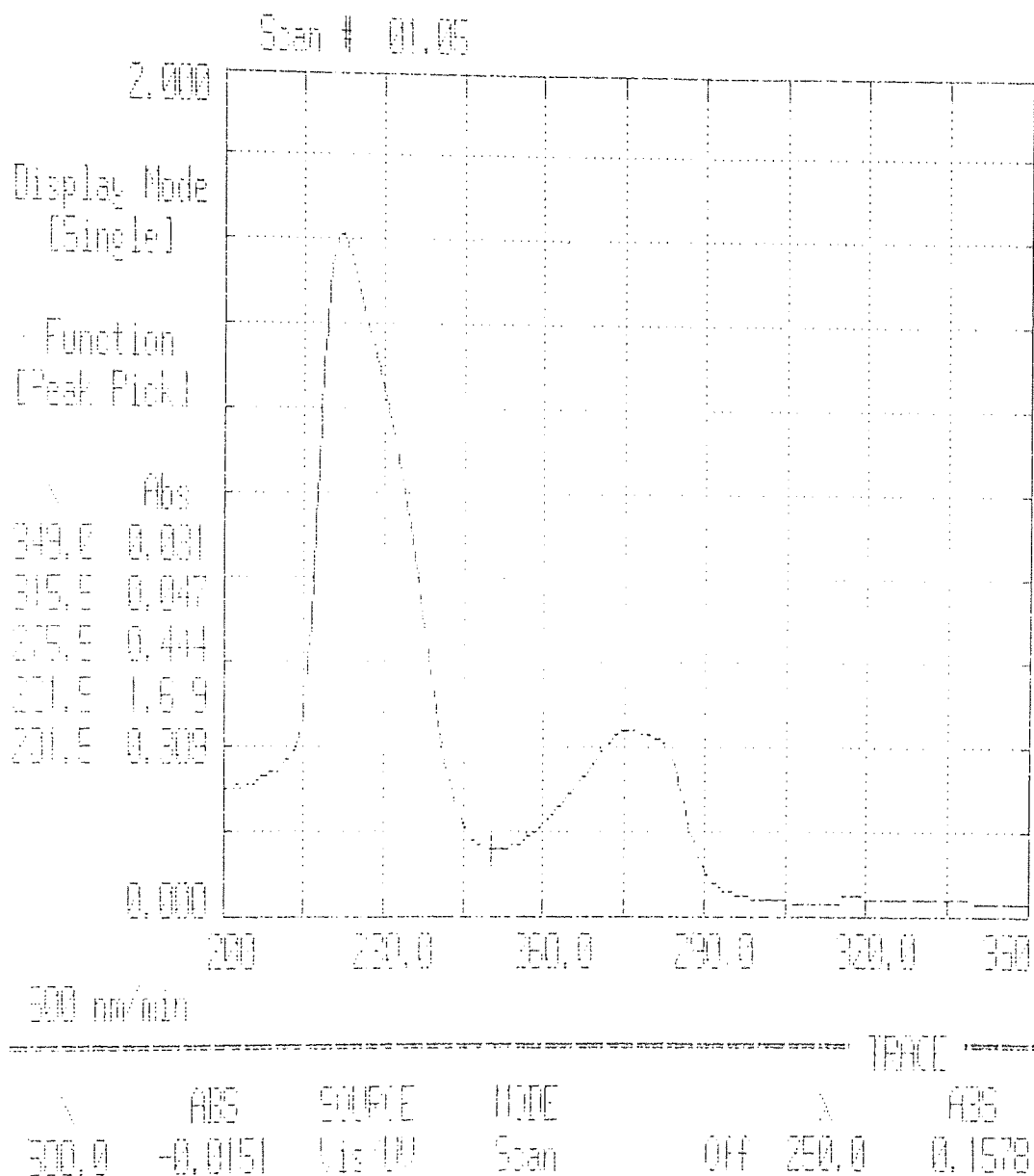


Figure 2.14a UV spectrum of Vinyl-3-(3',5'-di-tert-butyl-4-hydroxy phenyl) propionate, VDBP in DCM solution.

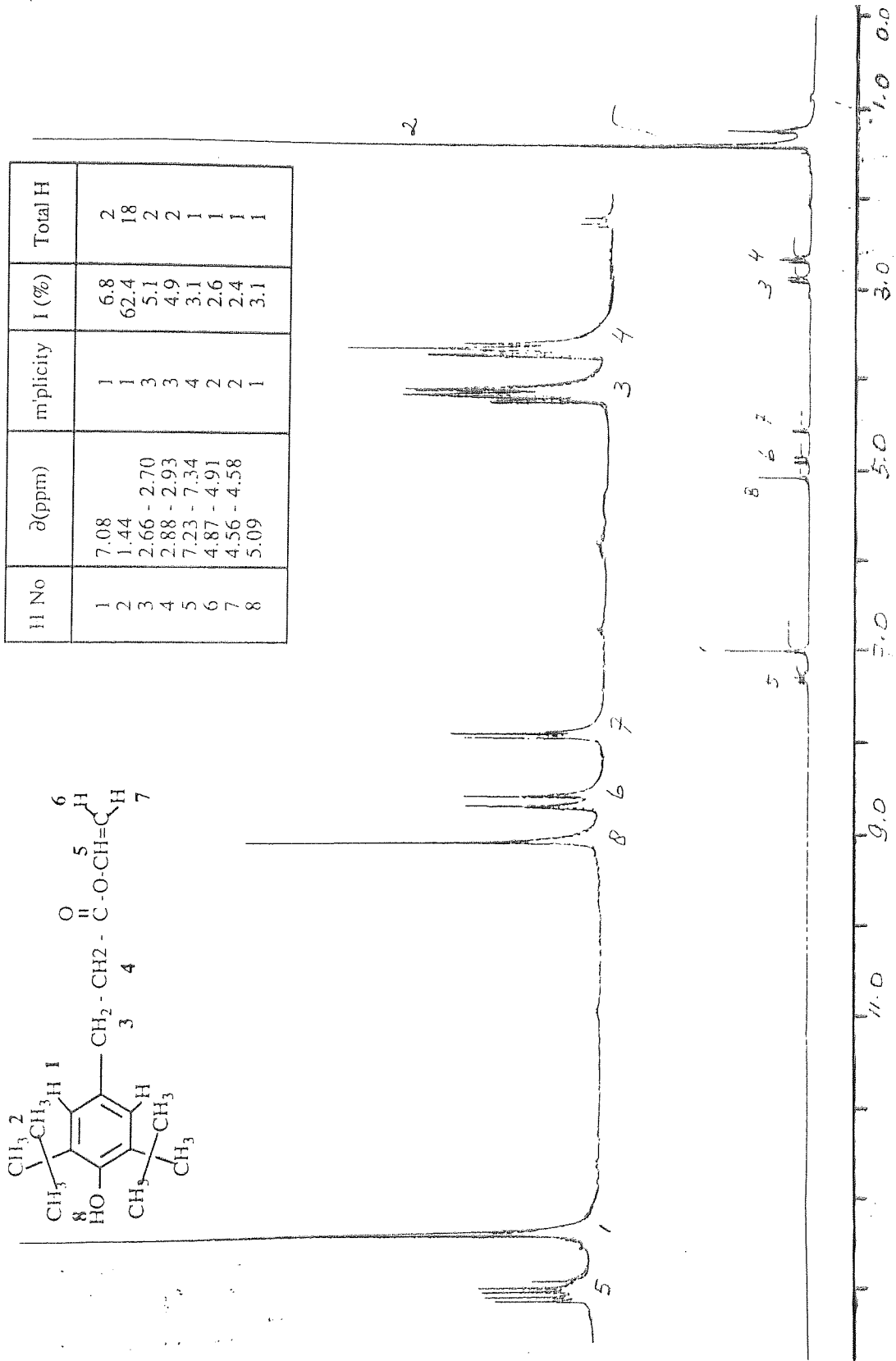


Figure 2.15 Proton NMR spectrum of Vinyl-3-(3,5-di-tert-butyl-4-hydroxy phenyl) propionate, VDBP in CDCl₃.

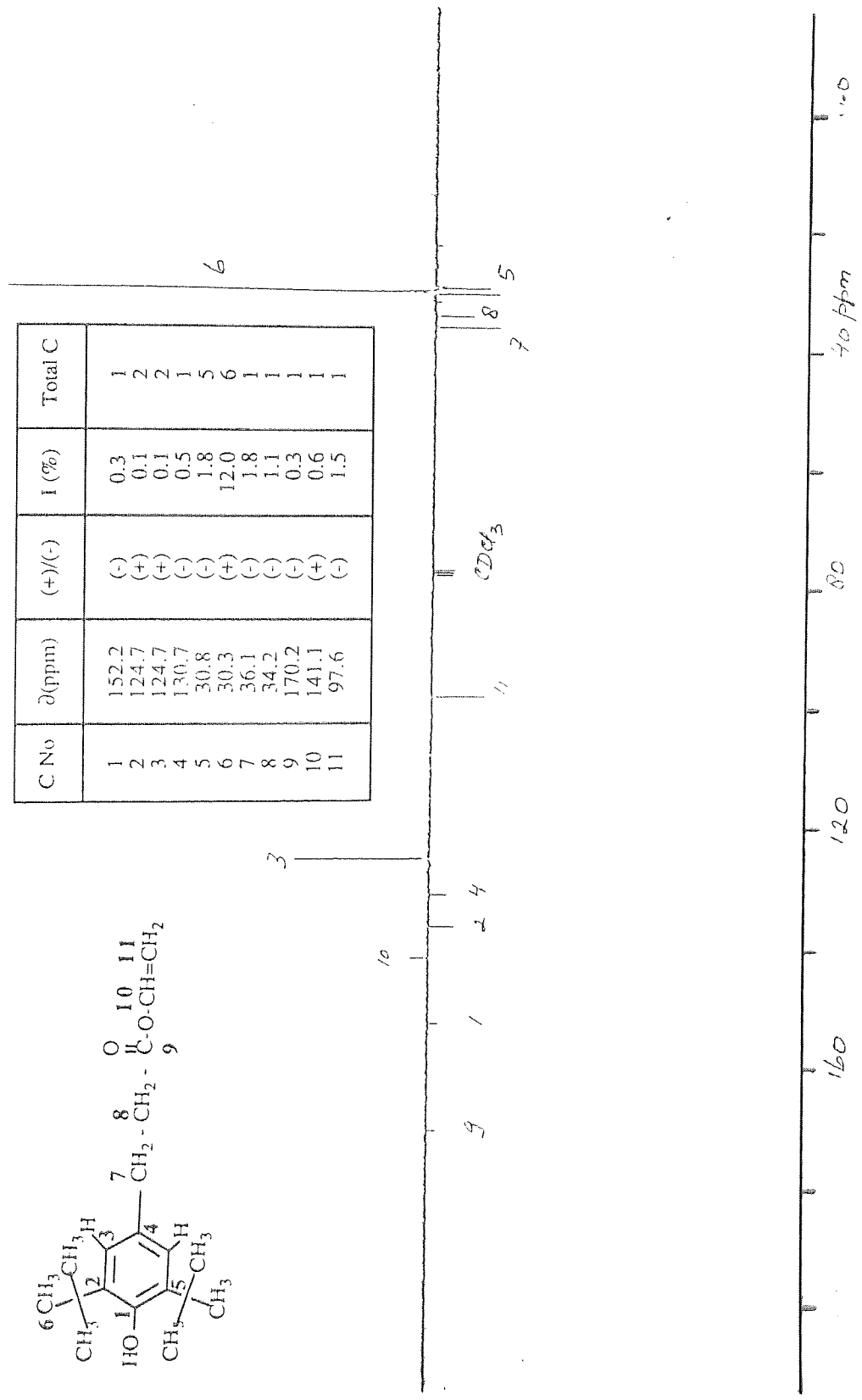


Figure 2.16 Carbon-13 NMR spectrum of Vinyl-3-(3',5'-di-tert-butyl-4-hydroxy phenyl) propionate, VDBP in CDCl₃.

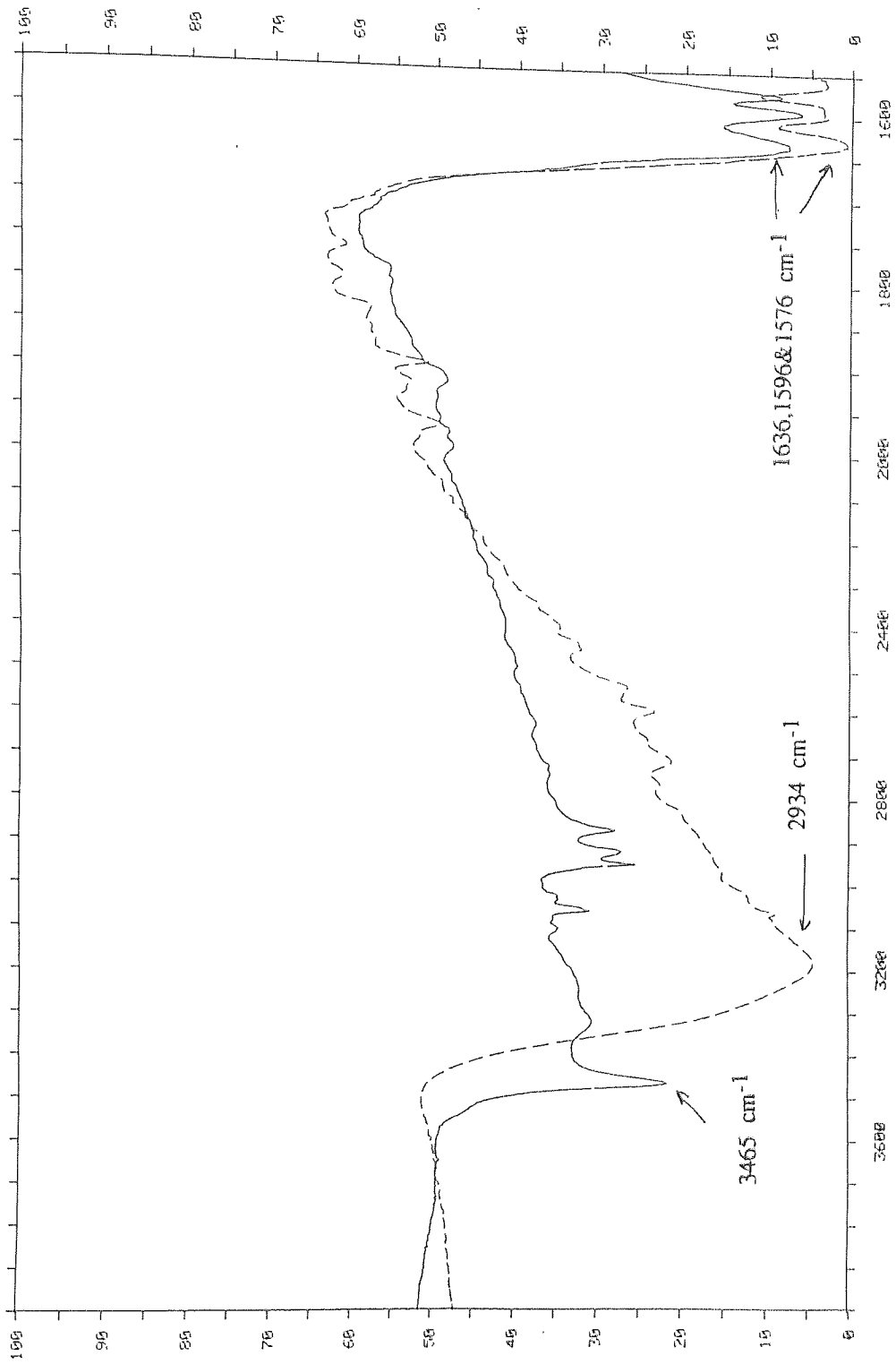


Figure 2.17 Comparison FTIR spectra in region 4000-1400 cm^{-1} of 2-hydroxy-4-(beta hydroxy ethoxy) benzophenone, HHBP (—) with that of DHBP (---) in KBr disc.

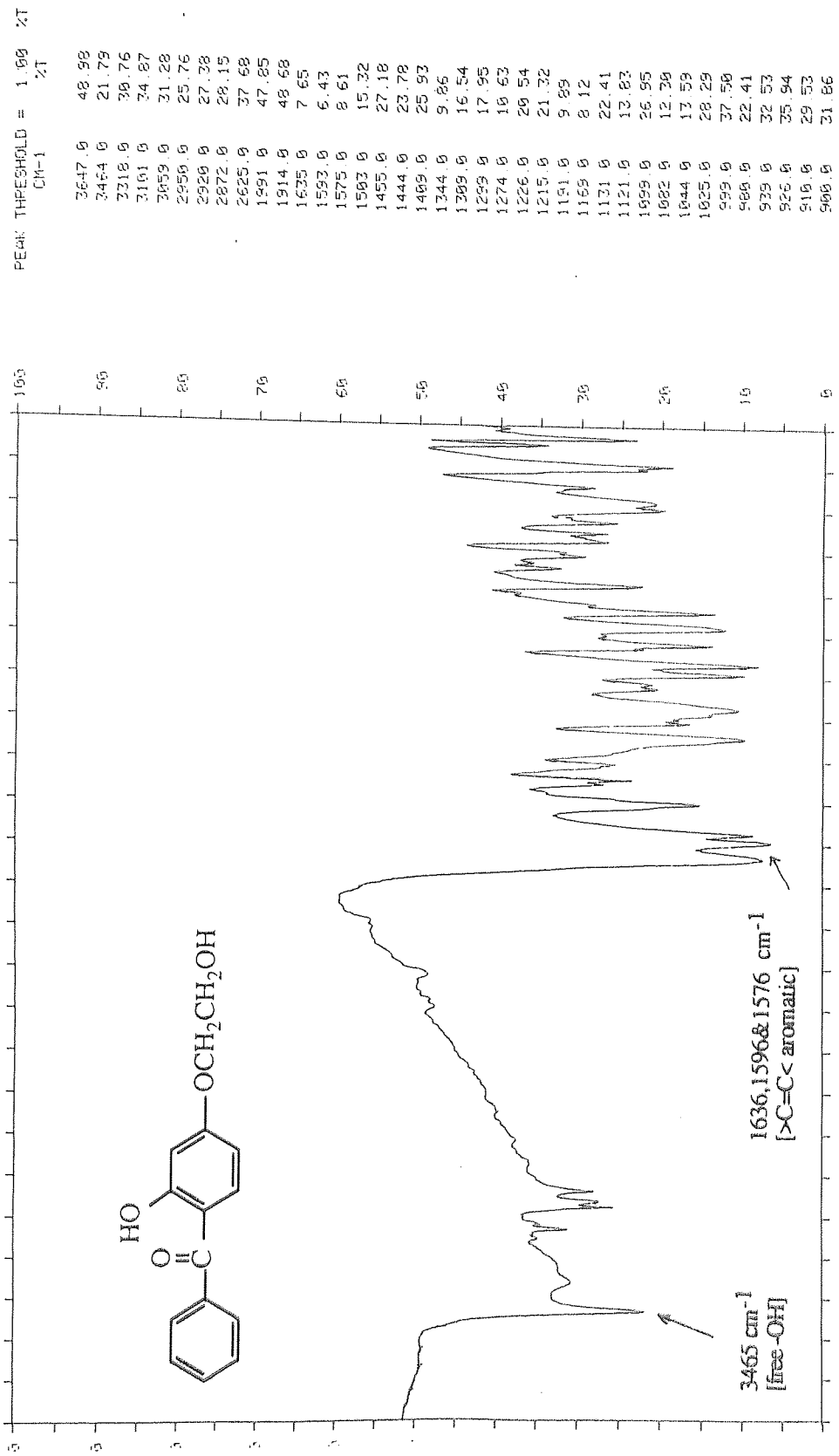


Figure 2.18 FTIR spectrum of 2-hydroxy-4-(beta hydroxy ethoxy) benzophenone, HHBP in KBr disc.

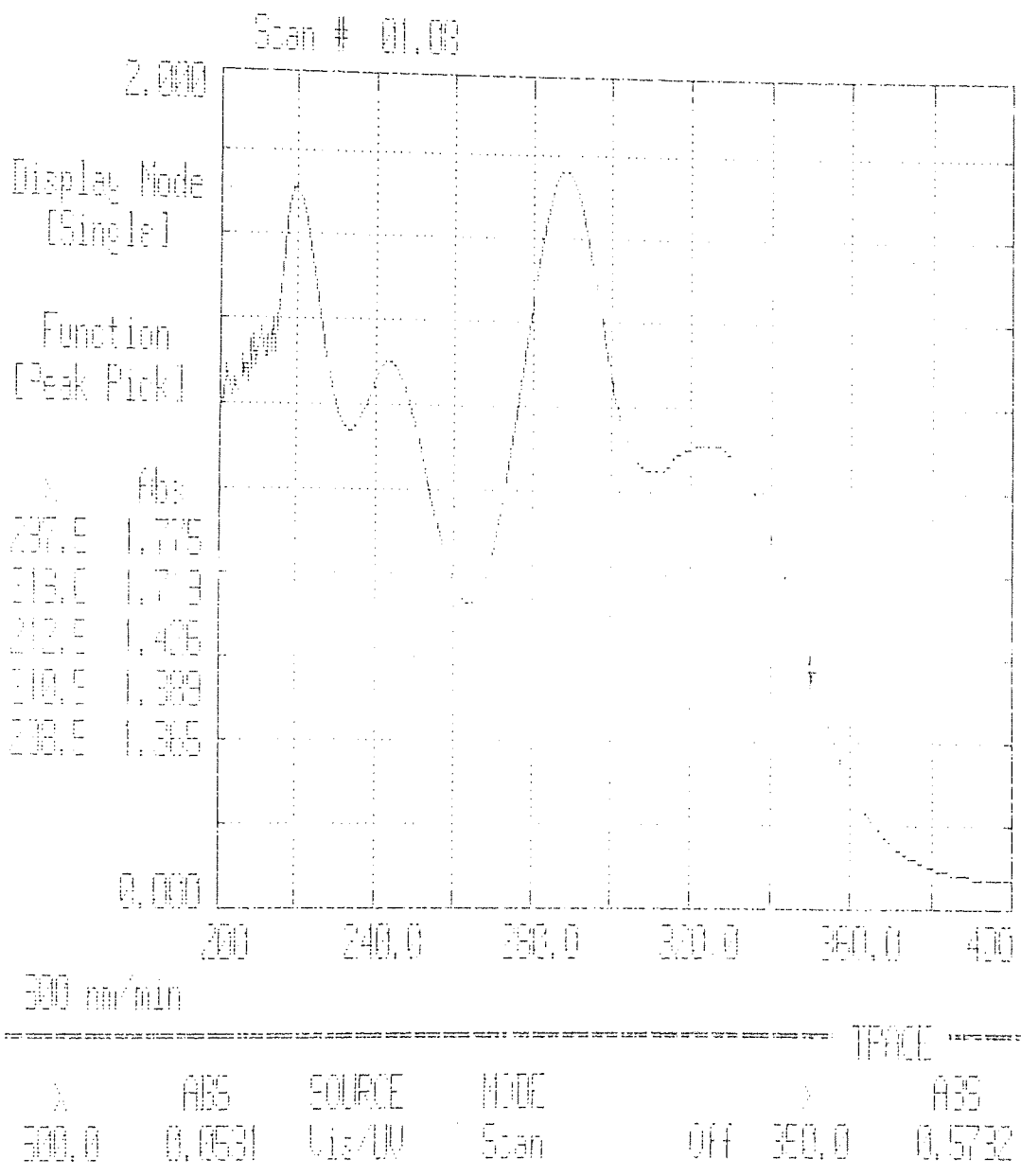


Figure 2.18a UV spectrum of 2-hydroxy-4-(beta hydroxy ethoxy) benzophenone, HHBP in DCM solution.

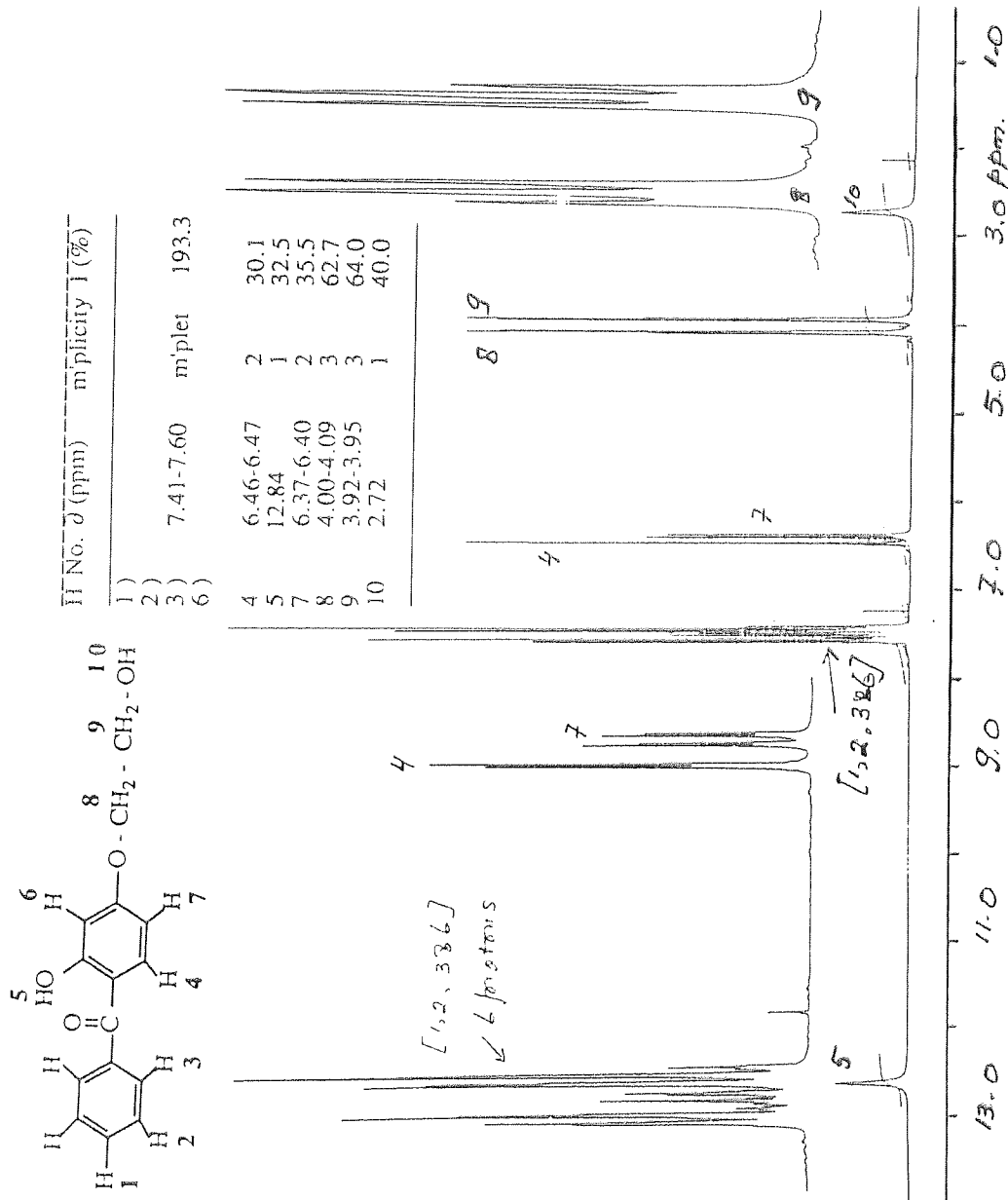


Figure 2.19 Proton NMR spectrum of 2-hydroxy-4-(beta hydroxy ethoxy) benzophenone, HHP in deuterated chloroform.

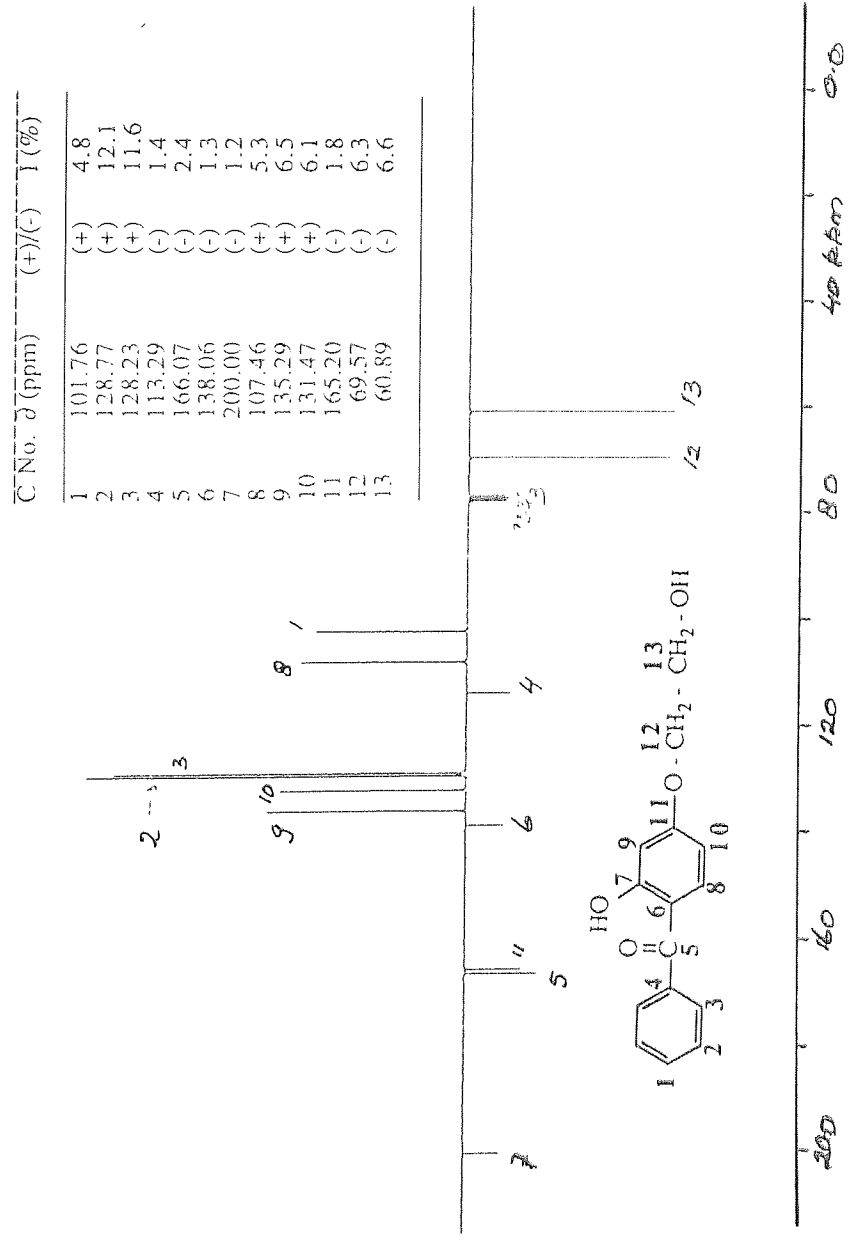


Figure 2.20 Carbon-13 NMR spectrum of 2-hydroxy-4-(beta hydroxy ethoxy) benzophenone, HHPB in deuterated chloroform.

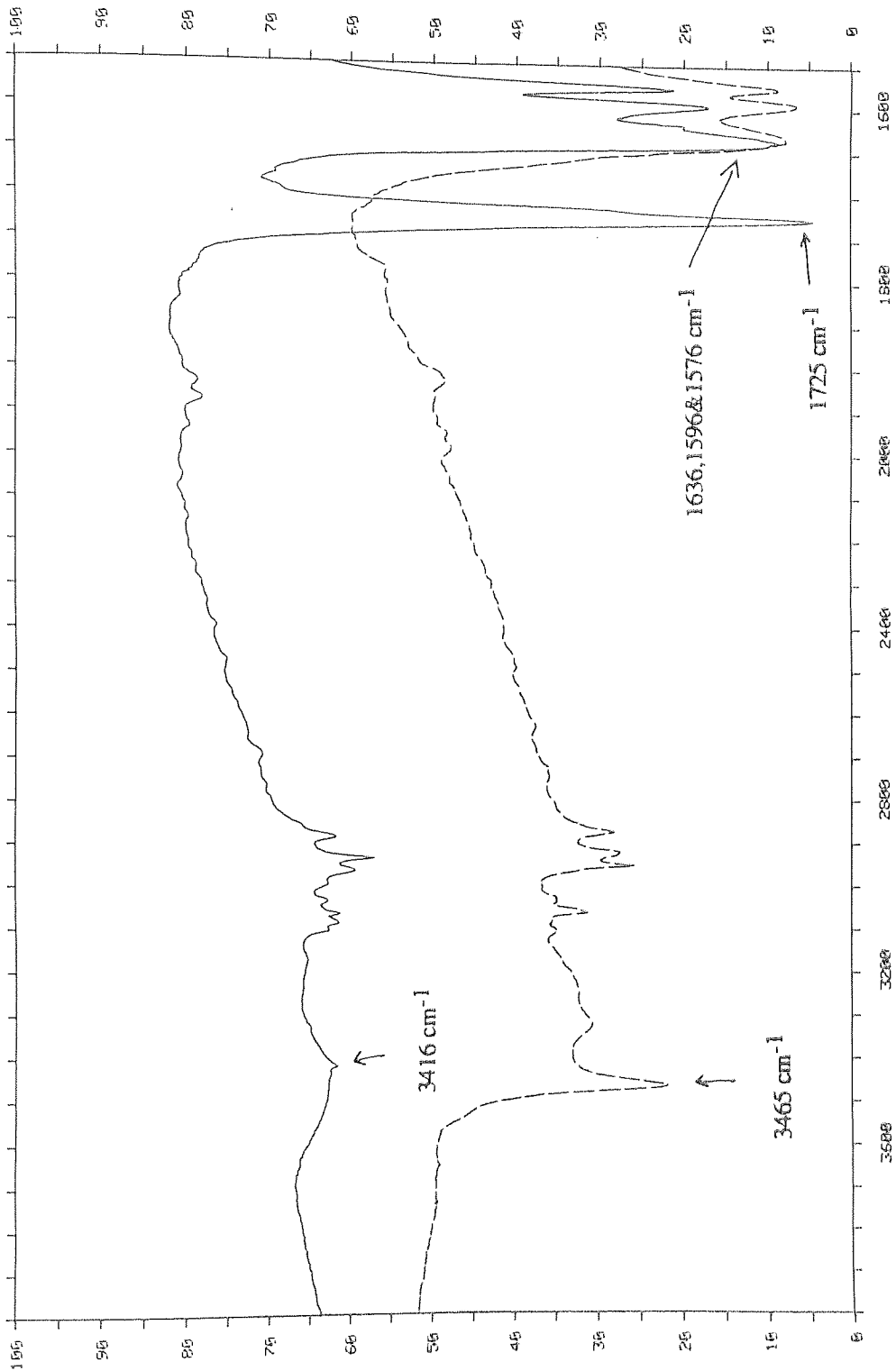


Figure 2.21 Comparison FTIR spectra in region 2500-1400 cm⁻¹ of 2-hydroxy-4-(beta acrylate ethoxy) benzophenone, HAEB (---) with that of HHPB (—) in KBr disc.

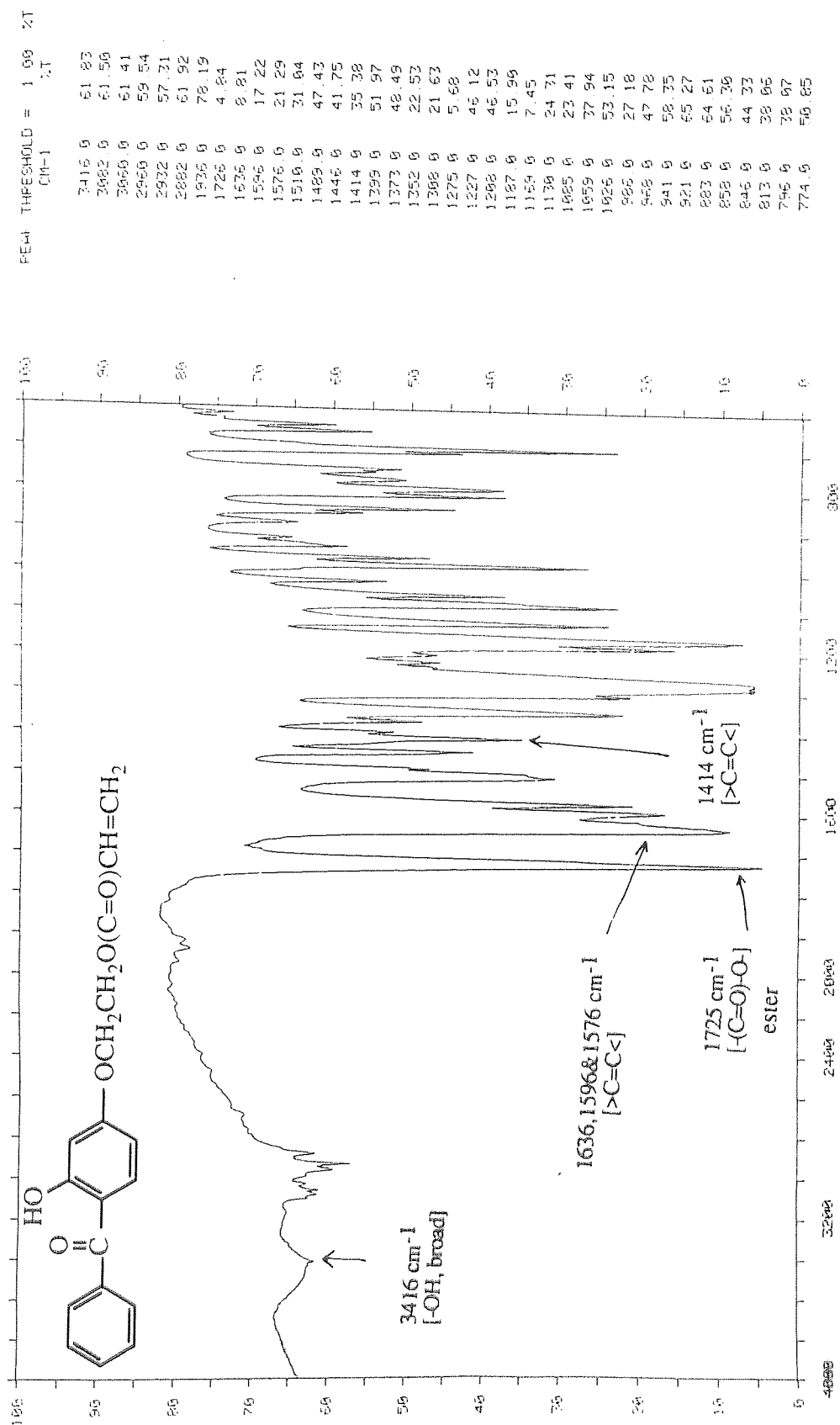


Figure 2.22 FTIR spectrum of 2-hydroxy-4-(beta acrylate ethoxy) benzophenone, HAEB in KBr disc.

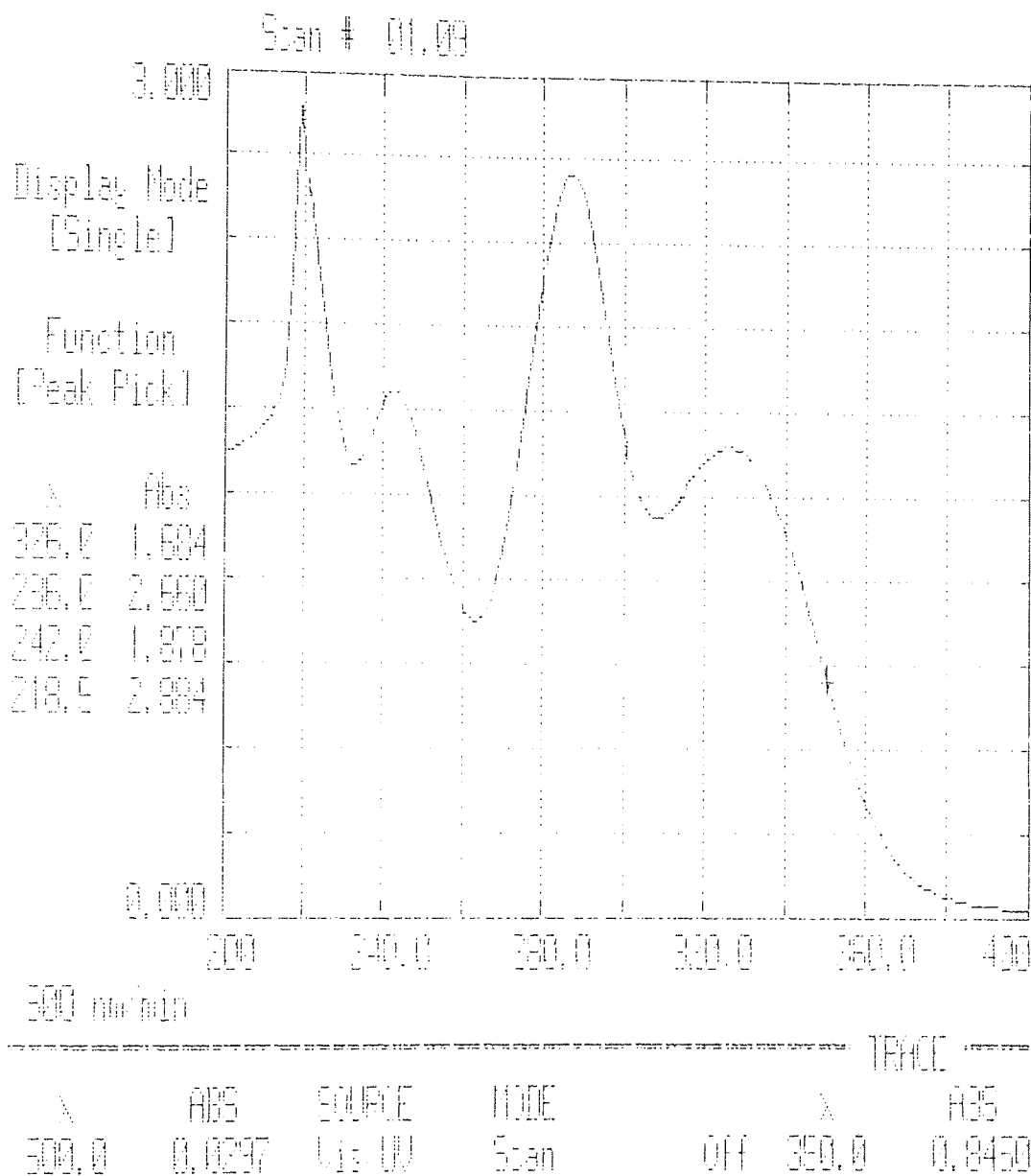


Figure 2.22a UV spectrum of 2-hydroxy-4-(beta acrylate ethoxy) benzophenone, HAEB in DCM solution.

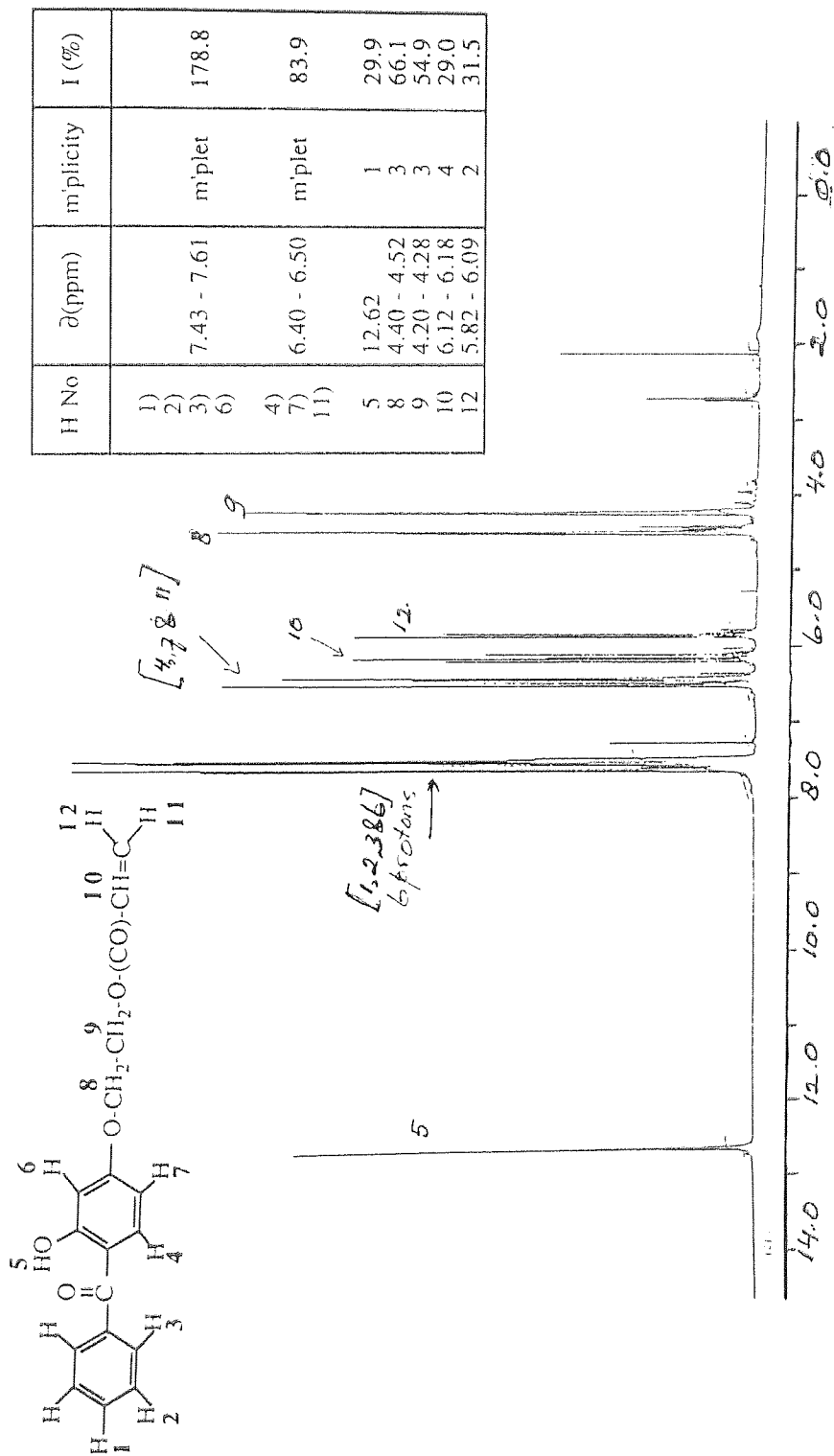


Figure 2.23 Proton NMR spectrum of 2-hydroxy-4-(beta acrylate ethoxy) benzophenone, HAEB in deuterated chloroform.

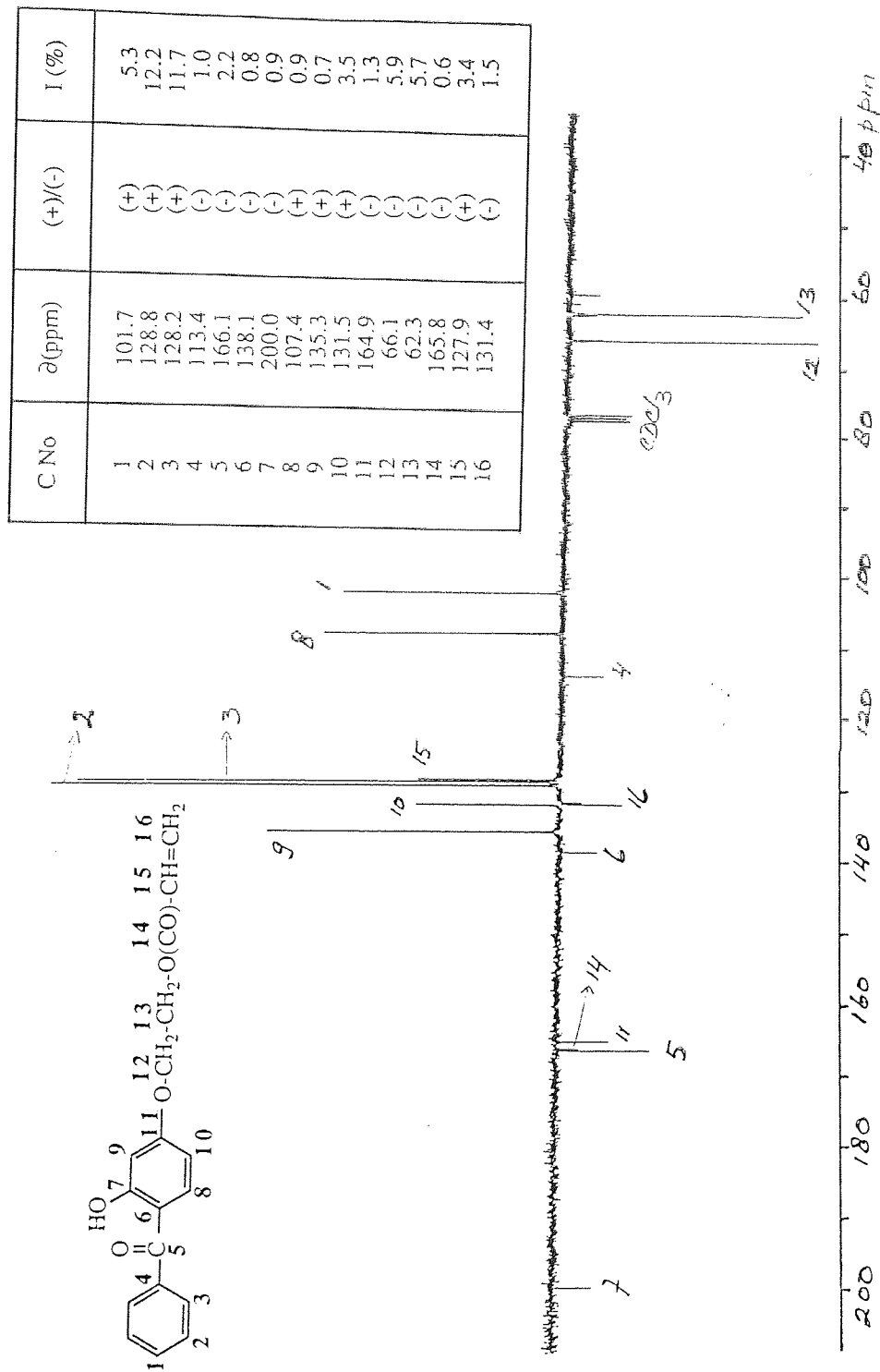


Figure 2.24 Carbon-13 NMR spectrum of 2-hydroxy-4-(beta acrylate ethoxy) benzophenone, H.A.E.B. in deuterated chloroform.

CHAPTER THREE

OPTIMISATION OF GRAFTING EFFICIENCY OF ANTIOXIDANTS CONTAINING HINDERED PHENOL AND BENZOPHENONE FUNCTIONS IN POLYPROPYLENE USING REACTIVE PROCESSING PROCEDURE

3.1 OBJECT AND METHODOLOGY

Two reactive antioxidants containing hindered phenol and benzophenone functions (DBBA and HAEB see Table 3.1) were synthesised (see Chapter 2 section 2.2). One of the ways in which the substantivity of antioxidants in polymers may be maximised is by chemically attaching the antioxidant to the polymer backbone^(107,113,114,157,177-182). In this chapter, the above reactive antioxidants are chemically attached to polypropylene using a reactive processing procedure. Here, the reactive processing is defined as a chemical reaction of reactive antioxidant onto the polymer backbone in the melt using a free radical initiator. Previous works^(107,113,114,157,177-182) indicate that more than 40% of the antioxidant is lost from the polymer matrix following Soxhlet extraction using DCM or acetone. The binding efficiency is usually low (~ 20 - 30%). Earlier works at Aston^(12,13) have shown that the binding efficiency of functionalised additives can be extended up to 100% in the presence of an enhancing agent (coagent) which contains more than one polymer reactive groups. Table 3.1a gives a list of the coagents used in the present work to improve the binding efficiency of DBBA and HAEB in polypropylene. Masterbatches containing "bound" antioxidants are prepared, and their binding efficiency is examined as a function of the different processing parameters, e.g. temperature and time processing, antioxidant concentration, concentration of peroxide and coagents.

3.1.1 Evaluation of Binding Efficiency of Antioxidants in Masterbatch Films

The general experimental procedure used for the work described in this chapter is summarised below. Unstabilised polypropylene was tumble mixed at room temperature in small amount of dichloromethane with various concentrations (3 - 20%, w/w) of DBBA or HAEB antioxidants (see Table 3.1), free radical initiator, FRI (molar ratio of FRI to antioxidant of 0 - 0.02) and a multi functionalised coagent (concentration 1 - 4%, w/w). The mixture was then vacuum evaporated at room temperature. 35 gram of the mixture was then processed in a Hampden Rapra Torque Rheometer at 180° C (setting temperature of the machine's heater) for 10 minutes, under closed mixing condition (this is the standard processing condition used throughout the work unless otherwise stated) to form masterbatch (concentrate) of antioxidant. These masterbatches were then characterised for melt viscosity (melt flow index, MFI), gel content and molecular weight distribution. Compression moulded films (identical thickness 0.1 - 0.2 mm) were used to measure binding efficiency of antioxidants, described previously (see Section 2.4). The extraction of polymer samples film to remove all unbound antioxidants was carried out in DCM (good solvent for the antioxidants) using a Soxhlet extractor until no more antioxidants could be extracted. The calculation of the binding efficiency of DBBA and DBBA+DVB in masterbatch films was based on measuring the ratio of carbonyl indices before and after extraction in DCM using FTIR spectroscopy (see Section 2.4 and Figures 3.1 and 3.1b). The binding efficiency of DBBA in the presence of Tris coagent was calculated from FTIR measurements of the hydroxyl indices (without interfering absorption of Tris compound) of masterbatch films before and after extraction (see Section 2.4 and Figure 3.1a). The binding efficiency of HAEB masterbatch film can be calculated either using FTIR or UV spectroscopy, by comparing the carbonyl index or absorption area, respectively, before and after Soxhlet extraction in DCM (see Section 2.4 and Figure 3.2a). In the presence of Tris the binding efficiency of HAEB was determined by comparing the UV spectra absorption of HAEB before and after extraction (see Section 2.4 and Figure 3.2b), to avoid the

problem of interference of the carbonyl function of Tris in FTIR measurement of HAEB-containing masterbatch films. A flow diagram describing the procedure of reactive processing used is shown in Scheme 3.1.

Table 3.1 Acrylic ester derivatives of hindered phenol and benzophenone antioxidants used

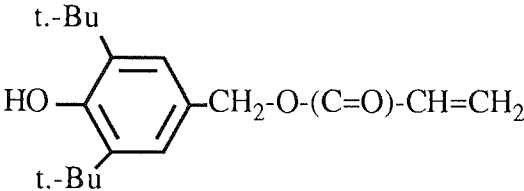
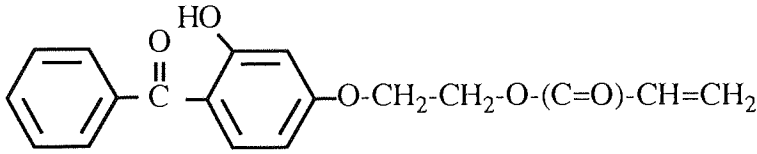
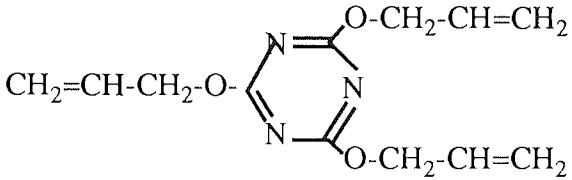
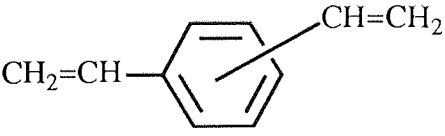
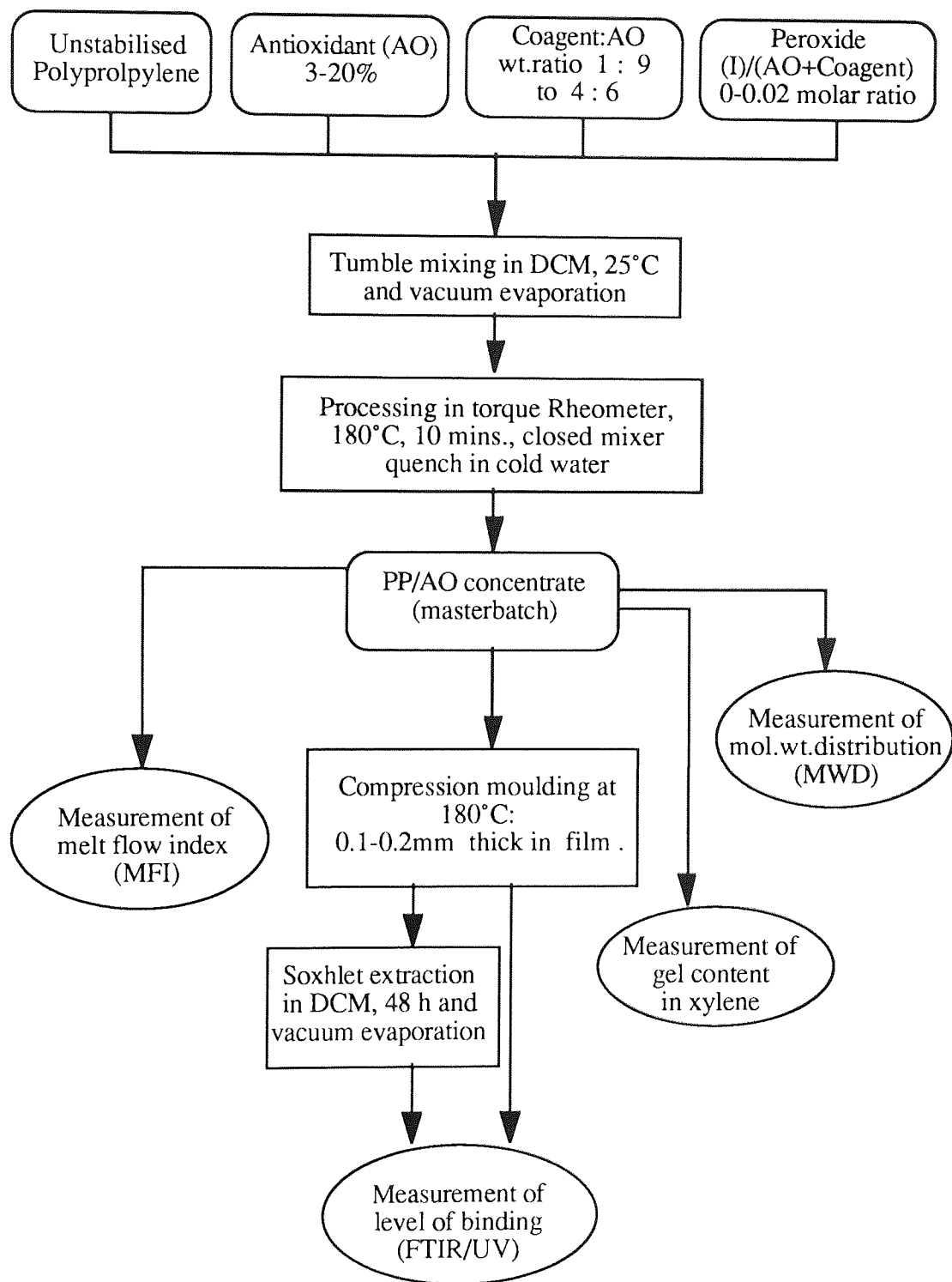
Structure number	Chemical structure, name and molecular weight (MW)	Abreviation
I	 <p>3,5-di-tert.-butyl-4-hydroxy benzyl acrylate (MW =296)</p>	DBBA
II	 <p>2-hydroxy-4-(beta acrylate ethoxy) benzophenone (MW=312)</p>	HAEB

Table 3.1a Various coagent used to extend the binding efficiency of antioxidants

Structure number	Chemical structure, name and molecular weight (MW)	Abreviation
III	$\left[\text{CH}_2=\text{CH}-(\text{C}=\text{O})-\text{O}-\text{CH}_2 \right]_3-\text{C}-\text{CH}_2-\text{CH}_3$ <p>Tri-methylol propane tri-acrylate (MW = 296)</p>	TMPTA (Tris)
IV	 <p>2,4,6-tri-allyl-oxy 1,3,5- triazine (MW = 250)</p>	TAC
V	 <p>Divinyl benzene (MW = 131)</p>	DVB



Scheme 3.1 Flow chart for a typical Reactive Processing Procedure and polymer test and characterisation

3.2 RESULTS

3.2.1 Optimisation of Conditions to Achieve High level of Binding of 3,5-di tert.-butyl-4-hydroxy benzyl acrylate (DBBA) in Polypropylene.

Assessment of the binding efficiency of antioxidants in polypropylene were calculated as has been mentioned in Section 2.4 and 3.1. To examine the binding efficiency of 3,5-di tert.-butyl-4-hydroxy benzyl acrylate (DBBA), this antioxidant was reactively processed in unstabilised polypropylene (PP) using the general procedure described in Scheme 3.1 stage B, C and D and see Section 2.3 & 2.4 and 3.1.1 for more detail. In order to optimise the efficiency of binding reactions the effect of processing parameters and the effect of chemical composition of the agents (antioxidants and peroxide) and coagent (additional functional monomers) were examined. Processing parameters (time and temperature) were optimised to achieve most efficient binding of the antioxidant. Similarly, the concentration of DBBA, peroxide initiator (Trigonox 101) and the type and concentration of the coagent used were optimised to achieve high binding level of the antioxidant.

3.2.2 Effect of Processing Condition on Efficiency of Binding of DBBA on Polypropylene During Melt Processing

Temperature and time are the two main process parameters which can effect the efficiency of binding of antioxidants on the polypropylene melt

3.2.2.1 Effect of processing temperature on the binding efficiency of DBBA in polypropylene

Table 3.1b and Figure 3.3 show that temperature plays an important role on the binding efficiency of DBBA in the polypropylene melt. Generally, the binding efficiency of DBBA increases with temperature up to 180°C, after which the level of binding decreases with further increase of temperature. The MFI values of masterbatches show an increase at

higher processing temperatures which suggests the occurrence of chain scission and polymer degradation. The optimum processing temperature of 180°C was chosen because high binding efficiency was obtained with acceptable MFI values.

Table.3.1b Binding efficiency and Melt flow index (MFI) of masterbatches (MB's) containing 10% DBBA in polypropylene in the presence of 0.02 molar ratio, m.r.(I/DBBA) Trigonox 101, processed at different temperatures for 10 minutes under closed mixer condition

No sample	Processing Temperature, °C	[Trig.101]/[AO] (m.r.)	Binding* (%)	MFI (g/10 mins)
1	160	0.02	17	0.99
2	170	0.02	28	1.02
3	180	0.02	40	1.65
4	190	0.02	35	1.95
5	200	0.02	30	2.45

* Measured ratio of carbonyl area indices by IR spectroscopy, see Fig.3.1

3.2.2.2 Effect of processing time on the binding efficiency of DBBA in polypropylene

Processing time also influences the binding efficiency of DBBA in a polypropylene melt. Table 3.2 and Figure 3.3a shown that different binding levels can be achieved during processing of 10% DBBA in polypropylene for different of time, e.g. 5, 10, 15 and 20 minutes in Torque Rheometer under closed conditions. Generally, the binding efficiency of DBBA increases with processing time, but at the same time the MFI values decrease, indicating chain scission and polymer degradation. The optimum processing time which gives a high levels of binding and an acceptable MFI value was found to be 10 minutes and was used throughout this work.

Table.3.2 Binding efficiency and Melt flow index (MFI) of masterbatches (MB's) containing 10% DBBA in polypropylene in the presence of 0.02 molar ratio, m.r.(I/DBBA) Trigonox 101, processed at various processing time at 180°C under closed mixer condition

No sample	Processing Time (mins)	[Trig.101]/[AO] (m.r.)	Binding* (%)	MFI (g/10 mins)
1	5	0.02	20	1.09
2	10	0.02	40	1.65
3	15	0.02	43	2.12
4	20	0.02	45	3.10

* Measured ratio of carbonyl area indices by IR spectroscopy, see Fig.3.1

3.2.3 Effect of Chemical Composition on Efficiency of Binding of DBBA on Polypropylene During Melt Processing

Some chemical compositions also play very important role on determination of the binding efficiency of DBBA in polypropylene. Effects of initiator, DBBA concentration, type and coagent concentration are investigated under this section.

3.2.3.1 Effect of free radical initiator (Trigonox 101) on the binding efficiency of DBBA in polypropylene

Effect of varying the concentration of the free radical initiator on the binding efficiency of DBBA is shown in Table 3.3. In the absence of FRI no binding occurs while increasing peroxide concentration increases the binding level. However, it is important to note that while highest peroxide molar ratio (m.r.) of FRI to antioxidant, I/AO, (e.g. 0.03), increases the efficiency of binding, the MFI values also increase, indicating chain scission and polymer degradation, see Figure 3.4. Molecular weight distribution data (see Table 3.4 and Figure 3.5) support this and shows that the increase in initiator concentration lowers MW obtained. From Table 3.3 it is shown that the optimum binding with minimum effect on thermal degradation was therefore achieved by using initiator molar ratio (I/AO) of 0.02, see Figure 3.4 and 3.4a.

3.2.3.2 Effect of DBBA concentration on the binding efficiency

Table 3.5 and Figure 3.6 show that increasing the DBBA concentration up to a certain concentration (6-10%), is accompanied by an increase in efficiency of binding, after which the binding efficiency decreases with further increases in concentration. Table 3.5 and Figure 3.7 does not show any significant change in MFI values with increasing the DBBA concentration.

Table. 3.3 Binding efficiency and Melt flow index (MFI) of masterbatches (MB's) containing 6% &10% DBBA in polypropylene in the presence of (0-0.03 molar ratio,m.r.) Trigonox 101, processed in standard condition.

No sample	DBBA conc. (%)	[Trig.101]/[AO] content (m.r.)	Binding* (%)	MFI (g/10 mins)
	PP, processed	-	-	0.58
	PP, processed	0.002	-	1.34
	PP, processed	0.020	-	17.37
1	6	0.00	0	0.39
2	6	0.002	2	0.42
3	6	0.01	15	0.82
4	6	0.02	40	1.63
5	6	0.03	63	4.00
5	10	0.002	2	0.43
6	10	0.02	40	1.65
7	10	0.03	65	4.12

* Measured ratio of carbonyl area indices by IR spectroscopy, see Fig.3.1

Table 3.4 Molecular weight distribution data of polymer samples (masterbatches)

No	Polymer samples (masterbatches)	[FRI]/[AO] (m.r.)	Mw ($\times 10^{-5}$)	Mn ($\times 10^{-4}$)	D(MWD) Mw/Mn
1	PP, unprocessed	0.00	4.17	5.13	8.128
2	PP, processed	0.00	3.62	5.53	6.546
3	PP, processed	0.02	1.75	4.34	4.032
4	PP + DBBA 6%	0.00	4.10	5.75	7.130
5	PP + DBBA 6%	0.02	2.57	4.82	5.332
6	PP + DBBA 6%	0.03	2.01	4.15	4.843

Table. 3.5 Effect of DBBA concentration on the binding efficiency and Melt flow index (MFI) in polypropylene in the presence of 0.02 molar ratio (m.r.) Trigonox 101, processed in closed mixing condition at 180°C for 10 minutes

No	DBBA conc. (%)	[Trig.101]/[AO] (m.r.)	Binding* (%)	MFI (g/10 mins)
1	3	0.02	15	1.46
2	6	0.02	40	1.63
3	10	0.02	40	1.65
4	15	0.02	31	1.78
5	20	0.02	27	1.86
6	3	0.03	18	2.50
7	6	0.03	63	4.00
8	10	0.03	65	4.12
9	15	0.03	49	4.17
10	20	0.03	43	4.21

* Measured ratio of carbonyl area indices by IR spectroscopy, see Fig.3.1

3.2.4 Effect of Coagent on Binding Efficiency of DBBA in Polypropylene.

The binding levels of DBBA in polypropylene processed in the presence of 0.02 m.r Trigonox 101 was shown to be 40% (see Table 3.5), i.e. up to 60% of reactively processed DBBA can be lost from a masterbatch film when subjected to an aggressive environment, e.g. in the presence of DCM or acetone. To extend the binding efficiency of DBBA, different enhancing agents (coagent) were used (see Table 3.3).

Table 3.6 shows that binding efficiency up to 15% was achieved when DBBA was processed with various co-agents in the presence of a free radical initiator (Trigonox 101) at 0.002 m.r. (no binding was found in the absence of co-agent under the same conditions). To optimise the binding of DBBA using (Tris or DVB) coagents, the coagent ratio and the concentration of the free radical initiator (Trigonox 101) were varied, (experiments using co-agent Tac were discontinued due to low binding results).

Table. 3.6 Binding efficiency of DBBA in polypropylene (3%) processed with various co-agents (2%), in the presence of Trigonox 101 (0.02 m.r), in closed mixing condition at 180 C for 10 minutes.

No	[Trig.101]/[AO] m.r.	Coagents	Binding* (%)
1	0.002	None	0
2	0.002	Tris	9
3	0.002	Tac	4
4	0.002	DVB	15

* Measured both ratio of hydroxyl or carbonyl area indices by IR spectroscopy, see Fig. 3.1, 3.1a, and 3.1b

3.2.4.1 Optimisation of the binding efficiency of DBBA in polypropylene using DVB as a coagent

Further optimisation of the binding efficiency of DBBA using DVB as a coagent was carried out at various DBBA/DVB weight ratios and initiator concentrations. Table 3.7 shows that at a DBBA/DVB ratio of 5/5 and higher initiator concentration (0.02 m.r.) the binding efficiency of DBBA is increased quite sharply (up to 95%). The MFI value of the masterbatch in this case, however, decreases as DVB ratio increases (MFI is 0.10 g/10 minutes at DBBA/DVB ratio 5/5), which even much lower than that of processed unstabilised polypropylene (0.58 g/10 minutes, see Figure 3.8). Therefore, the optimum DBBA/DVB ratio which gives high binding efficiency and acceptable MFI value was taken to be 6/4, at 0.02 molar ratio [I]/[DBBA] peroxide, see Table 3.7.

Table 3.7 Binding efficiency of DBBA in Polypropylene film processed with various ratio of DVB coagent (total concentration of DBBA+DVB=10%) in the presence of FRI Trigonox 101 (0.002 or 0.02 m.r.), under standard condition.

No	[Trig.101]/[AO] (m.r.)	DBBA/DVB ratio	Binding* %	MFI g/10 mins
1	0.002	5/5	15	0.23
2	0.002	6/4	13	0.24
3	0.002	7/3	11	0.27
4	0.002	8/2	7	0.28
5	0.002	10/0	2	0.42
6	0.02	5/5	95	0.10
7	0.02	6/4	93	0.16
8	0.02	7/3	84	0.22
9	0.02	8/2	68	0.30
10	0.02	10/0	40	1.65

* Measured ratio of carbonyl area indices by IR spectroscopy, see Fig.3.1b

Table 3.8 shows the effect of initiator concentration on the binding efficiency of 10% masterbatches containing DBBA-DVB (ratio 6/4). The higher the concentration of the initiator, the higher the extent of binding but the lower the MFI values, see Figure 3.9. Results from molecular weight distribution show the opposite trend: i.e. an increase in free radical initiator concentration, leads to a decrease in the molecular weight (see Table 3.9 and Figure 3.9a). It is important to mention that molecular weight distribution measurement were carried out after filtration of the polymer sample solution. The insoluble fraction of the polymer sample, which contains high molecular weight cannot be analysed. On the other hand, MFI values were measured based on the entire polymer masterbatch.

Table 3.8 Effect of FRI concentration on the binding efficiency and MFI of 10% masterbatches (MB's) polypropylene containing DBBA-DVB ratio 6/4, processed in closed mixing condition at 180°C for 10 minutes

No	[Trig.101]/[AO] (m.r.)	Binding* (%)	MFI (g/10 mins)
1	PP processed no additive	-	0.58
2	0.000	5	0.45
3	0.005	17	0.35
4	0.010	70	0.22
5	0.020	93	0.16
6	0.030	97	0.07

* Measured ratio of carbonyl indices by IR spectroscopy, see Fig.3.1b

Table 3.9 Molecular weight distribution data of polymer samples of 10% masterbatches (MB's) polypropylene containing DBBA-DVB ratio 6/4, processed in closed mixing condition at 180°C for 10 minutes

No	Polymer samples (masterbatches)	[FRI]/[AO] (m.r.)	Mw (x10 ⁻⁵)	Mn (x10 ⁻⁴)	D(MWD) Mw/Mn
1	PP, unprocessed	0.00	4.17	5.13	8.128
2	PP, processed	0.00	3.62	5.53	6.546
3	PP, processed	0.02	1.75	4.34	4.032
4	PP + DBBA 6% + DVB 4%	0.00	3.35	4.84	6.921
5	PP + DBBA 6% + DVB 4%	0.005	3.31	5.47	6.029
6	PP + DBBA 6% + DVB 4%	0.02	2.22	5.02	4.422
7	PP + DBBA 6% + DVB 4%	0.03	1.59	3.51	4.530

3.2.4.2 Optimisation of binding efficiency of DBBA using TMPTA (Tris) as a coagent

Further experiments were carried out to find the optimum condition of binding efficiency of DBBA+Tris system at various weight ratios of DBBA/Tris. Table 3.10 shows that at the ratio of DBBA/Tris of 5/5 and the initiator concentration 0.02 molar ratio the highest binding is achieved (up to 94%). On the other hand, higher Tris concentration causes the increase in MFI values of the masterbatches. Results in Table 3.10, indicated that the optimum ratio of DBBA/Tris which gives high binding efficiency and acceptable MFI value is 6/4, see Figure 3.10.

Table 3.10 Binding efficiency of DBBA in Polypropylene film processed with various ratio of Tris coagent (total concentration of DBBA+Tris = 10%) in the presence of FRI Trigonox 101 0.02 m.r. [I]/[DBBA+Tris], under standard condition.

No	DBBA/Tris ratio	Binding* (%)	MFI (g/10 mins)
1	5/5	94	1.74
2	6/4	91	1.19
3	7/3	84	0.95
4	8/2	65	0.78
5	9/1	54	0.76
6	10/0	40	1.65
7	PP processed no additives	-	0.58
8	PP proc'd +0.02 m.r. FRI	-	17.37

* Measured ratio of hydroxyl area indices by IR spectroscopy, see Fig.3.1a

This ratio (4 to 6) was used to prepare polymer samples with a total concentration of DBBA+Tris of 6% and 10% (w/w), see Table 3.11 and Figure 3.11. The concentration of Trigonox 101 was varied from 0 to 0.03 molar ratio with respect to [DBBA+Tris], i.e. [I]/[DBBA+Tris]. In general, the higher the initiator (Trigonox 101) concentration, the higher the binding efficiency. However, at high initiator concentrations, the polymer masterbatches underwent degradation as revealed from the increase of MFI values and changes in molecular weight distribution data, (see Table 3.12 and Figure 3.13). Optimal binding levels and minimal degradation effects were achieved with molar ratio of initiator to antioxidant of 0.02.

Table 3.11 Effect of FRI concentration on the binding efficiency and MFI of 6% or 10% masterbatches (MB's) polypropylene containing DBBA-Tris ratio 6/4, processed in closed mixing condition at 180°C for 10 minutes

No	% MB, containing DBBA/Tris (6/4)	[Trig.101]/[AO] (m.r.)	Binding* (%)	MFI (g/10 mins)
1	6	0.000	3	0.31
2	6	0.001	9	0.32
3	6	0.002	31	0.35
4	6	0.010	75	0.63
5	6	0.020	91	1.09
6	6	0.030	93	2.15
7	10	0.000	3	0.44
8	10	0.001	11	0.48
9	10	0.002	35	0.53
10	10	0.010	76	0.78
11	10	0.020	91	1.19
12	10	0.030	97	1.93
14	PP, processed no additives	-	-	0.58
15	PP processed	0.002	-	1.34
16	PP processed	0.02	-	17.37

* Measured ratio of hydroxyl area indices by IR spectroscopy, see Fig.3.1a

Table 3.12 Molecular weight distribution data of polymer samples 10% masterbatches (MB's) polypropylene containing DBBA-Tris ratio 6/4, processed in closed mixing condition at 180°C for 10 minutes

No	Polymer samples (masterbatches)	[FRI]/[AO] (m.r.)	Mw x 10 ⁻⁵	Mn x 10 ⁻⁴	D(MWD) Mw/Mn
1	PP, unprocessed	0.00	4.17	5.13	8.128
2	PP, processed	0.00	3.62	5.53	6.546
3	PP, processed	0.02	1.75	4.34	4.032
7	PP + DBBA 6% + Tris 4%	0.00	4.10	5.75	7.130
8	PP + DBBA 6% + Tris 4%	0.005	2.74	4.99	5.491
9	PP + DBBA 6% + Tris 4%	0.02	1.59	3.24	4.907
10	PP + DBBA 6% + Tris 4%	0.03	1.51	3.54	4.265

3.2.4.3 Effect of FRI (Trigonox 101) on the MFI of various polypropylene film controls (unprocessed and processed) and containing 4 % Tris or 4 % DVB

Table 3.13 shows the effect of various concentration of the initiator on melt viscosity of polypropylene containing 4% of the coagents Tris and DVB. The MFI of unstabilised polypropylene processed in absence of peroxide is slightly higher than that of unprocessed polypropylene. In the presence of peroxide, the MFI values show an increase which parallels to the peroxide concentration and corresponds to the increased levels of chain scission and degradation of the polymer. The high MFI values observed for polypropylene processed with 4% Tris at high initiator concentration is attributed to the degradation of the polymer (see Table 3.13, sample no. 6-10 and Figure 3.12). On the other hand, polypropylene processed with 4% DVB in the presence of increasing amounts of initiator showed a decreasing trend in MFI values which is indicative of crosslinking via DVB (see Table 3.13, sample no. 11-15 and Figure 3.12).

Table 3.13 Effect of FRI on the MFI of various polypropylene film controls (unprocessed and processed) and containing 4% Tris or 4% DVB in various concentration of Trigonox 101, processed under standard condition.

No	PP sample	[Trig. 101]/[coagent] (m.r.)	MFI (g/10 mins)
1	PP, unprocessed	0.000	0.40
2	PP, processed	0.000	0.58
3	HWM 25, processed*	0.000	0.58
4	PP, processed	0.002	3.34
5	PP, processed	0.020	17.37
6	PP + 4% Tris	0.000	0.65
7	PP + 4% Tris	0.001	0.72
8	PP + 4% Tris	0.002	0.95
9	PP + 4% Tris	0.010	2.65
10	PP + 4% Tris	0.020	5.62
11	PP + 4% DVB	0.000	0.26
12	PP + 4% DVB	0.001	0.21
13	PP + 4% DVB	0.002	0.19
14	PP + 4% DVB	0.010	0.17
15	PP + 4% DVB	0.020	0.14

* HMW 25 is a stabilised commercial PP

3.2.5 Optimisation of Conditions to Achieve High Level of Binding Efficiency of 2-hydroxy-4(beta acrylate ethoxy) benzophenone (HAEB) in Polypropylene

To examine the binding efficiency of 2-hydroxy-4-(beta acrylate ethoxy) benzophenone (HAEB) this antioxidant was reactively processed in unstabilised polypropylene using the general procedure described in Scheme 3.1. Two different initiators were used in this case; dicumyl peroxide (DCP) and 2,5-dimethyl 2,5-di-tertiary butylperoxy hexane (Trigonox 101). Both processing conditions and chemical composition were optimised to achieve a high level of binding of HAEB in PP. The processing operation was optimised by varying processing time and temperature. The concentration of initiator, HAEB and coagent were varied to achieve optimum chemical composition for high binding efficiency and polymer stability.

3.2.5.1 Effect of processing time on the binding efficiency of HAEB in polypropylene.

The effect of processing time on the binding efficiency of HAEB is shown in Table 3.14. Although, longer processing time does not influence the significant extent of binding of HAEB in polypropylene, it affects the melt viscosity adversely as can be seen from MFI values (see Table 3.14 and Figure 3.16). Changes in the viscosity of the masterbatches during the processing operation was recorded, as shown in Figure 3.17. Initially, a decrease of the torque is observed during softening and melting of the polymer which is followed by a sharp rise to a peak at about 2.5 minutes. Further processing causes a gradual drop which reacts as the typical value for PP melt control at the specified temperature. Furthermore, both gel content and polydispersity (MWD) decrease with longer processing time (see Table 3.14).

Table 3.14 Effect of various processing times on binding efficiency of 10% HAEB in polypropylene, in the presence of Trigonox 101 (0.005 m.r., I/HAEB), processed in closed mixing condition at 180°C.

No	Processing time (minutes)	Binding* (%)	MFI (g/10 mins)	Gel content %	Molecular weight distribution of MB's fraction		
					Mw x 10 ⁻⁵	Mn x 10 ⁻⁴	MWD (Mw/Mn)
1	2.5	71	1.15	16	2.39	3.47	6.887
2	5	71	1.54	6	2.22	3.29	6.747
3	10	72	1.82	0	1.59	2.86	5.559
4	15	72	2.62	-	-	-	-
5	20	72	2.91	-	-	-	-

* Measured by both IR and UV spectroscopy, see Fig.3.2a and 3.2b

3.2.5.2 Effect of processing temperature on the binding efficiency of HAEB in polypropylene.

Table 3.15 shows the effect of processing temperature on the binding efficiency of HAEB in polypropylene; i.e. binding efficiency increases with processing temperature, with maximum binding efficiency at 190°C. Furthermore, higher temperatures cause greater chain scission and thermal degradation as revealed by increasing values of MFI. The optimum processing temperature (180°C) of HAEB in polypropylene showed a high binding level and acceptable MFI value.

Table 3.15 Effect of processing temperature on the binding efficiency of HAEB (10% MB) in propylene, in the presence of DCP (0.005 m.r.,I/HAEB), processed in closed mixer condition for 10 mins

No	Processing Temperature (°C)	Binding* (%)	MFI (g/10 mins)
1	160	30	1.10
2	170	56	1.32
3	180	72	1.82
4	190	73	2.31
5	200	70	3.42

* Measured by both IR and UV spectroscopy, see Fig.3.2a and 3.2b

3.2.5.3 Effect of antioxidant's concentration on the binding efficiency of HAEB in polypropylene.

Table 3.16 shows that changing the initial antioxidant concentration does not effect the binding efficiency of HAEB in poppypropylene. However, higher concentration of HAEB gave higher MFI values of the masterbatches which suggests the occurrence of chain scission and polymer degradation.

Table 3.16 Effect of HAEB concentration on binding efficiency in polypropylene, in the presence of DCP (0.005 m.r., I/HAEB), processed in closed mixing condition at 180°C for 10 minutes.

No	HAEB concentration (% w/w)	Binding* (%)	MFI (g/10 mins)
1	5	70	1.62
2	10	72	1.82
3	15	72	2.37
4	20	72	3.65

* Measured by both IR and UV spectroscopy, see Fig.3.2a and 3.2b

3.2.5.4 Effect of initiator concentration on the binding efficiency of HAEB in polypropylene.

Masterbatches containing 10% HAEB were processed in the presence or absence of a free radical initiator (DCP or Trigonox 101) for 10 minutes at 180°C in a Torque Rheometer under closed mixing condition. Four different molar ratios of FRI ([DCP]/[HAEB] or [Trig.101]/[HAEB]), 0.003, 0.005, 0.010 and 0.020 were used. The effect of the different FRI is shown in Table 3.17, in which the effect of mechanochemical shear alone (no FRI) leads to a grafting efficiency of 30%, but this can be enchanced up to 83% by addition of FRI. However, at high FRI concentration, the melt flow index values of the masterbatches increases indicating polymer degradation. Optimum binding was, therefore, considered when minimal effect on thermal degradation was achieved and this resulted when using initiator molar ratio (I/AO) of 0.005 in the case of both FRI's used. 10% HAEB masterbatches processed with Trigonox 101 gave slightly

higher binding efficiency of HAEB in polypropylene than with DCP initiator, under similar condition.

Table 3.17 Binding efficiency and MFI of MB's containing 10% HAEB in polypropylene in the presence of various concentrations of FRI dicumyl peroxide or Trigonox 101, processed under standard condition.

Sample No	[DCP]/[AO], (m.r.)	Binding (%)*	MFI (g/10 mins)
1	0.000	24	1.01
2	0.003	61	1.32
3	0.005	72	1.82
4	0.010	78	4.13
5	0.020	80	6.83
	[Trig. 101]/[AO], (m.r.)		
6	0.000	30	1.00
7	0.003	65	1.22
8	0.005	73	1.80
9	0.010	80	4.02
10	0.020	83	6.71

*Measured by both IR and UV spectroscopy, see Fig.3.2a and 3.2b

Changes in the polymer viscosity during processing were followed by recording the changes in the torque. Polypropylene and HAEB masterbatches processed in the absence of initiator shows gradual decrease of torque value with time. However, the presence of FRI leads to the appearance of a torque peak which shifts to a shorter processing times with increasing peroxide concentration, see Figure 3.20. The effect of the initiator (DCP) concentration on binding efficiency of HAEB masterbatches in polypropylene is shown in Figure 3.21.

3.2.6 Effect of a Coagent, TMPTA (Tris) on the Binding Efficiency of HAEB in Polypropylene.

Optimisation of processing conditions of HAEB-Tris system was carried out using various HAEB/Tris ratios in the presence of the optimum concentration of peroxide of 0.005 m.r,

(I)/(HAEB+Tris). Figure 3.22 shows that the height of the torque peak increases as the concentration of Tris was increased. This suggests higher contribution of a crosslinking reaction on the torque value. Results in Table 3.18 show that at a HAEB/Tris ratio of 9/1 the binding efficiency of DBBA increased up to 93%, the other ratios did not show any significant increase in level of binding. Torque data shows that the height of peak curves at 3.5 minutes increases with Tris content in the masterbatches. The optimum condition giving high level binding was achieved at the HAEB/Tris ratio of 9/1.

Table 3.18 Binding of HAEB in Polypropylene with Tris co-agent at various ratios HAEB/Tris in masterbatches containing 10% of mixture in the presence 0.005 m.r. of FRI Trig.101, processed in closed mixing condition at 180°C for 10 minutes.

No	HAEB/Tris ratio	Binding* (%)	MFI (g/10 mins)
1	10/0	73	1.80
2	9/1	93	1.72
3	8/2	94	1.68
4	7/3	95	1.59

* Measured by UV spectroscopy, see Fig.3.2b

Further experiment was carried out to find the optimum FRI concentrations of HAEB-Tris system. The ratio of HAEB/Tris, temperature and time processing were fixed at optimum condition, whereas the concentration of Trigonox 101 was varied. Table 3.19 shows that the higher the concentration of Trigonox 101 was used in that system the higher binding efficiency was achieved. On the other hand, the MFI value shows increasing with the increase of initiator concentration. The increase of MFI values indicating the chain scission and polymer degradation had occurred in this system. Results from Table 3.19 also show that at the ratio of HAEB/Tris of 9/1 and initiator concentration of 0.005 molar ratio the achieved binding efficiency was 93% and this was chosen as the optimum concentration which leads to minimal effect on the degradation.

Table 3.19 Effect of FRI Trigonox 101 concentration in binding efficiency and MFI of Polypropylene MB's containing 10 % mixture of HAEB/Tris ratio 9/1 processed in closed mixing condition at 180°C for 10 minutes.

No	[Trig.101]/[AO], (m.r.)	Binding* (%)	MFI (g/10 mins)
1	0.003	90	1.45
2	0.004	91	1.50
3	0.005	93	1.72
4	0.008	96	2.78
5	0.010	99	4.61

* Measured by UV spectroscopy

The torque peak (see Figure 3.22) observed suggest the formation of crosslinked material, hence, gel content test was carried out for a masterbatch (MB) sample containing HAEB/Tris (9 : 1) processed with optimum peroxide concentration at different processing time i.e. at 3.5 minutes (the maxima torque peak), 5 minutes and 10 minutes. The maximum gel content was found after 3.5 minutes coinciding with the torque peak maximum. At the end of the reaction (after 10 minutes) all the gel has disappeared. Further analysis and elucidation of the structure of the graft will be discussed in Chapter-5.

Table 3.20 Effect of processing time on binding efficiency and gel content of PP film containing (9% HAEB+1% Tris) in presence 0.005 m.r. of Trigonox 101, processed in closed mixing condition at 180°C.

No	Processing Time (mins)	Binding* (%)	gel content (%)
1	3.5	72	8
2	5.0	81	3
3	10	93	0

* Measured by UV spectroscopy, see Fig.3.2b

3.3 DISCUSSION

3.3.1 Reactive Processing Containing DBBA System

High levels of binding the two antioxidants (DBBA and HAEB) examined was achieved in polypropylene melt using initiator and a coagent (e.g. Tris). In the case of DBBA, quite a high concentration of peroxide (0.02 molar ratio) was needed to achieve a high level of binding. The optimum conditions for binding of (DBBA+Tris) samples were observed in 10% total concentration of (DBBA+Tris) with ratio 6 to 4, and a processing temperature of 180°C in the presence of 0.02 molar ratio Trigonox 101 as initiator, processed for 10 minutes under closed mixing conditions, see Table 3.10 and Figure 3.10.

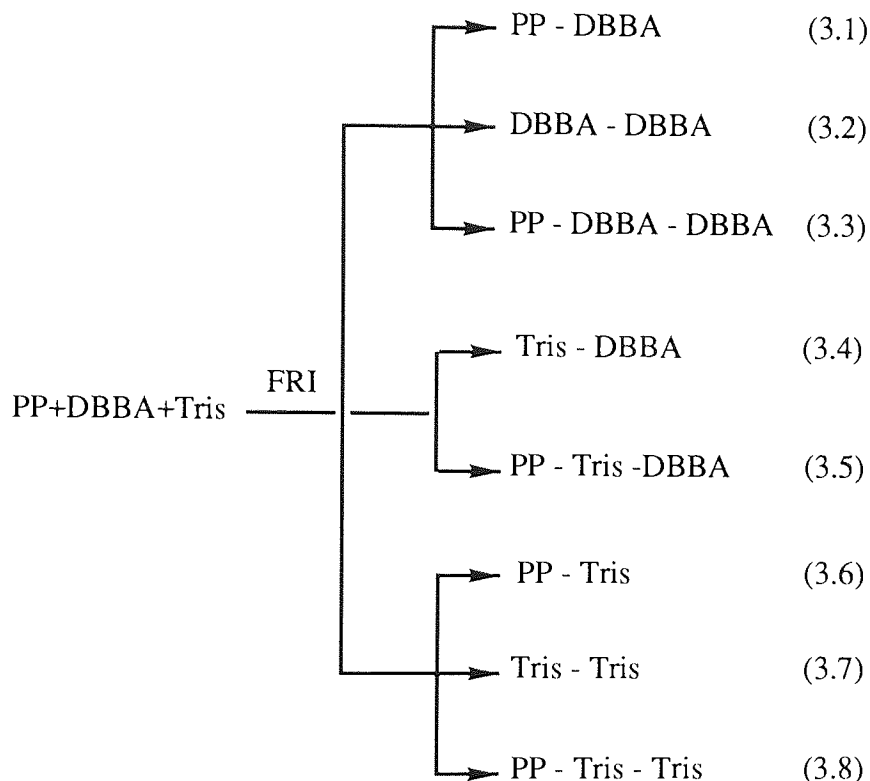
The concentration of antioxidant plays an important role in determining the binding efficiency. The binding level increases (up to 40%) with the increasing DBBA concentration (up to 10%), but when the DBBA concentration more than 10%, the binding efficiency decreases with increasing the concentration. In any reactive processing procedure of an AO with polypropylene both grafting of AO DBBA onto the polymer backbone (desired reaction) and side reactions such as AO homopolymerisation (undesired reaction) take place^(93,98,97,100,113). The efficiency of the binding reaction of the antioxidant onto the polymer backbone depends on the extent of competition between desired and undesired reactions. At high DBBA concentration (more than 10%), it's likely that competition of homopolymerisation reaction is higher compared to the grafting reaction, resulting in lower binding levels, see Figure 3.6.

Figure 3.4 shows that the initiator concentration also plays a very important role in the level of binding of DBBA onto polypropylene. The reaction rate of grafting as well as homopolymerisation depend on the concentration of peroxide, polymer radical (R.) and antioxidant radical (A.) formed during the melt reaction. Increasing initiator concentration

has resulted in a higher binding efficiency of DBBA in PP (see Figure 3.4), this should be due to more initiator radicals being formed which generates more grafting and homopolymerisation processes^(111,112,125,180). The need for higher peroxide concentration in the DBBA system (0.02 molar ratio, [I]/[AO]) compared to that of HAEB (0.005 molar ratio, [I]/[AO]) is almost certainly due to the fact that hindered phenols are very effective radical scavengers^(47,49). Hence, the initiator's radical formed does not only initiate formation of polypropylene radicals and polymerisation via vinyl group of DBBA, but can also be deactivated by the hindered phenol group of DBBA. It is clear from the results, however, that although higher grafting efficiency can be achieved at higher peroxide concentration, the melt stability of the polymer decreases, reflected by high MFI values, see Figures 3.4 and 3.4a. This is in agreement with the molecular weight data (see Table 3.3), which shows that molecular weight decreases with increasing peroxide concentration^(168,169).

Reactive processing of DBBA in the presence of different coagents (which contain more than one reactive function), may lead to number of possible reactions as shown in Scheme 3.2, reaction 3.1 to 3.8^(183,184).

1. DBBA can graft onto the polypropylene without or with coagent (see reaction 3.1 and 3.5).
2. DBBA may homopolymerise or oligomerise and then this is grafted onto the polypropylene backbone (see reaction 3.2 and 3.3).
3. DBBA can copolymerise with the coagent, and then this can be followed by grafting onto the polypropylene backbone (see reaction 3.4 and 3.5).
4. The coagents themselves can also graft onto polypropylene (see reaction 3.6), or homopolymerise themselves either linearly or non-linearly (normally forming crosslinking, see reaction 3.7 and 3.8).



Scheme 3.2 The possible reactions of DBBA+Tris in polypropylene using reactive processing procedure in the presence of 0.02 m.r Trigonox 101 under standard condition.

The effect of coagents (DVB or Tris) as interlinking agents have been shown to play an important role in extending the level of binding of DBBA and HAEB onto the PP backbone; the level of binding has increased with increasing concentration of DVB or Tris. This confirms earlier results based on work at Aston using these coagents to look the whole range of agents including AO's and other modifiers (111,112,127-130).

In the case of DBBA+DVB system, results have shown that higher DVB concentrations not only give high level of binding but also lead to lower MFI values (see Table 3.7). It is well known that DVB acts as a crosslinking agent and forms a polymer network of styrene during radical copolymerisation (183,184). When 4% DVB with or without DBBA was processed in PP, it shows that MFI values decrease with increasing initiator concentration (see Tables 3.8 & 3.13 and Figures 3.12 & 3.15). Compounds (such as DVB) with high grafting and homopolymerisation activity will consume more peroxide during processing,

leaving less peroxide to react with the polymer. This may be one of the reasons, that the order of the binding efficiency of DBBA+DVB is in the opposite direction to the order of MFI values, see Figure 3.9. Possible reactions in the reactive processing of the DBBA-DVB system includes homopolymerisation of DBBA which may or may not be attached onto polymerised DVB, copolymerisation of DBBA-DVB, which may become attached to the polymer matrix. In addition, the crosslinking of DVB alone or with the polymer is also possible. However, Table 3.9 shows that the molecular weight distribution gives a different trend (see Figure 3.9a). The molecular weight distribution measurement was carried out after filtration of the polymer sample solution, the insoluble fraction of the polymer sample which contains high molecular weight can not be measured. Further analysis of DBBA-DVB masterbatch will be discussed in Chapter-5.

In the case of the DBBA-Tris system, Table 3.10 and Figure 3.10 show that the level of binding increases with higher Tris concentration. However, the MFI values of the masterbatches also increases slightly, as shown in Table 3.11 and Figure 3.11. Higher Tris concentration (meaning lower concentration of DBBA, melt stabiliser) in the system, causes more thermal degradation. This was supported by the molecular weight distribution of those masterbatches, see Table 3.12 and Figure 3.13. On the other hand, a less amounts of Tris, may decrease the compatibility of the DBBA in that system, which leads to less grafting of DBBA onto the polypropylene backbone, as reflected by the low binding level of DBBA, see Table 3.10. When Tris alone was reactively processed with polypropylene the MFI values increased with increasing peroxide concentration, see Table 3.13 and Figure 3.12, indicating chain scission and polymer degradation. Unlike using DVB coagent, the presence of Tris coagent can enhance the level of binding of DBBA without changing the polymer's properties (e.g. no crosslinked formation). Further analysis and model reaction of (DBBA+Tris) system to understand its mechanism will be discussed later in Chapter-5.

3.3.2 Reactive Processing Containing HAEB System

HAEB was successfully bound at high levels in unstabilised polypropylene (10%), when processed in the presence of Tris as a coagent (at a AO:Tris ratio of 9:1) and in the presence 0.005 molar ratio ($[I]/[AO+Tris]$) Trigonox 101 using reactive processing procedure.

Differently from DBBA, in the HAEB system the processing time has very important role on the changes of reaction during processing. Table 3.14 and Figures 3.16 & 3.17 show that in the early stage of processing (2.5 minute) the crosslinked (non permanent) product were formed. However, at the end of processing (after 10 minutes) all crosslinked products had broken down and were soluble in xylene. However, this structural change during processing does not change the level of binding of HAEB in PP (see Table 3.14), this should be due to that graft HAEB in PP underwent re-structuring. The concentration of antioxidant in the HAEB system does not affect the extent of binding efficiency, however, greater HAEB concentration causes an increase in the degradation of the masterbatches, which was reflected by increasing MFI values, see Table 3.16 and Figure 3.19. This degradation may be due to the increased in the amount of FRI in the system in relation to the rise in HAEB concentration.

Like DBBA, the HAEB system also used the Tris coagent to enhance its binding efficiency onto PP, to protect the escape of antioxidants from the polymer matrix. The binding levels increase as the Tris concentrations increases. On the other hand, the torque value shows that at higher concentrations of the Tris coagent the intensity of the peak became higher, which indicates that the binding during processing was very high due to grafting or crosslinking (see Figure 3.22). However, these crosslinked products also break down at the end of processing (after 10 minutes), which was indicated by a decrease in the torque and their MFI values (see Table 3.19 and Figure 3.22). Further analysis will be carried out in Chapter-5.

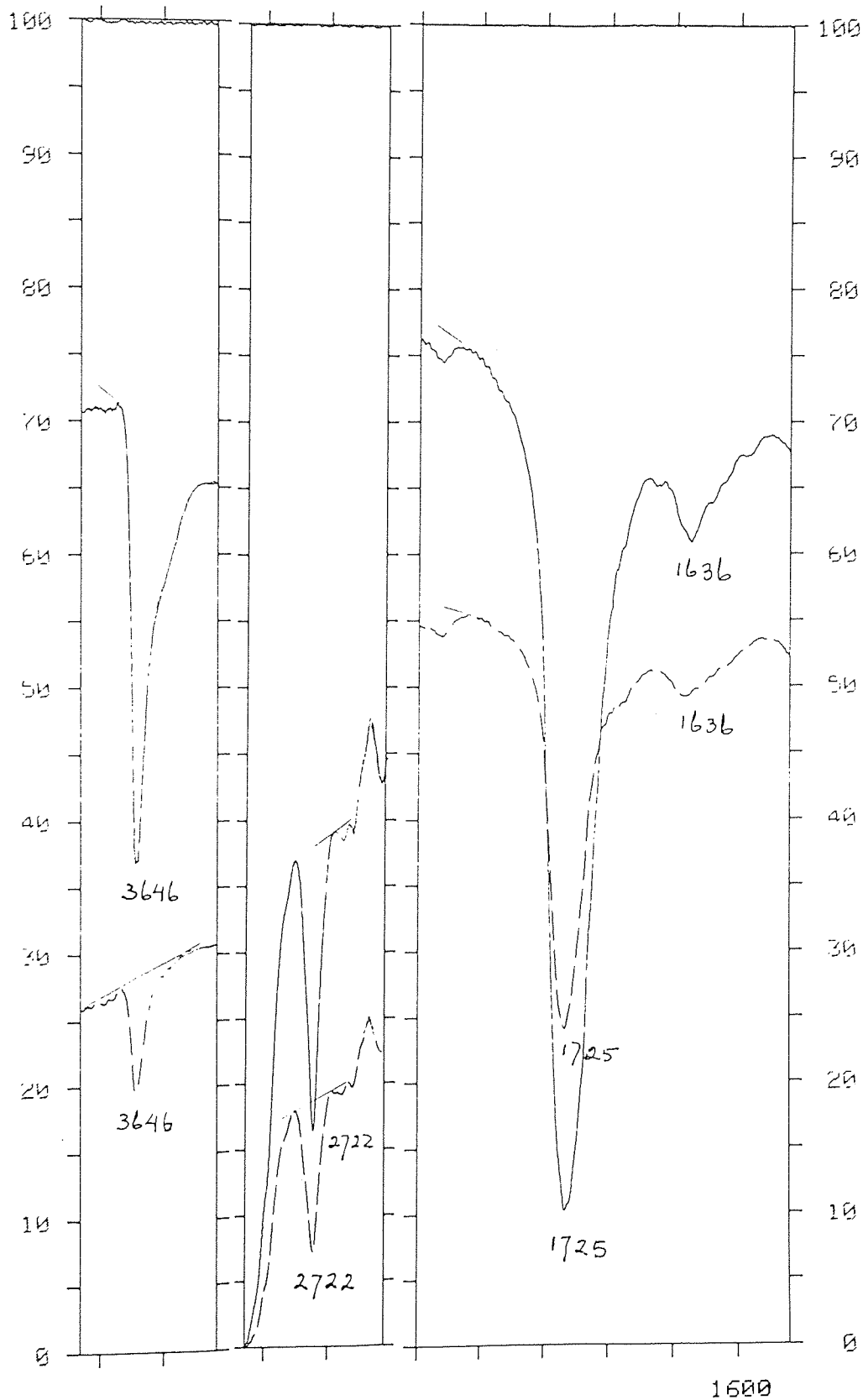


Figure 3.1 Infra red spectra of PP film processed in presence of 6% DBBA and 0.02 m.r (I/DBBA) of Trigonox 101, before (—) and after (-----) exhaustive Soxhlet extraction.

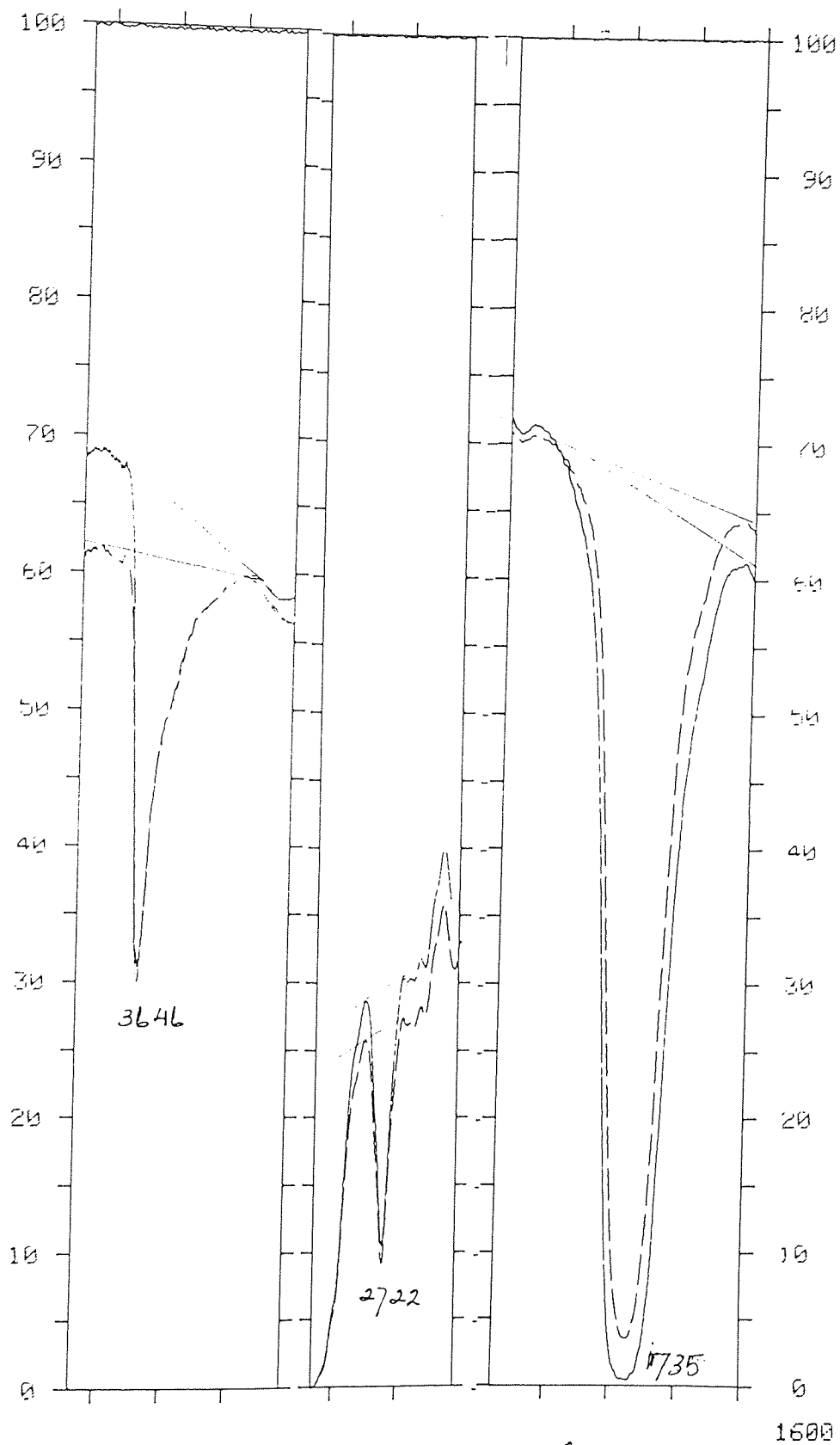


Figure 3.1a Infra red spectra of PP film processed in presence of 6% DBBA + 4% Tris and 0.02 m.r (I)/(DBBA+Tris) of Trigonox 101, before (—) and after (-----) exhaustive Soxhlet extraction.

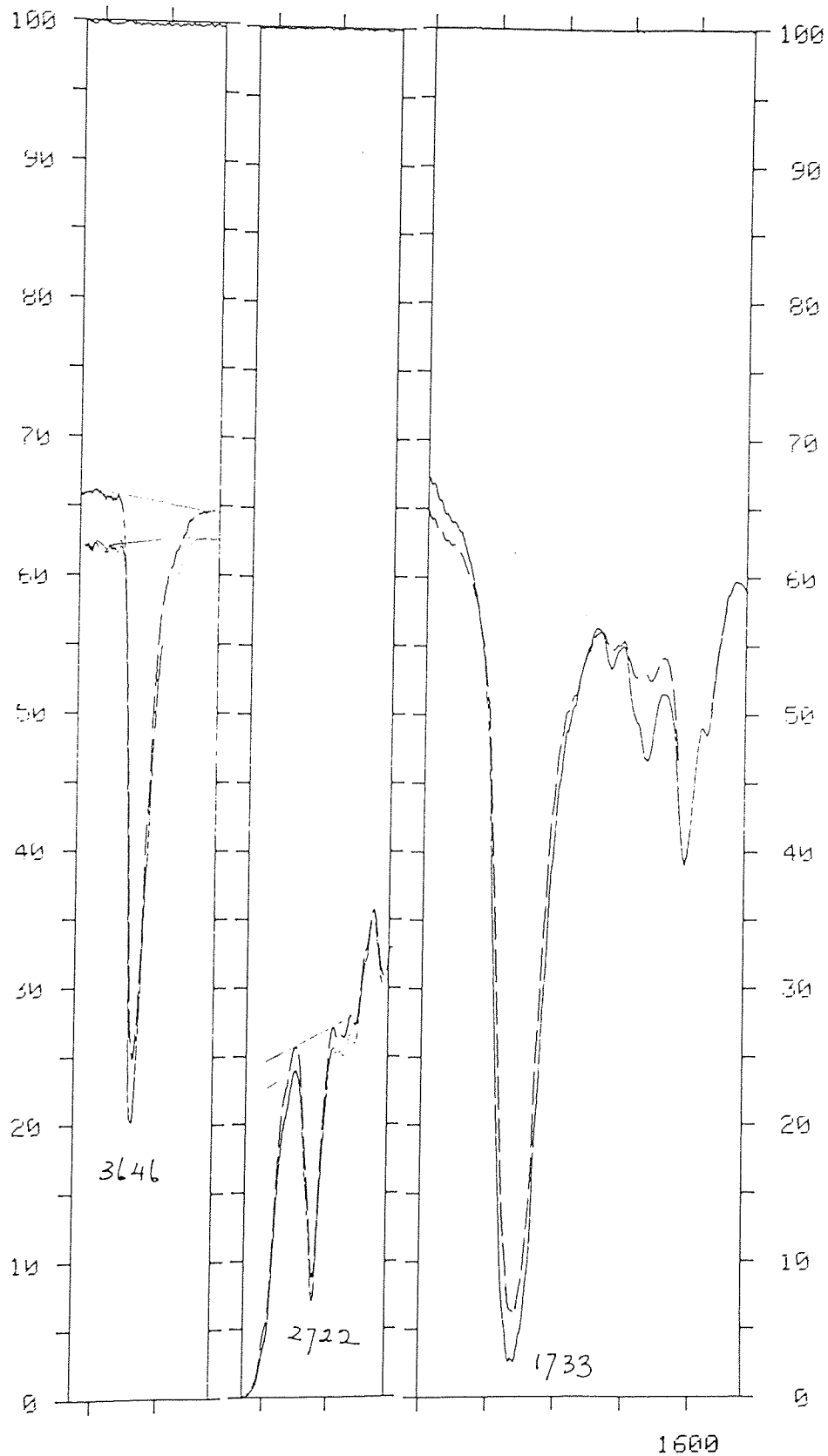


Figure 3.1b Infra red spectra of PP film processed in presence of 6% DBBA + 4% DVB and 0.02 m.r (I)/(DBBA+DVB) of Trigonox 101, before (—) and after (-----) exhaustive Soxhlet extraction.

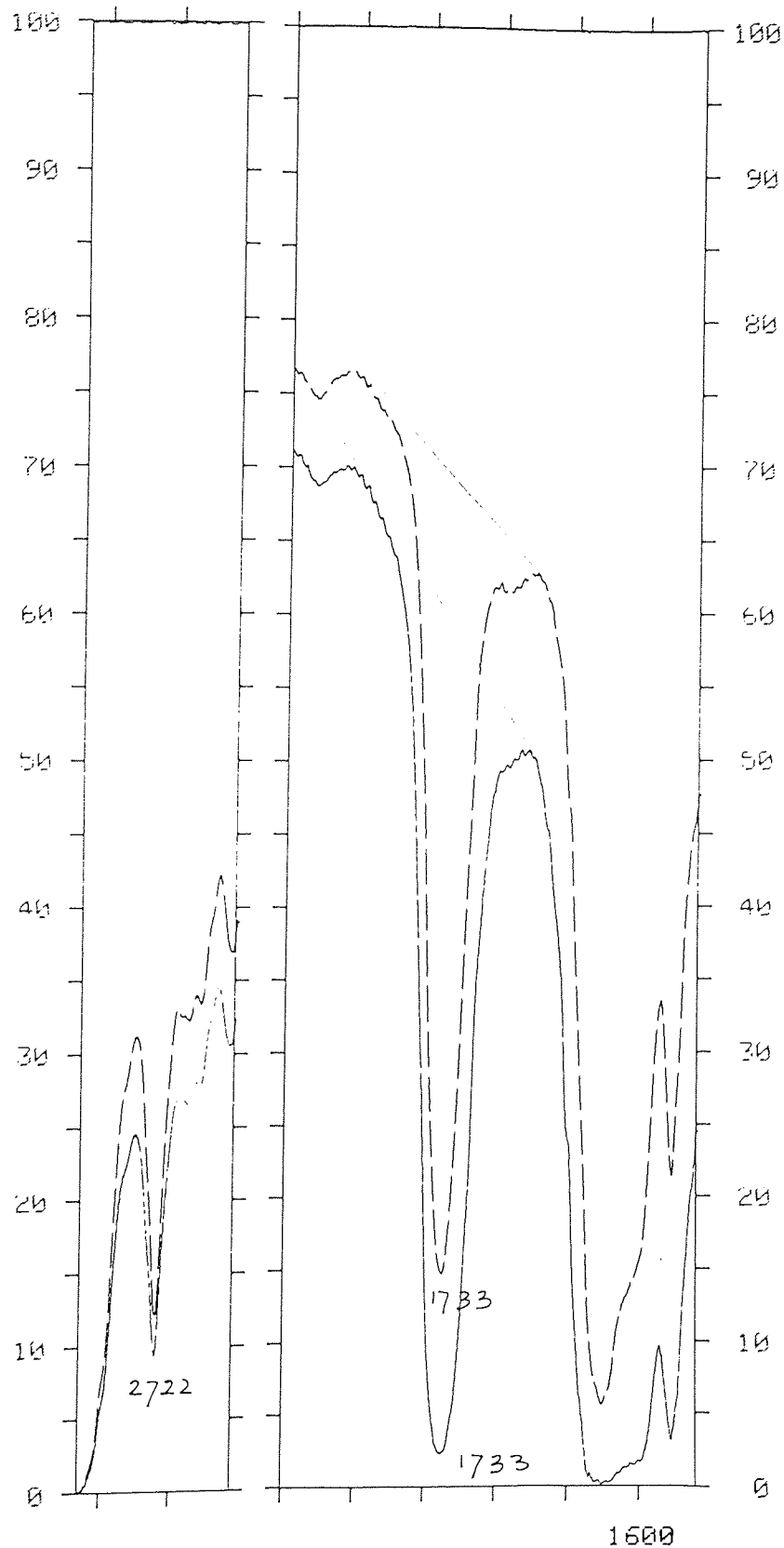


Figure 3.2a Infra red spectra of PP film processed in presence of 10% HAEB and 0.005 m.r (I)/(HAEB) of Trigonox 101, before (—) and after (----) exhaustive Soxhlet extraction.

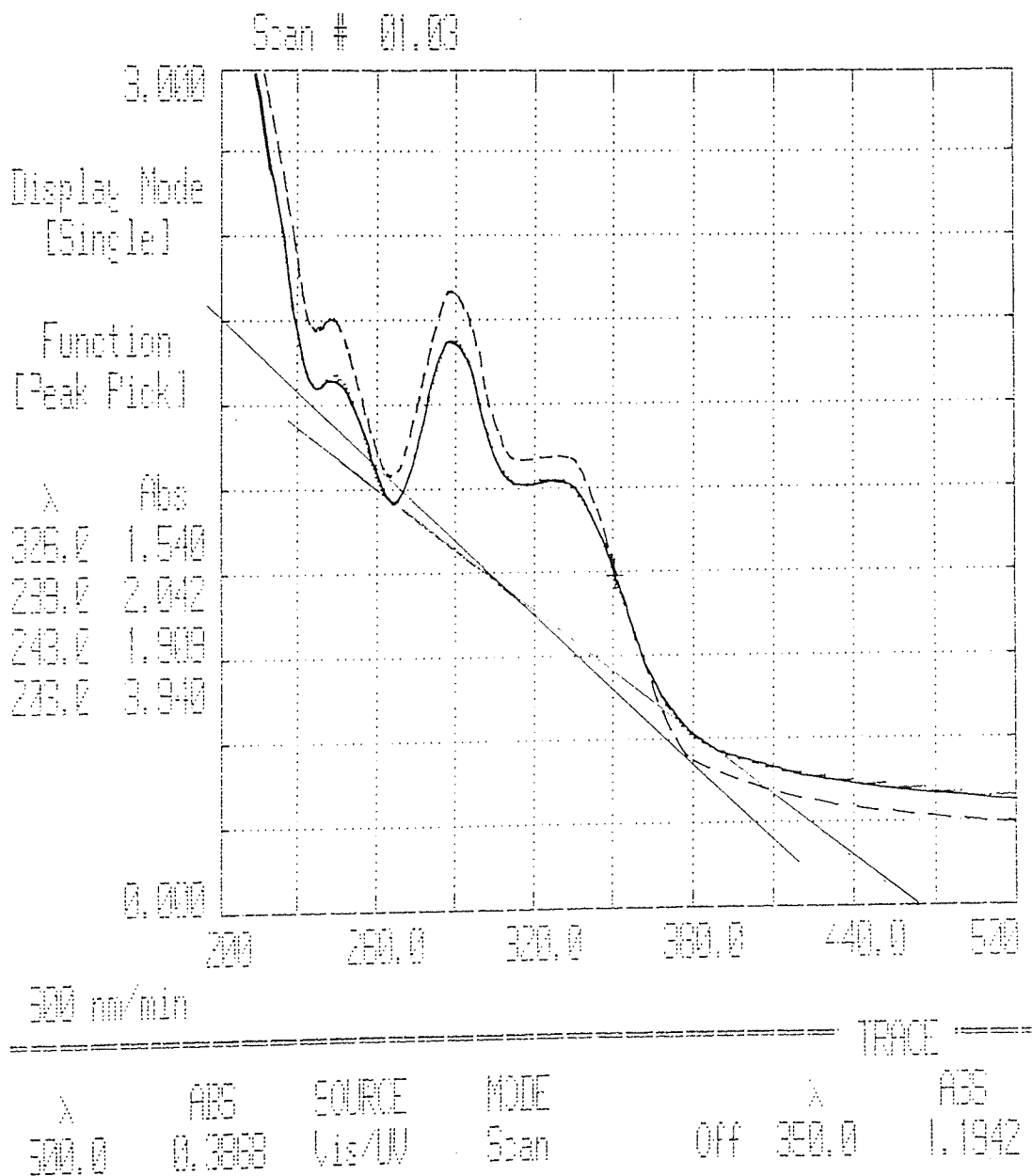


Figure 3.2b UV spectra of PP film processed in presence of 9% HAEB+1%Tris and 0.005 m.r (I)/(HAEB+Tris) of Trigonox 101, before (—) and after (-----) exhaustive Soxhlet extraction.

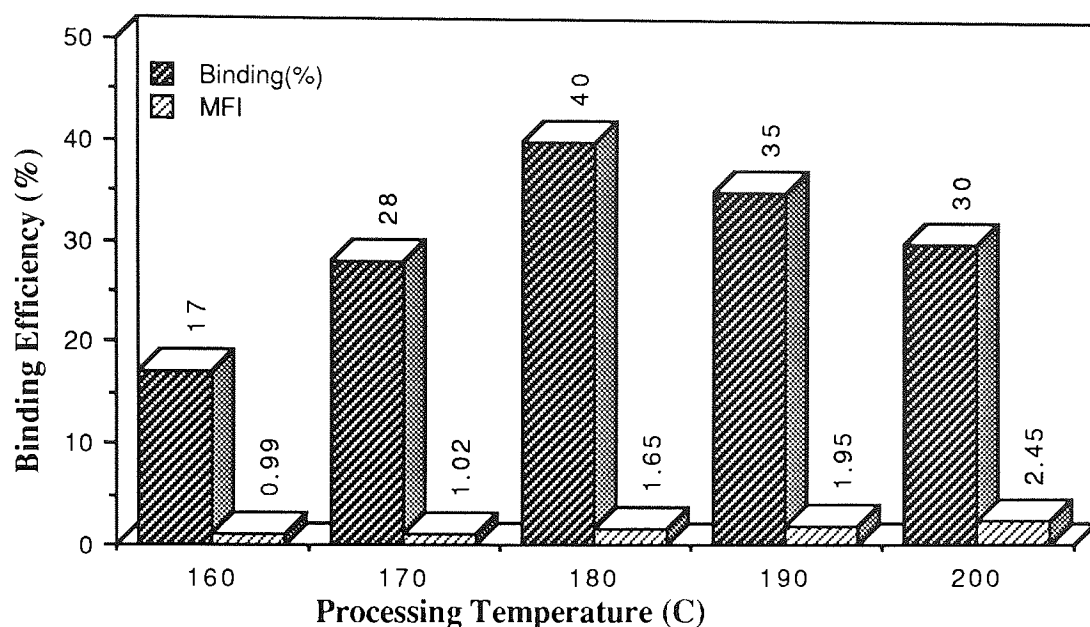


Figure 3.3 Binding efficiency and Melt flow index (MFI) of masterbatches (MB's) containing 10% DBBA in polypropylene in the presence of 0.02 molar ratio, m.r.(I/DBBA) Trigonox 101, processed at various processing temperature for 10 minutes under closed mixer condition

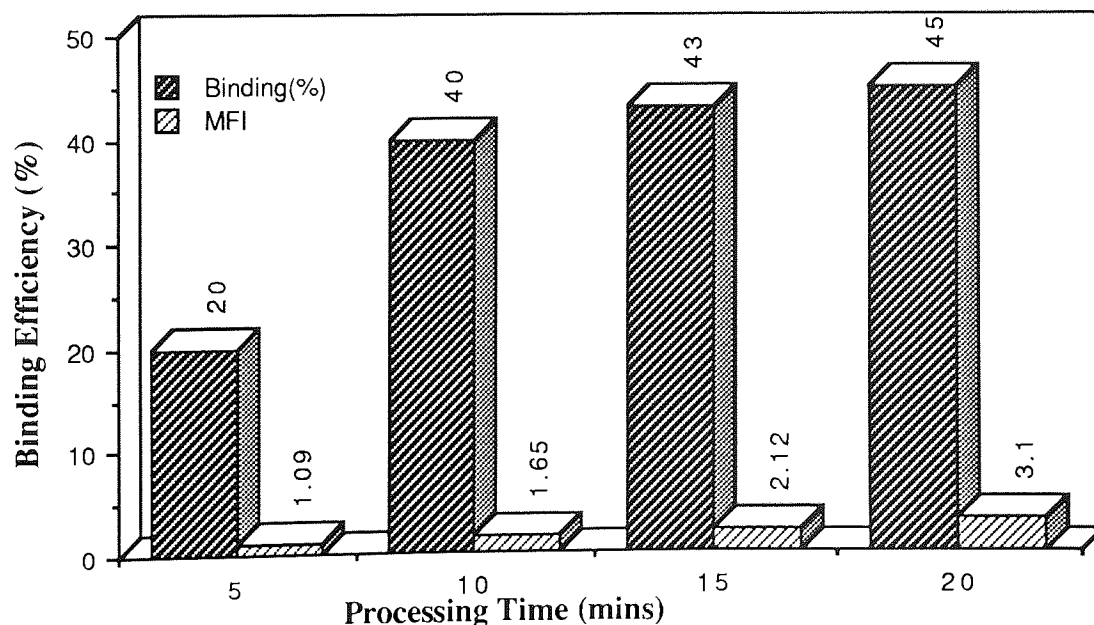


Figure 3.3a Binding efficiency and Melt flow index (MFI) of masterbatches (MB's) containing 10% DBBA in polypropylene in the presence of 0.02 molar ratio, m.r.(I/DBBA) Trigonox 101, processed at various processing time at 180°C under closed mixer condition

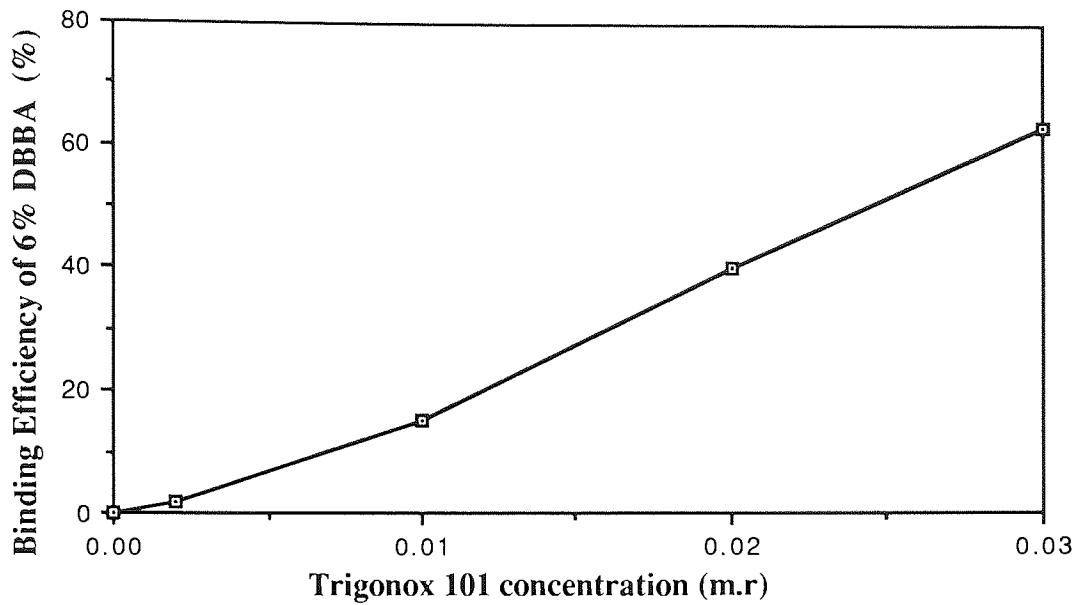


Figure 3.4 The effect of various Trigonox 101 concentration on binding level of 6% DBBA MB's with PP processed under standard condition.

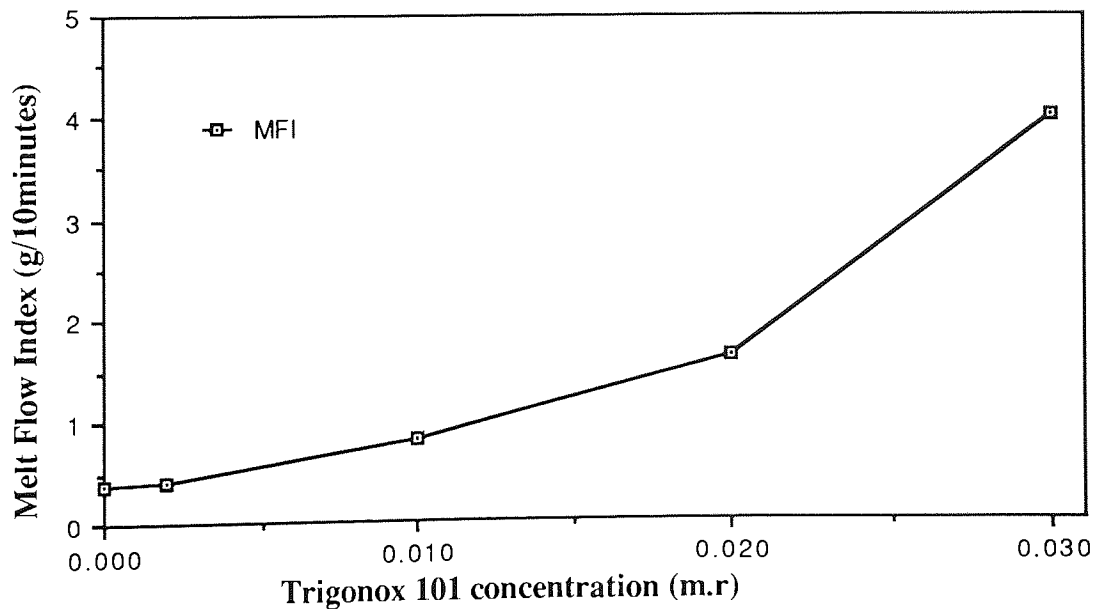


Figure 3.4a The effect of various Trigonox 101 concentration on MFI of 6% DBBA MB's with PP processed under standard condition.

B337

<14> DBCU-3 (9312)

ENDED: 04/09/90 10:1

MOLECULAR WEIGHT DISTRIBUTION

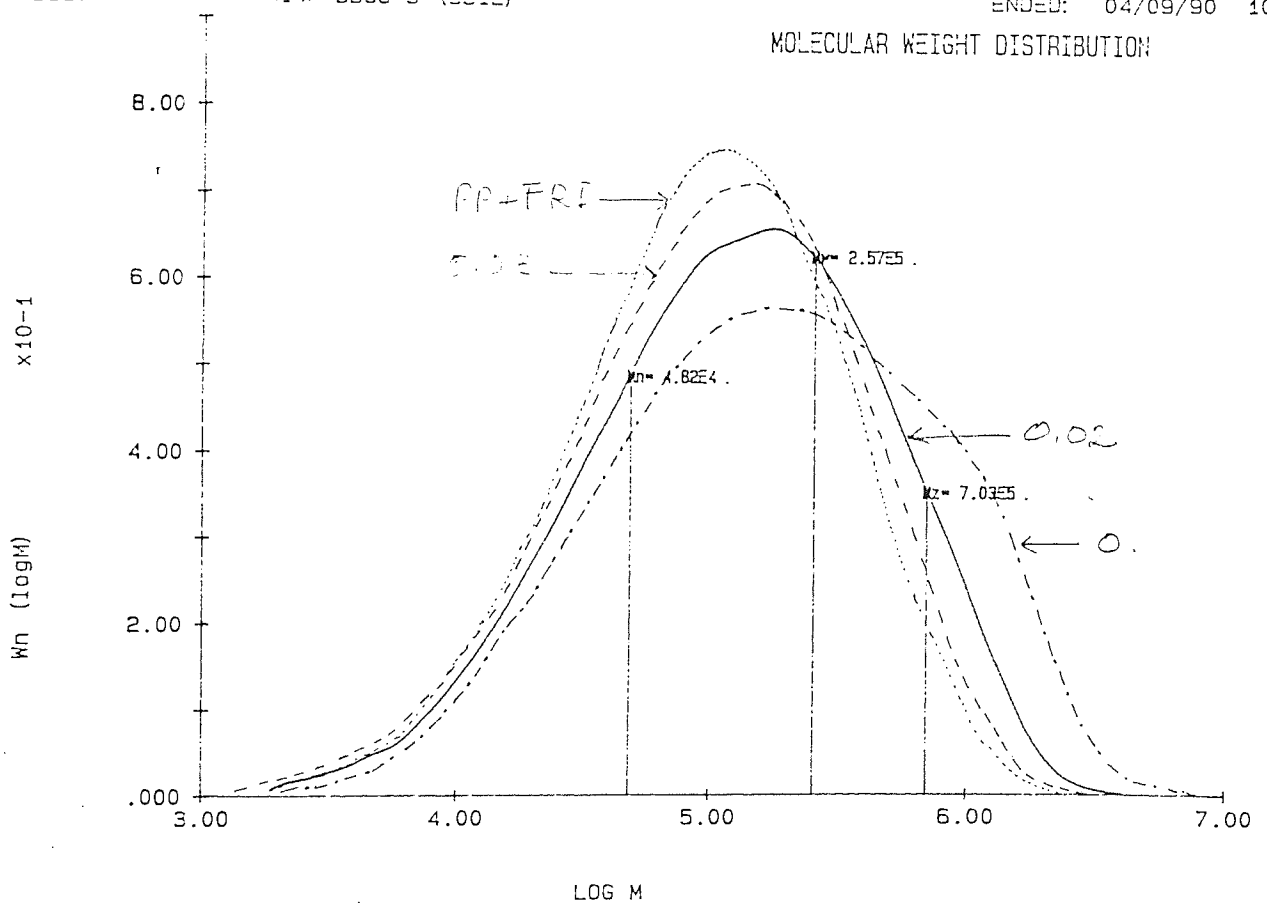


Figure 3.5 Molecular weight distribution curves for, PP processed in the presence of 0.02 m.r Trig. 101 (.....), in the presence of 10% DBBA (-.-.-), in the presence of 10% DBBA+Trig.101 0.02 m.r (____), and in the presence of 10% DBBA+Trig.101 0.03 m.r (-.-.-), refer to Table 3.3

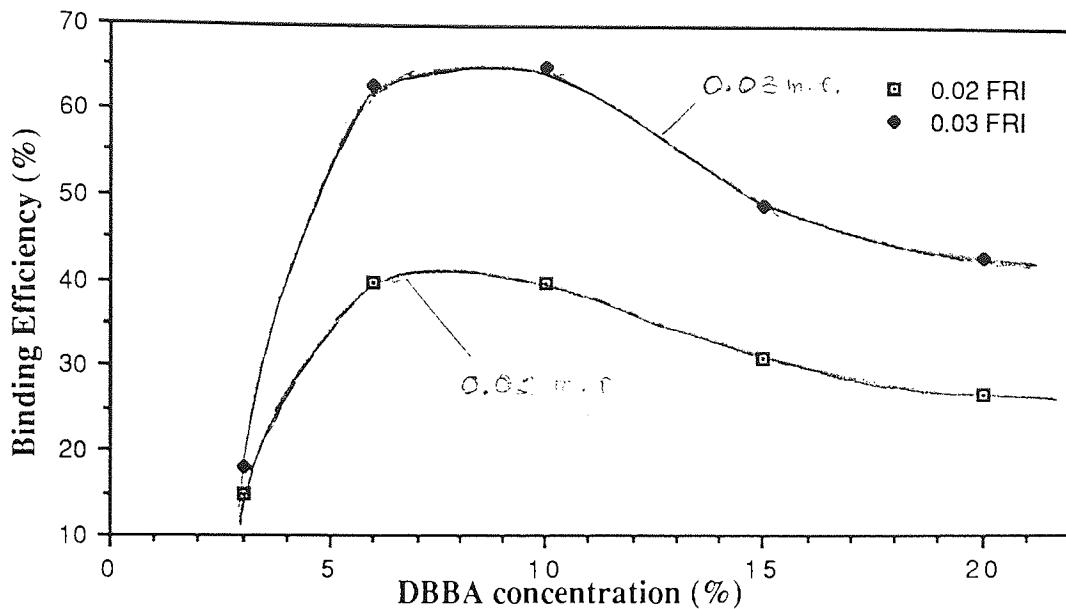


Figure 3.6 Effect of DBBA concentration on binding efficiency in polypropylene processed in the presence of 0.02 and 0.03 m.r. Trigonox 101, under standard condition.

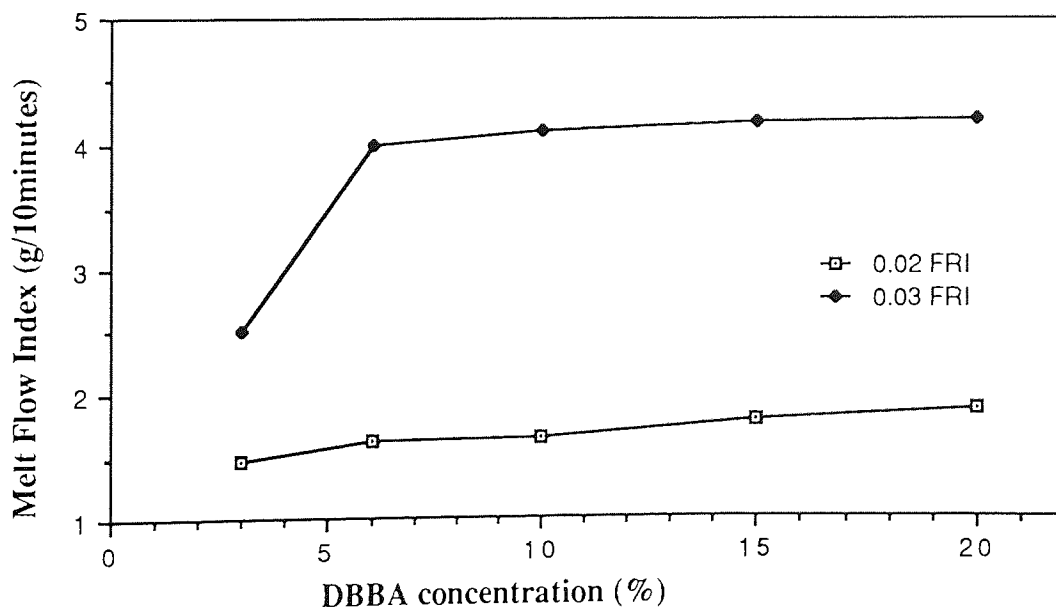


Figure 3.7 The effect of DBBA concentration on MFI in polypropylene processed in the presence of 0.02 and 0.03 m.r. Trigonox 101, under standard condition.

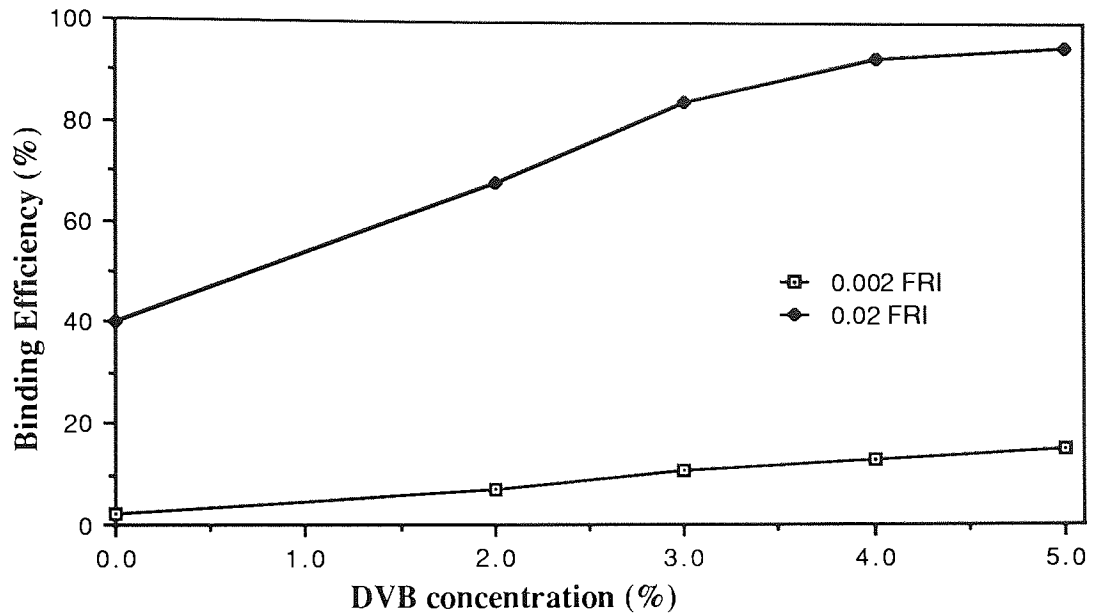


Figure 3.8 The effect of DVB as a coagent on binding level of antioxidant in polypropylene, in the presence of 0.002 or 0.02 m.r. Trigonox 101, processed under standard condition.

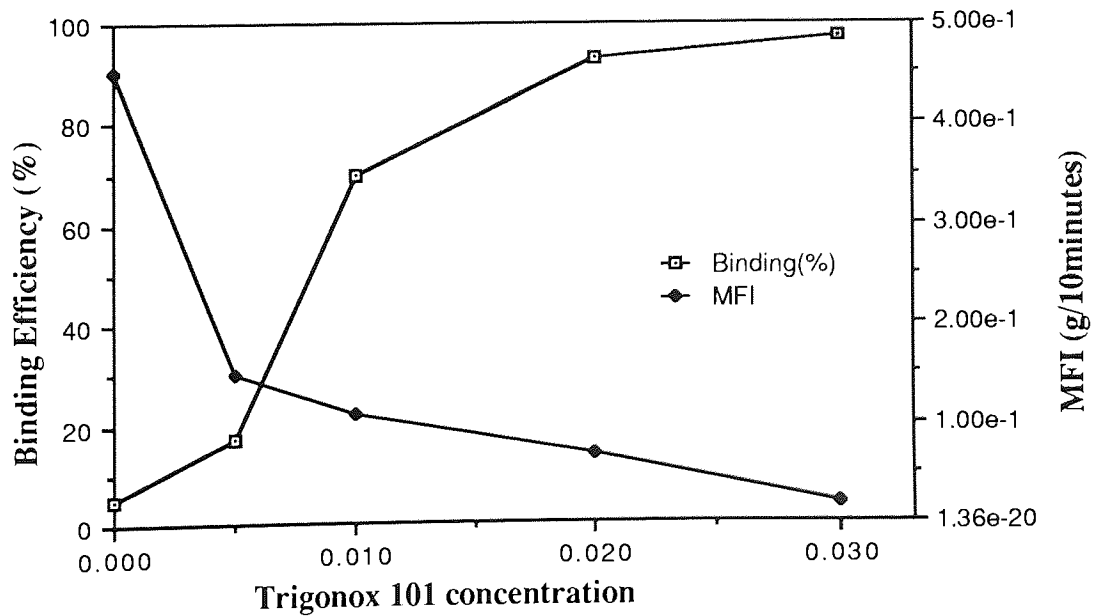


Figure 3.9 The effect of Trigonox 101 concentration (m.r.) on the binding efficiency and MFI of 10% MB's containing DBBA+DVB ratio 6 to 4, processed under standard condition.

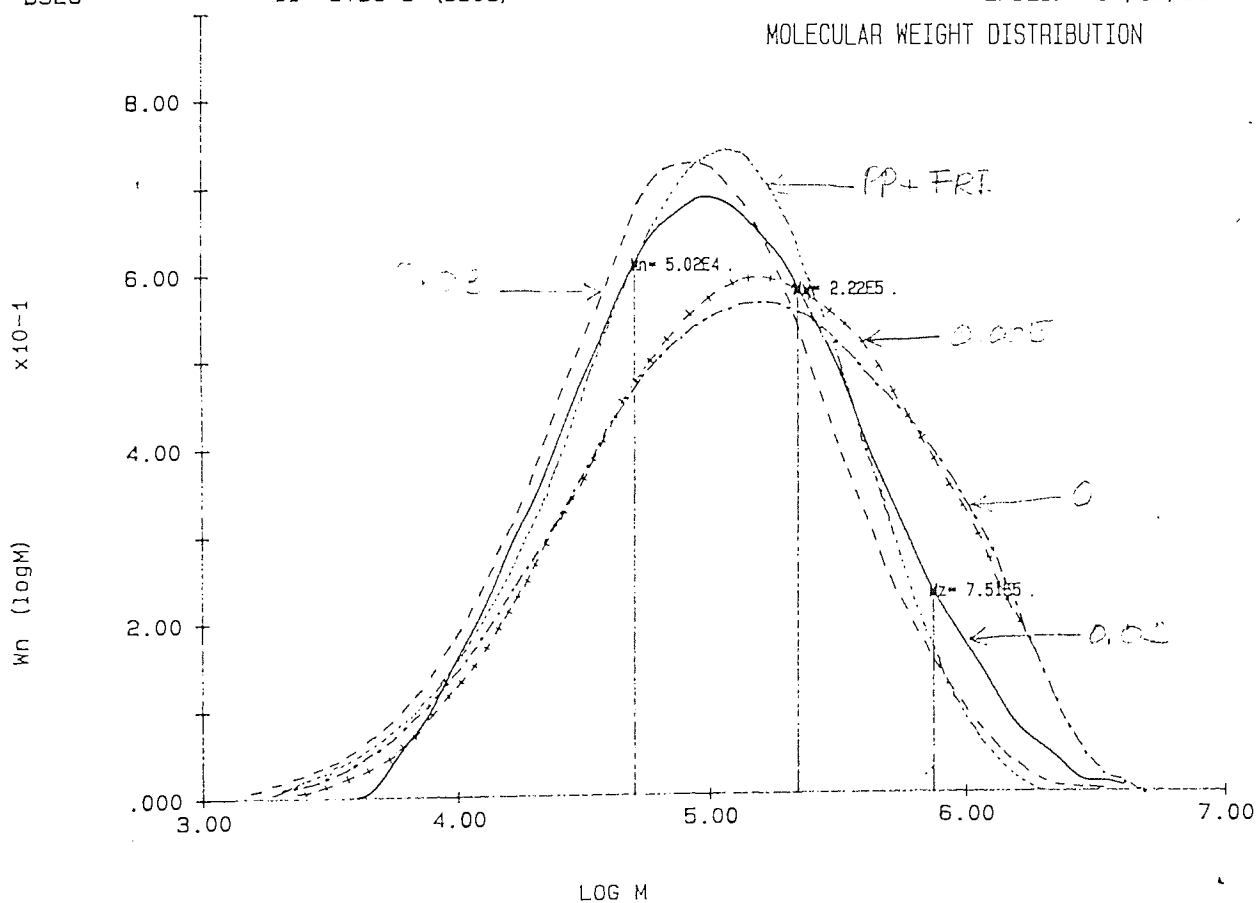


Figure 3.9a Molecular weight distribution curves for, processed PP in the presence of 0.02 m.r FRI (.....), in the presence of 6%DBBA +4%DVB (-.-.-), in the presence of 6%DBBA+4%DVB+FRI 0.005 m.r (++++), in the presence of 6%DBBA+4%DVB+FRI 0.02 m.r (-----), in the presence of 6%DBBA+4%DVB+FRI 0.03 m.r (.....), (refer to Table 3.9)

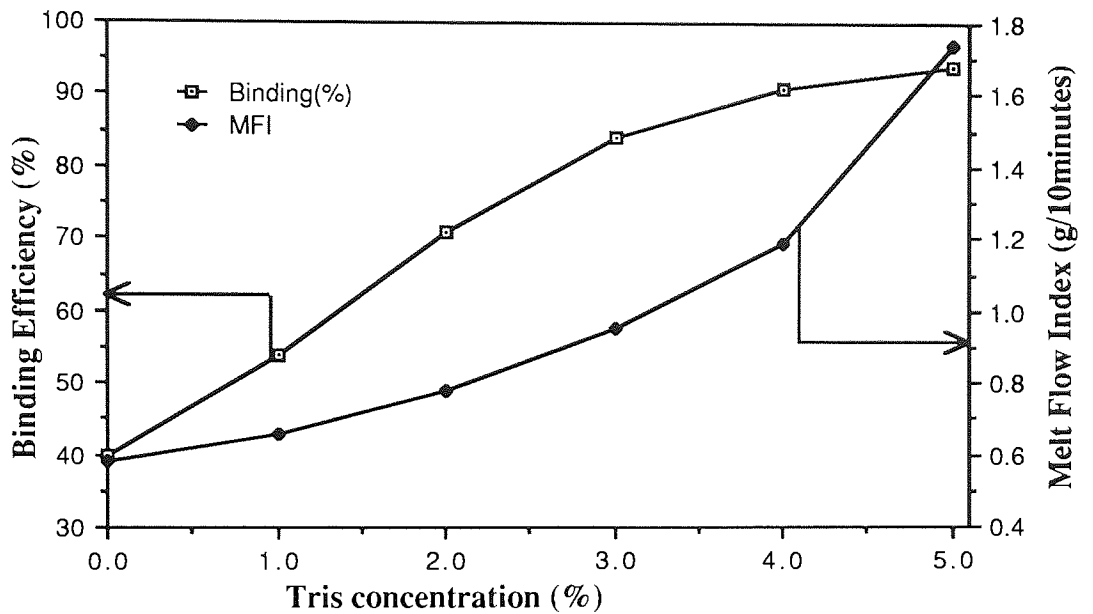


Figure 3.10 The effect of Tris concentration on the binding efficiency and MFI of 10% masterbatches containing at various ratio (DBBA+DVB), processed under standard condition.

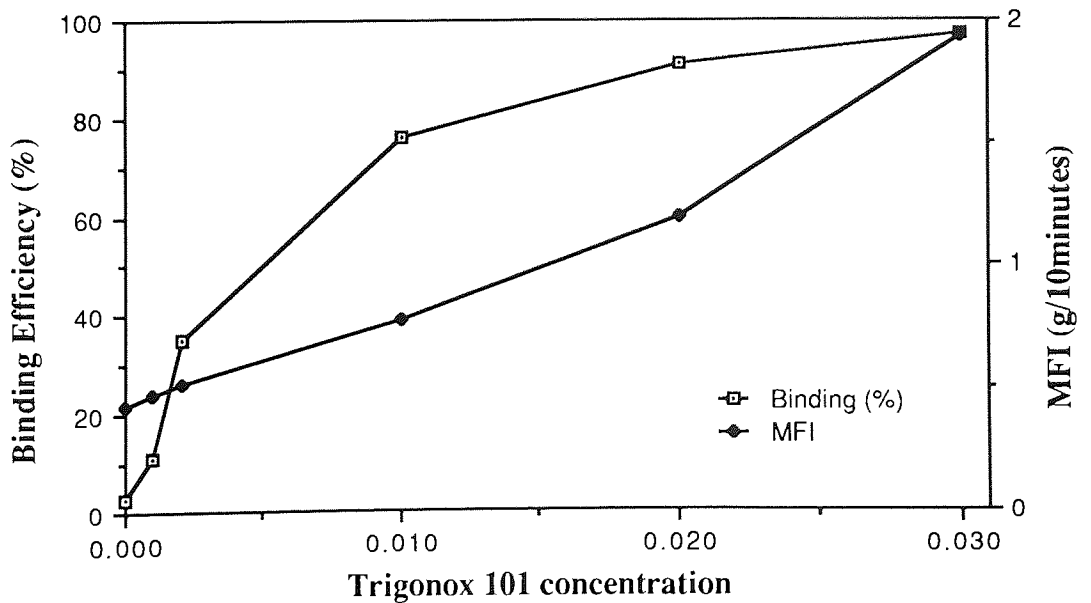


Figure 3.11 The effect of Trigonox 101 concentration (m.r.) on the binding efficiency and MFI of 10% masterbatches containing DBBA+Tris ratio 6/4, processed under standard condition.

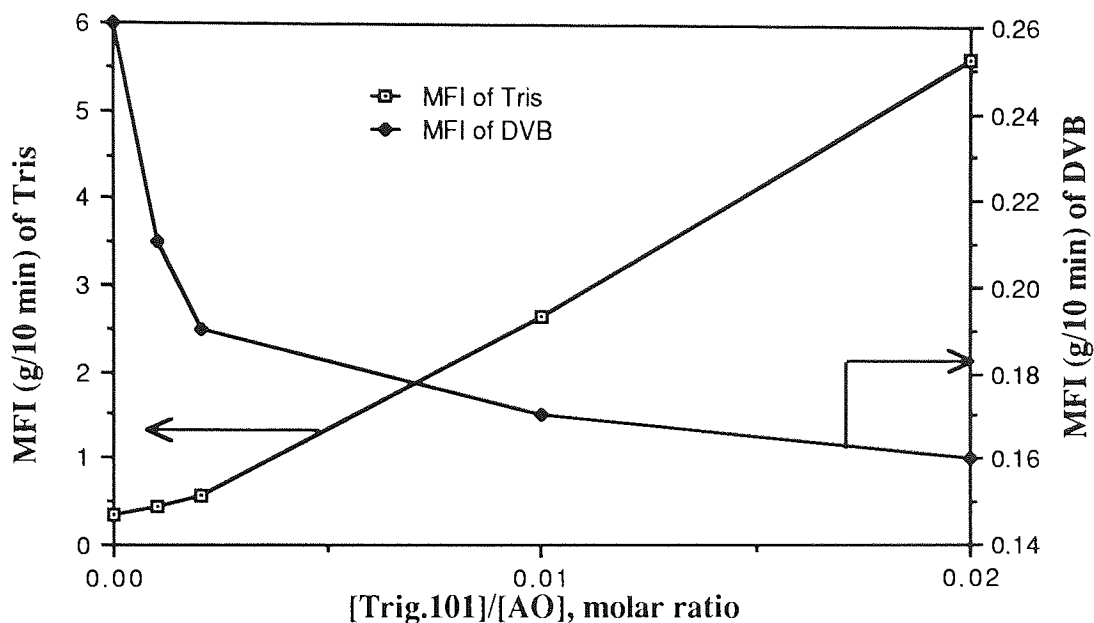


Figure 3.12 Effect of various concentration of Trigonox 101 on the MFI of polypropylene film containing 4% Tris or 4% DVB processed in closed mixing condition at 180°C for 10 minutes.

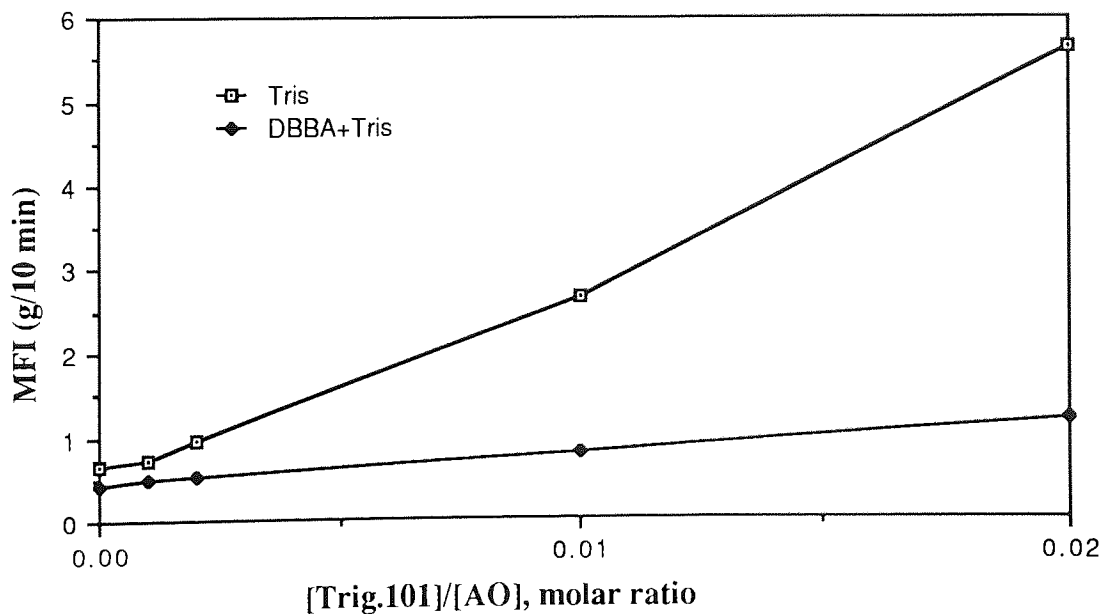


Figure 3.14 MFI values of 10% (DBBA+Tris) and 4% Tris masterbatches processed in the presence of different amounts of Trig.101, under standard condition.

B325

<7> TRDU-3 (9305)

ENDED: 04/06/90 10:1

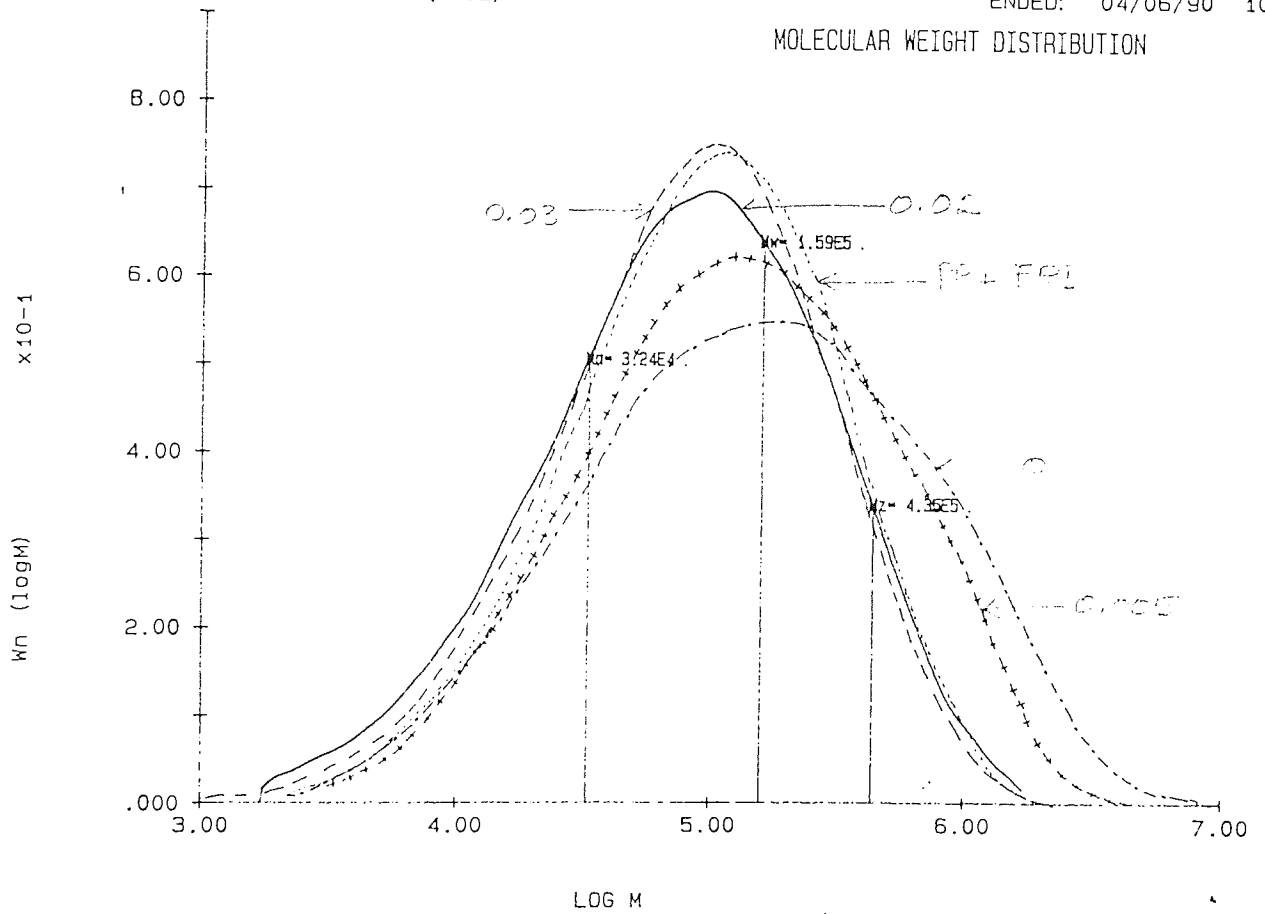


Figure 3.13 Molecular weight distribution curves for processed PP in the presence of 0.02 m.r Trig.101 (.....), in the presence of 6% DBBA+4% Tris (-.-.-.-), in the presence of 6% DBBA +4% Tris+FRI 0.005 m.r (++++), in the presence of 6% DBBA +4% Tris+FRI 0.02 m.r (____), in the presence of 6% DBBA +4% Tris+FRI 0.03 m.r (-----), (refer to Table 3.12)

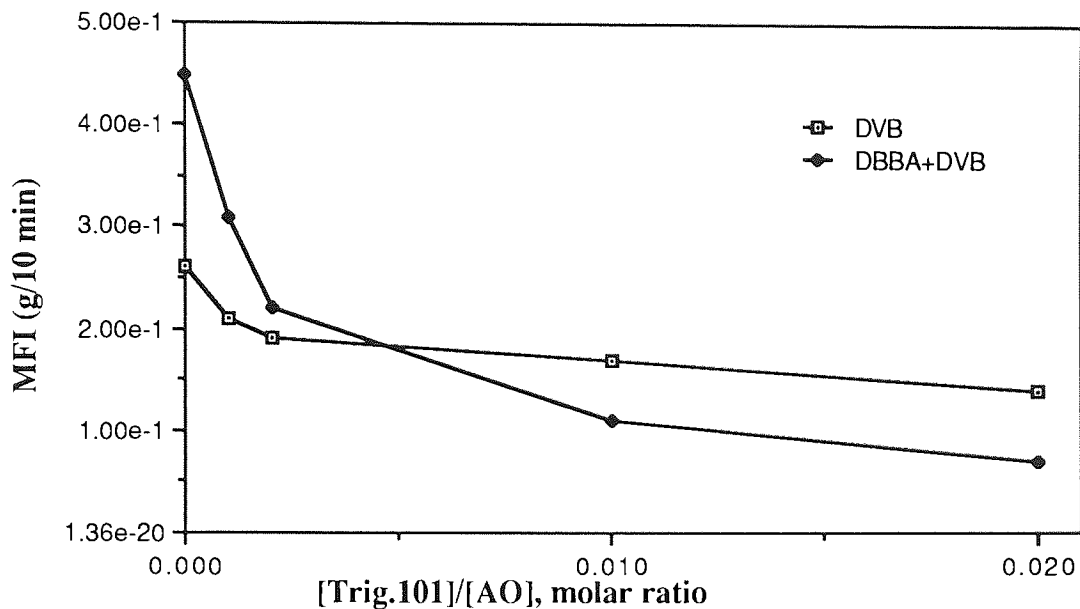


Figure 3.15 MFI values of 10% (DBBA+DVB) and 4% Tris masterbatches processed in the presence of different amounts of Trig.101, under standard condition.

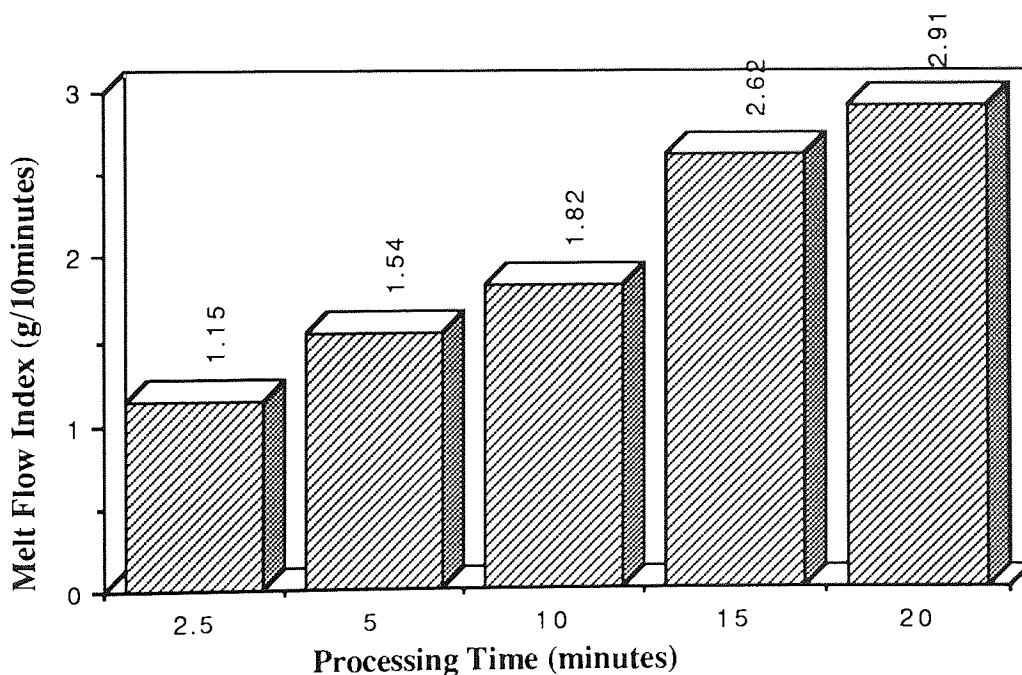


Figure 3.16 Effect of various processing time on MFI of 10% HAEB masterbatches, processed in the presence of Trigonox (0.005 m.r., I/HAEB), at 180°C under closed mixing condition.

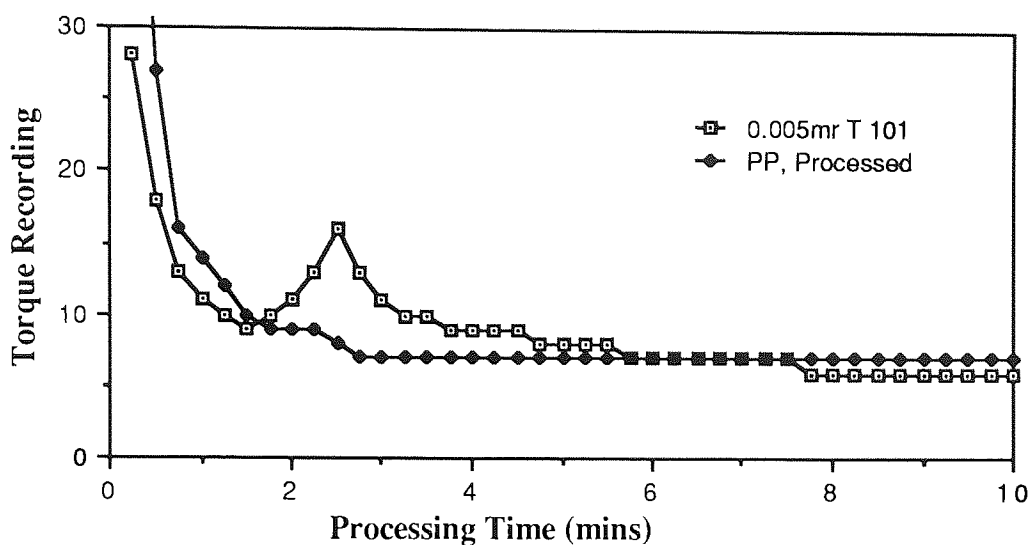


Figure 3.17 Effect of various processing time on the Torque changes of 10% MB's of HAEB in Polypropylene in the presence of 0.005 m.r. (I/HAEB) Trigonox 101, processed at 180°C under closed mixing condition.

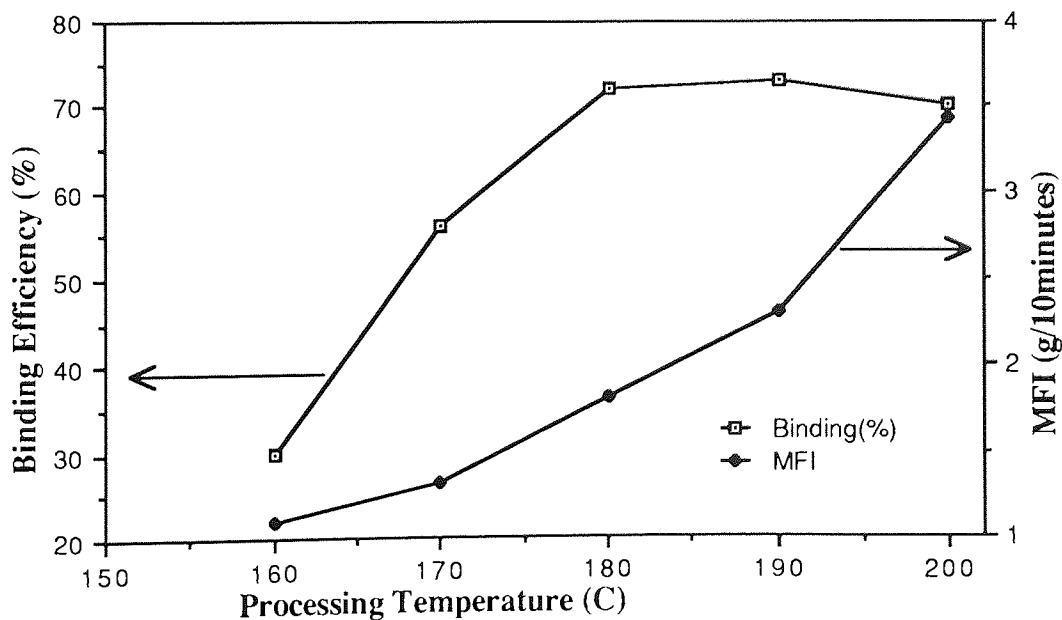


Figure 3.18 Effect of processing temperature on the binding efficiency of HAEB (10% MB) in propylene, in the presence of DCP (0.005 m.r., I/HAEB), processed in closed mixing condition for 10 minutes.

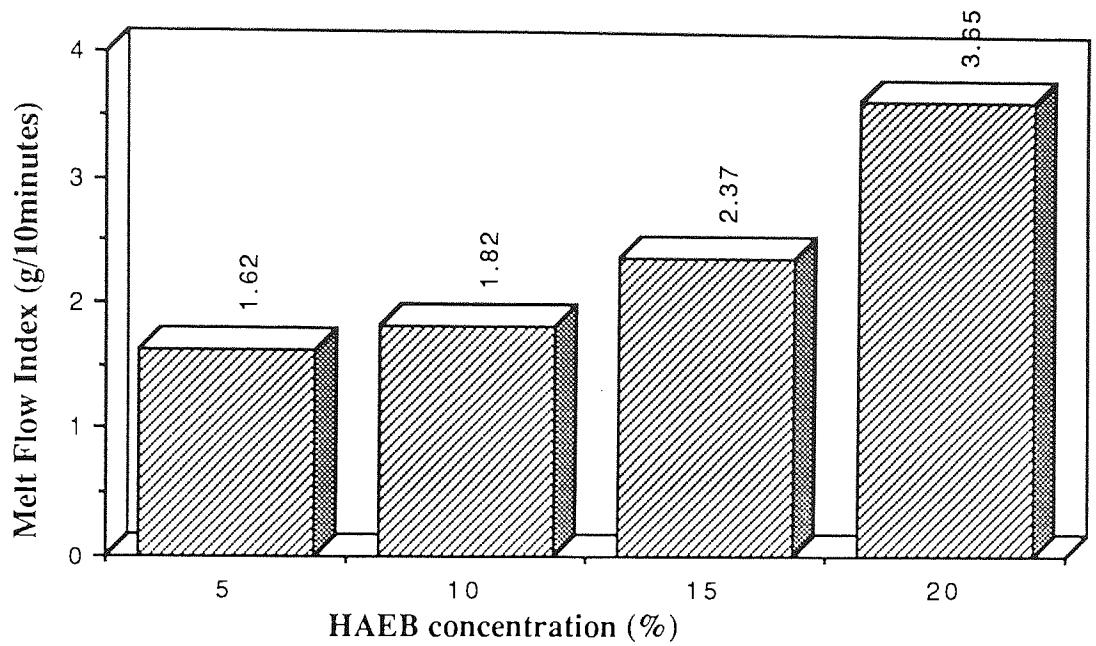


Figure 3.19 Effect of HAEB concentration on MFI masterbatches, processed in the presence of DCP (0.005 m.r, I/HAEB), under closed mixing condition at 180°C for 10 minutes.

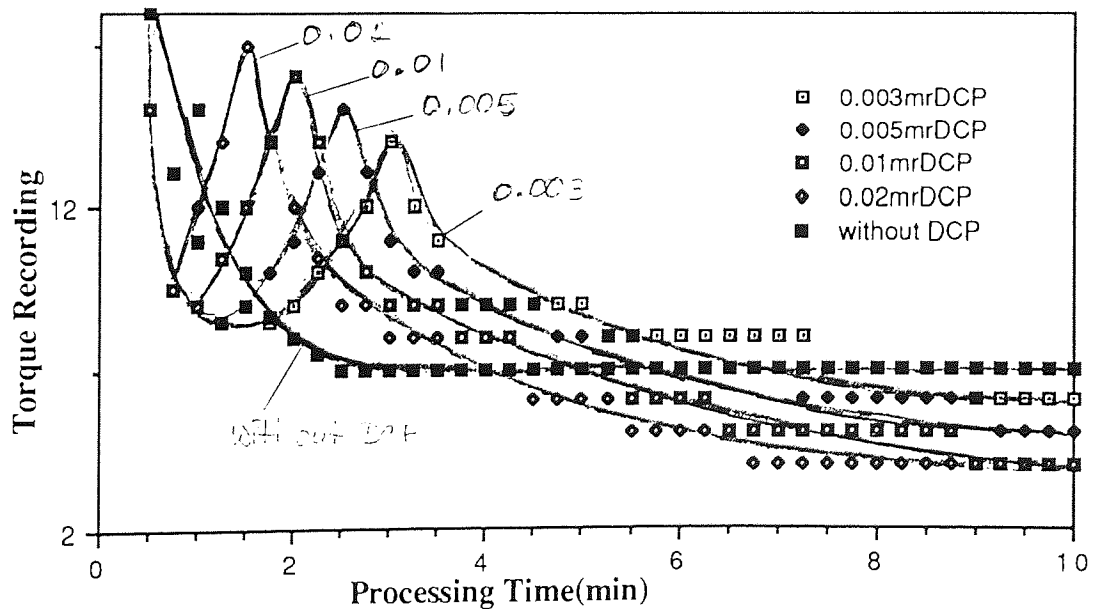


Figure 3.20 Changes in torque during processing of HAEB (10%) in PP in the presence of various concentrations of DCP, processed under standard condition

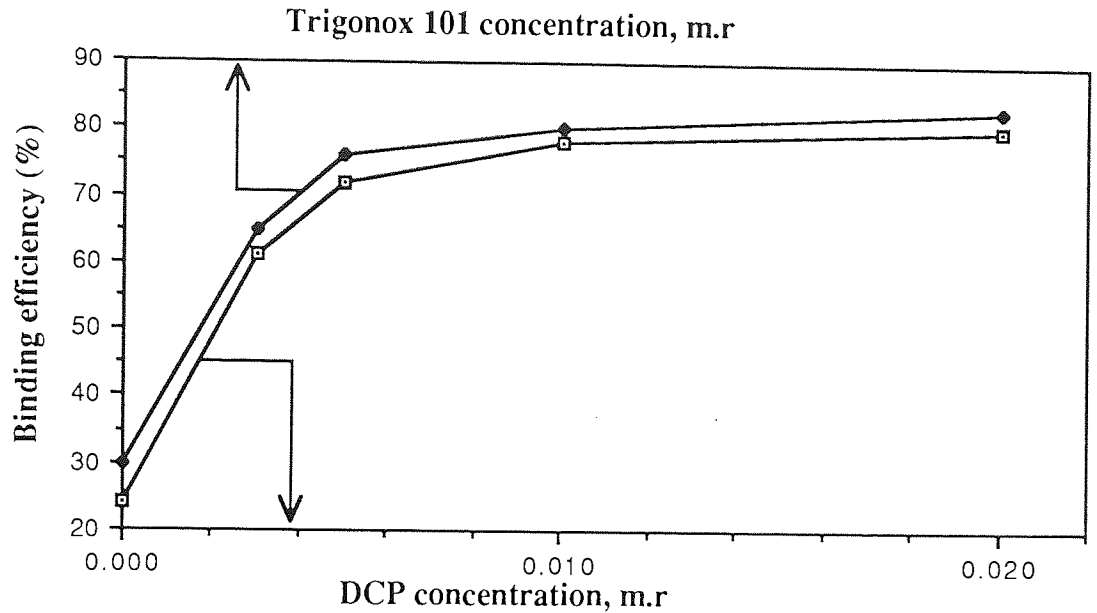


Figure 3.21 Binding efficiency of masterbatches containing 10% HAEB in polypropylene in the presence of various concentrations of FRI dicumyl peroxide or Trigonox 101, processed under standard condition.

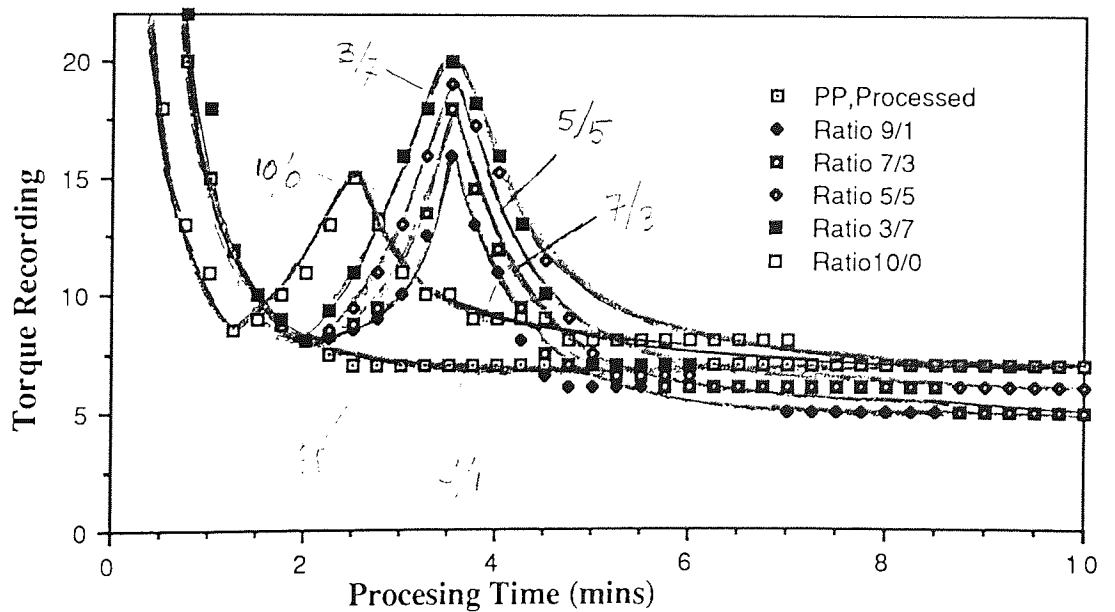


Figure 3.22 Changes in Torque during processing of 10% (HAEB/Tris) at various ratios with PP in the presence of 0.005 m.r., (I)/(HAEB+Tris) Trigonox 101 processed under standard condition.

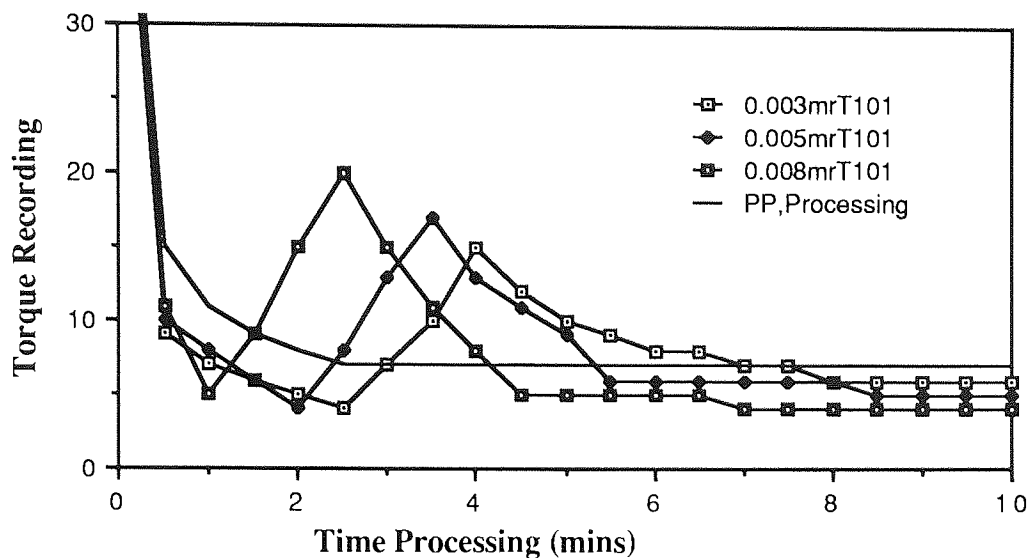


Figure 3.23 Torque recording of various concentration of FRI Trigonox 101 in binding efficiency and MFI of Polypropylene MB's containing 10 % mixture of HAEB/Tris ratio 9/1 processed in closed mixing condition at 180°C for 10 minutes.

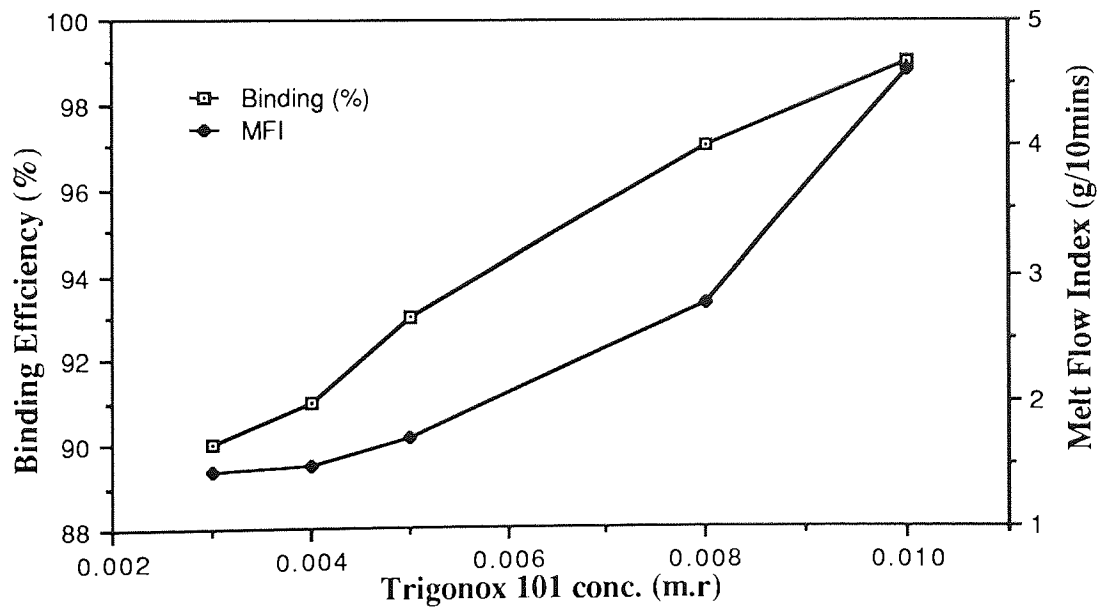


Figure 3.24 Effect of Trigonox 101 concentration on binding efficiency and MFI of MB's containing HAEB/Tris ratio 9/1, processed under standard condition

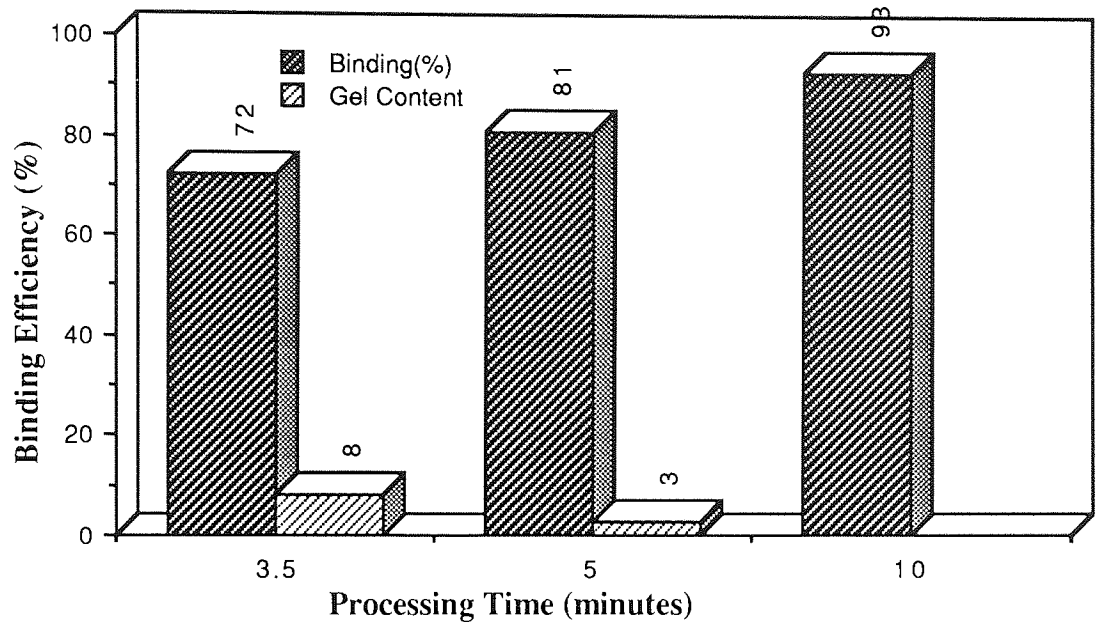


Figure 3.25 Effect of processing time on binding efficiency and gel content of MB's containing 10% (HAEB+Tris) at ratio 9/1 processed in the presence of 0.005 m.r. Trigonox 101, under standard condition.

CHAPTER FOUR

STABILISING ACTIVITY OF HINDERED PHENOL AND BENZOPHENONE CONTAINING ACRYLIC GROUP IN POLYPROPYLENE EITHER AS A SINGLE OR AS A MIXTURE OF ANTIOXIDANTS

4.1 OBJECT AND METHODOLOGY

The optimum conditions to achieve high binding efficiency of DBBA or HAEB in polypropylene have been discussed in the previous chapter. In this chapter the stabilising activity of highly bound DBBA and HAEB will be examined and compared with the effect of commercial antioxidants containing the same antioxidant functions. The combined effect of two highly grafted antioxidants containing hindered phenol (DBBA) and a UV stabiliser (HAEB) functions on their UV and thermal stabilising activity will also be examined.

The general experimental procedure used in this chapter is described in Scheme 4.1 - 4.4. Masterbatches containing different antioxidants (see Table 4.1) were processed (following procedure described in Scheme 3.1) and were subsequently diluted down in a torque rheometer (180°C, 10 minutes, closed mixer) in fresh polypropylene to different concentrations up to 0.4%. These dilute masterbatches were then compression moulded at 180°C and under a pressure of 85 kg/cm² into film of identical thickness (~0.1 - 0.2 mm), see Section 2.3.2 and Scheme 4.1. To study the combination effect, more than one AO (e.g. HAEB and DBBA) were reactively processed together in the presence of a coagent to produce a masterbatch which was then diluted down in fresh polypropylene to 0.4% (total AO's content), see Scheme 4.2. Another method involved the preparation of a masterbatch of each of the antioxidants, and more than one masterbatch which were diluted together in fresh polypropylene to 0.4% (total antioxidants content), see Scheme 4.3. Some masterbatches containing the bound antioxidants were also diluted in polypropylene

in addition to small concentrations of fresh commercial antioxidant (to 0.4% total antioxidants content), see Scheme 4.4. To investigate the uv-stabilising effect of these antioxidant combinations, both extracted and unextracted diluted films were then uv-irradiated. Results were compared with those of unstabilised polypropylene and that containing unbound commercial AO's containing similar antioxidant function (e.g. HOBP and Tinuvin 770, see Table 4.2). The extent of stabilising activity of these antioxidants was assessed by measuring embrittlement time (ET), and changes in carbonyl index (ΔCI) of the polymer sample during uv-irradiation. For thermal stabilisation both extracted and unextracted films were aged in separate cells of a Wallace oven at 140°C and air flow 85 l/h (more detail see Subsection 2.6.2) and their activity was compared with that of commercial antioxidants, e.g. Irganox 1076 and Irganox 1010, see Table 4.1. The schematic procedure's diagram of testing stability are described as in Scheme 4.1- 4.4.

Table 4.1 Various antioxidants were used in reactive processing

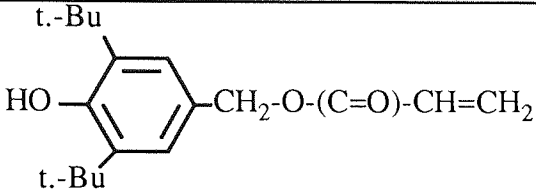
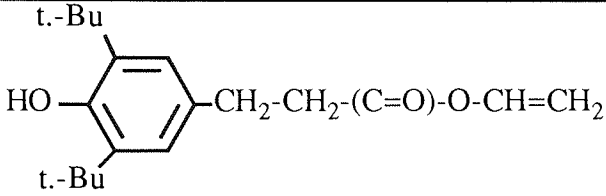
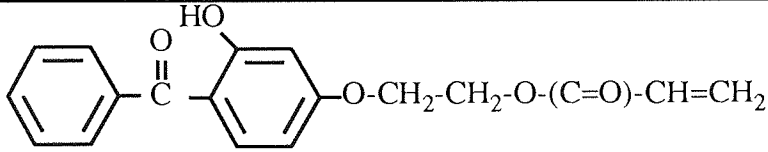
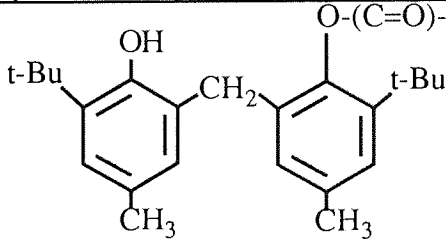
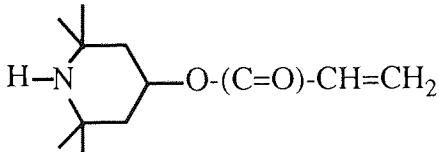
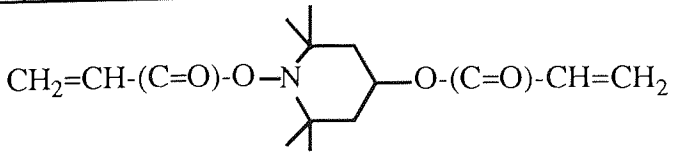
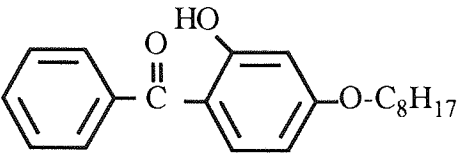
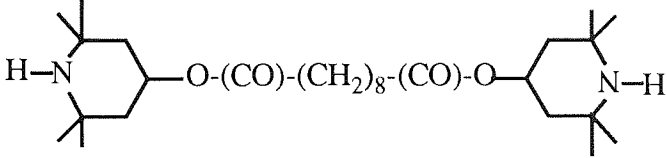
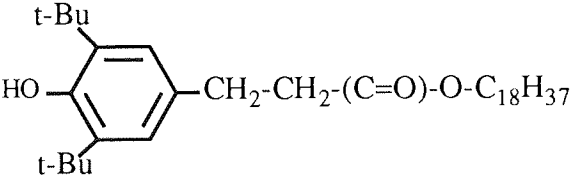
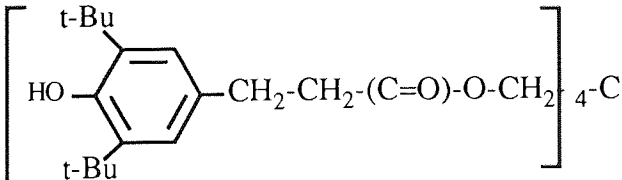
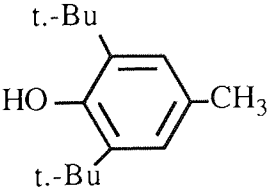
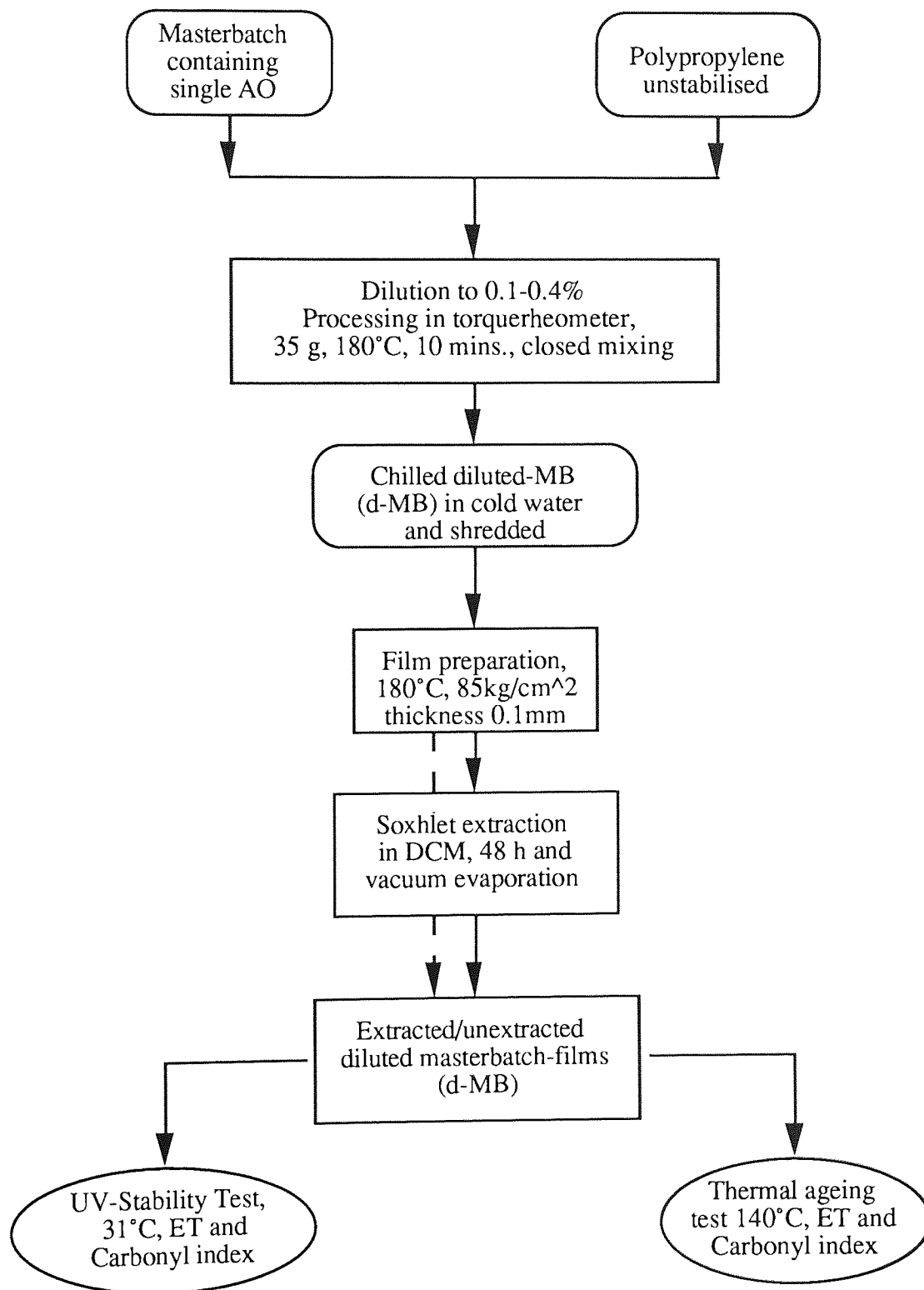
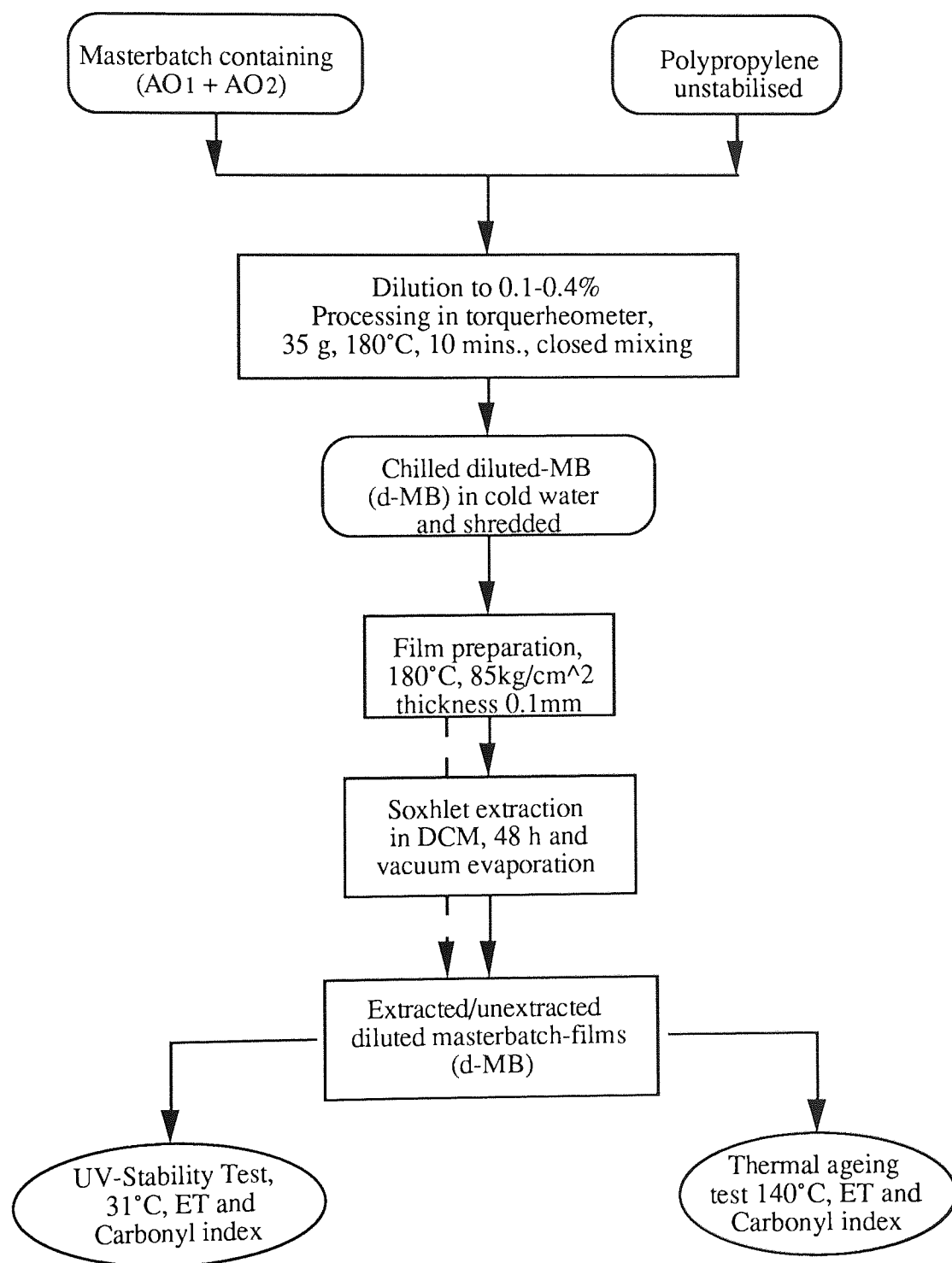
Structure number	Chemical structure, name and molecular weight (MW)	Abreviation
I	 <p>3,5 - di-tert.-butyl-4-hydroxy benzyl acrylate (MW=296)</p>	DBBA
II	 <p>Vinyl - (3,5-di-tert.-butyl-4-hydroxy) propionate (MW=310)</p>	VDBP
III	 <p>2-hydroxy-4-(beta acrylate ethoxy) benzophenone (MW=312)</p>	HAEB
IV	 <p>2,2'-methylene-bis-(4-methyl-6-tert.-butyl phenol monoacrylate (MW=394)</p>	SGM
V	 <p>4-acryloyloxy 2,2,6,6-tetra methyl piperidine (MW=211)</p>	AOTP
VI	 <p>1-acryoyl 4-acryloyloxy 2,2,6,6-tetra methyl piperidine (MW=265)</p>	AATP

Table 4.2 Various commercial antioxidants were used in reactive processing

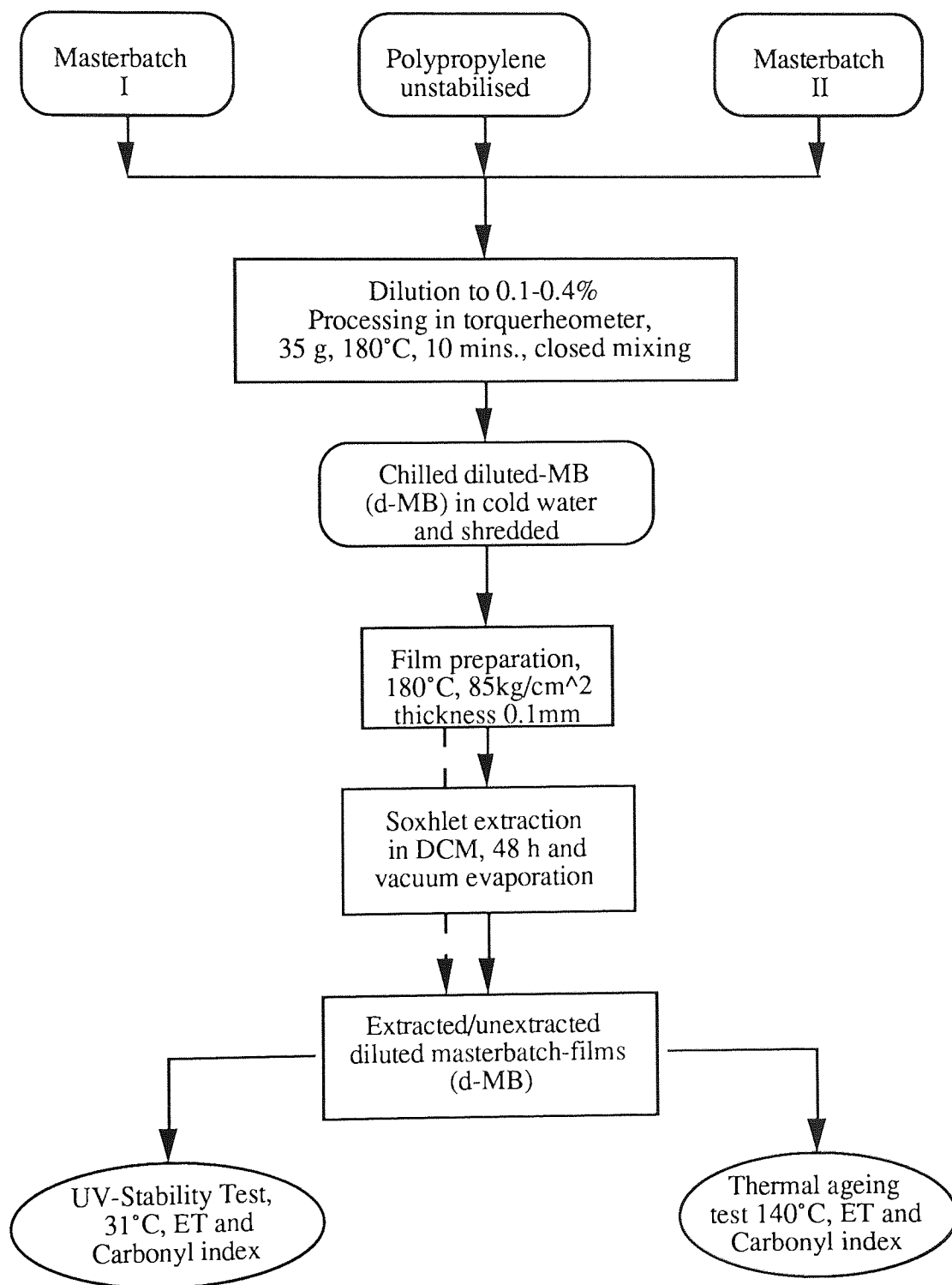
Structure number	Chemical structure, name and molecular weight (MW)	Abreviation
I	 <p>2-hydroxy-4-octyloxy-benzophenone (MW=326)</p>	Cyasorb UV-531 (HOBP)
II	 <p>Bis-(2,2,6,6-tetra methyl piperidine) sebacate (MW=506)</p>	Tinuvin 770
III	 <p>n-octadecyl-3-(3',5'-di-tert.-butyl-4-hydroxyphenyl) propionate (MW=521)</p>	Irganox 1076
IV	 <p>Pentaerythrityl tetrakis-(3,5,-di-tert.-butyl-4-hydroxyphenyl) propionate (MW=1095)</p>	Irganox 1010
V	 <p>3,5-di-tert.-butyl-4-hydroxy toluene (MW=220)</p>	BHT



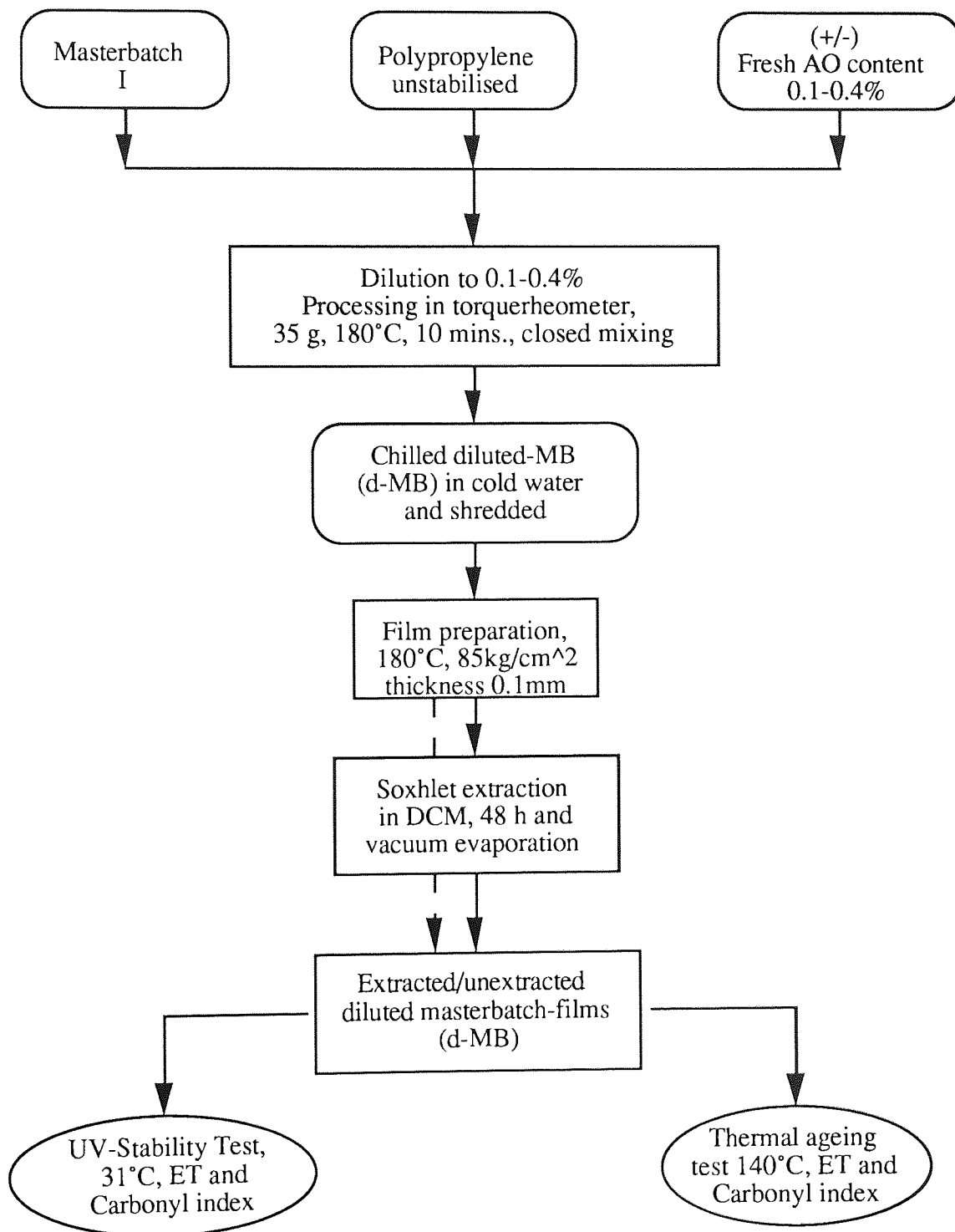
Scheme 4.1 Flow diagram for preparation of MB film containing single antioxidant for stabilising activity test



Scheme 4.2 Flow diagram for preparation MB film containing mixture antioxidants (one stage synergistic system) for stabilising activity test



Scheme 4.3 Flow diagram for preparation MB film containing mixture antioxidants from different MB's, processing separately (two stage synergistic system) for stabilising activity test



Scheme 4.4 Flow diagram for preparation MB film containing mixture antioxidants from MB and fresh AO, processing separately (two stage synergistic system) for stabilising activity test

4.2 RESULTS

4.2.1 Effect of Reactive Processing on the Photo Stabilising Activity of Derivatives of Hindered Phenol and Benzophenone Antioxidants Containing Acrylic Group.

Table 4.3 and Figure 4.1 show that the embrittlement time (ET) of diluted masterbatch films containing bound antioxidants (DBBA, VDBP, HAEB, AATP and AOTP) before extraction were higher than their extracted analogues, but in general they retain their antioxidant activity (even if it is low), see Figure 4.2. Table 4.4 and Figure 4.3 show that when the antioxidants (DBBA, VDBP, HAEB) were used as conventional antioxidant (unbound) before extraction their embrittlement time were higher compared to that of unbound one, but after extraction, they were very low similar to that of the polypropylene control processed without any additive. In the case of bound-VDBP sample due to difficulties in synthesis (very low yield), the masterbatch was prepared only 3%.

Table 4.3 Binding and uv-stability of bound AO's in PP-films containing 0.4% of AO's (before and after extraction), diluted from 10% masterbatches processed in the presence of 0.02 m.r. [I]/[AO] Trigonox 101. (* diluted from 3% masterbatch)

No	Film Sample	Binding (%)	UV Embrittlement Time (hours)	
			Before Extraction	After Extraction
1	DBBA	40	190	160
2	VDBP*	25	150	130
3	HAEB	72	310	140
4	AATP	100	550	350
6	AOTP	50	1375	475

The commercial photostabilisers (HOBP and Tinuvin 770) used as conventional antioxidants (see Table 4.4 and Figure 4.1) show very high stabilising activity in polypropylene as expected, but their activity is reduced to that of unstabilised polypropylene after extraction (see Figure 4.1 and 4.2).

Table 4.4 UV-stability of PP-films containing 0.4% of unbound AO's (before and after extraction) processed without peroxide as conventional additive.

No	Film Sample	UV Embrittlement Time (hours)	
		Before Extraction	After Extraction
1	PP, processed	75	70
2	HMW-25, processed	145	70
3	Tinuvin 770	1500	70
4	HOBP (Cyasorb UV-531)	1200	70
5	Irganox 1076	185	70
6	Irganox 1010	200	70
8	Irg.1010 + HOBP (0.2/0.2)	1450	70
9	Tin.770 + HOBP (0.2/0.2)	1750	70
10	Irg.1076 + HAEB (0.2/0.2)	285	70
11	DBBA, Ub	205	80
12	VDBP, Ub	185	70
13	HAEB, Ub	330	70

The effect of an enhanced level of binding (by using coagents, Tris or DVB) on the stabilising efficiency of antioxidants was investigated. 10% masterbatches of DBBA/Tris, DBBA/DVB and VDBP/Tris (all at weight ratio 6/4), 10% masterbatch of HAEB/Tris (weight ratio 9/1) and 10% masterbatch of AOTP/Tris (weight ratio 8/2) were all diluted down in unstabilised polypropylene to 0.4%. Films of these masterbatches were then uv-

irradiated and aged in a Wallace oven (at 140°C) before and after soxhlet extraction in DCM. In the case of VDBP/Tris film sample, due to synthesis difficulties, it is diluted from a 3% masterbatch. Table 4.5 and Figure 4.4 show that the UV embrittlement time (ET) of these antioxidants were all low (except AOTP/Tris), although, extraction with DCM does not cause much change (except for AOTP/Tris), this was clearly stated by previous workers⁽¹¹²⁾. It can be seen generally, that the stabilising activity of these antioxidants in polypropylene in the presence of coagent, even though they have improved the binding efficiency, show no improvement.

Table 4.5 Binding and UV stability of PP-film containing 0.4% of AO in the presence of coagent (before and after extraction), diluted in fresh polypropylene from 10% masterbatches processed in the presence of 0.02 m.r.[I]/[AO+Coagent) under standard condition. * diluted from 3% masterbatch

No	Film sample (0.4%)	Ratio of AO/Coagent	MB's conc.(%)	Binding (%)	UV Embrittlement Time(hours)	
					Before Extraction	After Extraction
1	DBBA+Tris	6/4	10	91	160	150
2	DBBA+DVB	6/4	10	93	140	110
3	VDBP+Tris*	6/4	3	67	150	110
4	HAEB+Tris	9/1	10	93	195	115
5	AOTP+Tris	8/2	10	85	1635	425

4.2.2 Effect of Reactive Processing on the Thermal Stabilising Activity of Derivatives of Hindered Phenol and Benzophenone Containing Acrylic Group as a Single Antioxidant.

Table 4.6 shows that bound antioxidants (e.g. DBBA, VDBP and SGM), used without a coagent, before extraction have the highest thermal ET at 140°C and after extraction the

bound DBBA shows much better performance compared to the rest, see Figures 4.5 and 4.7. In the case of VDBP (diluted from 3% masterbatch) the ET of bound antioxidant as shown in Tables 4.6 & 4.7 was higher than that of the unbound one, even higher than that of bound DBBA. For bound Sumiliser GM in polypropylene it was also shown that their ET before and after extraction were low. Generally, before extraction the thermal stabilising activity of bound AO's (DBBA, VDBP, DBBA/Tris, DBBA/DVB, and VDBP/Tris) is much lower compared to those of commercial antioxidants (Irganox 1076 and Irganox 1010). However, after exhaustive DCM soxhlet extraction the ET of bound AO's was much higher than that of commercial antioxidants, see Figure 4.6.

**Table 4.6 Thermal stability of PP-films containing 0.4% of bound and unbound AO's (before and after extraction) diluted from 10% MB's processed without and with 0.02 m.r. [I]/[AO+Coagent] Trigonox 101 under standard condition.
* diluted from 3% masterbatches**

No	Film sample (0.4%)	Trig.101 m.r.	Ratio of AO's	MB's conc.(%)	Binding (%)	Embrittlement Time (hours) at 140°C	
						Before Extraction	After Extraction
1	DBBA	0.02	-	10	40	60	50
2	VDBP	0.02	-	3	25	90	10
3	SGM	0.02	-	10	15	20	10
4	DBBA+Tris	0.02	6/4	10	91	40	30
5	DBBA+DVB	0.02	6/4	10	93	30	20
6	VDBP+Tris	0.02	6/4	3	67	110	15
7	DBBA,Ub	0	-	10	0	50	3
8	VDBP,Ub	0	-	3	0	50	3
9	SGM,Ub	0	-	10	0	25	3

Table 4.7 Thermal stability (at 140°C) of PP-films containing 0.4% of unbound commercial AO (before and after extraction) and PP processed as control.

No	Film sample (0.4%)	Embrittlement Time (hours) at 140°C	
		Before Extraction	After Extraction
1	PP, processed	2	2
2	DTBP	20	3
3	DBHBA	25	3
4	DBBA, Ub	50	3
5	Irganox 1076	350	3
6	Irganox acid	40	3
7	VDBP, Ub	50	3
8	Irganox 1010	1350	3
9	BHT	30	3
10	SGM	25	3

4.2.3 Effect of Mixture Antioxidant Activity of Hindered Phenol and Benzophenone Containing Acrylic Group as Mixture AO's ('one-stage' synergistic system) on Thermal Stabilising Activity of PP

To investigate the synergistic effect of bound DBBA on the thermal stabilising activity, mixtures of DBBA with other antioxidants were prepared (following the procedure described in Scheme 4.2) as masterbatches, see Table 4.8. 10% masterbatches containing bound DBBA/AO₂/Tris at different weight ratio (see Table 4.8) were prepared in the presence of 0.02 molar ratio [I]/[DBBA+AO₂+Tris] Trigonox 101 and were then diluted down in fresh polypropylene to 0.4% total concentration antioxidant (AO₁+AO₂) and tested for their thermal stabilising effectiveness in polypropylene at 140°C (Wallace oven). Table 4.8 shows that all AO have low stabilising activity when compared to that of commercial hindered phenols (Irganox 1010 and Irganox 1076)

Table 4.8 Thermal stability of PP-films containing 0.4 % of bound mixture of AO's (before and after extraction) diluted from 10% masterbatches processed in the presence of 0.02 molar ratio [I]/[AO₁+AO₂+Coagent] Trigonox 101 under standard condition. (* diluted from 3% masterbatch)

No	Film sample containing 0.4%, (AO ₁ +AO ₂)	Weight ratio AO's & coagent in 10% MB	Embrittlement Time (hours) at 140°C	
			Before Extraction	After Extraction
1	(DBBA/HAEB)/Tris	(4/4)/2	120	75
2	(DBBA/AATP)/Tris	(4/4)/2	45	20
3	(DBBA/AOTP)/Tris	(4/4)/2	100	35
4	(VDBP/HAEB)/Tris*	(4/4)/2	150	40
5	(DBBA/HAEB)/Tris	(2.7/5.3)/2	85	45
6	(DBBA/HOBP)/Tris	(2.7/5.3)/2	40	10
7	(DBBA/Tin.770)/Tris	(2.7/5.3)/2	70	10
8	DBBA/Tris	6/4	40	30
9	VDBP/Tris*	6/4	110	15
10	HAEB/Tris	9/1	15	3
11	Irganox 1010	-	1350	3
12	Irganox 1076	-	350	3

4.2.4 Effect of Mixture Antioxidant Activity of Hindered Phenol and Benzophenone Containing Acrylic Group as Mixture AO's on UV-Stabilising Activity of Polypropylene.

To study the combined effect of bound DBBA (thermal antioxidant) with UV stabilisers, some bound UV stabilisers such as HAEB, AATP and AOTP were used as synergists. Films containing various ratios of mixtures of antioxidants were prepared in two different ways. The first (see procedure in Scheme 4.2) involved 10% total antioxidant mixtures and coagent which were reactively processed in polypropylene at different ratios of antioxidants (agents) to coagent in the presence of 0.02 molar ratio ([I]/[agent+coagent]) Trigonox 101. To investigate the effect of Tris content and UV stabiliser (AO₂) content in DBBA (AO₁) masterbatches, the masterbatches containing different concentrations of

antioxidant mixture (e.g. [AO1+AO2] to [Tris] and [AO1] to [AO2]) were varied, see Table 4.8a. In the case of the VDBP/HAEB/Tris system only a 3% masterbatch was prepared due to the difficulties in the synthesis of VDBP and the very low yield obtained, thus only one ratio, containing 0.6% Tris and ratio of antioxidants to coagent of 1.2/1.2/0.6 = 4/4/2 was used. Table 4.9 and Figure 4.7 show that generally the ET of the masterbatch films containing mixture of antioxidants is higher at higher HAEB concentration. Table 4.9 and Figure 4.9 show that ET of diluted masterbatch films of mixtures of DBBA/HAEB/Tris at a weight ratio 2/6/2 (containing 2% Tris coagent) give the highest ET before and after extraction compared with that of other ratios (i.e. very high retention of activity, see Figure 4.8).

Table 4.8a The combination of antioxidant mixtures and coagent in 10% masterbatches.

No	[AO1+AO2], (%)	[A1], (%)	[A2], (%)	[Coagent], (%)
1	9	4.5	4.5	1
2	9	3	6	1
3	9	2.2	6.8	1
4	8	4	4	2
5	8	2.7	5.3	2
6	8	2	6	2
7	7	3.5	3.5	3
8	7	2.3	4.7	3
9	7	1.8	5.2	3

Table 4.9 UV Stability of PP-films containing 0.4% of mixture AO's in varied composition (before and after extraction), diluted in PP from 10% masterbatches processed in the presence of 0.02 molar ratio [I]/[AO1+AO2+AO3+Tris] Trigonox 101, under standard condition. (* diluted from 3% masterbatch)

No	Film sample (0.4%)	Ratio of AO's	UV Embrittlement Time (hours)	
			Before Extraction	After Extraction
1	(DBBA/HAEB)/Tris	(4.5/4.5)/1	685	430
2	(DBBA/HAEB)/Tris	(3/6)/1	1120	560
3	(DBBA/HAEB)/Tris	(2.2/6.8)/1	1340	730
4	(DBBA/HAEB)/Tris	(4/4)/2	1160	1130
5	(DBBA/HAEB)/Tris	(2.7/5.3)/2	1810	1650
6	(DBBA/HAEB)/Tris	(2/6)/2	2210	1970
7	(DBBA/HAEB)/Tris	(3.5/3.5)/3	720	470
8	(DBBA/HAEB)/Tris	(2.3/4.7)/3	1230	610
9	(DBBA/HAEB)/Tris	(1.8/5.2)/3	1395	830
10	(VDBP/HAEB)/Tris*	(4/4)/2	1050	560
11	(DBBA/HAEB/AOTP)/Tris	(2.7/2.7/2.6)/2	1180	830
12	(DBBA/HAEB/AATP)/Tris	(2.7/2.7/2.6)/2	1040	830

A different method was used to prepare synergistic masterbatches containing bound antioxidants involving initially, the preparation of a single antioxidant masterbatch containing DBBA, HAEB, AOTP or AATP (separately processed with or without Tris coagent in the presence of an optimum concentration of Trigonox 101). To study the combined effect, the ratio of AO's content in every masterbatch was varied. Two masterbatches were chosen and then were diluted together in fresh polypropylene to 0.4% total antioxidant content. Extracted and unextracted films were then irradiated in a UV-cabinet to test their stabilising activity.

The photo stabilising activity results (see Table 4.10), show clearly that when masterbatches containing different bound antioxidants {(DBBA/Tris) and (HAEB/Tris)} were prepared separately and then diluted together (two stage preparation, see Scheme 4.3), they gave lower embrittlement times compared to the effect if they were processed together (one stage preparation, see Scheme 1.2). On the other hand, the masterbatch films containing bound AO's mixtures with AOTP {(DBBA/HAEB/Tris) and (AOTP/Tris)} prepared following a two stage preparation, gave an embrittlement times higher compared to that of a single processing (one stage preparation).

To examine whether there is any combination effect of HOBP with hindered phenolic antioxidants, the masterbatches containing bound-DBBA and fresh HOBP were diluted down together in fresh PP to 0.4% of total AO's (see procedure in Scheme 4.4). The concentration of both antioxidants were varied (see table 4.12). Table 4.12 shows that in the presence of HOBP before extraction, the embrittlement times were high, even than the sum of those of the single antioxidants. However, after soxhlet extraction, the uv-stabilising activity of remaining bound DBBA does not exhibit any considerable improvement compared to that of bound DBBA without HOBP.

Table 4.10 UV Stability of PP-films containing 0.4% AO's of mixture masterbatches in varied composition (before and after extraction), diluted from 10% masterbatches processed in the presence of 0.02 molar ratio Trigonox 101, under standard condition.

No	Film sample cont'g 0.4% total AO's (d-MB I) + (d-MB II)	0.2% AO's d-MB I Ratio AO's &coagent	0.2%AO's d-MB II Ratio AO &coagent	UV Embrittlement Time (hrs)	
				Before Extraction	After Extraction
1	[DBBA/Tris] + [HAEB/Tris]	6/4	9/1	320	160
2	[(DBBA/HAEB)/Tris] + [AATP]	(4 / 4) / 2	10	630	520
3	[(DBBA/HAEB)/Tris] + [AATP]	(2.7/5.3)/2	10	840	550
4	[(DBBA/HAEB)/Tris] + [AATP]	(2 / 6) / 2	10	510	480
5	[(DBBA/HAEB)/Tris] + [AOTP/Tris]	(4 / 4) / 2	(8/2)	1330	730
6	[(DBBA/HAEB)/Tris] + [AOTP/Tris]	(2.7/5.3)/2	(8/2)	1560	840
7	[(DBBA/HAEB)/Tris] + [AOTP/Tris]	(2 / 6) / 2	(8/2)	1040	670

Table 4.11 UV Stability of PP-films containing different single AO using various ratio Tris coagent in varied concentration (before and after extraction), diluted from 10% masterbatches processed in the presence optimum Trig.101, under standard condition.

No	Film sample	Ratio of AO's	d-MB containing AO (%)	UV-Embrittlement Time (hours)	
				Before Extraction	After Extraction
1	(DBBA/Tris)	6/4	0.20	130	110
2	(DBBA/Tris)	6/4	0.13	120	105
3	(DBBA/Tris)	6/4	0.10	115	105
4	(HAEB/Tris)	9/1	0.20	120	100
5	(HAEB/Tris)	9/1	0.27	140	120
6	(HAEB/Tris)	9/1	0.30	140	120

Table 4.12 Effect of UV-stabiliser (HOBP) on the uv-irradiated of PP films containing bound DBBA with coagent at 0.4% total AO's mixture MB's (before and after extraction), diluted from 10% masterbatches processed in standard condition.

No	Film sample contain (0.4%) AO's (MB I) + (fresh HOBP)	d-MB I containing AO (%)	Fresh HOBP (%)	UV Embrittlement Time (hrs)	
				Before Extraction	After Extraction
1	[DBBA/Tris] + [HOBP]	0.1	0.3	1310	110
2	[DBBA/Tris] + [HOBP]	0.2	0.2	850	120
3	[DBBA/DVB]+ [HOBP]	0.1	0.3	1120	100
4	[DBBA/DVB]+ [HOBP]	0.2	0.2	750	105
5	[DBBA/Tris]	0.1	-	90	100
6	[DBBA/Tris]	0.2	-	140	120
7	[DBBA/DVB]	0.2	-	120	110
8	HOBP	-	0.2	640	70
9	HOBP	-	0.3	960	70

4.3 DISCUSSION

4.3.1 Effect of Reactive Processing on Stabilising Activity of Hindered Phenol and Benzophenone in Polypropylene Containing Acrylic Group

It was found that the stabilising activity of bound DBBA either as a thermal antioxidant or uv-stabiliser is lower compared to that of unbound DBBA as shown in Tables 4.3, 4.4 & 4.6 and Figures 4.3 & 4.5. Use of peroxide in reactive processing is not only to initiate grafting reaction of antioxidants or polymers but will also initiate melt and thermal degradation. During processing, therefore, some of the radical scavenger antioxidant will act mainly to protect the polymer from degradation, which in turn, can decrease the stabilising activity of the antioxidants in service (188). Allen and Chmela(189,190) reported that polymerised antioxidants in polypropylene exhibit lower photo stabilising activity compared to the unpolymerised antioxidants. In the case of DBBA, even though the level of binding is very high, the thermal stabilising efficiency is very low when compared to that of Irganox 1076 or Irganox 1010. This should be due to the fact that DBBA does not have any propionate group which can form a regenerative mechanism like commercial antioxidants (e.g. Irganox 1010 and 1076). Gugumus⁽¹⁴¹⁾ has reported that the mechanism of hindered phenol substituted with a propionate group there is a chain breaking regenerative character step for the formation of a phenoxyl radical with a second alkyl radical to form a resonance stabilising structure which is then a regenerated hindered phenol (see reaction no. 1.30 in Chapter-1).

A sample film containing bound-VDBP (diluted from 3% MB), having a propionate group substituent, exhibited a lower stabilising activity, both in thermal ageing and photo irradiation, see Tables 4.3 to 4.7. This should be due to the preparation of the masterbatch using a very low VDBP concentration (3%). Yachigo and workers⁽¹⁴⁶⁾ have demonstrated that a hindered phenol containing an acrylic group (Sumiliser GM, see Table

4.1) is a very effective stabiliser for thermal degradation of a butadiene type polymers by trapping radicals. However, in this work neither bound nor unbound Sumiliser GM resulted in a good thermal stabilisation in polypropylene using a reactive processing procedure.

4.3.2 Synergistic of Hindered Phenol and Benzophenone in Polypropylene Containing Acrylic Group

In this work a very high synergistic action of reactively processed bound DBBA/HAEB systems which retained their stabilising activity after extraction was achieved, see Tables 4.9 & 4.11 and Figure 4.9. This effect is due primarily to the non removal of the bound antioxidants under these conditions. The reason for this high antioxidant synergistic activity can be suggested to be due to cooperative action of the free radical scavenger (DBBA) which protects the UV stabiliser (HAEB) during processing and the UV stabiliser which offers the UV stability and protects the DBBA and polymer from the adverse effect of UV light⁽¹⁹¹⁾. The UV-screening action of benzophenone is due to a keto-enol tautomerisation of carbonyl and hydroxyl groups, see Chapter-1 Scheme 1.9^(61,62). Furthermore, it is reported^(48,149) that the benzophenone may also function as a radical scavenger for alkoxy radicals and this, in turn, is responsible for the subsequent destruction of the stabiliser function. Some previous work at Aston⁽¹¹²⁾ has shown that HOBP (as UV-screen and radical scavenger) synergises with bound AATP (UV-stabiliser) in polypropylene. Similarly, bound AOTP (UV-stabiliser) and HOBP led to a very effective synergism⁽¹¹²⁾. It was suggested that HOBP protects AATP from UV light during the early stages of polymer degradation until AATP or AOTP are ready to produce a nitroxyl radical ($>NO\cdot$) and undergoes a regenerative mechanism⁽¹¹²⁾. Scott and Evan⁽¹⁰⁷⁾ have successfully grafted DBBA and HAEB by UV irradiation onto the surface polypropylene which gave effective synergism.

On the other hand, samples of bound DBBA and bound HAEB prepared using a two stage synergism (see procedure Scheme 4.4) show low stabilising activity compared to that of using one stage synergism (Scheme 4.2), see Table 4.10. In this case, DBBA should not protect the destruction of HAEB during the first separate processing, but the former only protects further destruction of HAEB in the second processing during dilution. In the first stage processing some of the HAEB as a UV-stabiliser was lost due to a transformation reaction and subsequently there is a decrease in its stabilising activity. This is in agreement with the previous work which had been reported by Allen and coworkers⁽¹⁸⁷⁾ that re-processing of Tinuvin 770 in polypropylene can decrease its uv-stabilising activity, compared to that of a single processing. Chakraborty and Scott^(67,149) have reported that the benzophenone may function as a radical scavenger for alkoxy radicals and could destroy the stabiliser's function.

The mixture of bound DBBA (radical scavenger) and fresh HOBP (UV-stabiliser) before extraction also shows the synergistic effect (see Table 4.12). However, after extraction when the unbound HOBP was removed from the bound DBBA in polypropylene film, the stabilising activity was found to be very low. This low stability in the system may be due to the removal of unbound HOBP antioxidant after aggressive soxhlet extraction in DCM.

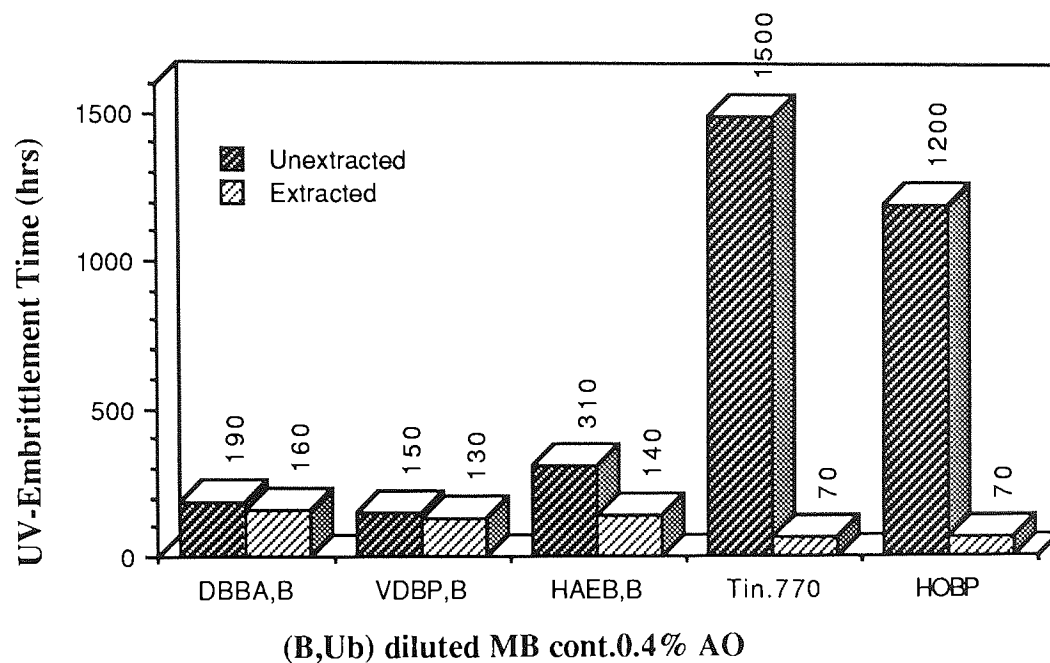


Figure 4.1 Embrittlement time of uv-irradiated diluted-films containing 0.4% of various bound (B) antioxidants and commercial AO's before (Unextracted) and after extraction (Extracted).

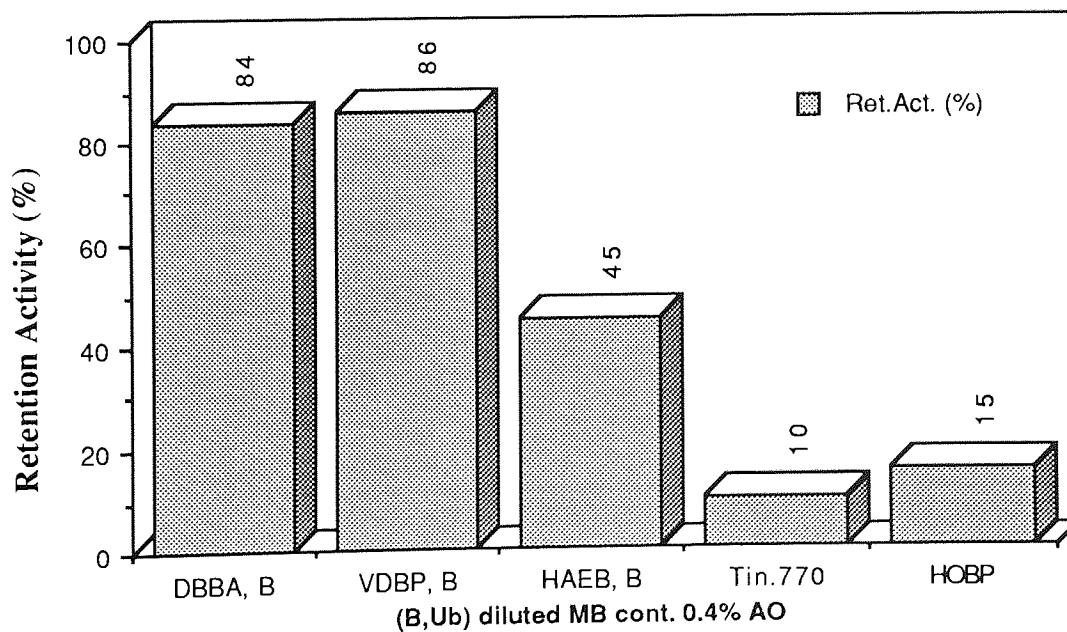


Figure 4.2 Retention activity of uv-irradiated diluted-films containing 0.4% of bound (B) antioxidants and commercial AO's.

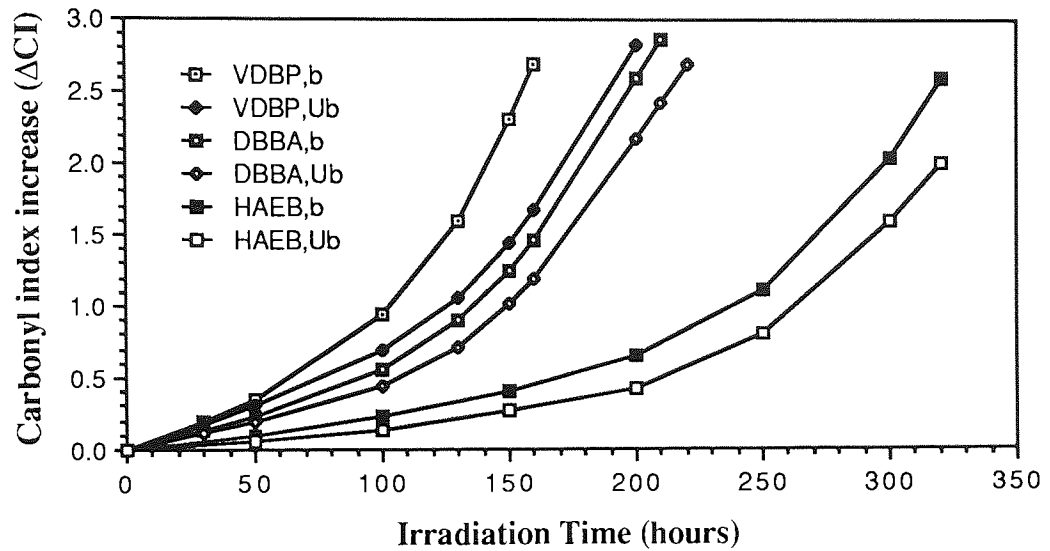


Figure 4.3 Carbonyl index increase during uv-irradiation of diluted masterbatch film containing 0.4% of bound and unbound VDBP, DBBA, and HAEB before extraction, refer to Table 4.3 sample no 1-3 and Table 4.4 sample no.11-13

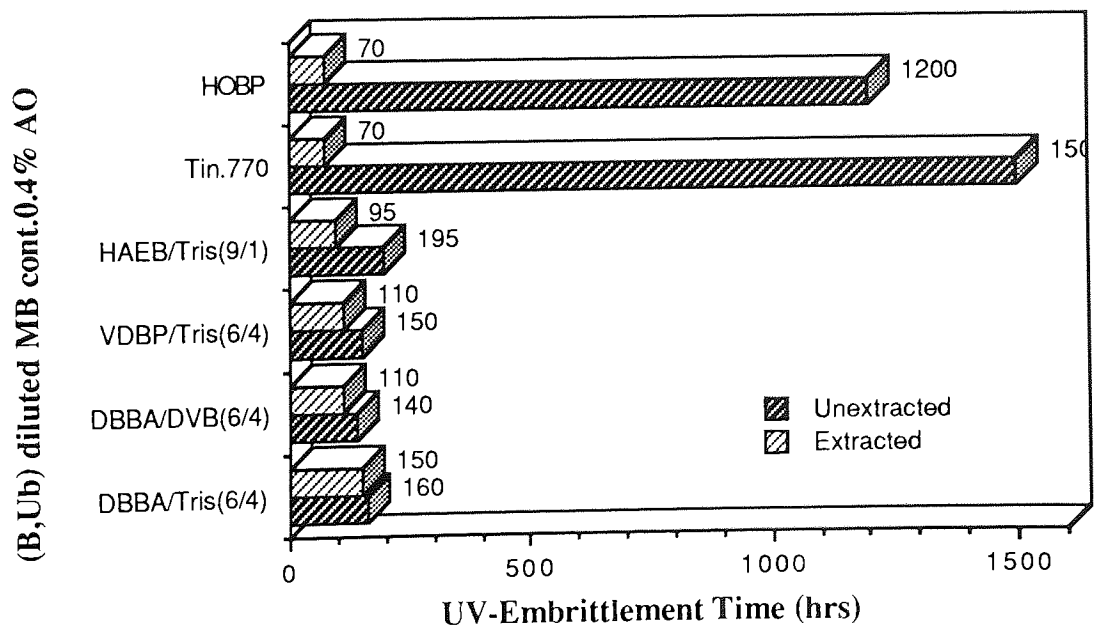


Figure 4.4 Embrittlement time of uv-irradiated diluted masterbatch films containing 0.4% of various bound (B) antioxidants in the presence of coagent and commercial antioxidants, before and after extraction.

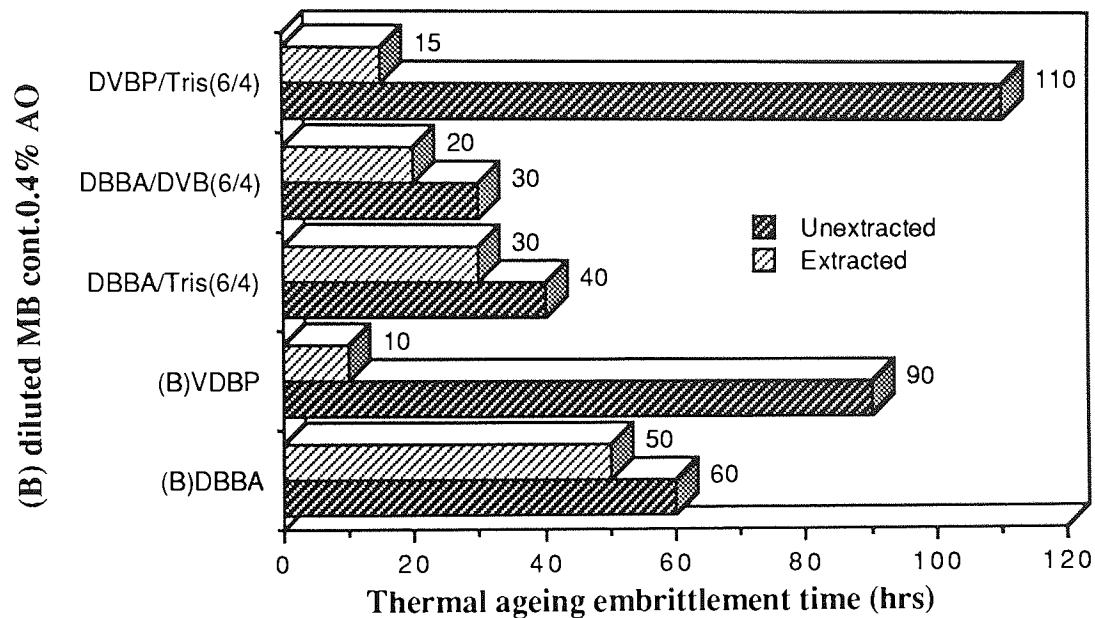


Figure 4.5 ET of thermally aged diluted MB films containing 0.4% of various bound (B) antioxidants with or without coagent, before and after extraction.

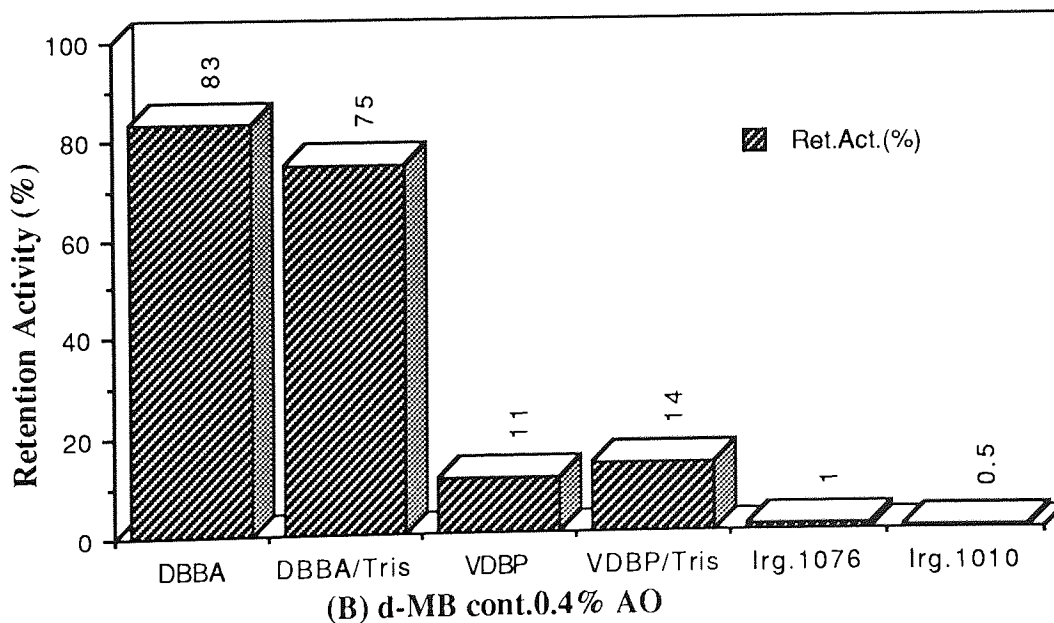


Figure 4.6 Retention Activity of thermal ageing diluted masterbatch films containing 0.4% of various bound (B) antioxidants compared with commercial AO's, see Table 4.6 and 4.7.

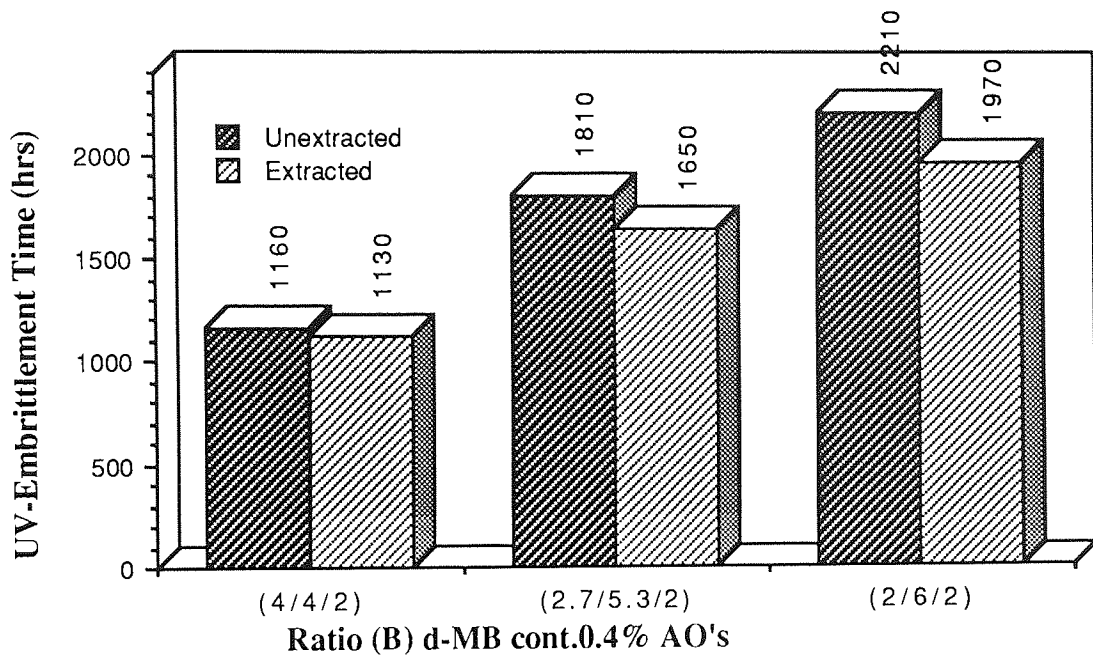


Figure 4.7 Embrittlement time of UV-irradiated films of (DBBA/HAEB/Tris) masterbatches having the same concentration of Tris (2%), but at various ratios of DBBA/HAEB (1/1, 1/2, 1/3) processed in the presence of 0.02 molar ratio Trigonox 101, diluted to 0.4% of total AO's content, see Table 4.9.

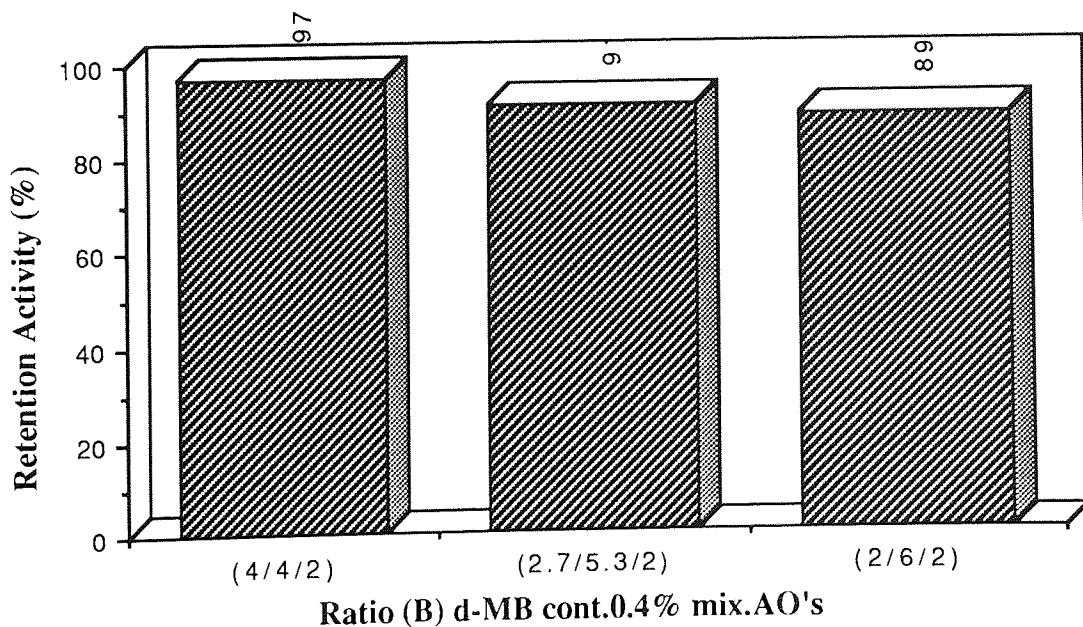


Figure 4.8 Retention Activity of UV-irradiated films of (DBBA/HAEB/Tris) masterbatches having the same concentration of Tris (2%), but at various ratios of DBBA/HAEB (1/1, 1/2, 1/3) processed in the presence of 0.02 molar ratio Trigonox 101, diluted to 0.4% of total AO's content, see Table 4.9.

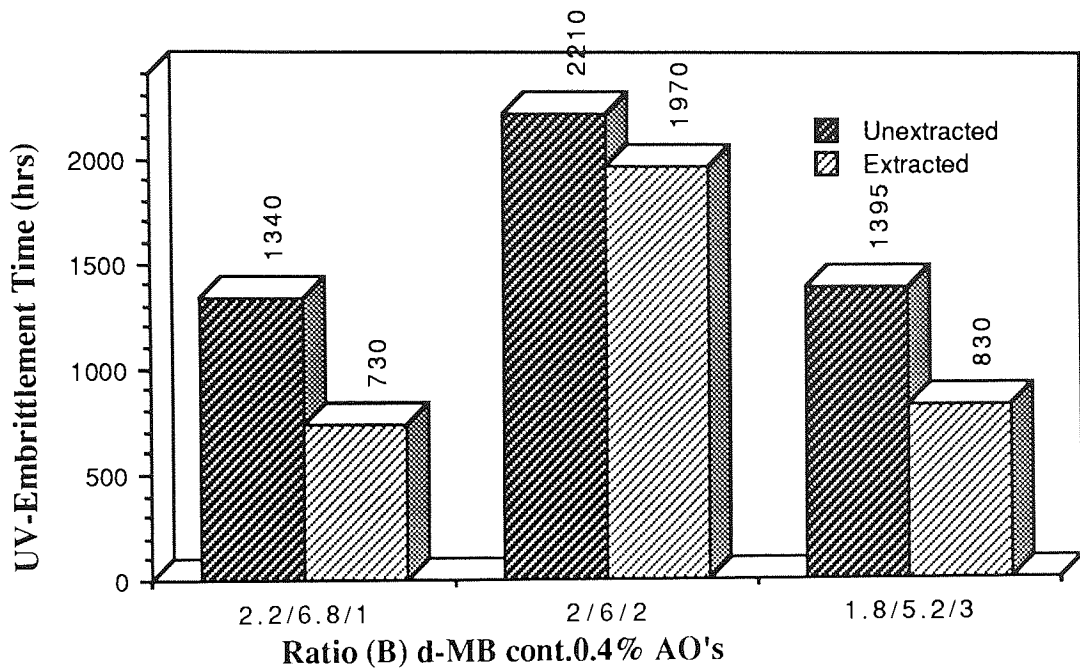


Figure 4.9 The Embrittlement Time of UV-irradiated films of (DBBA/HAEB/Tris) masterbatches have the same ratio (1/3) of DBBA/HAEB in the presence of different concentration of Tris coagent content, diluted to 0.4% of total AO's content.

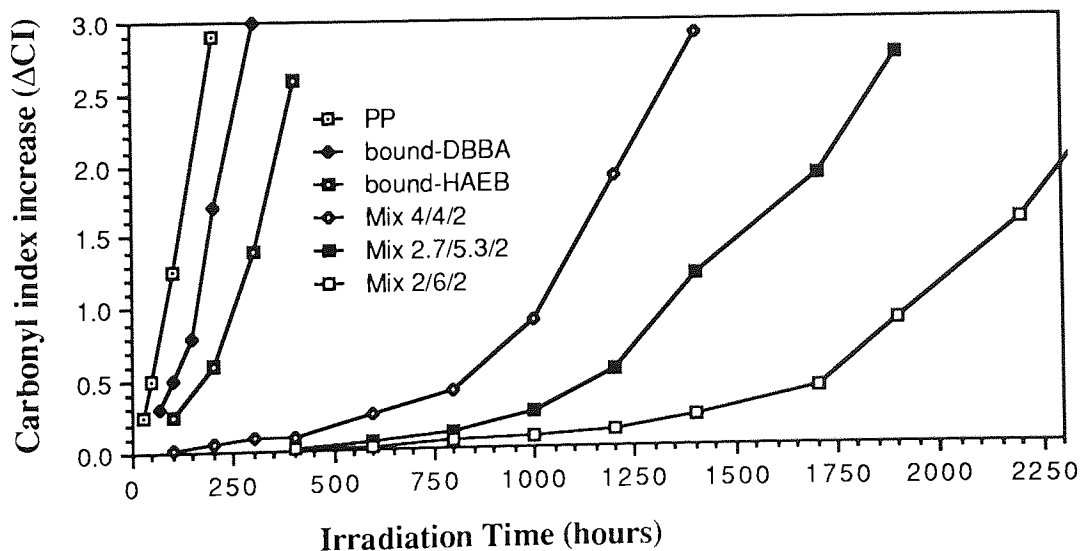


Figure 4.10 Carbonyl index increase during uv-irradiation of diluted masterbatch films containing 0.4% of bound-DBBA, bound-HAEB and mixtures DBBA/HAEB/Tris weight ratio: 4/4/2, 2.7/5.3/2, and 2/6/2 before extraction, refer to Table 4.3 sample no 1&3, Table 4.4 sample no.1 and Table 4.9 sample no.4-6

CHAPTER FIVE

ANALYSIS OF MASTERBATCHES CONTAINING DBBA AND HAEB IN POLYPROPYLENE AND MODEL REACTION OF DBBA IN SOLUTION

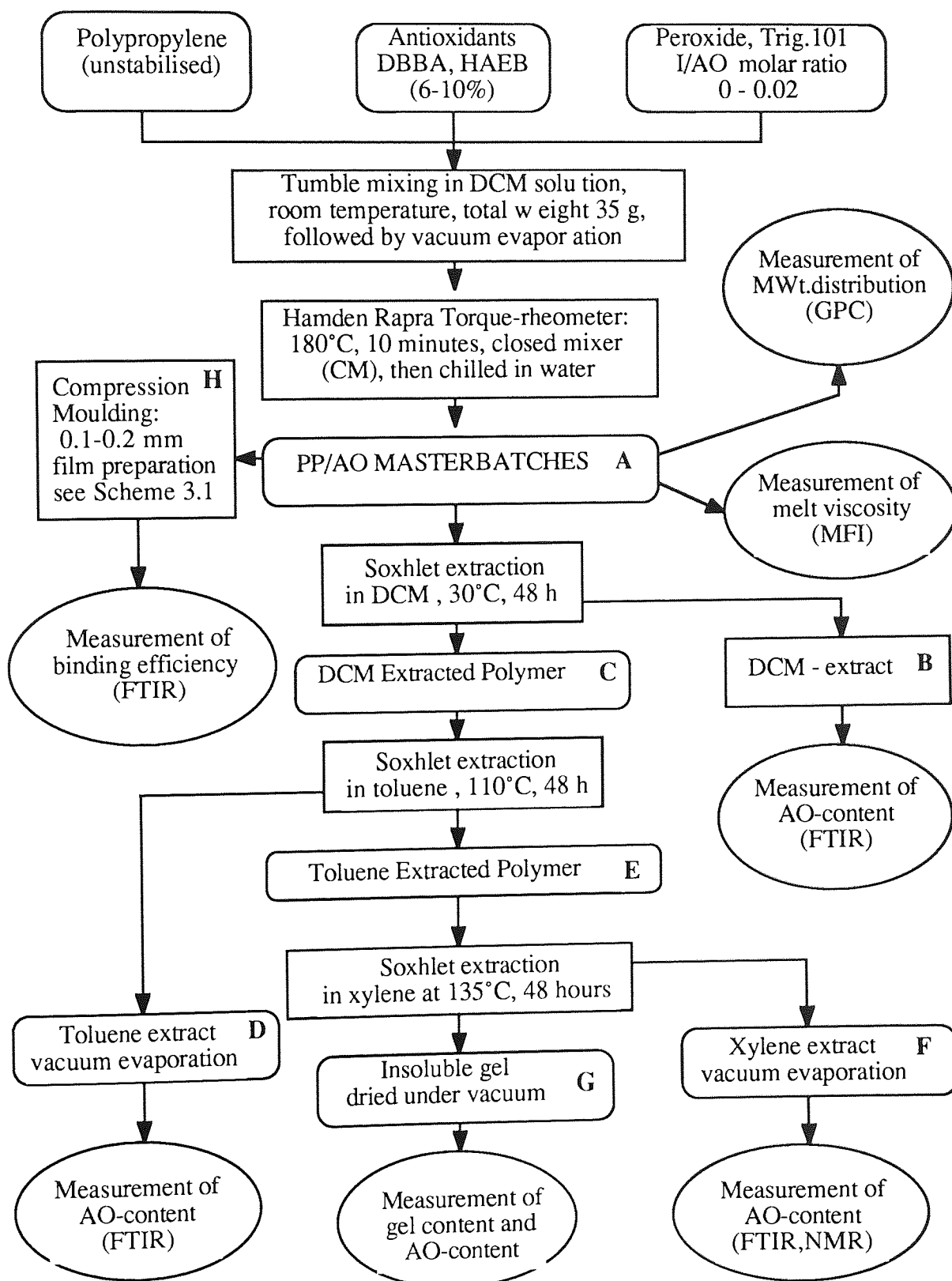
5.1 OBJECT AND METHODOLOGY

The high binding efficiency of DBBA and HAEB when processed in PP have been demonstrated in Chapter-3. The stabilising activity of these antioxidants alone and in synergistic combinations has also been illustrated in Chapter-4. In this chapter the binding mechanism of DBBA and HAEB will be examined in the polymer melt as well as in liquid hydrocarbon models in the case of the former.

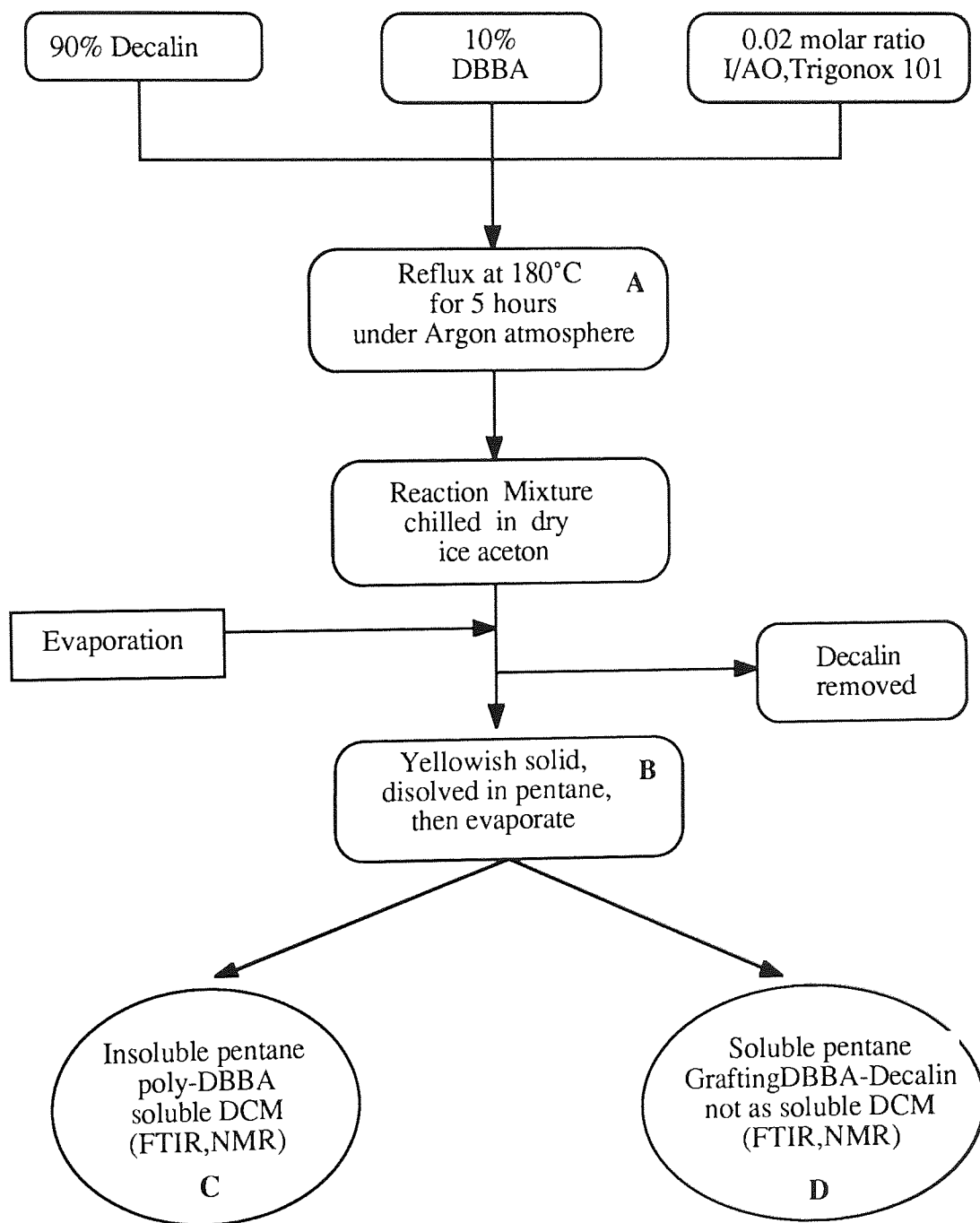
The overall procedure used to analyse polymer concentrates (masterbatches) of DBBA and HAEB by extraction and spectroscopic techniques is shown in Scheme 5.1. Unstabilised polypropylene containing 6-10% antioxidant (AO), DBBA or HAEB in the presence of the initiator (I), 0 - 0.02 molar ratio, m.r. ($[I]/[AO]$) Trigonox 101 were tumble mixed together in DCM at room temperature, and followed by vacuum evaporation. This was then processed in a Hampden Rapra Torquerheometer at 180°C for 10 minutes under closed mixing condition (this is the standard processing condition used throughout the work unless otherwise stated), to produce antioxidant concentrates (masterbatches, MB's), see Scheme 5.1 stage A. The melt viscosity (melt flow index, MFI) and molecular weight distribution, GPC (see Section 2.5 and 2.10) were examined for those concentrates. Thin films were compression moulded from the processed concentrates in order to assess the binding efficiency, see Scheme 5.1 stage H. Quantitatively, 5 gram of shredded concentrates were exhaustively Soxhlet extracted in DCM (see Scheme 5.1 stage C) and after drying at room temperature, the antioxidant content was examined (see Scheme 5.1 stage B). The DCM-extracted polymer was further Soxhlet extracted in toluene and the

antioxidant content in the toluene extract was measured again (see Scheme 5.1 stage D). The toluene-extracted polymer was further Soxhlet extracted in xylene, the xylene-extract was vacuum evaporated and the remaining antioxidant concentration was examined (see Scheme 5.1 stage F). Furthermore any insoluble gel was measured (as gel content) after the xylene extraction (see Scheme 5.1 stage G).

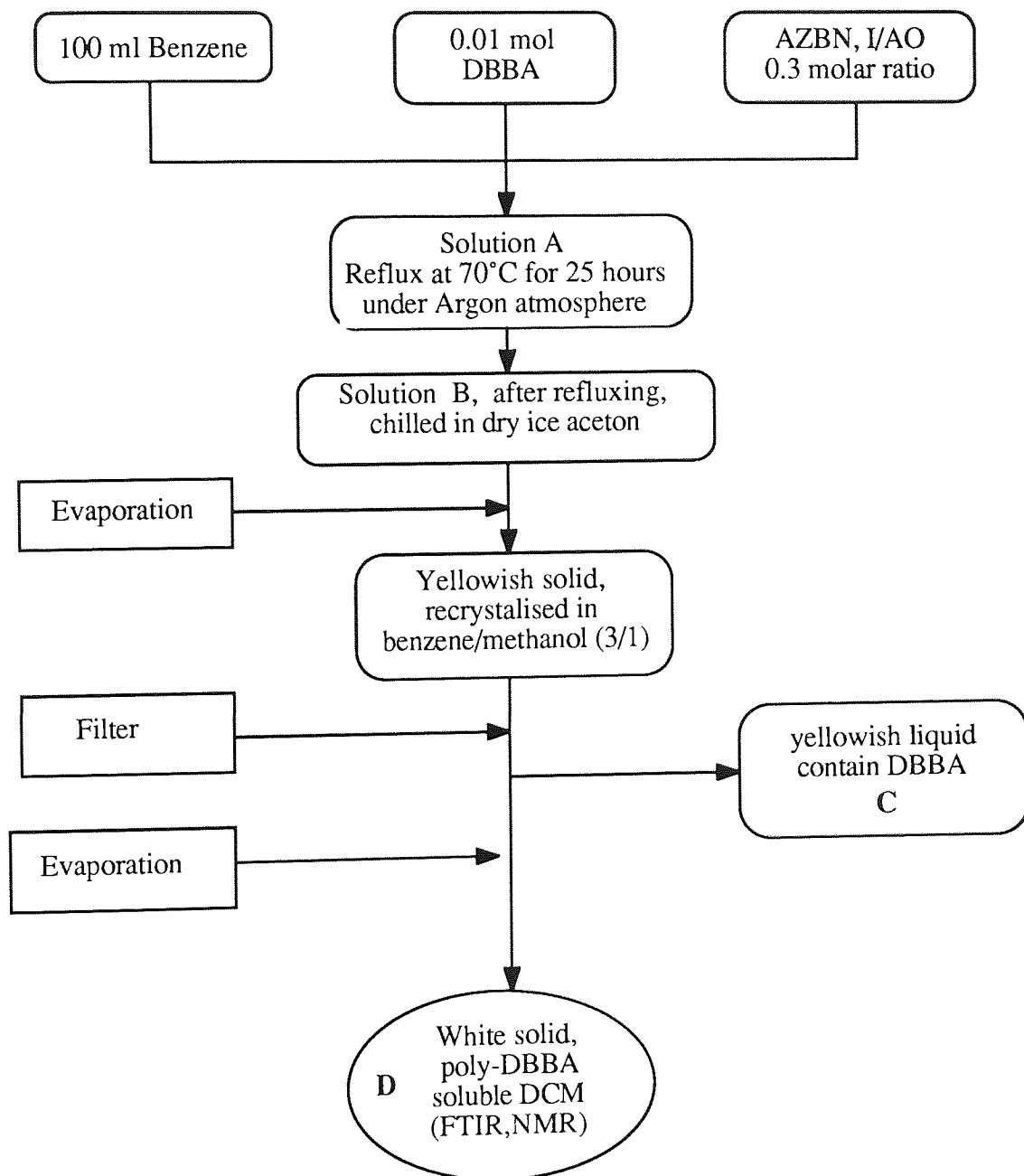
For model reactions, decaline was used as a substrate (containing labile proton, hence used as a model for polypropylene) for further examination of the binding mechanism of DBBA as shown in Scheme 5.2. 10% DBBA in decalin (b.p. 190°C) in the presence of 0.02 molar ratio (I/AO) of Trigonox 101, was refluxed at 190°C for 5 hours under Argon atmosphere (see Scheme 5.2 stage A). After reflux, the reaction mixture was chilled in dry ice to stop further reaction, followed by vacuum evaporation (to evaporate any unreacted decalin). The residue, a yellowish solid, was then dissolved in pentane (see Scheme 5.2 stage B). Both soluble and insoluble pentane fractions (after drying in vacuum evaporation), were examined by FTIR and NMR spectroscopy (see Scheme 5.2 stage C and D). Control for polymerisation of DBBA in the presence of a free radical initiator, in this case azobisisobutyronitrile (AZBN), but in the absence of the substrate (decalin), was also examined for comparison, see Scheme 5.3.



Scheme 5.1 Schematic presentation of procedure used for analysis of MB's containing 6-10% of DBBA or HAEB processed in the presence of various concentration of Trigonox 101 (molar ratio=0-0.02) at 180°C for 10 minutes in a closed mixer torque rheometer.



Scheme 5.2 Schematic procedure of polymerisation DBBA-Decalin in the presence of 0.02 molar ratio (I/DBBA) Trigonox 101 at 180°C for 5 hours.



Scheme 5.3 Schematic procedure of DBBA polymerisation in benzene in the presence of 0.3 molar ratio (I/DBBA) AZBN at 70°C for 25 hours under Argon atmosphere

5.2 RESULTS

5.2.1 Analysis of Masterbatches Containing DBBA and HAEB

5.2.1.1 Spectroscopic investigation using infra red

The FTIR spectrum of fresh DBBA in a KBr disc (see Figure 5.1) shows clearly the major absorptions of the antioxidant in the polymer at 3588 cm^{-1} (OH group), 1714 cm^{-1} (C=O unsaturated ester group), the peak at 1636 cm^{-1} ($>\text{C}=\text{C}<$ for aromatic and acrylic double bond), 1408 cm^{-1} which appears in the window between the two major polypropylene absorptions (at 1456 cm^{-1} and 1358 cm^{-1}) is due mainly to the acrylic double bond. This peak can therefore be conveniently used to monitor changes in $>\text{C}=\text{C}<$ of the acrylic group. The comparison of an IR spectra of a PP film containing 10% DBBA (masterbatch, MB) processed in the absence of peroxide with that of fresh DBBA in a KBr disc (see Figure 5.1) shows the absorption at 1408 cm^{-1} while absorptions at 1714 cm^{-1} (shifts up to 1725 cm^{-1}) and 3588 cm^{-1} (shifts up to 3646 cm^{-1}) shift to higher wave numbers. Exhaustive Soxhlet extraction of this MB with DCM (see Figure 5.2), led to the complete disappearance of the major DBBA absorptions (e.g. 1408 , 1725 and 3646 cm^{-1}) and the overall IR spectrum is very similar to that of a control PP film processed in the absence of any additive. When the IR spectrum of DBBA (10% MB) processed in the presence of peroxide is compared with that of fresh DBBA (in KBr disc, see Figure 5.3) the 1408 cm^{-1} absorption disappears completely, while the 1636 cm^{-1} broadens, and the 1714 and 3588 cm^{-1} absorptions shift to higher wave numbers (1731 and 3648 cm^{-1} , respectively). Soxhlet extraction of this MB in DCM, see Figure 5.4, led to a reduction of the intensities of both absorptions at 1731 and 3646 cm^{-1} , otherwise, the overall spectrum of the extracted sample is similar to that of the unextracted sample. Comparison of IR spectra of 10% DBBA masterbatch films processed in the presence and absence of peroxides (see Figure 5.5) highlights the major differences shown above (in the presence of peroxide the 1408 cm^{-1} band disappears, 1636 broadens and 1725 shifts to 1731 cm^{-1}).

In the case of the DCM extract of 10 % DBBA MB processed with peroxide (Scheme 5.4 stage B, see Figures 5.6 and 5.7) the spectrum of the extract shows that the major absorptions are different to that of fresh DBBA (1408 disappears, both the 3588 and 1714 cm^{-1} absorptions shift up to higher wave numbers, 3639 and 1735 cm^{-1} , respectively). Contribution from absorptions at 3639 and 1735 cm^{-1} and the disappearance at 1408 cm^{-1} leads to an overall spectrum which is very similar to that of the grafted DBBA concentrate (the same 10% DBBA MB film before and after DCM extraction, Scheme 5.4 stage A and C), see Figure 5.7 and 5.8.

In the presence of DVB coagent during DBBA processing (MB containing 10% [DBBA+DVB]) we can improve the binding efficiency of DBBA onto PP up to 93%. The FTIR spectrum of 10 % (DBBA+DVB) MB film compared with fresh DBBA shows that the absorption at 1408 cm^{-1} disappears completely, while the 1636 cm^{-1} broadens and has a lower intensity, the 1714 and 3588 cm^{-1} absorptions shift up to higher wave numbers (1731 and 3646 cm^{-1} , respectively), see Figure 5.8a. Comparison of the IR spectra of 10% (DBBA+DVB) masterbatch films processed in the presence of peroxides, before DCM extraction (Scheme 5.6 stage A), after DCM extraction (Scheme 5.6 stage C) and DCM extract (Scheme 5.6 stage B) show that all spectra have similar major absorptions, see Figure 5.8b.

In the presence of Tris coagent during DBBA processing (MB containing 10% [DBBA+Tris]) the binding efficiency of DBBA onto PP can be increased by up to 91%. The FTIR spectrum of 10 % (DBBA+Tris) MB film compared with fresh DBBA shows that the absorption at 1408 cm^{-1} disappear completely, while the 1636 cm^{-1} broadens and has a lower intensity, the 1714 and 3588 cm^{-1} absorptions shift up to higher wave numbers (1735 and 3646 cm^{-1} , respectively), see Figure 5.8c. Comparison of the IR spectra of 10% (DBBA+Tris) masterbatch films processed in the presence of peroxides, before DCM extraction (Scheme 5.5 stage A), after DCM extraction (Scheme 5.5 stage C) and DCM extract (Scheme 5.5 stage B) show that all spectra have similar saturation, see Figure 5.8d.

Similarly, in the case of HAEB, the FTIR spectrum of fresh HAEB in a KBr disc (Figure 5.9) shows clearly the major absorptions of the antioxidant at 1725 cm^{-1} (C=O unsaturated ester group) at 1625 to 1577 cm^{-1} ($>\text{C}=\text{C}<$ for aromatic and acrylic double bond), at 1414 cm^{-1} which appears in the window between the two major polypropylene absorptions (at 1456 and 1358 cm^{-1}) is due mainly to the acrylic double bond. This peak can therefore be conveniently used to monitor changes in the $>\text{C}=\text{C}<$ of the acrylic group. The comparison of an IR spectra of a PP film containing 10% HAEB (masterbatch, MB) processed in the absence of peroxide with that of fresh HAEB in a KBr disc (see Figure 5.9) shows that the absorption at 1414 cm^{-1} was still observed while the absorption at 1725 shifts to higher wave numbers, 1731 cm^{-1} . Exhaustive Soxhlet extraction of this MB with DCM (see Figure 5.10), leads to the complete disappearance of the 1414 cm^{-1} absorption and a reduction of the major HAEB absorptions (e.g. 1577 , 1625 and 1731 cm^{-1}). When the IR spectrum of HAEB (10% MB) processed in the presence of peroxide is compared to that of fresh HAEB (in KBr disc, see Figure 5.11), the 1414 cm^{-1} absorption disappears completely, while the 1725 cm^{-1} absorption shifts to higher wave length numbers (1733 cm^{-1}). Soxhlet extraction of this MB in DCM, see Figure 5.12, led to a reduction in the intensities of absorptions at 1733 , 1636 and 1577 cm^{-1} . Comparison of the IR spectra of 10% HAEB masterbatch films processed in the presence and absence of peroxides (see Figure 5.13) highlights the major differences shown above (in the presence of peroxide the absorption at 1414 cm^{-1} disappears, and the 1731 band shifts to 1733 cm^{-1}). Examination of figures 5.14 and 5.15 which compare the IR of the DCM extract of 10% HAEB MB processed with peroxide, with that of the same MB but before extraction (see Figure 5.15) and with fresh HAEB (in KBr disc) reveals that the extract spectrum is different from that of fresh HAEB (note absorptions at 1725 shifts up to 1738 cm^{-1} and 1414 cm^{-1} absorption completely disappears). This could suggest that both HAEB monomer and homopoly-HAEB are being extracted. This extract spectrum is similar to that of the extracted polymer i.e. grafted HAEB concentrate (see Figure 5.16).

5.2.1.2 Analysis of antioxidant concentration in masterbatches and the gel content

Solubility of polypropylene and the antioxidants used, DBBA and HAEB, was examined in xylene, toluene and DCM. Polypropylene was found to be completely soluble in boiling xylene (b.p = 135°C), partially (up to 66%) soluble in boiling toluene (b.p = 110°C) but not soluble in boiling DCM (b.p = 30°C), whereas both antioxidants were found to be completely soluble in all three solvents. DCM was, therefore, used for the initial extraction of the polymer to remove any free antioxidant while the concentration of any crosslinked (gel) material was determined by treating the polymer samples with boiling xylene. Furthermore, stepwise fractional separation of antioxidant concentrates (AO = 6 - 10% in polypropylene) was carried out in the above three solvents and samples were taken out for further analysis, see Scheme 5.4 to 5.9

The binding efficiency, MFI, gel content and changes in torque during processing of polypropylene containing DBBA (10%) in the absence and presence of two different coagents, Tris and DVB are shown in Table 5.1 and Figures 5.17 and 5.18. Figure 5.17 shows that for all different DBBA samples examined there is a general decrease in the torque with no appearance of peaks at any processing time in the torque curves. The torque curves were all lower than that of a polypropylene control sample (with no additive), except for one sample which was processed in the presence of DVB (used as a coagent) which showed a higher torque curve. The MFI for the DVB-containing sample was very low (see Table 5.1 and Figure 5.19) when compared to polypropylene control and to the other samples, suggesting the crosslinked product was formed. This was confirmed from the formation of a gel (tests in xylene, see Section 2.6) in this sample, see Table 5.1. Furthermore, this was the only sample which became hard very soon after processing (much harder than the other DBBA samples).

Similar analysis was carried out for HAEB masterbatches processed in the presence of peroxide ([I/AO] 0.005 molar ratio Trigonox 101) as that used for DBBA, except that in the case of HAEB samples, they were not only analysed at the end of the processing operation (after 10 minutes) but also samples were removed at intervals (2.5 and 5 minutes) during the processing and were subjected to further analysis. Changes in torque of HAEB masterbatch is very different from that shown for DBBA; a pronounced torque peak was observed after 2.5 minutes of processing in the former case, see Figure 5.20. This torque peak was also observed by previous researchers (128). Table 5.2 and Figure 5.21 show that maximum amount of insoluble material (gel) was found after 2.5 minutes, coinciding with the torque peak. Further processing leads to reductions in the gel content and at the end of the processing (after 10 minutes) there was no gel left in the sample corresponding to the decreasing of the torque curve to approximately the same value of the polypropylene control. Furthermore, the decrease in gel content with processing time is paralleled by an increase in MFI, see Figure 5.22.

Table 5.1 Binding efficiency, MFI and gel content of 10% masterbatches containing DBBA in polypropylene without and with coagents, in the presence of 0.02 m.r. [I] /([DBBA]+[Coagent] Trigonox101 (processed at 180°C for 10 minutes under closed mixer).

No	Code	MB's Sample	Binding (%)	MFI (g/10 mins)	Gel content (%)
1	-	PP only, processed	-	0.58	none
2	-	PP+peroxide	-	17.37	none
3	DBCUC	DBBA (10%)	40	1.65	none
4	TRDU	DBBA+Tris (6/4)	91	1.19	none
5	DVBU	DBBA+DVB(6/4)	93	0.16	6

Table 5.2 Effect of processing time on binding efficiency, MFI and gel content of 10% HAEB in polypropylene, in the presence of 0.005 molar ratio [I]/[AO] Trigonox 101 processed at 180°C under closed mixer condition at different processing time.

No	Processing Time (minutes)	Binding (%)	MFI (g/10 mins)	Gel content (%)
1	2.5	73	1.15	16
2	5.0	73	1.54	6
3	10	73	1.82	0

Scheme 5.4 to 5.6 show flow diagrams of the fractional separation (according to solubility in solvents) of various DBBA masterbatches. In order to calculate the concentration of DBBA in the various masterbatches calibration curves, based on polypropylene containing different known concentrations of DBBA (see Figures 5.23 to 5.25), were constructed with respect to hydroxyl (OH) absorption index (reference to a PP peak which does not change, at 1722 cm^{-1}) and carbonyl (C=O) absorption index, for detail see Section 2.4, 2.9 and 2.10. The hydroxyl index for the sample containing Tris was used since this coagent has itself a large carbonyl absorption.

The concentration of DBBA in the masterbatches can be measured by using the calibration curves of masterbatches containing known concentration of DBBA (see Figure 5.23) obtained empirically, which follows as a linear equation:

$$C = 3.2636 (CI) + 0.133 \quad 5.1$$

where, C is DBBA concentration (% w/w) and CI is carbonyl area index of DBBA. The carbonyl area index is defined as the area absorption ratio of carbonyl and a polymer (peak reference, at 2722 cm^{-1}).

In the case of calculating antioxidant content in masterbatches of (DBBA+Tris) system, the carbonyl area of DBBA is overlapping with the carbonyl area of Tris. Hence, to measure

the DBBA content in masterbatches the calibration curve used is the hydroxyl area index of masterbatches containing known concentration of DBBA (see Figure 5.24) is needed which follows the linear equation:

$$C = 7.3982 (HI) - 0.1548 \quad 5.2$$

where, C is DBBA concentration (% w/w) and HI is hydroxyl area index of DBBA. Since the hydroxyl area index is defined as the area absorption ratio of the hydroxyl and the polymer (reference peak).

To measure HAEB content in masterbatches, the calibration curve used is the carbonyl area index of masterbatches containing known concentrations of HAEB was used (see Figure 5.25). This was similarly calculated using the linear equation:

$$C = 3.2489 CI + 0.1498 \quad 5.3$$

where, C is the HAEB concentration (% w/w) and CI is the carbonyl area index of HAEB, since the carbonyl index is defined as the area absorption ratio of the carbonyl and the polymer (reference peak).

The results on the analysis of the amount of soluble polymer at different stages of extraction and the concentration of DBBA in the extract of different solvents (see Scheme 5.4 - 5.6) are shown in Tables 5.3 and 5.4. The very high initial loss (in the DCM-extract), of DBBA when processed in the presence of peroxide but in the absence of the co-agent contrasts with the very low initial loss of DBBA in the presence of both co-agents, (Tris and DVB), hence the very high level of binding (calculated after DCM extraction), see Table 5.3. It is interesting to note that in the case of DVB, 7% gel was found in the sample and some of the DBBA ($\approx 1\%$) was found to be present in the gel, no other sample gave a gel, see Table 5.3. It is also important to point out that when DBBA was processed in the absence of a co-agent, a larger proportion became soluble in the toluene fraction compared to the xylene fraction (73:21); this was the reverse of what happened when co-agents were present, see Table 5.3. In the absence of a coagent, the polymer is quite soluble in toluene (upto 73%), comparable to 66% solubility of PP. However, when

a coagent is used, the polymer became more "crosslinked" and less soluble in toluene. However, this is not permanent crosslinking (mobile crosslinking) which breaks down when heated further at the xylene boiling point temperature.

Table 5.3 Percentage weight of soluble and insoluble fractions (after continuous extraction in different solvents) of masterbatches containing 10% AO's processed in the presence of optimum concentration of Trig.101, at 180°C in closed mixing at different processing times

No	% conc. of DBBA + Coagent	Binding %	MFI	% (A) Before ext'ion	% (w/w) polymer soluble in different fractions (of original 100%)			
					(B) DCM extract	(D) Toluene-Extract	(F) Xylene-extract	(G) Gel
1	PP (no additive)	-	0.58	100	0	66	44	0
2	DBBA (10/0)	40	1.65	100	6	73	21	0
3	DBBA+Tris (6/4)	91	1.19	100	0.5	22.5	77	0
4	DBBA+DVB(6/4)	93	0.16	100	0.5	22.5	70	7

* Solubility of PP in toluene is 66%
Solubility of PP in xylene is 100%

The results on the analysis of the concentration of HAEB in the different solvents (see Scheme 5.7 - 5.9) is shown in Table 5.5 and 5.6. The very high initial loss (in the DCM-extract), of HAEB when processed in the presence of peroxide with high level of binding 73%, see Table 5.5. It is interesting to note that in the case of 2.5 minutes processing time 16% the gel content was found in the sample and a very high proportion of the HAEB ($\approx 4.5\%$) was found to be in the gel see Table 5.6. When the processing time increased (5 minutes) the gel content decreased (6%) and less of the HAEB ($\approx 1.1\%$) was found in this gel, see Table 5.6. It is also important to point out that when HAEB is processed for 10 minutes, no gel content was found and a larger proportion become soluble in the xylene fraction compared to the toluene fraction (66:32), see Table 5.5. In the latter case, very high HAEB (4.8%) was found in the xylene fraction.

Table 5.4 Percentage of DBBA in different fractions (after continuous separation in different solvents) of 10% total (DBBA with or without coagent) masterbatches processed with 0.02 m.r. (I/DBBA+Coagent) Trigonox 101, at 180°C, for 10 minutes under closed mixer condition.

No	% conc. of DBBA + Coagent	Binding %	% gel	% (w/w) conc. of DBBA (of original 10%) in different fractions			
				(B) DCM extract	(D) Toluene-Extract	(F) Xylene-extract	(G) Gel
1	DBBA (10/0)	40	0	6	1	3	0
2	DBBA+Tris (6/4)	91	0	0.5	0.5	5	0
3	DBBA+DVB(6/4)	93	7	0.5	1.5	3	1

Table 5.5 Percentage weight of soluble and insoluble fractions (after continuous extraction in different solvents) of masterbatches containing 10% HAEB processed in the presence of 0.005 m.r. (I/AO) Trig.101, at 180°C under closed mixer condition at different processing times

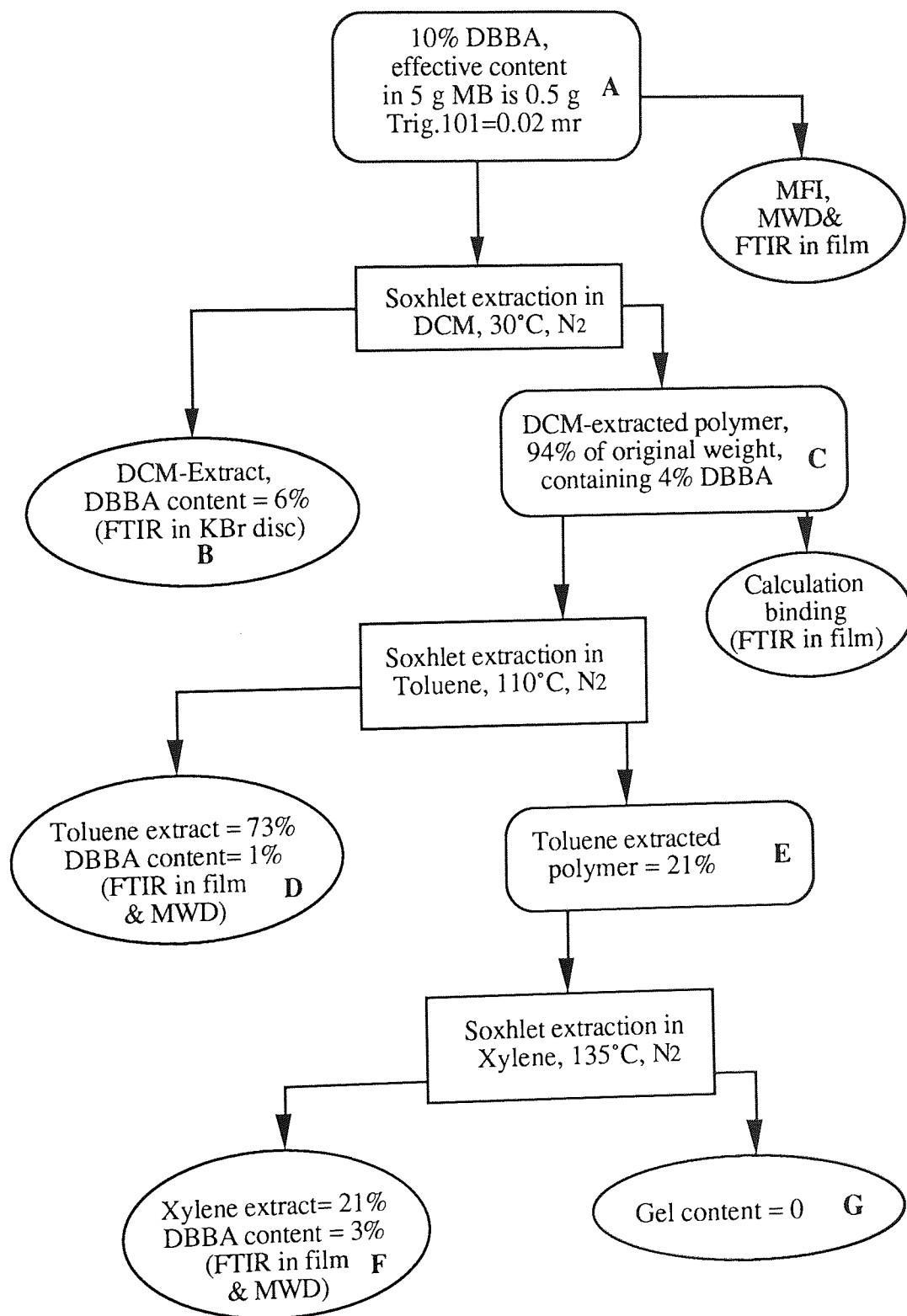
No	MB's (processing time, minutes)	Binding %	MFI	% (A) Before ext'ion	% (w/w) polymer soluble in different fractions (of original 100%)			
					(B) DCM extract	(D) Toluene-Extract	(F) Xylene-extract	(G) Gel
1	HAEB, 2.5 mins	73	1.15	100	2.7	11	71	16
2	HAEB, 5 mins	73	1.54	100	2.7	18	73	6
3	HAEB, 10 mins	73	1.82	100	2.7	32	66	0

Table 5.6 Percentage of HAEB in different fractions (after continuous separation in different solvents) of 10% HAEB masterbatches processed with 0.005 m.r. (I/AO) Trig.101, at 180°C, under closed mixer condition, for various processing time (2.5, 5 and 10 minutes).

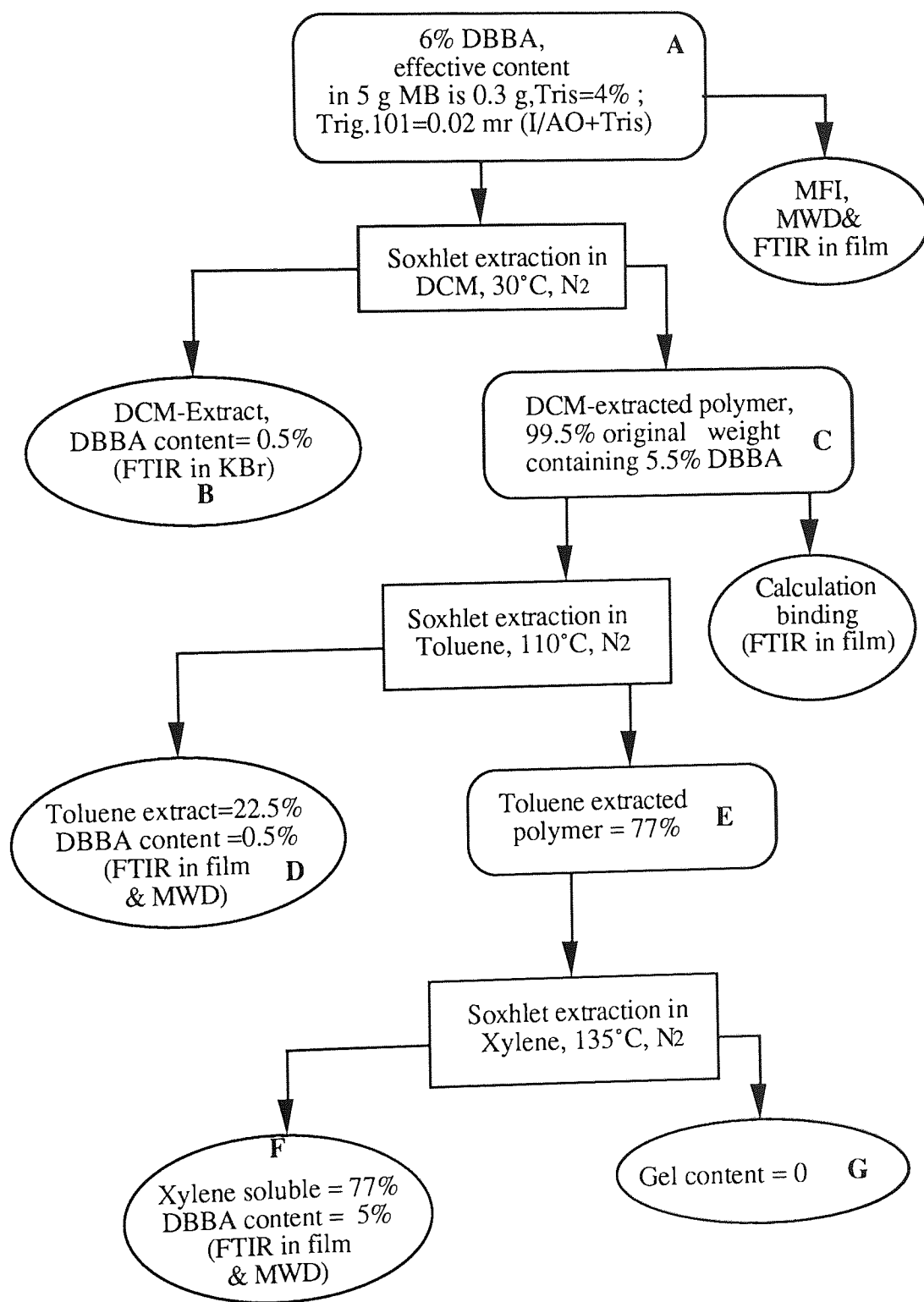
No	MB's (processing time, minutes)	Binding %	gel %	% (w/w) conc. of HAEB (of original 10%) in different fractions			
				(B) DCM extract	(D) Toluene-Extract	(F) Xylene-extract	(G) Gel
1	HAEB, 2.5 mins	73	16	2.7	0.6	2.2	4.5
2	HAEB, 5 mins	73	6	2.7	1.9	4.3	1.1
3	HAEB, 10 mins	73	0	2.7	2.5	4.8	0

Table 5.7 The MFI of original MB's, soluble and insoluble fractions (after continuous extraction in different solvents) of MB's containing 10% AO's processed in the presence of optimum concentration of Trig.101, at 180°C in closed mixer condition at different processing times.

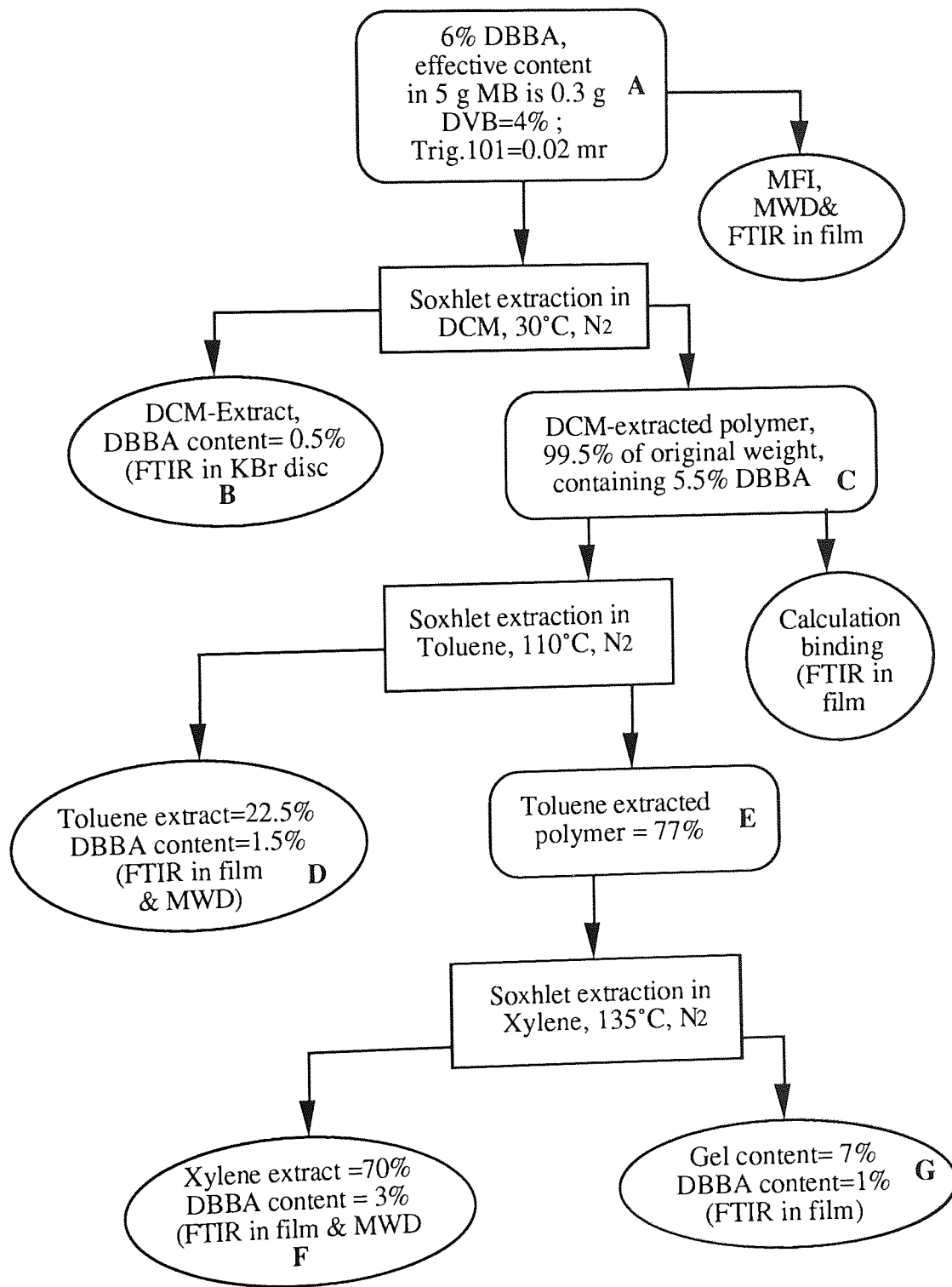
No	Sample	Processing Time(mins)	Original MB's	MFI gram/10 minutes		
				(Stage D) Toluene-Extract	(Stage F) Xylene-Extract	(Stage G) Xylene-Insoluble
1	HAEB	2.5	1.15	0.72	0.59	0.01
2	HAEB	5.0	1.54	0.81	0.47	0.02
3	HAEB	10	1.82	0.98	0.35	-
4	DBBA	10	1.65	0.91	0.28	-
5	DBBA+Tris (6/4)	10	1.19	0.83	0.02	-
6	DBBA+DVB(6/4)	10	0.16	0.06	0	0



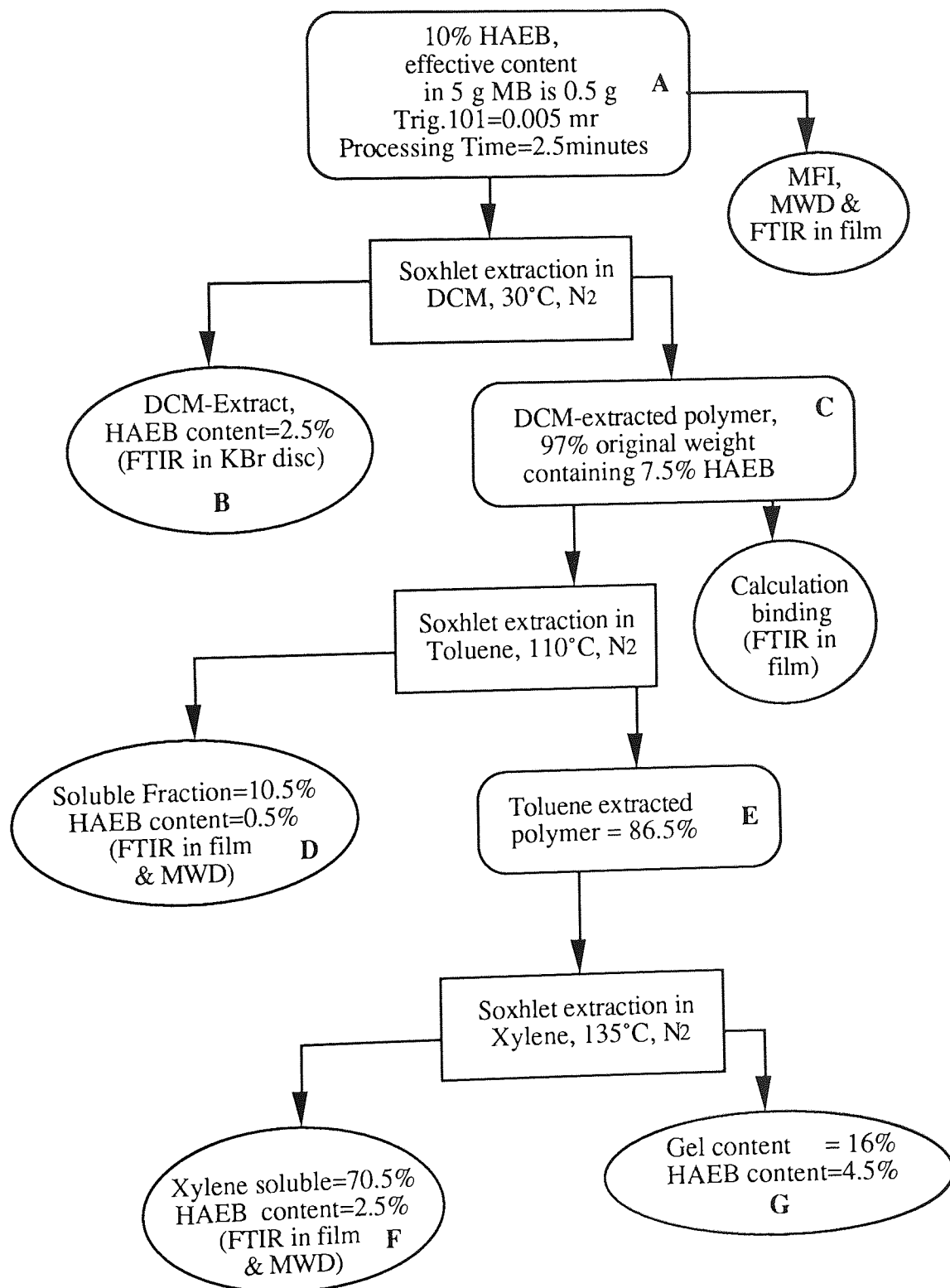
Scheme 5.4 Diagram analysis of 5 gram masterbatch containing 10% DBBA in the presence of 0.02 molar ratio of Trigonox 101.



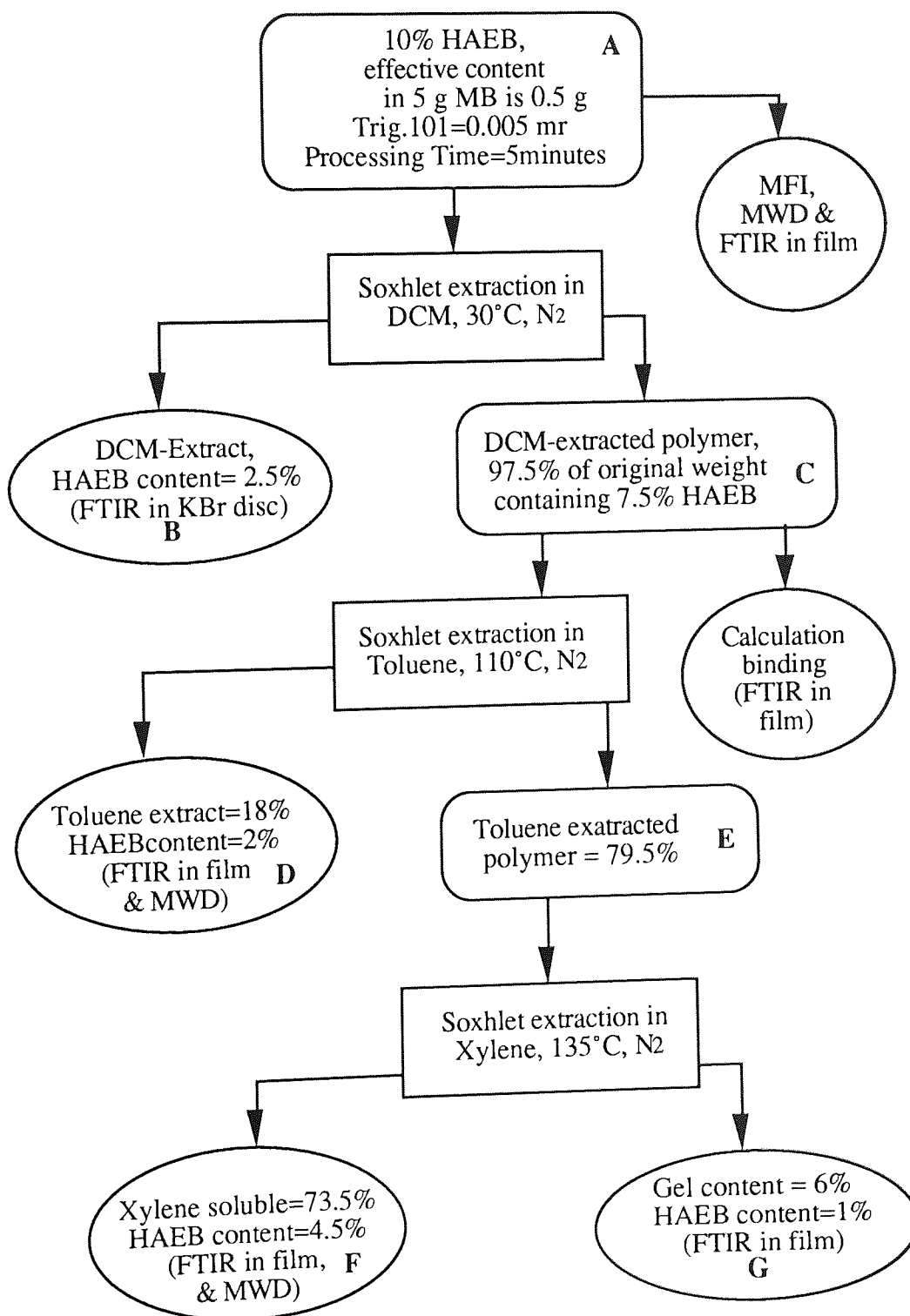
Scheme 5.5 Diagram analysis of 5 gram masterbatch containing 6% DBBA and 4% Tris, processed in the presence of 0.02 molar ratio Trigonox 101



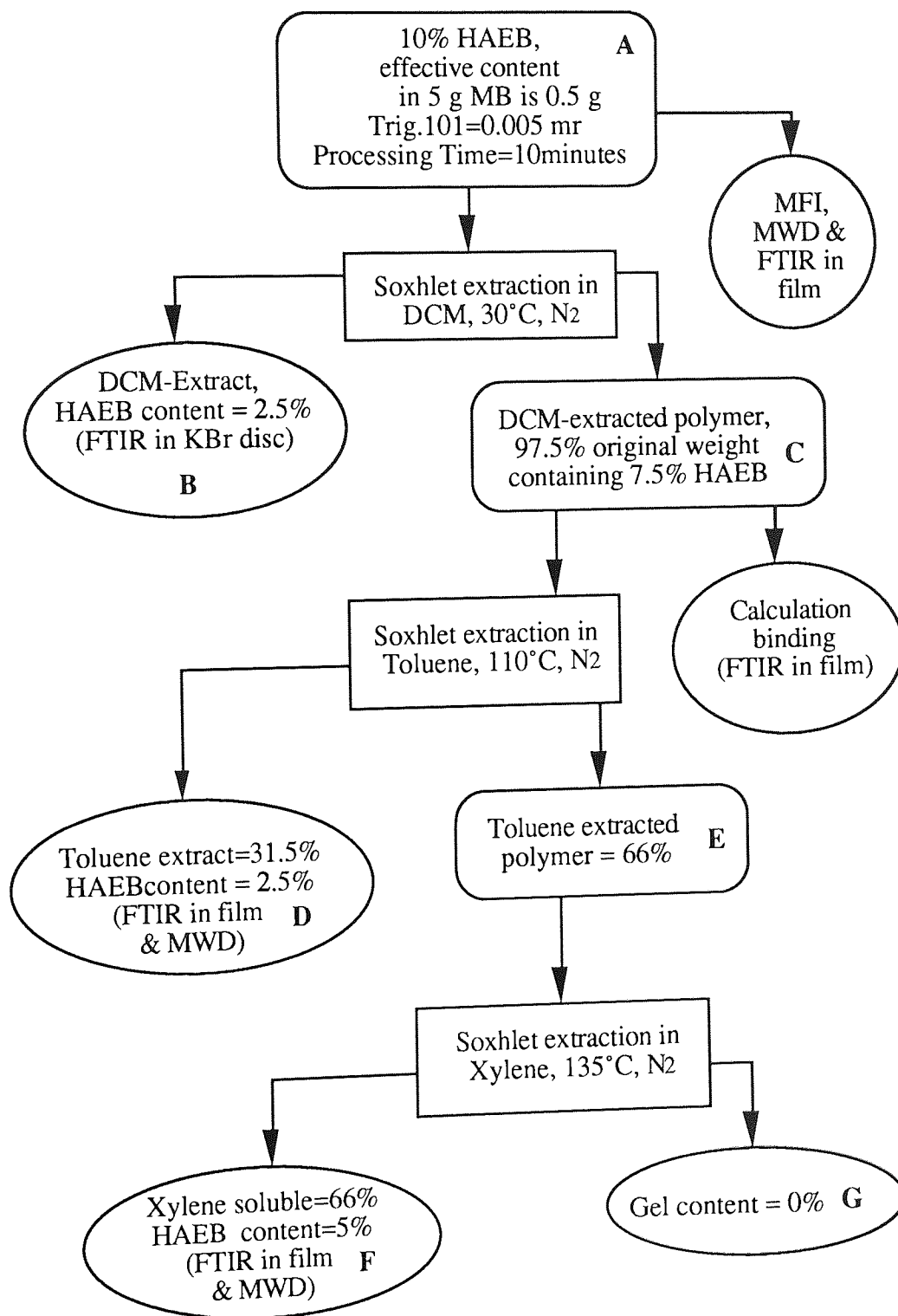
Scheme 5.6 Diagram analysis of 5 gram masterbatch containing 6% DBBA and 4% DVB processed in the presence of 0.02 molar ratio of Trigonox 101



Scheme 5.7 Diagram analysis of 5 gram masterbatch containing 10% HAEB processed for 2.5 minutes, in the presence of 0.005 molar ratio Trigonox 101



Scheme 5.8 Diagram analysis of 5 gram masterbatch containing 10% HAEB processed for 5 minutes, in the presence of 0.005 molar ratio Trigonox 101



Scheme 5.9 Diagram analysis of 5 gram masterbatch containing 10% HAEB processed for 10 minutes, in the presence of 0.005 molar ratio Trigonox 101

5.2.1.3 Molecular weight distribution (MWD) data of masterbatches containing DBBA or HAEB

Table 5.8 and Figure 5.27 show the molecular weights of PP in the presence and absence of DBBA. Polypropylene processed with peroxide gives lower molecular weight (MW) values and has a narrower MWD than PP processed in the absence of peroxide. The shape of the MWD curve of the 10% DBBA masterbatch is more similar to that of unprocessed PP but the sample has slightly lower MW -values.

Processing polypropylene in the presence of peroxide can cause degradation by chain scission(11-13). In the presence of DBBA some peroxide was used up to initiate grafting of the antioxidant. When Tris or DVB were used as a coagent in 10% (DBBA+coagent) masterbatches (see Table 5.8 & 5.9 and Figure 5.28), the molecular weight (MW) of the polymer was lower than that of 10% DBBA masterbatch without any coagent. The MWD curves of these masterbatches (with coagents) were also shifted towards lower MW values and their intensities were higher compared to that of the 10% DBBA masterbatch in the absence of a coagent. On the other hand, the number average molecular weight (M_n) of the 10% (DBBA+DVB) masterbatch was very high compared to the other two.

Further analysis of the molecular weight distribution of different fractions of DBBA masterbatches extracted with different solvents (DCM, toluene and xylene) is shown in Tables 5.8 & 5.9 and Figures 5.30 - 5.32. The toluene extract fractions of 10% (DBBA without and with coagent) masterbatches have a molecular weight (e.g. M_n) much lower than that of the xylene extract fractions (see Figure 5.29).

Similarly, the molecular weight distribution of 10% HAEB masterbatches processed at various processing times was measured, as shown in Table 5.10 and Figures 5.33 and 5.33a. It is clear that the molecular weight of 10% HAEB masterbatches decreases with increasing processing time as expected, but the molecular weight (e.g. M_n) of this sample

is lower than that of DBBA samples. This means the longer the processing time the more chain scission occurs in these systems. This is in agreement with the viscosity changes by their MFI values for original masterbatches (see Figure 5.26).

Table 5.8 Molecular weight distribution (MWD) data of masterbatches containing 10% (DBBA without or with coagent), processed in the presence of 0.02 m.r. (I/DBBA+coagent) Trigonox 101 at 180°C for 10 minutes under closed mixer condition.

No	Masterbatches	Processing Time(mins)	Binding %	Molecular weight distribution of MB's fractions		
				Mw x10 ⁻⁵	Mn x10 ⁻⁴	D, (MWD) (Mw/Mn)
1	PP, unproc'd	-	-	4.17	5.13	8.128
2	PP, proc'd	10	-	3.62	5.53	6.546
3	PP+0.02m.r. FRI	10	-	1.75	4.34	4.032
4	DBBA	10	40	2.57	4.82	5.332
5	DBBA+Tris (6/4)	10	91	1.59	3.24	4.907
6	DBBA+DVB(6/4)	10	93	2.22	5.02	4.422

Table 5.9 Molecular weight distribution (MWD) data of masterbatch's fractions after Soxhlet separation of DBBA MB's containing 10% total (DBBA with or without coagent) processed in the presence of 0.02 m.r. Trig. 101, at 180°C for 10 minutes, in closed mixer condition.

No	Sample	Proc'g Time (mins)	Binding (%)	Molecular weight distribution of MB's fractions	
				Toluene-Extracted	Xylene-Soluble
				Mw : Mn : D, x10 ⁻⁵ : x10 ⁻⁴ : (Mw/Mn)	Mw : Mn : D, x10 ⁻⁵ : x10 ⁻⁴ : (Mw/Mn)
1	DBBA	10	40	1.51 : 2.82 : 5.354	3.37 : 9.12 : 3.695
2	DBBA+Tris(6/4)	10	91	1.29 : 3.11 : 4.148	2.78 : 9.71 : 2.863
3	DBBA+DVB(6/4)	10	93	1.03 : 2.34 : 4.402	2.63 : 6.61 : 3.979

Table 5.10 Molecular weight distribution (MWD) data of MB's containing 10% HAEB, processed in the presence of 0.005 m.r. (I/HAEB) Trig. 101 at 180°C in closed mixing condition at various processing time

No	Sample	Processing Time(mins)	Binding %	Molecular weight distribution of MB's fractions		
				Mw x10 ⁻⁵	Mn x10 ⁻⁴	D,(MWD) (Mw/Mn)
1	PP, unproc'd	-	-	4.17	5.13	8.128
2	PP, proc'd	10	-	3.62	5.53	6.546
3	PP+0.02m.r.FRI	10	-	1.75	4.34	4.032
4	HAEB	2.5	73	2.39	3.47	6.887
5	HAEB	5.0	73	2.22	3.29	6.747
6	HAEB	10	73	1.59	2.86	5.559

5.2.2. Homopolymerisation of DBBA using benzene as a substrate

Some polymerised DBBA may have formed during processing of DBBA masterbatch in polypropylene. Polymerisation of DBBA on the bench is therefore examined using a suitable initiator (AZBN, see Scheme 5.3) in an inert liquid hydrocarbon substrate (benzene with boiling point 86°C). 100 ml benzene solution containing 0.01 mol DBBA and 0.3 molar ratio of initiator AZBN were mixed together in 250 ml in three neck round bottom flask. After assembling with a thermometer, and a condenser, the solution was purged with Argon gas and was then refluxed at 70°C (constant temperature) for 25 hours. After refluxing the reaction mixture was chilled in dry ice-acetone to stop further reaction, and then was evaporated exhaustively at room temperature (to remove benzene). The residue was recrystallised in benzene/methanol mixture at ratio 3/1. After filtration a white solid residue, was formed which was subsequently evaporated at 40°C to constant weight. The residue (white solid, see Scheme 5.3 stage D) was then identified using IR and Proton

&Carbon-13 NMR spectroscopy and results were compared with fresh DBBA, and DCM-extract of the 10% DBBA masterbatch. Both poly-DBBA (white solid product) and monomer DBBA are soluble in DCM.

The FTIR spectrum of fresh DBBA in KBr disc (see Figure 5.34) shows the major absorptions at 3588 cm^{-1} (OH group), 1714 cm^{-1} (C=O unsaturated ester group), 1636 cm^{-1} ($>\text{C}=\text{C}<$ for aromatic and acrylic double bond) and 1408 cm^{-1} ($>\text{C}=\text{C}<$ for typical double bond of an acrylic group). After polymerisation for 25 hours the FTIR spectrum of the polymerised DBBA (see Scheme 5.3 stage D and Figure 5.34), shows a very different spectrum to that of fresh DBBA. The hydroxyl of hindered phenol has shifted up to higher wave length numbers (to 3642 cm^{-1}), the carbonyl ester absorption band broadened and shifted up (to 1734 cm^{-1}), the intensity of the double bond absorption for aromatic and acrylic groups at 1636 cm^{-1} decreased and the double bond acrylic group at 1408 cm^{-1} disappeared. Comparison of the FTIR spectrum of the DCM-extract from 10% DBBA masterbatch processed with 0.02 m.r. Trigonox 101 (see Scheme 5.4 stage B) with that of polymerised DBBA without decalin (Scheme 5.3 stage D), shows that the two spectra are very similar, see Figure 5.35.

The polymerised DBBA is identified using Proton NMR spectroscopy in CDCl_3 . The proton NMR of fresh DBBA (see Figure 2.7 in Chapter-2), clearly shows the characteristic absorption peaks of (H no.1) aromatic proton at δ (ppm) = 7.23 (singlet), (H no.2) tertiary butyl protons at 1.50 (singlet), (H no.3) methylenic proton at 5.16 (singlet), (H no.7) proton of hydroxyl hindered phenol at 5.35 (singlet). The acrylic proton ($>\text{CH}=\text{CH}_2$), with the proton chemical shifts (H no.5) at 6.44-6.50 (doublet), (H no.4) at 6.15-6.23 (quartet) and (H no.6) at 5.82-5.86 (doublet). After polymerisation for 25 hours in the presence of initiator AZBN (see Table 5.11 and Figure 5.36), it was found that the typical absorption peak of the acrylic proton in NMR spectra had disappeared. The new saturated proton (C no. 4', 5' and 6' of $>\text{CH}-\text{CH}_2-$) were found at $\delta = 2.37$ and 1.70 ppm .

The ^{13}C NMR spectrum of fresh DBBA (shown at Figure 2.8 in Chapter-2), exhibits specific peaks of interest at carbon chemical shifts (δ , ppm): carbon aromatic, (C no.1, =COH-) at (-) 154.0; (C no.2, >C=) at (-) 136.0; (C no.3, =CH-) at (+) 125.8; (C no.4, >C=) at (-) 128.4, carbon of tertiary butyl (C.no.5, >C<) at (-) 34.3, carbon of methyl (C no.6, -CH₃) at (+) 30.2, carbon methylene (C no.7, -CH₂-O-) at (-) 67.2, carbon of carbonyl (C no.8, -O-(C=O)-) at (-) 166.1 and carbon of double bond acrylic group (C no.9, -CH=) at (+) 128.6; (C no.10, =CH₂) at (-) 130.1. After 25 hours polymerisation, some of the particular absorption peaks mentioned above, have changed as shown in Table 5.7 and Figure 5.37. It was found that both carbon absorption of vinyl acrylic (Carbon number 9 and 10 of fresh DBBA) have completely disappeared (see Figures 2.8 and 5.37). The new absorption peaks were formed as the results of saturated carbons, with carbon chemical shift (δ , ppm): carbon number 9' (>CH-) at (+) 41.4 and carbon number 10' (>CH₂) at (-) 22.3 (see Table 5.12 and Figure 5.37).

Table 5.11 Proton NMR spectra of polymerised DBBA without decalin in CDCl₃ (using AZBN in benzene, see Scheme 5.3 stage D)

H No	δ (ppm)	m'plicity	I (%)	Total H
1	7.06	1	2.3	2
2	1.31	1	23.0	18
3	4.84	1	0.8	2
4'	2.37	1	1.5	1
5', 6'	1.70	1	0.5	2
7	5.14	1	1.2	1

Table 5.12 ^{13}C NMR spectra of polymerised DBBA without decalin in CDCl_3 (using AZBN in benzene, see Scheme 5.3 stage D)

C No	$\delta(\text{ppm})$	(+)/(−)	I (%)	Total C
1	153.6	(−)	0.4	1
2	135.7	(−)	1.0	2
3	126.0	(+)	1.1	2
4	126.6	(−)	0.5	1
5	34.1	(−)	2.8	2
6	30.2	(+)	12.1	6
7	67.1	(−)	0.5	1
8	174.1	(−)	0.2	1
9'	41.4	(+)	0.2	1
10'	22.3	(−)	0.1	1

5.2.3 Polymerisation of DBBA-Decalin

Another model reaction was investigated in order to simulate the grafting of DBBA onto the polypropylene backbone. DBBA was polymerised in the presence of decalin (substrate which can donate a proton, similar to the condition of polypropylene) on the bench, see Scheme 5.2. Solution of 10% fresh DBBA in decalin (mixture of cis/trans, decahydro-naphthalene, b.p. 190°C) in the presence of 0.02 molar ratio Trigonox 101 (as initiator) was placed in a three-neck round bottom flask. After assembling with a thermometer, a condenser and a mechanical stirrer, the solution was then refluxed at 180°C (in constant temperature oil bath) under Argon atmosphere for 5 hours. However, the effect of shear cannot be simulated in the model compound studies. The reaction mixture in decalin was then chilled instantly in dry ice-acetone to stop any further reaction. After the unreacted decalin had been evaporated at room temperature under Argon atmosphere, a yellowish

solid "gum-like" residue resulted, see Scheme 5.2 stage B. This residue was then dissolved in pentane, both the soluble and insoluble fractions were then vacuum evaporated to constant weight at room temperature. The yellowish solid residue from the soluble pentane fraction (see Scheme 5.2 stage D) and the white solid residue from the insoluble pentane fraction (see Scheme 5.2 stage C) were then identified using FTIR, and Carbon-13 spectroscopy and their spectra were compared with that of fresh DBBA, polymerised DBBA, decalin grafted DBBA (10% MB) in a polymer film.

The FTIR spectrum of the white solid polymerised DBBA-decalin (see Scheme 5.2 stage D) was compared with that of fresh DBBA in a KBr disc, see Figure 5.38. The polymerised DBBA-Decalin sample shows major differences associated with shifts in the main absorption bands, for example, the hydroxyl group of the hindered phenol shifted to higher wave length numbers (to 3642 cm^{-1}) but the 3588 cm^{-1} band is also present as a shoulder. The carbonyl ester absorption band broadened and shifted up (to 1734 cm^{-1}). The absorption of the double bond for the aromatic and acrylic groups at 1636 cm^{-1} have decreased in intensity and the absorption of the double bond acrylic group at 1408 cm^{-1} has disappeared. In addition, some new absorptions were found in the region between $2600 - 3000\text{ cm}^{-1}$. Comparison of FTIR spectra of the polymerised DBBA-Decalin (grafted DBBA) with that of polymerised DBBA (poly-DBBA) without decalin (in KBr disc), see Figure 5.39, reveals that the overall absorption spectra are quite similar, except the appearance of new absorptions at $2859, 2736, 2709$ and 2664 cm^{-1} , in the case of the former was found to be due to decalin absorptions in this region, see Figure 5.40. Comparison of FTIR spectra of the polymerised DBBA-Decalin with that of grafted DBBA (10%) masterbatch film processed in the presence of 0.02 m.r. Trigonox 101 after DCM or xylene extraction, reveals also that the major absorptions of two spectra are similar, see Figure 5.41 and 5.42.

Examination of the ^{13}C NMR of polymerised DBBA-Decalin (Scheme 5.2 stage D) as shown in Table 5.13 and Figure 4.43 reveals major changes when compared to that of

fresh DBBA (see Figure 2.8 Chapter-2). It was found that both carbon absorptions of vinyl acrylic groups completely disappeared. The new absorptions were found as saturated carbon are formed (grafting to decalin), with carbon chemical shift (δ , ppm): carbon number 9' (>CH-) at (+) 43.3 and carbon number 10' (>CH₂) at (-) 21.7. Other new absorptions were found at (-) 34.2 (C no. D4) and (+) 36.2 (C no. D2), these should be carbon absorptions of decalin, which is bound to the DBBA. Other absorptions of decalin should be overlapped to that of Carbon of DBBA, i.e. C no. 9' and D1 overlapped at (+) 43.3 and C no. 5 and D3 overlapped at (-) 34.2 ppm. Figure 5.44 shows the ¹³C NMR spectrum of fresh Decalin in CDCl₃ at room temperature.

Table 5.13 ¹³C NMR spectrum of polymerised DBBA-decalin in CDCl₃ (see Scheme 5.2 stage D)

C No	δ (ppm)	(+)/(-)	I (%)	Total C
1	153.8	(-)	0.3	1
2	135.9	(-)	0.6	2
3	125.7	(+)	1.3	2
4	125.9	(-)	0.2	1
5/D3	34.2	(-)	1.7	2+1
6	30.1	(+)	12.0	6
7	67.2	(-)	0.7	1
8	174.7	(-)	0.1	1
9'/D1	43.5	(+)	0.2	1+1
10'	21.7	(-)	0.7	1
D2	36.2	(+)	0.9	1

D = Carbon of decalin

5.2.4 "Insitu" polymerisation of DBBA in NMR sample tube

^{13}C NMR investigation has also been carried out "in-situ" in the sampling cavity of the NMR machine. The measurement was not carried out at temperatures higher than 373°K , for safety reasons. Solutions of 10% DBBA and 0.02 molar ratio Trigonox 101 in decalin (mixture cis and trans) in the presence of a small amount of deuterated decalin was placed in an NMR sample tube at 296°K (23°C), its ^{13}C spectrum was recorded (see Figure 5.45). The sample tube was then removed from the NMR cavity and the temperature of the sample cavity of the NMR machine was increased up to 373°K (100°C). The sample tube was then inserted back into the sample cavity, its ^{13}C NMR spectrum was recorded every hour during a 25 hour reaction.

^{13}C NMR spectrum of the DBBA solution in decalin before reaction was recorded using a J-modulated (JMOD) method, where the spectrum with resonances was displayed in a positive (+) and negative (-) manner. This spectrum (see Figure 5.45 and Table 5.14) shows all similar peaks of its corresponding spectrum of fresh DBBA (as shown in Figure 2.8), in addition to decalin peaks at $\delta = (-) 24.0$ [C no. D4 of $-\text{CH}_2-$], $(-) 33.8$ [C no. D3 of $-\text{CH}_2-$], $(+) 35.7$ [C no. D2 of cis $>\text{CH}-$] and $(+) 43.1$ [C no. D1 of trans $>\text{CH}-$] ppm, see also Figure 5.44 for comparison.

When the decalin solution was heated up to 373°K , both $-\text{CH}_2-$ peaks (C no. D3 and D4 before heating up) of the decalin splitted to four new peaks at $\delta = 25.2$ (C no. D3), 27.9 (C no. D4), 30.9 (C no. D5) and $(-) 35.4$ ppm (C no. D6), see Table 5.15 and Figure 5.46. This splitting also occurred when fresh decalin was heated and recorded at a similar temperature (see Figure 5.47), which must be due to a reversible chain rotation of both decalin rings at high temperature, since when the decalin was cooled down and recorded at room temperature again the four peaks became two peaks, similar to that in Figure 5.44. After 1 hour heating at 373°K (in this case the ^{13}C NMR spectrum was recorded with a routine single pulsing method, where all the absorption peaks appear only on [+] value),

both unsaturation peaks of DBBA at δ (ppm) = (+) 129.7 (C no. 9) and (+) 130.3 (C no 10) still appeared, see Table 5.10a and Figure 5.46. Further reaction after 25 hours (see Table 5.11 and Figure 5.48) gives a similar spectrum to that of after 1 hour reaction (Figure 5.46), except that both unsaturation peaks of unreacted DBBA have completely disappeared. The appearance of the peak at $\delta = 24.4$, must be due to saturation of acrylic group (Carbon no. 10' of $-\text{CH}_2-$), another new saturated methine group (C no. 9') should be overlapped with that of carbon number D1 of decalin.

Table 5.14 ^{13}C NMR spectra of DBBA with decalin in NMR sample tube before reaction at 296°K, using Trigonox 101 as initiator.

C No	δ (ppm)	(+)/(-)	I (%)	Total C
1	153.6	(+)		1
2	135.5	(-)		2
3	125.4	(+)		2
4	126.0	(-)		1
5/D3	33.8	(-)		2+2
6	29.7	(+)		6
7	66.7	(-)		1
8	165.6	(-)		1
9	128.2	(+)		1
10	130.0	(-)		1
D1	43.1	(+)		1
D2	35.7	(+)		1
D4	24.0	(-)		2

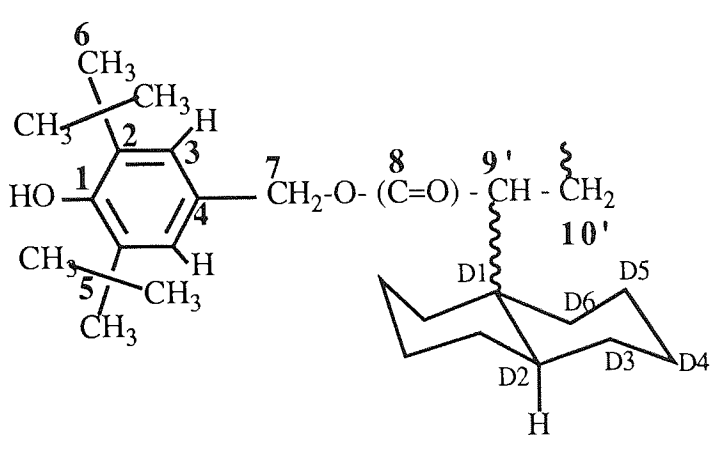
Like the spectrum of polymerised DBBA without and with decalin (see Figure 5.37 and 5.43) the spectrum of the in-situ polymerised DBBA in decalin for 25 hours shows also doublet peaks at $\delta = (+) 126.4$ ppm (C no 3). On the other hand, one of the

>CH₂- groups due to decalin at $\delta = (+) 44.9$ ppm (C no. D₁), which is recognised as that of trans >CH- (more susceptible to radical attack than the cis), decreased slightly. This indicates that the decalin substrate is also involved in the polymerisation reaction with the acrylate through hydrogen elimination from the >CH- group, which in turn may form a grafted structure onto the polymerised DBBA backbone.

Table 5.15 ¹³C NMR spectra of DBBA with decalin in NMR sample tube at 373°K, using Trigonox 101 as initiator after 1 hour reaction

C No	δ (ppm)	(+)/(-)	I (%)	Total C
1	154.7	(+)	0.26	1
2	137.4	(+)	0.60	2
3	126.3	(+)	1.41	2
4	129.2	(+)	0.59	1
5/D6	35.4	(+)	23.88	2+2
6	31.3	(+)	4.57	6
7	67.2	(+)	0.67	1
8	165.6	(+)	0.26	1
9	129.7	(+)	0.10	1
10	130.3	(+)	0.53	1
D1	44.9	(+)	11.0	1
D2	37.7	(+)	10.75	1
D3	25.2	(+)	22.34	2
D4	27.9	(+)	23.02	2
D5	30.5	(+)	21.18	2

Table 5.16 ^{13}C NMR spectra of DBBA with decalin in NMR sample tube at 373°K, using Trig.101 as initiator after 25 hours reaction.



C No	$\delta(\text{ppm})$	(+)/(-)	I (%)	Total C
1	154.7	(+)	0.07	1
2	137.4	(+)	0.07	2
3	126.4	(+)	0.23	2
4	129.2	(+)	0.10	1
5/D6	35.4	(+)	24.59	2+2
6	31.4	(+)	1.83	6
7	67.2	(+)	0.89	1
8	173.9	(+)	0.05	1
9'/D1	44.9	(+)	8.88	1+1
10'	24.4	(+)	0.11	1
D2	37.7	(+)	10.79	1
D2	25.2	(+)	22.87	2
D3	27.9	(+)	25.55	2
D4	30.5	(+)	21.55	2

5.2.5 Homopolymerisation of Tris Coagent in Benzene Substrate

To study the polymerised Tris that could occur during processing, this was simulated by the polymerisation of the Tris on a bench using AZBN as an initiator (see Scheme 5.10) in an inert liquid hydrocarbon substrate (benzene with boiling point 86°C). 100 ml of benzene solution containing 10% (w/w) Tris and 0.3 molar ratio (I/Tris) of initiator AZBN were mixed together in a 250 ml three necked round bottomed flask. After assembling with thermometer, condenser, and purged with Argon gas, this was then refluxed at constant temperature (70°C) for 5 hours. After refluxing the reaction mixture

was chilled in dry ice-acetone to stop further reaction, and was then exhaustively evaporated at room temperature (to remove benzene). The residue was then washed with DCM. After filtration white crystals insoluble DCM were found (see Scheme 5.10 stage C). This was then identified using IR and ^{13}C NMR spectroscopy to be compared to that of fresh Tris.

The FTIR spectrum of fresh Tris in neat liquid (see Figure 5.49) shows the interesting absorption at 1729 cm^{-1} ($\text{C}=\text{O}$ unsaturated ester group), 1636 , 1619 and 1408 cm^{-1} ($>\text{C}=\text{CH}_2$ for acrylic double bond). After polymerisation for 5 hours the FTIR spectrum of polymerised Tris, an insoluble DCM white crystal (see Scheme 5.10 stage C and Figure 5.49a) shows a changes in some absorptions, i.e. the saturated carbonyl, which shifts up to 1742 cm^{-1} due to saturation and most of the absorption of the acrylic double bond disappeared.

The ^{13}C NMR spectrum of fresh Tris as shown in Table 5.17 and Figure 5.50 exhibits specific peaks of interest at carbon chemical shifts (δ , ppm): methyl carbon (C no. T₁, of $-\text{CH}_3$) at (+) 7.1; two methylenic carbons (C no. T₂ and T₄ of $-\text{CH}_2-$) at (-) 22.9 and 63.8 respectively; quaternary carbon (C no. T₃, of $>\text{C}<$) at (-) 40.6; carbonyl carbon (C no. T₅, of $>\text{C}=\text{O}$) at (-) 165.3; methine carbon of acrylic (C no. T₆, of $-\text{CH}=>$) at (+) 128.1 and methylenic carbon of acrylic (C no. T₇, of $=\text{CH}_2$) at (-) 130.9. ^{13}C NMR of polymerised Tris was measured using solid state NMR and recorded in a routine method (which displayed all resonance as [+] value), since the poly-Tris was very difficult to dissolve in any solvent. The ^{13}C NMR spectrum of Tris after polymerisation (see Table 5.18 and Figure 5.51) exhibits carbon chemical shifts (δ , ppm): of methyl carbon, (C no. T₁, of $-\text{CH}_3$) at $\delta = 8.1$ ppm; methylenic carbons (C no. T₂) at 26.0; new methylenic saturated and quaternary carbons (C no. T_{7'} and T₃) overlapped at 41.5; methylenic and new methine saturated carbon (C no. T₄ and T_{6'}) overlapped at 66.0 and carbonyl carbon (C no. T₅) at 173.9 ppm. The carbon absorption of acrylic group at 128.0 and 130.9 ppm have almost completely disappeared.

Table 5.17 ^{13}C NMR of fresh Tris in CDCl_3

C No	$\delta(\text{ppm})$	(+)/(-)	I (%)	Total C
T1	7.1	(+)	4.6	1
T2	22.9	(+)	4.4	1
T3	40.6	(+)	2.3	1
T4	63.8	(+)	13.1	3
T5	165.3	(+)	3.4	3
T6	128.1	(+)	1.5	3
T7	130.9	(+)	11.1	3

Table 5.18 Solid state ^{13}C NMR of polymerised Tris in benzene substrate using AZBN as initiator.

C No	$\delta(\text{ppm})$	(+)/(-)	I (%)	Total C
T1	8.1	(+)	7.9	1
T2	26.0	(+)	3.6	1
T3/T7'	41.5	(+)	1.5	1+3
T4/T6'	66.0	(+)	5.5	3+3
T5	173.9	(+)	14.1	3

5.2.6. Polymerisation of DBBA with Tris in benzene substrate

In order to further understand the reaction of DBBA with Tris during processing, model reactions of DBBA+Tris were carried out using 0.02 molar ratio (I/DBBA+Tris) of AZBN (see Scheme 5.11) in an inert liquid substrate (benzene with boiling point 86°C). 100 ml benzene solution containing 6% (w/w) DBBA, 4% (w/w) Tris and 0.02 molar ratio (I/DBBA+Tris) of AZBN as initiator were mixed together in a 250 ml three neck round bottom flask. After assembling with a thermometer and condenser the solution was purged with Argon gas and was then refluxed at constant temperature of 70°C for 5 hours. After refluxing the reaction mixture was chilled in dry ice-acetone to stop the further reaction, and then was evaporated exhaustively at room temperature (to remove benzene). The residue (Scheme 5.11 stage B) was dissolved in DCM, both insoluble (white solid, see Scheme 5.11 stage C) and soluble DCM compounds (yellowish solid, see Scheme 5.11 stage D) were evaporated to remove the DCM solvent. The compound which soluble in DCM were then identified using IR and ^{13}C NMR spectroscopy compared with that of fresh DBBA and fresh Tris.

The FTIR spectrum of polymerised DBBA+Tris (soluble DCM residue part, see Scheme 5.11 stage D) shows very different spectral characteristics to that of fresh DBBA (see Figure 5.52). In the former, the hindered phenol hydroxyl absorption shifted to higher wave numbers (3642 cm^{-1}), the carbonyl ester absorption band broadened and shifted (to 1741 cm^{-1}), whereas the double bond for aromatic and acrylic groups at 1636 cm^{-1} weakened drastically in intensity and the absorption of the double bond of the acrylic group at 1408 cm^{-1} disappeared. When the spectrum of DBBA-Tris copolymer was compared with that of Tris, it reveals the appearance of new absorptions at 3639 cm^{-1} , disappearance of the double bond at 1636 and 1619 cm^{-1} and shift of carbonyl absorption to 1741 cm^{-1} . Comparison of FTIR spectra of DBBA-Tris copolymer with that of poly DBBA (polymerised without decalin), found that the absorptions of saturated carbonyl

were at different wave numbers, the former was at 1741 cm^{-1} whereas the latter was at 1735 cm^{-1} (see Figure 5.53). However, comparison of that of DBBA-Tris copolymer with poly Tris, shows absorption at similar wave number of saturated carbonyl at 1741 cm^{-1} , see Figure 5.54.

When the ratio of the carbonyl area of FTIR spectra of fresh DBBA after polymerisation was compared with that of Tris (using hydroxyl area as a referency of), it was found that the carbonyl area after polymerisation increased by 140%. This means that the increasing of the carbonyl area may be not only due to the polymerised DBBA alone but also that the Tris is involved in the polymerisation with DBBA.

Furthermore, the polymerised DBBA+Tris was examined by ^{13}C NMR in the solid state. The ^{13}C NMR spectra of fresh Tris and fresh DBBA are shown in Figures 5.50 and 2.8 respectively. After 5 hours polymerisation of DBBA+Tris using benzene substrate in the presence of an initiator (see Scheme 5.11 stage D, see Table 5.19 and Figure 5.55) solid state NMR analysis, reveals that carbon absorptions of aromatic DBBA appears at δ (ppm) 154.3 (C no.1), at 136.3 (C no. 2), while other aromatic carbons, (C no. 3 and 4) overlapped at 127.1 ppm. Quaternary carbons of tert. butyl (C no.5) appear at 34.3, methyl carbons of tert.butyl (C no. 6) appear at 30.3, methylenic carbon (C no. 7 overlapped with C no. T4 and T6') appears at 66.1, two carbonyl carbons (C no. 8 and T5) appear at 173.9. Both acrylic group carbons of DBBA or Tris disappeared and were replaced with a new methine saturated carbon (C no. 9' overlapped with C no.T3 and T7') and new methylenic saturated carbon (C no. 10' overlapped with C no. T2), and methyl carbon of Tris (C no. T1) at 7.7 ppm.

Table 5.19 Solid state ^{13}C NMR of polymerised DBBA+Tris in benzene substrate using AZBN as initiator.

C No	$\delta(\text{ppm})$	(+)/(-)	I (%)	Total C
1	154.3	(+)	2.2	1
2	136.3	(+)	2.7	2
3/4	127.1	(+)	3.8	2+!
5	34.3	(+)	6.6	2
6	30.3	(+)	15.0	6
7/T4/T6'	66.1	(+)	2.3	1+3+3
8/T5	173.9	(+)	4.7	1+3
9'/T3/T7'	40.3	(+)	5.4	1+3+3
10'/T2	22.9	(+)	2.7	1+1
T1	7.7	(+)	2.7	1

5.2.7 Polymerisation of DBBA+Tris with Decalin

Reaction of DBBA+Tris was further investigated but in the presence of a labile substrate (decalin) to simulate polypropylene and the reaction was carried out under condition similar to that of polymer processing, i.e. at temperature 180°C (see Scheme 5.12). Solution of 6% (w/w) fresh DBBA and 4% (w/w) Tris in decalin (decahydronaphthalene, b.p. 190°C) in the presence of 0.02 molar ratio (I/DBBA+Tris) of Trigonox 101 as initiator was placed in a three necked round bottomed flask. After assembling with a thermometer and a condenser the reaction mixture was stirred and then refluxed at 180°C (a constant temperature oil bath) under Argon atmosphere for 5 hours. However, the effect of shear

cannot be simulated in the model compound studies. The reaction mixture in decalin was then chilled instantly in dry ice-acetone to stop any further reaction. After the unreacted decalin had been evaporated at room temperature under Argon atmosphere, a yellowish solid "gum-like" residue was found, see Scheme 5.12 stage B. The residue was dissolved in hot-DCM, both insoluble (see Scheme 5.12 stage C) and soluble hot-DCM compounds (see Scheme 5.12 stage D) were evaporated to remove DCM. The soluble DCM residue was then dissolved in pentane, both of the soluble and insoluble fractions were then vacuum evaporated to a constant weight at room temperature. The yellowish solid residue from soluble pentane (see Scheme 5.12 stage F) was then identified using FTIR and ^{13}C spectroscopy and their spectra were compared with that of fresh DBBA or copolymer DBBA-Tris.

The FTIR spectrum of polymerised DBBA-Tris-Decalin (Scheme 5.12 stage F), see Figure 5.55a and 5.56, shows carbonyl ester absorption at 1741 cm^{-1} and the disappearance of the absorption of the double bond of the acrylic group at 1408 cm^{-1} . Overall the IR spectrum of polymerised DBBA-Tris-Decalin is very similar to that of DBBA-Tris copolymer, except for the persistence of the decalin peaks in the former ($2922, 2854, 2736, 2709$ and 2644 cm^{-1}) which suggests that the decalin is involved in the copolymerisation reaction. Figure 5.58 shows the comparison between grafted DBBA-Tris-Decalin and copolymer DBBA-Tris without decalin. When the former was compared with that of MB film containing 10% (DBBA+Tris) after DCM extraction (see Scheme 5.5 stage C, Figure 5.59) and also with that of a similar MB but for the soluble xylene fraction (see Scheme 5.5 stage F, Figure 5.60), it gave similar absorptions of hydroxyl and carbonyl groups (at 3642 and 1741 cm^{-1} respectively).

When the ratio of the carbonyl and hydroxyl areas of fresh DBBA and after polymerisation with Tris and decalin were compared, it was found that the carbonyl area increased up to 40%. The ratio of methylene ($3118.8 - 2765.0\text{ cm}^{-1}$) and hydroxyl absorption areas ($3639.1 - 3510.5\text{ cm}^{-1}$) of fresh DBBA and after polymerisation with Tris and decalin

were compared, it was found that the methylene area increases up to 250% (see Figure 5.61), this is much higher than when compared to that of polymerised DBBA+Tris without decalin (~57%), see Figure 5.55a and 5.56. This high increase in the area should be due to the decalin involvement in the copolymerisation reaction.

Table 5.20 Solid state ^{13}C NMR of polymerised DBBA-Tris-Decalin using Trigonox 101 as initiator.

C No	$\delta(\text{ppm})$	(+)/(-)	I (%)	Total C
1	154.2	(+)	1.3	1
2	135.6	(+)	2.2	2
3/4	126.7	(+)	2.7	2+1
5/D2/D3	34.6	(+)	9.9	2+1+2
6/D4	30.4	(+)	18.0	6+2
7/T4/T6'	67.3	(+)	3.3	1+3+3
8/T5	173.9	(+)	9.9	1+3
9'/D1/T3/T7'	40.6	(+)	7.1	1+1+3+1
10'/T2	24.7	(+)	2.9	1+1
T1	8.2	(+)	1.9	1

The pentane soluble fraction of the polymerised DBBA-Tris-Decalin (Scheme 5.12 stage F) was further characterised by ^{13}C NMR in the solid state, see Table 5.14 and Figure 5.62. When this polymerised DBBA-Tris-Decalin ^{13}C NMR spectrum was compared with that of polymerised DBBA-Tris (no decalin), similar peaks were shown, except that in the area

of 20.00 - 50.00 ppm, the absorption peaks were more crowded. In the former case, this is presumably due to the decalin absorption in this region, i.e. at δ (ppm) = 40.6 (C no. D1 overlapped with C no. 9', T3 and T7'); at δ (ppm) = 34.6 (C no. D2 overlapped with C no D3 and 5); at δ (ppm) = 30.4 (C no. D4 overlapped with C no. 6).

Figure 5.63 and Table 5.21 show solid state NMR of polymerised DBBA with decalin. It was found that both the carbon absorptions of the vinyl acrylic groups completely disappeared. The new absorptions were found as saturated carbon are formed (grafting to decalin), with carbon chemical shift (δ , ppm): C no. 9' overlapped with C no.D1 at 40.0 and C no. 10' at 22.5. Other new absorptions were found at 34.4 (C no. 5, D2 and D3) and at 30.5 (C no. 6 and D4).

Table 5.21 Solid state ^{13}C NMR of polymerised DBBA with Decalin using AZBN as initiator, see Scheme 5.2 stage D.

C No	δ (ppm)	(+)	I (%)	Total C
1	154.1	(+)	4.7	1
2	135.9	(+)	6.7	2
3/4	127.0	(+)	7.5	2+1
5/D3/D2	34.4	(+)	9.0	2+2+1
6/D4	30.5	(+)	23.0	6+2
7	67.3	(+)	1.6	1
8	174.5	(+)	1.7	1
9'/D1	40.0	(+)	1.6	1+1
10'	22.5	(+)	0.5	1

Figure 5.64 and Table 5.22 show solid state NMR of the xylene soluble fraction of MB containing 10% DBBA (see Scheme 5.4 stage F). It was found that both carbon absorptions of vinyl acrylic groups of fresh DBBA completely disappeared. The new absorptions were found as saturated carbons are formed (grafting to PP), with carbon chemical shift (δ , ppm): C no. 9' overlapped with PP at 43.6, carbon number 10' overlapped with PP resonance at 22.5, carbon no. 5, 6 overlapped with PP at 26.2.

Table 5.22 Solid state ^{13}C NMR of xylene soluble MB containing 10% DBBA, see Scheme 5.4 stage F.

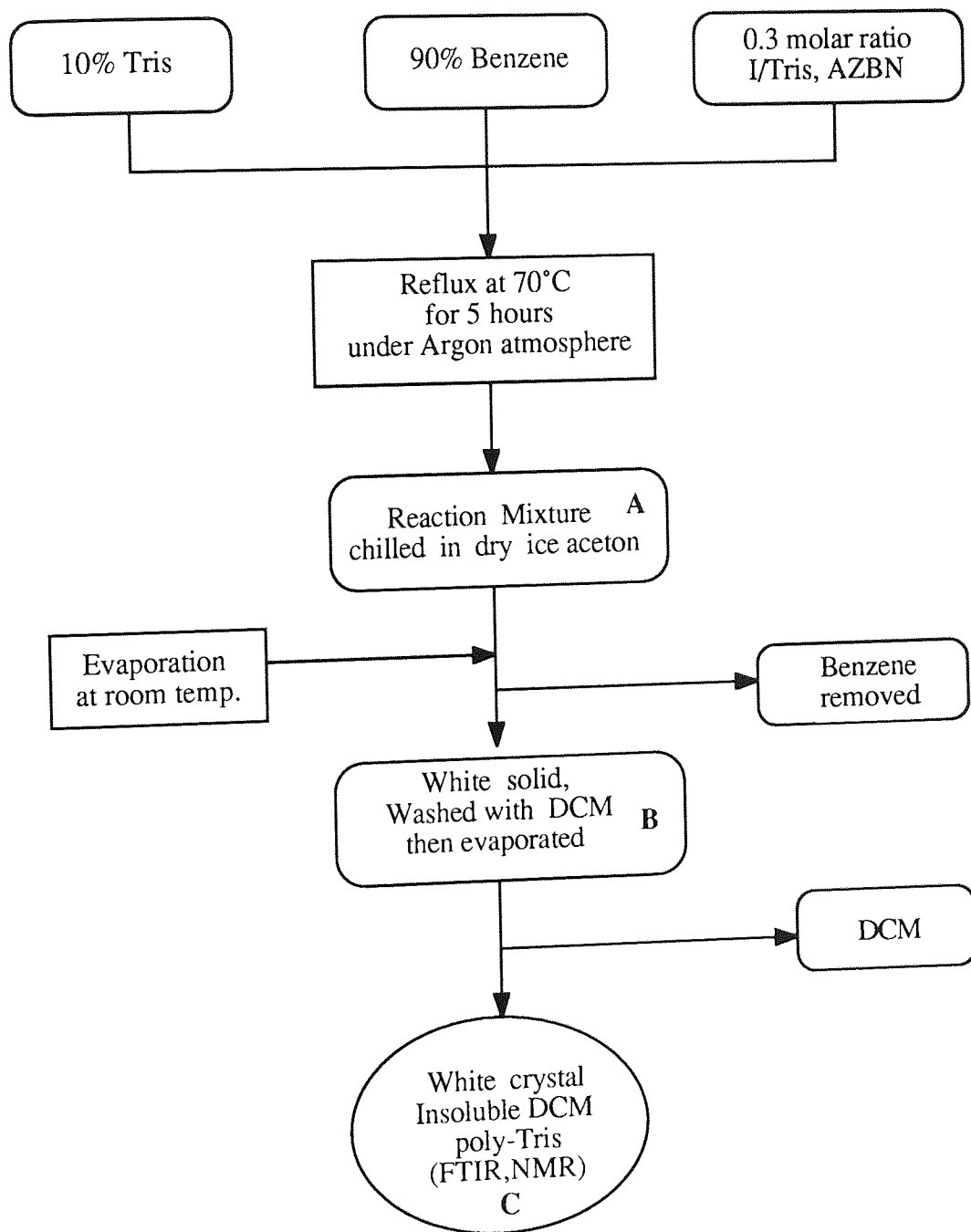
C No	δ (ppm)	(+)/(-)	Total C
1	154.1	(+)	1
2	135.9	(+)	2
3/4	127.0	(+)	2+1
5/6/PP	26.2	(+)	2+6
7	67.3	(+)	1
8	174.9	(+)	1
9'/PP	43.6	(+)	1
10'/PP	22.5	(+)	1

Figure 5.65 and Table 5.23 show solid state ^{13}C NMR spectrum of xylene soluble fraction of MB containing 10% (DBBA+Tris), see Scheme 5.5 stage F. Like polymerised DBBA-Tris in Decalin, it was found that both absorptions of vinyl acrylic groups of fresh DBBA and Tris completely disappeared. The new absorptions were found as the saturated carbons are formed (grafting to PP), with carbon chemical shift (δ , ppm): C no. 9', T3, carbons are formed (grafting to PP), with carbon chemical shift (δ , ppm): C no. 9', T3, T7' overlapped with PP at 40.6, carbon number 10' overlapped with PP resonance at 22.5,

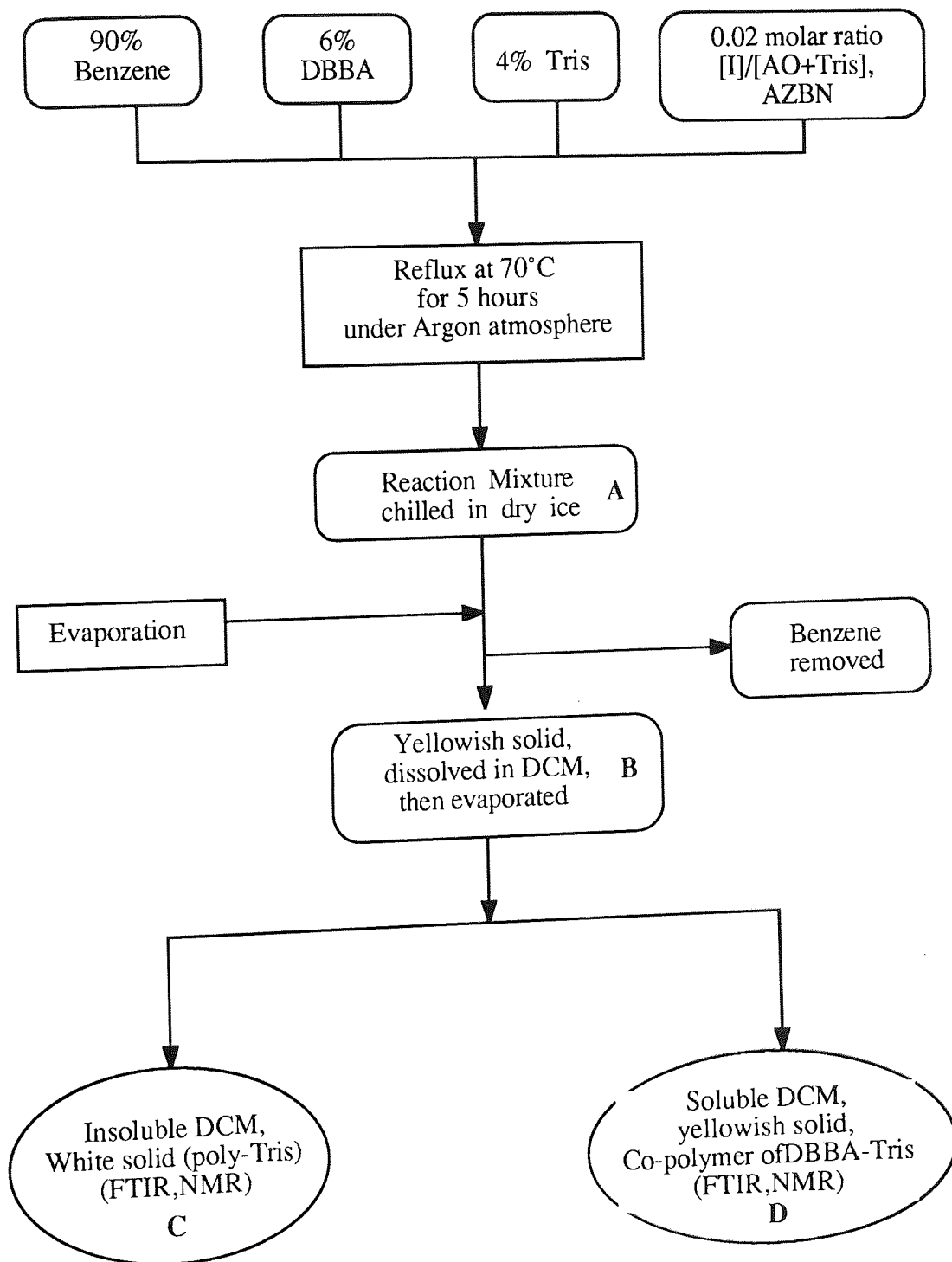
carbon no. 5, 6 overlapped with PP at 26.2. The spectrum of antioxidant (DBBA-Tris) is not very clear, compared to that of PP, this should be due to the concentration of DBBA-Tris which grafted onto PP is very low.

Table 5.23 Solid state ^{13}C NMR of xylene soluble MB containing 10% (DBBA+Tris), see Scheme 5.5 stage F.

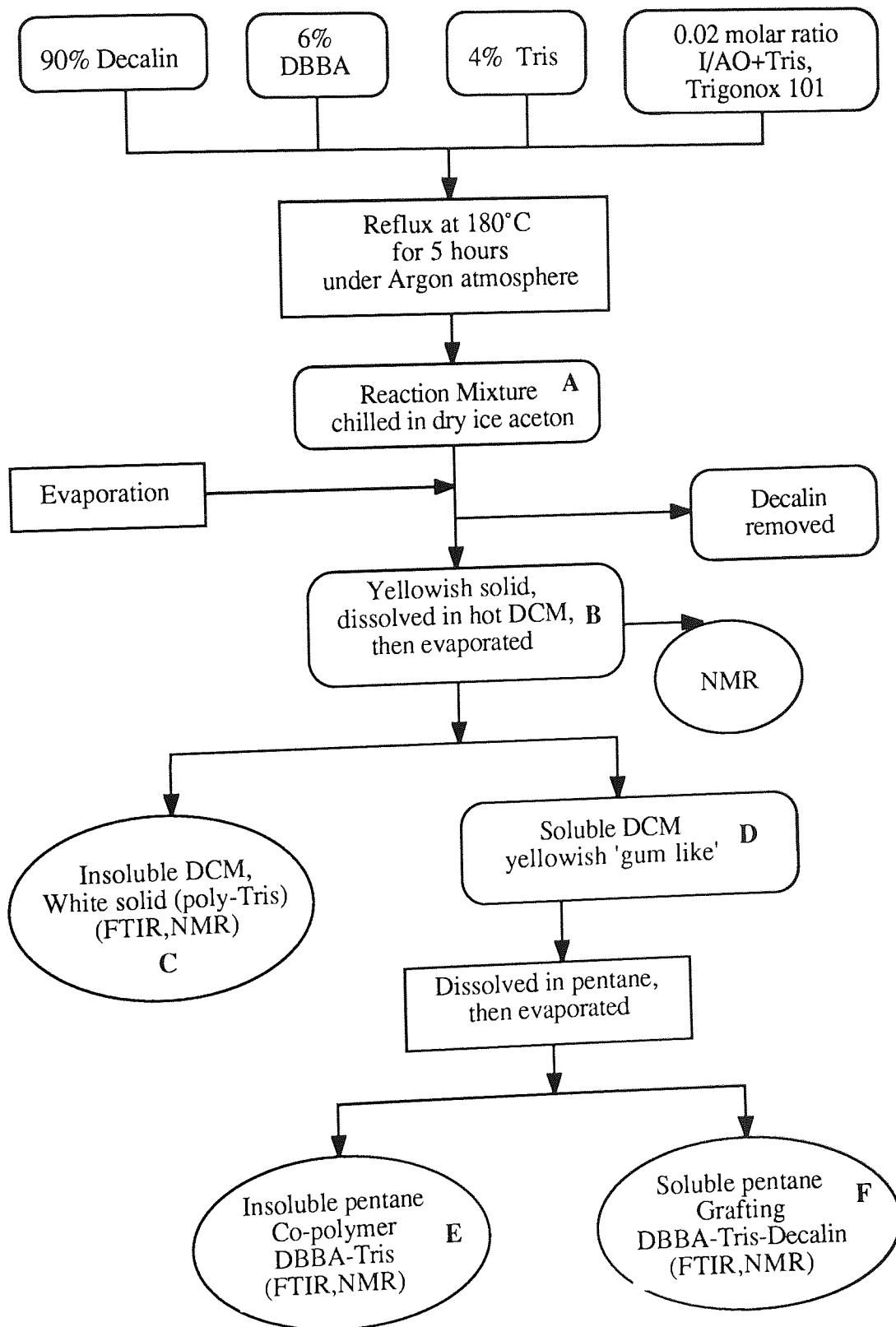
C No	$\delta(\text{ppm})$	(+)/(-)	Total C
1	154.1	(+)	1
2	135.9	(+)	2
3/4	127.0	(+)	2+1
5	34.6	(+)	2
6	30.7	(+)	6
7/T4/T6'	67.3	(+)	1+3+3
8/T5	174.5	(+)	1+3
9'/PP/T3/T7'	40.6	(+)	1+1+3
10'/T2	43.6	(+)	1+1
PP	26.2	(+)	-
PP	22.2	(+)	-
PP	22.2	(+)	-
T1	6.3	(+)	1



Scheme 5.10 Schematic procedure of polymerisation Tris in benzene in the presence of 0.03 m.r. (I/Tris), AZBN at 70°C for 5 hours.



Scheme 5.11 Schematic procedure of polymerisation DBBA+Tris (ratio 6/4) in benzene in the presence of 0.02 m.r.(I/DBBA+Tris) AZBN at 70°C for 5 hours.



Scheme 5.12 Schematic procedure of polymerisation DBBA+Tris (ratio 6/4) with decalin in the presence of 0.02 molar ratio (I/DBBA+Tris) Trigonox 101 at 180°C for 5 hours.

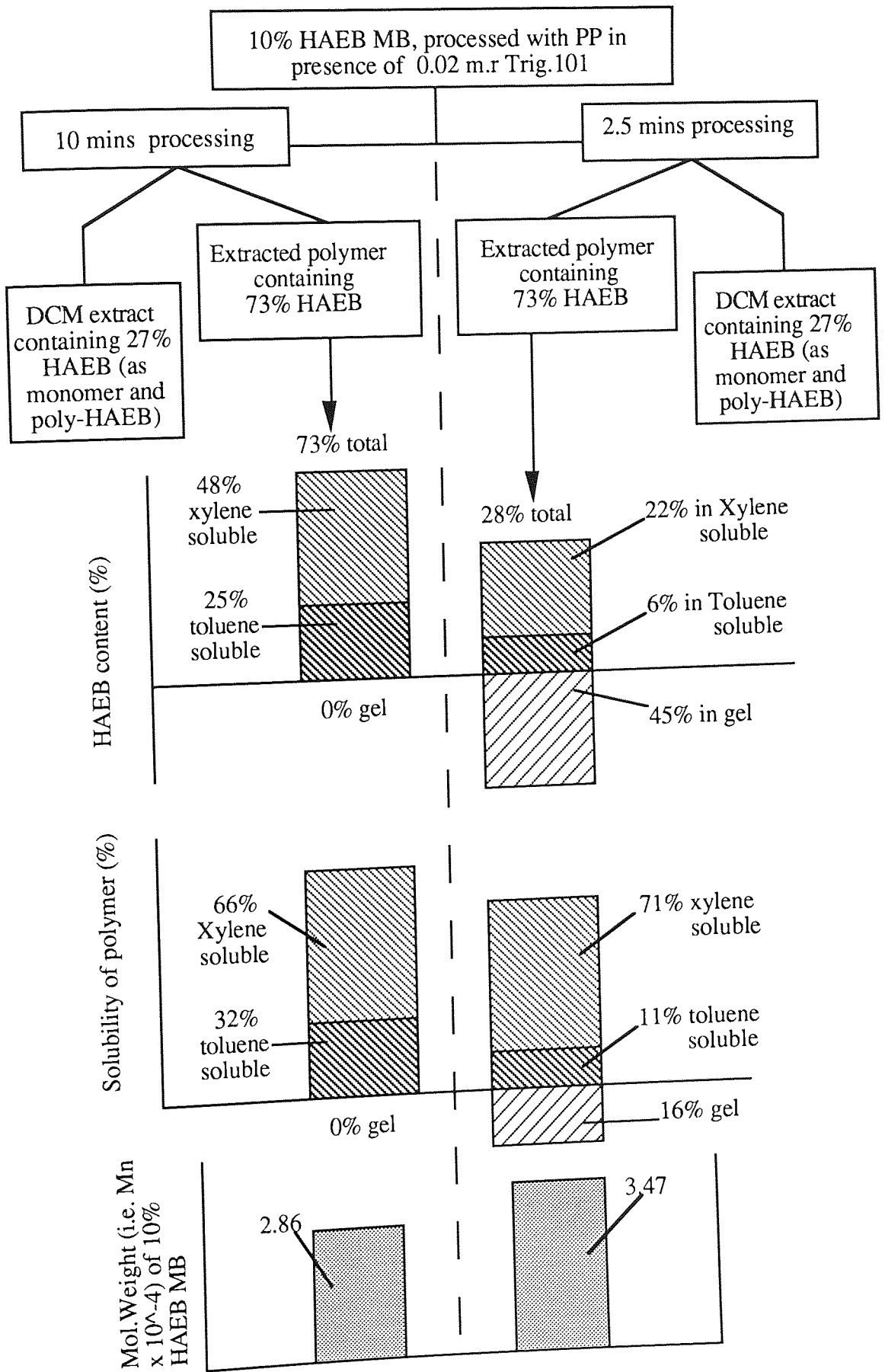
5.3 DISCUSSION

5.3.1 Reactive Processing Mechanism of HAEB and DBBA in Polymer Melts

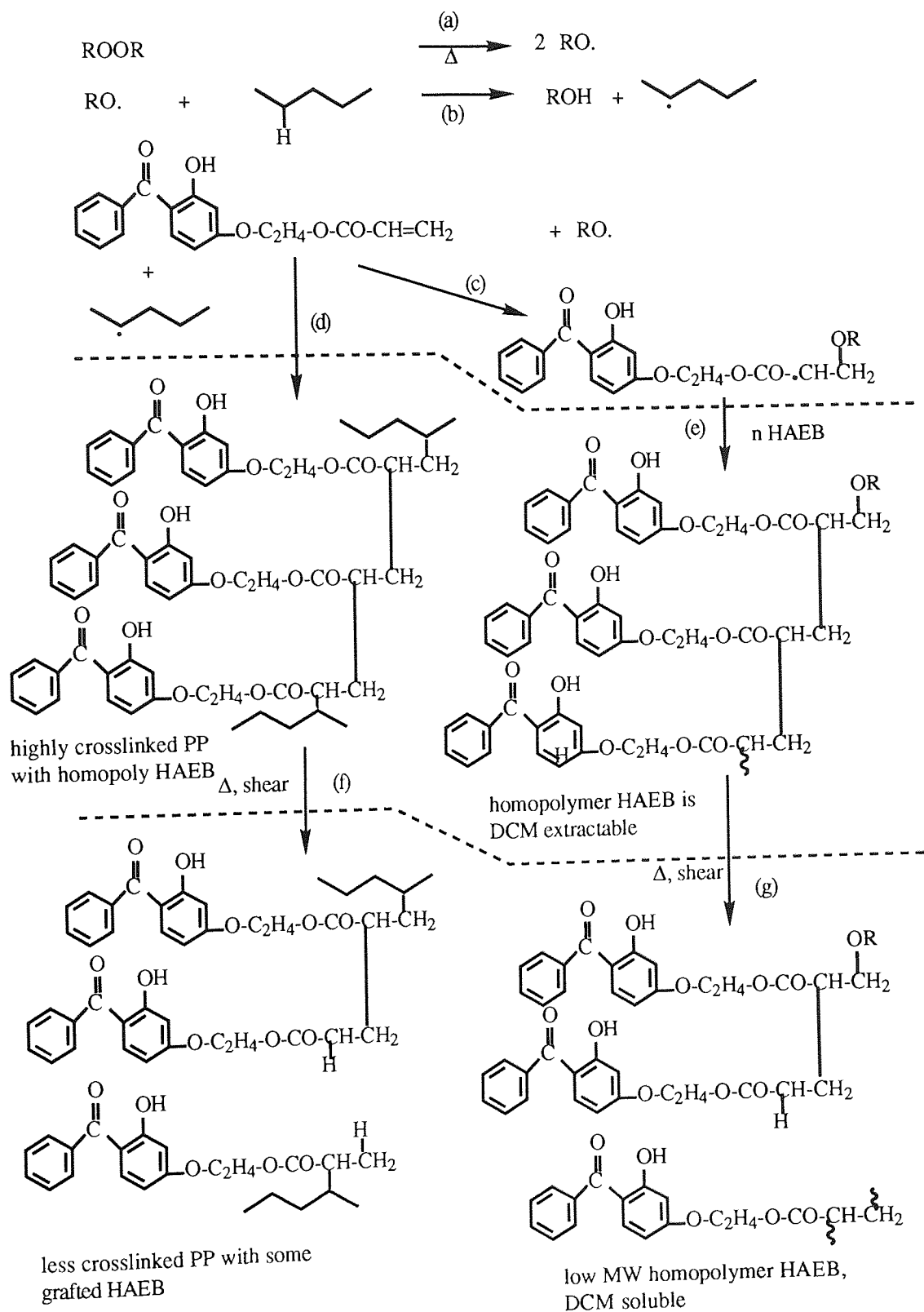
Both HAEB and DBBA have a polymer reactive function (acrylic groups) which can react with polypropylene during processing leading not only to the grafting of AO's onto polymer backbones but also to many other side reactions. The acrylic double bond group in both molecules can undergo homopolymerisation as was clearly described in the literature (192). Further reaction of the linear homopolymerised AO can occur in the form of a random attack onto the polypropylene backbone, leading to crosslinking or a high molecular weight polymer matrix (112,182,192).

Processing of HAEB with polypropylene in the presence of peroxide suggests that high molecular weight and crosslinked products are formed. These occur, initially, at the beginning of the melt reaction (initial stage of processing), as indicated by the high torque peak and corresponding with the gel formation (see Figures 3.19 and 5.23). As processing continues, the crosslinked product and high molecular weight product undergo chain scission leading to a drop of the torque to almost the level of PP (see Figure 5.22). Analysis of HAEB MB's after various reaction times reveals that in both cases during the initial melt reaction with PP (after 2.5 minutes processing) and at the end of the reaction (after 10 minutes processing), 73% of HAEB is retained in the polymer (after DCM extraction) and 27% HAEB is in the form of poly-HAEB which is well extracted out by DCM. The DCM extract shows clearly (see Figure 5.16) the characteristic absorptions for a poly HAEB, most certainly low molecular weight homopolymer reflected in the shift in $>C=O$ absorption from the unsaturated carbonyl at 1725 cm^{-1} to a saturated carbonyl at 1738 cm^{-1} .

The behaviour of the 73% HAEB retained in the polymer at the early stages of the reaction (2.5 minutes) and at the end of reaction (10 minutes) is, however, very different. At the early stages of reaction 45% of HAEB becomes a xylene insoluble gel, suggesting a very high MWt structure. While of the rest, 22% is xylene soluble (but toluene insoluble) and only 6% toluene soluble (xylene soluble fraction must certainly have higher molecular weight (MW) structure than the toluene soluble fraction). At the end of the reaction, however, all the xylene insoluble gel disappears and 48% becomes xylene soluble, while 25% is toluene soluble, suggesting that some high molecular weight is not retained. The structure must be different due to different solubilities; lower overall molecular weight which is toluene soluble and high molecular weight which is xylene soluble. This is further confirmed by examination of changes in MW (see Scheme 5.13) whereby high molecular weight (e.g. Mn) at 2.5 minutes, decreases after 10 minutes processing and also there is a clear narrowing of MWD as reflected in the decrease of dispersity, suggesting breaking of the crosslinked structure, possibly some crosslinked PP. However, the binding efficiency of HAEB does not change for different times of processing. It can be suggested that grafted HAEB undergoes re-structuring during processing. Previous work at Aston (112) reported that grafted AATP undergoes re-structuring during reactive processing with PP. The suggested mechanism of reactive processing of HAEB in polypropylene in the presence of peroxide, is that at the beginning of the reaction, HAEB homopolymer is formed, this was then followed by high crosslinking of HAEB with PP. Finally due to the shearing and thermal effects, after 10 minutes processing, the crosslinking decreased, and grafted HAEB was the major product at the end of the reaction (see Scheme 5.14).



Scheme 5.13 Structure of HAEB in polymer (10%) MB's processed with PP in the presence of 0.02 m.r Trig.101, for 2.5 and 10 minutes under standard condition



Scheme 5.14 Suggested mechanism of reactive processing of HAEB in PP in the presence of 0.005 m.r. Trig.101, processed at 180°C for 10 minutes in closed mixing condition.

Analysis of DBBA MB (10 minutes processing) indicates that, 40% of DBBA is retained in the polymer (after DCM extraction) and 60% DBBA is in the form of monomer and poly-DBBA, which were well extracted out by DCM. DCM extract contains mainly poly-DBBA, note shift of unsaturated carbonyl of fresh DBBA to saturated carbonyl (from 1714 to 1735 cm^{-1}). The DCM extract shows clearly (see Figure 5.8) that the characteristic absorptions for a DBBA monomer at 1408 cm^{-1} completely disappear (small contribution from vinyl, $>\text{C}=\text{C}<$) suggesting very little or no monomer left to be extracted. This is confirmed by the similarity of the IR of the DCM extract (poly-DBBA which is very DCM soluble) and that of the grafted DBBA-PP (completely DCM insoluble), see Figure 5.9. Furthermore, the almost identical IR spectrum of the polymerised DBBA on the bench (poly-DBBA of model reaction) compared with that of the DCM extract, see Figure 5.34, confirms that the DCM extract is mainly a poly-DBBA. Synthesised poly-DBBA is very soluble in DCM, while grafted DBBA-Decalin is less soluble compared with the former. DCM extracted DBBA masterbatch (completely DCM insoluble) mainly contains grafted DBBA-PP (see Figure 5.4) as indicated from unsaturated carbonyl (1714 cm^{-1}) shift to saturated carbonyl (1725 cm^{-1}) and complete disappearance of 1408 cm^{-1} ($>\text{C}=\text{C}<$ of vinyl). When this DCM extracted DBBA masterbatch (see Scheme 5.4 stage C) is compared with both model reactions of poly-DBBA and grafted DBBA-decalin, they exhibit similar saturation of acrylic groups (see Figure 5.39 and 5.41). This is supported by the fact that the poly-DBBA model reaction was found to be very DCM soluble (see Scheme 5.2 and 5.3), while the model grafted DBBA-Decalin was comparatively less DCM soluble than the former. When solid state ^{13}C NMR of xylene soluble 10% grafted DBBA MB is compared with that of models grafted DBBA-decalin, it was shown that both of them also have similar saturation, even though the latter was lower in intensity (see Figure 5.63 and 5.64). Almost 60% of initial DBBA that undergoes homopolymerisation is extracted by DCM. The structure of the remaining 40% in the polymer is as follows: The structure of DBBA-polymer contains a greater amount of lower MWt fraction (which is toluene soluble (73% polymer) containing 10% out of total 40% remaining DBBA), than the higher MW fraction (which is xylene soluble (21% polymer) containing 30% out of

total 40% remaining DBBA). The xylene soluble polymer, however, has a much higher MW (e.g. Mn) as clearly illustrated in Scheme 5.15. The results discussed above may be used to elucidate a mechanism of the reactive processing of DBBA in PP in the presence of 0.02 m.r. ratio of Trigonox 101, processed at 180°C for 10 minutes under closed mixing condition, see Scheme 5.18.

A model reaction for reactive processing of DBBA with decalin can be carried out at 180°C, a temperature similar to that used for standard processing of PP. The FTIR spectra of polymerised DBBA-Decalin and poly DBBA without decalin exhibited the disappearance of the acrylic double bond group and similar absorptions of saturated carbonyl at 1735 cm⁻¹. However, in the former some new absorption was found which was typical of decalin compounds in the region of 2600 - 3000 cm⁻¹, reflecting that decalin was involved in this polymerisation reaction. The proton and ¹³C NMR spectra of polymerised DBBA-Decalin shows the disappearance of a typical acrylic double bond absorption. The appearance of new absorptions is the result of saturation of the acrylic double bonds and the modification of decalin. Polymerised DBBA without decalin is very DCM soluble, however, grafted DBBA-Decalin is less DCM soluble compared to that of the former. The reaction mechanism of polymerisation of DBBA in decalin (in the presence of 0.02 molar ratio Trigonox 101 as initiator at 180°C for 5 hours under argon atmosphere) is shown in Scheme 5.19.

Only 40% binding efficiency of DBBA in PP in the presence of peroxide is achieved, hence, to enhance the reaction other functional monomers are used (called coagents, i.e. Tris and DVB)(183,184). Analysis of 10% (DBBA+Tris) MB (10 minutes processing) demonstrates that 91% of DBBA is retained in the polymer (after DCM extraction) and 9% DBBA is in the form of poly-DBBA is extracted out by DCM. The DCM extract contains poly-DBBA; note shift of unsaturated carbonyl of fresh DBBA to saturated carbonyl (from 1714 to 1735 cm⁻¹). The DCM extract clearly shows (see Figure 5.8d) the characteristic absorptions for a DBBA monomer at 1736 and 1619 cm⁻¹ which are broader and less

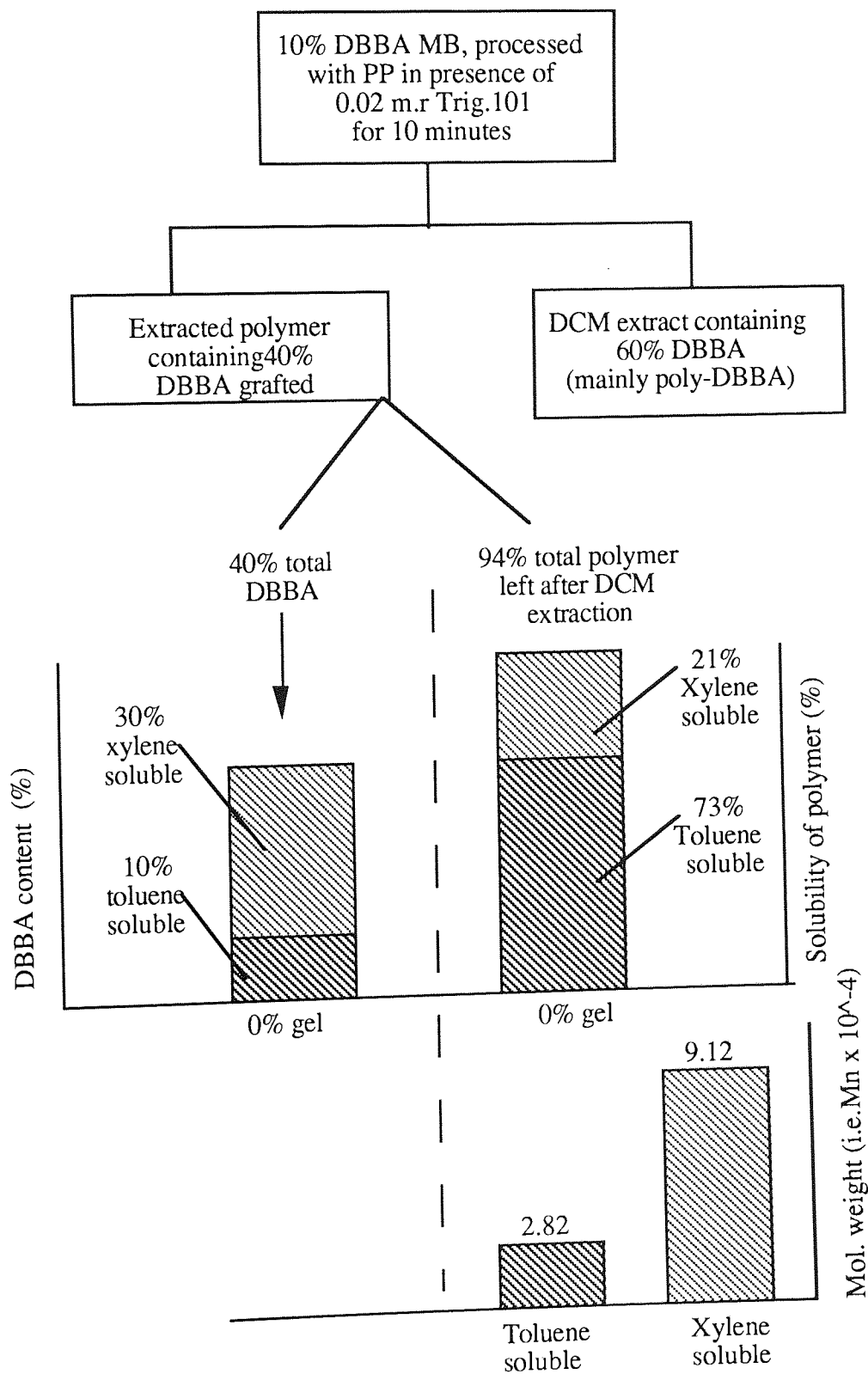
intense. The 1408 cm^{-1} absorption completely disappears (although there may be a negligible contribution from vinyl, $>\text{C}=\text{C}<$) suggesting that no monomer is left to be extracted. This is confirmed by the similarity of the IR spectra of the DCM extract (poly-DBBA which is very DCM soluble) and that of the grafted DBBA-Tris-PP (completely insoluble in DCM), see Figure 5.8d and 5.60. Furthermore, the almost identical IR spectra of the polymerised DBBA on the bench (poly-DBBA model reaction) with that of the DCM extract, see Figure 5.35, confirms that the DCM extract is mainly a poly-DBBA. Synthesised poly-DBBA is very soluble in DCM, while grafted DBBA-Tris-Decalin is less soluble compared with the former. DCM extracted DBBA+Tris masterbatch (completely insoluble in DCM, Scheme 5.5 stage C) is mainly composed of grafted DBBA-Tris-PP (see Figure 5.59) as indicated from the unsaturated to saturated carbonyl shift (1714 to 1741 cm^{-1}) and complete disappearance of the 1408 cm^{-1} ($>\text{C}=\text{C}<$ of vinyl) absorptions. The suggested mechanism of reactive processing of DBBA+Tris in PP (in the presence of 0.02 m.r. ratio of Trigonox 101, processed at 180°C for 10 minutes under closed mixing condition) can be seen in Scheme 5.20.

FTIR spectra of the model reaction of grafted DBBA-Tris-Decalin, copolymer DBBA-Tris and grafted DBBA-Tris-PP have similar saturation absorption (i.e. saturated carbonyl at 1741 cm^{-1}). The ratio of carbonyl and hydroxyl area of DBBA-Tris-Decalin shows 40% increase compared to that of fresh DBBA. This means that the increase of carbonyl area should be due to that the Tris involved in that copolymerisation reaction with DBBA (see Figure 5.52), with saturated carbonyl absorption at 1741 cm^{-1} , since saturated carbonyl of poly DBBA is at 1735 cm^{-1} . The increasing ratio of the methylene and hydroxyl area of the model reaction of polymerised DBBA-Tris-Decalin compared to that of the DBBA-Tris copolymer gives evidence that the decalin is involved in copolymerisation with the DBBA. When the DCM extracted DBBA+Tris masterbatch (see Scheme 5.5 stage C and F) is compared with both model reactions DBBA-Tris copolymer and grafted DBBA-Tris-Decalin, it exhibits similar saturation of acrylic groups spectra (see Figure 5.56, 5.59 and 5.60). Like in the FTIR spectra, the solid state of ^{13}C NMR spectra of

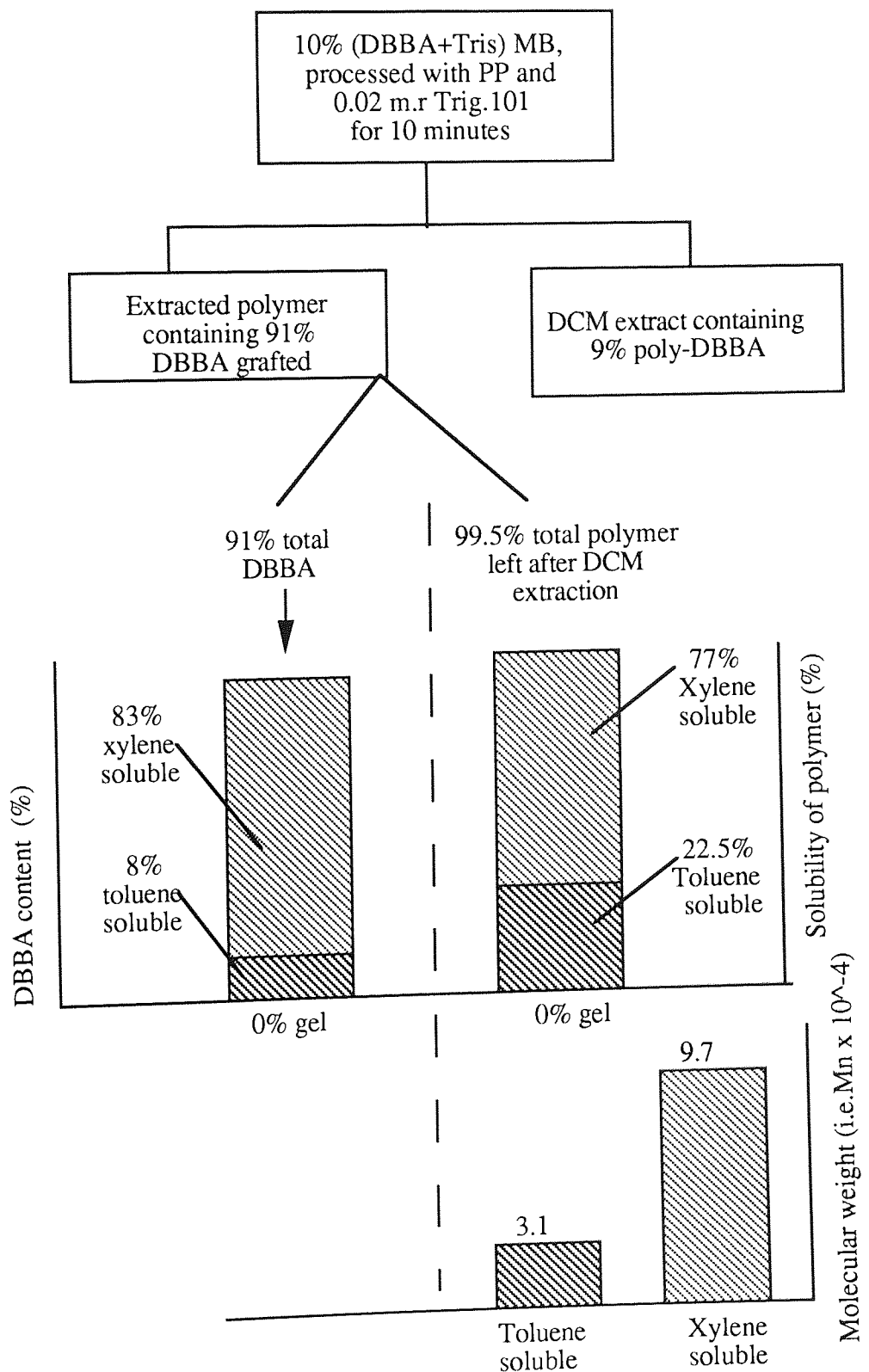
xylene soluble component of MB containing 10% (DBBA+Tris) and the model reaction of grafted DBBA-Tris-Decalin reveal that after excluding all the decalin and polypropylene absorptions⁽¹⁹³⁾, it has similar characteristics as that of the model reaction of DBBA-Tris copolymer (see Figure 5.55, 5.62 and 5.65). From the above discussion, it can be suggested that the mechanism of polymerised DBBA+Tris in decalin in the presence of 0.02 m.r. of Trigonox 101 as initiator (at 180°C for 5 hours under Argon atmosphere) as described in Scheme 5.21.

Comparison of MB containing 10% DBBA (Scheme 5.15) and 10% (DBBA+Tris), Scheme 5.16 shows:

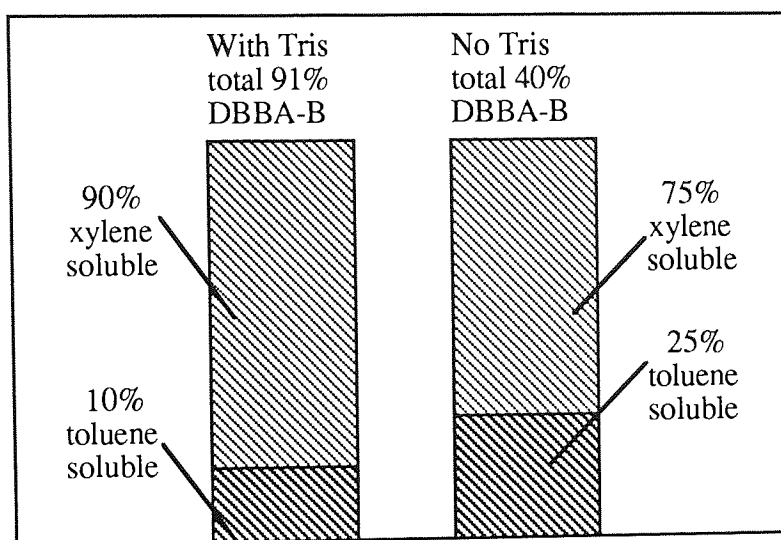
1. Binding efficiency with Tris is 91%, whereas no Tris is only 40%
2. DCM extract masterbatches in both cases is in the form of poly DBBA, even though, in the case of with Tris only 9% , compared to 60% without Tris.
3. Carbonyl saturated in DCM extracted masterbatch with Tris at 1741 cm^{-1} (it is similar to that of model reaction of DBBA-Tris copolymer and grafted DBBA-Tris-Decalin), whereas without Tris is at 1731 cm^{-1} .
4. Structure of grafted DBBA in DCM extracted polymer in the presence of Tris, however, is very different than when Tris is absent. In the absence of Tris, a higher amount of lower MW structure was found (toluene soluble, 73%) but this contains only 25% of total DBBA, i.e. 10% based on 40% remaining polymer (see Figure 5.64a). Around 90% of total remaining DBBA in polymer is tied up in a higher MW structure contained in 77% of the total polymer. In the presence of Tris, a higher MW structure was also found (xylene soluble, 77%) and this contains most of the DBBA, 90% of total (i.e. 83% based on remaining 91% in polymer) see Scheme 5.15 and 5.16. The MW of the xylene soluble structure in both cases is high and quite similar, and in both cases no gel content was found.



Scheme 5.15 Structure of grafted DBBA in polymer (10% MB, processed with polypropylene in presence of 0.02 m.r Trig.101, under standard condition)



Scheme 5.16 Structure of grafted DBBA with Tris coagent in polymer (10% MB, processed with polypropylene in the presence of 0.02 m.r. Trig.101, under standard condition)



% Distribution of bound-DBBA from total in each case toluene and xylene fractions, in presence and absence of Tris

Figure 5.64a Grafted DBBA content of toluene soluble and xylene soluble of 10% MB containing DBBA without and with Tris coagent processed in the presence of 0.02 m.r. Trig.101, under standard condition.

In the presence of DVB as coagent having two reactive polymer groups, in the masterbatch (6%DBBA+4%DVB) gave higher binding efficiency (93%) compared to that using the Tris coagent. The FTIR spectrum of this masterbatch shows that the absorption of the acrylic double bond completely disappears, see Figure 5.8a. After xylene extraction, it was found that the gel content is 7.2%. Surprisingly the torque recording did not show any maxima peak during 10 minutes processing. The FTIR spectra of DCM-extract of this masterbatch also did not show typical absorption of acrylic double bond (see Figure 5.8b). It can be suggested that the remain DBBA in (DBBA+DVB) masterbatch after DCM extraction may contain the grafted and crosslinked DBBA-polypropylene.

The overall structure of grafted DBBA with DVB is very similar to that of with Tris in which a higher amount of higher MW structure (xylene soluble) is found and the amount of lower MW structure is the same as for Tris (~22.5%). However, here there is an additional 7% gel which is completely absent in the Tris. Although the total amount of DBBA left in polymer after DCM extraction is the same in the case of Tris and DVB, the

distribution of DBBA in different structural fractions is different in the two cases. In the case of DVB, only 46% of DBBA is present in the higher MW structure which is xylene soluble (compared to 83% in case of Tris), and the remaining ~40% is divided between lower MW, toluene soluble (~23%) and in the xylene insoluble gel (~16%). In the case of Tris only 10% DBBA is in the soluble toluene fraction and no gel is formed. Furthermore, the xylene soluble fraction in the case of DVB has a lower MW than the xylene soluble fraction in the presence of Tris (see Scheme 5.15 & 5.16 and Figure 5.64b). Since the MW of the xylene soluble fraction of Tris is very similar to that of the 10% DBBA MB without any coagent, it is suggested that the DBBA sample processed with DVB undergoes more degradation leading to a polymer with a lower MW. The very low MFI in the presence of DVB suggests the some crosslinked material is formed as reflected by the formation of the gel.

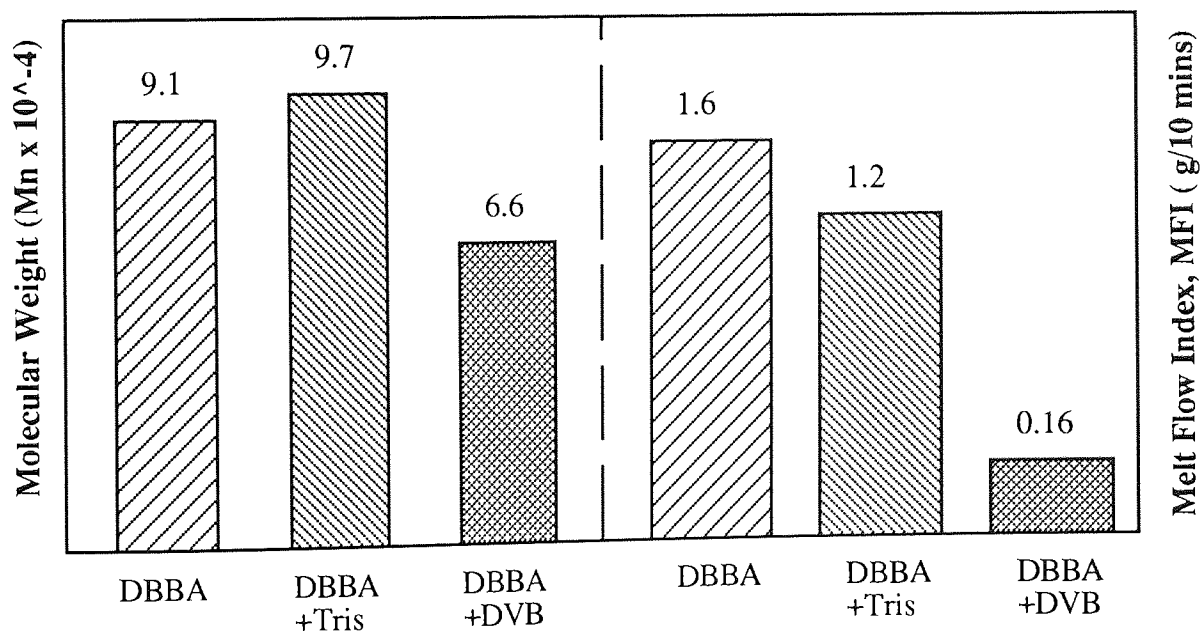
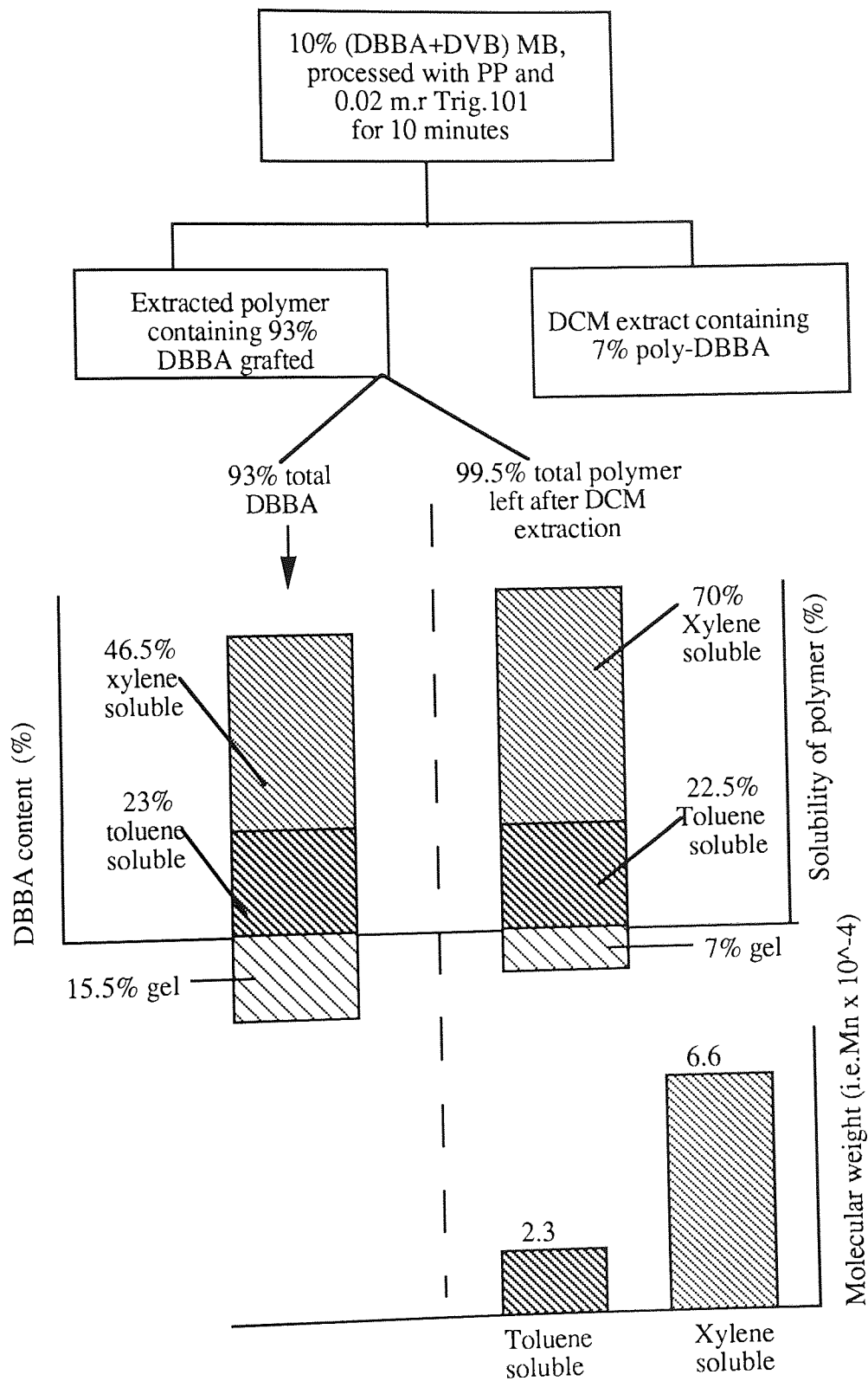
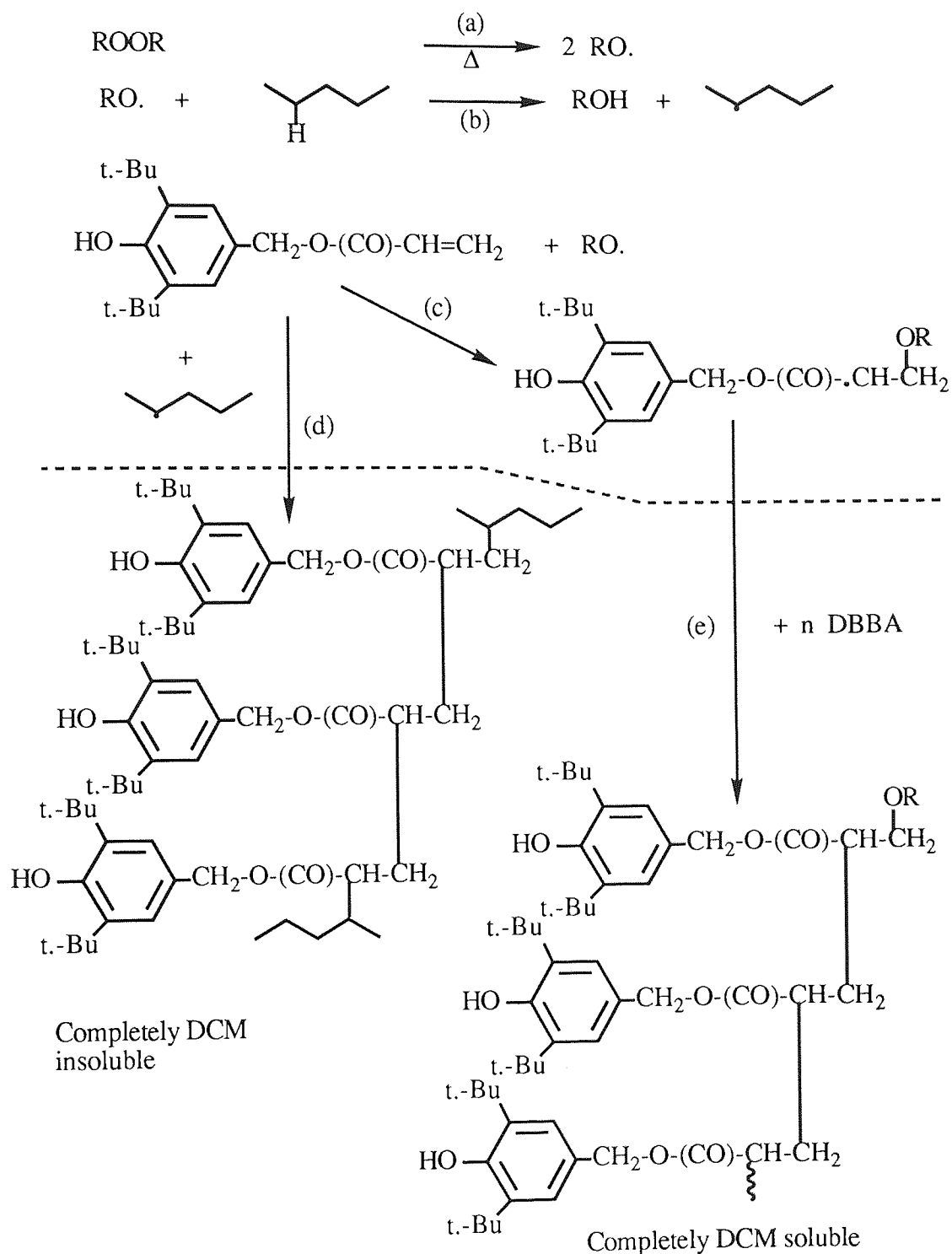


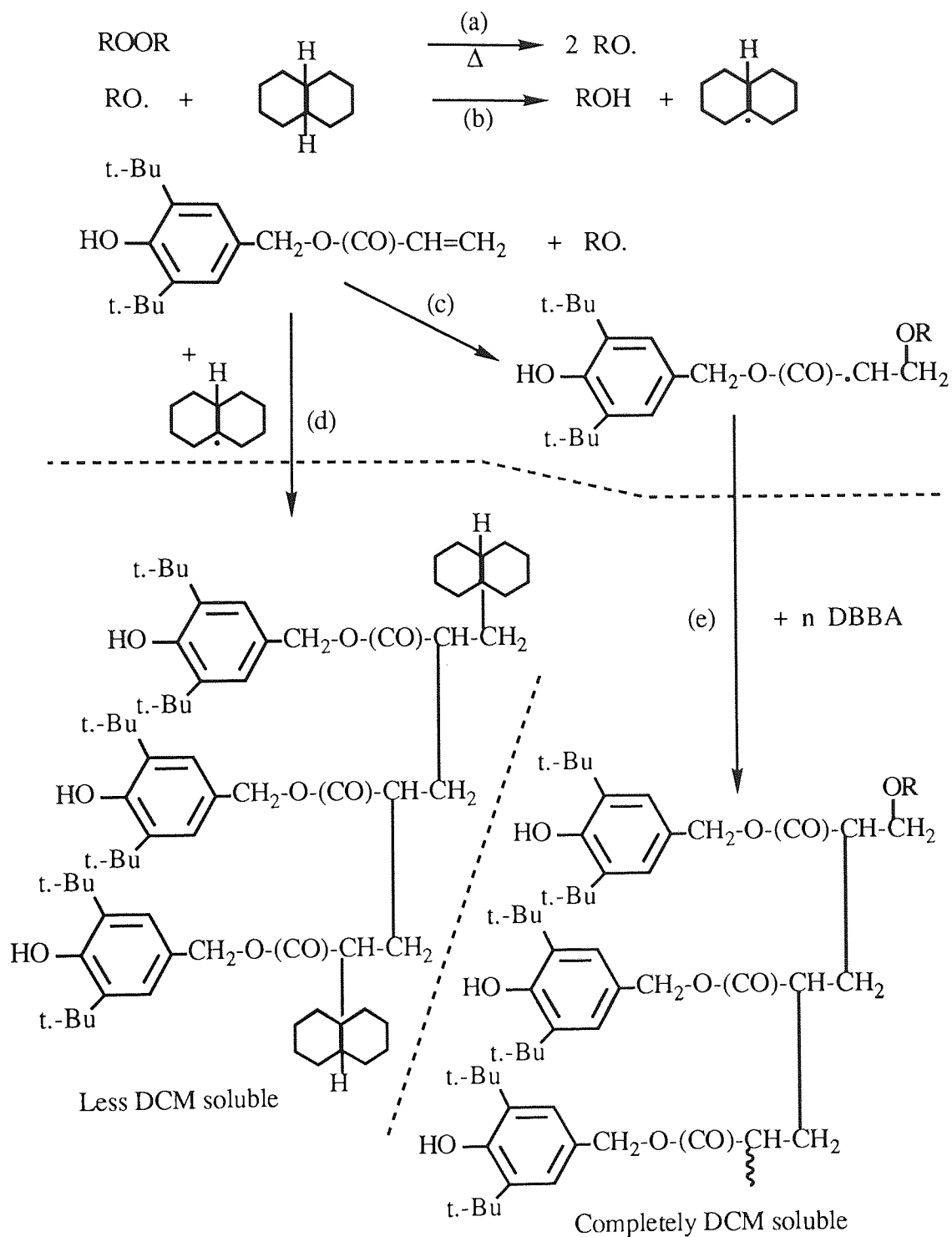
Figure 5.64b. Molecular weight (e.g. Mn x 10⁻⁴) and MFI of 10% MB's containing DBBA without and with coagents (Tris or DVB) processed in the presence of 0.02 m.r. Trigonox 101, under standard condition.



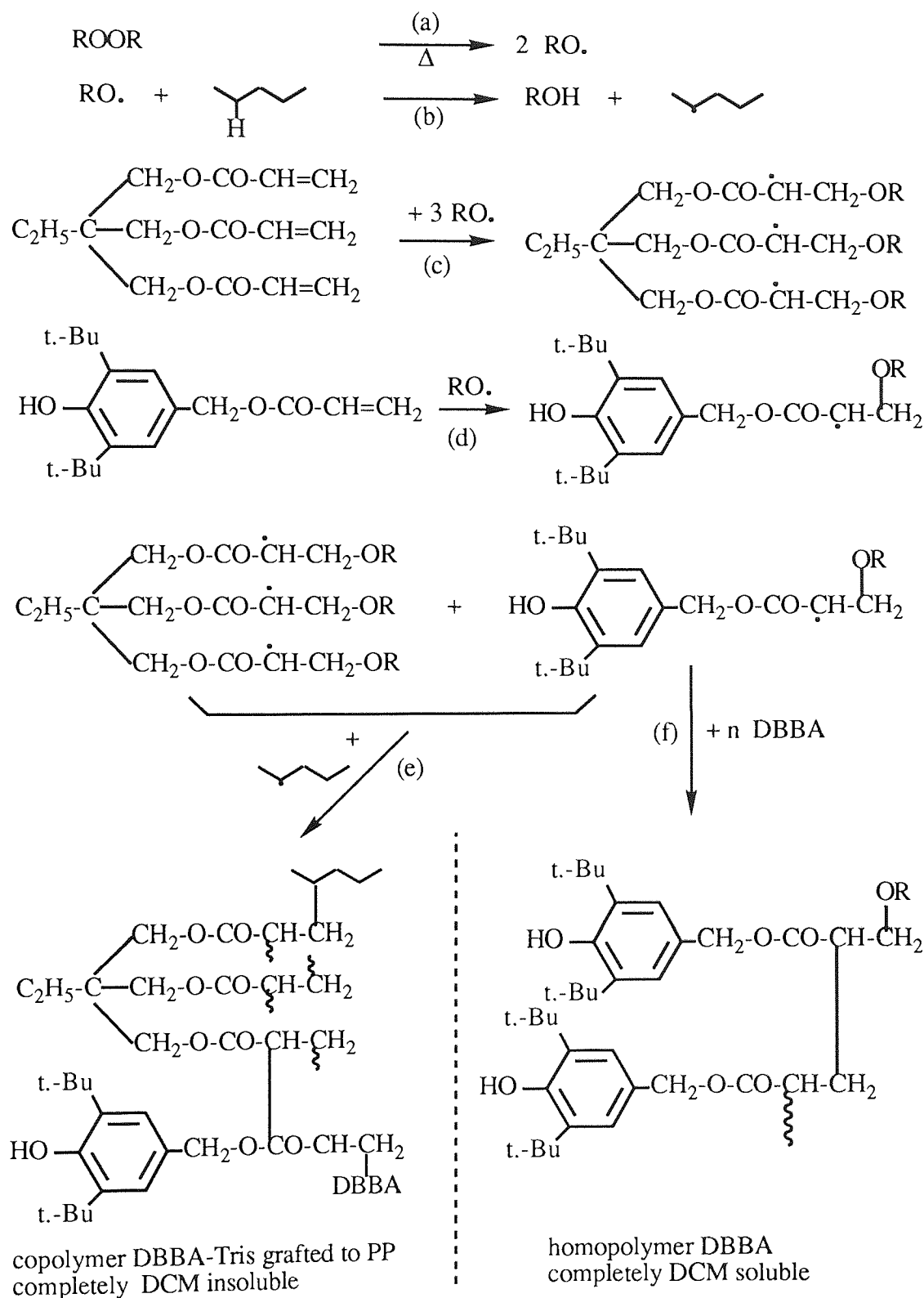
Scheme 5.17 Structure of grafted DBBA with DVB coagent in polymer (10% MB, processed with polypropylene in the presence of 0.02 m.r. Trig.101, under standard condition)



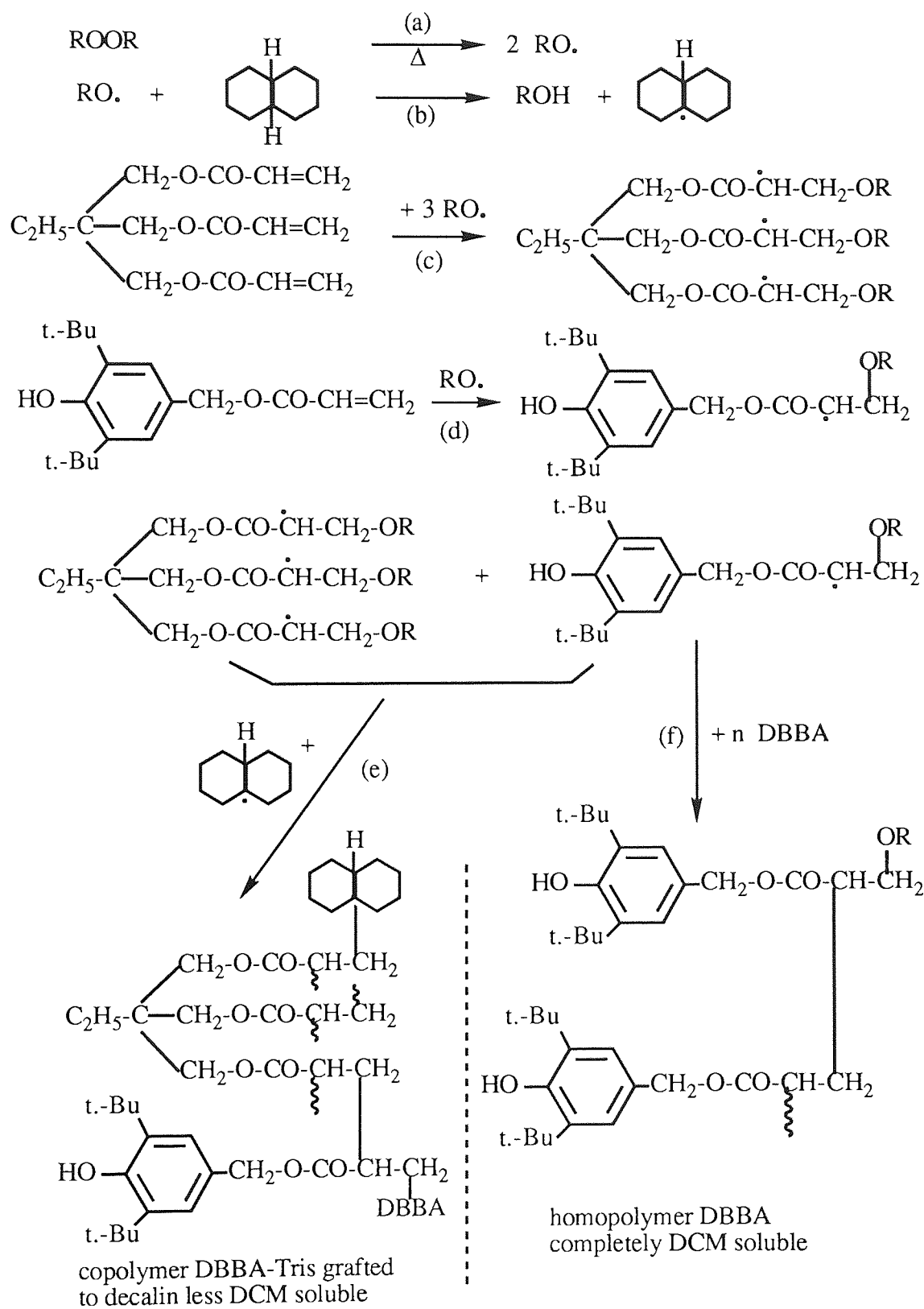
Scheme 5.18 Suggestion mechanism of reactive processing of grafted DBBA in PP in the presence of 0.02 m.r. of Trig.101, processed at 180°C for 10 minutes in closed mixing condition.



Scheme 5.19 Suggestion mechanism of polymerised DBBA with Decalin in the presence of 0.02 m.r.Trig.101 as initiator at 180°C for 5 hours under Argon atmosphere



Scheme 5.20 Suggestion mechanism of reactive processing of grafted DBBA+Tris in PP, in the presence of 0.02 m.r.Trig.101, processed at 180°C for 10 minutes in closed mixing condition.



Scheme 5.21 Suggestion mechanism of polymerised DBBA+Tris with Decalin in the presence of 0.02 m.r.Trig.101 as initiator at 180°C for 5 hours under Argon atmosphere

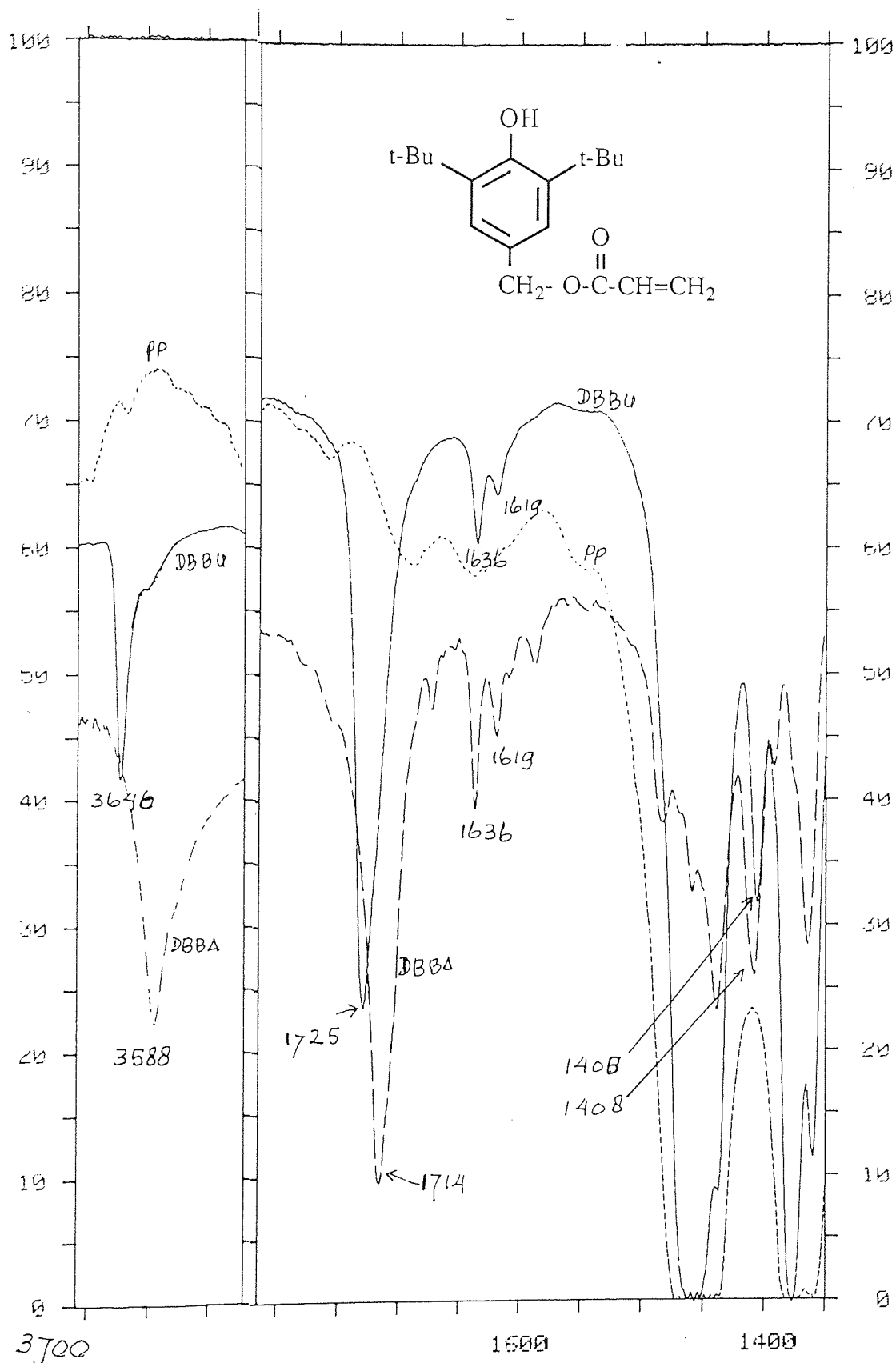


Figure 5.1 Comparison of FTIR spectra of PP film containing 10% DBBA processed without peroxide (—) in regions 3720-3420 cm^{-1} and 1815 - 1350 cm^{-1} (see A in Scheme 5.1), with that of fresh DBBA using KBr disc (-----). PP processed in absence of peroxides under same condition is also shown (.....).

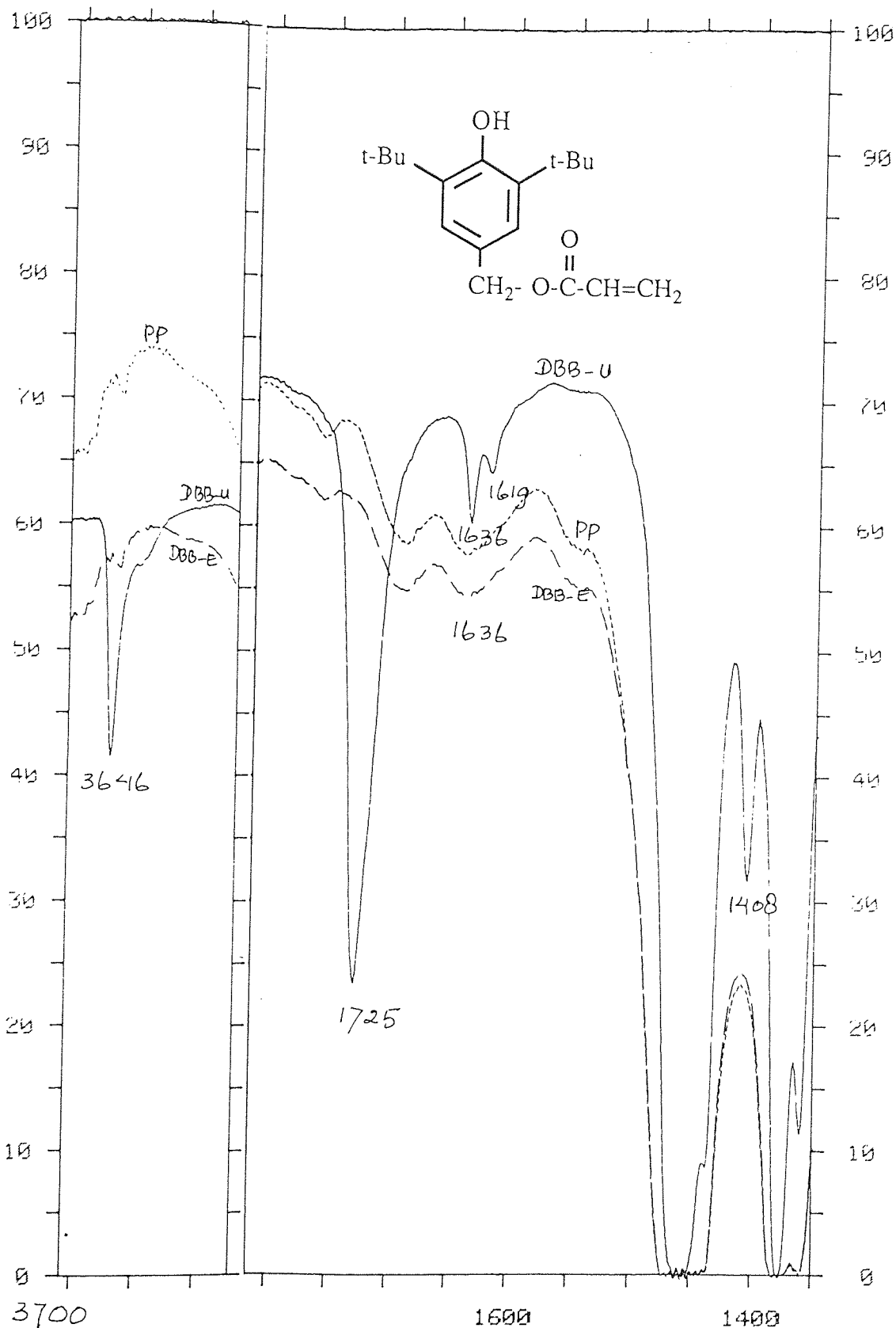


Figure 5.2 Comparison of FTIR spectra of PP film containing 10% DBBA processed without peroxide in regions $3720-3420\text{ cm}^{-1}$ and $1815-1350\text{ cm}^{-1}$ (see A in Scheme 5.1), before DCM extraction (—) and after extraction (-----). PP processed in absence of peroxides under same condition is also shown (.....).

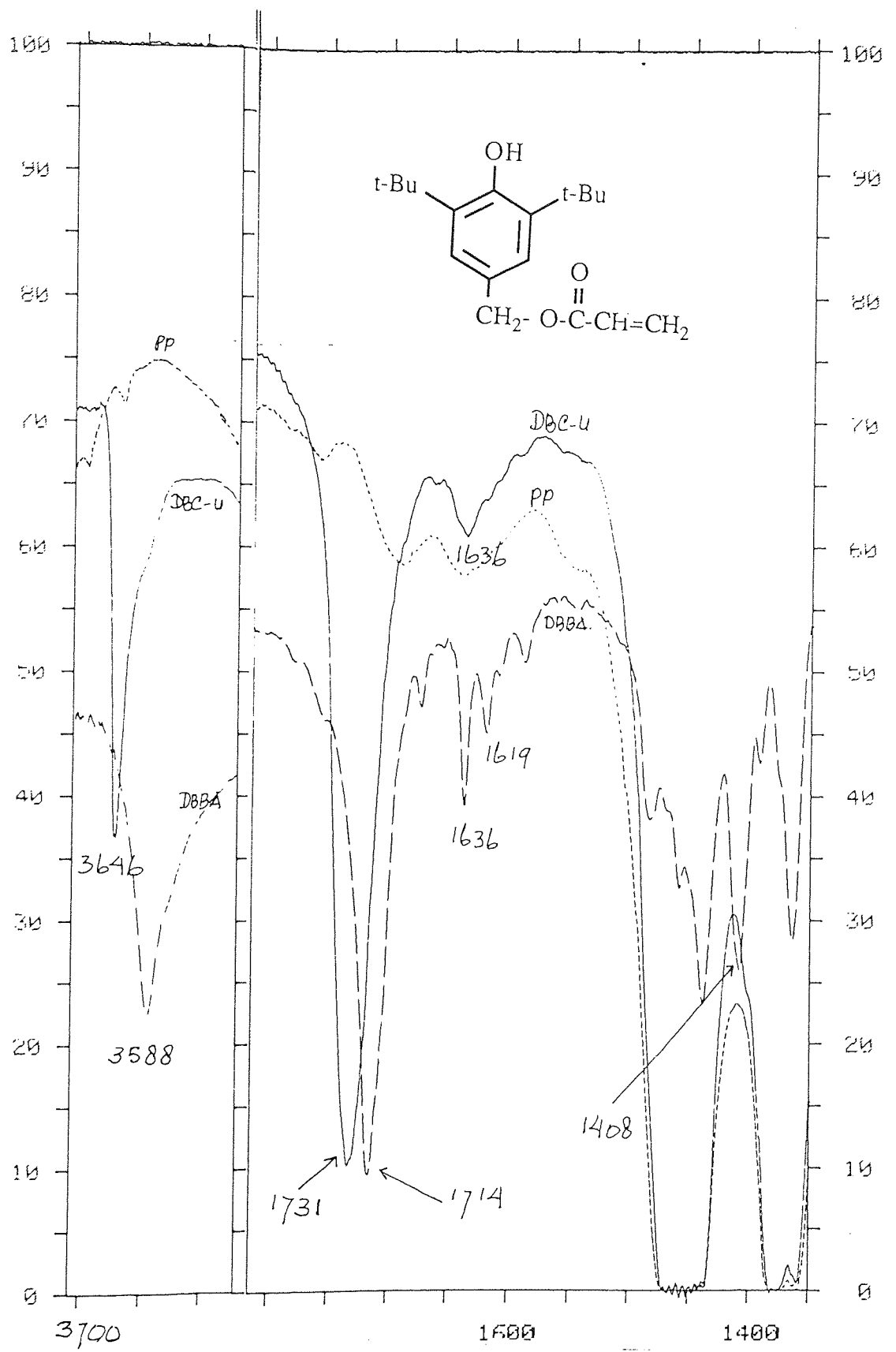


Figure 5.3 Comparison of FTIR spectra of PP film containing 10% DBBA processed with 0.02 m.r Trigonox 101 (____) in the regions 3720 - 3420 cm⁻¹ and 1815 - 1350 cm⁻¹ (see A in Scheme 5.1), with that of fresh DBBA using KBr disc (-----) and PP processed in absence of peroxide under same condition is also shown (.....).

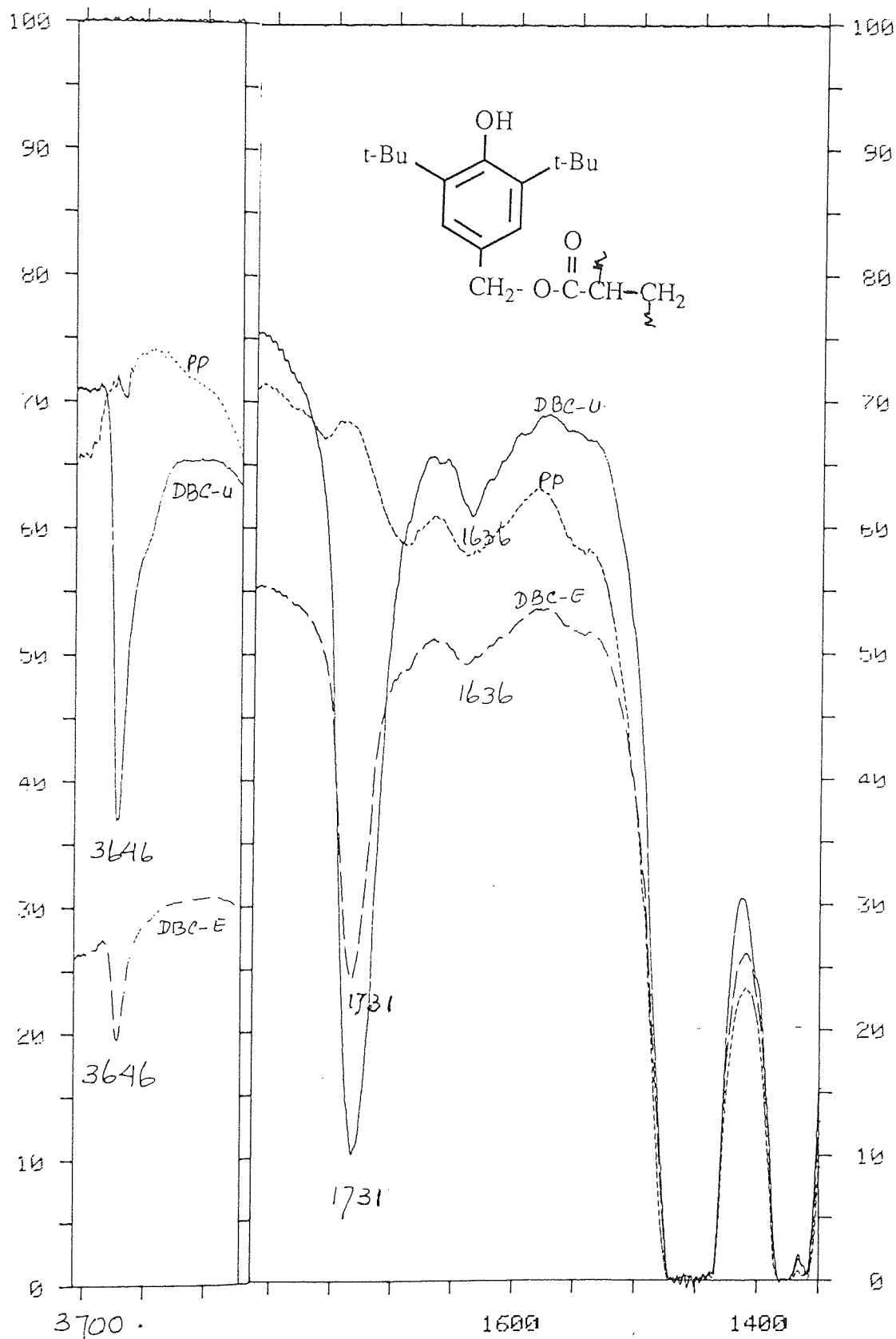


Figure 5.4 Comparison of FTIR spectra of PP film containing 10% DBBA processed with 0.02 m.r. Trigonox 101 in the regions 3720-3420 cm⁻¹ and 1815-1350 cm⁻¹ (see A in Scheme 5.1), before DCM extraction (—) with that after extraction (-----). PP processed in absence of peroxide under same condition is also shown (.....).

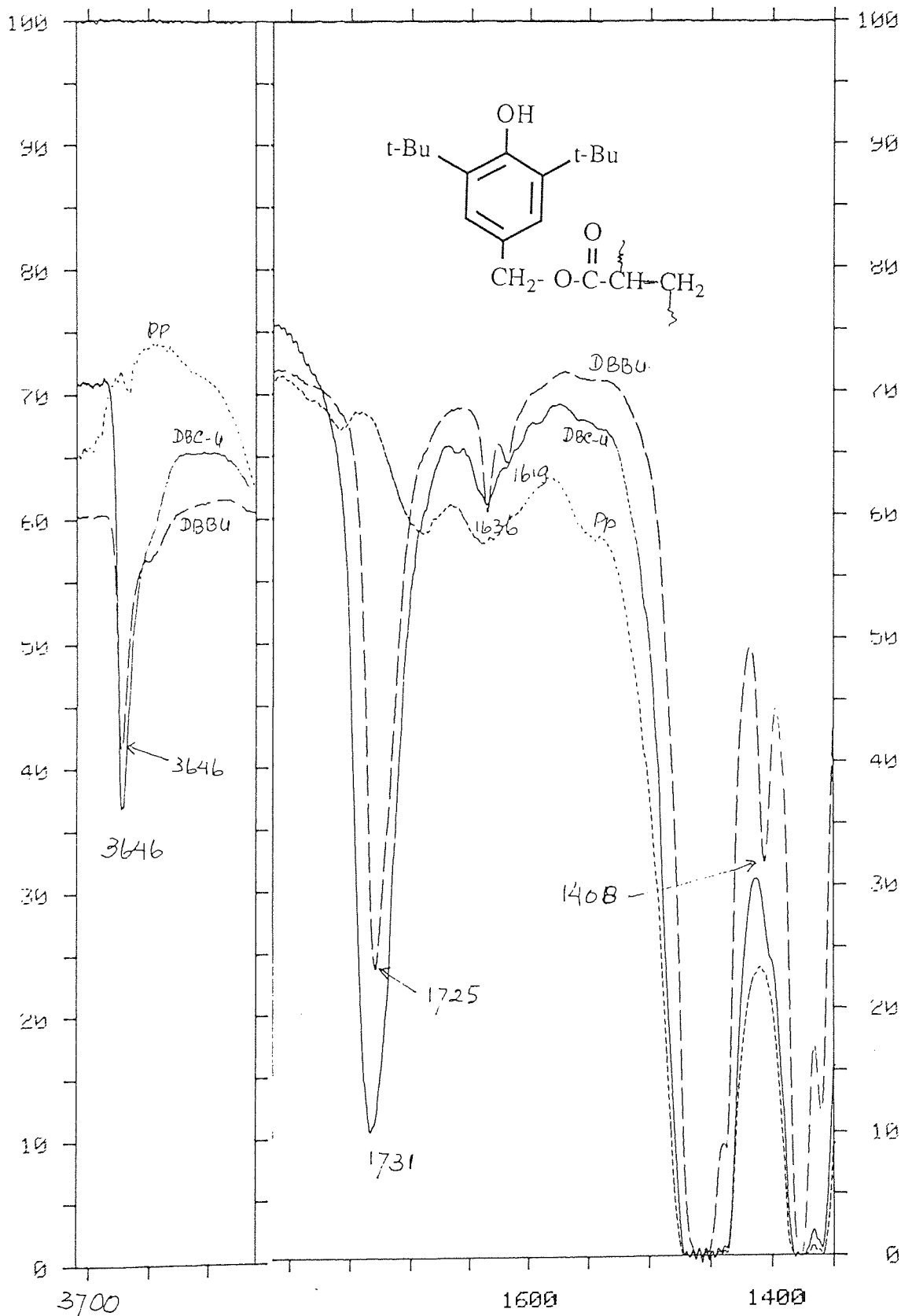


Figure 5.5 Comparison of FTIR spectra of PP film containing 10% DBBA processed with (—) and without (-----) 0.02 m.r. Trigonox 101 in the regions 3720-3420 cm^{-1} and 1815-1350 cm^{-1} under standard condition.

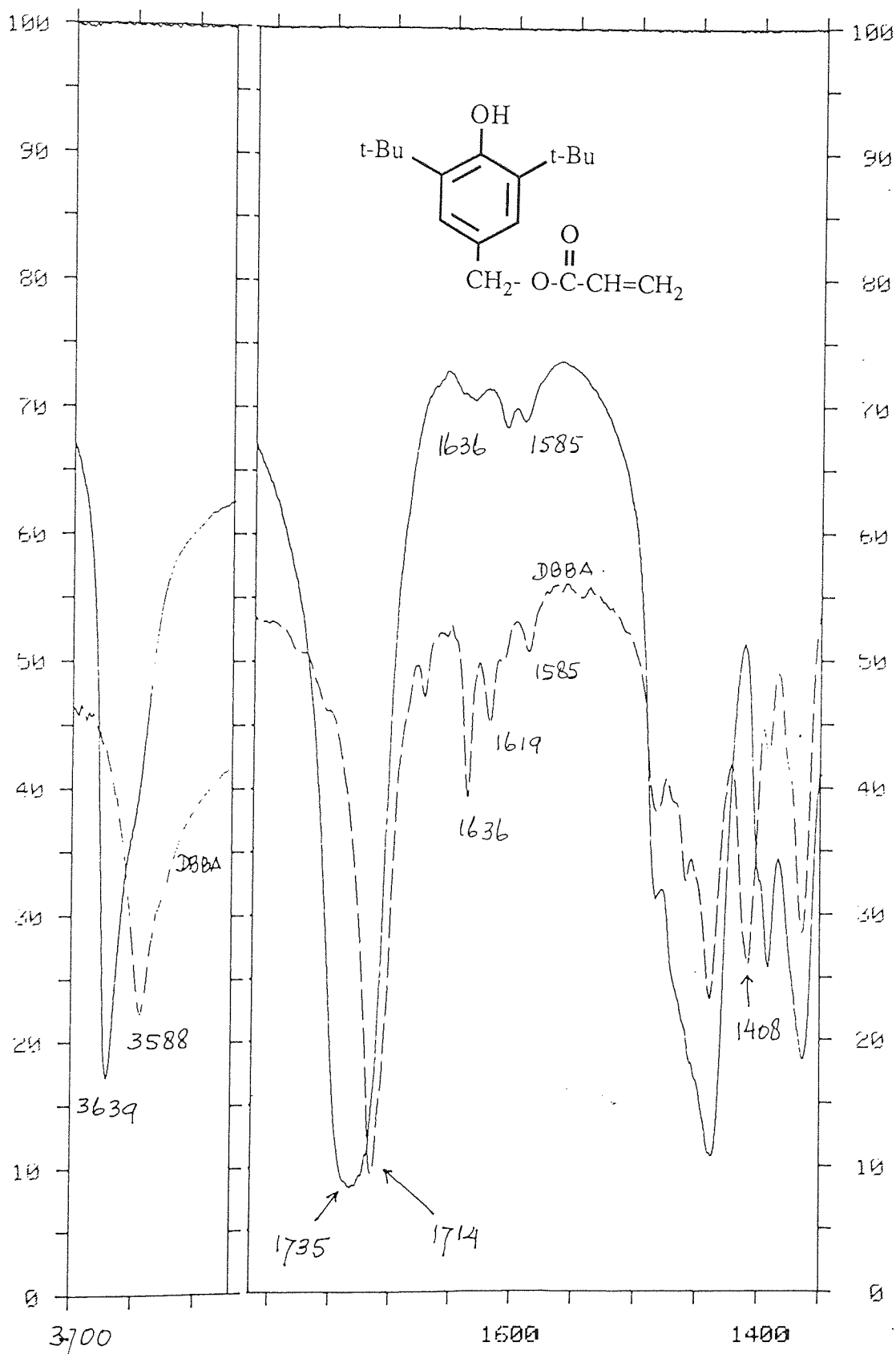


Figure 5.6 Comparison of FTIR spectra of cold DCM-extract of 10% DBBA processed with 0.02 m.r. Trigonox 101 (see stage C in Scheme 5.1) in the regions $3720-3420 \text{ cm}^{-1}$ and $1815-1350 \text{ cm}^{-1}$ (___), with fresh DBBA both in KBr disc (-----).

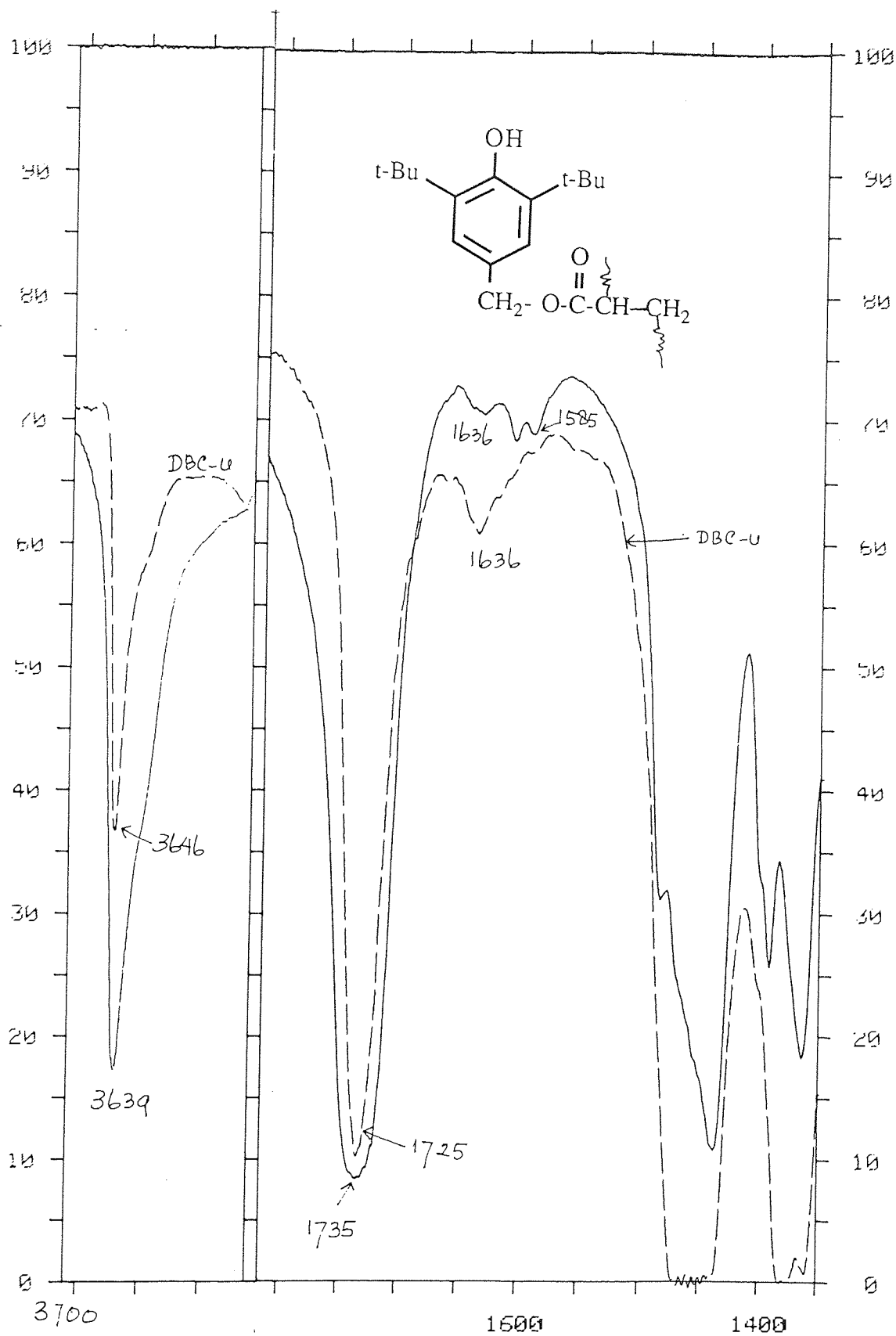


Figure 5.7 Comparison of FTIR spectra of cold DCM-extract in KBr disc (—) of 10% DBBA processed with 0.02 m.r. Trigonox 101, see stage C in Scheme 5.1, in the regions 3720-3420 cm^{-1} and 1815-1350 cm^{-1} with the same MB film, but before extraction (-----).

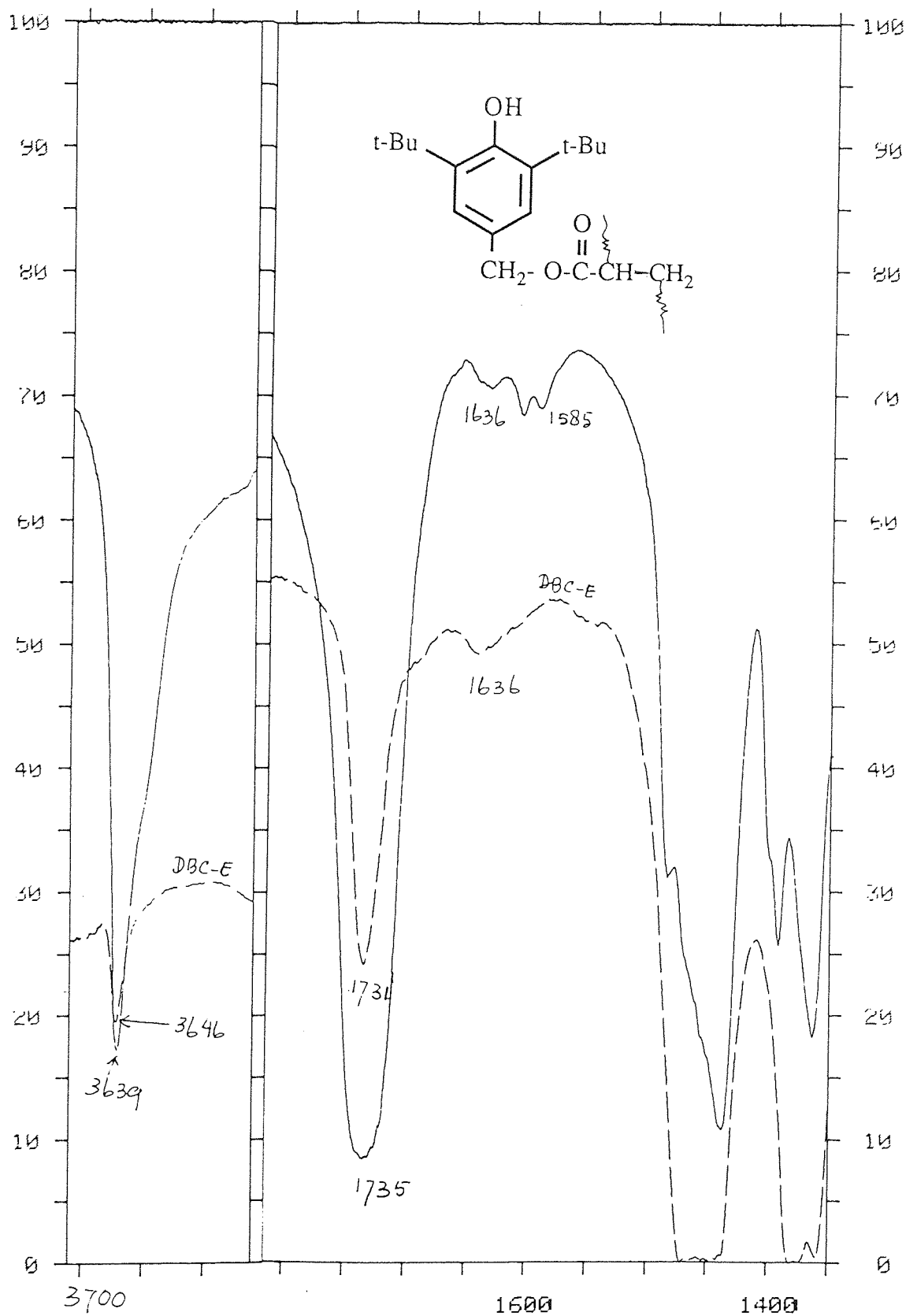


Figure 5.8 Comparison of FTIR spectra of cold DCM-extract in KBr disc (—), of 10% DBBA processed with 0.02 m.r. Trigonox 101, see stage C in Scheme 5.1, in the regions 3720 -3420 cm^{-1} and 1815 -1350 cm^{-1} with that of the same MB film, but after extraction (-----).

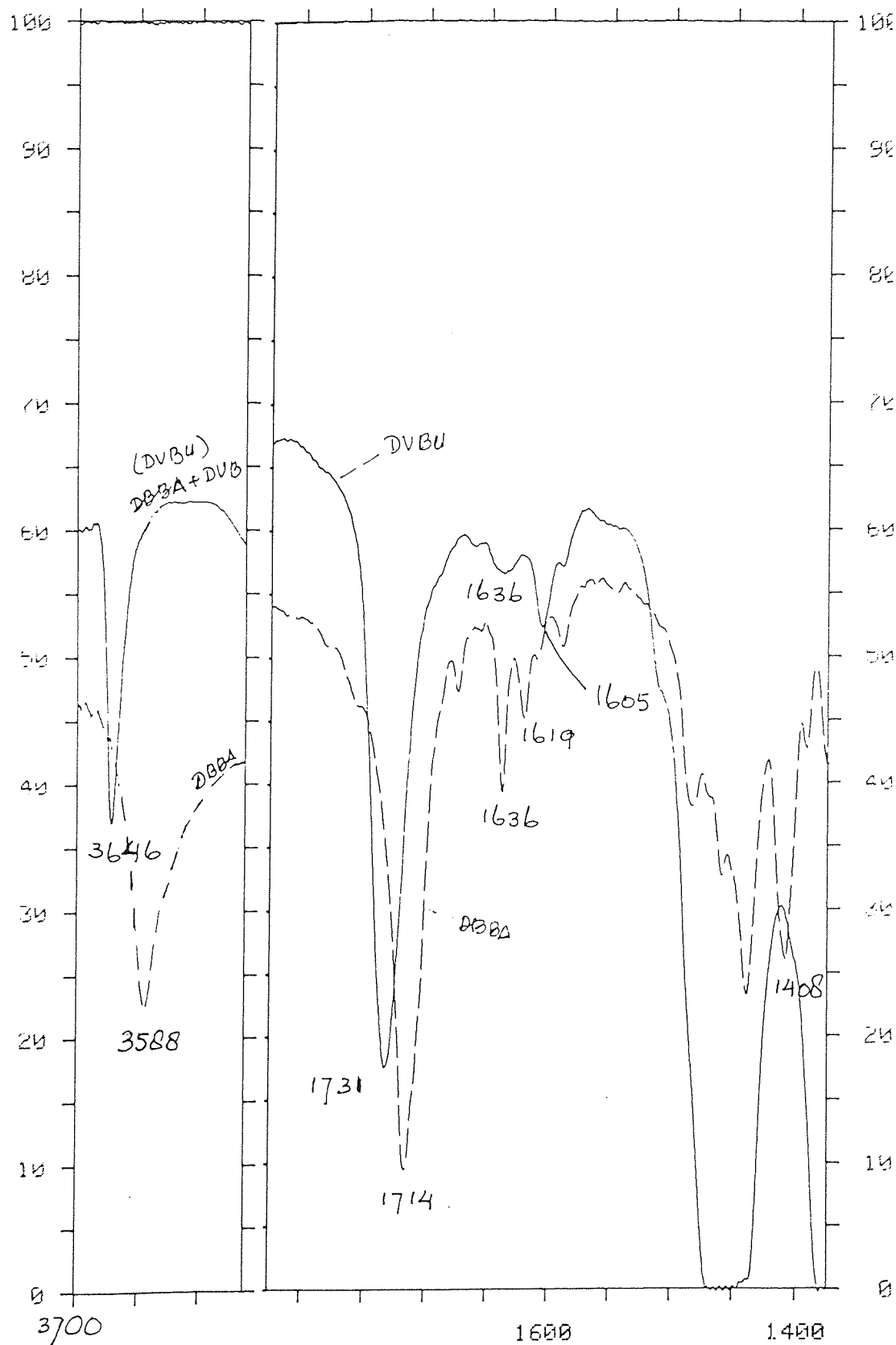


Figure 5.8a Comparison of FTIR spectra of 10% MB film containing (DBBA+DVB) processed with 0.02 m.r. Trigonox 101, see stage C in Scheme 5.1 before extraction (—), in the regions 3720-3420 cm^{-1} and 1815-1350 cm^{-1} with that of fresh DBBA in KBr disc (-----).

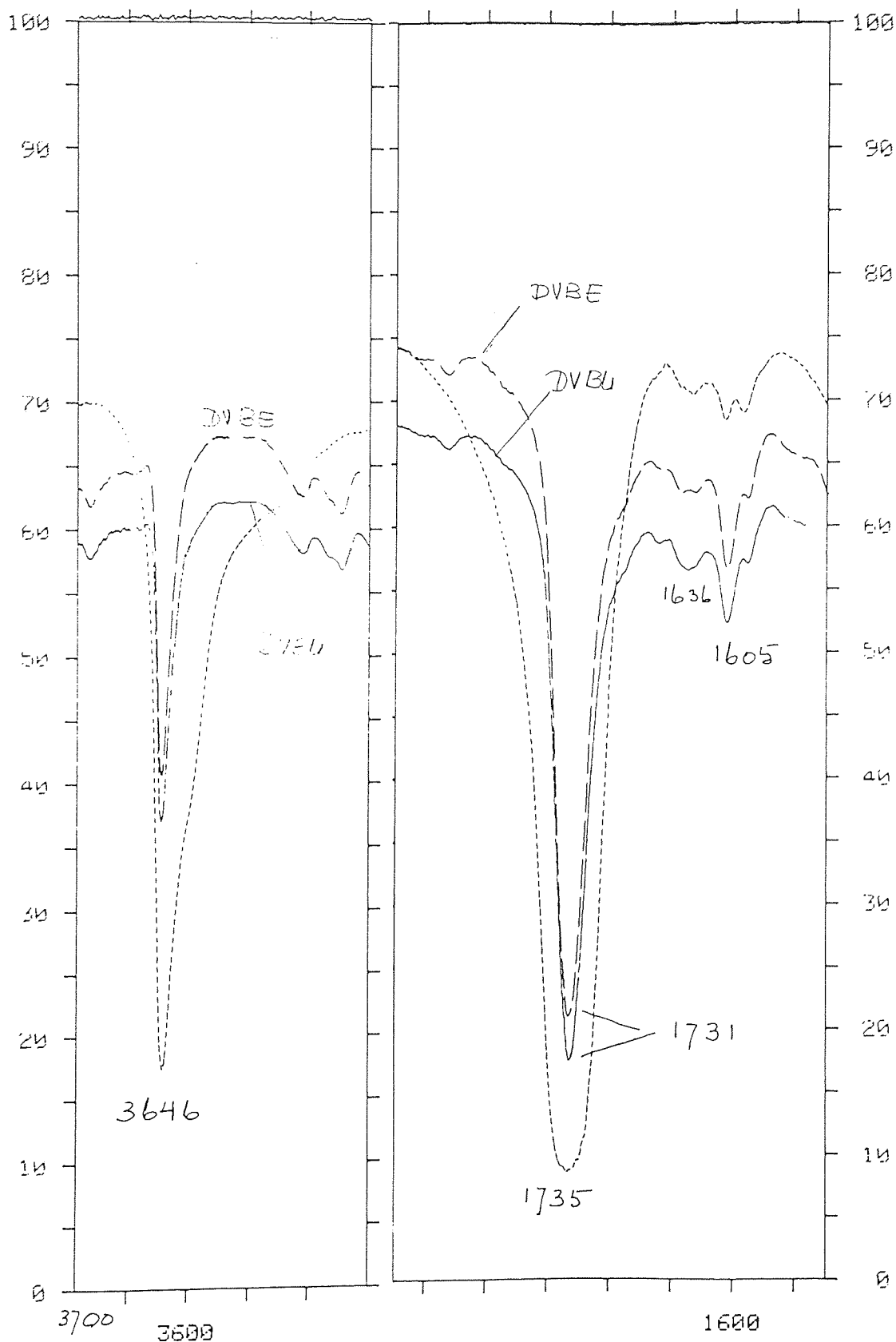


Figure 5.8b Comparison of FTIR spectra of 10% MB film containing (DBBA+DVB) processed with 0.02 m.r. Trigonox 101, see stage C in Scheme 5.1 before extraction (—), in the regions 3720 -3420 cm^{-1} and 1815 -1350 cm^{-1} with that the same MB film but after extraction (-----) and DCM extract from the same MB in KBr disc (.....).

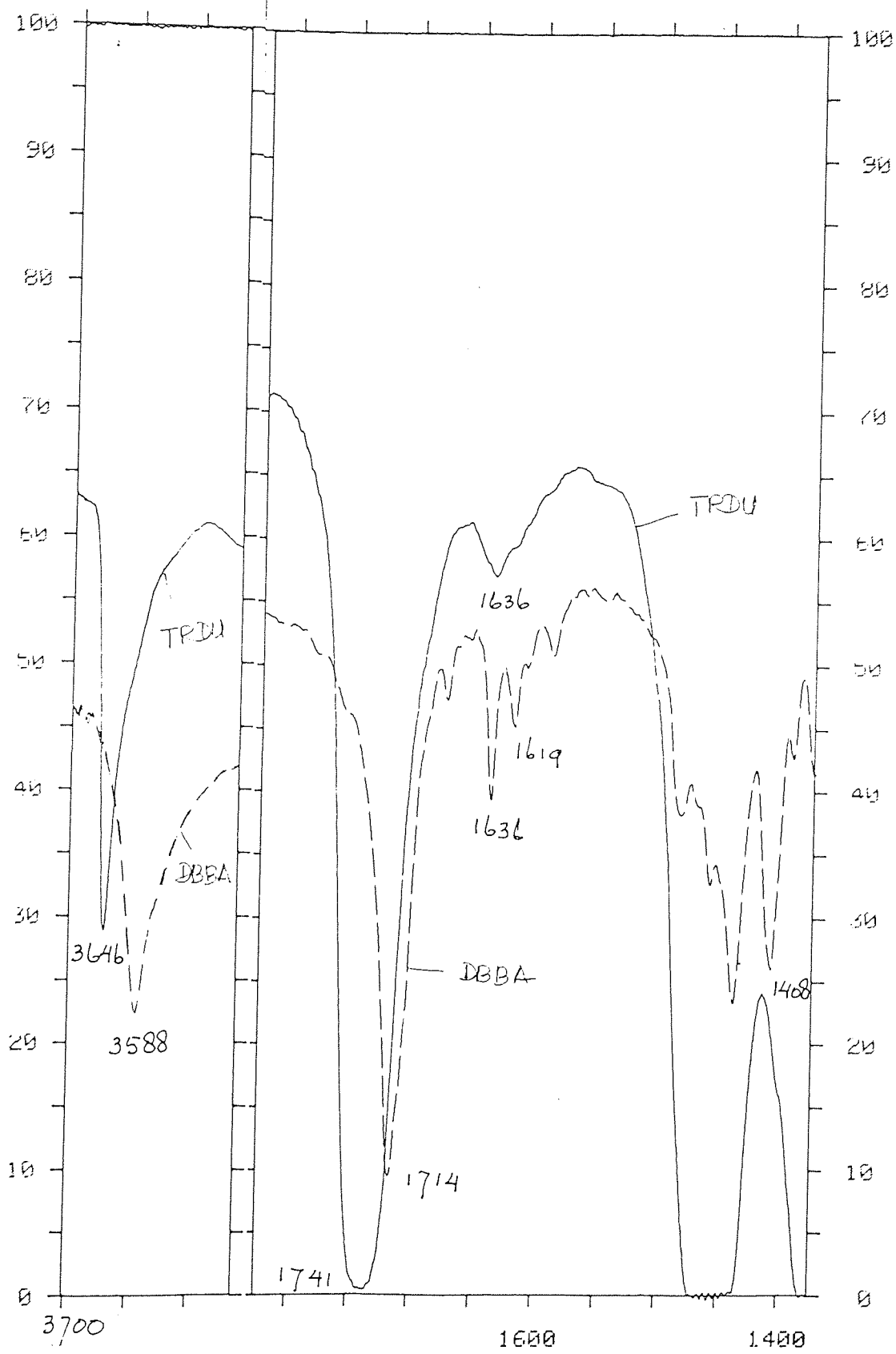


Figure 5.8c Comparison of FTIR spectra of 10% MB film containing (DBBA+Tris) processed with 0.02 m.r. Trigonox 101, see stage C in Scheme 5.1 before extraction (—), in the regions 3720 -3420 cm^{-1} and 1815 -1350 cm^{-1} with that of fresh DBBA in KBr (-----).

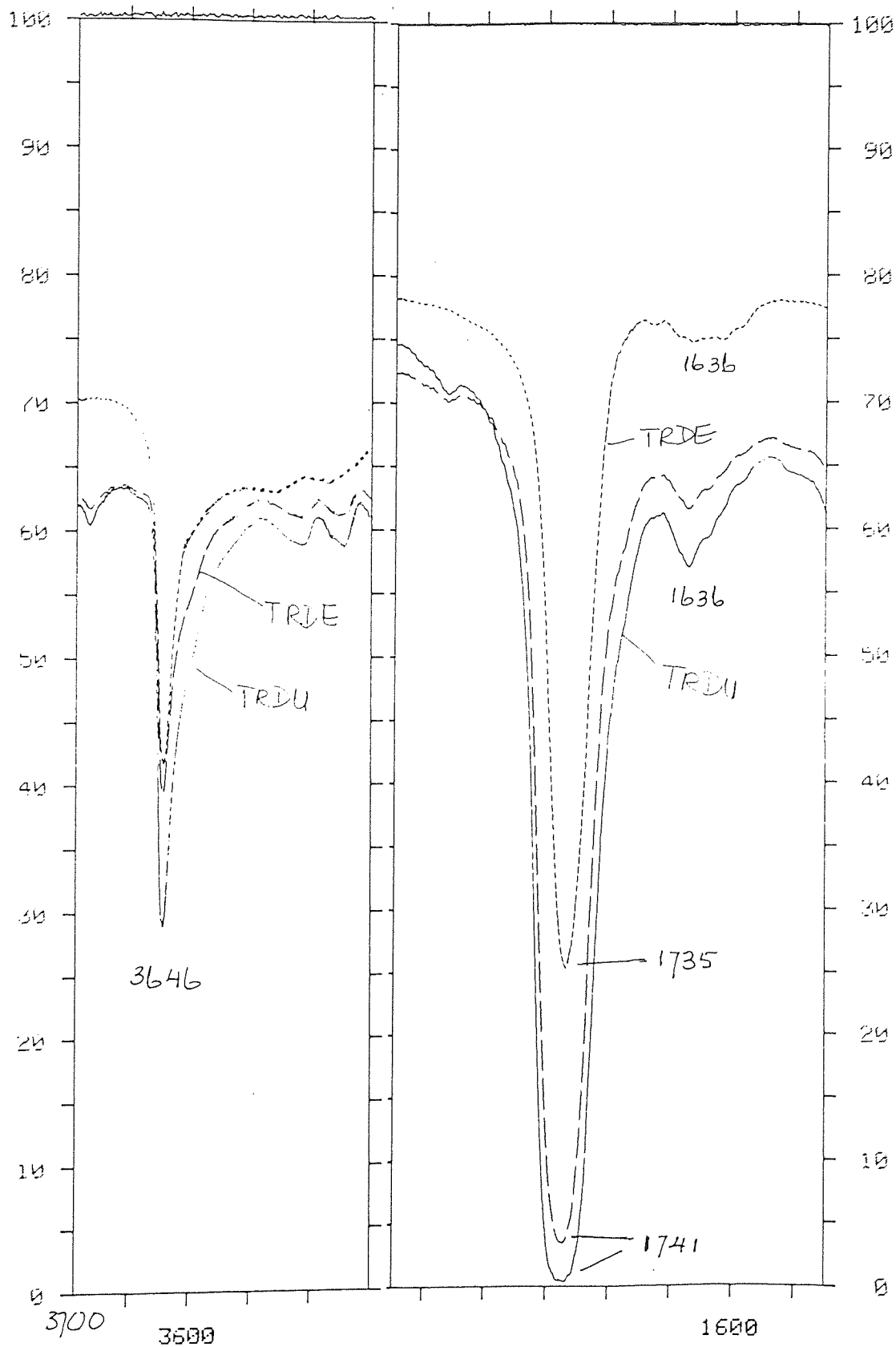


Figure 5.8d Comparison of FTIR spectra of 10% MB film containing (DBBA+Tris) processed with 0.02 m.r. Trigonox 101, see stage C in Scheme 5.1 before extraction (—), in the regions 3720 -3420 cm^{-1} and 1815 -1350 cm^{-1} with that the same MB film but after extraction (---) and DCM extract from the same MB in KBr disc (.....) .

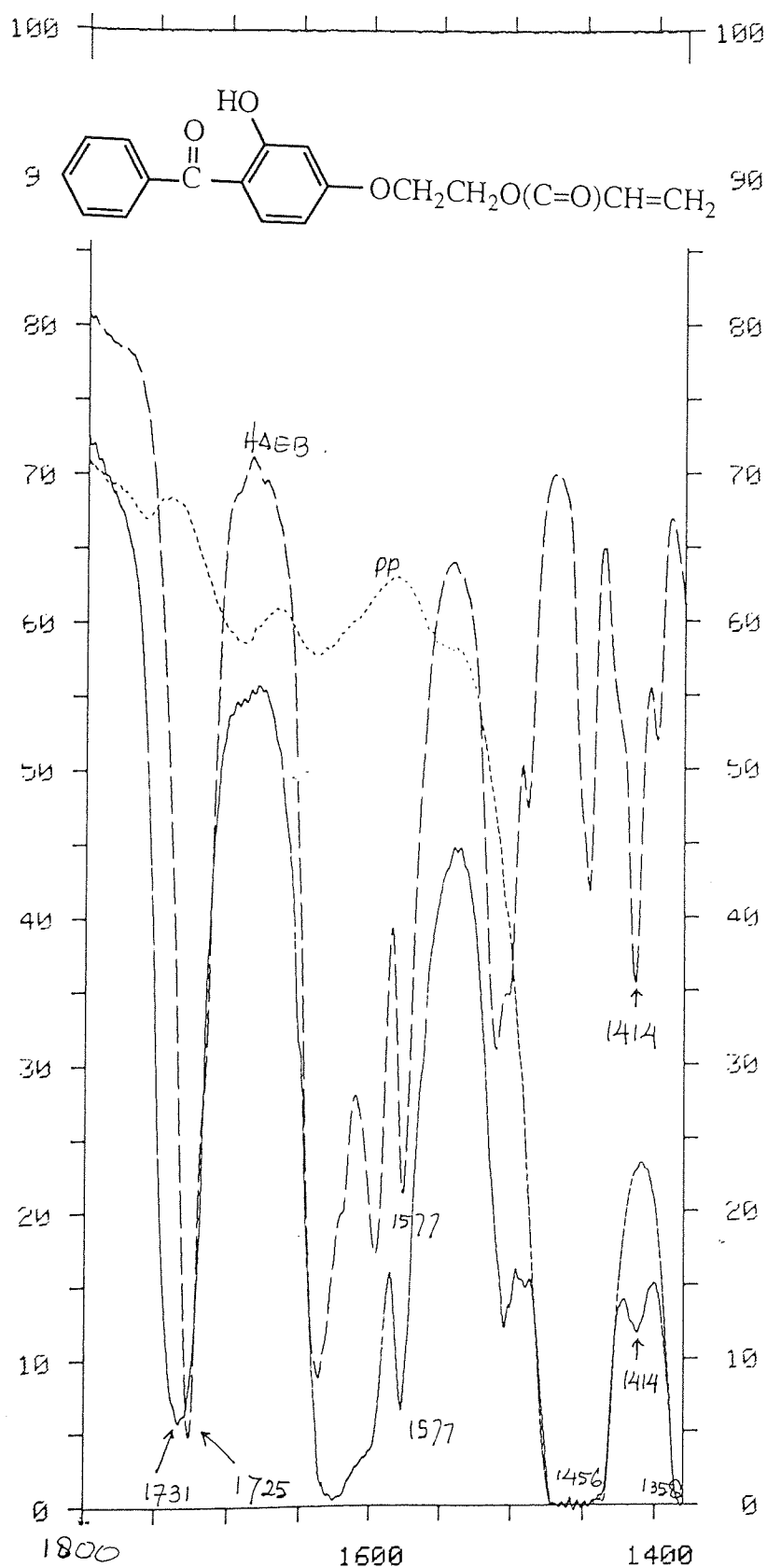


Figure 5.9 Comparison of FTIR spectra of PP film containing 10% HAEB processed without peroxide (—) in regions 1800-1380 cm^{-1} (see stage A in Scheme 5.1), with that of fresh HAEB using KBr disc (-----). PP processed in absence of peroxides under same condition is also shown (.....).

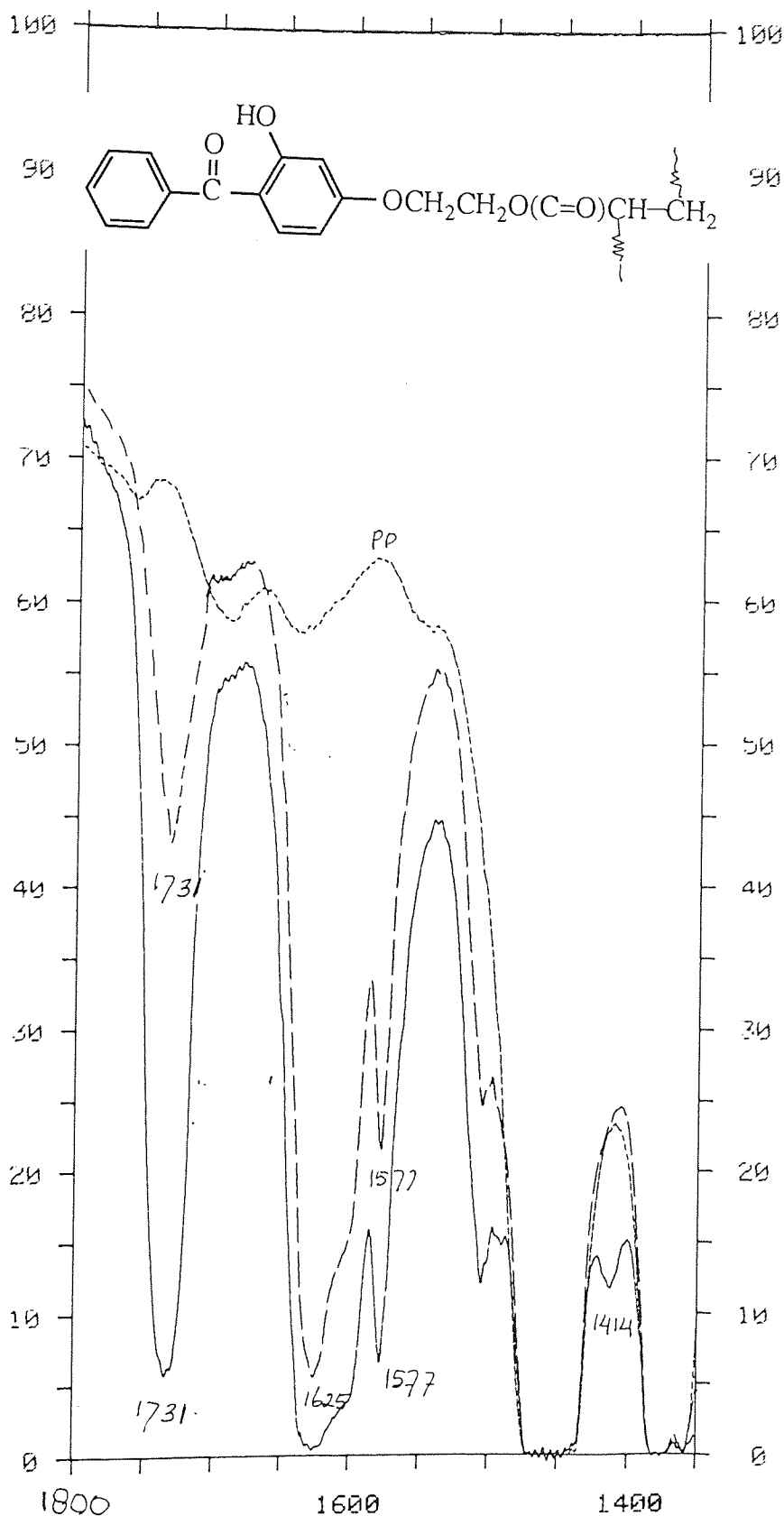


Figure 5.10 Comparison of FTIR spectra of PP film containing 10% HAEB processed without peroxide in regions 1800-1380 cm⁻¹ (see A in Scheme 5.1), before DCM extraction (—) with that after extraction (-----). PP processed in absence of peroxides under same condition is also shown (.....).

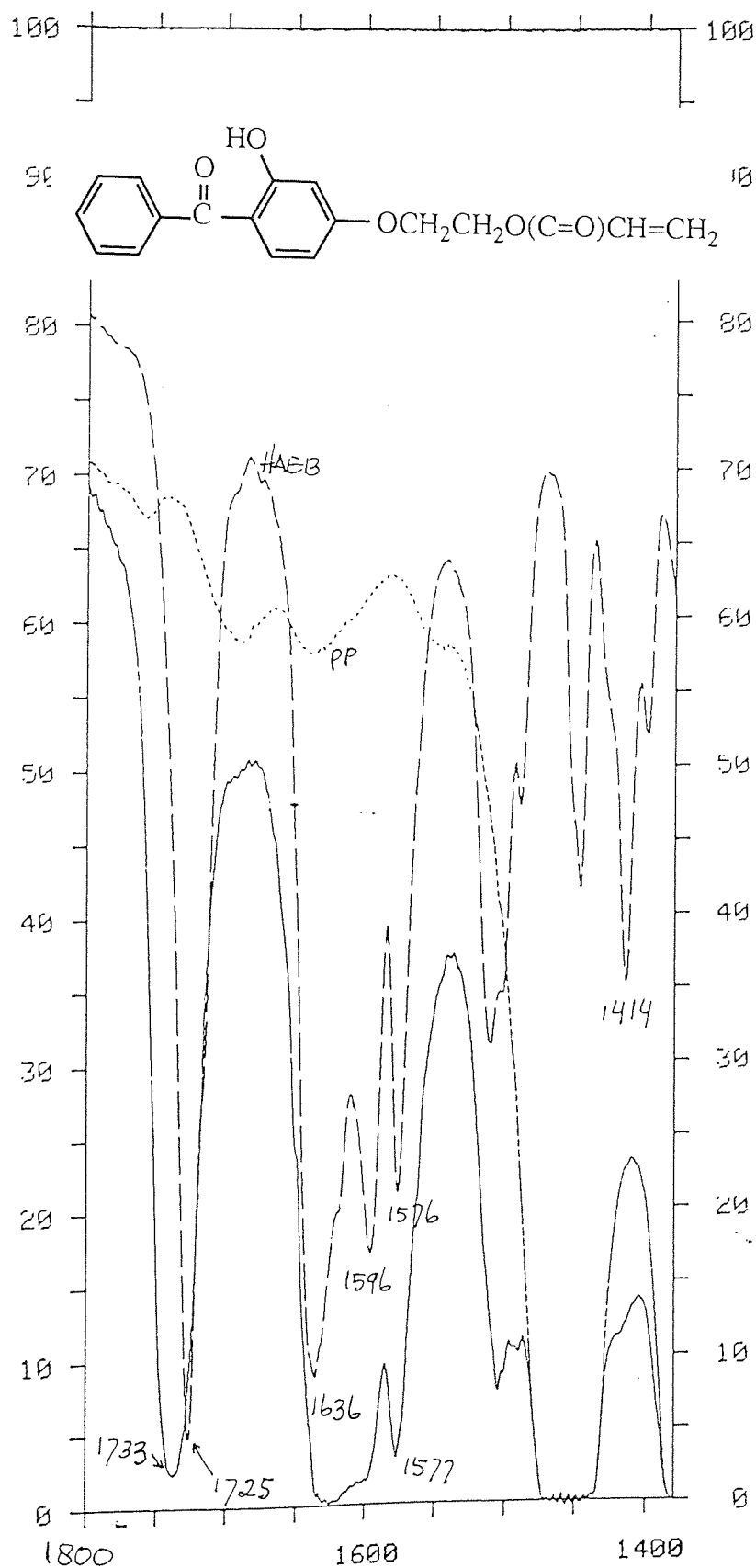


Figure 5.11 Comparison of FTIR spectra of PP MB film containing 10% HAEB processed with 0.005 m.r Trigonox 101 (—), in the regions 1800-1380 cm^{-1} (see A in Scheme 5.1), with that of fresh HAEB using KBr disc (-----). PP processed in absence of peroxide under same condition is also shown (.....).

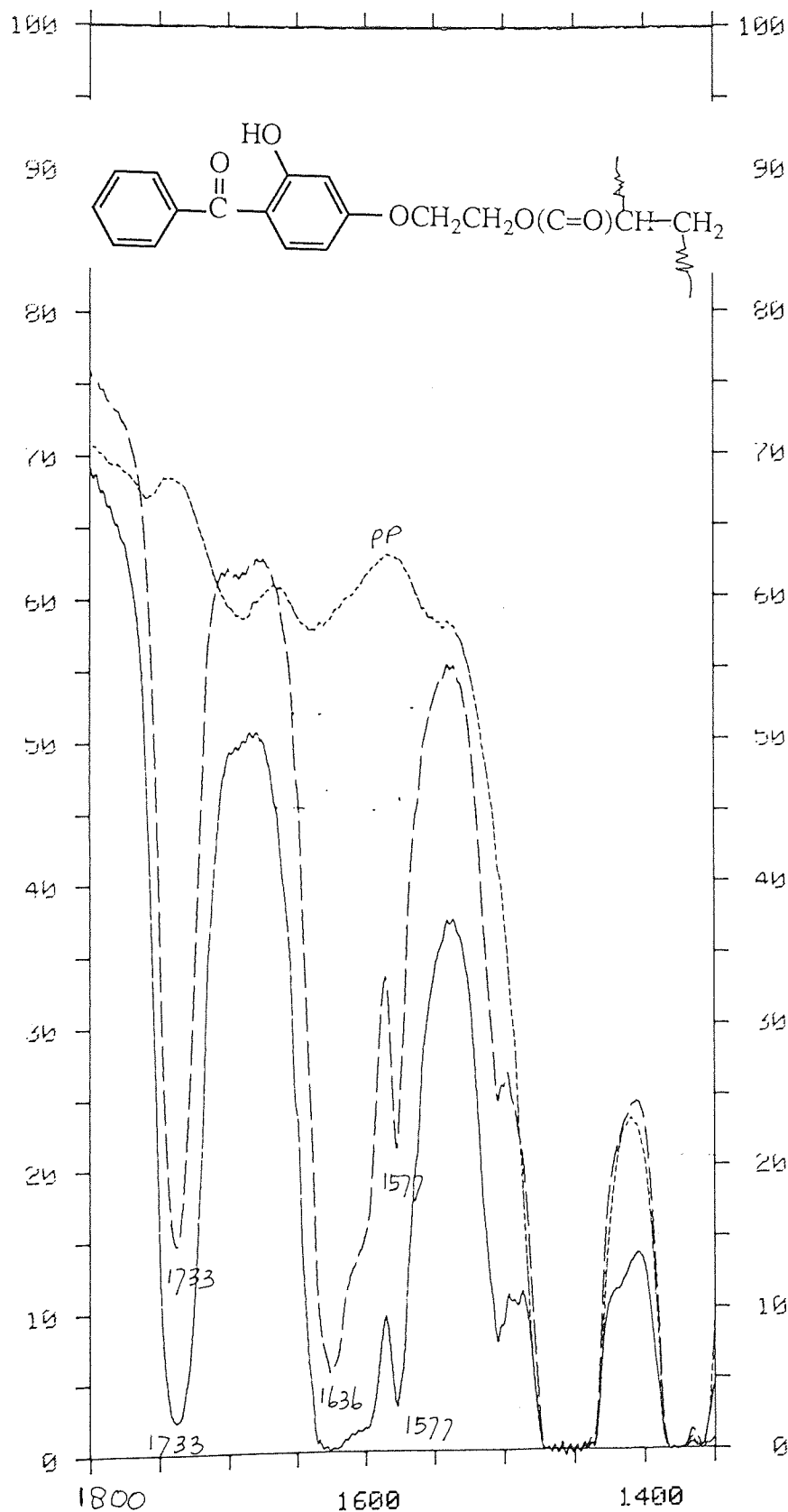


Figure 5.12 Comparison of FTIR spectra of PP film containing 10% HAEB processed with 0.005 m.r. Trigonox 101 in the regions 1800-1380 cm⁻¹ (see A in Scheme 5.1), before DCM extraction (—) with that after extraction (-----). PP processed in absence of peroxide under same condition is also shown (.....).

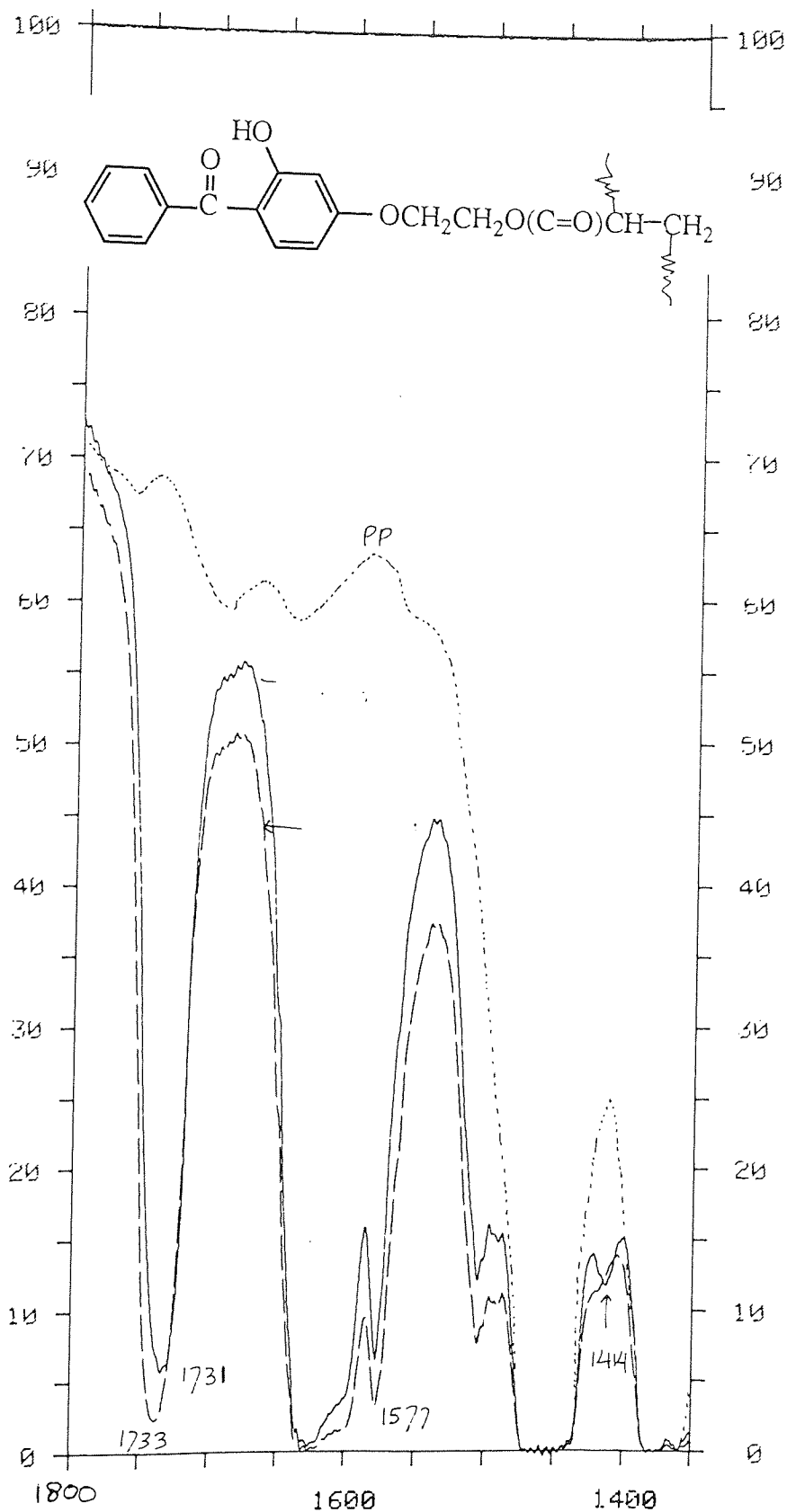


Figure 5.13 Comparison of FTIR spectra of PP film containing 10% HAEB processed with (—) and without (-----) 0.005 m.r. Trigonox 101 in the regions 1800-1380 cm⁻¹ (see stage A in Scheme 5.1), PP processed in absence of peroxide under same condition is also shown (.....).

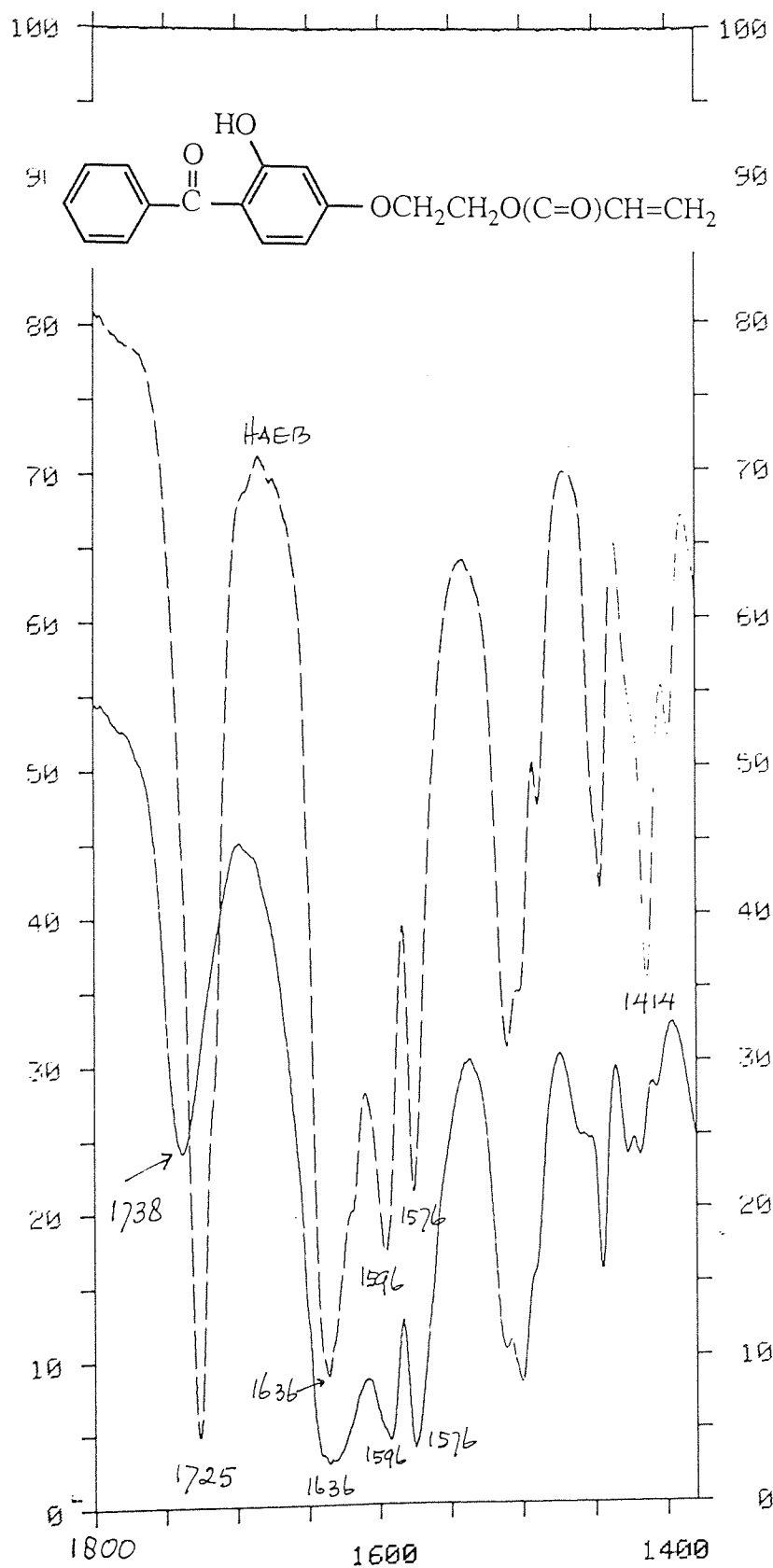


Figure 5.14 Comparison of FTIR spectra of cold DCM-extract of 10% HAEB processed with 0.005 m.r Trigonox 101 (see stage C in Scheme 5.1) in the regions 1800-1380 cm^{-1} (—), with that of fresh HAEB using KBr disc (-----).

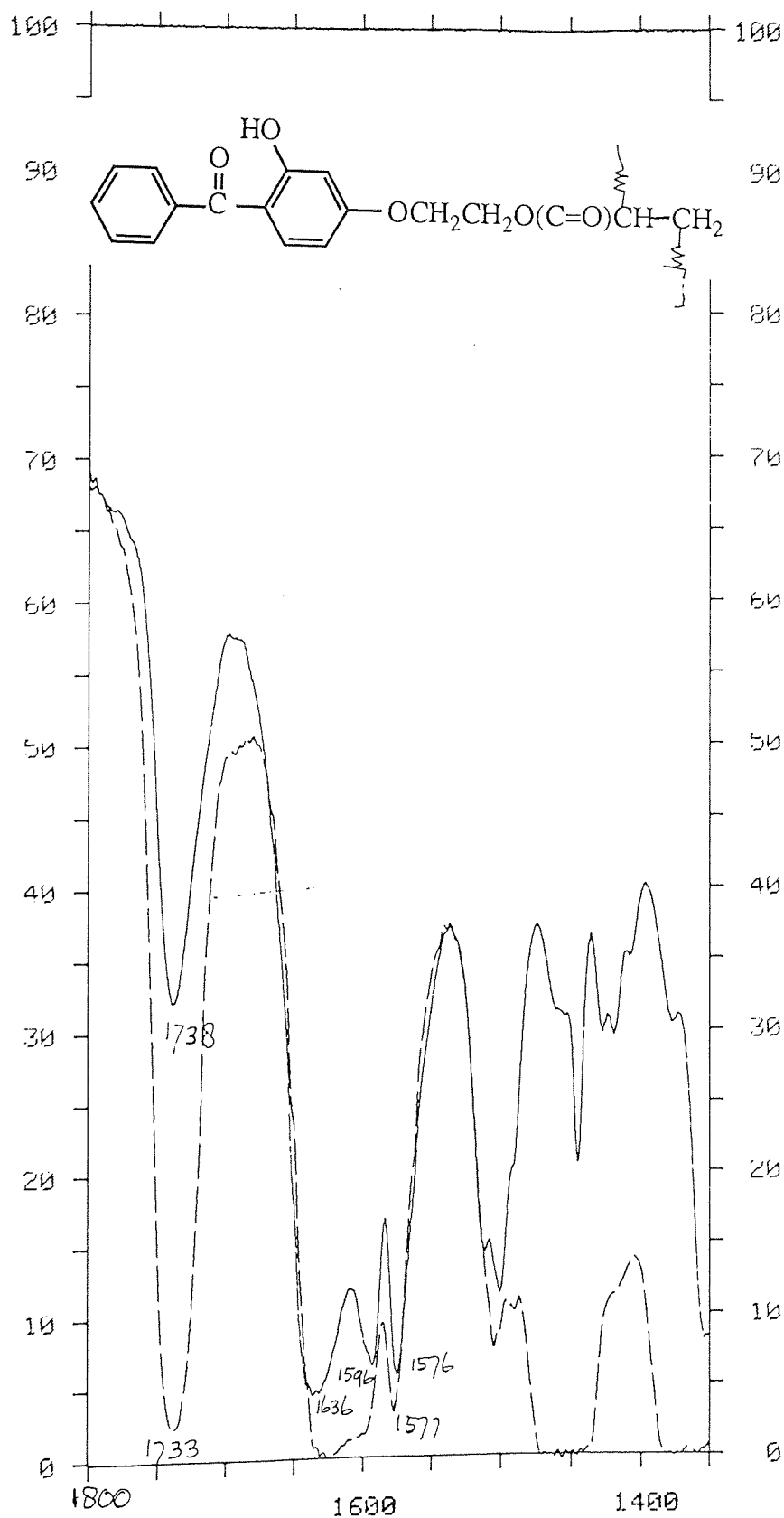


Figure 5.15 Comparison of FTIR spectra of cold DCM-extract in KBr disc (—), of 10% HAEB processed with 0.02 m.r Trigonox 101 (see stage C in Scheme 5.1), in the regions $3720-3420\text{ cm}^{-1}$ and $1815-1350\text{ cm}^{-1}$ with the same MB's film but after DCM extraction (-----).

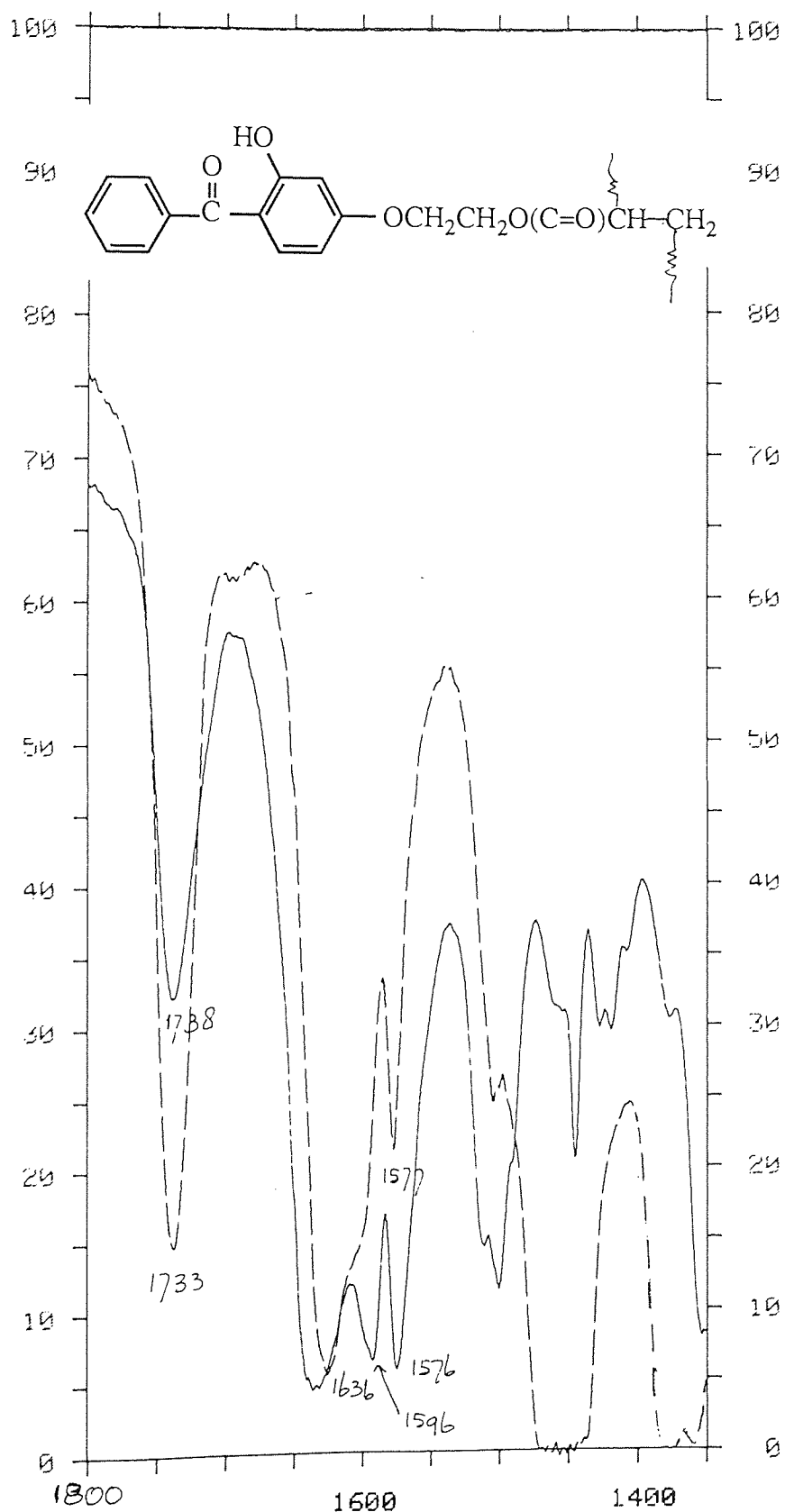


Figure 5.16 Comparison of FTIR spectra of cold DCM-extract (—), of 10% HAEB processed with 0.02 m.r Trigonox 101, (see stage C in Scheme 5.1), in the regions 3720 -3420 cm^{-1} and 1815 -1350 cm^{-1} with the same MB's film but after DCM extraction (-----).

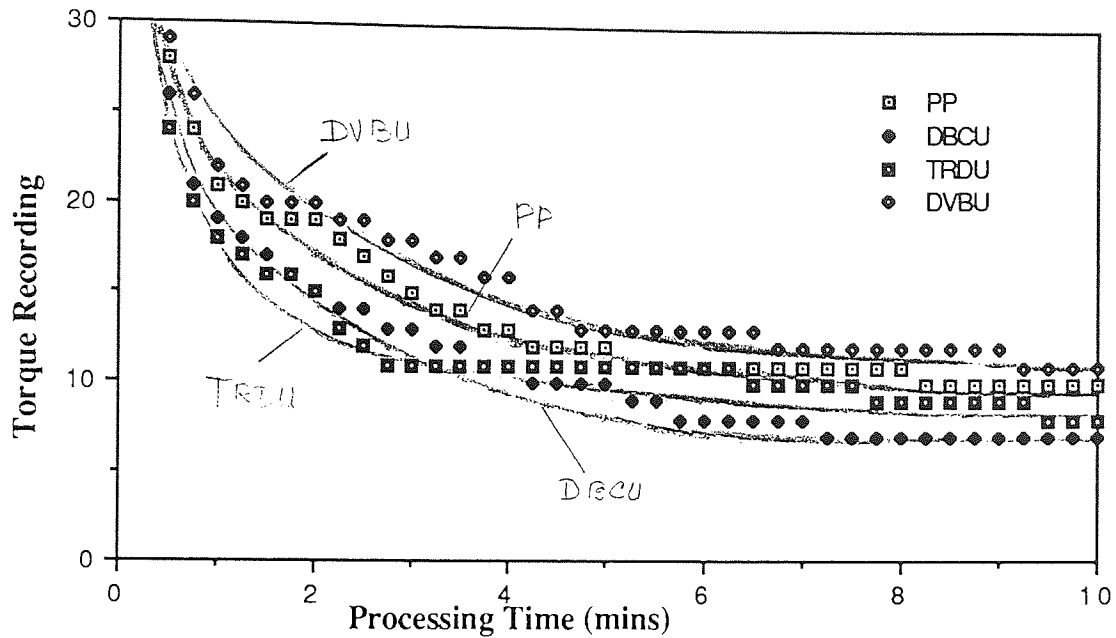


Figure 5.17 Torque recording of various masterbatches,
 PP = PP processed alone
 DBCU = PP +10% DBBA + 0.02 mr Trig.101,
 TRDU = PP + 6% DBBA + 4%Tris + 0.02m.r.Trig.101, and
 DVBU = PP + 6% DBBA + 4%DVB + 0.02 m.r. Trig.101.

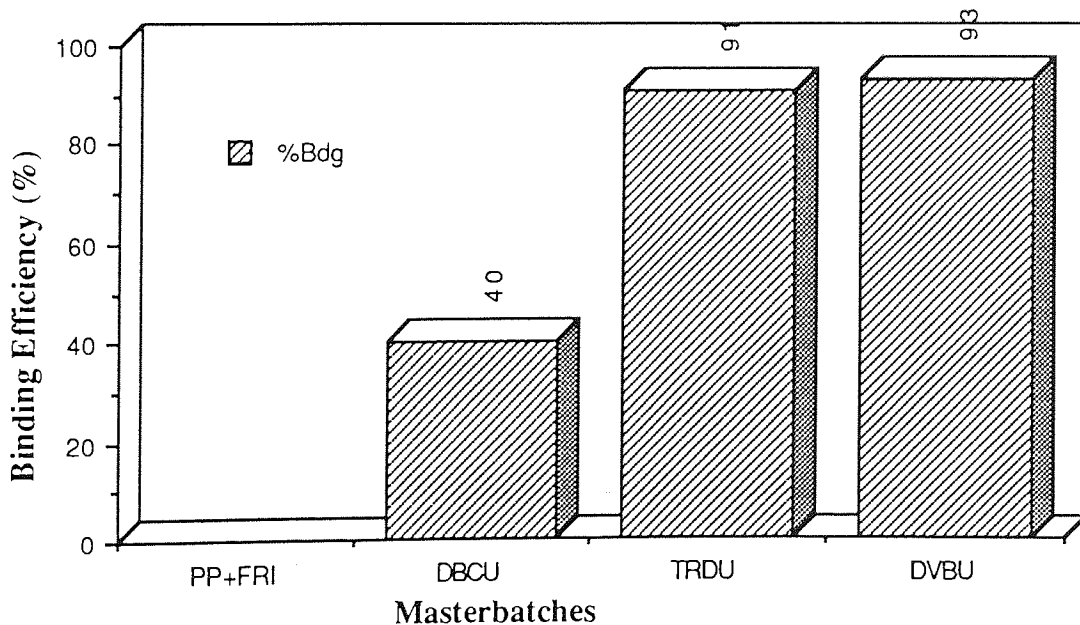


Figure 5.18 Binding Efficiency of various masterbatches, refer to Table 5.1 i.e.
 PP+FRI = PP + 0.02 m.r Trig.101,
 DBCU = PP +10% DBBA + 0.02 mr Trig.101,
 TRDU = PP + 6% DBBA + 4%Tris + 0.02m.r.Trig.101, and
 DVBU = PP + 6% DBBA + 4%DVB + 0.02 m.r.Trig.101.

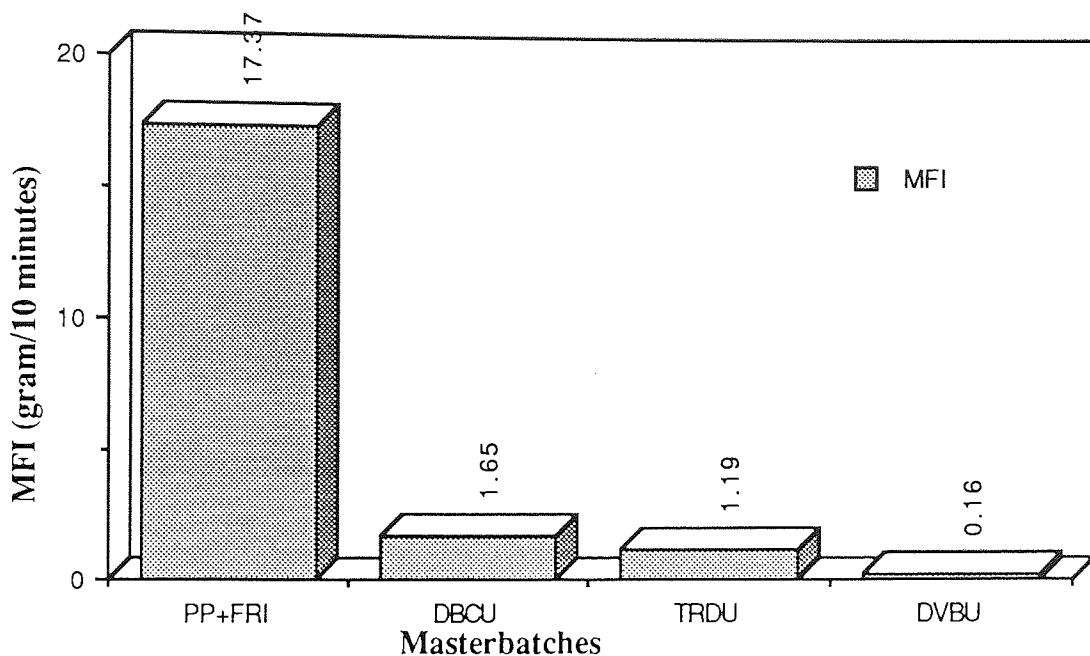


Figure 5.19 MFI of various masterbatches, refer to Table 5.1, i.e.
 PP+FRI = PP + 0.02 m.r Trig.101,
 DBCU = PP + 10% DBBA + 0.02 mr Trig.101,
 TRDU = PP + 6% DBBA + 4% Tris+0.02m.r.Trig.101, and
 DVBU = PP + 6% DBBA + 4% DVB+0.02 m.r. Trig.101.

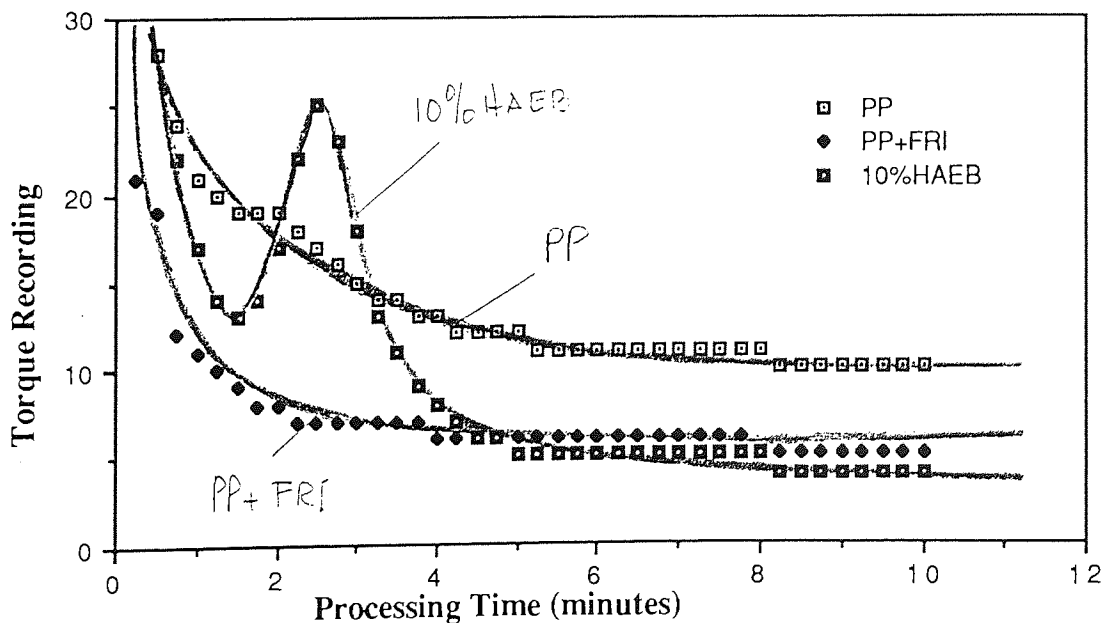


Figure 5.20 Changes in torque during processing of masterbatches containing 10%HAEB + 0.005 m.r. [I]/[AO] Trigonox 101, PP processed without AO in absence and presence 0.005 m.r. of Trigonox 101 is also shown for comparison processing condition, under closed mixer, 10 minutes at 180°C.

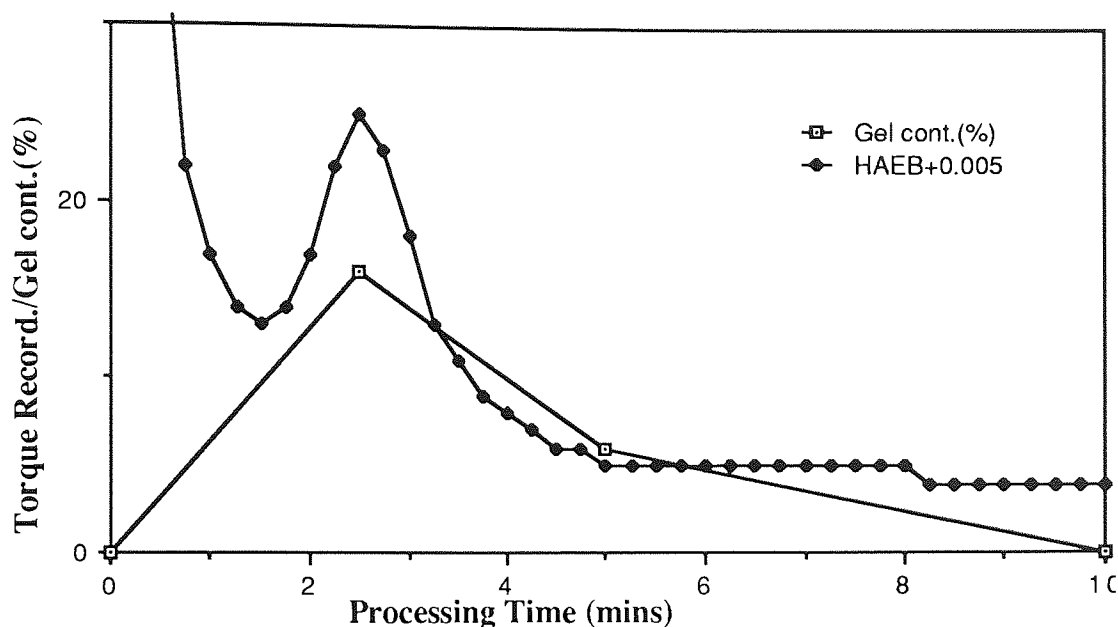


Figure 5.21 Changes in torque during processing and gel content of MB's containing 10% HAEB in the presence of 0.005 m.r.Trig.101, processed at various time (2.5, 5 and 10 minutes) under closed mixer condition at 180°C.

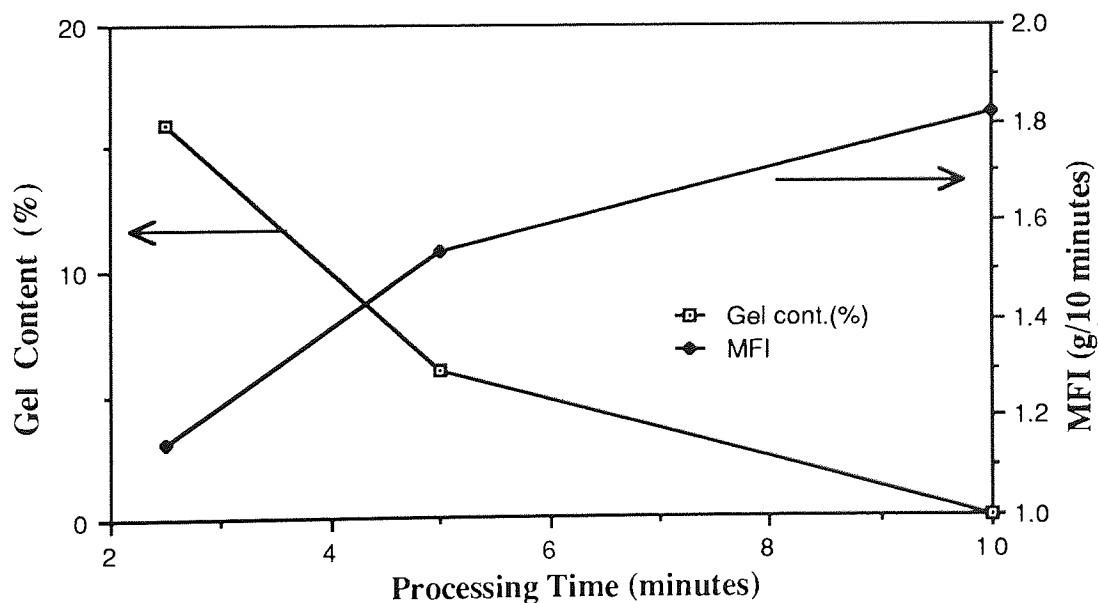


Figure 5.22 MFI and Gel content of 10% HAEB masterbatches processed in the presence of 0.005 m.r. [I/[AO] Trigonox 101, at various time processing (2.5, 5 and 10 minutes) under closed mixer condition at 180°C.

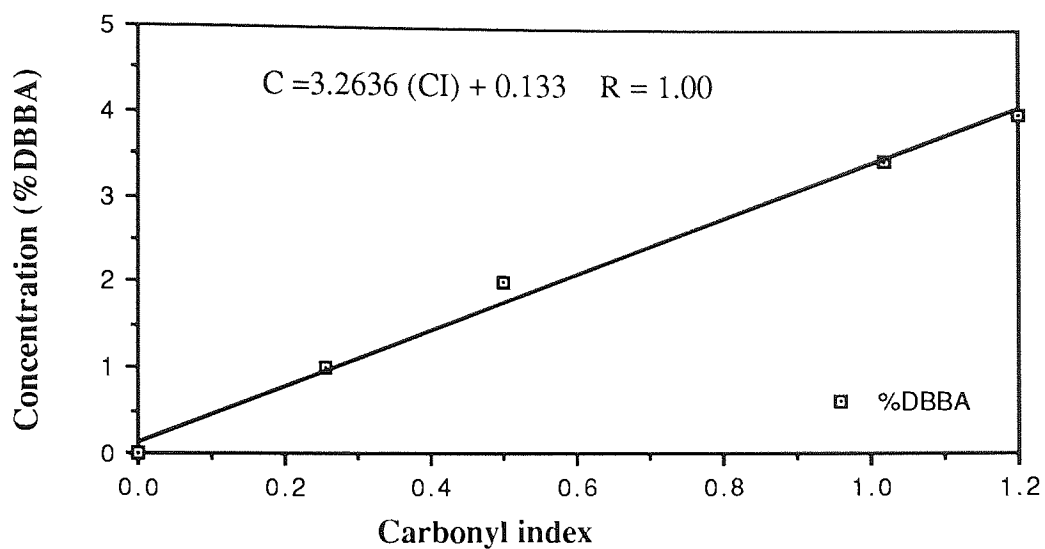


Figure 5.23 Calibration curve of DBBA masterbatches in various concentration

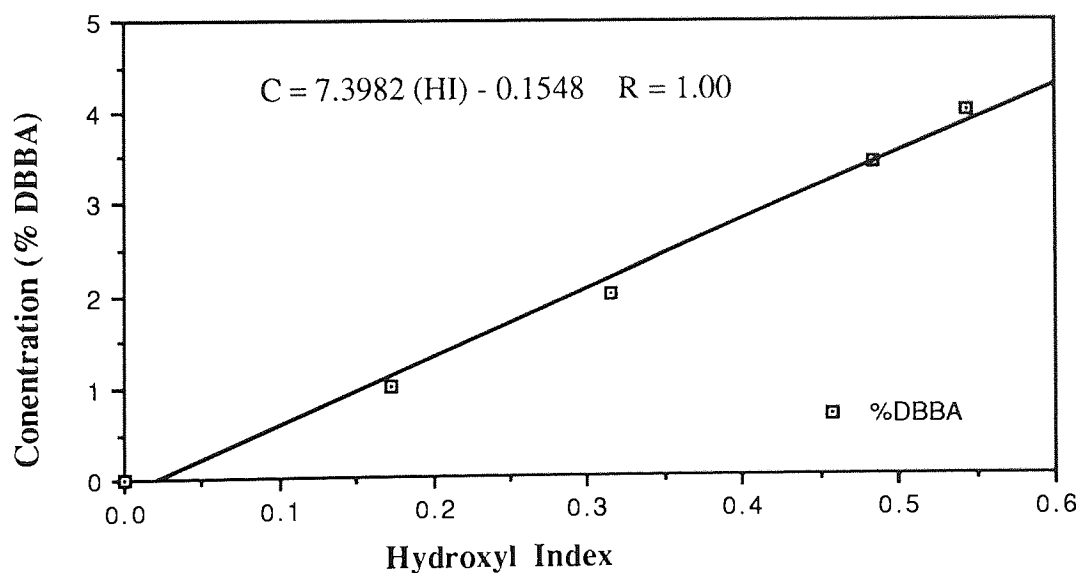


Figure 5.24 Calibration curve of DBBA masterbatches in various concentration

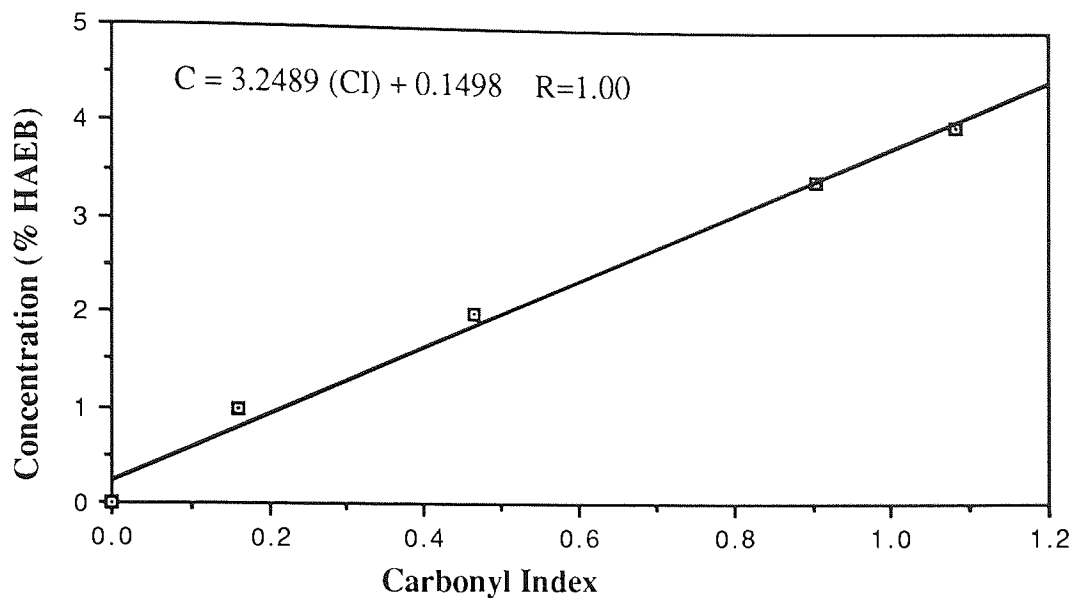


Figure 5.25 Calibration curve of HAEB masterbatches in various concentration

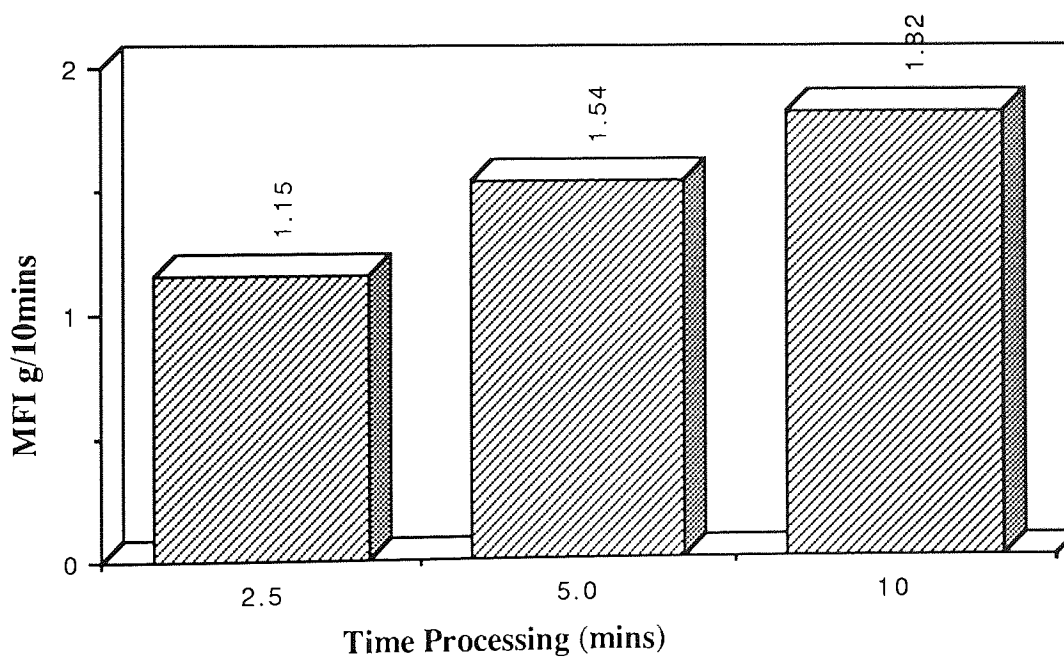


Figure 5.26 The MFI of original masterbatches, containing 10% HAEB processed in the presence of optimum concentration of Trigonox 101, at 180°C in closed mixer condition at different processing times.

B300

<S> PPTG (9301)

ENDED: 04/04

MOLECULAR WEIGHT DISTRIBUTION

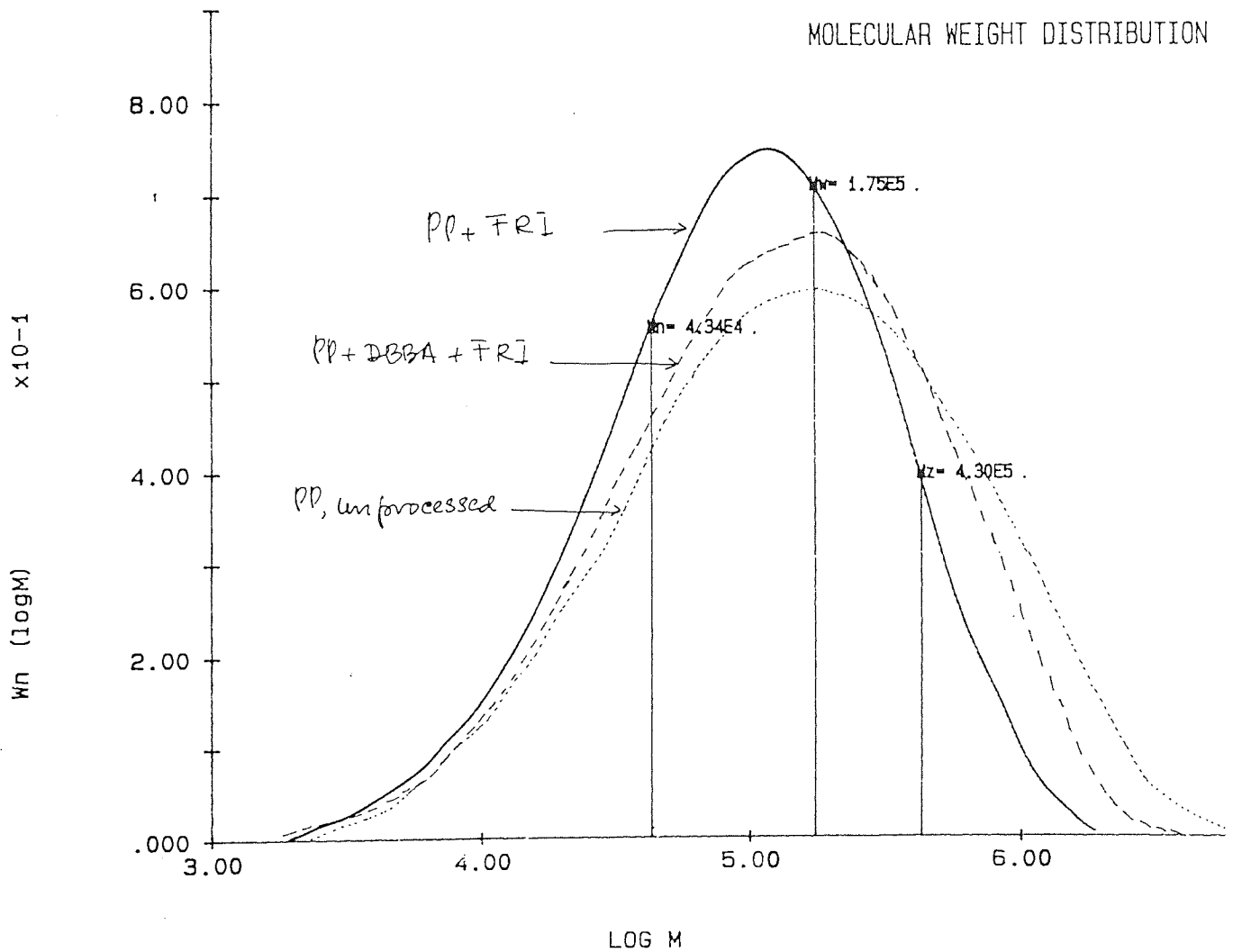


Figure 5.27 Molecular weight distribution curves of masterbatches containing 10% of DBBA, see Scheme 5.4 stage A (-----) processed in the presence of 0.02 molar ratio Trigonox 101, compared to that of PP processed with similar amount of peroxide, 0.02 m.r Trigonox 101 (—) and unprocessed PP (.....)

MOLECULAR WEIGHT DISTRIBUTION

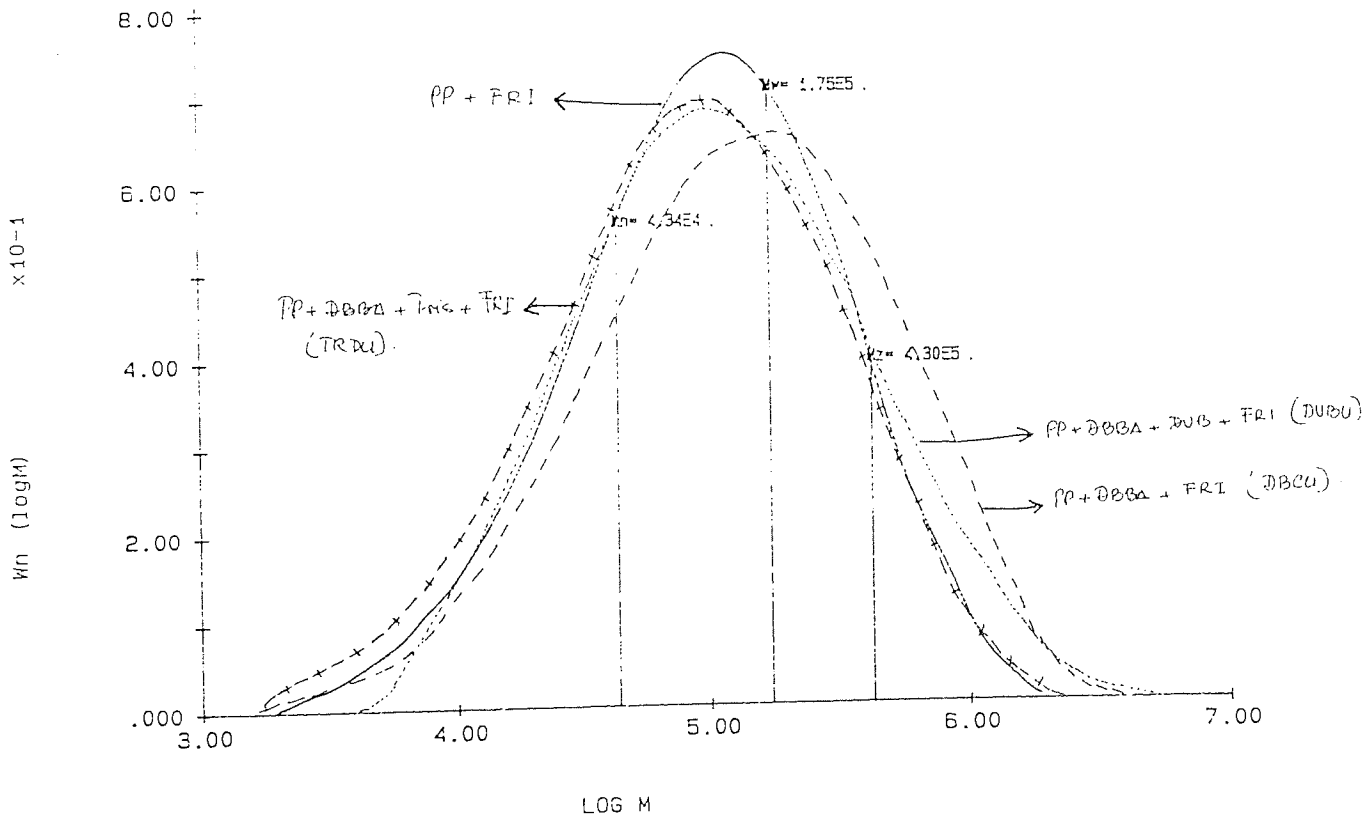


Figure 5.28 Molecularweight distribution curves of masterbatches containing: 10% of DBBA, see Scheme 5.4 stage A (-----); 10% (DBBA+Tris), see Scheme 5.5 stage A (-+--+); 10% (DBBA+DVB), see Scheme 5.6 stage A (.....) all were processed in the presence of 0.02 molar ratio Trigonox 101. PP processed with similar amount of peroxide, 0.02 m.r Trigonox 101 (___)

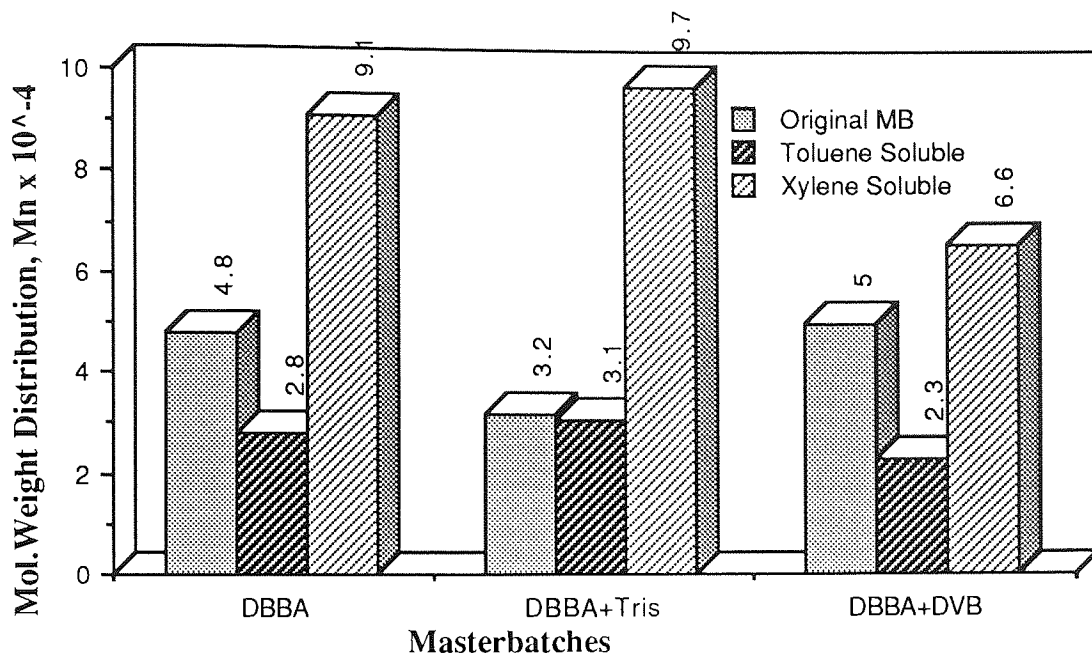


Figure 5.29 Molecular weight distribution (Mn) data of MB's fractions (after Soxhlet separation) of DBBA MB's containing 10% total (DBBA without or with coagent ratio 6/4) processed in the presence of 0.02 m.r.Trig.101, at 180°C for 10 minutes, in closed mixing condition.

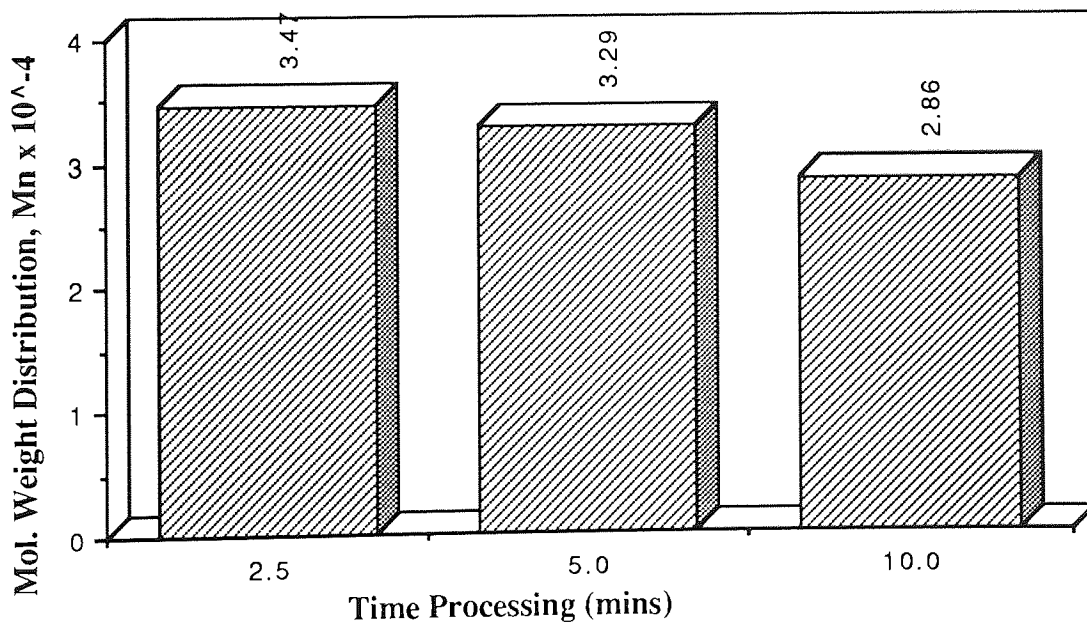


Figure 5.33 Molecular weight distribution, [Mn x10⁻⁴] data of MB's containing 10% HAEB, processed in the presence of 0.005 m.r. (I/HAEB) Trigonox 101 at 180°C in closed mixing condition at various processing time, see Table 5.10

B337

<14> DBCU-3 (9312)

ENDED: 04/09/

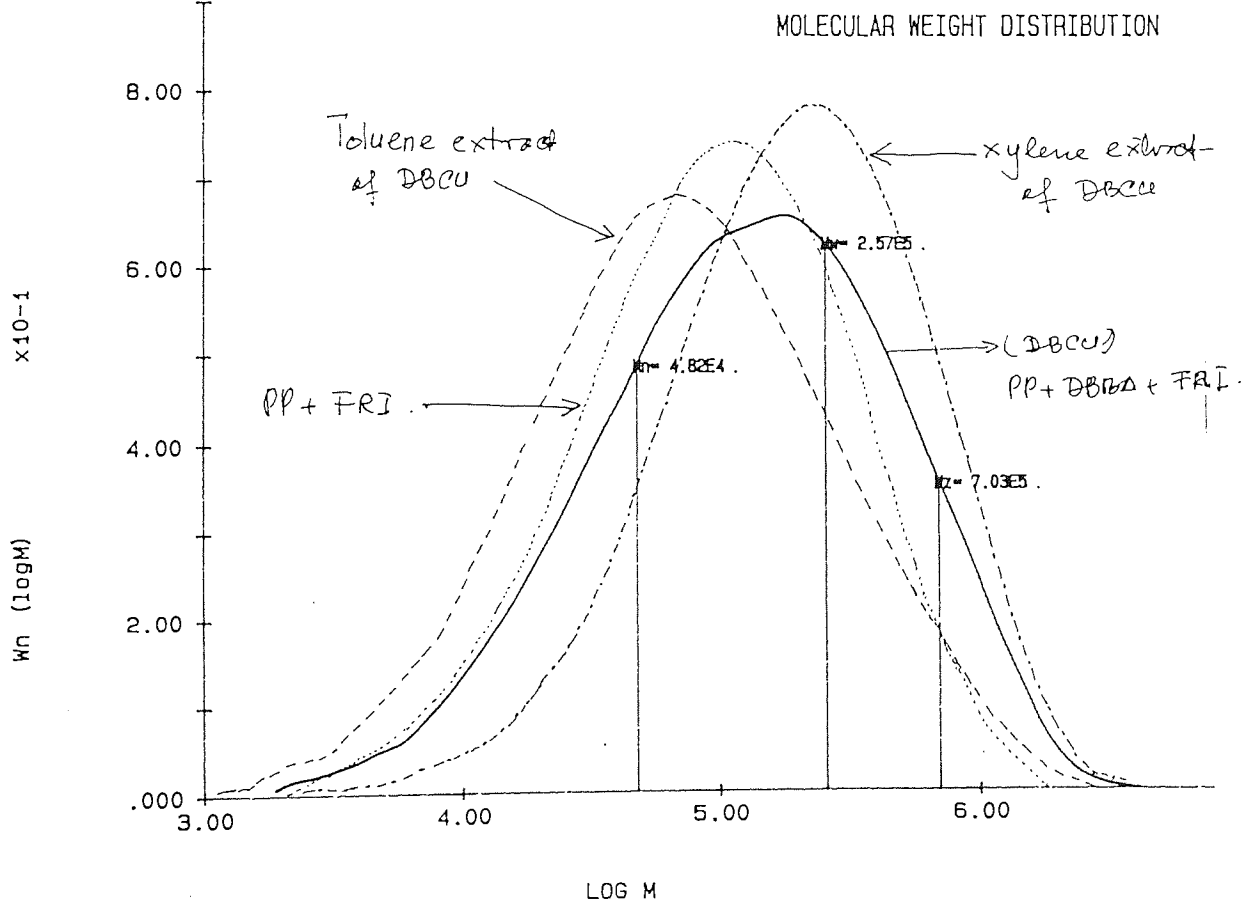


Figure 5.30 Molecular weight distribution curves of masterbatches containing 10% DBBA before extraction, see Scheme 5.4 stage A (—), toluene extract fraction, see Scheme 5.4 stage D (-----), xylene extract fraction, see Scheme 5.4 stage F (· · · ·), compared to that of PP processed with 0.02 molar ratio Trigonox 101 (— · — ·).

B325

<7> TRDU-3 (9305)

ENDED: 04/06/90

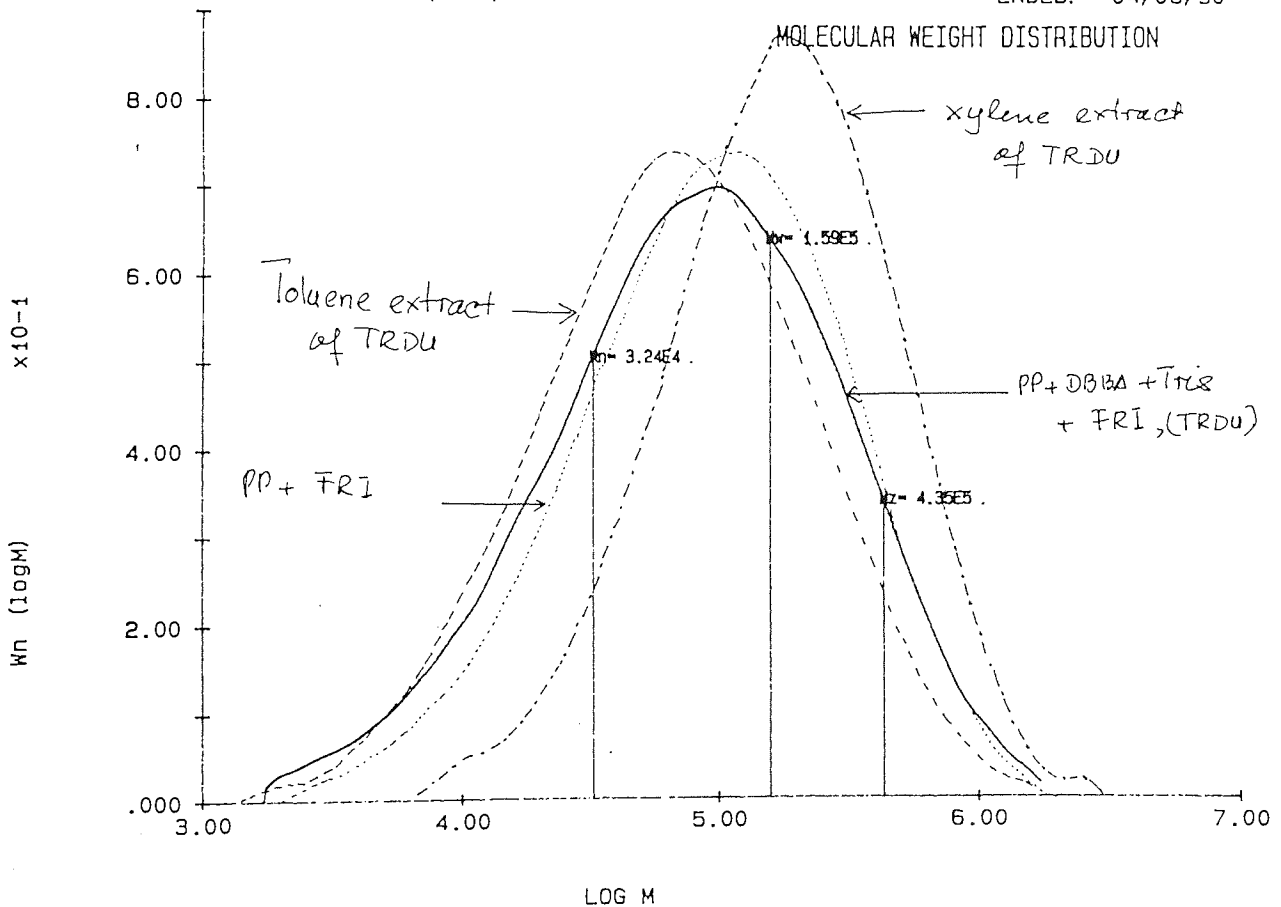


Figure 5.31 Molecular weight distribution curves of masterbatches containing 10% (DBBA+Tris) before extraction, see Schem 5.5 stage A (____), toluene extract fraction, see Schem 5.5 stage D (-----), xylene extract fraction, see Schem 5.5 stage F (.....), compared to that of PP processed with 0.02 m.r trigonox 101 (.....).

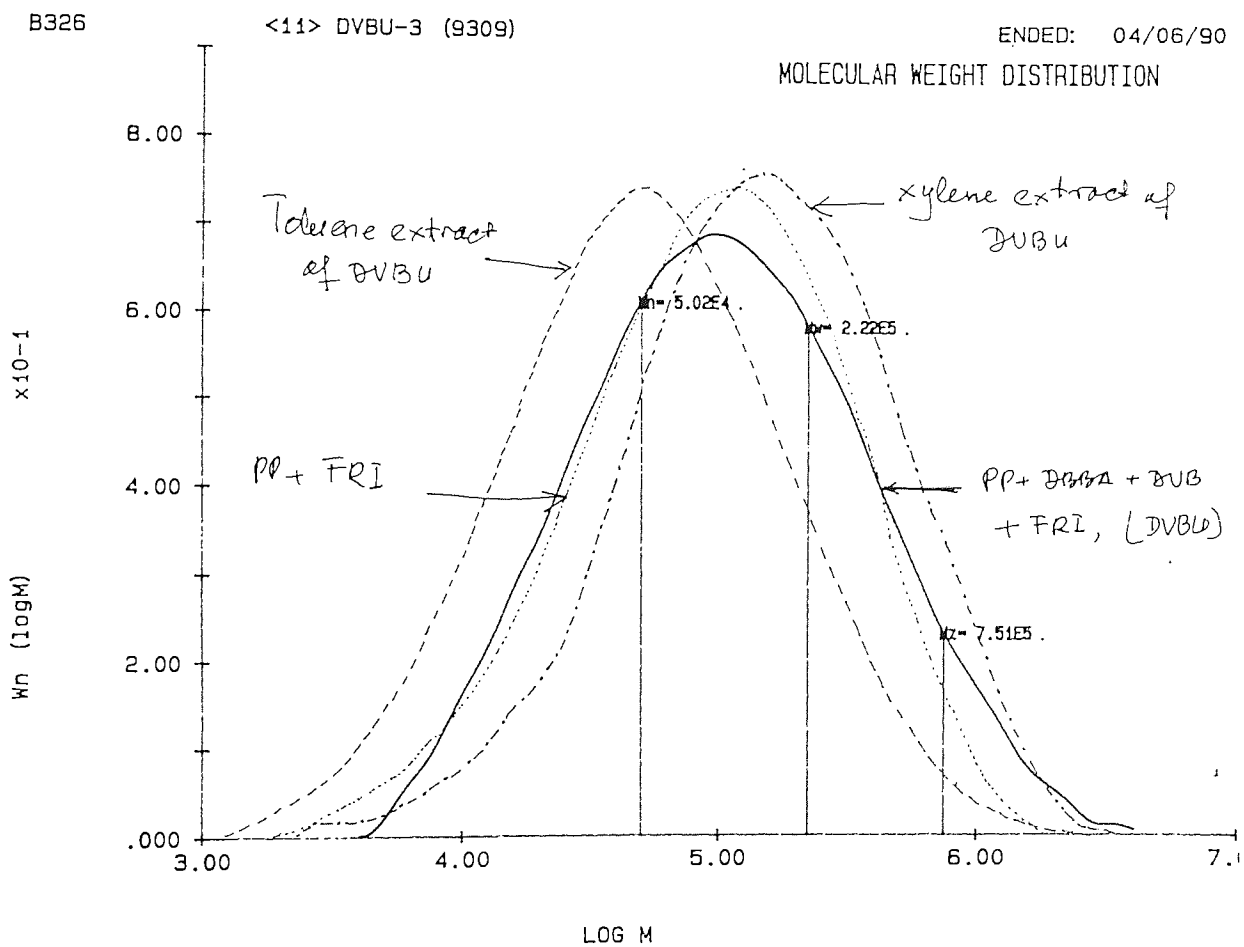


Figure 5.32 Molecular weight distribution curves of masterbatches containing 10% (DBBA+DVB) before extraction, see Scheme 5.6 stage A (____), toluene extract fraction, see Scheme 5.6 stage D (-----), xylene extract fraction, see Scheme 5.6 stage F (._._.), compared to that of PP processed with peroxide (.....).

SAMPLE 17 (3429)

ENDED: 09/

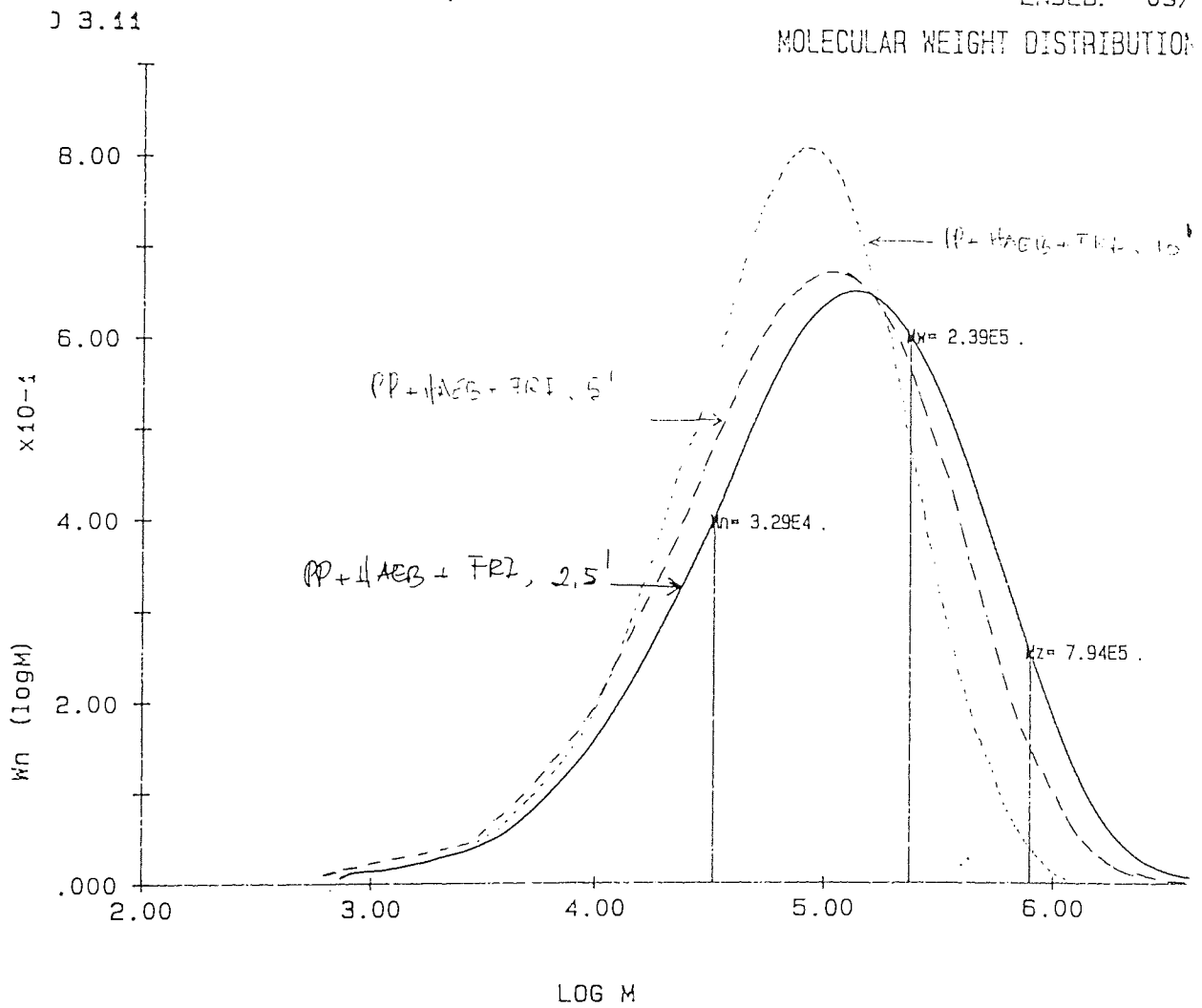


Figure 5.33a Molecular weight distribution curves of masterbatches containing 10% HAEB processed in the presence 0.005 m.r. Trigonox 101, for 2.5 minutes (.....), for 5 minutes (-----), and for 10 minutes (_____),

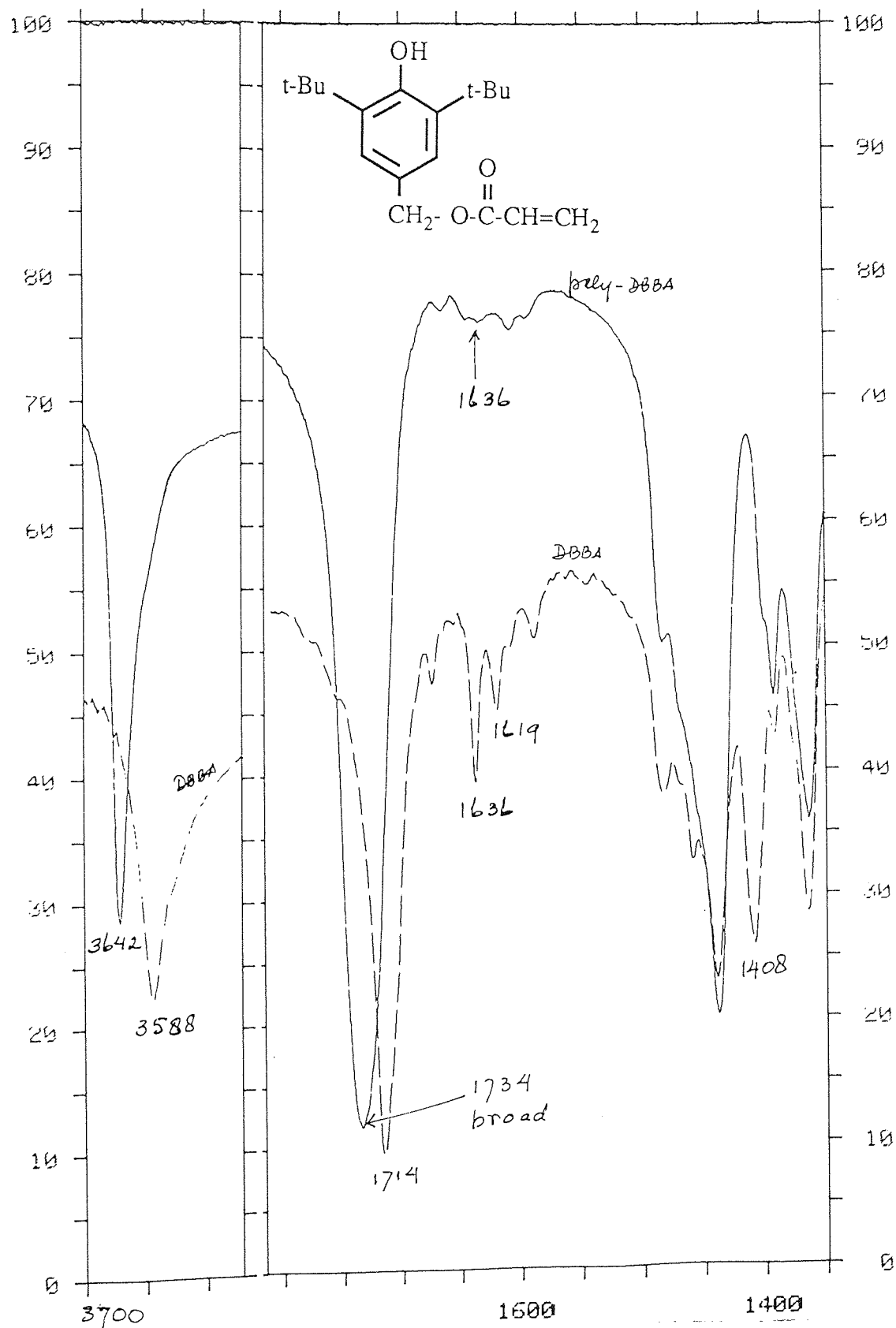


Figure 5.34 Comparison of FTIR spectra (in region 3700-1300 cm^{-1}) of polymerised DBBA without decalin (in benzene), refluxed at 70°C for 25 hours in the presence of initiator AZBN, see Scheme 5.3 stage D (—), with that of fresh DBBA (-----) both in KBr disc.

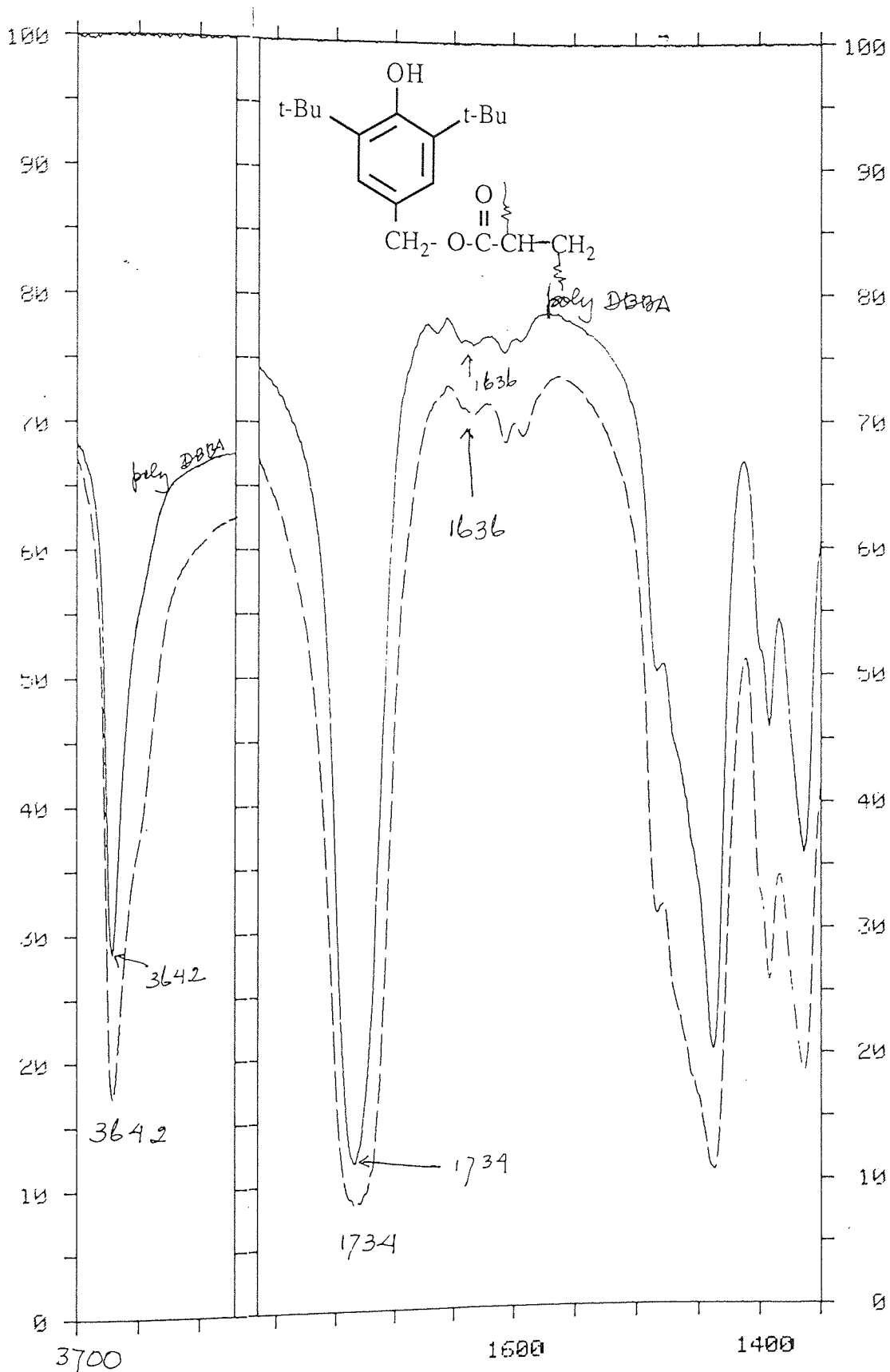


Figure 5.35 Comparison of FTIR spectra (in region 3700-1300 cm⁻¹) of polymerised DBBA without decalin (in benzene), see Scheme 5.3 stage D (—), with that of DCM-extract from 10% DBBA MB, see Scheme 5.4 stage B (-----) both in KBr disc.

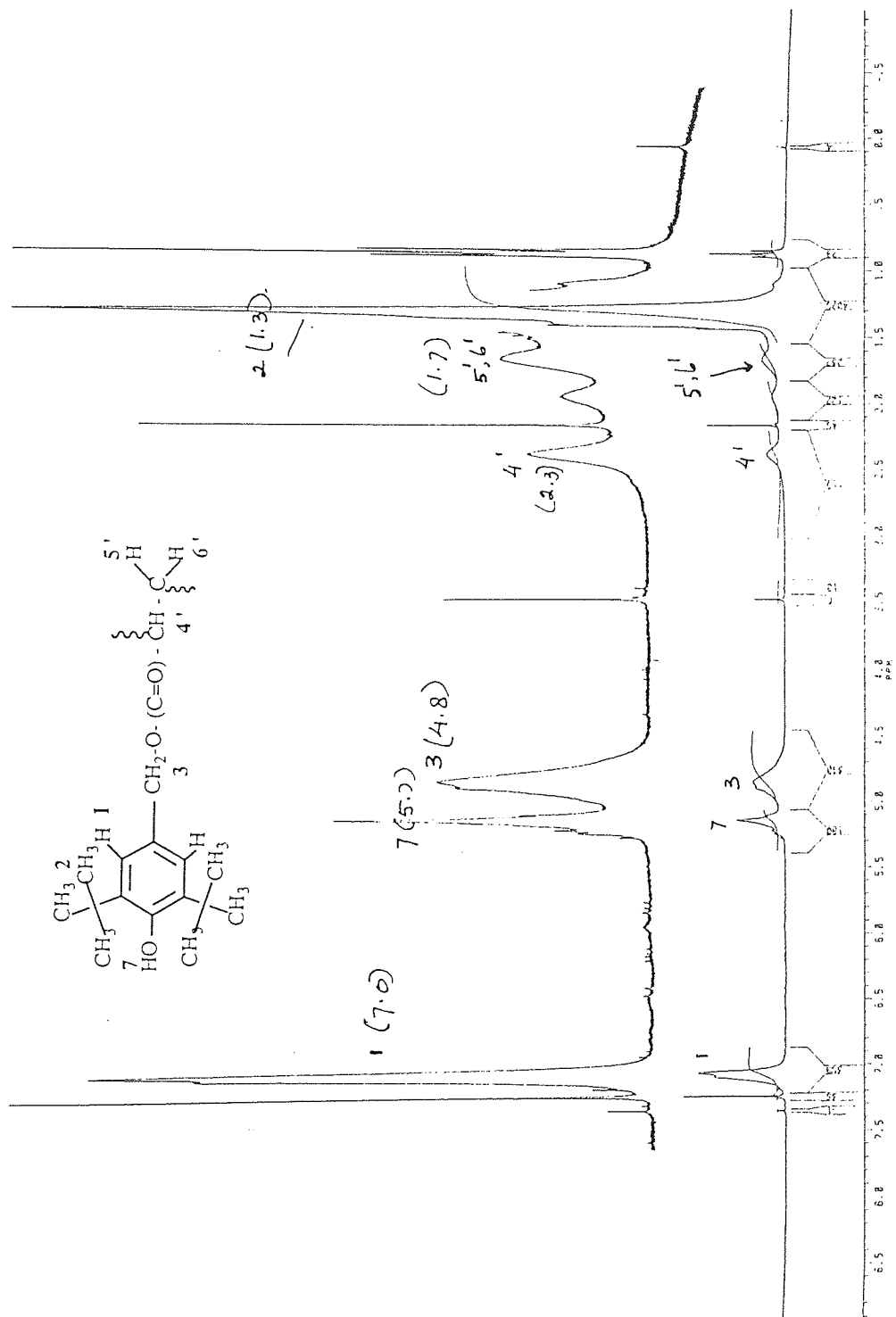


Figure 5.36 Proton NMR spectrum of polymerised DBBA without decalin (refluxed at 70°C for 25 hours in the presence of initiator AZBN, see Scheme 5.3 stage D) in CDCl₃.

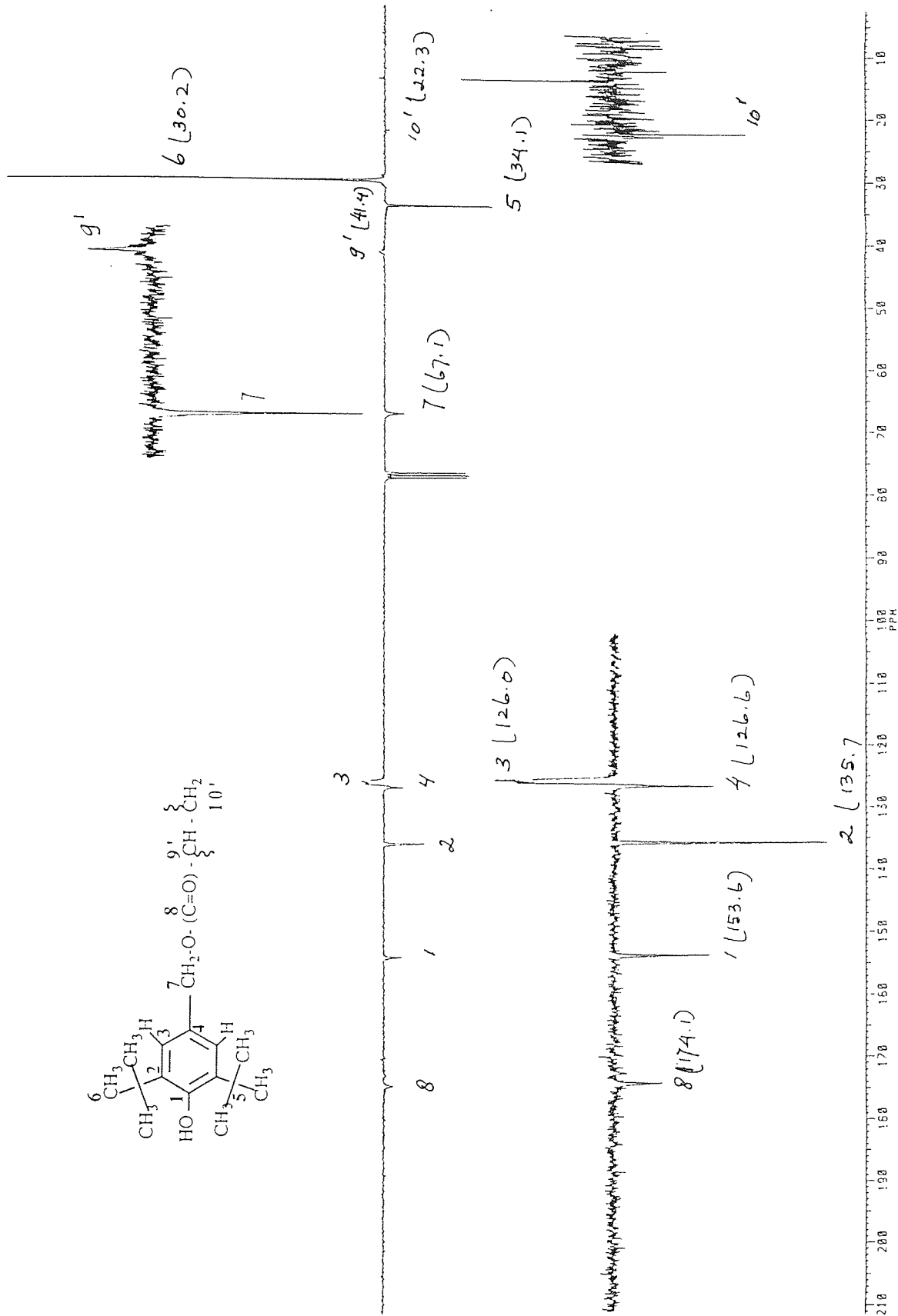


Figure 5.37 Carbon-13 NMR spectrum of polymerised DBBA without decalin (refluxed at 70°C for 25 hours in the presence of initiator AZBN, see Scheme 5.3 stage D) in CDCl₃.

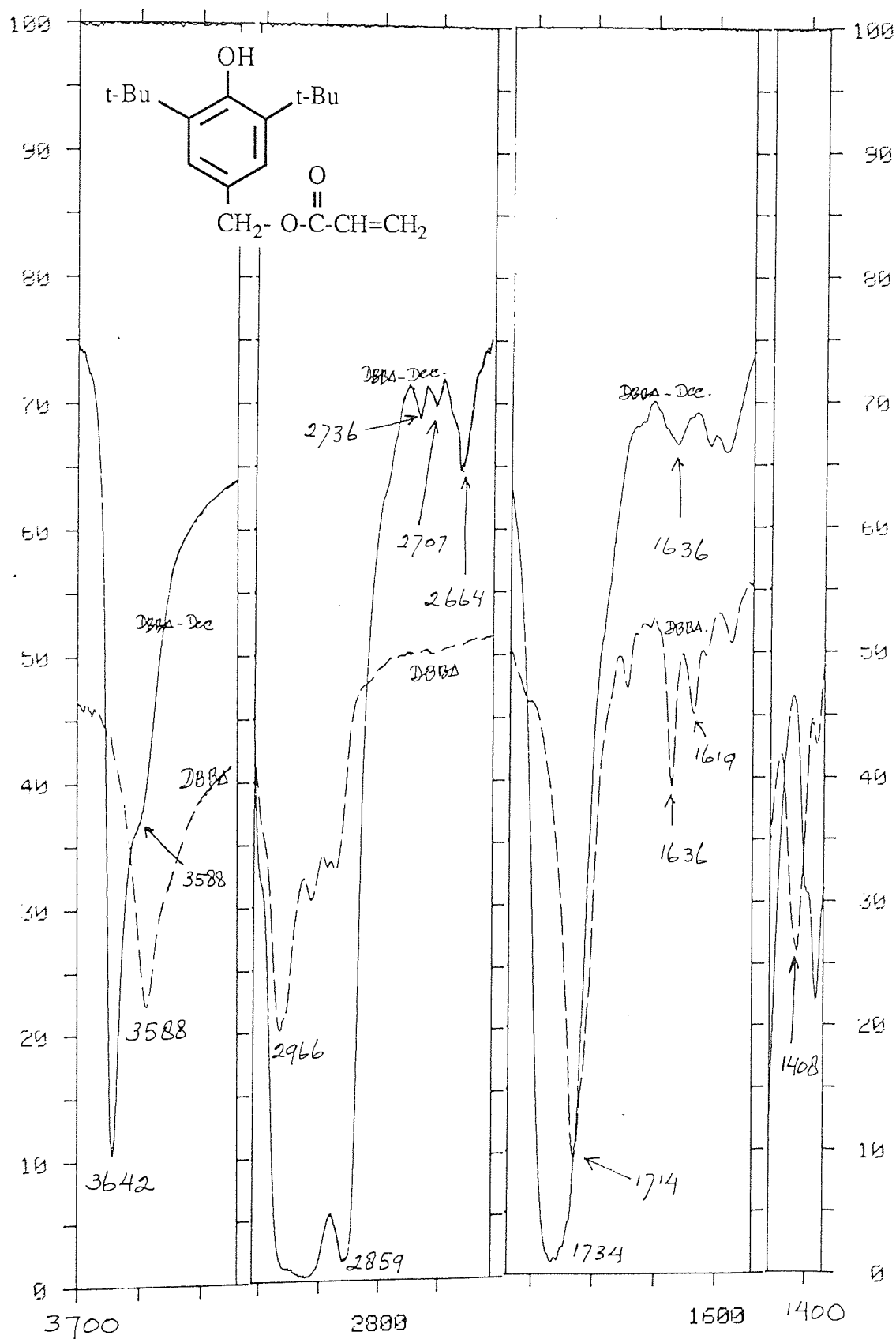


Figure 5.38 Comparison of FTIR spectra (in region 3700-1300 cm^{-1}) of polymerised DBBA-Decalin, see Scheme 5.2 stage D (—), with that of fresh DBBA (-----) both in KBr disc.

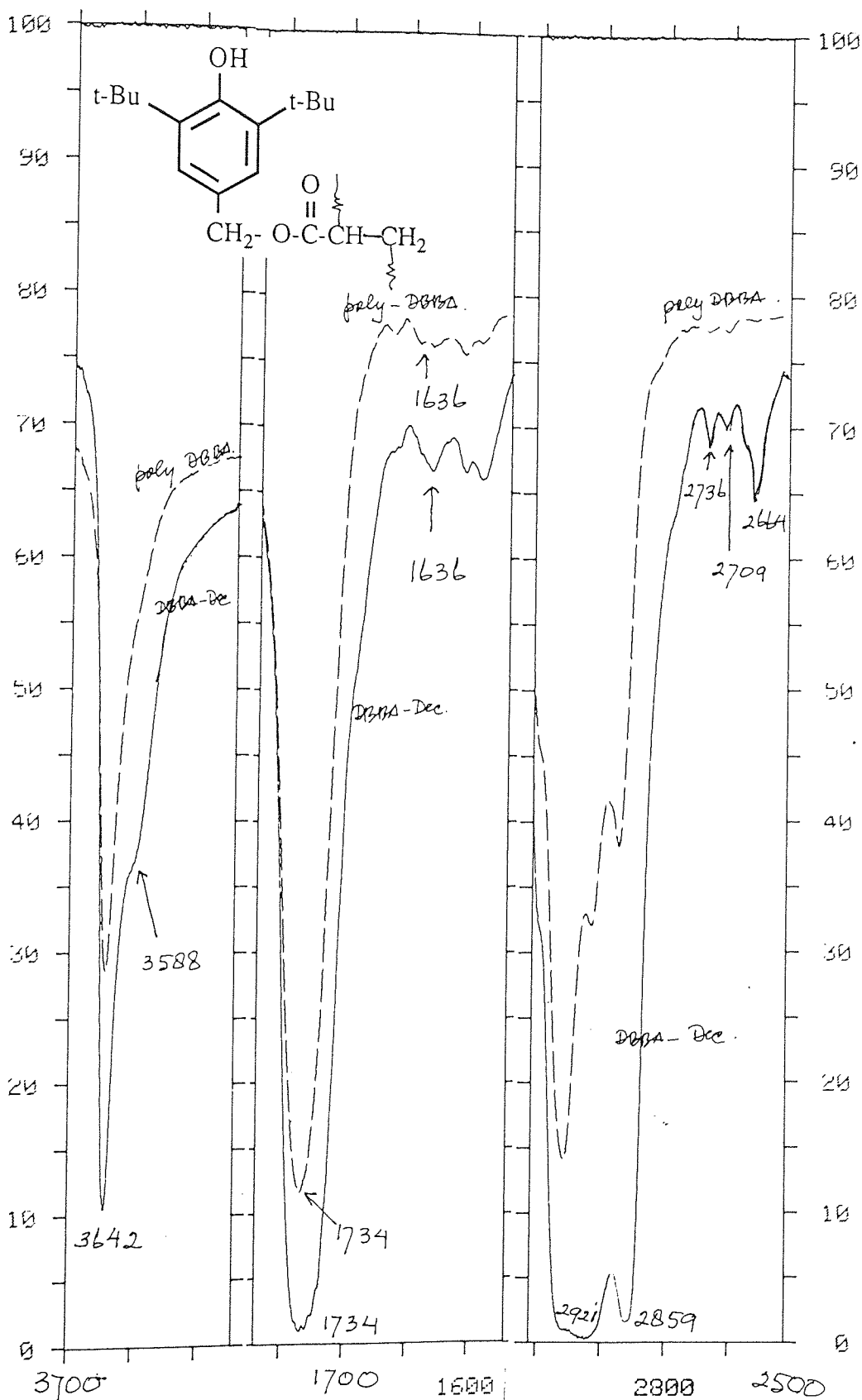


Figure 5.39 Comparison of FTIR spectra (in region 3700-1300 cm^{-1}) of polymerised DBBA-Decalin, see Scheme 5.2 stage D (—), with that of polymerised DBBA without decalin, see Scheme 5.3 stage D (-----) both in KBr disc.

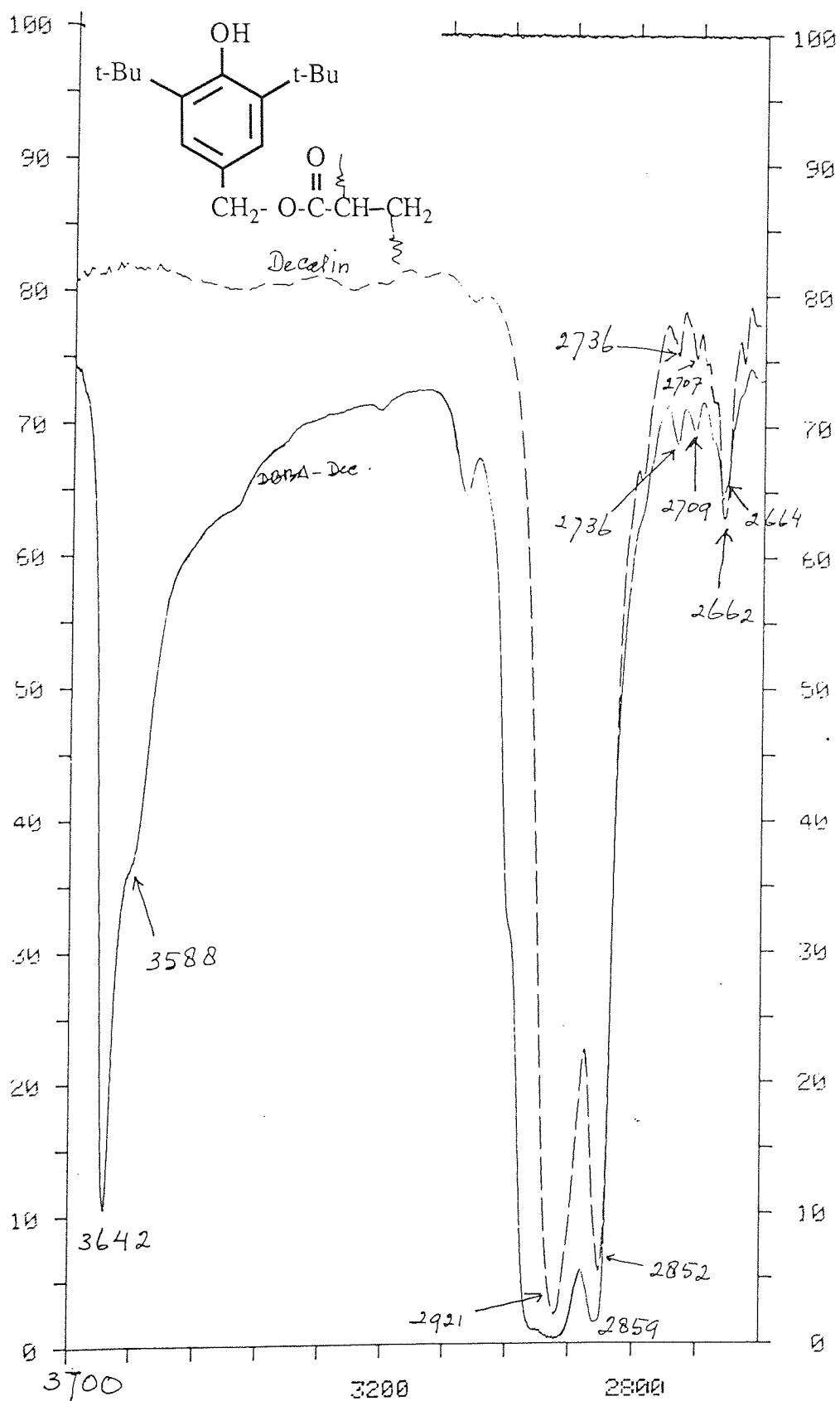


Figure 5.40 Comparison of FTIR spectra (in region 3700-2500 cm⁻¹) of polymerised DBBA-Decal using KBr disc, see Scheme 5.2 stage D (—), with that of neat liquid decalin (-----).

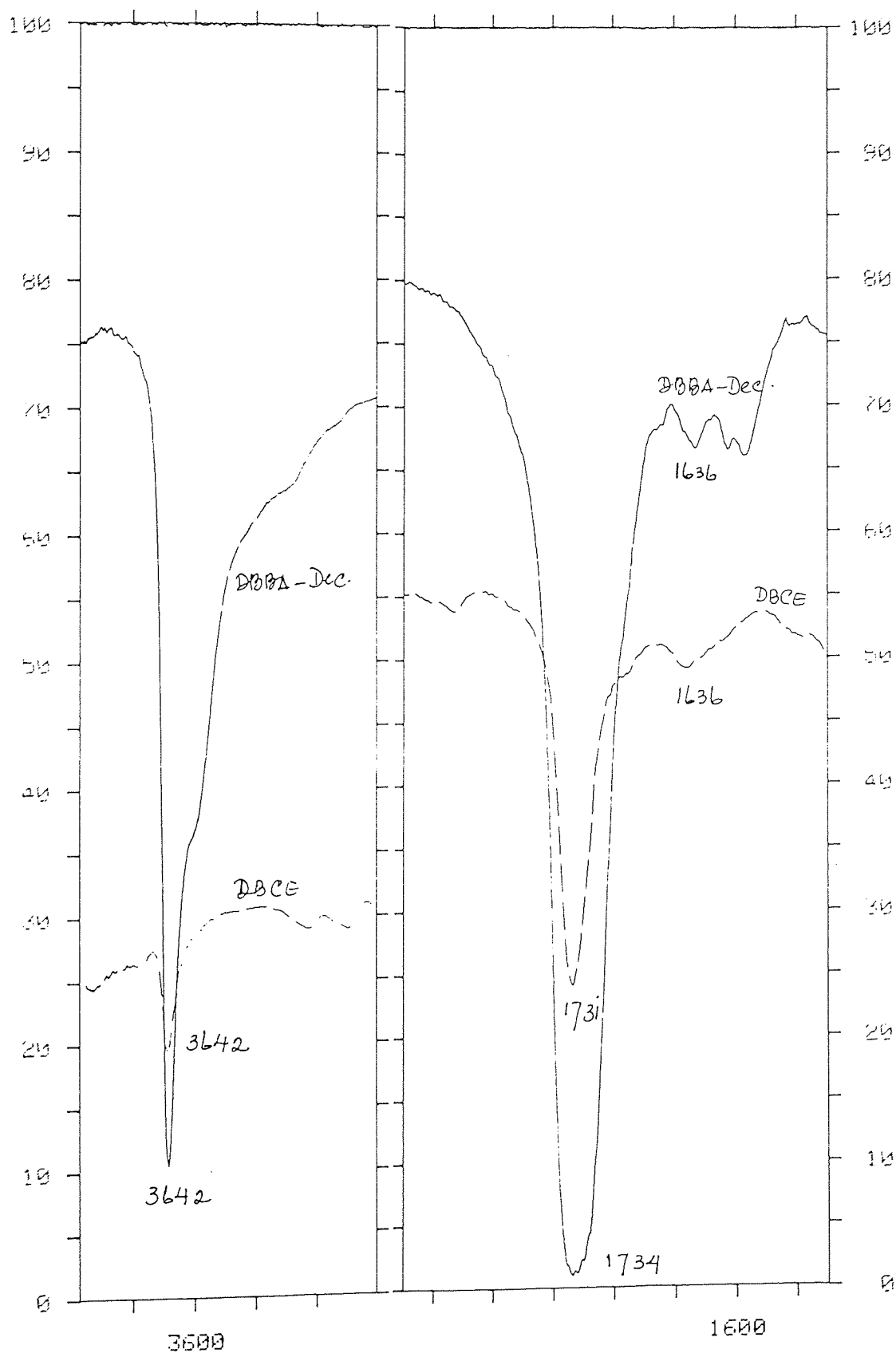


Figure 5.41 Comparison of FTIR spectra (in region 3700-1300 cm^{-1}) of polymerised DBBA-Decalin, see Scheme 5.2 stage D, in KBr disc (—), with that of PP MB film containing 10% DBBA after DCM extraction see Scheme 5.4 stage C (-----).

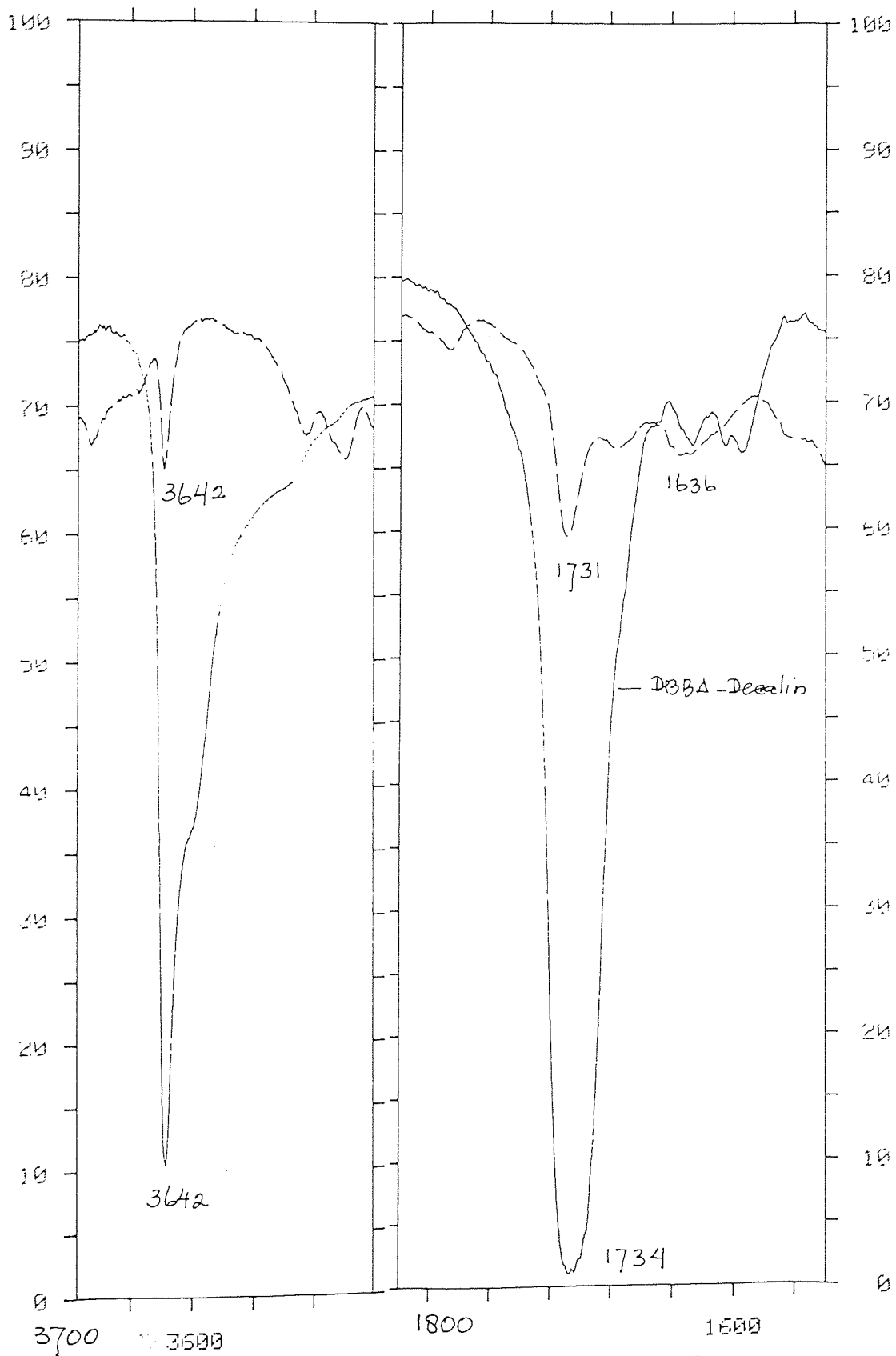


Figure 5.42 Comparison of FTIR spectra (in region 3700-1300 cm⁻¹) of polymerised DBBA-Decalin, see Scheme 5.2 stage D, in KBr disc (—), with that of xylene soluble of MB film containing 10% DBBA, see Scheme 5.4 stage F (-----).

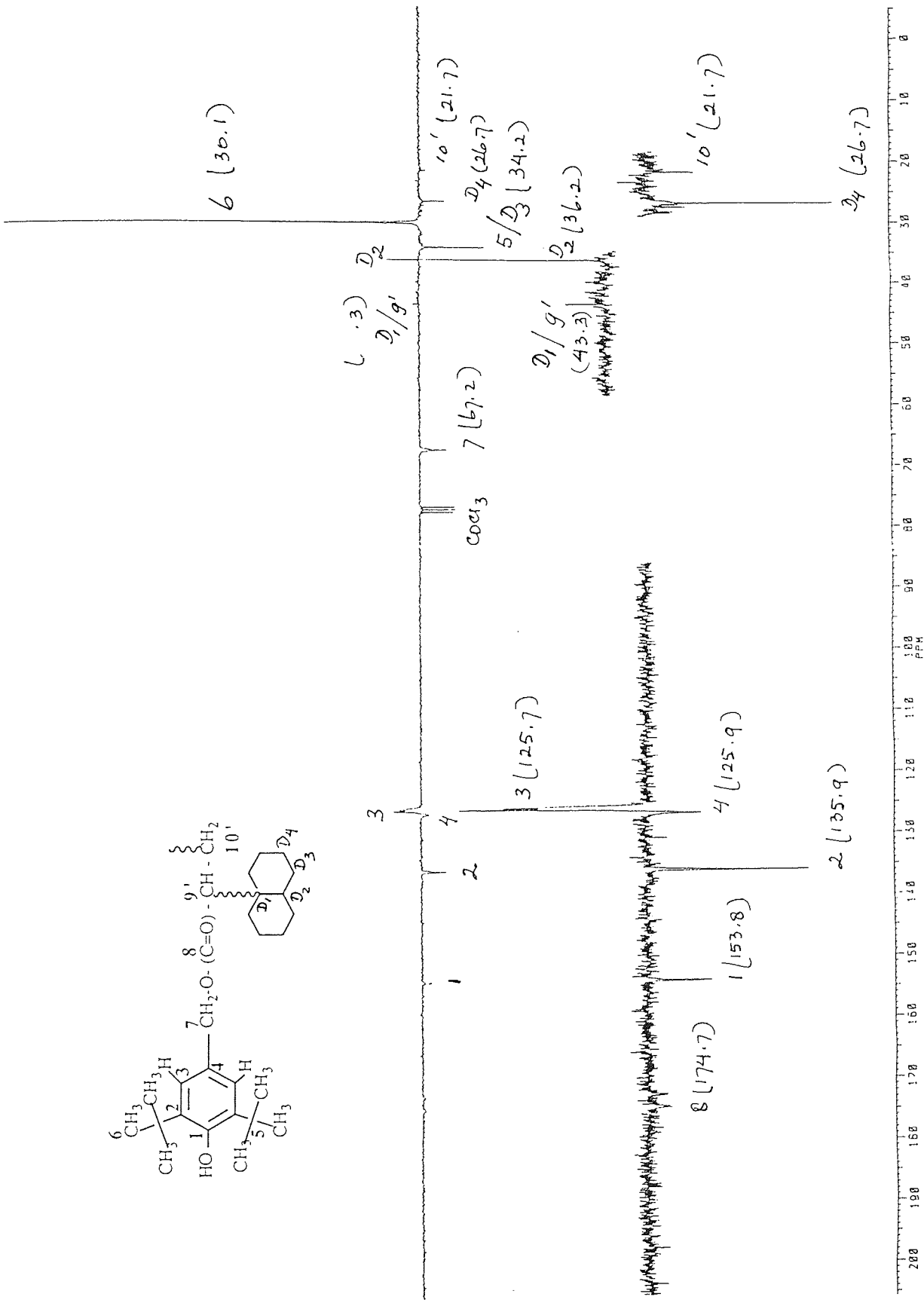


Figure 5.43 Carbon-13 NMR spectrum of polymerised DBBA-Decalin, see Scheme 5.2 stage D, run in deuterated chloroform (CDCl₃).

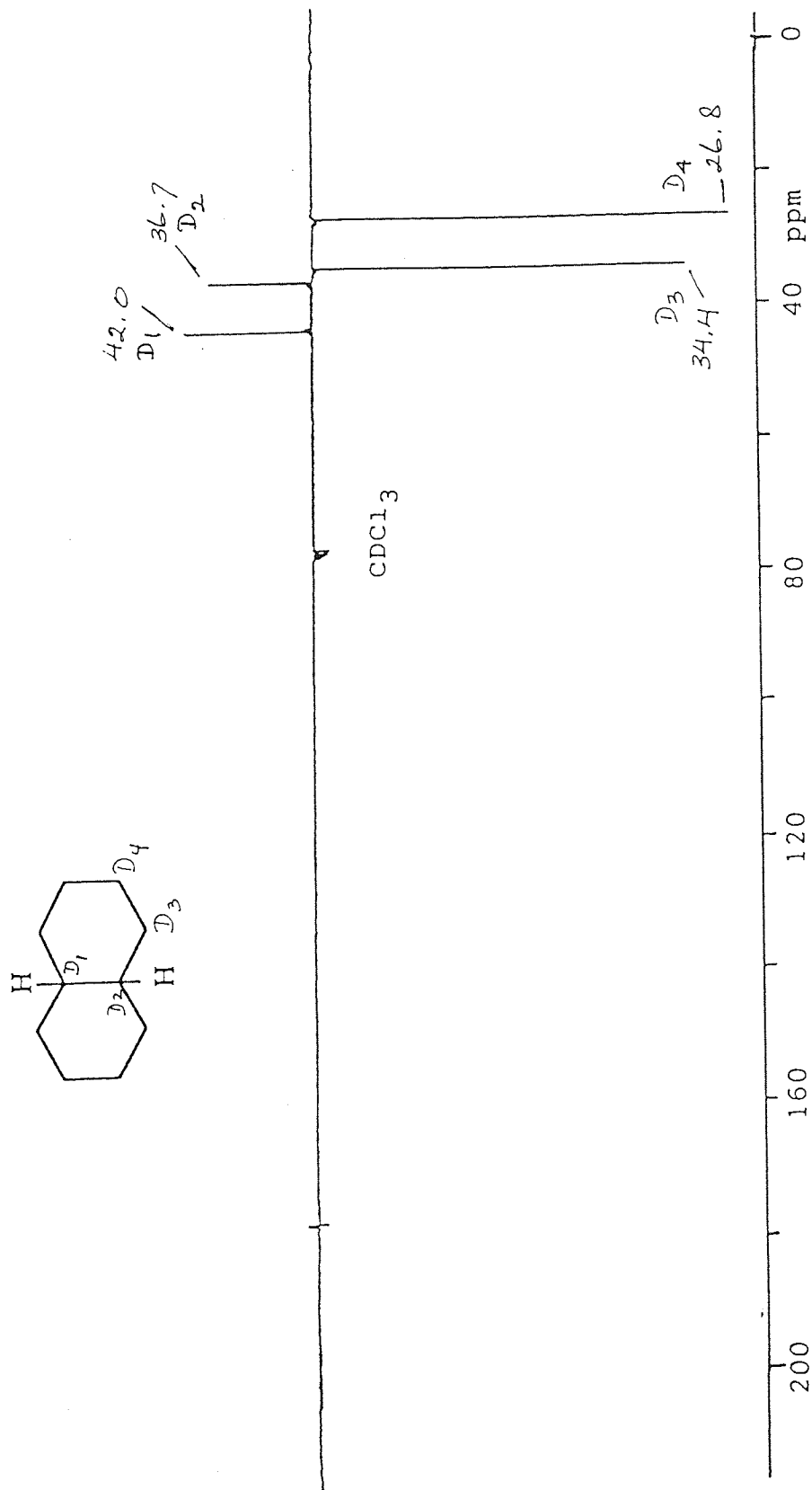


Figure 5.44 Carbon-13 NMR spectrum of fresh Decalin, run in deuterated chloroform (CDCl_3).

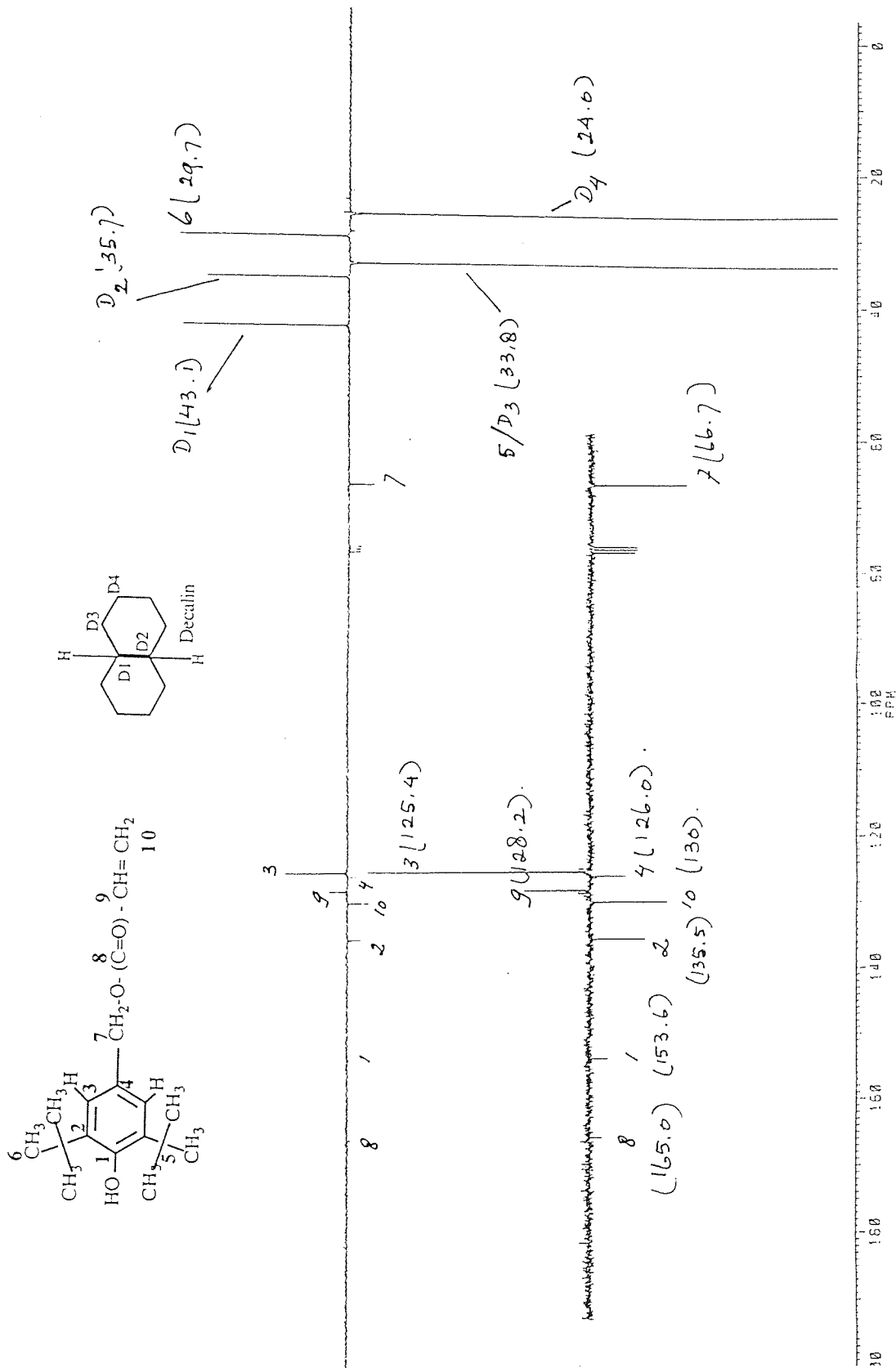


Figure 5.45 Carbon-13 NMR spectrum of 10% DBBA solution in decalin at 296 °K in the presence of 0.02 m.r [I/AO] Trigonox 101 and small amount of deuterated decalin, before reaction.

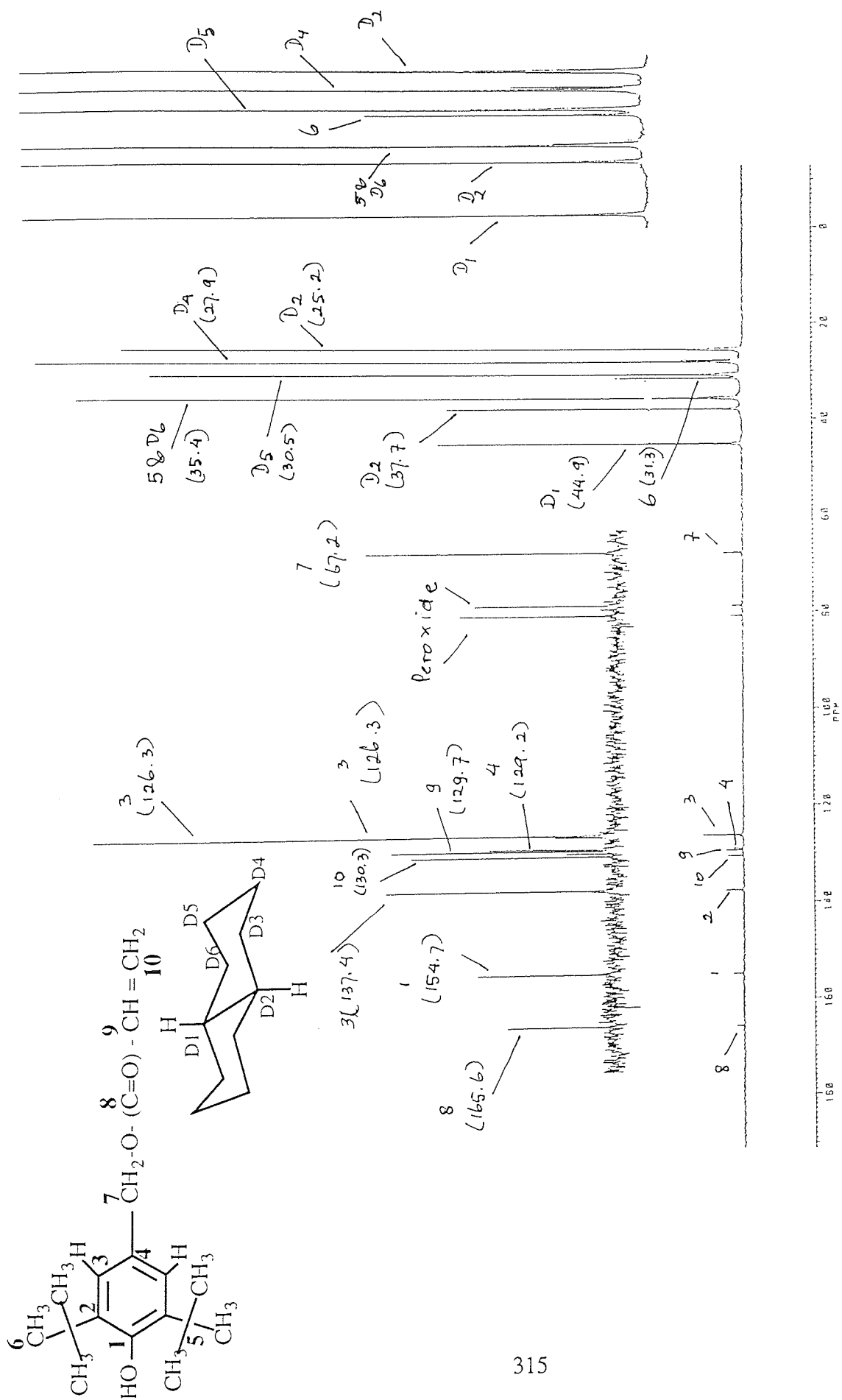


Figure 5.46 Carbon-13 NMR spectrum of 10% DBBA solution in decalin at 373°C after 1 hour reaction in the presence of 0.02 m.r [I/AO] Trigonox 101 and small amount of deuterated decalin.

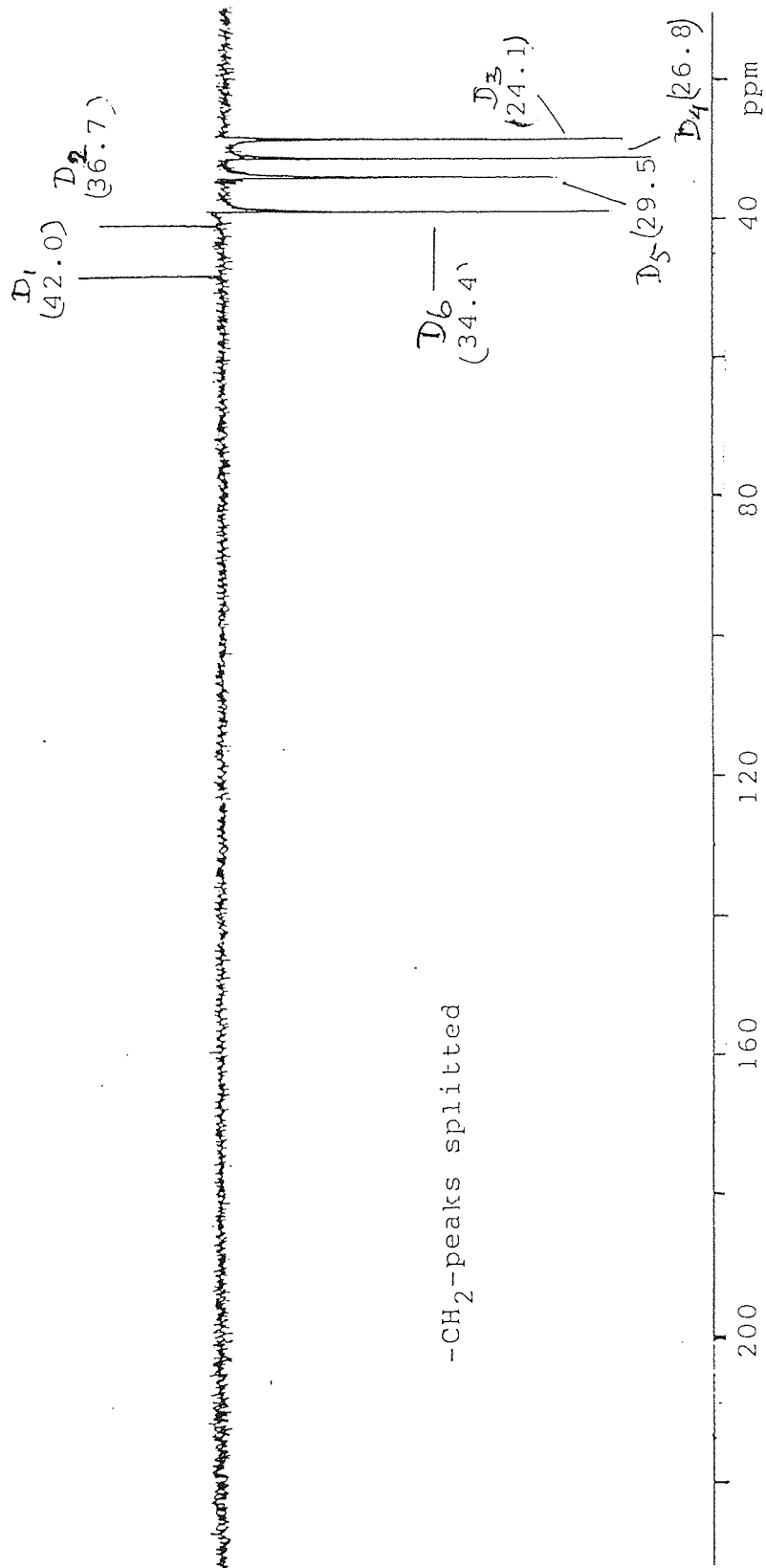
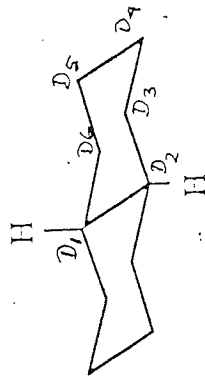


Figure 5.47 Carbon-13 NMR spectrum of fresh decalin at 373°K heated in NMR cavity for 1 hour in the presence of small amount of deuterated decalin.

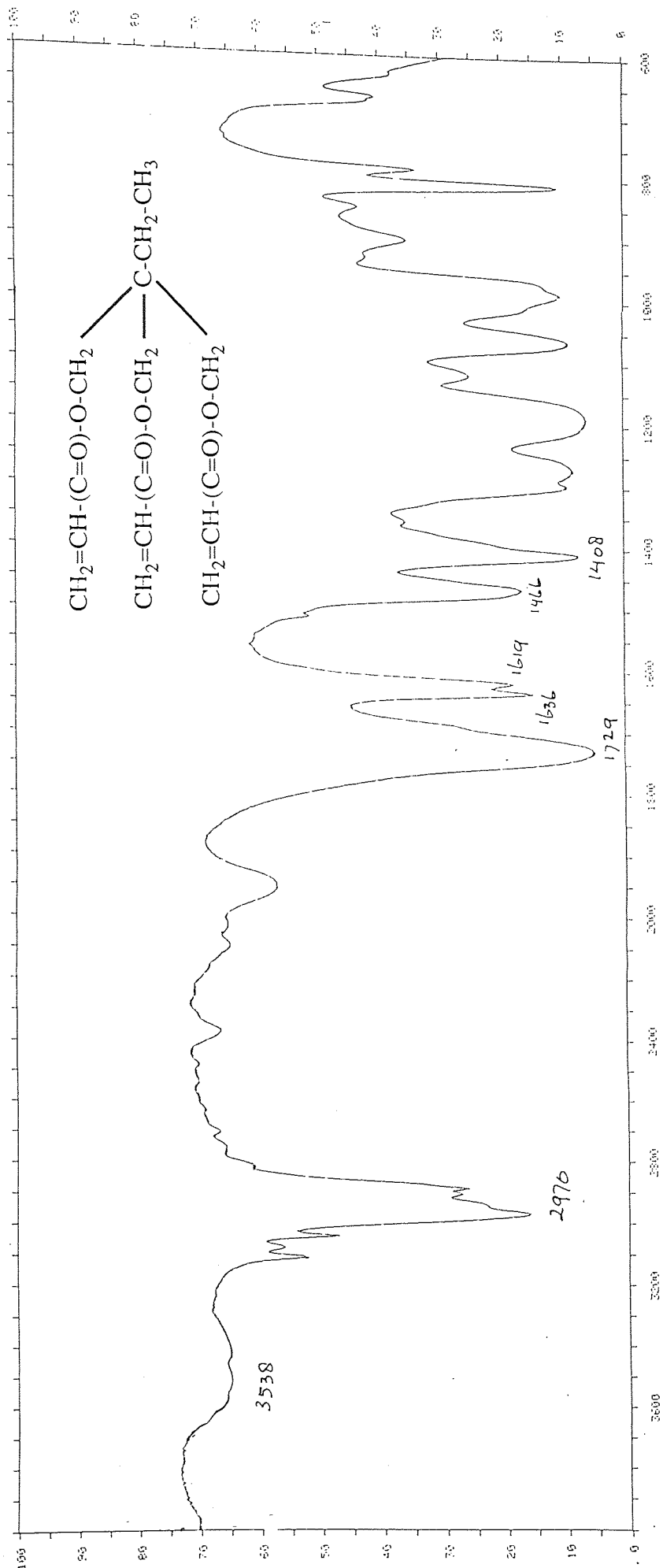


Figure 5.49 The FTIR spectrum of fresh Tris in neat liquid

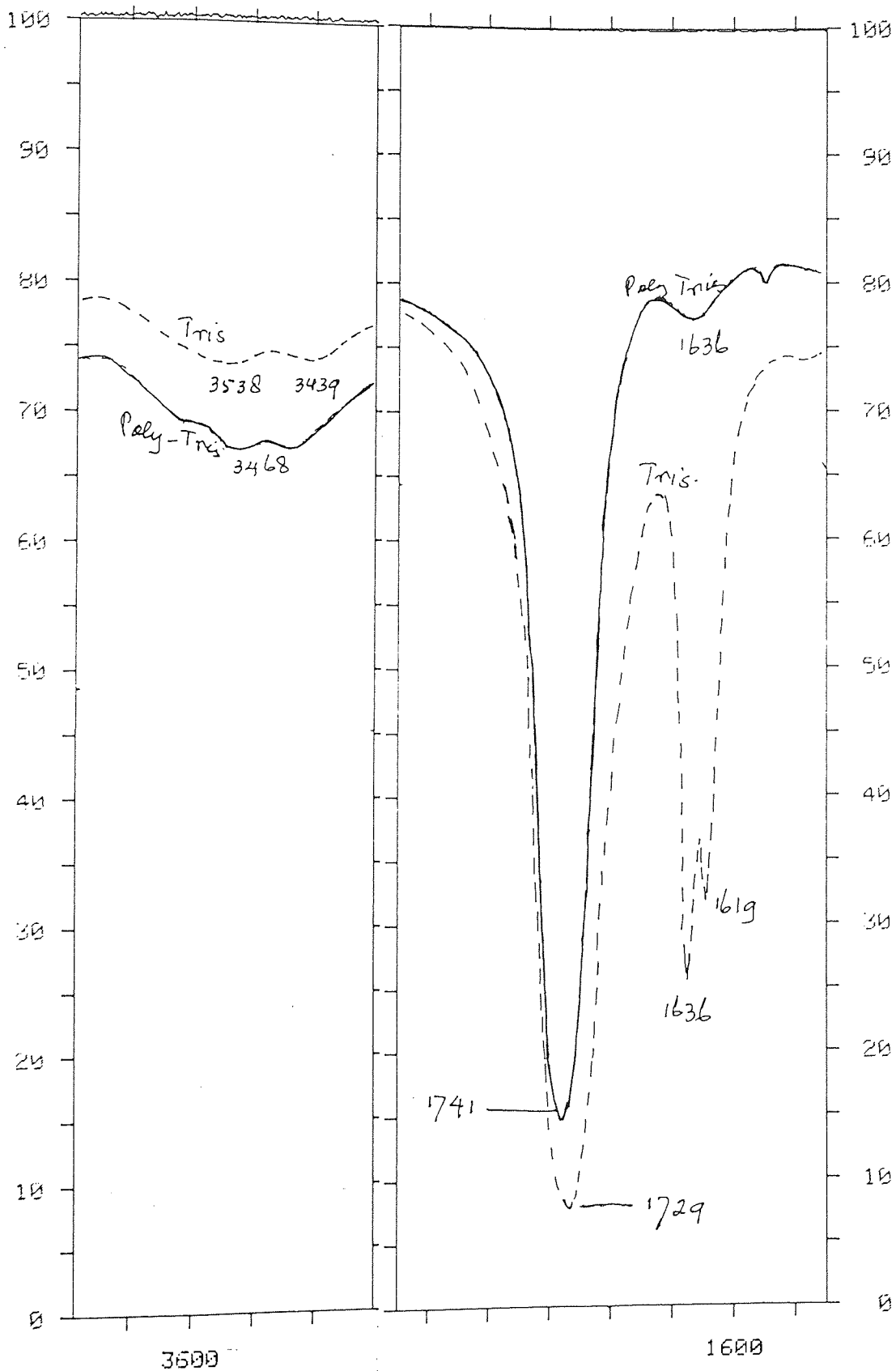


Figure 5.49a Comparison of FTIR spectra (in region 3700-1300 cm^{-1}) of polymerised Tris in the presence of 0.02 m.r initiator Trigonox 101, see Scheme 5.10 stage C, in KBr disc (—), with that of fresh Tris as neat liquid (-----).

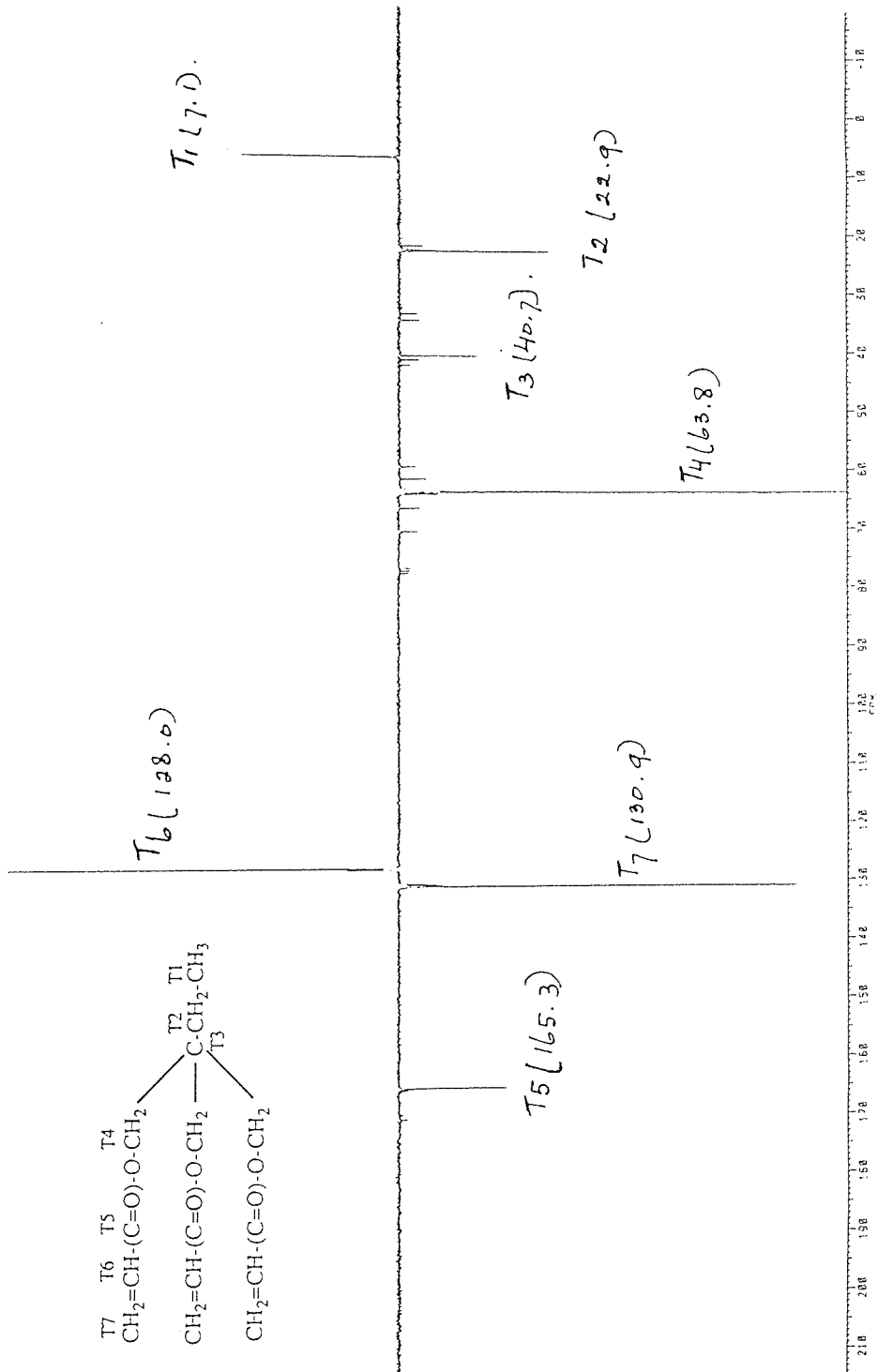


Figure 5.50 Carbon-13 NMR spectrum of fresh Tris in CDCl₃

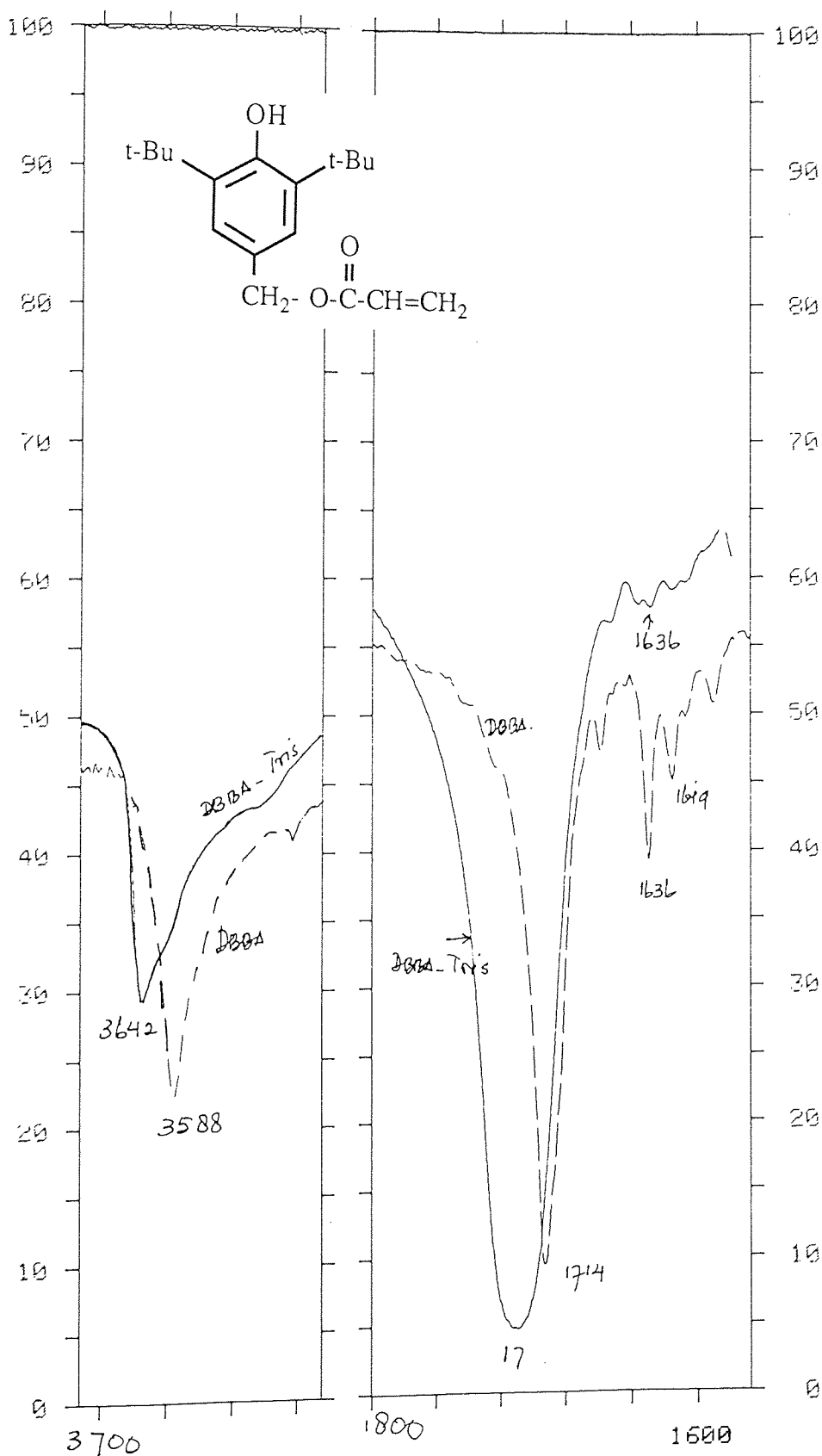


Figure 5.52 Comparison of FTIR spectra (in region 3700-1300 cm⁻¹) of polymerised DBBA-Tris in the presence of 0.02 m.r (I/DBBA+Tris) initiator AZBN, see Scheme 5.11 stage D (—), with that of fresh DBBA (-----), both using KBr disc.

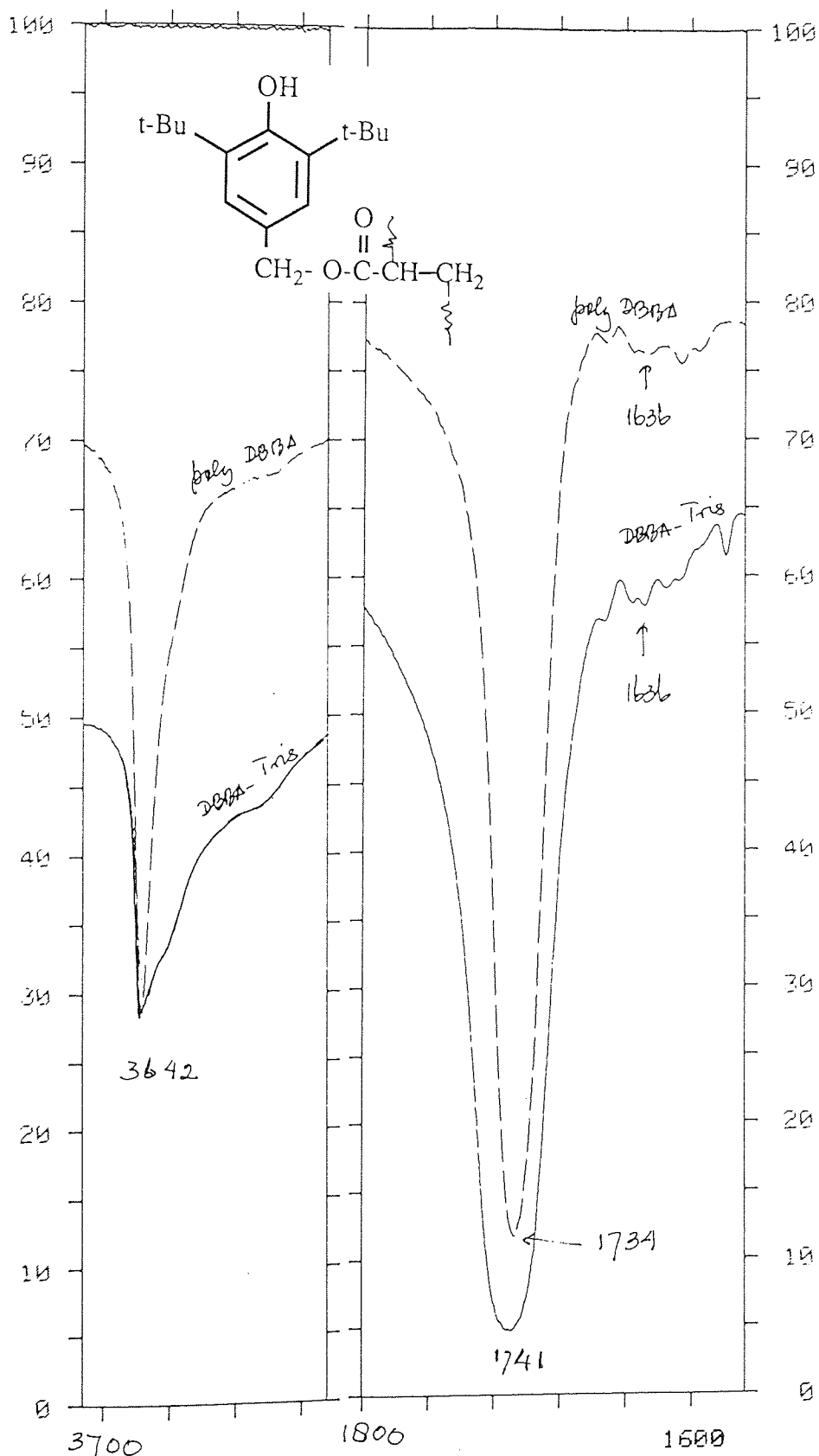


Figure 5.53 Comparison of FTIR spectra (in region 3700-1300 cm^{-1}) of polymerised DBBA-Tris in the presence of 0.02 m.r. (I/DBBA+Tris) initiator AZBN, see Scheme 5.11 stage D (—), with that of polymerised DBBA without decalin, see Scheme 5.2 stage D (-----), both using KBr disc.

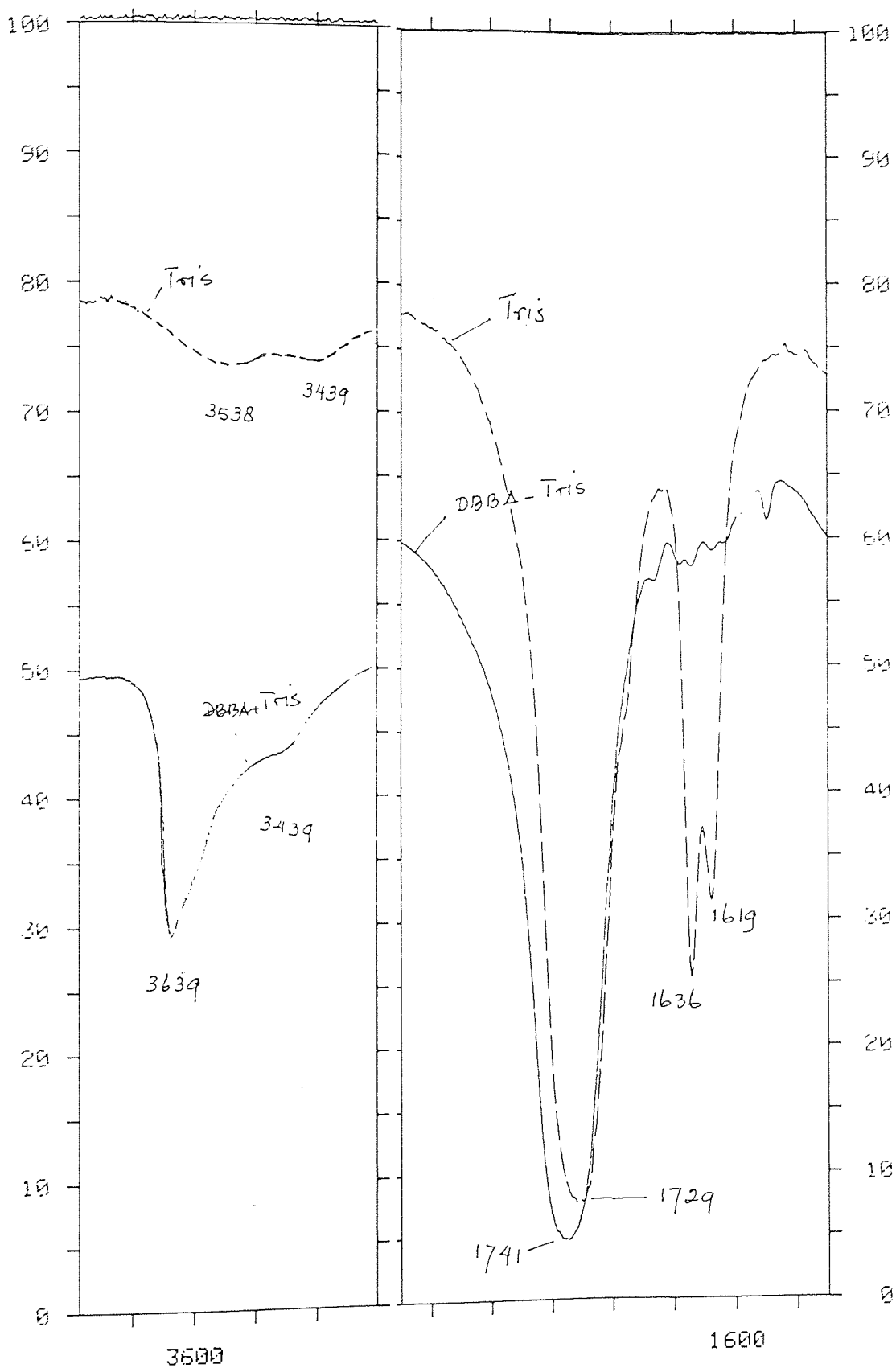


Figure 5.53a Comparison of FTIR spectra (in region 3700-1300 cm^{-1}) of polymerised DBBA-Tris in the presence of 0.02 m.r (I/DBBA+Tris) initiator AZBN, see Scheme 5.11 stage D in KBr disc (—), with that of fresh Tris as neat liquid (-----).

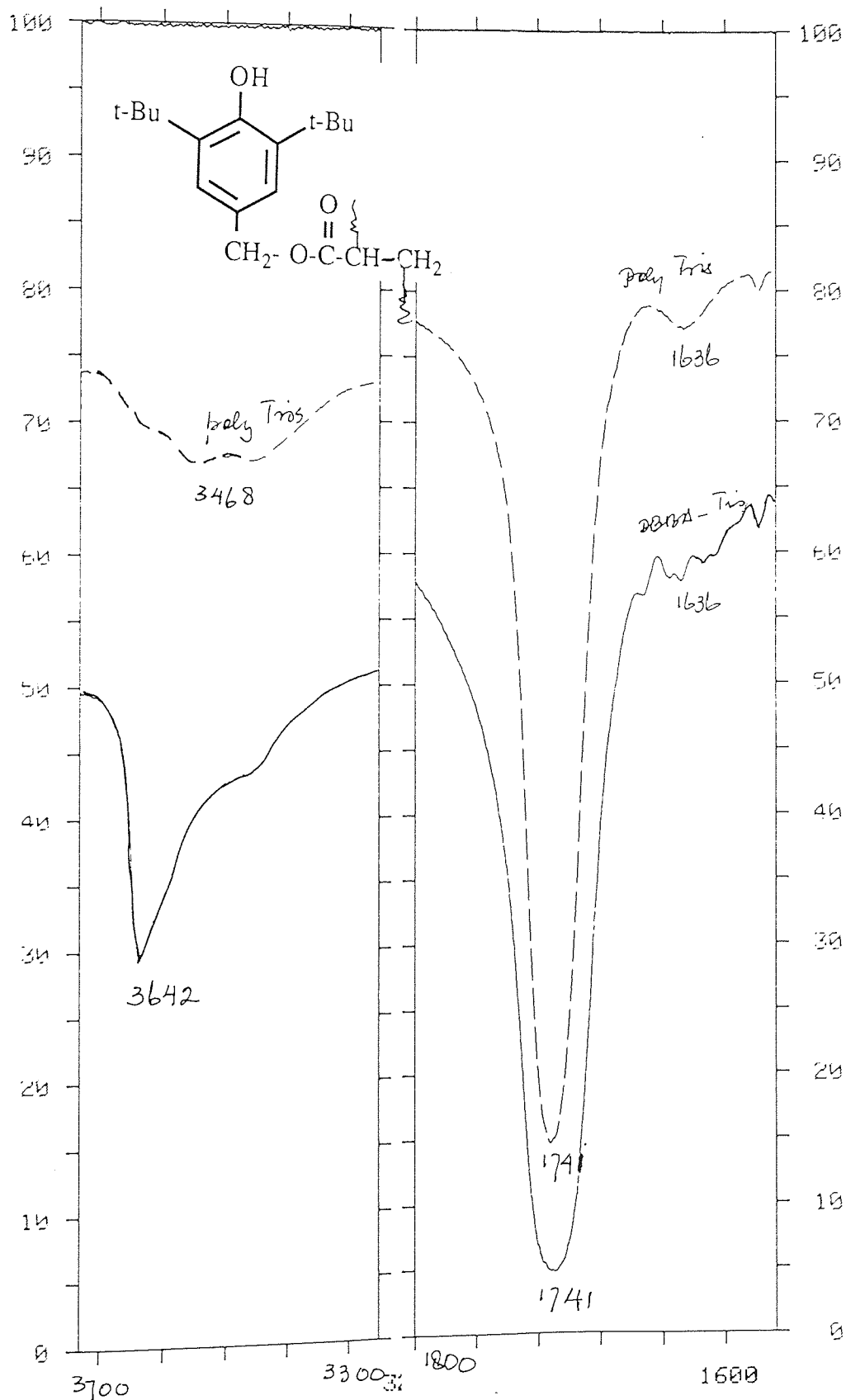


Figure 5.54 Comparison of FTIR spectra (in region 3700-1300 cm^{-1}) of polymerised DBBA-Tris in the presence of 0.02 m.r (1/DBBA+Tris) initiator AZBN, see Scheme 5.11 stage D (—), with that of polymerised Tris, see Scheme 5.10 stage C (-----) both in KBr disc.

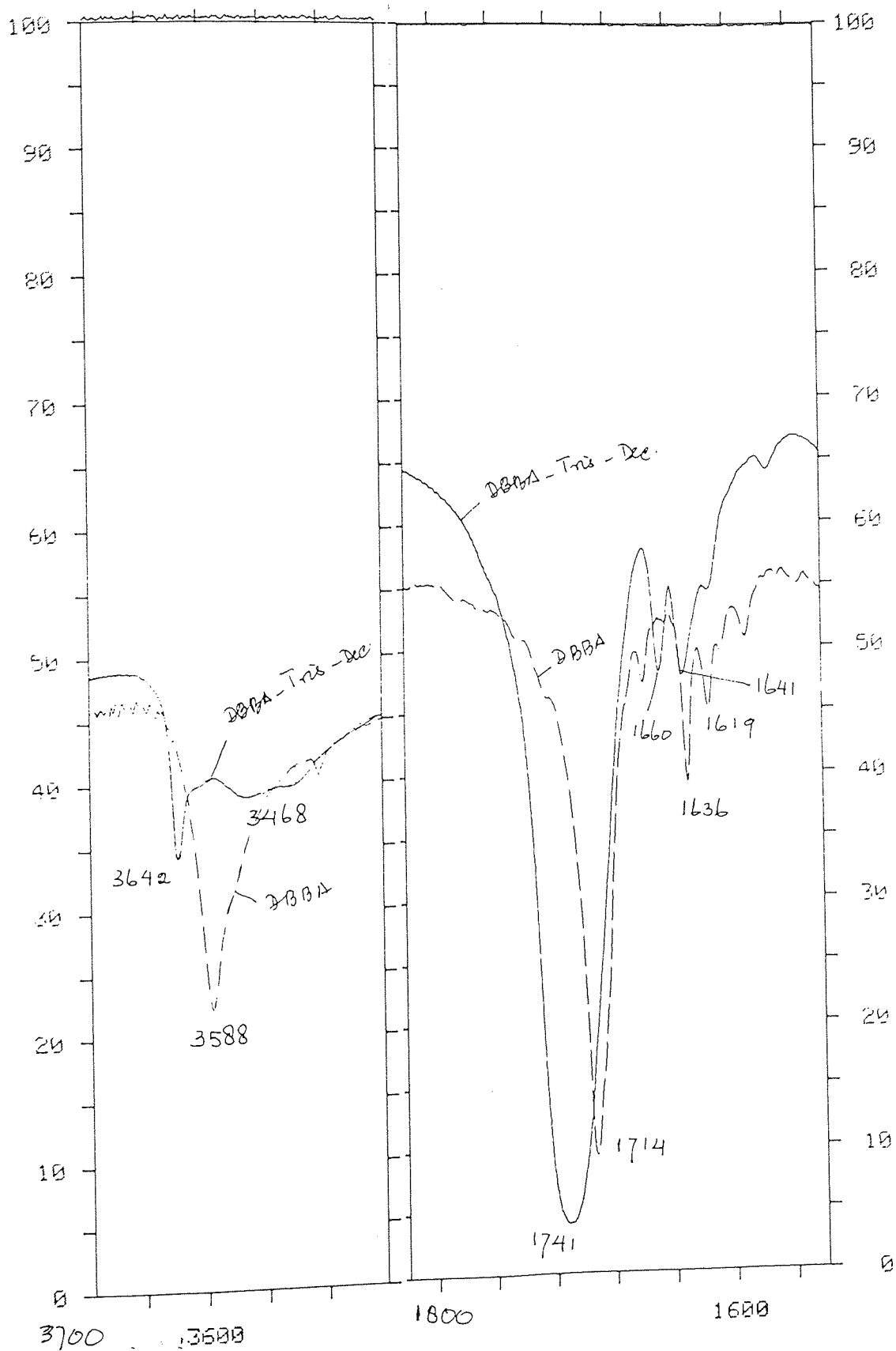


Figure 5.55a Comparison of FTIR spectra (in region 3700-1300 cm^{-1}) of polymerised DBBA-Tris in the presence of 0.02 m.r. (I/DBBA+Tris) initiator AZBN, see Scheme 5.11 stage D (—), with that of fresh DBBA (-----) both in KBr disc.

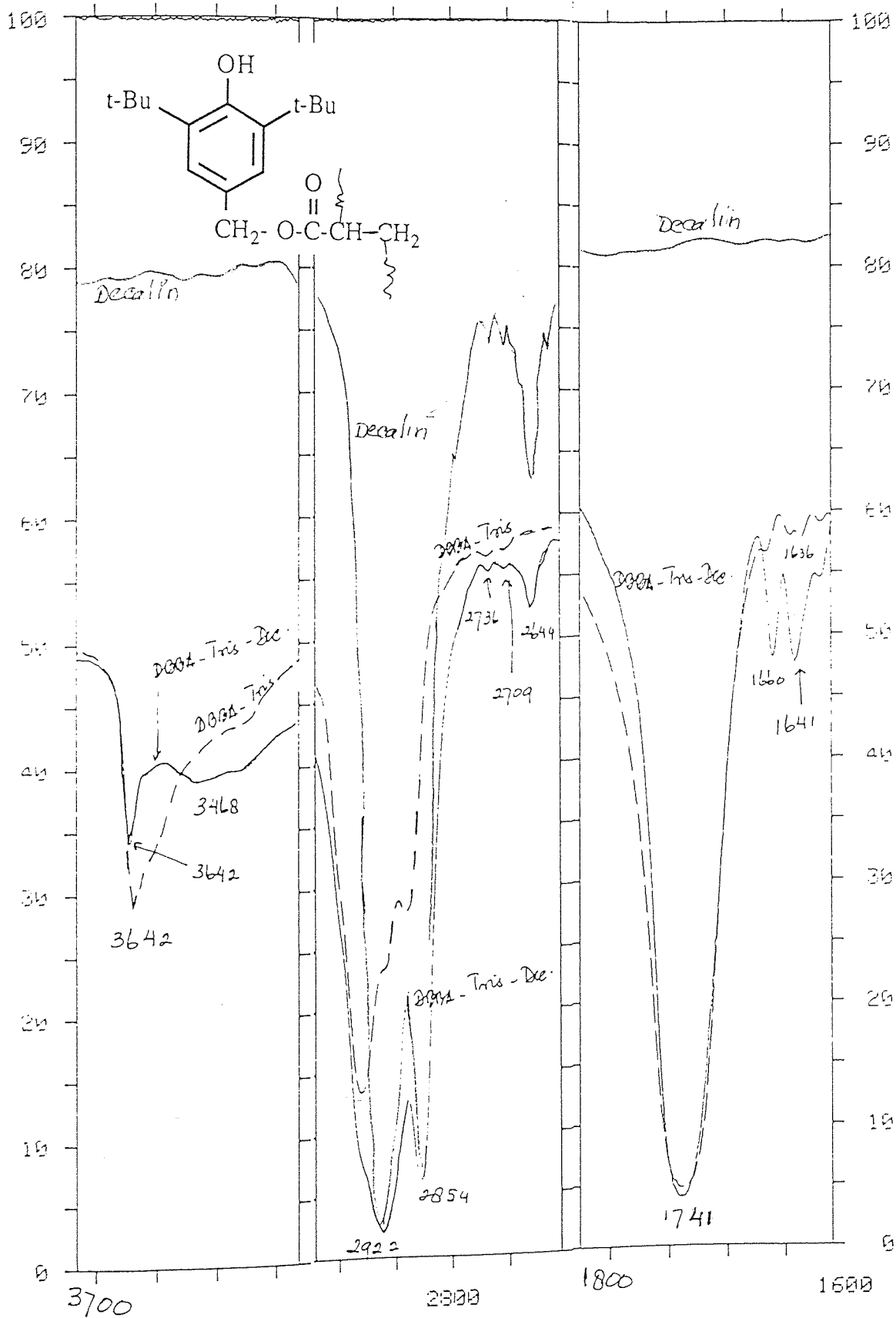


Figure 5.56 Comparison of FTIR spectra (in region 3700-1300 cm⁻¹) of polymerised DBBA-Tris-Decalin in the presence of 0.02 m.r (I/DBBA+Tris) Trigonox 101, see Scheme 5.12 stage F(—), with polymerised DBBA+Tris without decalin, see Scheme 5.11 stage D (-----), both using KBr disc.

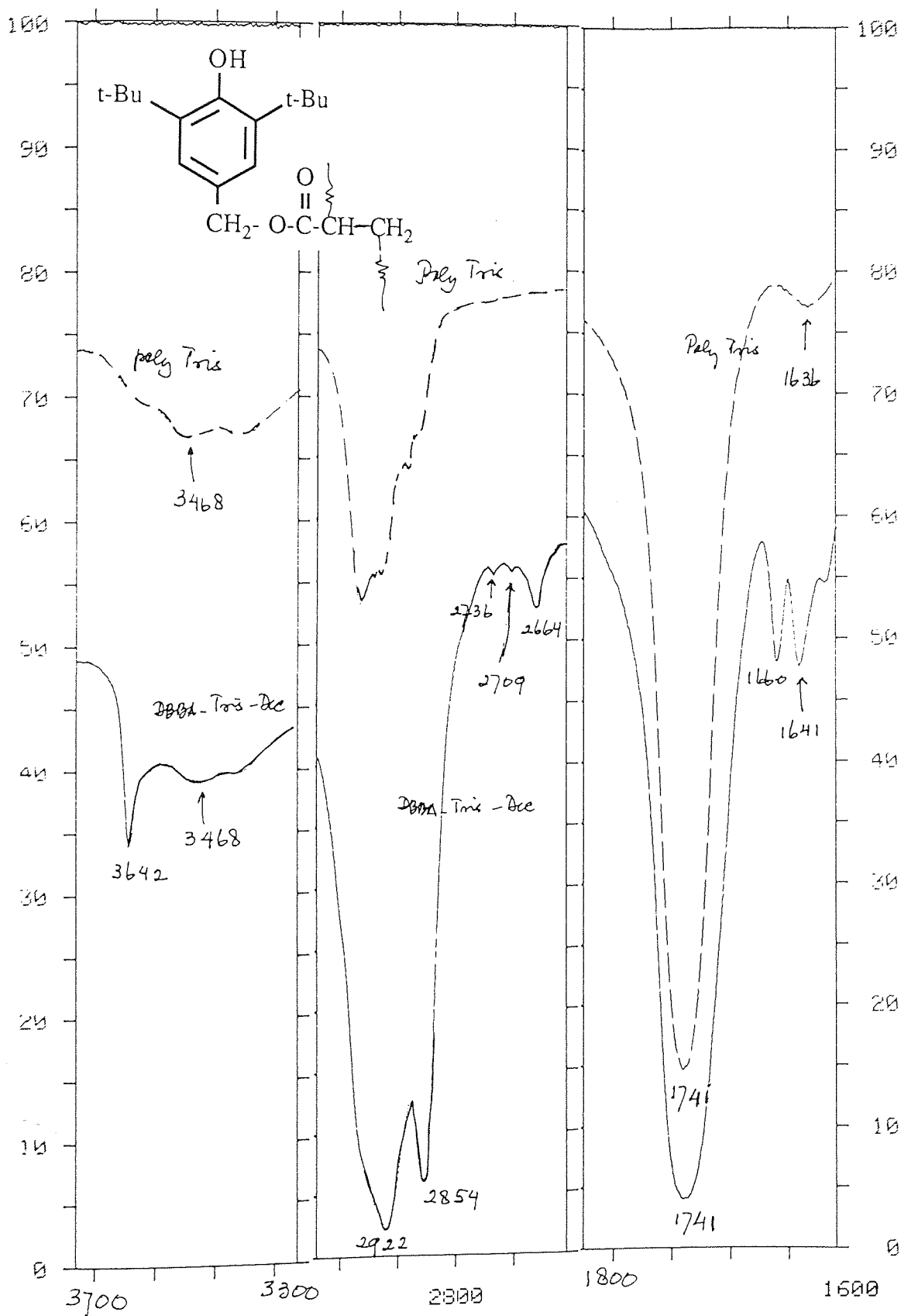


Figure 5.57 Comparison of FTIR spectra (in region 3700-1300 cm⁻¹) of polymerised DBBA-Tris-Decalin in the presence of 0.02 m.r (I/DBBA+Tris) Trigonox 101, see Scheme 5.12 stage F(—), with polymerised Tris (-----), both using KBr disc.

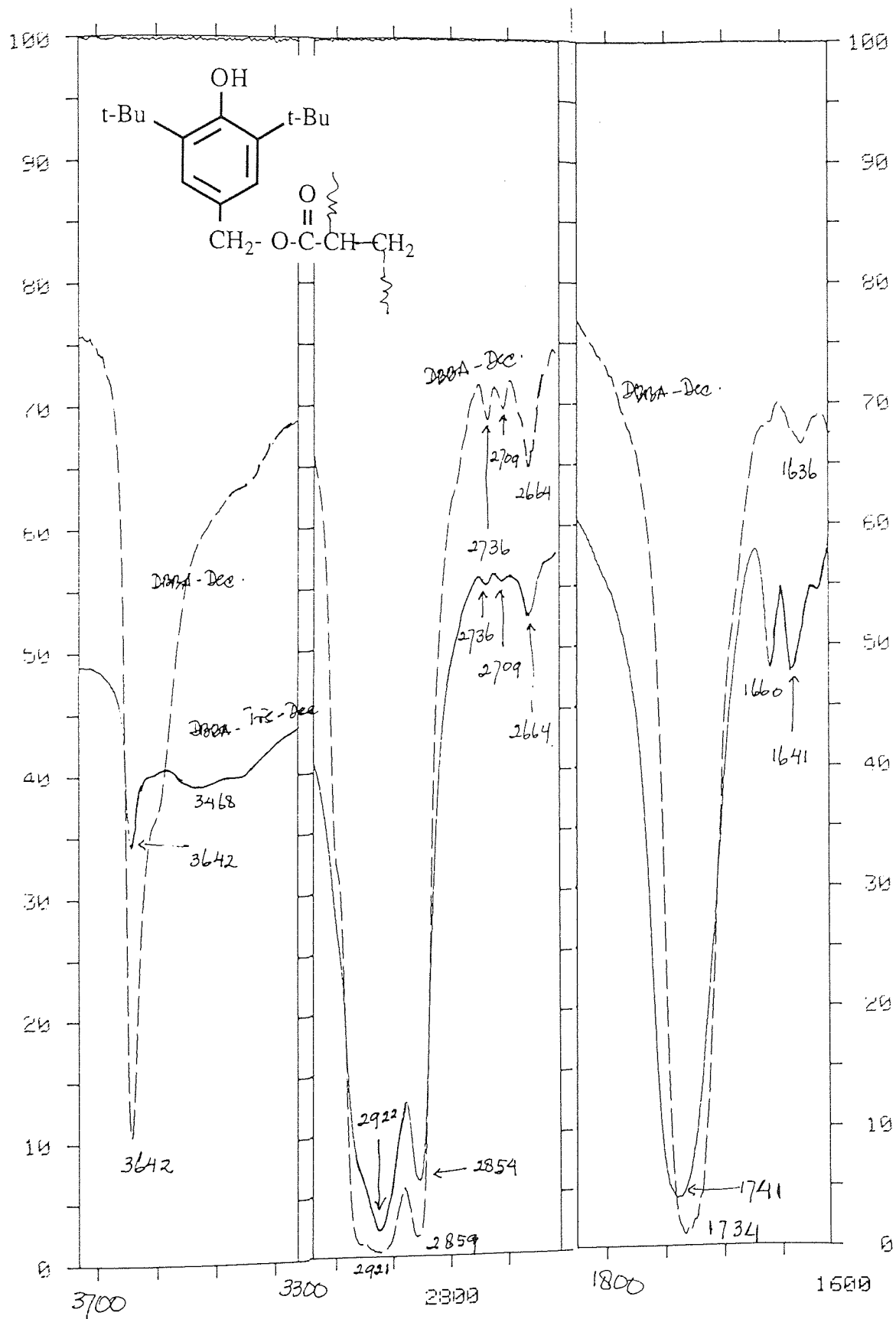


Figure 5.58 Comparison of FTIR spectra (in region $3700\text{-}1300\text{ cm}^{-1}$) of polymerised DBBA-Tris-Decalin in the presence of 0.02 m.r (I/DBBA+Tris) Trigonox 101, using KBr disc, see Scheme 5.12 stage F (—), with that polymerised DBBA-Decalin, see Scheme 5.2 stage D (-----) both in KBr disc.

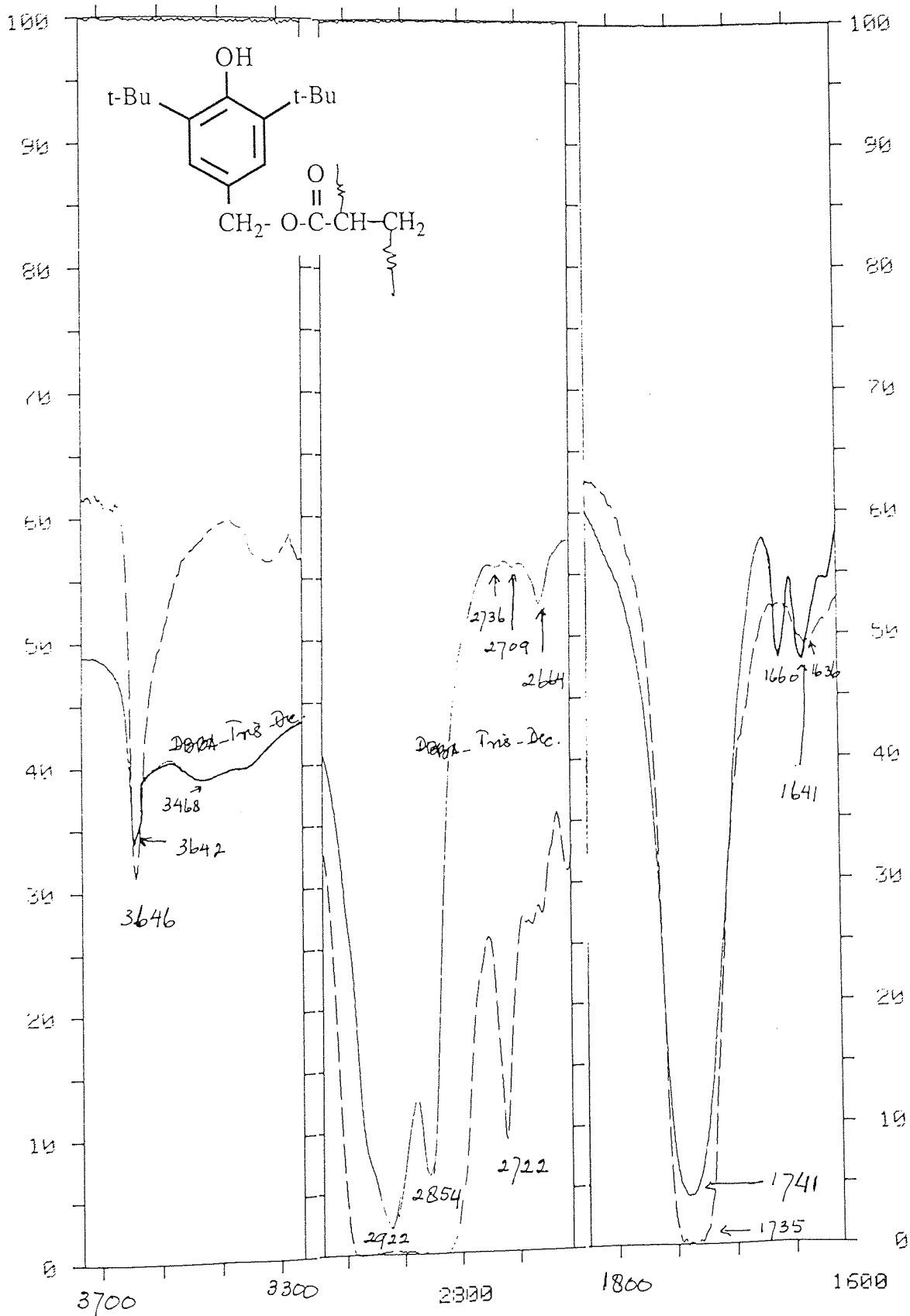


Figure 5.59 Comparison of FTIR spectra (in region 3700-1300 cm^{-1}) of polymerised DBBA-Tris-Decalin in the presence of 0.02 m.r (I/DBBA+Tris) Trigonox 101, see Scheme 5.12 stage F using KBr disc (—), with 10%MB's film containing (DBBA+Tris) processed in the presence of 0.02 m.r Trigonox 101, after DCM extraction see Scheme 5.5 stage C (-----).

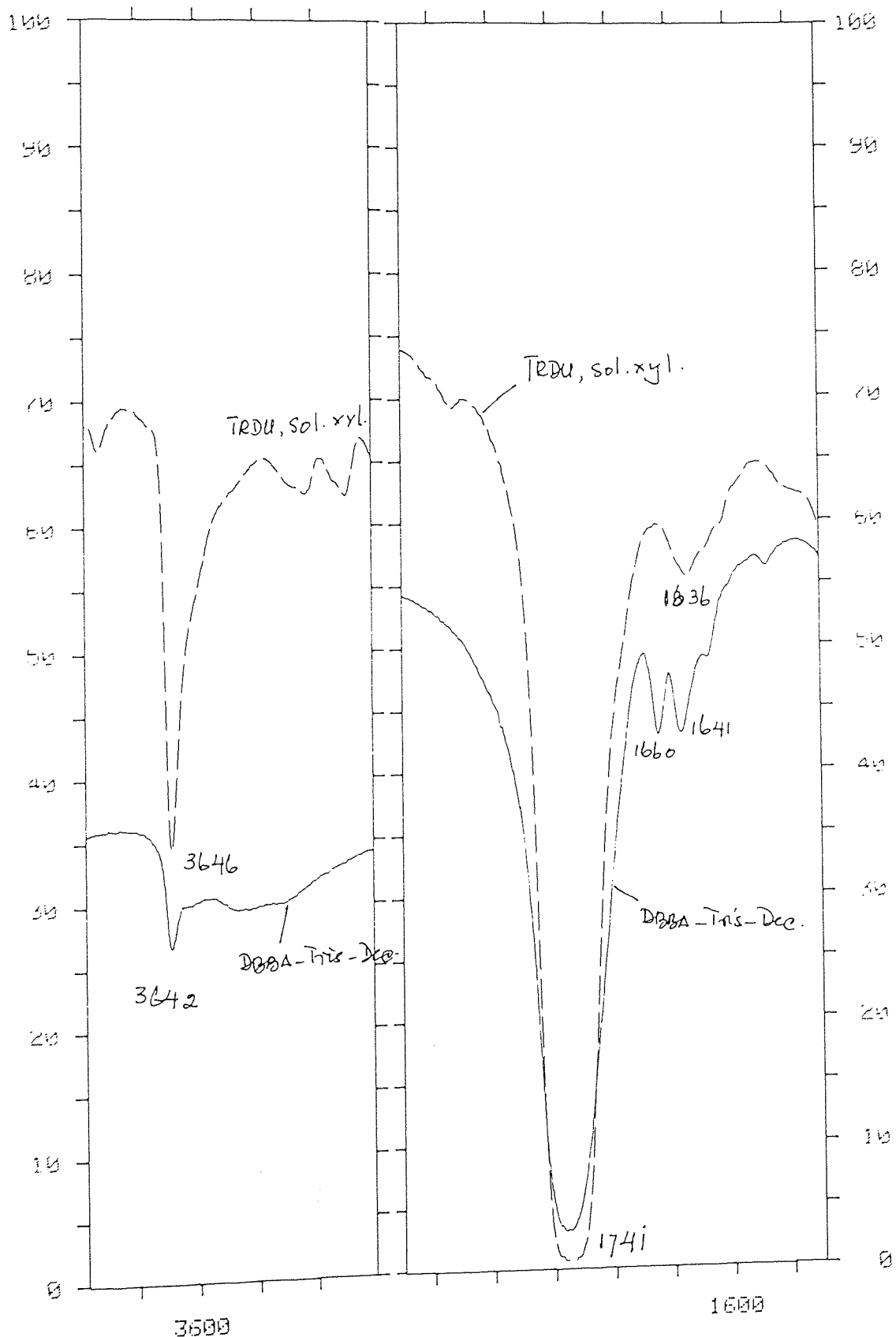


Figure 5.60 Comparison of FTIR spectra (in region 3700-1300 cm^{-1}) of polymerised DBBA-Tris-Decalin in the presence of 0.02 m.r (I)/(DBBA+Tris) Trigonox 101, see Scheme 5.12 stage F using KBr disc (—), with xylene soluble of 10% MB's film containing (DBBA+Tris) processed in the presence of 0.02 m.r Trigonox 101, see Scheme 5.5 stage F (-----).

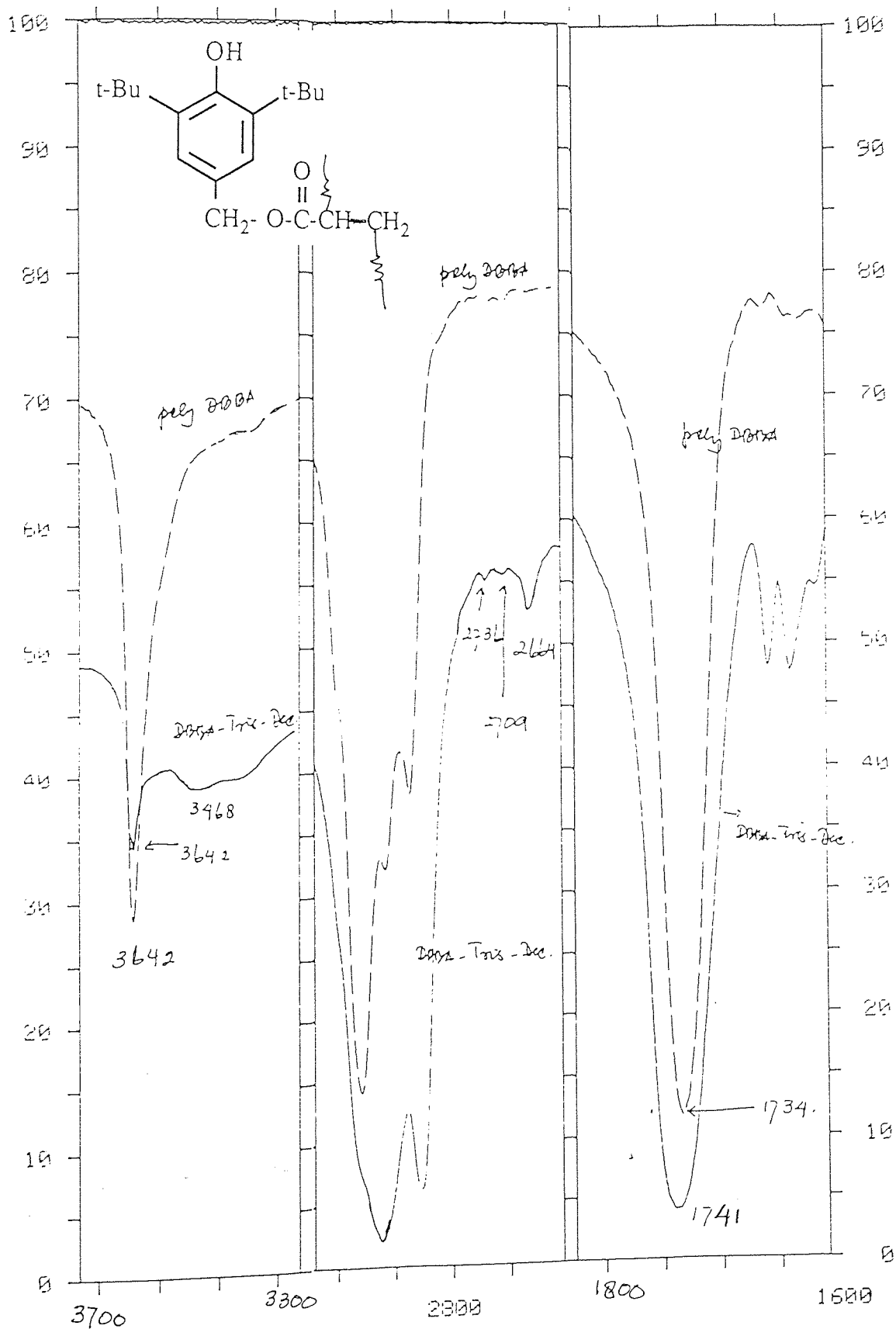


Figure 5.61 Comparison of FTIR spectra (in region 3700-1300 cm⁻¹) of polymerised DBBA-Tris-Decalin in the presence of 0.02 m.r (I/DBBA+Tris) Trigonox 101, using KBr disc, see Scheme 5.12 stage F (—), with that polymerised DBBA without Decalin, see Scheme 5.3 stage D (-----) both in KBr disc.

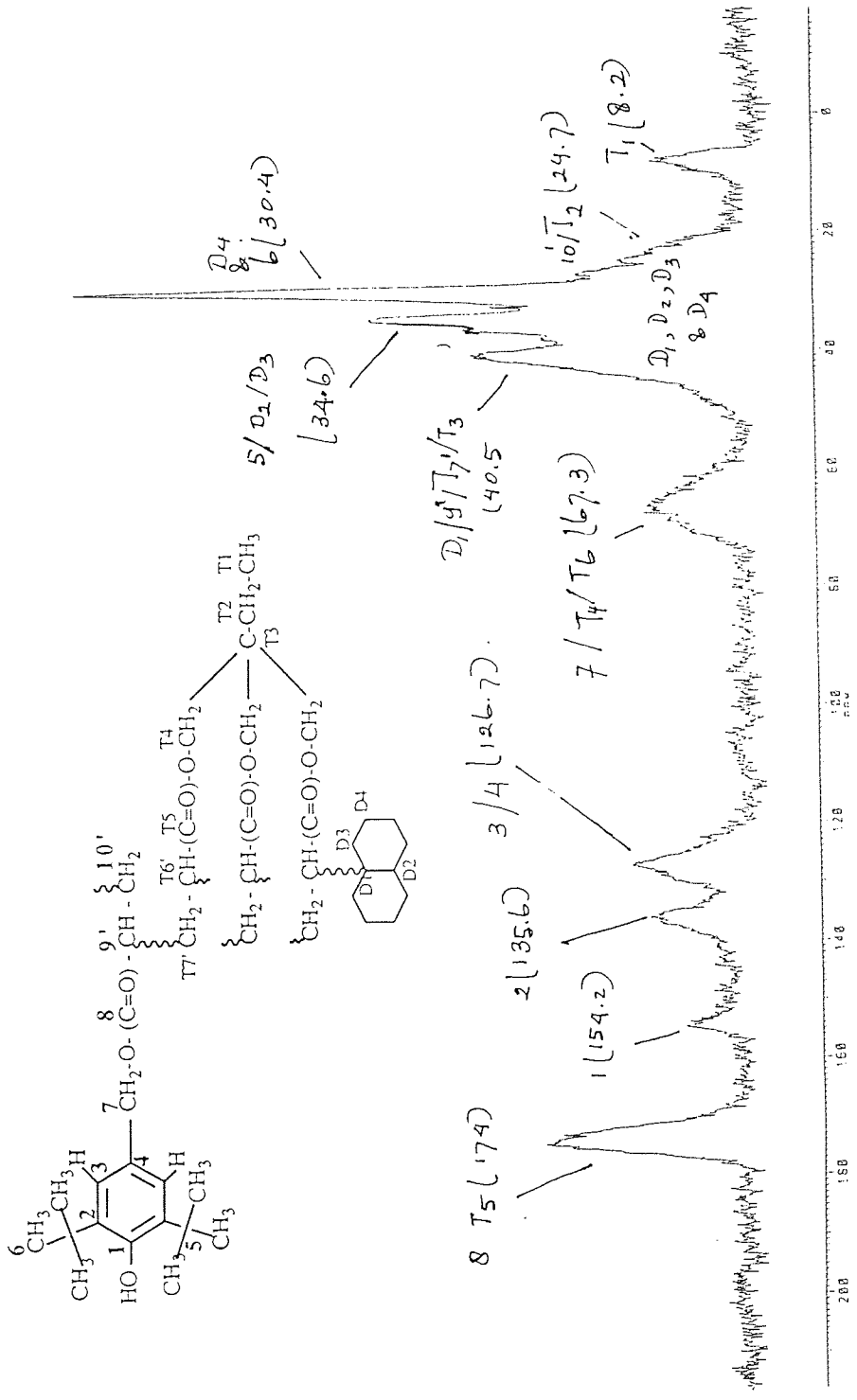


Figure 5.62 Solid state Carbon-13 NMR spectrum of polymerised DBBA+Tris with Decalin in the presence of 0.02 m.r (I)/(DBBA+Tris), see Scheme 5.12 stage F.

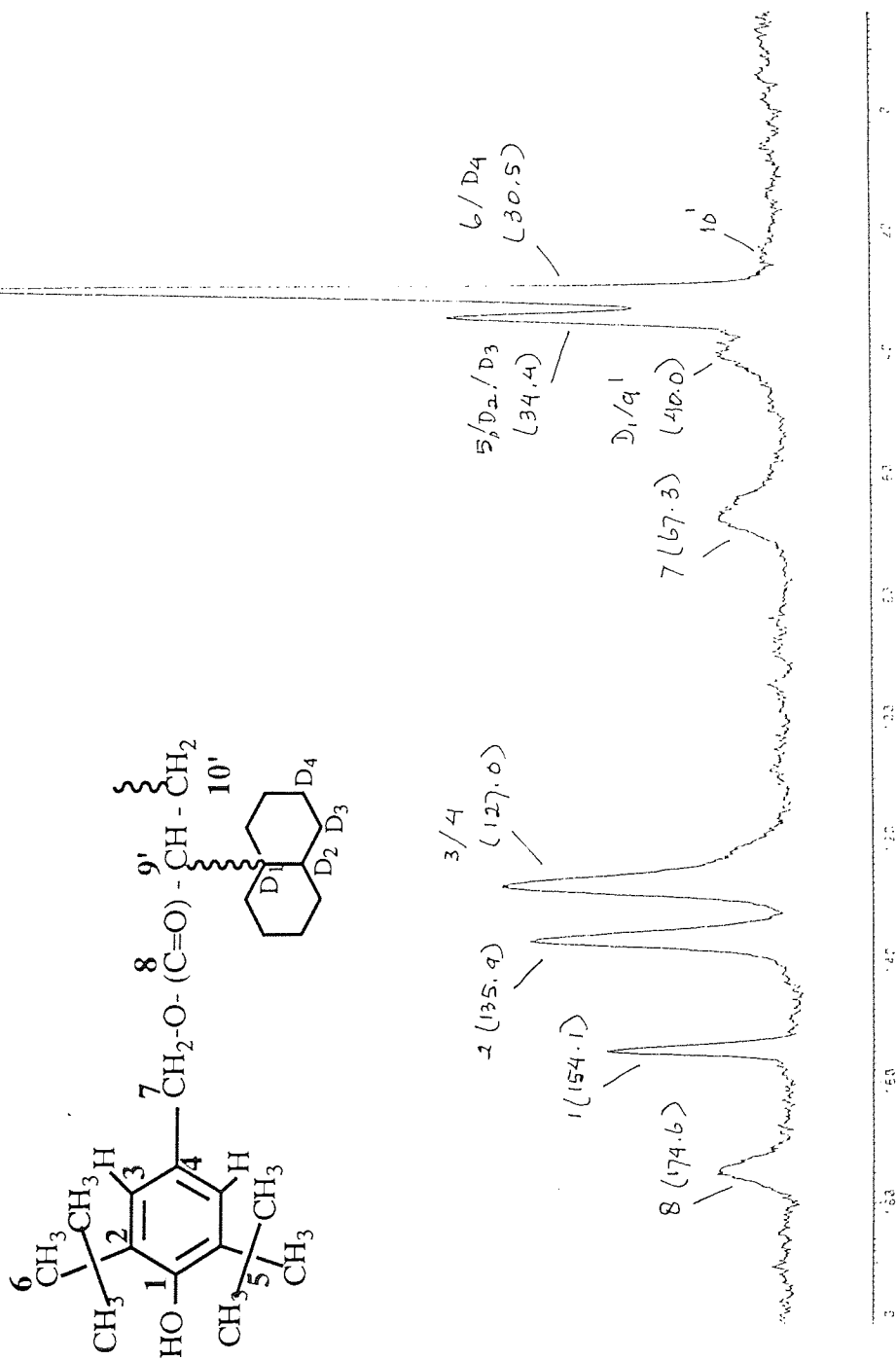


Figure 5.63 Solid state Carbon-13 NMR spectrum of polymerised DBBA with Decalin in the presence of 0.02 m.r (I)/(DBBA), see Scheme 5.2 stage D.

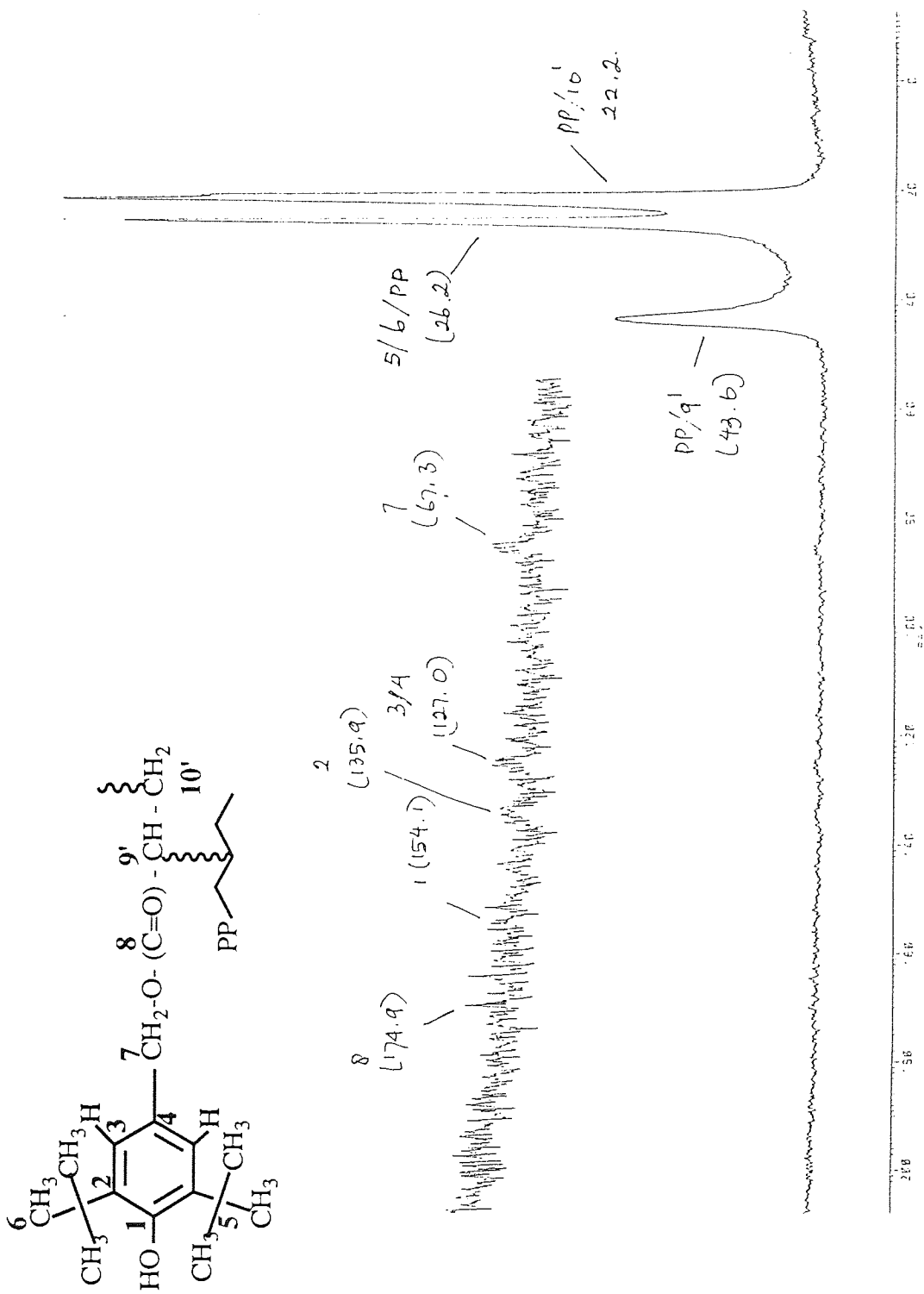


Figure 5.64 Solid state Carbon-13 NMR spectrum of xylene soluble of 10% MB containing DBBA in the presence of 0.02 m.r (I)/(DBBA), see Scheme 5.5 stage F.

CHAPTER SIX

CONCLUSIONS AND RECOMENDATIONS FOR FURTHER WORK

6.1 CONCLUSIONS

The following conclusions can be drawn from results discussed in Chapters 3 to 5:

1. In a typical reactive processing procedure, various acrylic containing hindered phenol antioxidants (e.g. DBBA, VDBP, SGM) which were reacted with polypropylene in the presence of FRI, lead to low level of binding, up to a maximum of 40%. Increasing the antioxidants concentration from 3 to 10%, improved the binding efficiency, but when the concentration was increased to more than 10% the level decreased slightly. At higher peroxide concentrations (up to 0.03 [I]/[AO] molar ratio) the binding level increased considerably, but this was achieved at the expense of melt stability of the polymer, as was reflected by an increase in melt flow index. For the above hindered phenols an optimum binding level ~40% was achieved with 6-10% AO processed in the presence of 0.02 molar ratio peroxide. In the case of acrylic containing benzophenone, HAEB, these conditions lead to binding efficiency of HAEB up to 72% (10% HAEB with 0.005 molar ratio peroxide). The higher concentrations of peroxide needed for hindered phenols compared to benzophenones, is almost certainly due to the fact that hindered phenols act as very effective radical scavengers during processing and this would be expected to reduce the capacity of peroxides in the system.

2. To enhance the efficiency of binding of DBBA and HAEB, various coagents containing multi functional polymer reactive groups, such as DVB and Tris (TMPTA) were used. It was found that the binding level of DBBA can be improved up to 91%, using Tris coagent at a ratio of 4 : 6, in the presence of 0.02 molar ratio of Trigonox 101. DVB can also

improve the binding level (upto 93%), but the MFI of the polymer samples were very low compared to that of Tris, indicating that some crosslinking occurs in this case. In the case of HAEB, the binding efficiency can be extended by using Tris coagent with a ratio of 1 to 9 in the presence of 0.005 molar ratio Trigonox 101, processed for 10 minutes. In this system the processing time plays an important role to determine the final structure of the grafted HAEB onto the PP backbones. At the early stages of processing (short processing time) dramatic increase in gel and molecular weight occurs, but this 'break down' with increasing processing time and after 10 minutes in an internal mixer, the gel content decrease dramatically, becomes similar to that of a control PP. Processing time, however, did not change on level of 'binding'.

3. Photo stabilising activity of bound acrylic hindered phenols or acrylic benzophenone antioxidants processed with or without Tris coagent was found to be lower than that of their corresponding unbound analogous before extraction. However, the retention activity of the bound antioxidants was much higher compared to that of the unbound antioxidants or commercial AO's having similar AO function used as conventional additives (i.e. much higher retention of activity in the case of bound AO's after extraction). Both the hindered phenols (a melt stabilisers) and the benzophenone (a UV absorber) can act, to varying extent, as radical scavengers, during the reactive processing reaction, and this may contribute to the reduction of their stabilising activities. However, when the bound DBBA was processed with a coagent, e.g Tris and in the presence of small amount of a UV-screen (HOBP), the excellent UV stabilising activity of the antioxidant was recovered. Extraction of this sample, however, removed all the HOBP, and the stabilising activity was similar to that of the AO when used without HOBP.

4. When (DBBA+HAEB/Tris) system was used (at a weight ratio of total antioxidants to Tris, 8 to 2) very high synergism in photo stabilising activity was achieved. This photo stabilising activity increased with increasing HAEB concentration. This synergism is almost certainly due to the fact that the hindered phenol has the ability to trap the radicals

during processing to protect the degradation of the UV absorber (HAEB), which in turn protect the phenol during the UV-irradiation stage. This synergism is retained even under aggressive environments such as DCM Soxhlet extraction. In contrast, when (DBBA+Tris) and (HAEB+tris) were processed as two separate AO concentrates (MB's), and then both MB's were diluted together in fresh PP (second processing step), it was found that their photo stabilising activity was much lower when compared with the (DBBA+HAEB/Tris) system which undergone a single processing step. In this case of the former, DBBA can not protect the HAEB as UV screen during processing and the HAEB may act as radical scavenger which could in turn destroy the stabilisation function of HAEB.

5. Thermal stabilising activity (at 140° C with air flow at a rate of 85 l/hours) of bound acrylic hindered phenols (i.e. DBBA, VDBP) processed with or without Tris was found to be higher than the corresponding unbound analogues. This is attributed to evaporation of the unbound antioxidants. The substantivity of the antioxidants become more important when the polymer is used at high temperature as a high surface-weight ratio materials, such as film or fibre. The thermal stabilising activity of commercial stabilisers (i.e. Irganox 1076, Irganox 1010) have very high performance compared with bound acrylic hindered phenol. However the retention of activity of the bound DBBA and VDBP processed with Tris was shown to be much higher when compared with the commercial antioxidants (e.g. Irganox 1010 and 1076).

6. Investigation of the progress of the reaction of HAEB with PP melt during processing in the absence of a coagent was carried out, using both physical and spectroscopic methods. From torque recorder, gel content, and molecular weight data, it was shown that at the beginning of the processing (2.5 minutes), crosslinked (non permanent) and high molecular weight products were formed. However, at the end of the processing (10 minutes) most of the product almost certainly undergo chain scission to give a polymer with lower molecular weight (similar to that of a processed PP control). The evidence

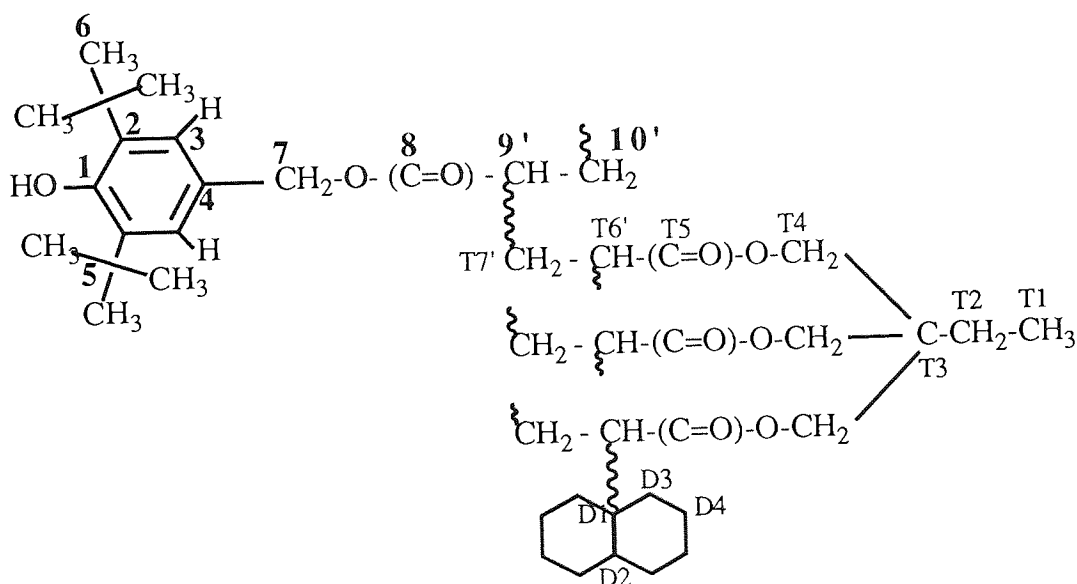
suggests that the changes in the structure during processing is most likely to be due to restructuring of the graft polymer as shown in Schemes 5.13 and 5.14. Most of the extractable HAEB in DCM (27%) was shown to be a homopolymer of HAEB. At the early stage of the reaction e.g after 2.5 minutes processing, 45% of the HAEB content was found to be present in the polymer gel; 22% of HAEB content was found to be present in the xylene soluble polymer (higher molecular weight); and 6% of HAEB content was in the toluene soluble polymer (lower molecular weight). At the end of reaction, after 10 minutes processing, the picture was completely different, no gel in the polymer was found; 48% of HAEB content was found in the xylene soluble (higher molecular weight) polymer; and 25% of HAEB content was found in the toluene soluble (lower molecular weight) polymer.

7. Investigation of the course of the reaction of DBBA in the presence and absence of coagent in polypropylene was carried out using both physical and spectroscopic methods. The binding efficiency of DBBA without coagent was shown to be 40%; however, in the presence of Tris coagent the binding efficiency increased up to 91% and the Soxhlet DCM extract of these concentrate was shown in both cases to be almost entirely the homopolymer of DBBA. The structure of DBBA graft in the extracted polymer processed in absence and presence of Tris were shown to be very different (see Scheme 5.15 and 5.15). In the absence of Tris, only 40% of DBBA was retained in the polymer. 30% of DBBA content was found in the xylene soluble polymer (making ~21% of the total), 10% of DBBA content was found in toluene soluble polymer (making ~73% of the total). In the presence of Tris, on the other hand, 91% of DBBA remained in the polymer, after Soxhlet extraction, out of which 83% of DBBA content was found in the xylene soluble polymer and 10% of DBBA content was found in the toluene soluble polymer. However, in both cases, no gel was found to be in the polymer. It is important to point out the finding that the presence of Tris as a coagent in a DBBA system, can improve the binding efficiency of DBBA, but does not change the property of polymer (e.g. no crosslinking was formed). In the presence of DVB coagent enhanced binding efficiency of DBBA was achieved, up to 93%, and the overall structure of the DBBA graft is most likely to be similar to that formed

when using similar Tris as coagent, see Scheme 5.17. However, DVB differs from the case of the Tris, in that the former lead to ~7% crosslinking product in the final processed polymer, and this crosslinking material contains 15.5% of the total DBBA content.

8. FTIR analysis of polymerised DBBA in decalin solution at 180°C for 5 hours, showed the disappearance of all the typical absorptions of the acrylic double bound in the DBBA structure (at 1408 cm^{-1} and decreasing intensity of 1636 cm^{-1} absorptions), and the appearance of new absorptions at 2922, 2854, 2736, 2709 and 2644 cm^{-1} (these absorptions are due to decalin). The FTIR spectra of the homopolymer of DBBA, grafted DBBA-Decalin model reaction product and grafted DBBA masterbatch, showed very similar spectra with C=O absorption shift, suggesting a saturated C=O (e.g. saturated carbonyl absorption at 1735 cm^{-1}). Analysis of the polymerised DBBA by proton NMR spectroscopy, showed that the protons of the acrylic double bound ($-\text{CH}=\text{CH}_2$) at δ (ppm) = 6.15-6.23, 6.44-6.50 and 5.82-5.86 has disappeared, and proton saturated were formed as the result of saturation acrylic ($>\text{CH}-\text{CH}_2-$) were found at δ (ppm) = 0.85-0.95 and 2.04-2.35. However protons of decalin were not found clearly, because of overlap with other protons at chemical shift between 1.0-2.0 ppm. ^{13}C NMR spectrum of the polymerised DBBA showed the complete disappearance of acrylic carbon at δ (ppm) = 128.6 and 130.1, and appearance of the new saturated carbon at δ (ppm) = 43.1 and 21.7. Decalin carbons were found at δ (ppm) = 26.7 and 36.2, but the other two decalin carbons did overlap with other DBBA carbon at δ (ppm) = 43.3 and 34.2 (see Figure 5.43). In situ ^{13}C NMR investigation, of polymerisation of DBBA in decalin at 100°C (in the NMR cavity) gave similar results. In addition, after 25 hours polymerisation at 100°C, one of the $>\text{CH}-$ peak of decalin at δ (ppm) = 43.1 decreased sharply. This peak is known as that of the trans $>\text{CH}-$ which is more susceptible to hydrogen elimination than the cis. Therefore, the peroxide used in polymerisation may also attack the trans $>\text{CH}-$ of the decalin solvent, which then grafts to the DBBA polymer.

9. In the presence of Tris, the FTIR analysis of polymerised (DBBA+Tris) in decalin showed the disappearance of the typical acrylic absorptions; double bond of DBBA at 1408 cm^{-1} and decreasing intensity of 1636 cm^{-1} absorption, and the appearance of new absorptions at $2922, 2854, 2736, 2709$ and 2644 cm^{-1} . The FTIR spectra of a copolymer DBBA-Tris, grafted DBBA-Tris-Decalin model reaction product and grafted DBBA-Tris masterbatch, showed also very similar overall results in that the unsaturated C=O becomes saturated (saturated carbonyl absorption at 1741 cm^{-1}). Solid state of ^{13}C NMR spectrum of copolymerised DBBA-Tris showed the complete disappearance of acrylic carbon groups of DBBA overlaps to that of Tris at δ (ppm) = 128.6 and 130.1ppm, and was replaced with the new methyn saturated carbons (C no.9' overlapped with C no. T4 and T6') appears at 66.1ppm. The new methylenic saturated carbon (C no. 10' overlapped with C no. T2) and methyl carbon of Tris (C no. T1) at 7.7 ppm. When solid state ^{13}C spectrum of model reaction of a copolymer of DBBA-Tris was compared with that of model reaction of polymerised DBBA-Tris-Decalin, it was revealed that similar resonance peaks occurred, except in the area between 20.00 to 40.00 ppm which was more crowded. In the latter case, should be due to that the decalin absorption in this region, i.e. C no. D1 overlapped with C no. 9', T3 and T7' at 34.6 ppm; C no.D2 overlapped with C no. D3 and 5 at 34.6 ppm, and at 30.4 ppm, C no.D4 overlapped with C no.6.



Grafted copolymer DBBA-Tris with Decalin

10. Analysis using physical technique (Soxhlet extraction with different solvent) and GPC for molecular weight distribution showed that bound-DBBA xylene soluble polymer processed with Tris as coagent, has higher molecular weight (M_n), compared to that of processed without coagent, however, still lower than that of processed PP without any additive. This indicates that Tris coagent may inhibits further melt degradation of polymer. Model reaction of DBBA in liquid hydrocarbon (decalin) and analysis of products using FTIR and NMR spectroscopy showed the formation of grafted DBBA onto decalin molecules, as well as homopolymerisation of antioxidant. in the presence of Tris coagent, copolymerisation of DBBA with Tris inevitably occurred, which was followed by grafting of the copolymer onto decalin. FTIR and NMR results of the polymer concentrates containing bound-DBBA processed with and without Tris coagent, showed similar behaviour as the above model reactions. This evidence supports the effect of Tris coagent in enhancing the efficiency of the reaction of DBBA in polymer melt.

6.2 RECOMENDATIONS FOR FURTHER WORKS

1. This work advanced our understanding of the nature of the grafting reaction of reactive hindered phenol AO's in PP melt and the structure of the antioxidant-grafted polymer through model compound reactions, under conditions very closed to that used during processing. However, so far, estimation of the binding efficiency, has been limited only in systems where the homopolymerised antioxidant is extractable from the polymer matrix. Further investigations of these reactions, using high sensitivity analytical techniques (i.e. ESR, HPLC, UV, solid state NMR ect.) are required to be carried out on the polymer in order to analyse the polymer products formed during processing.
2. Synthesis of VDBP from Irganox Acid using procedure described in this work gave low yield. Further work can be carried out to modify the synthetic procedure to enhance the yield of this AO may be very promising.

3. In this work, 3% MB containing VDBP was shown to give low binding efficiency in polypropylene. Further work to optimise conditions of VDBP in PP are needed, as well as to examine its stabilising activity in PP under these optimum reaction conditions.

4. In this work, preliminary analysis of the structure of graft HAEB in PP was carried out. Further investigation, may be conducted using model reactions and identification of products formed from the reactively processed HAEB using various spectroscopic techniques especially solid state NMR, may lead to a better understanding of the nature of the graft HAEB reaction.

5. The reactive processing procedure, in this work was carried out in polypropylene. Further work, the reactive processing using multifunctional coagent and reactive antioxidants can be investigated in other polyolefins (e.g. polyethylene, polystyrene, polyvinyl chloride).

REFERENCES

1. Smith.P.I., *Plastic as Metal Replacement*, Chapter-7,10,14 & 15, Scientific Publications (G.B) Ltd., (1968).
2. Scott .G., *in Atmospheric Oxidation and Antioxidants*, Chapter-1, Elsevier Publishing Company, Amsterdam, (1965).
3. Al-Malaika.S., *Comprehensive Polymer Science, Ed.*, G.C.Eastmond, A.Ledwith, S.Russo and P.Segwalt, Vol.6, Pergamon Press, New York, p. 539-579, (1989).
4. Briston.J.H. and Katan.L.L., *Plastic in Contact Food*, Food Trade Press Ltd, Part II, London, (1974).
5. Hardy.W.B., *in Developments in Polymer Photochemistry-3*, N.S.Allen (Ed.), App. Sci. Publ., London, p. 287, (1982).
6. Gould.R.W., Hennman.T.J. & Billingham.N.C., *Brit. Polym. J.*, 16, p. 284, (1984).
7. Lacallade.R., *Chem. Eng. News*, 16 (40), (Oct.24), p.18, (1983).
8. Al-Malaika.S., Scott.G. and Goonetilleka.R., *Polymer Degradation and Stability*, 32, p.231, (1991).
9. Al-Malaika.S., *in Free Radical & Food Additives: Toxicological Implications*, Chapter-7, O.Arouma and B.Halliwell (Ed.), Taylor & Francis, London, (1991).
10. Wall.L.A., Flynn.J.H., *Rubber Chem. Technol.*, 35, p. 1157, (1962).
11. Basedow.A.M., Ebert.K.H., Hunger.H., *Macromol. Chem.*, 180, p.411, (1970).
12. Sandner.M.R., Osborn.C.L., and Treckner.D.J., *Polym. Sci. Chem. Ed. J.*, 10, p. 3173, (1972).
13. Heller.H.J., and Blattmann.H.R., *Pure Appl. Chem.*, 30, p.145, (1972).
14. Casale.A., and Porter.R.S., *Polymer Stress Reaction*, Academic Press, New York, (1978) .
15. Goldberg.V.M. and Zaikov.G.E., *Polymer Degradation and Stability*, 19, p.221, (1978).
16. Sadrmoaghegh.C., and Scott.G., *Polymer Degradation and Stability*, 3, p.333, (1980-81).
17. Scott.G., *J. Polym. Sci. Symp.*, 57, p.357, (1976).
18. Scott. G., *Polym. Plast. Tech. Eng.*, 11, p.1, (1978).
19. Scott. G., *Polym.Eng. Sci.*, 24, p.1007, (1984).
20. Gilead.D., and Scott.G., *in Developments in Polymer Stabilisation-5*, G.Scott. (Ed.), Appl.Sci. Publ., London, p.71, (1982).
21. Henman.T.J., *in Developments in Polymer Stabilisation-6*, G.Scott. (Ed.), Appl.Sci. Publ., London, p.107, (1985).

22. Chakraborty.K.B., and Scott.G., *Eur. Polym. J.*, 13, p.731, (1977).
23. Gol'dberg.V.M. and Zaikov.G.E., *Polymer Degradation and Stability*, 19, p.221, (1987).
24. Al.Malaika.S., in *Encyclopedia of Engineering Mats*, Ed. N.P.Cheremisinoff, Vol-2, Marcel Dekker, New York, p.261, (1984).
25. Reich.L., Stivala.S.S., *Autoxidation of hydrocarbons and polyolefins*, Marcel Dekker, New York, (1968).
26. Bolland.J.L, *Quart. Rev.* , 3, p. 1₂ (1949).
27. Bolland.J.L, and Cooper.H.R., *Proc. Roy. Soc., A*, 225, p. 405, (1954).
28. Hiatt.R., Mill.T., and Mayo. F.R., *Org. Chem. J.*, 33, p. 1416, (1968).
29. Ingold.K.U., *Pure Appl. Chem.*, 15, p. 19, (1967).
30. Simoyi.M., and Tudos.F., *Adv. Phys. Org. Org.*, 9, p. 127, (1971).
31. Carlsson.D.J. and Wiles .D.M., *J. Macromol. Sci. Rev. Macromol. Chem.*, p. 66-103, (1976).
32. Rabek.J.F., *Photostabilisation of polymers*, Chap.5, Elsevier Sci.Publ., Essex, (1990).
33. Al-Malaika.S. and Scott.G., *Polymer Degradation and Stabilisation*, Chapter-7, Cambridge University Press, London, (1983).
34. Grassie.N., and Scott.G., *Polymer Degradation and Stabilisation*, Chap.3, Cambridge University Press, London, (1985).
35. Norrish.R.G.W., and Searby.M.H., *Proc. Roy. Soc. A*-237, p.464, (1956).
36. Scott.G., *British Polym. J.*, 16, p. 271 - 283, (1984).
37. Scott.G., *Polymer Degradation and Stability*, 10, p. 97 - 125, (1985).
38. Carlsson.D.J. and Wiles .D.M., *J. Rad. Curing*, 2 (4), p.2, (1975).
39. Hawkins.W.L., in *Polymer Stabilisation*, (Ed.) Wiley Inter. Sci., New York, p. 3, (1972).
40. Carlsson.J.R, Garlon.A., and Wiles.D.M., *Development in Polymer Stabilisation -I*, Chapter-7, G.Scott (Ed.), (1979).
41. Cooray.B.B., and Scott.G.,in *Eurp. Polym. J.*, 17, p. 379, (1981).
42. Chakraborty.K.B., and Scott.G., *Polymer*, 18, p. 98, (1977).
43. Carlsson.D.J. and Wiles .D.M., *Macromolecules*, 2, p.597, (1969).
44. Carlsson.J.R., and Wiles.D.M., *Macromolecules*, 2, p. 587-597, (1979).
45. Carvert and Pitts, *Photochemistry*, John Wiley and Sons, Chapter-4, p. 350, (1966).

46. Scott.G., in *Developments in Polymer Stabilisation-4*, Chapter-1, G.Scott. (Ed.), Appl.Sci. Publ., London, (1981).
47. Scott .G., in *Atmospheric Oxidation and Antioxidants*, Chapter-4 and 5 , Elsevier Publishing Company, Amsterdam, (1965).
48. Al-Malaika.S and Scott.G, in *Degradation and Stabilisation of Polyolefins* , N.S.Allen (Ed.), App. Sci. Publ. Ltd., London, p. 247, (1983).
49. Pospisil.J., in *Degradation and Stabilisation of Polymers*, Chapter-4, H.H.J. Jellinek (Ed), Vol.I, Elsevier, Amsterdam, (1983).
50. Grassie.N., and Scott.G., *Polymer Degradation and Stabilisation*, Chapter-5, Cambrigde University Press., London, (1985).
51. Scott.G., in *Developments in Polymer Stabilisation-7*, G.Scott. (Ed.), Appl.Sci. Publ., London, p.65, (1984).
52. Scott.G., Bhageri.R., and Chakraborty.K.B., in *Polymer Degradation and Stability*, **5**, p.145-160, (1983).
53. Holdsworth.J.D., Scott.G., and Williams.D., *J. Chem. Soc.*, p. 4692, (1964).
54. Schwetlick.K., in *Mechanism of Polymer Degradation and Stabilisation*, Chapter-2, G.Scott (Ed.), App. Sci. Publ. Ltd., London, (1990).
55. Al-Malaika.S., in *Mechanism of Polymer Degradation and Stabilisation*, Chapter-3, G.Scott (Ed.), App. Sci. Publ. Ltd., London, (1990).
56. Al-Malaika.S., and Scott. S., in *Eurp. Polym. J.*, **16**, p.7 09, (1980).
57. Dweik.H., *Ph.D. Thesis*, The University of Aston in Birmingham, 1982.
58. Konig.T., and Schwetlick.K., *Polymer Degradation and Stability*, **15**, p.151-160, (1986).
59. Al-Malaika.S., Chakraborty.K.B., and Scott. G., in *Developments in Polymer Stabilisation-6*, Chapter-3, G.Scott. (Ed.), Appl.Sci. Publ., London, (1983).
60. Scott.G., in *Developments in Polymer Stabilisation-6*, Chapter-2, G.Scott. (Ed.), Appl.Sci. Publ., London, (1983).
61. Allen.N.S., in *New Trends in the Photochemistry of Polymer*, Chapter-13, N.S.Allen & J.F.Rabek (Eds.), Elsevier App. Sci. Publ., London, (1985).
62. Vink.P., in *Developments in Polymer Stabilisation-3*, Chapter-4, G.Scott.(Ed.), Appl.Sci. Publ., London, (1980).
63. Ivanov.V.B., Shlyapintokh.V.Y.A., in *Developments in Polymer Stabilisation-8*, Chapter-2, G.Scott. (Ed.), Appl.Sci. Publ., London, (1987).
64. Toda.T., Kurumada.T., Murayama.K., *A.C.S. Symposium-28 Am. Chem. Soc.*, Chapter-3, Klemchuck (Ed.), A.C.S., Washinton, (1985).
65. De Jonge. C.R.H.I., and Hope. P., in *Developments in Polymer Stabilisation-3*, Chapter-2, G.Scott. (Ed.), Appl.Sci. Publ., London, (1987).

66. Shelton. J.R., *Rubb. Chem. and Tech.*, 45, p. 359, (1972).
67. Chakraborty.K.B., Scott.G., *Eur. Polym. J.*, 13, p. 1007, (1977).
68. Scott.G., Yusoff.M.F., in *Polymer Degradation and Stability*, 2, p. 309, (1980).
69. Mar'in.A.P., Cs, in *Polymer Degradation and Stability*, 36, p. 1, (1992).
70. Allen.N.S., *Chem. Soc. Rev.*, 15, p. 373, (1986).
71. Pospisil.J., in *Polymer Degradation and Stability*, 20, p. 181- 202, (1988).
72. Vyprachticky, D., Pospisil.J. & Sedlar.J., in *Polymer Degradation and Stability*, 27, p.49, (1990).
73. Pospisil.J., in *Polymer Degradation and Stability*, 34, p. 85-109, (1991).
74. Gomory.I, Gomoryova.A., Reya.R., and Stimel.J., in *Europ. Polym. J.*, 5 Supplement, p. 545-551, (1969).
75. Allen.N.S., *Macromol. Chem., Rapid. Commun.*, 1, p. 235, (1980).
76. Allen.N.S., McKellar.J.F., and Wilson.D., *Chem. Ind. (London)*, p. 887, (1978).
77. Chakraborty.K.B. and Scott.G., *Chem. Ind. (London)*, p. 237, (1978).
78. Allen.N.S., in *Polymer Degradation and Stability*, 2, p. 129, (1980).
79. Allen.N.S., in *Polymer Degradation and Stability*, 3, p. 73, (1980-81).
80. Vink.P. and Van Veen.Th.J., *Eur. Polym. J.*, 14, p.533, (1978).
81. Carlsson.D.J., Grattan.D.W., Suprunchuk.T., and Wiles.D.M., *J. Appl.Polym. Sci.*, 22, p. 2217, (1978).
82. Al-Malaika.S., Marogi.A., and Scott.G., in *J. App. Polym. Sci.*, 30, p.789-797, (1985).
83. Al-Malaika.S., Cooker.M., and Scott.G., in *Polymer Degradation and Stability*, 10, p.173-183, (1985).
84. Al-Malaika.S., Omikorade.E.O., and Scott.G., in *Polymer Communications*, 27, p.173-174, (1986).
85. Carlsson.D.J., Grattan.D.W., Suprunchuk.T., and Wiles.D.M., *J. Appl. Polym. Sci.*, 16, p.615, (1972).
86. Chakraborty.K.B. and Scott.G., in *Polymer Degradation and Stability*, 1, p.37, (1979).
87. Al-Malaika.S., Chakraborty.K., and Scott.G., in *Developments in Polymer Stabilisation-6*, G.Scott. (Ed.), Appl.Sci. Publ., London, p.73-120, (1983).
88. Scott.G., Sheena.H.H., and Harriman.A.M., in *Eur. Polym. J.*, 14, p.1071, (1978).

89. Scott.G., *Developments in Polymer Degradation-1*, N.Grassie-Ed., Appl. Sci. Publ., London, p. 205, (1977).
90. Ranaweera.R.P.R., and Scott.G., *Eur. Polym. J.*, 12, p.591, (1976).
91. Al-Malaika.S. and Scott.G., in *Eur. Polym. J.*, 19, p.235-240, (1983).
92. Al-Malaika.S. and Scott.G., in *Polymer*, 23, p.1711, (1983)
93. Luston.J., in *Developments in Polymer Stabilisation-2*, Chapter-5, Scott.G. (Ed.), Appl. Sci. Publ. Ltd., London, (1980).
94. Billingham.N.C., Calvert.P.D., in *Developments in Polymer Stabilisation-3*, Chapter-5, G.Scott. (Ed.), Appl.Sci. Publ., London,(1980).
95. Durmis.J., Cs., *Eur. Polym. J.*, 11, p. 219, (1975).
96. Amaraphathy.A.M.A., *Ph.D. Thesis*, The University of Aston in Birmingham, (1975).
97. Ambrovic.P. and Mikovic.J., *Eur. Polym. J., Supplement*, 5, p. 371, (1969).
98. Al-Malaika.S., in *Polymer Plastic Technology Engineering*, 29, (2), p.73, (1990)
99. Scott.G., in *Developments in Polymer Stabilisation-8*, Chapter-5, G.Scott. (Ed.), Appl.Sci. Publ., London, (1987).
100. Munteanu. D., in *Developments in Polymer Stabilisation-8*, Chapter-4, G.Scott. (Ed.), Appl.Sci. Publ., London, (1987).
101. Tucker.R.J., Susi.P.V., *A.C.S. Symposium-280*, Chapter-11, P.P.Klemchuk (Ed), A.C.S., Washinton, (1985).
102. Vogl.O., Cs., *New Trends in the Photochemistry of Polymer*, Chapter-15, N.A.Allen and J.F.Rabee (Eds.), Elsevier Appl. Sci. Publ., London, (1985).
103. Moysan.J.Y., in *Eur.Polym.J.* , 16 (10), p.979, (1980).
104. Hawkins.W.L., Worthington.M.A., Matreyek.W., *J.App.Polym.Sci.*, 3 (9), p.277, (1960).
105. Jackson.R.A., Oldland.S.R.D., Pajaczkowki, in *J.Appl.Polym.Sci.*, 12 (6), p.1297, (1968).
106. Schael.G.W., *J.Appl.Plym.Sci.*, 10 (4), p.653, (1966).
107. Evans.B.W., and Scott.G., *Eurp. Polym. J.*, 10, p. 453, (1974).
108. Cain.M.E., Knight. G.T., and Lewis.P.M., *Rubb.J.*, 150, (2), p. 204, (1968).
109. Cain.M.E., Gazeley.K.F., and Gelling.I.R., *Rubb. Chem. Tech.*, 45, p.20, (1972).
110. Al-Malaika.S., in *Polymer Degradation and Stability*, 34, p. 1-34, (1991).
111. Al-Malaika.S., Ibrahim.A.Q., and Scott.G., in *Polymer Degradation and Stability*, 22, p. 233, (1988).

112. Al-Malaika.S., and Wirjosentono.B., in *Polymer Degradation and Stability*, in Press.
113. Al-Malaika.S., in *Chemical Reactions in Polymers*, Ed.J.L.Benham & J.F.Kinslte, ACS Symp. Ser. 364, p.409, (1988).
114. Sharma.Y.N., Naqvi.M.K., Gawande.P.S., and Bhardwaj.I.S., in *J. of Appl. Polym. Sci.*, 27, p. 2605-2613, (1982).
115. Scott.G., Smith.K., *Rub. Chem. Tech.*, 52, p. 949, (1979).
116. Scott.G., *Plast. Rub. Process*, 2, p. 41, (1977).
117. Kaplan.M., Kelleher.P., Babbington.G., and Hartless.R., in *J. Polym. Sci., Polym. Lett. Ed.*, 11, p. 357, (1973).
118. Scott.G., *A.C.S. Symposium-280*, Chapter-14, P.P.Klemchuk (Ed), A.C.S., Washinton, (1985).
119. Ghaemy.M., and Scott.G., in *Polymer Degradation and Stability*, 3, p.405-422, (1980-81).
120. Ajiboye.O., and Scott.G., in *Polymer Degradation and Stability*, 4, p.415-425, (1982).
121. Scott.G., and Tavakoli.S.M., in *Polymer Degradation and Stability*, 4, p. 343-351, (1982).
122. Al-Malaika.S., and Scott.G., in *Polymer Degradation and Stability*, 5, p.415-424, (1983).
123. Al-Malaika.S. and Honggowongso.S., in *Polymer Degradation and Stability*, 16, p.25-34, (1986).
124. Scott.G., *Developments in Polymer Degradation-8*, N.Grassie-Ed., Appl. Sci. Publ., London, p. 209, (1987).
125. Al-Malaika.S., Ibrahim.A.Q., and Scott.G., *Brit. U.K. Pat. Appl. G.B.*, no. 2 202 226, March 1987.
126. Al-Malaika.S., and Scott.G., *Brit. Pat. Appl.* no. 8 818 880 (1989)
127. Al-Malaika.S., and Sheena.H.H., Unpublished work.
128. Al-Malaika.S., and Islam.S., Unpublished work.
129. Al-Malaika.S., and Hu.G., Unpublished work.
130. Al-Malaika.S., and Xing.X., Unpublished work.
131. Scott.G., in *Developments in Polymer Stabilisation-4*, Chapter-6, G.Scott (Ed.), App. Sci. Publ. Ltd., London, (1981).
132. Pospisil.J., Kotulak.L., Taimr.L., *Eur. Polym. J.*, 7, p. 255, (1971).
133. Scott.G., and Grassie.N., *Polymer Degradation and Stabilisation*, Chapter-5, Cambridge Univ. Press., London, (1985).

134. Grassie.N., and Scott.G., *Polymer Degradation and Antioxidants*, Chapter-5, Elsevier Publishing Company, Amsterdam, (1965).
135. Pospisil.J., in *Developments in Polymer Stabilisation-1*, G.Scott (Ed.), App.Sci.Publ. Ltd. London, p. 1, (1979).
136. Pospisil.J., *Advan. Polym. Sci.*, 36, p. 69, (1980).
137. Pospisil.J., in *Developments in Polymer Photochemistry-2*, N.S.Allen (Ed.), App. Sci.Publ. Ltd, London, p. 53, (1981).
138. Brede.O., *Radiat. Phys. Chem.*, 29, p. 369, (1967).
139. Denisov.E.T., in *Developments in Polymer Stabilisation-5*, G.Scott. (Ed.), Appl.Sci. Publ., London, p. 23, (1982).
140. Henman.T.J., in *Developments in Polymer Stabilisation-1*, G.Scott. (Ed.), Appl.Sci. Publ., London, p.39, (1979).
141. Gugumus.F., *Angew. Makromol. Chem.*, 137, p. 189, (1985).
142. Munteanu.D., Tincu.I., Csunderlik.C., and Iorga.I., *Proceedings of 29th IUPAC Symposium on Macromolecules*, Bucharest, p. 185, (1983).
143. Munteanu. D., Mracec.M., Tincul.I., and Csunderlik.C., *Polym. Bull.*, 13, p.77, (1985).
144. Scott.G., British Patent 1 503 501 (1975).
145. Hutson.G.V., and Scott.G., in *Eur. Polym. J.*, 10, p. 45, (1974).
146. Yachigo.S., Sasaki.M., Takahashi.Y., Kojima.F., Takada.T., and Okita.T., in *Polymer Degradation and Stability*, 22, p. 63-77, (1988).
147. Carlsson.D.J. and Wiles .D.M., *J. Macromol. Sci. Rev. Macromol. Chem.*, p. 155-188, (1976).
148. Allen.N.S., Gardette.J.L. and Lemaire.J., *Polym. Photochem.*, 3, p.251, (1983).
149. Chakraborty. K.B., and Scott.G., in *Eur. Polym. J.*, 15, p.35, (1979).
150. Vink.P., *J. Polym. Sci.*, 40, p.169, (1973).
151. Durmis.J., Karvas.M., Caucik.P. and Holcik.J., *Eur. Polym. J.*, 11, p.219, (1975).
152. Carlsson.D.J., Suprunchuk.T., and Wiles.D.M., *J. Appl. Polym. Sci.*, 16, p.615, (1972).
153. Sharma.Y.N., Naovi.M.K., Gawande.P.S., and Bhardwaj.I.S., *J. Appl. Polym. Sci.*, 27, p.2606, (1982).
154. Bahdwaj.I.S., Sharma.Y.N., and Naovi.M.K., *Proc. 28th IUPAC Symposium on Macromolecules*, p.331, (1982).
155. Pinkerton.D.M., *Weathering of Plastic and Rubbers, International Symposium of Plastic and Rubber Institute*, London, p.41, (1976).

156. Burchil.P.J., and Pinkerton.D.M., *J. Polym. Sci., Symp.*, 55, p.185, (1976).
157. Burchil.P.J., and Pinkerton.D.M., in *Polymer Degradation and Stability*, 2, p.239, 1980.
158. Mlinac.M., Ranogajec.F., Fles.D., and Dvornik.I., *Tech. Papers, Reg. Tech. Conf. Soc. Plast. Eng.*, p.481, (1981).
159. Ranogajec.F., Mlinac.M., and Dvornik.I., *Radiat. Phys. Chem.*, 18, , p.511, (1981).
160. Pradelock.W., Vogl.O., and Gupta. A., in *J. Polym. Sci., Polym. Chem. Ed.*, 19, p. 3307, (1981).
161. U.S. Patent, 893, 896. April 18 (1962)
162. U.S. Patent, 3, 116, 305. December 31 (1963)
163. U.S. Patent, 3, 391, 110. July 2 (1962)
164. Breslow.R, *The Organic Chemistry Monograph Series*, W.A.Benyamin, Inc. Philippines, p.387-392, (1972).
165. Robjohn.N., *Organic Synthesis*, John Wiley&Sons.Inc., New York, p.977-979, (1963).
166. Robinson.R., *Tetrahedron, Vol.23*, Pergamon Press Ltd.Northern Ireland, p.1395-1403, (1967).
167. British Standard Methods of Testing Plastics: BS 2782, Part 7, Method 720A, p.979
168. Hirt.R.C., and Searle.N.Z., *Appl.Polym. Symp.*, No.4, p.61, (1967).
169. Davis.A., and Gardiner.D., in *Polymer Degradation and Stability*, 4, p.145, (1982).
170. Cooley.J.W., and Tukey.J.W., *Math. Comput.*, 19, p.297, (1965).
171. Kemp.W., *Organic spectroscopy, NMR Spectroscopy*, The Macmillan Press Ltd., London, (1975).
172. Wexler.A.S., *Spectrochim., Acta.*, p.1725, (1965).
173. Kremmer.T., *Methods and techniques in gel chromatography*, T.Kremmer and L.Boross (Eds.), John Wiley&Sons, New York, (1979).
174. Johnson.L.T., Jankowski.W.C., *Carbon-13 NMR spectra*, Wiley, New York, (1972).
175. Sanders.J.M.K., and Hunter.B.K., *Modern NMR Spectroscopy*, Chapter 1&9, Oxford University Press, Oxford, (1987).
176. Tager.A., *Physical chemistry of polymers*, Chapter 18, MIR publishers, Moscow, 1972.

177. Kuleratna.K.W.S. and Scott.G., *Eur.Polym.J.*, **14**, Pergamon Press Ltd., p.835-843, (1978).
178. Scott.G., and Yusoff.M.F., in *Polymer Degradation and Stability*, **3**, p.53, (1980-81).
179. Adams.D., and Braun.D., *J. Polym. Sci., Polym. Lett Ed.*, **18**, p.629, (1980).
180. Al-Malaika.S., Ibrahim.A.Q., Rao.M.J., and Scott.G., *JAPS*, **44**, p.1287, (1992).
181. Scott.G. and Setoudeh.E., in *Polymer Degradation and Stability*, **5**, p.81, (1983).
182. Vogl.O., Cs., *J.Polym. Sci., Polym. Chem. Ed.*, **19**, p.3307, (1981).
183. Okasha.R., Hill.G., and Rempp.P., *Europ. Polym. J.*, Vol.15, Pergamon Press Ltd, Great Britain,p.975-982, (1979).
184. Bayard.T.Storey, in *J.of Polym.Sci., Part A*, Vol.3, p.265-282, (1965).
185. Al-Malaika.S., Ibrahim.A.Q., Rao.M.J., and Scott.G., in *J.Appl.Polym.Sci*, **44**, p.1287, (1992).
186. Scott.G., in *J.Appl.Polym. Sci.*, **35**, p.123-149, (1979)
187. Allen.N.S., Gardette.J.L., Lemarie.J., in *Polymer Degradation and Stability*, **8**, p.133, (1984)
188. Scott.G., Mellor.D.C., and Moir.A.B., in *Europ. Polym. J.*, **9**, p.219-225, (1973).
189. Chmela.S., Hrdlovic.P., Manasek.Z., in *Polymer Degradation and Stability*, **11**, p.233, 1985.
190. Allen.N.S., Kotecha.J.L., in *Polymer Degradation and Stability*, **11**, p.181,1985.
191. Pospisil.J., in *Developments in Polymer Stabilisation-7*, Chapter-1, G.Scott. (Ed.), Appl.Sci. Publ., London, 1984.
192. Flory.P., *Principles of Polymer Chemistry*, Chapter-12, Cornell, New York, (1953)
193. Bovey.F.A., *High Resolution NMR of Macromolecules*, Academic Press, New York, 1972, p.141.